



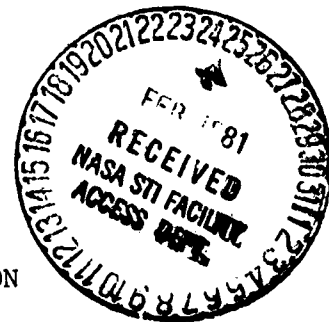
FINAL REPORT
LOW-THRUST CHEMICAL PROPULSION SYSTEM
PUMP TECHNOLOGY

by
J. W. Meadville

Rockwell International
Rocketdyne Division

prepared for
NATIONAL AERONAUTICS AND SPACE ADMINISTRATION

NASA-Lewis Research Center
Contract NAS3-21958
R. E. Connelly, Project Manager



(NASA-CR-165210) LOW-THRUST CHEMICAL
PROPULSION SYSTEM PUMP TECHNOLOGY Final
Report, Oct. 1979 - Sep. 1980 (Rocketdyne)
411 p HC A18/MF A01

CSCL 13K

NR1-17437

Unclas
43582
GJ/37

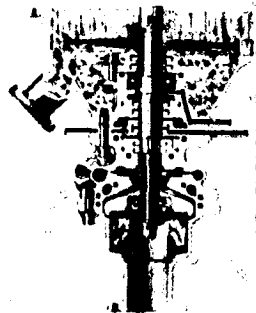
1. Report No. NASA CR-165210		2. Government Accession No.		3. Recipient's Catalog No.	
4. Title and Subtitle Low-Thrust Chemical Propulsion System Pump Technology				5. Report Date 20 October 1980	
				6. Performing Organization Code	
7. Author(s) J. W. Meadville				8. Performing Organization Report No. RI/RD80-222	
9. Performing Organization Name and Address Rocketdyne, Division of Rockwell International 6633 Canoga Avenue Canoga Park, Ca. 91304				10. Work Unit No.	
				11. Contract or Grant No. NAS3-21958	
				13. Type of Report and Period Covered Final Report (Oct. 1979 to Sept. 1980)	
12. Sponsoring Agency Name and Address National Aeronautics and Space Administration Washington, DC 20546				14. Sponsoring Agency Code	
15. Supplementary Notes Project Manager, Robert Connelly, NASA-LeRC, Cleveland, Ohio					
16. Abstract A study was conducted to evaluate the applicability and characteristics of dynamic and positive-displacement pumps and drives in low-thrust chemical propulsion feed systems within the thrust range 450 to 9000 N (100 to 2000 pounds). Performance analyses were made on centrifugal, pitot, Barske, drag, Tesla, gear, piston, lobe, and vane pumps with liquid hydrogen, liquid methane, and liquid oxygen as propellants. Gaseous methane and hydrogen driven axial impulse turbines, vane expanders, piston expanders, and electric motors were studied as drivers. Data are presented on performance, sizes, weights, and estimated service lives and costs.					
17. Key Words (Suggested by Author(s)) Small pumps, low specific speed, high speed, centrifugal, Barske, pitot, drag, Tesla, vane, piston, Gear, axial impulse, LOX pumps, methane pumps, hydrogen pumps.			18. Distribution Statement		
19. Security Classif. (of this report) Unclassified		20. Security Classif. (of this page) Unclassified		21. No. of Pages 411	22. Price*

* For sale by the National Technical Information Service, Springfield, Virginia 22151

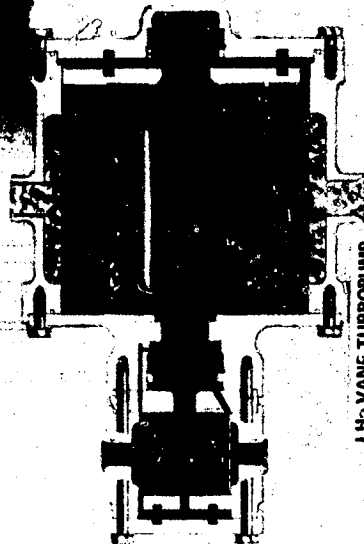
PRELIMINARY DESIGN SIZE COMPARISON



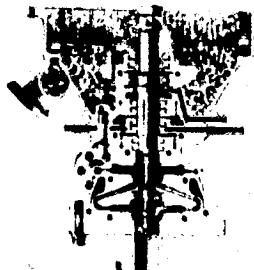
LH2 TURBOPUMP
N = 110,000 RPM
Q = 50 GPM



LO2 TURBOPUMP
N = 28,000 RPM
Q = 18 GPM



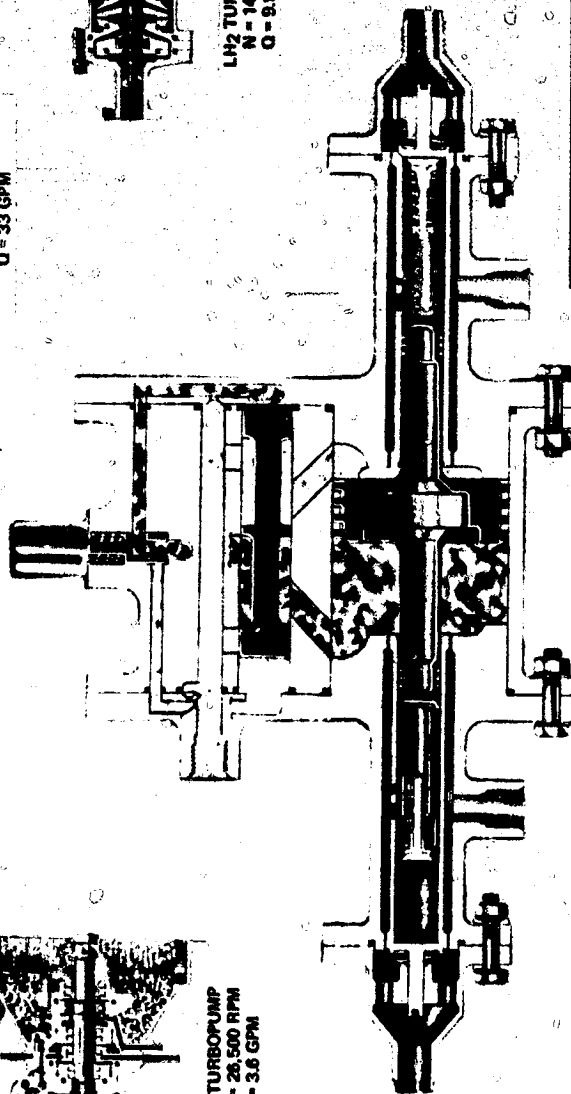
LH2 VANE TURBOPUMP
N = 2500 RPM
Q = 33 GPM



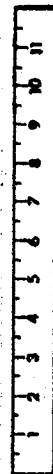
LO2 TURBOPUMP
N = 28,500 RPM
Q = 3.6 GPM



LH2 TURBOPUMP
N = 140,000 RPM
Q = 9.9 GPM



LH2 PISTON PUMP WITH PISTON DRIVE
CPM = 625
Q = 10 GPM



12" RULER - 1/2" SCALE

FOREWORD

The work herein was conducted from October 1979 to September 1980 by personnel from the Advanced Programs and Engineering units at Rocketdyne, a division of Rockwell International, under Contract NAS3-21958. Mr. Robert Connelly, Lewis Research Center, was NASA Project Manager. At Rocketdyne, Mr. Harold Diem, Program Manager, and Mr. James Meadville, Project Engineer, were responsible for the direction of the program.

Important contributions to the conduct of the program and to the preparation of the report material were made by the following Rocketdyne personnel:

Turbomachinery

Mr. A. Csomor
Dr. M. Subbaraman
Mr. S. Meng
Mr. F. O'Hern
Mr. R. Furst

Mechanical Design

Mr. R. Swain
Mr. J. Zorad

Consultant

Dr. O. E. Balje

PRECEDING PAGE BLANK NOT FILMED

TABLE OF CONTENTS

Summary	1
Introduction	7
Discussion: Task I, Analysis of Candidate Pumps	9
Candidate Pump Concepts and Assumptions	9
Centrifugal Pump	11
Barske Pump	11
Pitot Pumps	11
Drag Pump	11
Tesla Pump	16
Vane Pump	16
Gear Pump	16
Lobe Pump	16
Piston Pump	16
Diaphragm Pump	20
Screw Pump	20
Pump Performance Analysis	23
LOX Pump Performance Analysis	25
Methane Pump Performance Analysis	28
Hydrogen Pump Performance Analysis	31
Tesla - Centrifugal Hybrid Pump Analysis	31
Pump Mechanical Considerations	40
Pump Summary	43
Candidate Drive Concepts and Assumptions	43
Axial Impulse Turbines	44
Vane Expanders	44
Piston Expanders	44
Electric Motors	44
Drive Mechanical Considerations	51
Drive Summary	51
Recommended Concepts for Task III Preliminary Designs	65
Discussion: Task II, Trade Studies	67
Discussion: Task III, Preliminary Design	67
Concept Selections and Overview	71
Design 1 - Hydrogen Turbopump	72
Hydrodynamic Design and Performance	72
Aerodynamic Design and Performance	80
Mechanical Design.	86
Weight Analysis	86
Life Assessment	86
Performance Manufacturing Risk	87
Cost Analysis	88
Design 2 - Hydrogen Turbopump	88
Hydrodynamic Design and Performance	91
Aerodynamic Design and Performance	93
Mechanical Design.	93
Weight Analysis	104
Life Assessment	104
Performance and Manufacturing Risk	104
Cost Analysis	104

Design 3 - Oxygen Turbopump	105
Hydrodynamic Design and Performance	105
Aerodynamic Design and Performance	105
Mechanical Design	115
Weight Analysis	117
Life Assessment	117
Performance and Manufacturing Risk	117
Cost Analysis	121
Design 4 - Oxygen Turbopump	122
Hydrodynamic Design and Performance	122
Aerodynamic Design and Performance	125
Mechanical Design	127
Weight Design	127
Weight Analysis	137
Life Assessment	137
Performance and Manufacturing Risk	137
Cost Analysis	137
Design 5 - Hydrogen Vane Pump-Rotor	139
Hydrodynamic and Aerodynamic Design and Performance	139
Mechanical Design	143
Weight Analysis	146
Life Assessment	146
Performance and Manufacturing Risk	148
Cost Analysis	148
Design 6 - Methane Piston Pump-Drive	149
Hydrodynamic and Aerodynamic Design and Performance	149
Mechanical Design	153
Weight Analysis	156
Life Assessment	156
Performance and Manufacturing Risk	156
Cost Analysis	156
Task IV Discussion: Technology Assessment	159
Pump Hydrodynamic Performance	159
Goals	159
Approach	161
Recommended Test Articles	161
Program Schedule	162
Turbine Gas Dynamic Performance	162
Goals	162
Approach	162
Test Article	164
Program Schedule	164
Bearing Life	164
Approach and Test Articles	166
Program Schedule	166
Rotordynamics	166
Approach and Test Articles	168
Program Schedule	168
Dynamic Seal Efficiency	168
Approach and Test Articles	168
Program Schedule	170
Appendix A Task I, Curves	173
Appendix B Task III, Drawings	367
Appendix C Distribution List	389

LIST OF ILLUSTRATIONS

1.	Low Thrust Chemical Propulsion System Pump Technology Program Schedule	6
2.	Elements of a Centrifugal Flow Pump	10
3.	Barske Pump	12
4.	Pitot Pump	13
5.	Drag Pump	14
6.	Tesla Pump	15
7.	Positive-Displacement Pumps	17
8.	Piston Pump Schematic Nomenclature	18
9.	Wobble Plate Piston Pump	19
10.	Diaphragm Pump	20
11.	Screw Pump	21
12.	SOW Operating Requirements for Hydrogen, Methane, and Oxygen	22
13.	Operating Requirements of LOX Pumps	24
14.	Operating Requirements of Methane Pumps	26
15.	Operating Requirements of Hydrogen Pumps	29
16.	Centrifugal Pump	33
17.	Barske Pump	34
18.	Three Stage Pitot Pump	35
19.	LH ₂ Tesla Pump	36
20.	LO ₂ Tesla Pump	37
21.	Drag Pump	38
22.	LCH ₄ Vane Pump	39
23.	Hybrid Tesla-Centrifugal Pump	41
24.	Electric Motor/Alternator Efficiency Falls Off at Low Power	45
25.	Power vs Speed Relationship In Several Pump Candidates	46
26.	LO ₂ Vane Pump CH ₂ Expander (P/R=1.3)	47
27.	In-Line Piston Pump and Drive	48
28.	1000-Pound-Thrust Electric Motor Driven LH ₂ Pump	49
29.	1000-Pound-Thrust Turboalternator	50
30.	1000-Pound-Thrust Electric Motor Driven LO ₂ Pump	50

31.	Liquid Oxygen Pump and Drive Performance	52
32.	Liquid Oxygen Pump and Drive Performance	53
33.	Liquid Methane Drive and Pump Performance	54
34.	Liquid Methane Pump and Drive Performance	55
35.	Liquid Hydrogen Pump and Drive Performance	56
36.	Liquid Hydrogen Pump and Drive Performance	57
37.	LOX Pump Operating Ranges	58
38.	Recommended LOX Preliminary Design Points	59
39.	Liquid Methane Pump Operating Ranges	60
40.	Recommended Liquid Methane Pump Preliminary Design Points	61
41.	Liquid Hydrogen Pump Operating Range	62
42.	Recommended Liquid Hydrogen Pump Preliminary Design Points . .	63
43.	LTCPSPT Design No. 1 Centrifugal Pump-Axial Turbine	68
44.	LTCPSPT Design No. 2 Tesla-Centrifugal Pump-Axial Turbine	68
45.	LTCPSPT Design No. 3 Centrifugal Pump-Axial Turbine	68
46.	LTCPSPT Design No. 4 Tesla-Centrifugal Pump-Axial Turbine	69
47.	LTCPSPT Design No. 5 Vane Pump-Vane Expander	69
48.	LTCPSPT Design No. 6 Piston Pump-Piston Drive	69
49.	Designs 1 and 2 Cover Task I Envelope	70
50.	Designs 3 and 4 Cover Task I Envelope	70
51.	Hydrogen Turbopump Assembly	73
52.	Calculated Design and Off-Design Performance of the Four-Stage Pump	74
53.	HPFTP Turbine Low Thrust Propulsion System, Mean Diameter Optimization, Design 1	76
54.	HPFTP Turbine Low Thrust Propulsion System Velocity Vector Diagram, Design 1	78
55.	HPFTP Turbine Low Thrust Propulsion System Preliminary Turbine Blade Path Data, Design 1	79
56.	HPFTP Turbine Low Thrust Propulsion System Blade Path State Condition, Design 1	81

57.	Design 1, Fuel Turbopump (N = 140,000 rpm)	83
58.	Low Thrust Engine Turbopump Design No. 1 Critical Speed	84
59.	Low Thrust Engine Turbopump Design No. 1 Critical Speed Critical Speed vs Bearing Stiffness	85
60.	Design 1 Weighs 5.5 pounds.	87
61.	Operating Point for Design 2	89
62.	Predicted Pumphead, Flow, Efficiency Curve	90
63.	HPFTP Turbine Low Thrust Propulsion System, Mean Diameter Optimization, Design 2	92
64.	HPFTP Turbine-Low Thrust Propulsion System, Velocity Vector Diagram, Design 2	95
65.	HPFTP Turbine Low Thrust Propulsion System, Preliminary Turbine Blade Path Data, Design 2	96
66.	HPFTP Turbine Low Thrust Propulsion System, Blade Path State Condition, Design 2	97
67.	Design 2, Fuel Turbopump Tesla Inducer (N = 110,000 RPM).	100
68.	Low Thrust Engine Design No. 2 Critical Speed	101
69.	Low Thrust Engine Design No. 2 Critical Speed Critical Speed vs Bearing Stiffness	102
70.	Design 2 Weighs 10.0 Pounds	103
71.	Layout of Design 3	106
72.	Calculated Design and Off-Design Performance of the Two-Stage Pump	107
73.	HPOTP Turbine Low Thrust Propulsion System, Mean Diameter Optimization, Design 3	110
74.	HPOTP Turbine Low Thrust Propulsion System, Velocity Vector Diagram, Design 3	112
75.	HPOTP Turbine Low Thrust Propulsion System, Preliminary Turbine Blade Path Data, Design 3	113
76.	HPOTP Turbine Low Thrust Propulsion System, Blade Path State Condition, Design 3	114
77.	Design 3, LOX Turbopump (N = 26,500 RPM)	118
78.	Low Thrust Engine Turbopump Design 3 Critical Speed	119
79.	Low Thrust Engine Turbopump Design 3 Critical Speed Critical Speed vs Bearing Stiffness.	120

80.	Design 3 Weighs 12.0 Pounds	121
81.	Design 4, Liquid Oxygen Pump	123
82.	Predicted Pump Head, Flow, Efficiency Curve	124
83.	HPOTP Turbine Low Thrust Propulsion System, Mean Diameter Optimization, Design 4	126
84.	HPOTP Turbine Low Thrust Propulsion System, Velocity Vector Diagram, Design 4	129
85.	HPOTP Turbine Low Thrust Propulsion System, Preliminary Turbine Blade Path Data, Design 4	130
86.	HPOTP Turbine Low Thrust Propulsion System, Blade Path State Condition, Design 4	131
87.	Design 4 LOX Turbopump (Tesla Inducer N = 28,000 rpm)	134
88.	Low Thrust Engine Turbopump Design 4 Critical Speed	135
89.	Low Thrust Engine Turbopump Design 4 Critical Speed, Critical Speed vs Bearing Stiffness	136
90.	Design 4 Weighs 10.5 Pounds	138
91.	Vane Pump-Motor	140
92.	Vane Pump-Motor	141
93.	Design 5 Hydrogen Vane Pump-Motor	142
94.	Vane Pump-Motor	144
95.	Vane Pump-Motor Back Pressures	145
96.	Speed and NPSH as Functions of Flow	146
97.	Design 5 Weighs 94.0 Pounds	147
98.	Design Methane Piston Pump-Drive	150
99.	Design Relationship Methane Pump-Drive	151
100.	Methane Pump-Drive Part Load Data	152
101.	Methane Pump-Drive Back Pressures	154
102.	Cyclic Speed is Proportional to Flow Rate and Required NPSH Value Increases With the Square of Speed	155
103.	Design 6 Weighs 127.5 Pounds	157
104.	Flowrate vs Head for Pumps Manufactured by Rocketdyne	160
105.	Pump Technology Advancement Schedule	163
106.	Turbine Technology Advancement Program	165
107.	Bearing Technology Assessment Schedule	167
108.	Shaft Dynamic Assessment Schedule	169
109.	Seal Technology Assessment Schedule	171

LIST OF TABLES

1.	Hybrid Centrifugal-Tesla Performance	32
2.	Liquid Oxygen Pump Characteristics	40
3.	Liquid Methane Pump Characteristics	42
4.	Liquid Hydrogen Pump Characteristics	42
5.	Design 1, Low Thrust Propulsion System HPFTP Turbine Performance Parameters	75
6.	Design 1, Low Thrust-Propulsion System HPFTP Turbine Flange-to-Flange Efficiency and Performance	77
7.	Design 2, Low-Thrust Propulsion System HPFTP Turbine Performance Parameters	91
8.	Design 2, Low Thrust-Propulsion System Turbine Flange- to-Flange Efficiency and Performance	94
9.	Design 3, Low Thrust Propulsion System HPOTP Turbine Performance Parameters	109
10.	Design 3, Low Thrust-Propulsion System HPOTP Turbine Flange-to-Flange Efficiency and Performance	111
11.	Design 4, Low Thrust Propulsion System Turbine Performance Parameters	125
12.	Design 4, Low Thrust-Propulsion System Turbine Flange- to-Flange Efficiency and Performance	128

SUMMARY

A wide spectrum of possible pumps and drives for low thrust chemical rocket engine application has been studied in this program. Many potentially satisfactory pumps and drives were identified. The positive displacement pumps, notably the piston and vane, have high predicted performance. However, they tend to be large, heavy and difficult to fabricate. Dynamic pumps such as centrifugal offer much smaller and lighter units that are easier to fabricate. However, they are dramatically lower in performance, often requiring four times as much power to produce the same outlet conditions. Fortunately, the effect on overall engine performance is small because lost power primarily heats the propellant which is ultimately gasified and consumed during combustion. To provide the same impulse, the low thrust engine must operate for long periods of time. The long life of centrifugal pumps is well established. The life characteristics of vane and piston pumps must be determined by testing. Five classes of technology efforts are identified. Details are given on specific areas of knowledge required to successfully produce low thrust engine pumps. This program was completed on schedule and within budget.

This report covers effort performed at Rocketdyne, A Division of Rockwell International, from October 1979 through October 1980. The effort expended was focused on pump and drive technology for low thrust, 445-8900 N (100 to 2000 lbs.), chemical rocket engines using liquid oxygen and liquid hydrogen or liquid methane. This application required low flowrates and moderate to high pressures (low specific speed). Industry experience with such low specific speed pumps is limited. The program is divided into five tasks:

- I Analysis of Candidate Pumps
- II Trade Studies
- III Preliminary Designs
- IV Technology Assessment
- V Reporting

Task I, Analysis of Candidate Pumps, was established to survey the full range of possible pumps and drives, select promising candidates for parametric studies to determine performance and geometry trends over a specific range of flow and pressure. Minimum NPSH capabilities were specified at 0.6, 1.8, and 4.6 m (2, 6, and 15 feet) for oxygen, methane and hydrogen, respectively. Producibility limits were formulated to ensure that the parametric analysis would not yield impossibly small machines. Bearing life requirements were assessed and bearing DN (Diameter-Speed Product, mm-rpm) number limits were selected.

To adequately survey the range of possible pumps and drives, an in-depth literature search was performed. This search and Rocketdyne's own experience base yielded many unique and promising candidates for low thrust rocket engine application. Many others were eliminated. Some of the pumps and drives that were eliminated are listed as follows:

<u>Pump Type</u>	<u>Reason Eliminated</u>
Lobe	Lubrication System Required for Synchronizing Gears
Piston (Except In-Line)	Mechanically Complicated, Requires Lubrication
Diaphragm	Large Hold Over Volume, Diaphragm Fatigue
Screw	Difficult to Fabricate

<u>Drive Type</u>	<u>Reason Eliminated</u>
Single Acting Piston	Cannot Start If On Return Stroke
Terry Turbine	Low Performance
Re-entry Turbine	High Pressure Ratio Required
Drag Turbine	Too Large
Lobe Expander	Lubrication Required for Timing Gears
Gear Expander	Reduced Life of Gear Teeth

Pumps and drives selected as candidates were selected because they had desirable operating characteristics based on published information or Rocketdyne first hand experience. The pumps and drives selected fall into two categories; positive displacement and dynamic.

Candidate Pumps

<u>Dynamic</u>	<u>Positive Displacement</u>
Centrifugal	Vane
Pitot	Piston
Tesla	Gear
Drag	

Candidate Drives

<u>Dynamic</u>	<u>Positive Displacement</u>
Axial Impulse turbines	Vane Expander
	Piston Expander

In addition, electrical motors were studied as possible drives for any of the pumps.

Types of analysis performed include, parametric variations of number of stages, speed, diameter, percent emission and admission and efficiency. One-hundred-eighty-six curves were produced that show the study envelope consisting of minimum and maximum flow and minimum and maximum pressure rise. Superimposed on the envelopes are lines of constant value for parameters such as speed, efficiency and diameter. The results of the study are very briefly shown below.

Liquid Oxygen

- Centrifugal - 3 NPSH levels studied, 10,000 to 32,000 rpm, 25% to 65% efficient, 2 to 9.4 cm (0.8 to 3.7 in.) in diameter, 0.2 to 30 kW (0.25 to 40 hp)
- Pitot - 2 NPSH levels studied, 4,000 to 10,000 rpm, 4.3 to 15 cm (1.7 to 6.0 in.) in diameter, 0.2 to 13 kW (0.3 to 18 hp)
- Tesla - 0.6 m (2 ft.) NPSH, 10,000 to 40,000 rpm, 21% to 50% efficient, 2.5 to 7.0 cm (1.0 to 2.7 in.) in diameter, 0.4 to 16 kW (0.6 to 21 hp)
- Drag - 2 NPSH levels studied, 2 to 24 stages, 13 to 203 cm (5.0 to 80 in.) in diameter, 500 to 1,600 rpm.
- Vane - 3 NPSH levels studied, three clearance to diameter ratios evaluated 0.000025, 0.00050, 0.00075.
- Piston - 5,000 to 12,000 rpm, 90% to 94% efficient, 1.0 to 4.0 cm (0.4 to 1.6 in.) diameter, 0.08 to 7.5 kW (0.1 to 10 hp)

Liquid Methane

- Centrifugal - 3 NPSH levels studied, 30,000 to 60,000 rpm, 38% to 65% efficiency, 1.8 to 5.0 cm (0.7 to 2.0 in.) diameter, 0.37 to 19 kW (0.5 to 25 hp)
- Pitot - 2 NPSH levels, 12,000 to 40,000 rpm, 53% to 56% efficient, 2.5 to 10 cm (1.0 to 4.0 in.) in diameter, 0.2 to 15 (0.3 to 20 hp)
- Tesla - 62,000 to 108,000 rpm, 12% to 40% efficient, 2.5 to 3.2 cm (1.0 to 1.25 in.) diameter, 1.0 to 20 kW (1.3 to 27 hp)
- Drag - 2 NPSH levels studied, 2 to 6 stages, 30 cm (12 in.) diameter, 45% efficient
- Vane - 1,600 to 3,186 rpm, 88% to 96% efficient, 2.5 to 5.1 cm (1.0 to 2.0 in.) diameter.
- Piston - 2,700 to 10,000 rpm, 82% to 94% efficient, 0.8 to 2.8 cm (0.3 to 1.1 in.) diameter, 0.2 to 7.5 kW (0.25 to 10 hp)

Liquid Hydrogen

- Centrifugal - 3 NPSH levels studied, 40,000 to 140,000 rpm, 25% to 50% efficient, 1.8 to 8.9 cm (0.7 to 3.5 in.) diameter, 0.7 to 37 kW (0.9 to 50 hp)
- Pitot - 2 NPSH levels studied, 20,000 to 80,000 rpm, 3.0 to 13 cm (1.2 to 5.0 in.) diameter, 0.75 to 45 kW (1.0 to 60 hp)
- Tesla - 55,000 to 140,000 rpm, 25% to 53% efficient, 2.5 to 6.0 cm (1.0 to 2.4 in.) diameter, 1.1 to 52 kW (1.5 to 70 hp)
- Drag - 5 to 6 stages, 200 to 5,000 rpm, 38 to 500 cm (15 to 200 in.) diameter.
- Vane - 1,700 to 5,038 rpm, 87% to 93% efficient, 2.5 to 7.6 cm (1.0 to 3.0 in.) diameter
- Piston - 2,800 to 10,000 rpm, 80% to 93% efficient, 1.1 to 4.3 cm (0.45 to 1.7 in.) diameter, 0.4 to 30 kW (0.5 to 40 hp)
- Gear - 1,300 to 7,000 rpm, 52% to 75% efficient, 1.9 to 8.1 cm (0.75 to 3.2 in.) diameter

During the final part of Task 1, a hybrid pump consisting of a Tesla suction stage and a centrifugal was conceived. The use of the Tesla stage facilitated a substantial increase in pump speed. This increased the centrifugal stage efficiency enough to compensate for a relatively low Tesla stage efficiency. This hybrid combination was eventually selected for two of the preliminary designs in Task 111.

Task 11, Trade Studies, was modified during the Task 1 review at NASA-LeRC. The original objective was to study the effects of varying NPSH and head rise requirements. During Task 1, a substantial amount of this objective was accomplished. Some additional effort on low NPSH was performed in Task 111. Tank mounting was briefly examined. The primary effect of tank mounting is to reduce the required tank pressure in direct proportion to the reduction in inlet losses. By mounting turbomachinery on the tank, the inlet and discharge ducting for the drive is longer. This results in higher gas path losses and ultimately reduces engine P_c . Depending upon thrust chamber pressure levels, this can have very little to substantial effect on engine I_s .

Task 111, Preliminary Designs, was devoted to the design of six pump-drives selected by NASA/LeRC following the review of Task 1. The six design points and the pump-drive operating characteristics are described on the following page.

	<u>Design Point</u>		<u>Characteristics</u>
Design 1 Hydrogen Turbopump	6.2x10 ⁻⁴ m/s 6.55 Mpa 4.6 m NPSH	9.9 gpm 950 psi 15 ft NPSH	140,000 rpm 4-Stage Centrifugal 7% Admission Turbine 24.5 N (5.5 pounds)
Design 2 Hydrogen Turbopump	31.6x10 ⁻⁴ m/s 6.55 Mpa 4.6 m NPSH	50 gpm 950 psi 15 ft NPSH	110,000 rpm Tesla-Centrifugal Hybrid 30% Admission Turbine 44.5 N (10.0 pounds)
Design 3 LOX Turbopump	2.3x10 ⁻⁴ m/s 4.3 Mpa 0.6 m NPSH	3.6 gpm 625 psi 2 ft NPSH	26,500 rpm 2-Stage Centrifugal 5.6% Admission Turbine 53.4 N (12.0 pounds)
Design 4 LOX Turbopump	11x10 ⁻⁴ m/s 4.3 Mpa 0.6 m	18 gpm 625 psi 2 ft NPSH	28,000 rpm Tesla-Centrifugal Hybrid 30% Admission Turbine 53.4 N (10.5 pounds)
Design 5 Hydrogen Vane Pump- Motor	21x10 ⁻⁴ m/s 6.55 Mpa 4.6 m NPSH	33 gpm 950 psi 15 ft NPSH	2,500 rpm Double Flooded Floating End Plates 418 N (94.0 pounds)
Design 6 Methane Piston Pump- Drive	6.3x10 ⁻⁴ m/s 6.55 Mpa 1.8 m NPSH	10 gpm 950 psi 6 ft NPSH	625 cpm Double-Acting Drive Dual Pumps 567 N (127.5 pounds)

Task IV, Technology Assessment, concentrated on areas of technology that need improvement if pumps and drives for low thrust rocket engines are to be successfully developed. Three types of programs were proposed. First, Turbopump Development, where a specific thrust is desired and an entire turbopump or pump-drive is developed to satisfy the operating requirements. Second, Component Development, where specific components are developed to eventually be calibrated for turbopump development. Finally, Advanced Technology, where various components are studied and tested for possible application in future component development.

The last task, Task V, was devoted to reporting functions. Figure 1 shows the program schedule. All effort is completed.

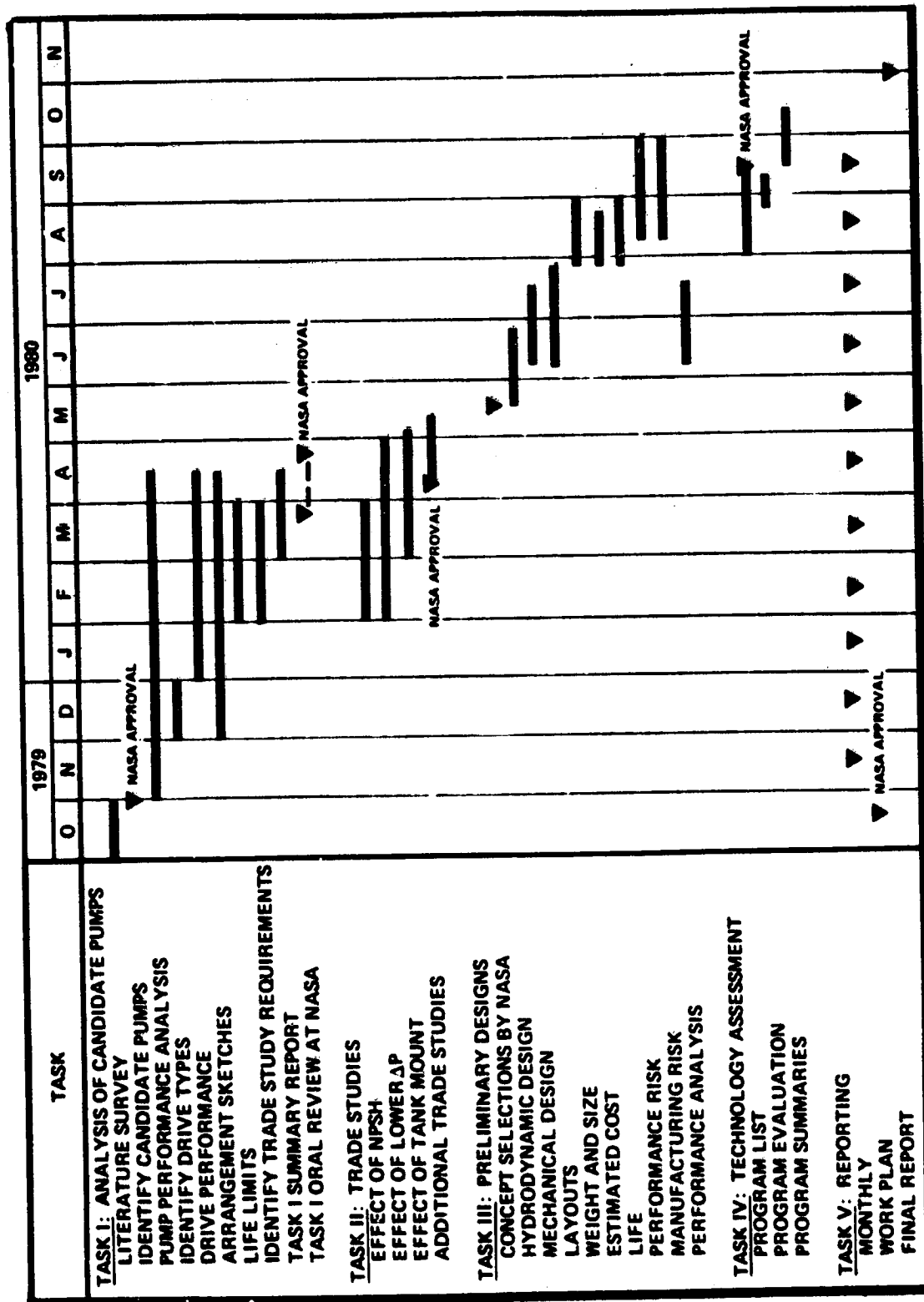


Figure 1. Low Thrust Chemical Propulsion System Pump Technology Program Schedule

ORIGINAL PAGE IS
OF POOR QUALITY

INTRODUCTION

Low thrust chemical propulsion is a candidate being considered for transferring acceleration-limited large space structures from low-earth-orbit or geosynchronous or other high-earth-orbits. The thrust values of interest for this purpose range from 445 N to 8900 N (100 to 2,000 pounds). The propellants, LH₂/LOX and hydrocarbon fuels/LOX, being considered for these systems and the pressure and flow requirements of the pump fed systems will require pumps that operate in a range for which little or no technology exists. The technical consensus before this study was that conventional dynamic type pumps (centrifugal) would be able to meet the maximum anticipated life requirement of 50 hours but may not be capable of achieving the pressure-flow requirements in the lower thrust range. In contrast, positive displacement type pumps were considered to have a well developed technology base for conventional fluids but may have serious problems meeting the engine service life requirements because of the non-lubricating properties of the cryogenic fluids.

This program was performed by Rocketdyne, under NASA-Lewis Research Center Contract No. NAS3-21958, to identify pumps and drives which could be used for low thrust application and study them in sufficient detail to define their performance and mechanical characteristics.

This study will provide information to the propulsion system designer on the current state of technology of applicable pumps, pump characteristics and performance information for making system trade studies and provide a base on which to start future pump technology programs.

DISCUSSION: TASK I, ANALYSIS OF CANDIDATE PUMPS

Task I was performed during the period October 1979 through April 1980. Results of the task were presented in an oral presentation to NASA-LeRC personnel on 23 April 1980. The purpose of the task was to examine all potential pumping devices applicable to low thrust chemical rocket engines in the 445-8900 N (100-2000 pound) thrust range. Two propellant combinations were of interest: oxygen-hydrogen (O_2-H_2) and oxygen-methane (O_2-CH_4). As a result, three propellant pump groups were studied (oxygen, methane, and hydrogen). A noteworthy operating requirement of these pumps is low flowrate/high pressure rise. Rocket industry experience in this area is very limited. To identify all potential pump types capable of performing in a rocket engine environment, a literature search was performed. From this and Rocketdyne's own experience base, a group of candidate pumps was selected. These pumps fall in two major categories: dynamic pumps and positive displacement pumps. Dynamic pumps are dependent upon fluid dynamics to accomplish the required pressure rise. The flow is accelerated to high velocity (thus adding kinetic energy) and is then diffused to the desired pressure. Dynamic pump operation is characterized by uniform discharge pressure (with time) and a continuous flow path through the machine. These characteristics lead to smooth engine operation and simple chilldown procedures. Positive displacement pumps perform by squeezing the flow. Discrete chambers or cells are formed in which the volume is variable with time. The fluid enters when the volume is large and exits when the volume is small (and the propellant is at a high pressure). Positive displacement pump operation is characterized by variable discharge pressure (with time) and a noncontinuous flow path. This creates a need for smoothing the discharge pressure and complicates the chilldown procedures. The following is a list of the dynamic (D) and positive (P) displacement pumps selected for concept analysis:

Centrifugal (D)	Drag (D)	Piston (P)
Barske (D)	Vane (P)	Diaphragm (P)
Pitot (D)	Gear (P)	Screw (P)
Tesla (D)	Lobe (P)	

CANDIDATE PUMP CONCEPTS AND ASSUMPTIONS

Centrifugal Pump

Centrifugal pumps are a prime candidate for low thrust application. They are the most common type of pump for rocket engine applications. Their performance is constant with time because of minimum rubbing contact. Long life capability has been demonstrated. They have smooth discharge characteristics and are easy to chill down.

PRECEDING PAGE BLANK NOT FILMED

Constraints imposed on the design are as follows: rotor diameter (DT) must be no less than 1.8 cm (0.7 in.) to facilitate fabrication of blade profiles. Discharge width (b_2) is limited to no less than 0.076 cm (0.03 in.) for fabrication ease. The bearings are 10 mm or larger and bearing DN (rpm-mm) is limited to 1.4×10^6 for oxygen and methane and 1.9×10^6 for hydrogen. Suction specific speed capability is assumed to be 30,000 for oxygen and methane and 40,000 for hydrogen. Figure 2 shows a cross-section of a typical single stage centrifugal pump.

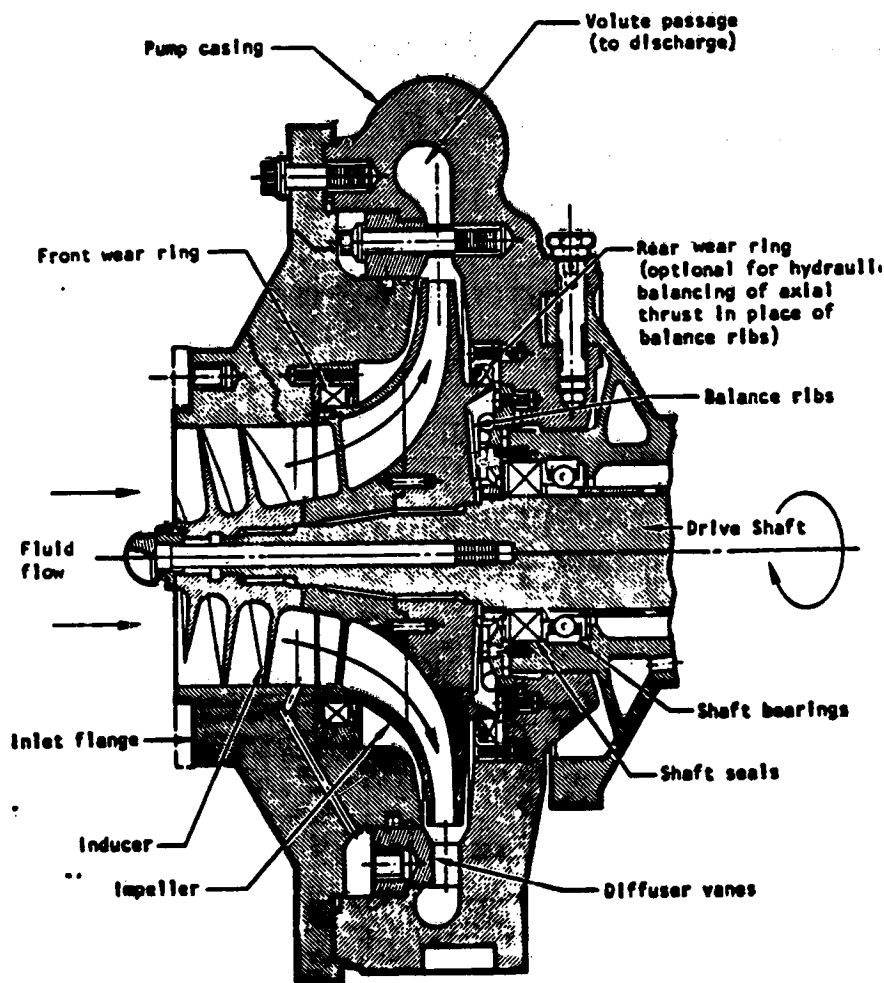


Figure 2. Elements of a Centrifugal Flow Pump

All centrifugal pumps are analyzed with an axial flow inducer integral to the first stage and impeller only for all successive stages.

Barske Pump

Barske pumps are a subset of centrifugal pumps. Their basic characteristic is that they are partial emission centrifugal pumps. Normally open (unshrouded) radial vanes make up the rotor. Their main advantages are ease of fabrication and low specific speed capability. Figure 3 shows a simple Barske pump with its axial inlet and tangential discharge. Performance analysis of Barske pumps is included in the centrifugal pump analysis sections to follow.

Pitot Pump

Pitot pumps use the pitot tube as a collection and pressure recovery device. The pump housing rotates, forcing the fluid into a stationary pitot tube. These pumps are low specific speed with constant performance (with time). No rubbing contact ensures long life, and an open flow path makes chilldown easy. Smooth discharge pressure makes engine operation better. Some constraints imposed on the design are: tube diameter (D) is limited to 2.5 cm (1 in.) minimum, tube ID(δ) must be no less than 0.076 cm (0.03 in.); single tube pickup per stage, D/δ , must be greater than 15, suction specific speed is 15,000 for oxygen and methane and 20,000 for hydrogen. Figure 4 shows a pitot pump (single stage) in schematic form.

Drag Pump

Drag pumps are characterized by radial inlet and outlet lines. Pumping is performed by a rotor which forces the fluid to flow tangentially by means of many small paddles machined in the outside diameter. A small clearance section of the housing isolates the high and low pressure regions. A large radial force is generated by this unequal circumferential pressure distribution; as a result stages are limited to no less than two with even numbers of stages preferred. Other constraints on the pump include: clearance to diameter ratio equals 0.001, minimum diameter equals 1.9 cm (0.75 in.), internal velocity head is limited to 1/2 NPSH at the inlet. Figure 5 shows a two-stage drag pump in schematic form.

Tesla Pump

Tesla pumps (or disc pump) achieve the pumping effect by means of viscous drag created by many thin discs assembled with close clearance and rotated at high speed. Fluid is drawn in at the inside diameter and expelled with higher energy at the outside diameter. The fluid is then diffused to the desired pressure. This type pump can operate at very low inlet NPSH and specific speed. Long life is probable because of no rubbing contact. Constraints placed on the design include: minimum inlet diameter 1.3 cm (0.5 in.), minimum outside diameter 2.5 cm (1 in.), maximum speed 160,000 rpm, number of discs 75, disc thickness and gap 0.13 mm (0.005 in.). Figure 6 shows a schematic of a tesla type pump.

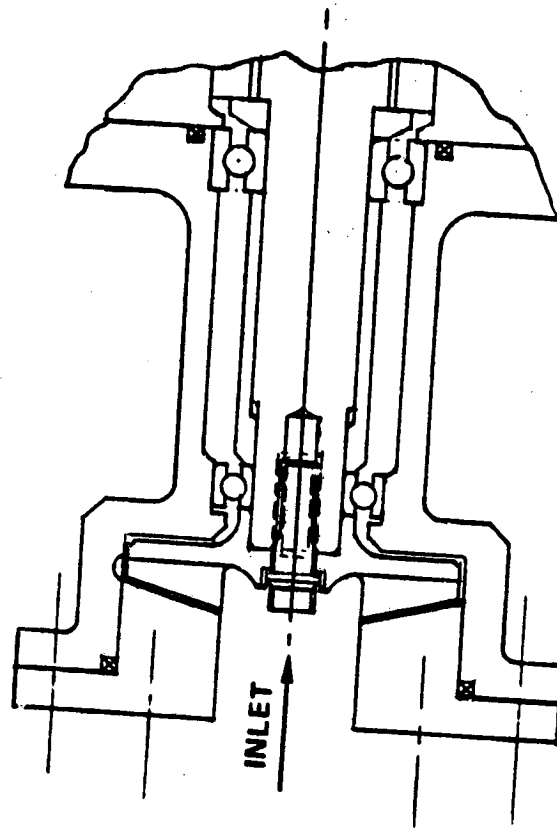
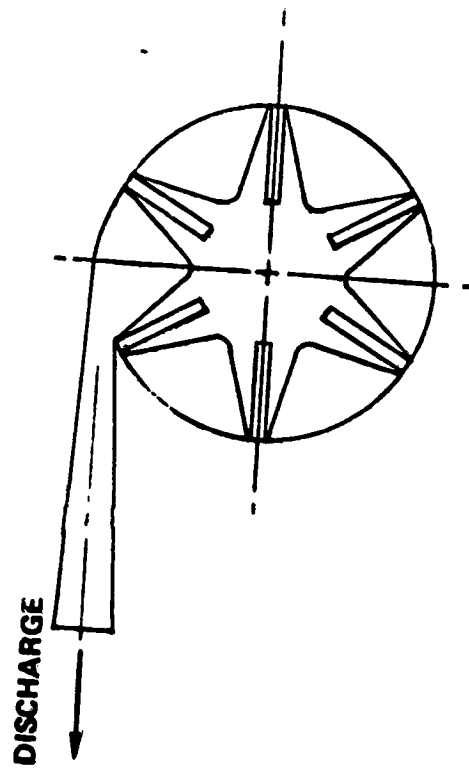


Figure 3. Barske Pump

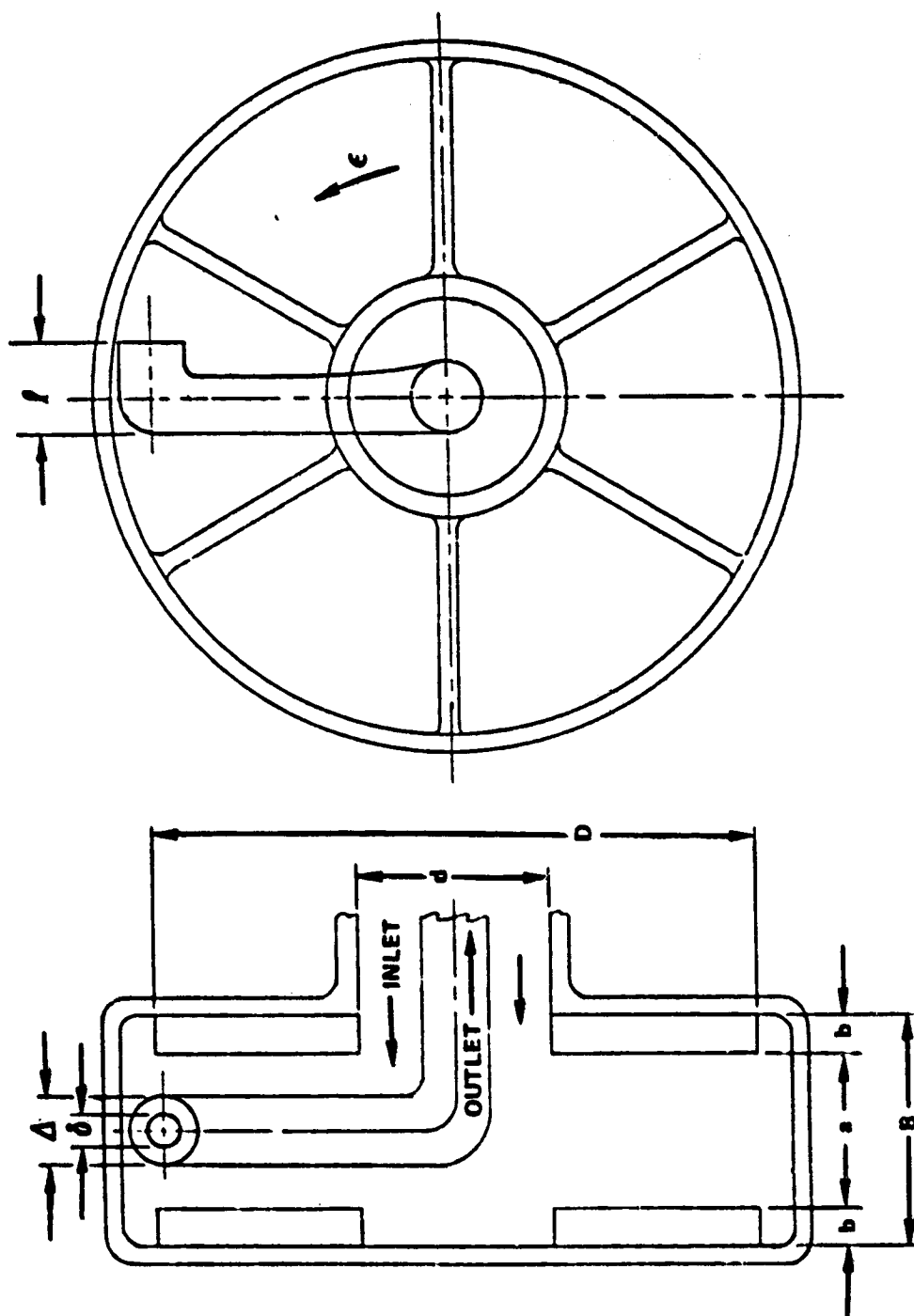


Figure 4. Pitot Pump

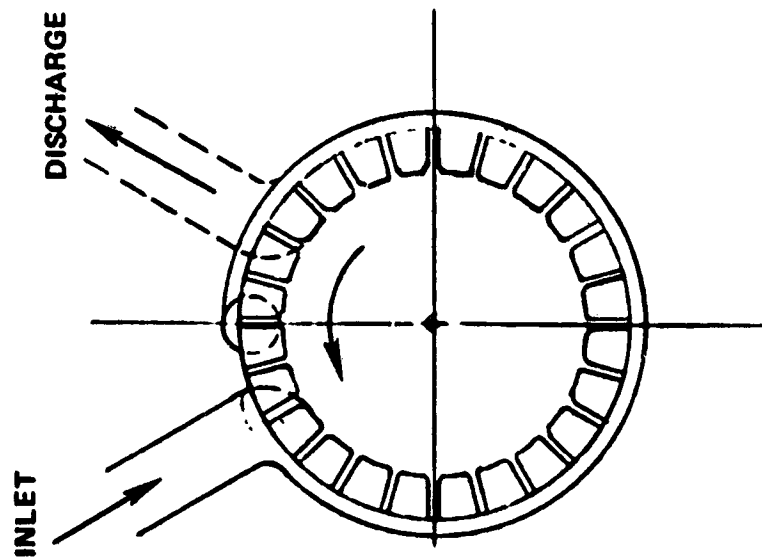
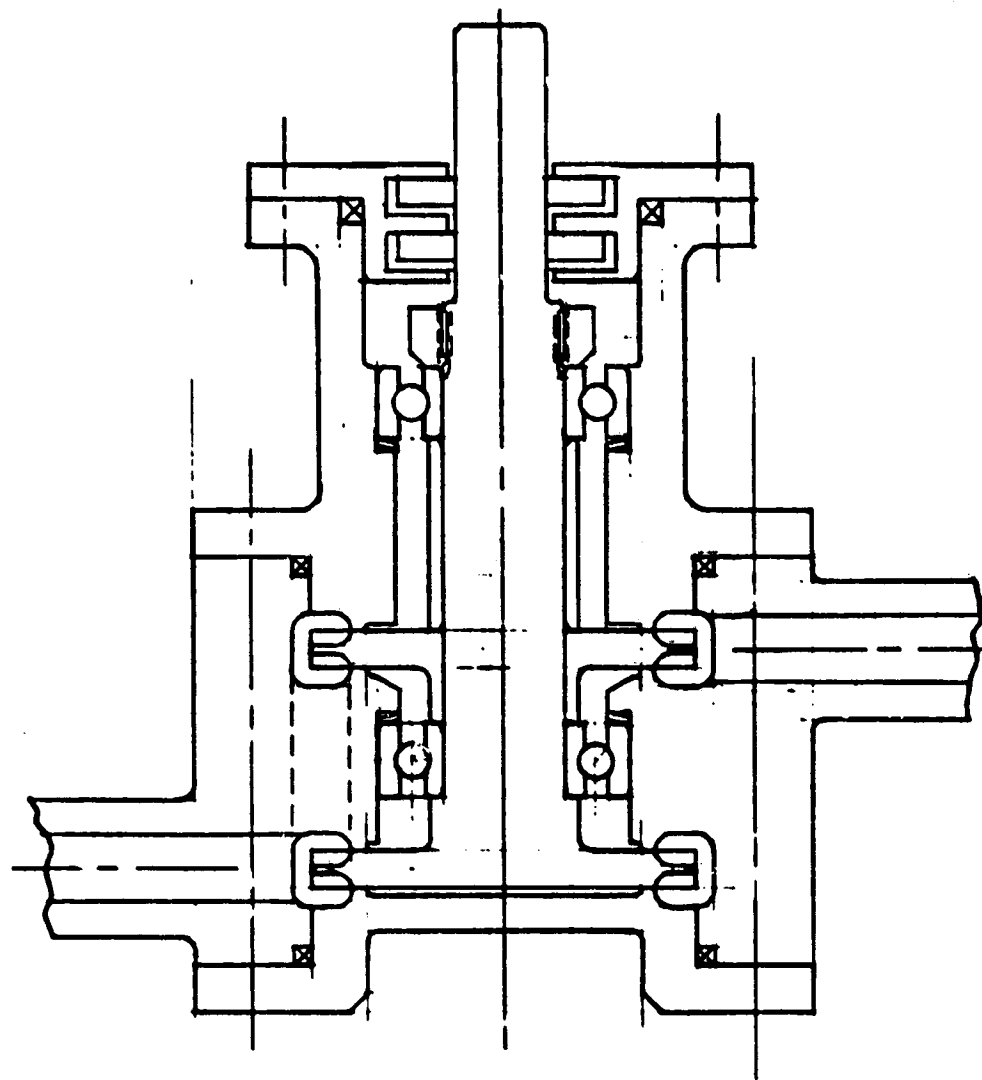


Figure 5. Drag Pump

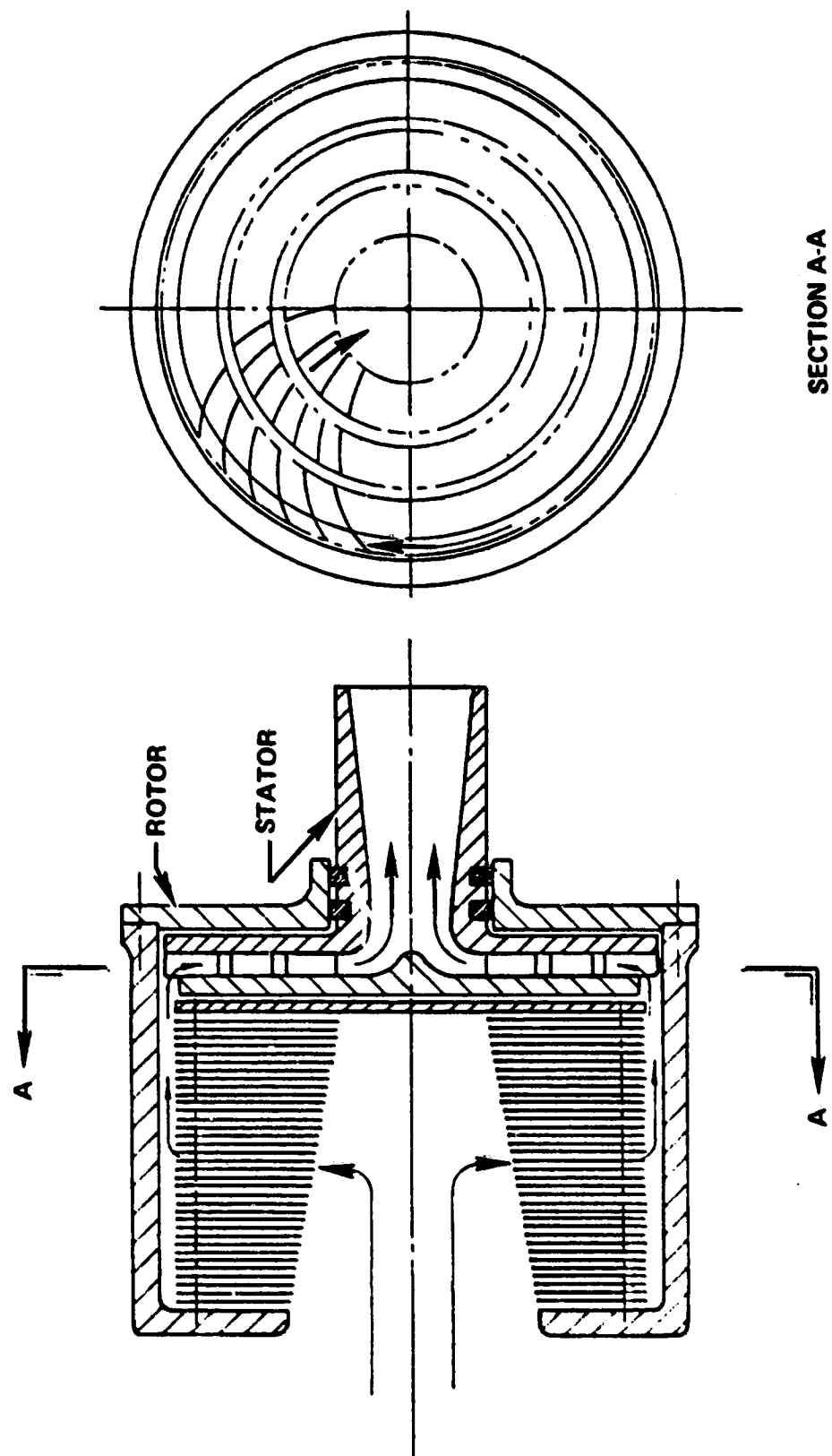


Figure 6. Tesla Pump

Vane Pump

Vane pumps have a segmented rotor with movable vanes (or dams) that trace the eccentric housing in which the rotor spins. The cavity created by two adjacent vanes, the rotor and the housing is largest at the inlet and smallest at the discharge. Very low specific speeds are possible with this and most positive displacement pumps. Figure 7 shows a vane pump schematic with three vanes; analysis performed during Task I was based upon a 16-vane configuration. Constraints imposed include: minimum diameter 2.5 cm (1 in.), vane thickness over rotor diameter ratio equals 0.05, clearance vs diameter varied from 0.00025 to 0.00075, internal velocity head was limited to one-half NPSH.

Gear Pump

Gear pumps force the fluid from inlet to discharge by trapping it between successive rows of gear teeth. Very low specific speeds are possible. Constraints imposed include: clearance over diameter ratio equals 0.00025, length over diameter ratio equals 1.5, clearance times length over diameter ratio equals 0.05, minimum diameter is 1.5 cm (0.6 in.), internal fluid velocity head limited to one-half NPSH. Figure 7 shows a gear pump.

Lobe Pump

Lobe pumps operate like gear pumps except that the lobe shape is optimized for pumping. Lobes are not self-synchronizing as are gears, therefore timing gears are required to maintain correct lobe operation. Lubrication of the gears with propellant as opposed to oil is required to simplify the engine system. Gear pump performance is nearly the same as lobe pumps, therefore only gear pumps will be considered further because they offer nearly the same performance with a much simpler design. Figure 7 shows a lobe pump with three lobes (timing gears not shown).

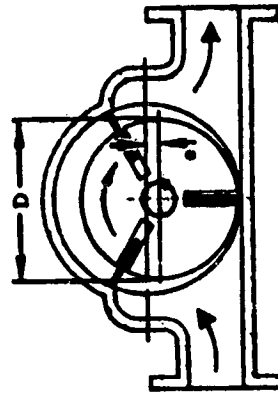
Piston Pump

The most common positive displacement pump is the piston pump. Several configurations are possible: crank operated (Fig. 8), radial, wobble plate operated (Fig. 9), and free piston (all axial motion). Analysis was performed assuming a free double acting piston. This eliminates top dead center starting problems with a crank drive. A single piston was selected to reduce complexity and weight. Constraints imposed include: stroke over diameter ratio between 0.75 and 1.0, length over diameter ratio equals 4.0, and clearance between 0.0025 and 0.008 cm (0.001 and 0.003 in.).

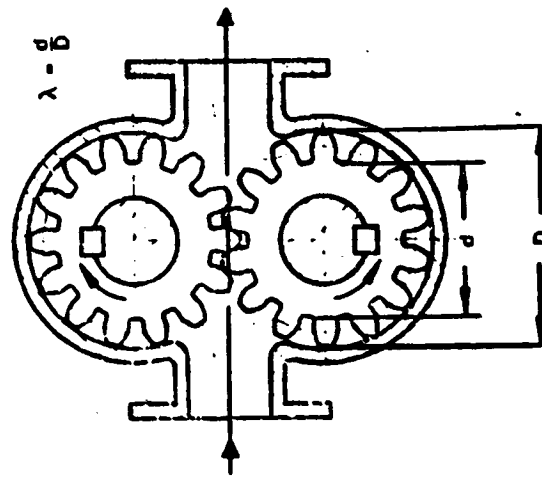
Diaphragm Pump

Diaphragm pumps were considered and then, for the following reasons, eliminated as a candidate. Figure 10 is a schematic sketch of a diaphragm pump actuated by an eccentric shaft. The flexible membrane required would have low life capability in a cryogenic environment. The relative size is large compared to other types of pumps. A large carry-over volume is present, which could be a problem if propellant gas bubbles were to collect in the pumping chamber.

VANE PUMP



GEAR PUMP



MULTILOBE PUMP

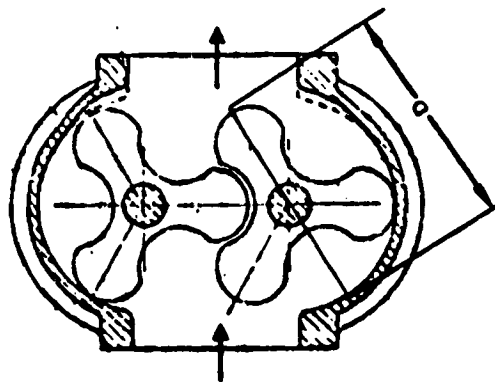


Figure 7. Positive-Displacement Pumps

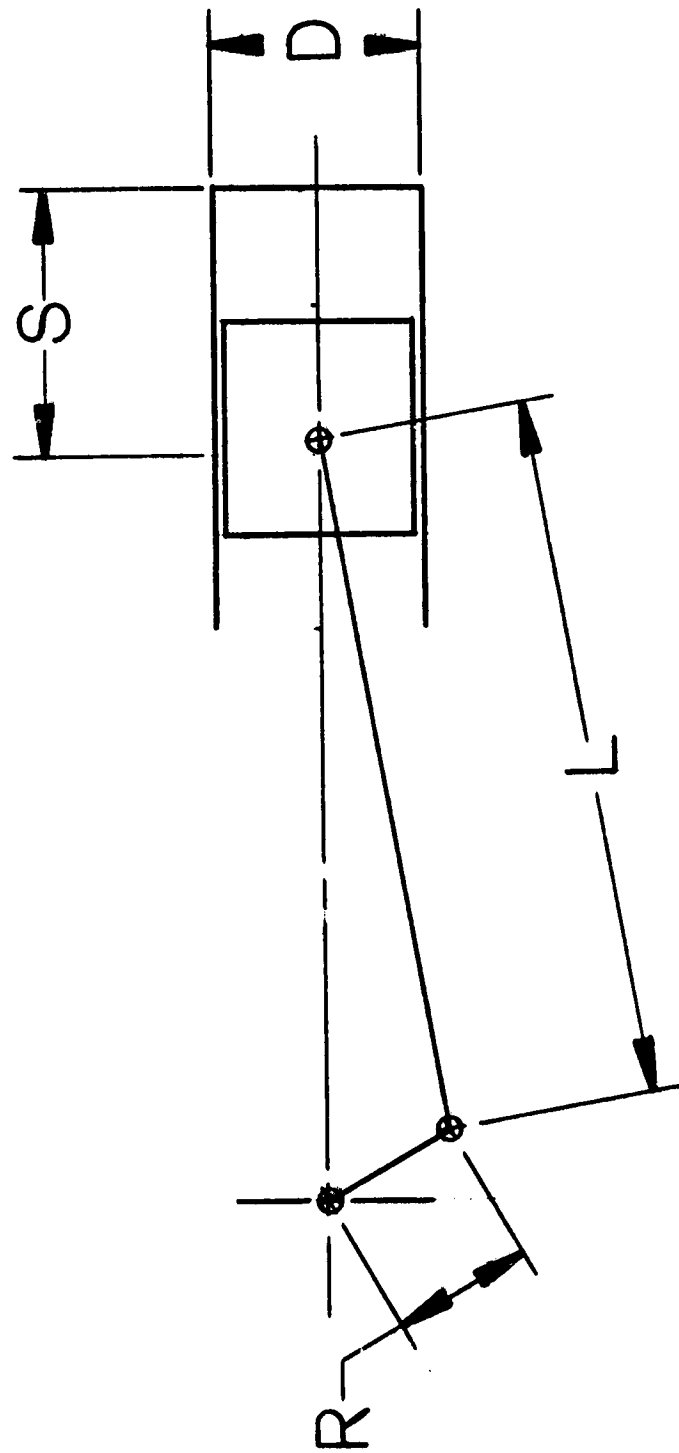


Figure 8. Piston Pump Schematic Nomenclature

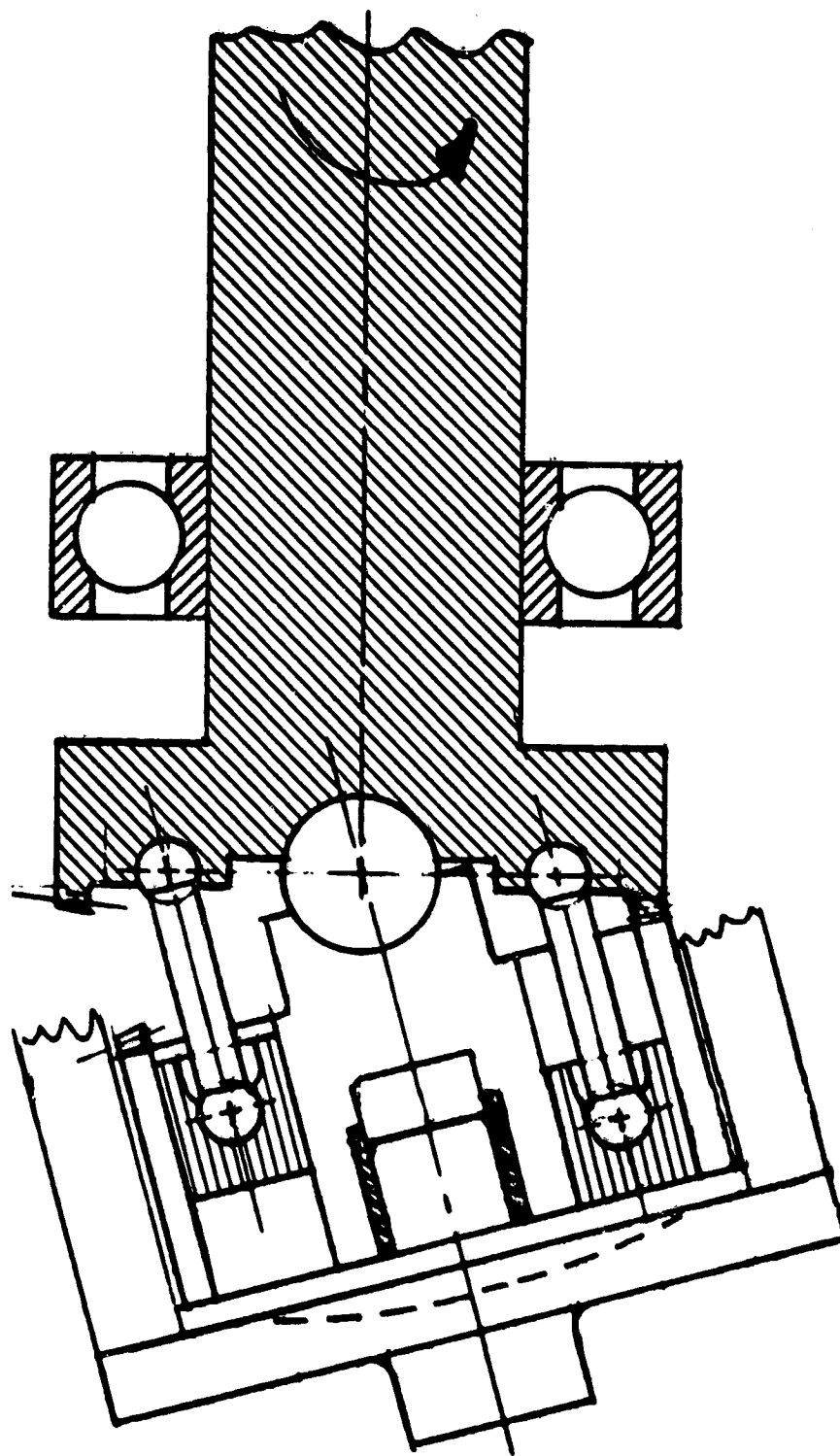


Figure 9. Wobble Plate Piston Pump

ORIGINAL PAGE IS
OF POOR QUALITY

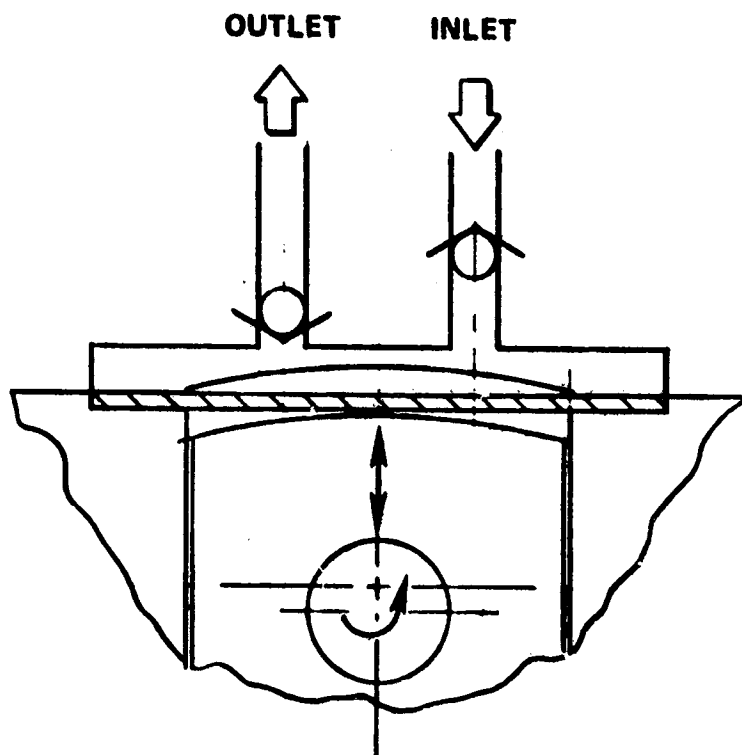


Figure 10. Diaphragm Pump

Screw Pump

Screw pumps operate by trapping fluid between the threads of grouped counter rotating screws. The concept is similar to a gear or lobe pump except the fluid moves in three dimensions rather than two. Complicated shapes and exacting tolerances are two reasons this pump was eliminated as a candidate. Figure 11 shows a schematic sketch of a screw pump.

PUMP PERFORMANCE ANALYSIS

Pump analysis was performed in three major categories: oxygen pumps, methane pumps and hydrogen pumps. Required pump performance was specified in the Statement-of-Work (SOW). Figure 12 shows the SOW pump operating requirements for hydrogen, methane, and oxygen. The propellant flowrates reflect rocket engine requirements for thrust levels from 100 to 2,000 pounds. The assumed engine specific impulse (ISP) is 452 seconds for oxygen/hydrogen and 398 seconds for oxygen/methane. An expander cycle type engine with fuel cooling of combustion chamber and nozzle and fuel powered propellant pumps is dictated by the higher fuel (hydrogen or methane) pump ΔP requirements. For this type engine all the oxygen is pumped directly into the combustion chamber injector. For the purpose of pump and drive analysis, pressure losses and fuel temperature were established based upon a parallel study being performed at Rocketdyne in which the overall engine performance was being analyzed.

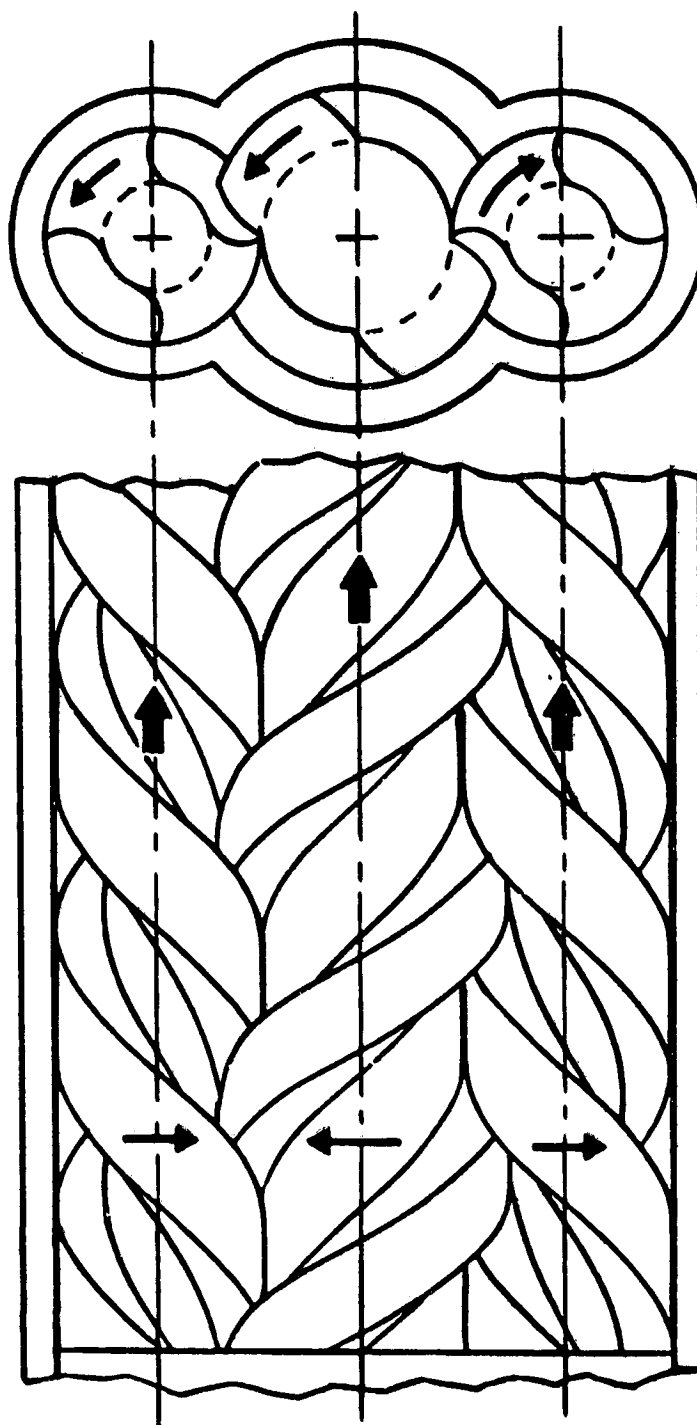


Figure 11. Screw Pump

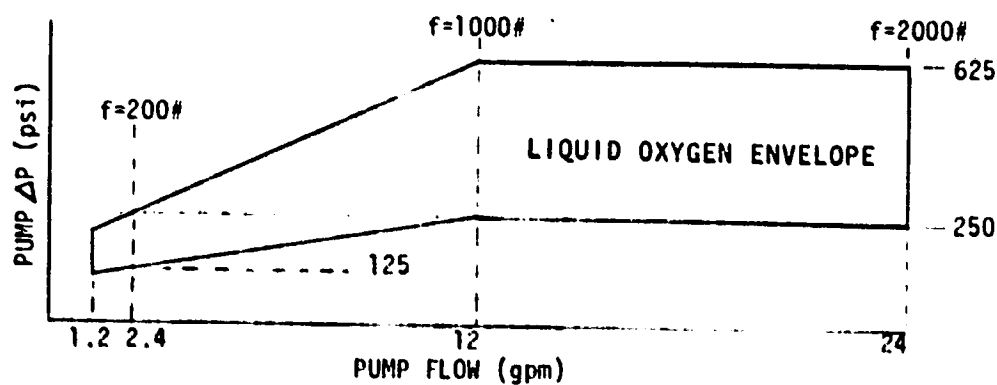
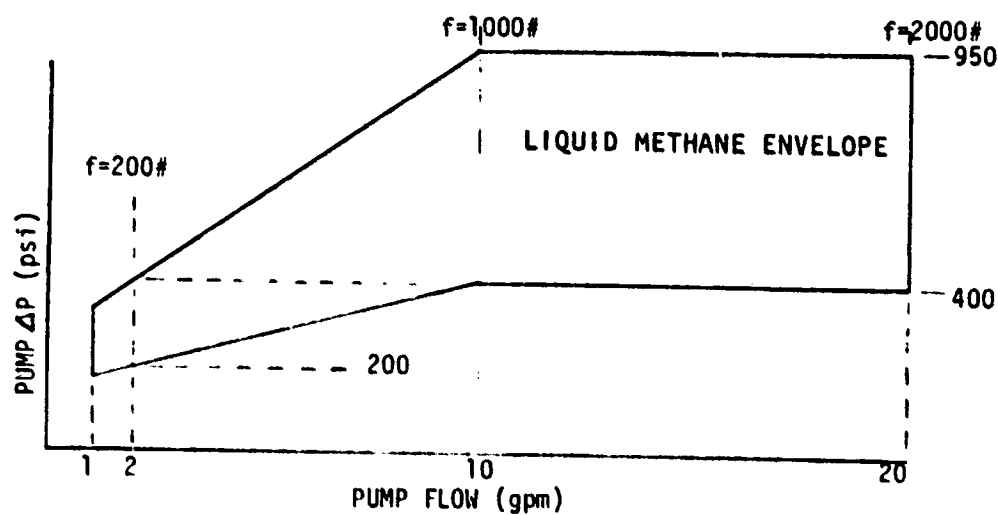
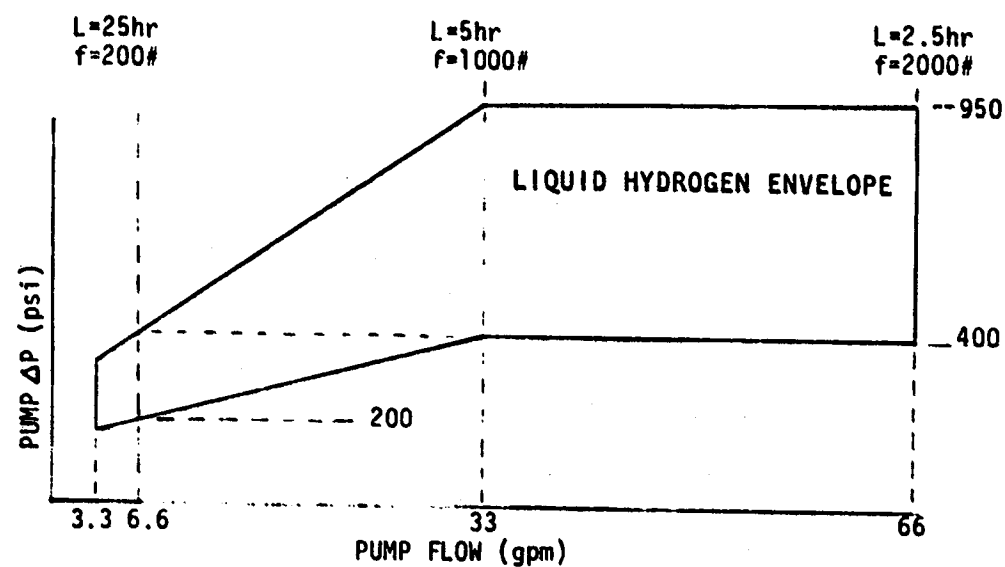


Figure 12. SOW Operating Requirements for Hydrogen, Methane, and Oxygen

The methodology employed to analyze the various types of pumps is as follows: where required, new computer programs were created in which a particular type pump could be optimized for a specified flowrate and pressure rise. The SOW envelope was then covered by a matrix of points at which the optimum pump geometry and performance were determined. From this data, isotropic lines of various parameters of interest were formed. These include: diameter, speed, power, efficiency and others. From these curves one can, at a glance, estimate the geometry and performance of an infinite number of pumps designed to operate in the specified envelop.

LOX Pump Performance Analysis

Liquid oxygen (LOX) pumps were analyzed using a fluid specific weight of 71.14 lb/ft³. The suction capability, size limitations and operating clearances were determined for each pump type. They were selected based on a thorough literature search and Rocketdyne's large experience base in liquid oxygen pumping. Figure 13 shows in more detail the operating requirements of the LOX pumps discussed below.

Centrifugal. Results of the analysis are shown in Fig. A-1 through A-27 (Appendix A). As mentioned previously, three inlet head cases were examined: the SOW, the SOW plus 2 psi, and unlimited. The parameters of interest are speed, rotor diameter, efficiency, power, discharge width and number of stages. The ranges of the parameters for the SOW case are as follows:

Speed 32,000 to 10,000 rpm

Efficiency 0.65 to 0.25

Diameter 2 to 9.4 cm (0.8 to 3.7 in.)

Discharge Width 0.076 to 0.36 cm (0.03 to 0.14 in.)

Power 0.19 to 30 kW (0.25 to 40 hp)

Pitot. Results of the analysis are shown in Fig. A-69 through A-75 (Appendix A). The SOW and 2 psi higher inlet head (NPSH) were analyzed. Speed, diameter and power were the parameters of interest. The ranges of the parameters are as follows:

Speed 10,000 to 4,000 rpm

Stages 1 to 5

Diameter 1.7 to 6.0 inch

Power 0.22 to 13 kW (0.3 to 18 hp)

Tesla. Results of the analysis are shown in Fig. A-96 through A-99 (Appendix A). Only the SOW NPSH case was examined. The Tesla pump performance is not affected

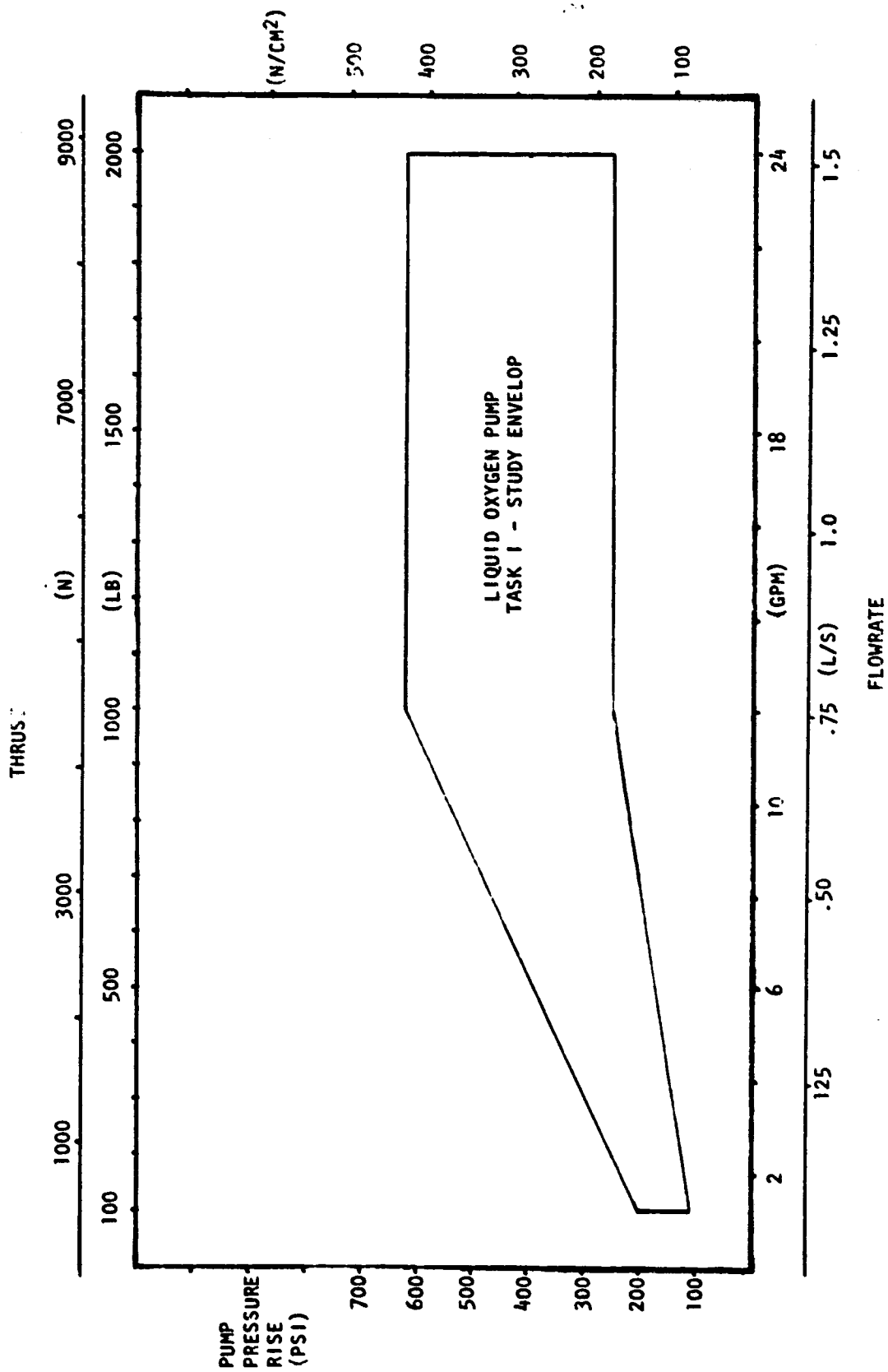


Figure 13. Operating Requirements of LOX Pumps

by NPSH as are the other pump types. Speed, efficiency, diameter and power were the parameters of interest. The ranges are as follows:

Speed 10,000 to 40,000 rpm

Efficiency 0.21 to 0.50

Diameter 2.5 to 6.9 cm (1.0 to 2.7 in.)

Power 0.45 to 15.7 kW (0.6 to 21 hp)

Drag. Results of the analysis are shown in Fig. A-108 through A-112 (Appendix A). Figure A-108 shows that the pump diameter is held constant at 16 inches, and that the required number of stages varies from 2 to 24. In Fig. A-109, the speed versus diameter relationship for 2 feet and 6.05 feet NPSH is shown. If the number of stages is limited to six, the required diameter increases to 80 inches (Fig. A-110). Figure A-111 shows that with reasonable limits on diameter and number of stages, only a portion of the study envelope can be covered by a drag type pump.

Vane. Results of the analysis are shown in Fig. A-119 through A-125 (Appendix A). Speed, efficiency and diameter were examined with clearance to diameter ratios (C/D) of 0.00025, 0.00050 and 0.00075. Vane length to diameter ratios (Vane L/D) were also examined. For C/D = 0.00025, the ranges are:

Speed 1,840 to 700 rpm

Efficiency 0.94 to 0.96

Diameter 2.5 to 6.9 cm (1.0 to 2.7 in.)

Piston. Results of the analysis are shown in Fig. A-140 through A-143 (Appendix A). Speed, efficiency, diameter and power are plotted. The ranges are as follows:

Speed 5,000 to 12,000 rpm

Efficiency 0.90 to 0.94

Diameter 1 to 4 cm (0.4 to 1.6 in.)

Power 0.07 to 7.5 kW (0.1 to 10 hp)

Methane Pump Performance Analysis

Liquid methane pumps were analyzed using a fluid specific weight of 27.5 lb/ft^3 . As with the LOX pumps, the operating and manufacturing limitations of each type of pump were based upon a literature search and Rocketdyne's broad experience with cryogenic pumps. Figure 14 shows in more detail the operating requirements of the methane pumps discussed below.

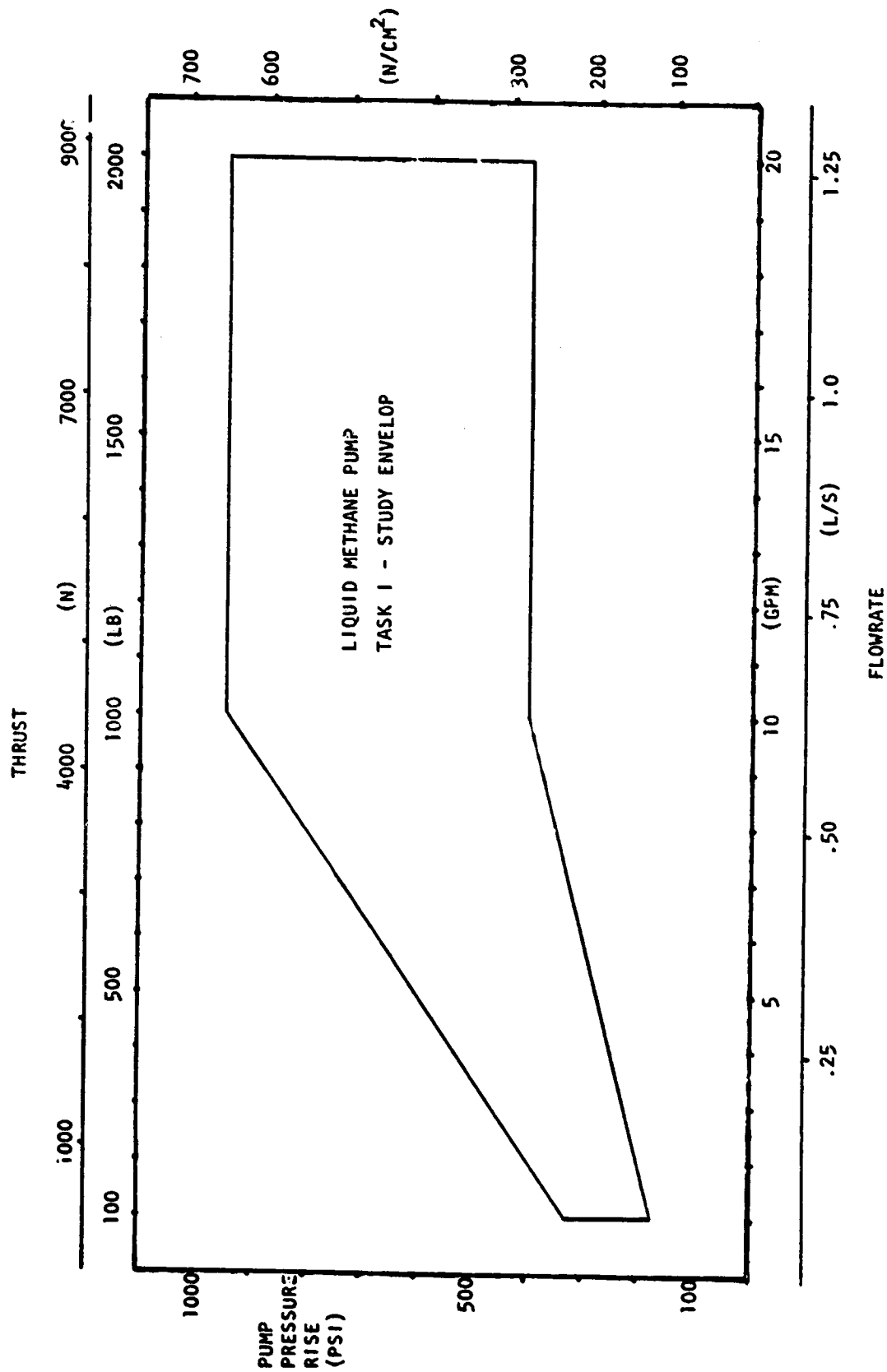


Figure 14. Operating Requirements of Methane Pumps

Centrifugal. Results of the analysis are shown in Fig. A-28 through A-49 (Appendix A). As with LOX, three NPSH cases were examined: 6 feet (from SOW), 16.47 feet (SOW plus 2 psi), and unlimited. Speed, efficiency, diameter, discharge width, and power were the parameters of interest. The ranges (at SOW NPSH) are as follows:

Speed 30,000 to 60,000 rpm

Efficiency 0.38 to 0.65

Diameter 1.8 to 5 cm (0.7 to 2.0 in.)

Discharge Width (b_2) 0.07 to 0.2 cm (0.03 to 0.08 in.)

Power 0.37 to 19 kW (0.5 to 25 hp)

Pitot. Results of the analysis are shown in Fig. A-76 through A-86 (Appendix A). SOW and SOW plus 2 psi NPSH cases were examined. Speed, efficiency, diameter and power were the parameters of interest. The ranges of these parameters (at SOW NPSH) are as follows:

Speed 45,000 to 12,000 rpm

Efficiency 0.53 to 0.56

Diameter 2.5 to 10 cm (1.0 to 4.0 in.)

Power 0.22 to 15 kW (0.3 to 20 hp)

Tesla. Results of the analysis are shown in Fig. A-100 through A-103 (Appendix A). Speed, efficiency, diameter and power were of interest. The ranges are as follows:

Speed 62,000 to 108,000 rpm

Efficiency 0.12 to 0.40

Diameter 2.5 to 3.2 cm (1.0 to 1.25 in.)

Power 1 to 20 kW (1.3 to 27 hp)

Drag. Results of the analysis are shown in Fig. A-113 through A-115 (Appendix A). Diameter versus speed is plotted in Fig. A-113. The effect of increasing NPSH by 2 psi is also included. Figure A-114 shows that with reasonable limits on size and number of stages (12 inches, 6 stages) a large part of the study envelope cannot be covered by a drag type pump.

Vane. Results of the analysis are shown in Fig. A-126 through A-132 (Appendix A). As with LOX, C/D ratios of 0.00025, 0.00050 and 0.00075 were investigated. The efficiency is a strong function of this clearance-to-diameter ratio. Speed, efficiency and diameter ranges for C/D = 0.00025 are as follows:

Speed 3,186 to 1,600 rpm

Efficiency 0.88 to 0.96

Diameter 2.5 to 5 cm (1.0 to 2.0 in.)

Piston. Results of the analysis are shown in Fig. A-144 through A-147 (Appendix A). Speed, efficiency, diameter and power were the parameters of interest. The ranges are as follows:

Speed 10,000 to 2,700 rpm

Efficiency 0.82 to 0.94

Diameter 0.8 to 2.8 cm (0.3 to 1.1 in.)

Power 0.19 to 7.5 kW (0.25 to 10 hp)

Hydrogen Pump Performance Analysis

Liquid hydrogen pumps were analyzed using a fluid specific weight of 4.2 lb/ft³. The suction capability, size limitations and operating clearances were determined for each type of pump. They were selected based upon a thorough literature search and Rocketdyne's large experience base in liquid hydrogen pumping. Figure 15 shows in more detail the operating requirements of the hydrogen pumps discussed below.

Centrifugal. Results of the analysis are shown in Fig. A-50 through A-58 (Appendix A). As with LOX and methane centrifugal pumps discussed earlier, three NPSH levels were examined: 15 feet, 83.6 feet (SOW plus 2 psi) and unlimited. Speed, efficiency, diameter, discharge width and power were the parameters of interest. The ranges (SOW NPSH) are as follows:

Speed 140,000 to 40,000 rpm

Efficiency 0.25 to 0.50

Diameter 1.8 to 9 cm (0.7 to 3.5 in.)

Discharge Width 0.076 to 0.18 cm
(0.03 to 0.07 in.)

Power 0.7 to 37 kW (0.9 to 50 hp)

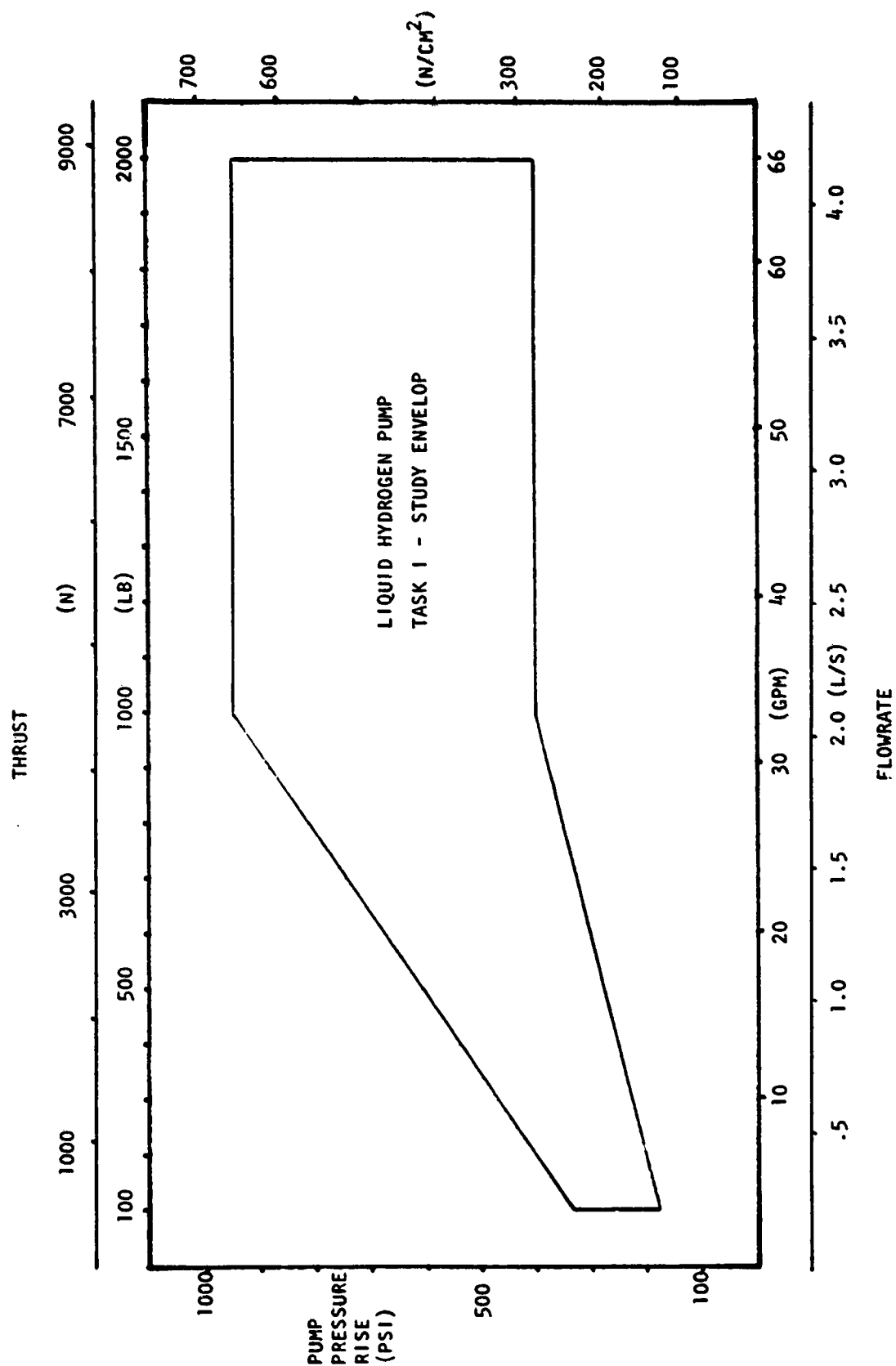


Figure 15. Operating Requirements of Hydrogen Pumps

Pitot. Results of the analysis are shown in Fig. A-87 through A-95 (Appendix A). SOW and SOW plus 2 psi NPSH cases were examined. Speed, diameter and power were the parameters of interest. The ranges (SOW NPSH) are as follows:

Speed 80,000 to 20,000 rpm
Diameter 3 to 13 cm (1.2 to 5 in.)
(2 to 9 stages)
Power 0.7 to 45 kW (1 to 60 hp)

Tesla. Results of the analysis are shown in Fig. A-104 through A-107 (Appendix A). Speed, efficiency, diameter and power were the parameters of interest. The ranges are as follows:

Speed 140,000 to 55,000 rpm
Efficiency 0.25 to 0.53
Diameter 2.5 to 6 cm (1.0 to 2.4 in.)
Power 1.1 to 52 kW (1.5. to 70 hp)

Drag. Results of the analysis are shown in Fig. A-116 through A-118 (Appendix A). Figure A-116 shows the effect of NPSH on the speed versus diameter relationship. Figure A-117 shows that if the diameter is limited to 16 inches and the number of stages limited to six, very little of the study envelope can be covered by a drag type pump.

Vane. Results of the analysis are shown in Fig. A-113 through A-139 (Appendix A). Clearance over diameter (C/D) ratios of 0.00025, 0.00050 and 0.00075 were studied. Speed, efficiency and diameter were the parameters of interest. The ranges (for C/D = 0.00025) are as follows:

Speed 5.038 to 1.700 rpm
Efficiency 0.87 to 0.93
Diameter 2.5 to 7.6 cm (1.0 to 3.0 in.)

Piston. Results of the analysis are shown in Fig. A-148 through A-152 (Appendix A). Speed, efficiency, diameter and power were the parameters of interest. The ranges are as follows:

Speed 10,000 to 2,800 rpm
Efficiency 0.80 to 0.93
Diameter 1.1 to 4.3 cm (0.45 to 1.7 in.)
Power 0.37 to 30 kW (0.5 to 40 hp)

Figure A-152 shows the effect of clearance upon piston pump efficiency.

Gear. Results of the analysis are shown in Fig. A-153 through A-155 (Appendix A). Speed, efficiency and diameter were the parameters of interest. The ranges are as follows:

Speed 7,000 to 1,300 rpm

Efficiency 0.75 to 0.52

Diameter 1.9 to 8 cm (0.75 to 3.2 in.)

Tesla Centrifugal Hybrid Pump Analysis

During the analysis it was noted that the centrifugal pump performance was downgraded significantly from what would normally be expected for this type of pump. This was due in part to the very low (for centrifugal pumps) rotating speeds that were required to meet the inducer suction specific speed limits. It was noted that Tesla pumps have shown exceptional suction capability, often operating at suction specific speeds two orders of magnitude higher than inducers. They have not been used in the past because they have a poor efficiency (about 40%). In a situation where the high-pressure pump is required to have exceptional suction capability, it is more attractive to use the Tesla because the efficiency lost in the first (or suction) stage is recovered. The pump can operate at much higher speed than would otherwise be possible. Table 1 shows the effect of adding a Tesla first stage to a multistage high pressure centrifugal pump. As can be seen, the benefit of the Tesla stage is at the mid and high flows. The increase in pump efficiency is from 6 to 37 points (12% to 148% improvement), depending upon the flow and propellant. In addition to the performance improvement, the size of the pump is reduced and the turbine performance is enhanced by the increased speed. With LOX and methane, the number of stages was halved and with hydrogen the number went from 4 to 3.

Pump Mechanical Considerations

The following section is devoted to mechanical consideration of the pumps as opposed to hydrodynamic performance as discussed above. A design life of 5,000 hours divided by engine nominal thrust has been established by the SOW. This translates to a life requirement of 50 hours at the lowest thrust (100 pounds) and to 2.5 hours at the highest thrust (2,000 pounds). Major concerns include bearings, seals, producibility, development confidence and projected mechanical reliability.

Centrifugal (including partial emission or Barske). Figure 16 and 17 are typical centrifugal and Barske pump cross-sections. The major factors affecting life in both types are bearing and seals. In the case of LOX and methane the bearing DN is moderate and presents no problem. The hydrogen DN, however, is fairly high. In some cases 1.9×10^6 RPM-MM. Some development is required but bearing life can be met. Shaft seals of the floating ring or hydrodynamic lift-off type would be required. With the size limitations selected, producibility is not a problem. Because of its large experience base with these type pumps, Rocketdyne has the highest confidence in successfully developing a small pump of this type. The projected mechanical reliability of this pump is excellent since it cannot seize under normal operating conditions.

TABLE 1. HYBRID CENTRIFUGAL-TESLA PERFORMANCE

HIGH HEAD						
	LOX		METHANE		HYDROGEN	
	CENTRIFUGAL	HYBRID	CENTRIFUGAL	HYBRID	CENTRIFUGAL	HYBRID
LOW FLOW						
SPEED, RPM	33,000	39,000	45,000	76,000	135,000	135,000
STAGES	3	3	4	2	4	4
EFFICIENCY, %	64	54	38	28	42	38
DIAMETER, INCHES	0.7	1.0	0.7	1.0	0.7	1.0
MID FLOW						
SPEED, RPM	14,500	38,000	36,000	100,000	52,000	137,000
STAGES	4	2	4	2	4	3
EFFICIENCY, %	49	57	38	46	25	62
DIAMETER, INCHES	2.3	1.8	1.7	1.0	2.8	1.0
HIGH FLOW						
SPEED, RPM	10,400	27,000	25,000	80,000	38,000	100,000
STAGES	4	2	4	2	4	3
EFFICIENCY, %	50	56	40	48	25	54
DIAMETER, INCHES	3.3	2.2	2.5	1.2	3.8	2.4

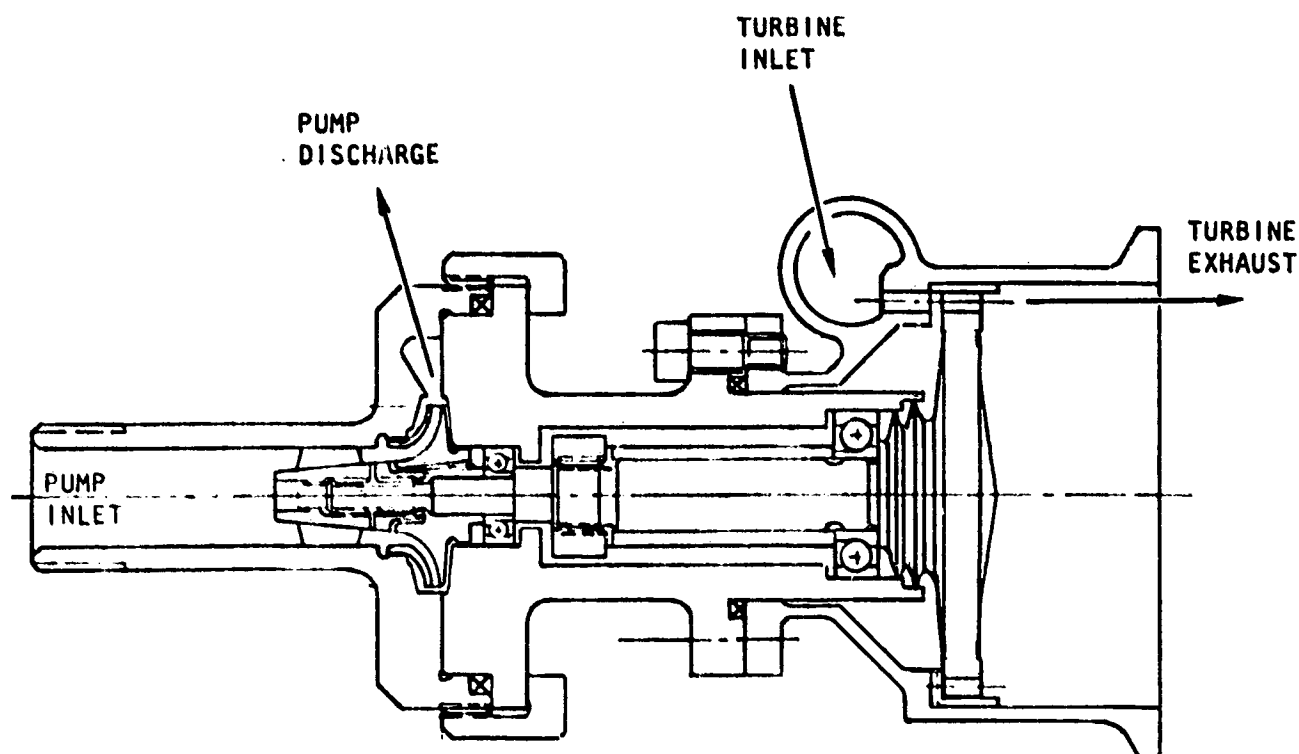


Figure 16. Centrifugal Pump

Pitot. The speed is low and the bearing DN is moderate on all the pitot pumps studied. No problem with bearing life is anticipated. Floating ring or hydrodynamic lift-off seals would be required. Producibility would be no problem since the original size constraints were selected to assure manufacturing of the pumps. Confidence in development is moderate because of limited industry experience. Excellent mechanical reliability is projected after development. Figure 18 is a typical cross-section of a three-stage pitot pump with radial inlet and axial discharge.

Tesla. As with the pitot pump, life is expected to be met with little or no advancement in the state of the art in bearing and seals. Producibility is no problem except for the very thin discs with small spacers between them (0.005 in each). Electrochemical machining would probably be employed to form integral discs and spacers. As with the pitot pump industry experience is limited, therefore, development confidence is only moderate. After development problems are overcome, good reliability would be expected. Figure 19 and 20 are two proposed tesla pump configurations.

Drag. Extremely low speeds facilitate roller bearings and face riding seals. High radial loads (even with multistaging) necessitate the use of higher radial load carrying bearings like rollers. No problem with the life requirement is foreseen. This type pump would be cheap and easy to produce. Its weight and size make it a poor candidate for a rocket engine pump. Once developed, high

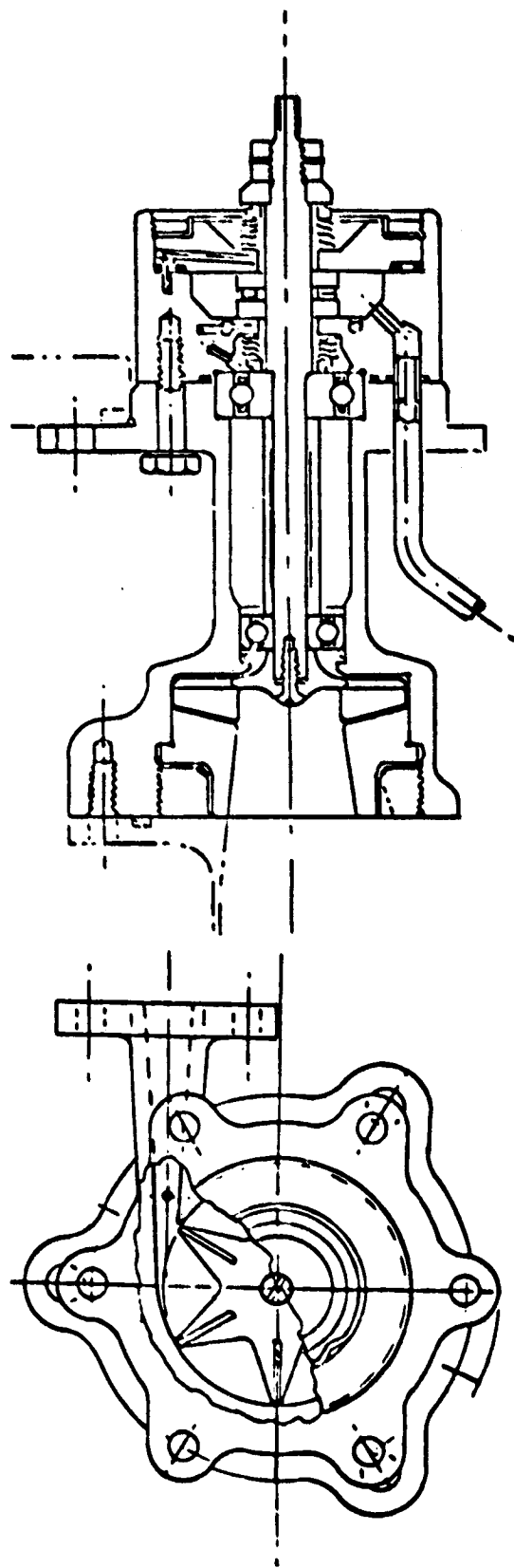


Figure 17. Barske Pump

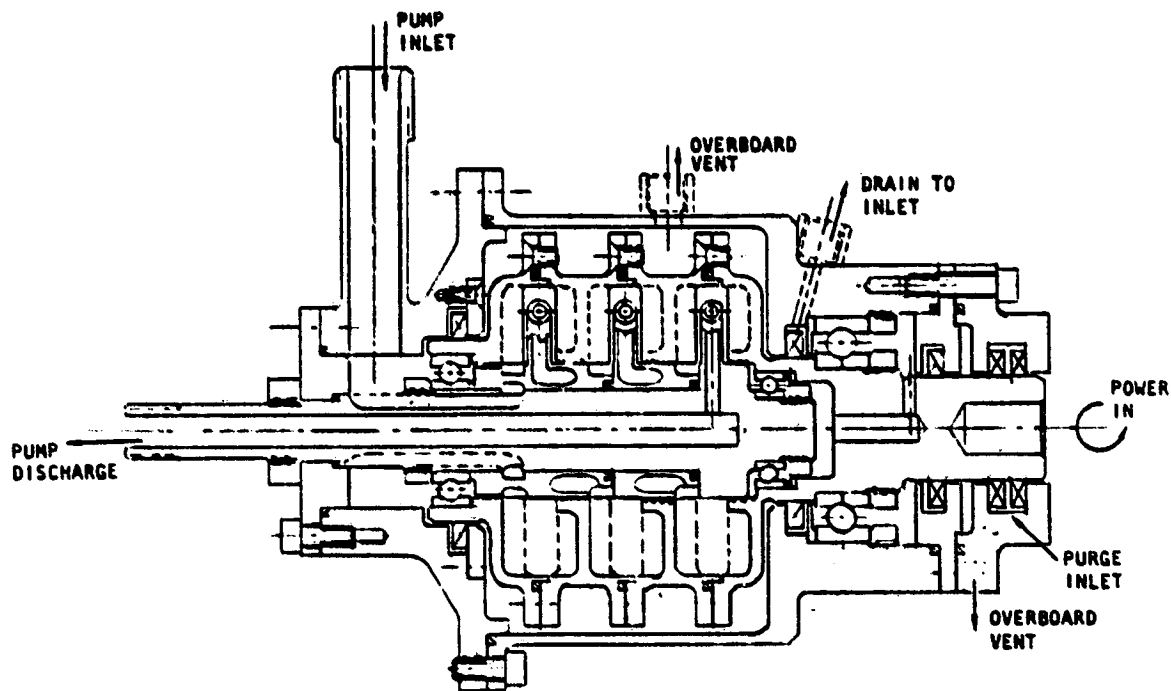
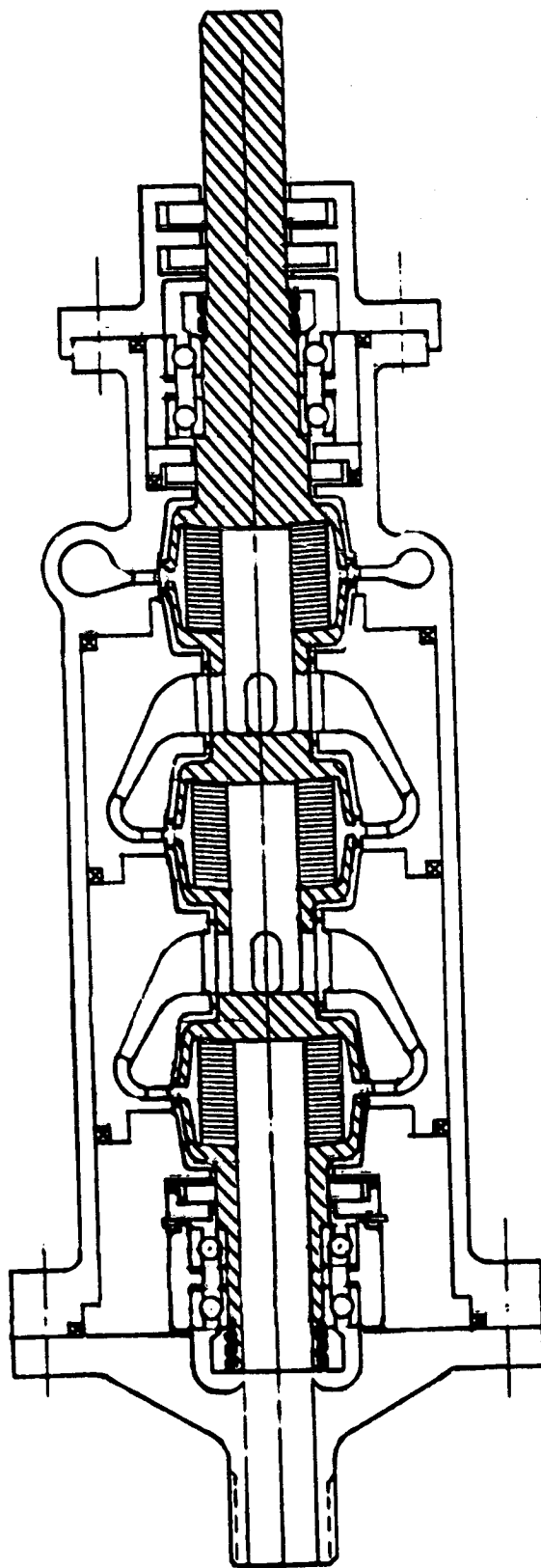


Figure 18. Three Stage Pitot Pump

confidence would be given to reliability. Figure 21 is a schematic cross-section of a two-stage drag pump.

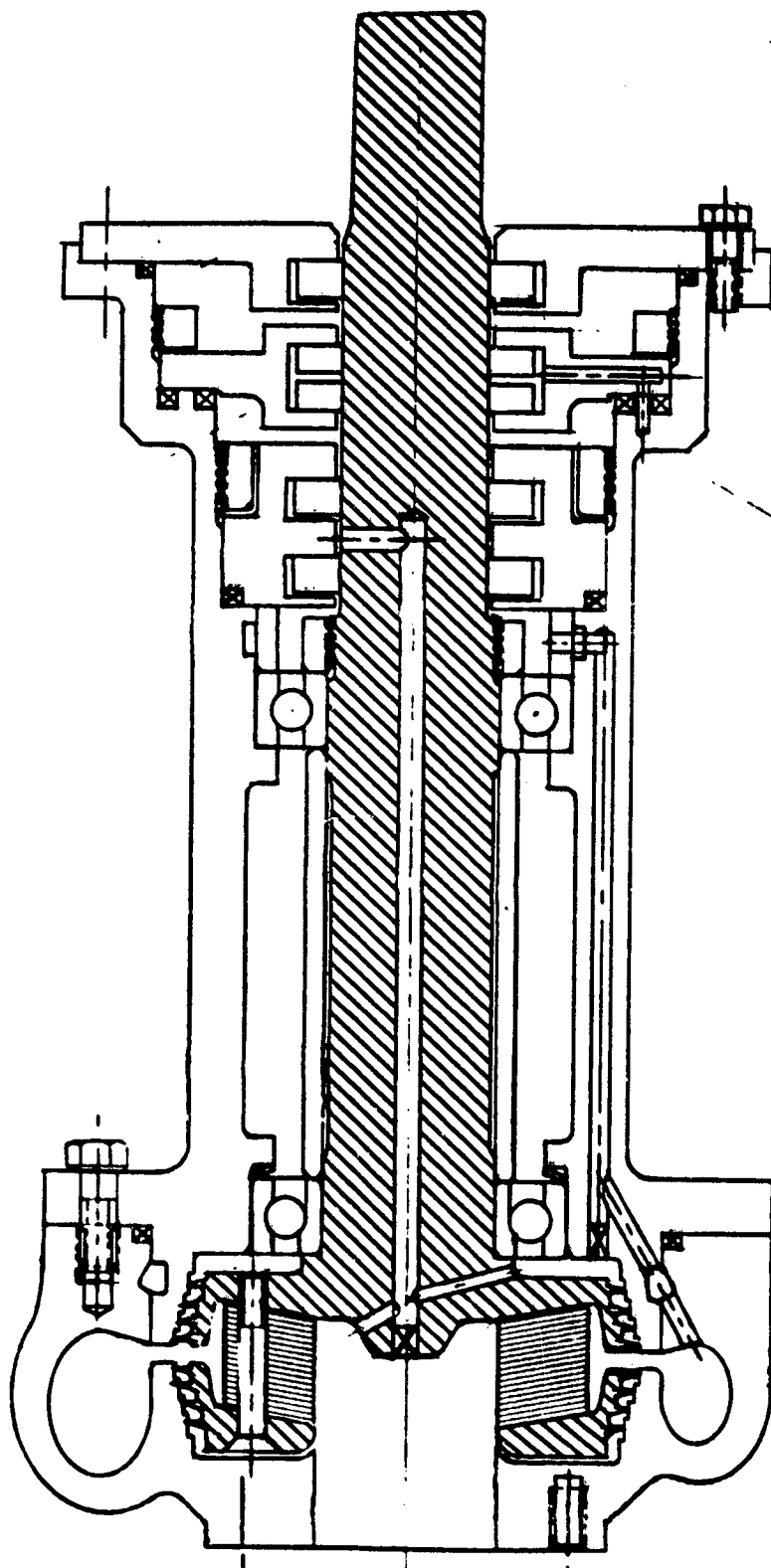
Vane. Life limiting factors for this type pump include vane wear, side plate wear, seizing or binding potential. This type positive displacement pump depends upon acceleration-loaded vanes which rub (or slide) along the outer housing as well as the guide slots of the rotor. Wear rate is a critical factor in predicting overall pump life. Side plate wear is also of concern (fixed sides) because it affects performance. Where movable side plates are employed, both wear and binding are potential failure modes. Life capability of this type pump must be verified by test. Manufacture of this pump is difficult because extremely small clearances are required. Substantial development is required to bring this type pump to the point where the moderate reliability could be expected. Figure 22 is a preliminary design of a vane pump.

Piston. Life limiting factors associated with piston pumps are piston wear and seizure and valve wear. Judicious selection of geometry and materials, combined with a thoroughly thought-out chilling and thermal management technique, the life of a piston type pump can meet the objectives of the SOW. As with the vane pump, precision machining is required to obtain the very small operating clearances necessary. Development confidence is moderate to good based on Rocketdyne micropump and diesel injector pump experience. Reliability is in question because of potential for valve or piston seizure. Pump performance is very sensitive to wear (Fig. A152, Appendix A). This also reduces reliability confidence.



140,000 RPM
15 GPM
3 STAGES
HEAD RISE 24,000 FT
ROTOR DIA. 1.0 IN.

Figure 19. LH₂ Tesla Pump



30,000 RPM
17 GPM
HEAD RISE 1500 FT
ROTOR DIA. 2.5 IN.

Figure 20. LO₂ Tesla Pump

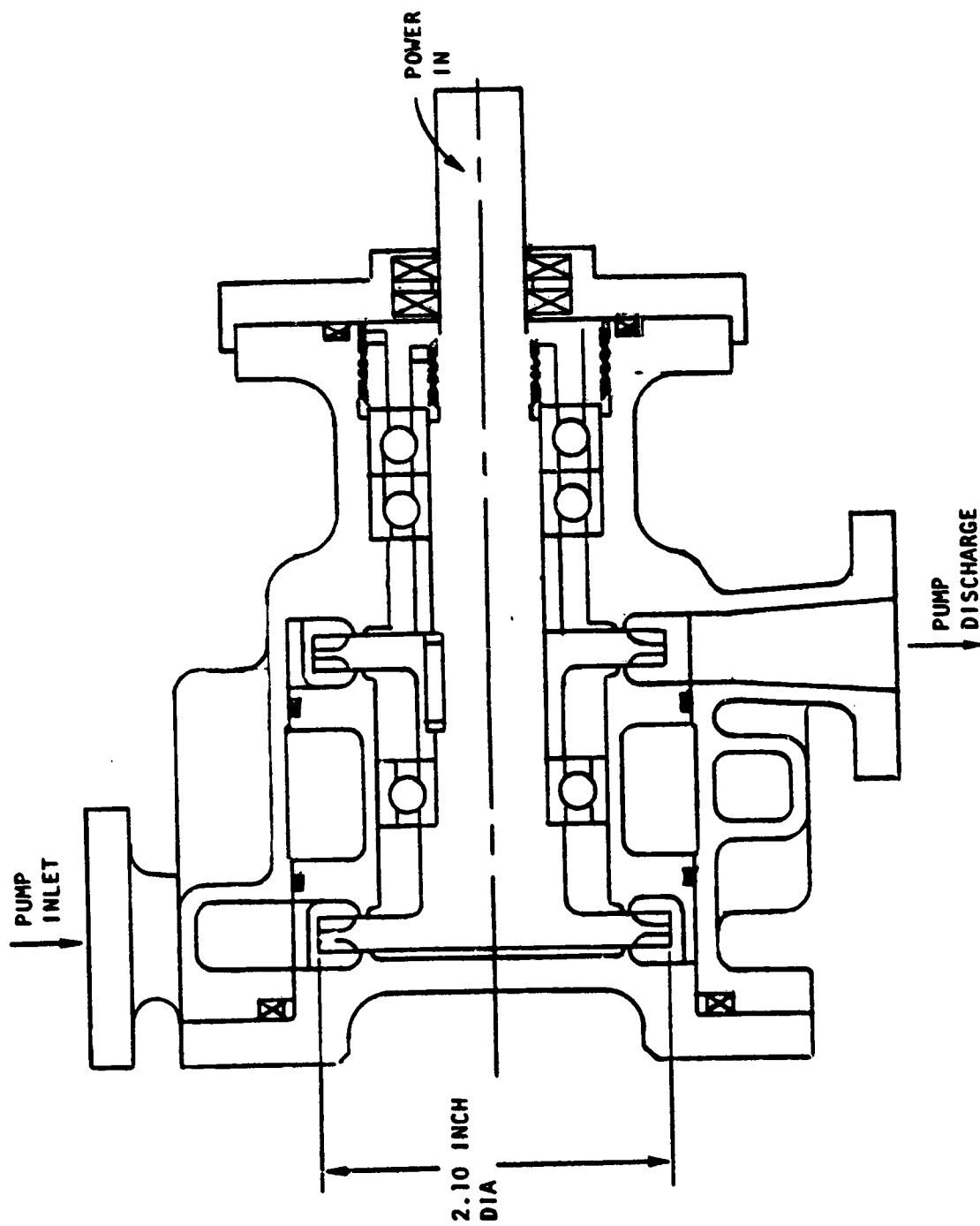


Figure 21. Drag Pump

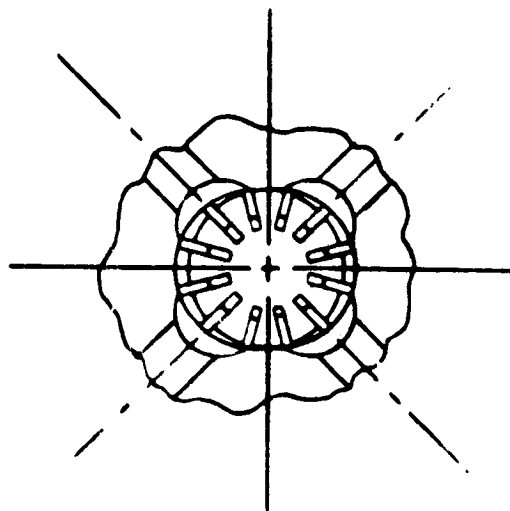
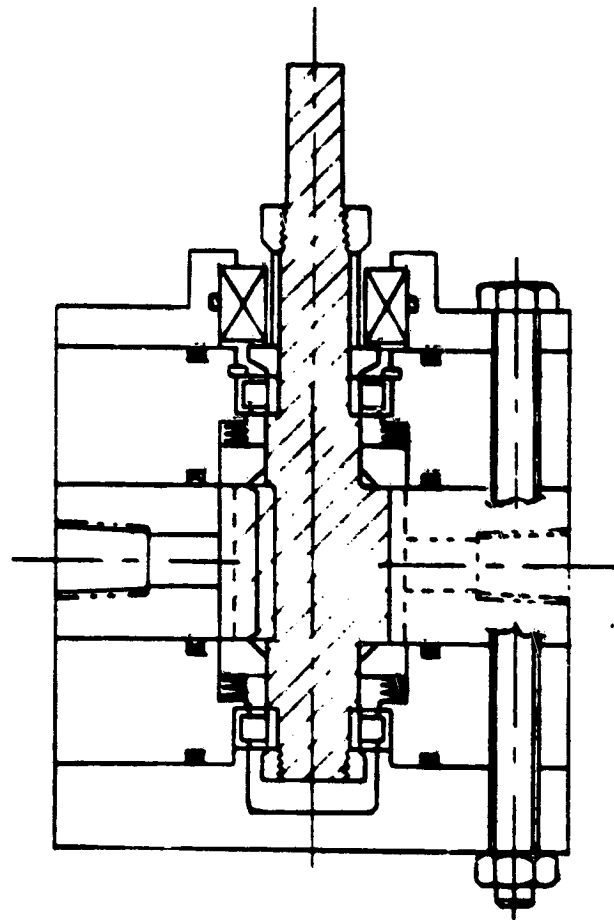


Figure 22. LCH₄ Vane Pump

Hybrid Tesla-Contrifugal. The mechanical considerations for each type pump remain, with the addition that the speed is higher, thus increasing bearing DN. The reduction in number of stages reduces complexity, cost and weight. Difficult to machine inducers are eliminated, partially balancing the machining difficulty of the thin discs. Figure 23 shows a Tesla-centrifugal hybrid in section.

Pump Summary

Oxygen pump characteristics are summarized in Table 2. Significant characteristics such as number of stages, operating speed, efficiency and power required are shown for the low and high flow cases of the study envelope. It is significant to note that the obvious poor performers are the drag pumps, with as many as 24 stages and low efficiency, and the pitot pump with as many as five stages and large diameter.

Methane pump characteristics are summarized in Table 3. The significant characteristics are listed as in the previous task. Again the drag and pitot pumps are identified as poor performers. The Tesla pump with its 15% to 40% efficiency is also an unlikely choice for space engine application.

Hydrogen pump characteristics are summarized in Table 4. The drag, pitot and Tesla pumps are the poorest performers of the group. The drag pump's diameter alone would make it unacceptable as a rocket engine component (200 inches). The pitot pump requires nine stages at the high flow end of the study envelope. This is a very complex mechanical design and would be avoided if possible. The Tesla pump has a reasonable number of stages (three) but its efficiency drops to about 20% at low flows.

TABLE 2. LIQUID OXYGEN PUMP CHARACTERISTICS

TYPE	CENTRIFUGAL		PITOT		TESLA		DRAG		VANE		PISTON	
FLOW	LOW	HIGH	LOW	HIGH	LOW	HIGH	LOW	HIGH	LOW	HIGH	LOW	HIGH
NUMBER OF STAGES	1	4	1	5	1	1	2	24	1	1	1	1
SPEED, RPM	32K	10K	15K	4K	40K	20K	1.6K	<.5K	2K	.6K	5K	1K
EFFICIENCY, %	73	50	56	56	25	50	45	45	96	89	90	94
DIAMETER, INCHES	0.8	3.0	1.7	6.0	1.0	2.5	5	80	1	3.0	0.4	1.6
POWER, HP	0.3	20	0.3	18	1	20	—	—	0.2	9.2	0.1	10
CLEARANCE, INCHES											0.001	
CLEARANCE/DIAMETER									0.00025			

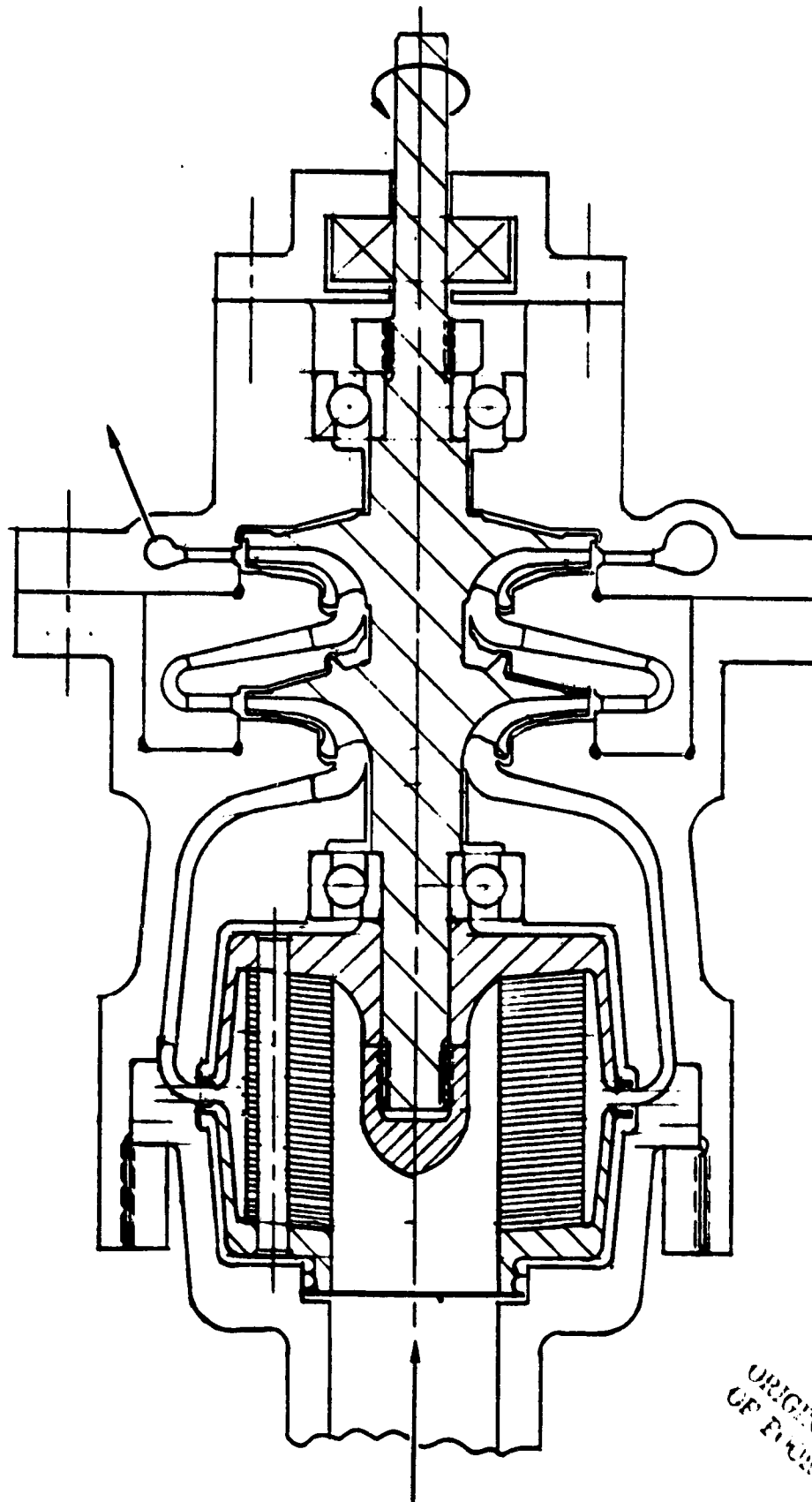


Figure 23. Hybrid Tesla-Centrifugal Pump

ORIGINAL PAGE IS
OF POOR QUALITY

TABLE 3. LIQUID METHANE PUMP CHARACTERISTICS

TYPE	CENTRIFUGAL		PITOT		TESLA		DRAG		VANE		PISTON	
FLOW	LOW	HIGH	LOW	HIGH	LOW	HIGH	LOW	HIGH	LOW	HIGH	LOW	HIGH
NUMBER OF STAGES	4	4	2	5	1	1	2	6	1	1	1	1
SPEED, RPM	60K	25K	45K	10K	70K	100K	.5K	.5K	3.2K	1.5K	27.5K	10K
EFFICIENCY, %	38	65	53	56	15	40	45	45	88	94	82	94
DIAMETER, INCHES	0.7	2.0	1.0	4.0	1.0	1.5	12	12	1	2	0.3	1.2
POWER, HP	0.5	25	0.3	20	1.2	27	—	—	0.1	12	0.25	10
CLEARANCE, INCHES											0.001	
CLEARANCE/DIAMETER									0.00025			

TABLE 4. LIQUID HYDROGEN PUMP CHARACTERISTICS

TYPE	CENTRIFUGAL		PITOT		TESLA		DRAG		VANE		PISTON		GEAR	
FLOW	LOW	HIGH	LOW	HIGH	LOW	HIGH	LOW	HIGH	LOW	HIGH	LOW	HIGH	LOW	HIGH
NUMBER OF STAGES	4	4	2	9	3	3	5	6	1	1	1	1	1	1
SPEED, RPM	150K	40K	80K	20K	140K	50K	.7K	<.2K	5K	1.7K	10K	3.5K	8K	1.2K
EFFICIENCY, %	60	25	56	56	20	55	45	45	90	76	80	93	85	50
DIAMETER, INCHES	0.7	3.5	1.2	5	1	2.5	15	200	1	3	0.4	1.7	0.7	3.5
POWER, HP	0.9	150	0.5	60	1.5	60	—	—	0.4	46	0.5	40	—	—
CLEARANCE, INCHES											0.001			
CLEARANCE/DIAMETER									0.00025				0.00025	

CANDIDATE DRIVE CONCEPTS AND ASSUMPTIONS

In general, the various type pumps studied can serve as drives with slight modification to their geometry, much the same as a generator can be made into a motor. Some potential drive candidates were eliminated very early in the analysis. Some examples follow.

Single Action Piston was eliminated because it can not start itself if it is on the return stroke or bottom or top dead center with a crankshaft.

Double Acting Piston with Crankshaft was also eliminated because it can potentially be top or bottom dead centered.

Terry Turbines have a low efficiency compared to others of similar size and weight. They were therefore eliminated as candidates.

Re-entry Turbines were also eliminated because they are actually partial admission multistage turbines applicable to high pressure ratio systems. Most low thrust drives require low to very low pressure ratios.

Drag Turbines are much too large just as are the pumps. The size of a drag pump and motor would dwarf the entire low thrust rocket engine (thrust chamber included).

Lobe Expanders were eliminated for the same reason lobe pumps were eliminated. They require gearing to maintain the proper orientation. They unduly complicate the engine since lubrication would have to be provided to the gears.

Gear Expanders eliminate the orientation problem but have uncertain life because of the high rubbing contact at even the moderate drive temperatures studied (680R).

Axial Impulse Turbines

Axial impulse turbines were selected to drive all high speed pumps (10,000 rpm and higher). Their performance is high and they are reasonably easy to fabricate. For design and analysis purposes, no gearbox was allowed. This required turbines to run at less than optimum speed but greatly simplified the system while increasing the probable reliability. Series turbines were assumed with the fuel first and the LOX Pump second (both driven by fuel gasified in the nozzle and combustion chamber cooling jackets). The pressure ratio was limited to a maximum of 1.4. For analysis purposes, the fuel drive gas temperature was assumed to be 900R for CH_4 and 1300R for C_2H_6 . For the LOX pump drive, both CH_4 and C_2H_6 were assumed to be 650R. Fuel pump drive inlet pressure was assumed to be 80% of the pump discharge pressure and LOX pump drive inlet pressure was assumed to be 85% of the LOX pump discharge pressure. Figures A156 through A169 (Appendix A) show the results of the analysis. In summary, the oxygen drive pressure ratio varied from 1.08 to 1.18 and the diameter varied from 2 to 6 inches. The methane drive pressure ratio varied from 1.07 to 1.15 and the diameter from 2 to 4 inches. Turbine admission percentage varied from 10 to 40%. The hydrogen drive pressure ratios varies from 1.05 to 1.4 while their diameters went from 2 to 6 inches. The maximum arc of admission on the hydrogen drives was 40%. The speed and output power of all the turbines was of course set by the pumps.

Vane Expander

Vane expanders were selected to drive vane pumps because the low speeds are incompatible with turbines. The same assumptions for the inlet pressures and temperatures were used as was the series arrangement for fuel and LOX pump drives. Figures A170 through A184 (Appendix A) show the results of the analysis. In summary, the oxygen pump drive had excellent efficiency (78 to 82%) but its size was rather large (8 to 20 inches). The methane drive had similar efficiency (71 to 79%) and its size was more acceptable (1.25 to 3.9 inches). The hydrogen drive efficiency was lower but still good at 67 to 69%. Its size varied from 2 to 7.5 inches in diameter.

Piston Expanders

Piston expanders were only considered for fuel pump application. The difficulty of providing a safe seal between the LOX and fuel negated the potential advantages of a fuel powered LOX pump. The same assumptions were used as with the turbines and vane expanders. The methane drives showed excellent efficiency at 93.5%. The diameters were small at 1.0 to 2.5 inches (Fig. A185, Appendix A). The hydrogen drives had even better efficiency at 94%. They were slightly larger at 1.5 to 4 inches in diameter (Fig. A186).

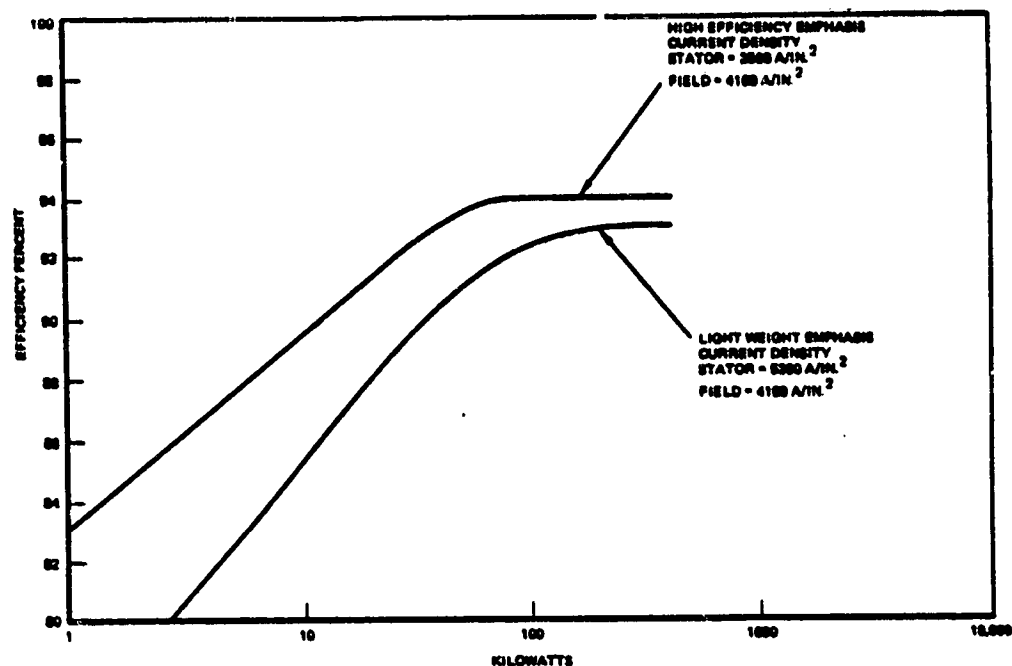
Electric Motors

Electric motors were examined as drives for any of the rotating pumps studied. Figure 24 shows that the efficiency of modern electric motors decreases at powers below 100 kilowatts (134 horsepower). Most pumps studied fall in the 0.2 to 60 horsepower range where electric motors have relatively lower efficiency. Figure 25 shows the power versus speed relationship for several of the pumps studied. The current technology in electric motors covers about half the candidate pumps. The others require a higher power and speed than currently available with electric motors. As a result, the application of electric motor drives is limited.

Drive Mechanical Considerations

Axial Flow Impulse Turbine. These turbines have high probability of meeting or exceeding the life goal. They operate in moderate temperatures (680R and lower) and at fairly low rotating speeds. Bearing DN's are held within proven limits, and seal requirements are state of the art or easier. Producibility is not expected to be a problem because the original ground rules were established to ensure producibility. Mechanical reliability of this type drive would be excellent.

Vane Expanders. Vane expanders operate at low speeds, therefore bearing life is not expected to be a problem. Vane (and housing) wear at drive gas temperatures is a concern. It is likely that the wear rate will be higher than the pump vanes which are immersed in liquid gas. This may cause an operating point shift as a result of the expander power reduction due to vane wear. Rotor end sealing will be difficult to control unless floating end plates are used. They can compensate for wear and will tend to maintain constant end leakage. Production of this type



Nadyne Parametric Data (Efficiency)

Figure 24. Electric Motor/Alternator Efficiency Falls Off at Low Power

drive is possible but requires very precise machining and grinding. Even when developed, this type drive would still have the potential for seizure due to foreign matter in the propellant or even wear products produced during operation. Figure 26 shows a preliminary sketch of a vane pump-drive.

Piston Expanders. Piston drives for piston pumps were considered for only the in-line case where the pump and drive pistons are on the same shaft. Sealing and bearing functions are performed by the piston to cylinder fit. Wear rate of the cylinder wall or piston will greatly effect both performance and life. Seizing is possible by either foreign matter or wear products. Valves and seats are subject to wear and seizure. As with the vane pump, precision machining is required. Very close fits are needed for good efficiency. Thermal distortion during start and cutoff transients is a potential problem in that the alignment of the pump might be effected causing seizure. Mechanical reliability would have to be verified by extensive testing. Figure 27 shows a preliminary sketch of an in-line free piston pump-drive.

Electric Motor. Electric motors below 10,000 rpm have demonstrated long life capability in many difficult environments including space. At higher speeds bearing, rotor and brush dynamics become increasingly difficult problems to solve. At very high speeds (above 70,000 rpm), special electronic development is probably required. Special manufacturing technology will have to be developed to produce high speed, high power motors. Once developed, this type drive would have very good reliability. Figure 28, 29, and 30 show potential arrangements of motors and pumps for a 1,000-pound (4430 newtons) thrust engine.

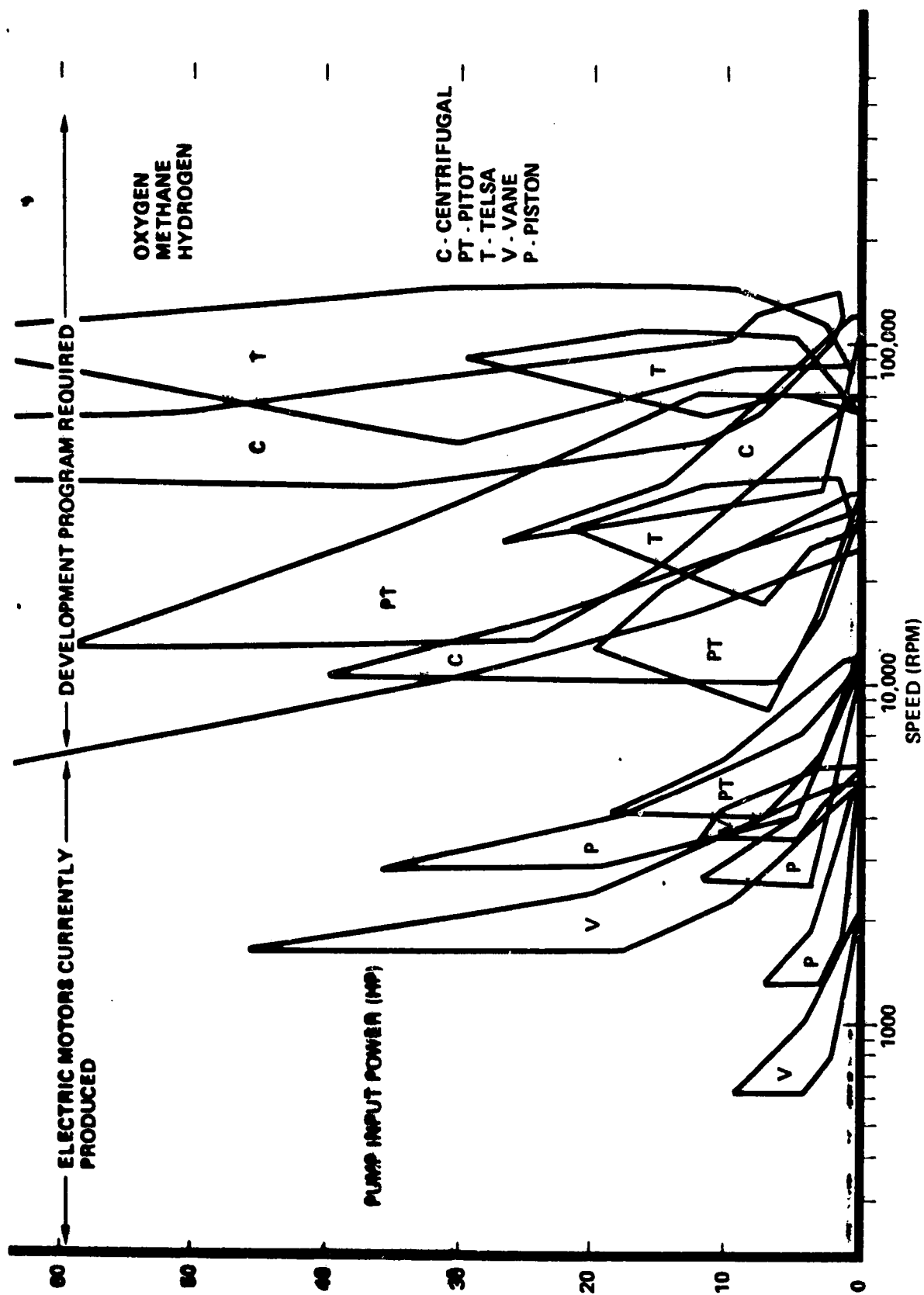
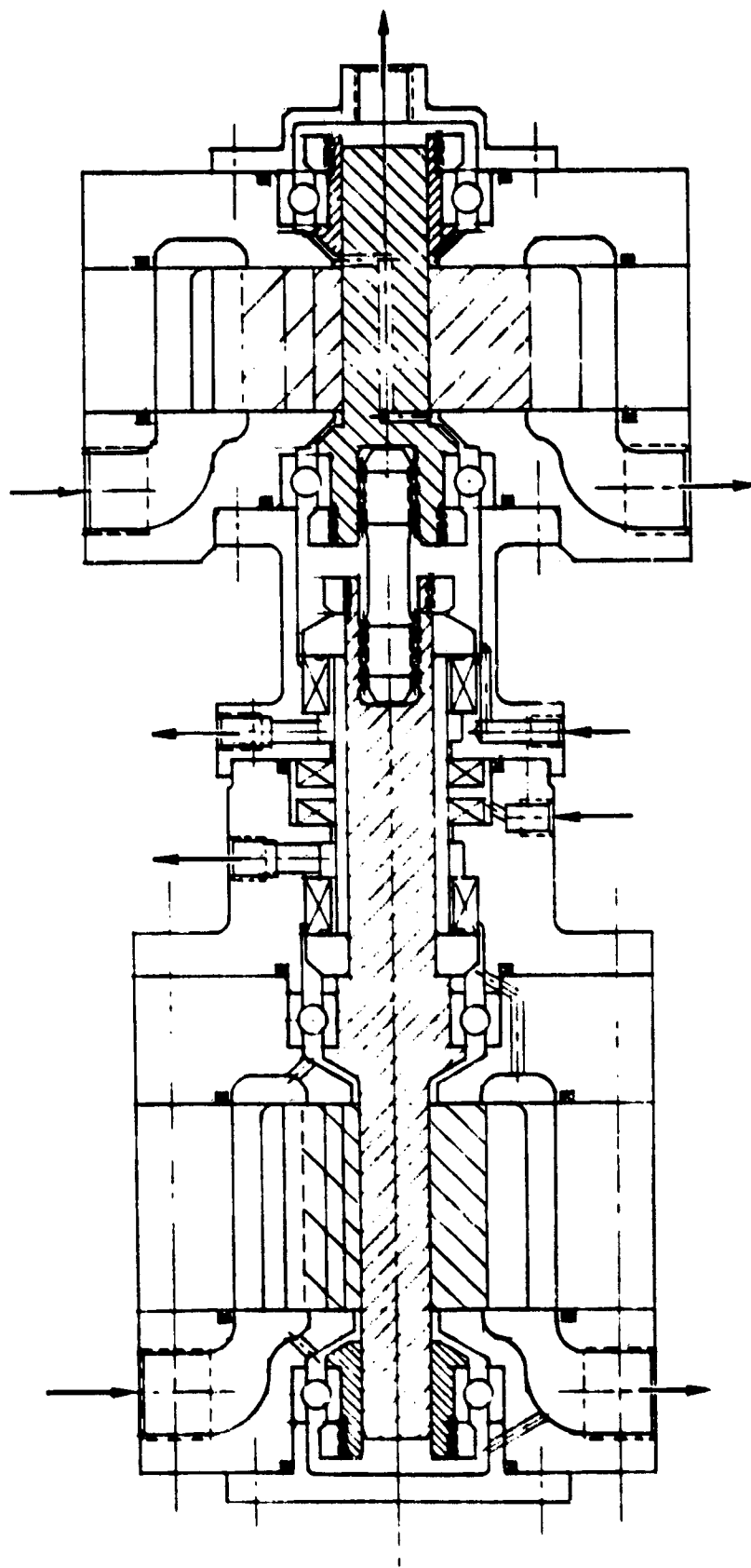


Figure 25. Power vs Speed Relationship In Several Pump Candidates



N = 1150 RPM
 Q = 3.79 RPM
 $\Delta P = 200 \text{ PSI}$

Figure 26. LO_2 Vane Pump GH_2 Expander ($P/R=1.3$)

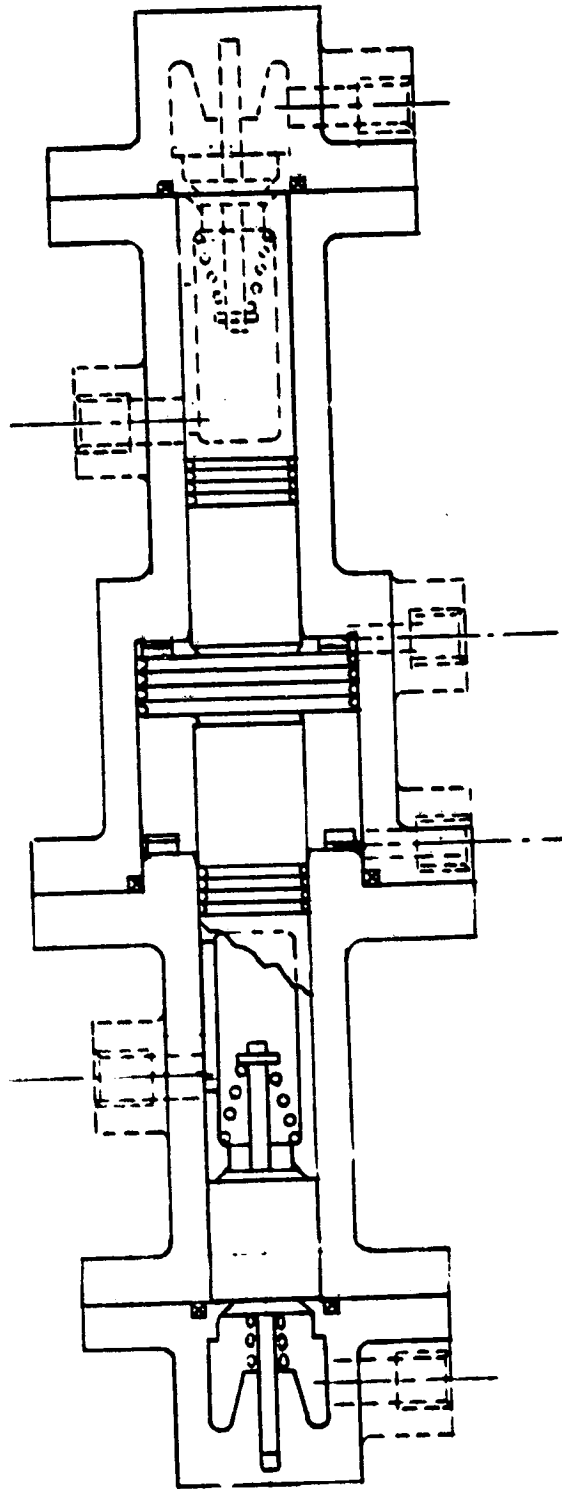


Figure 27. In-Line Piston Pump And Drive

ORIGINAL PAGE IS
OF 1000 QUALITY

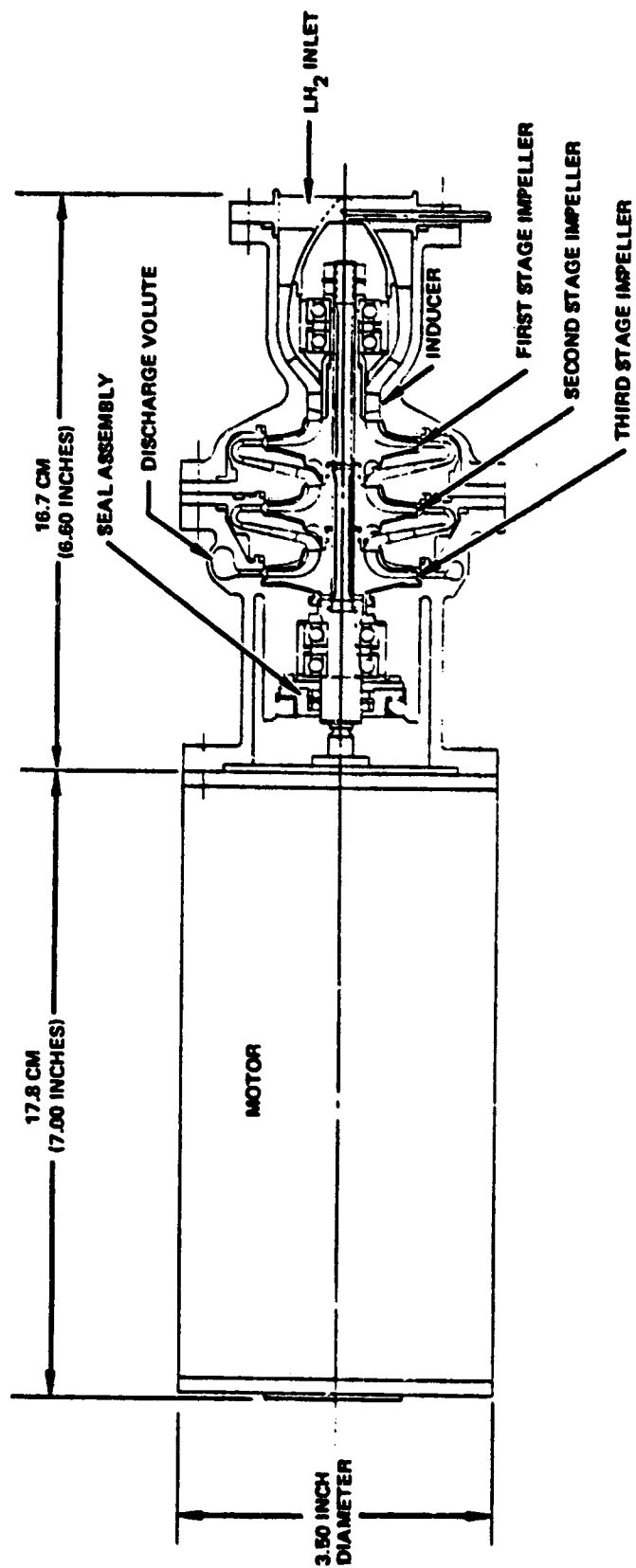


Figure 28. 1000-Pound-Thrust Electric Motor Driven LH₂ Pump

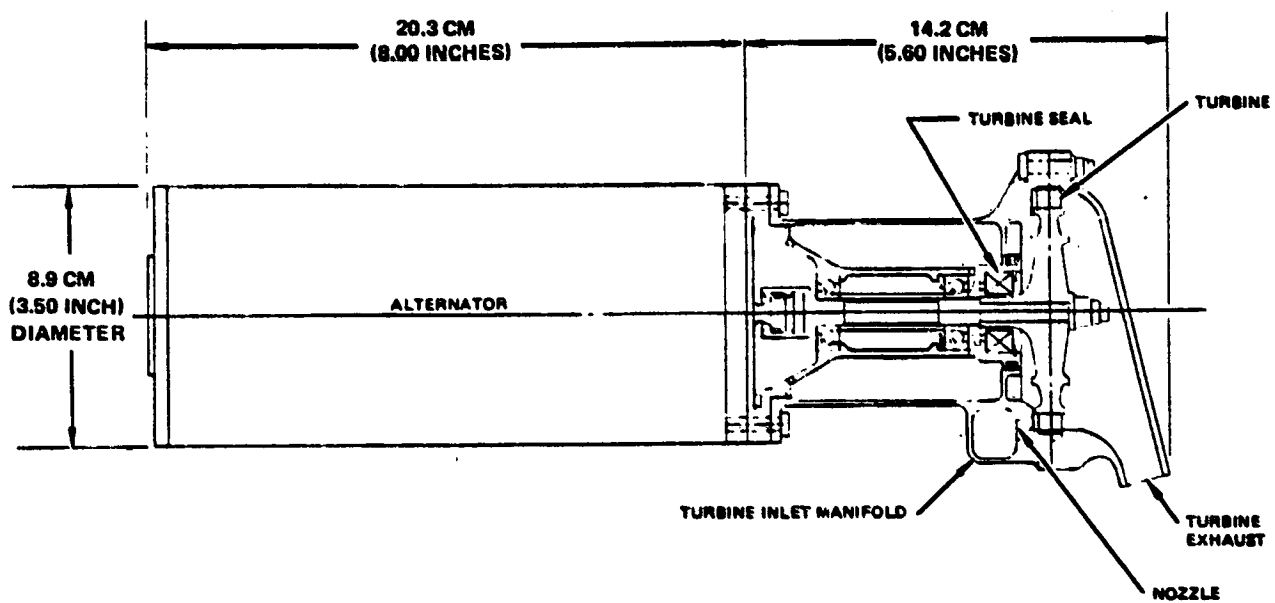


Figure 29. 1000-Pound-Thrust Turboalternator

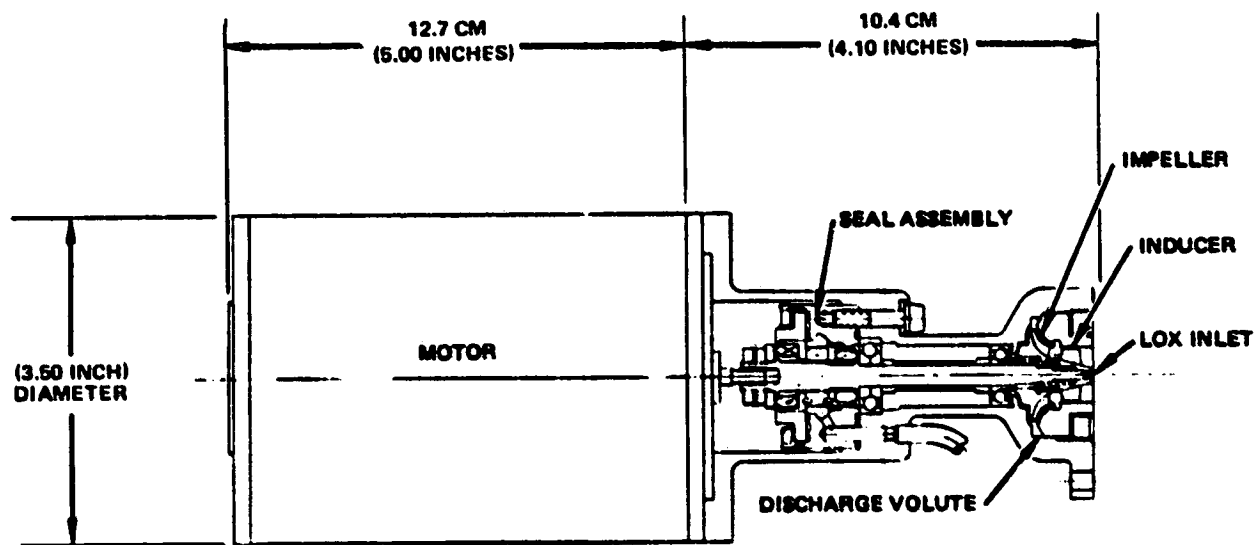


Figure 30. 1000-Pound-Thrust Electric Motor Driven LO_2 Pump

Drive Summary

The results of the drive analysis were plotted to show the efficiency versus rotating speed at various flowrates. Six points on each study envelope were examined. Low moderate and high flows with either high or low headrise. The pump characteristics were also plotted to show the range covered by the drive analysis. Figures 31 and 32 are for oxygen at low and high head, respectively. Note in general, the drive efficiency is lower than the pump. Methane and hydrogen curves are shown in Fig. 33 through 36.

Recommended Concepts for Task III, Preliminary Designs

A selection methodology was developed as a means of reducing the potential choices. A minimum of 45% efficiency in the pump was established. If the drive were no better than the pump (as in Fig. 31 through Fig. 36), a combined pump-drive efficiency of about 20% would be realized. In this case, the turbine would consume five times as much power as the pump produced. This leads to lower engine combustion pressure and ultimately to lower ISP. A limit of 5 inches (diameter) was set so the pumps would not dwarf the rest of the engine components and also to limit weight. Multistaging is a difficult mechanical problem. Four stages is a practical limit. In fact, very few rocket engine pumps have been more than three stages.

Oxygen. Figure 37 shows the oxygen study envelope (flowrate is logarithmic) with regions outlined for various type pumps. The four stage centrifugal, vane, piston and hybrid pumps are acceptable over the entire range. Tesla pumps are only applicable in the high flow-low head region. Drag pumps are only acceptable in the low flow-low head region. Pitot and two stage centrifugal pumps cover most of the range except high head.

It is felt that at a particular flow, the more difficult pumping job is always at highest head rise, therefore, the upper part of the envelope is of most interest in establishing technology. The piston and vane pumps offer higher potential performance than dynamic pumps if very close fits on rubbing parts can be maintained. The superior reliability of the centrifugal pumps outweighs this advantage, as a result, the following recommendations are made for LOX pump drive preliminary designs. At highest flow and head rise, a Hybrid Tesla-Centrifugal Pump powered by an axial impulse turbine; at lowest flow and highest head, a centrifugal pump and axial impulse turbine (Fig. 38).

Methane. Figure 39 shows the study envelope for methane. Both positive displacement pumps are acceptable over the entire range. The four-stage centrifugal and hybrid pumps cover most of the higher flow region and the pitot covers the entire flow range but not at high head rise. The recommended pump-drives for methane are: (1) at low flow-high head, a piston pump and drive and (2) at high flow-high head, a hybrid Tesla-centrifugal pump and axial impulse turbine (Fig. 40).

Hydrogen. Figure 41 shows the study envelope for hydrogen. The vane, piston, gear and hybrid pumps cover the entire range. Tesla pumps are only good for high flow. Pitot and centrifugal are only good for low head. The recommended pump-drives are: (1) at low flow-high head, a vane pump and electric motor, and (2) at high flow-high head, a hybrid Tesla-centrifugal pump with an axial impulse turbine (Fig. 42).

NPSH = 2FT LOW - HEAD

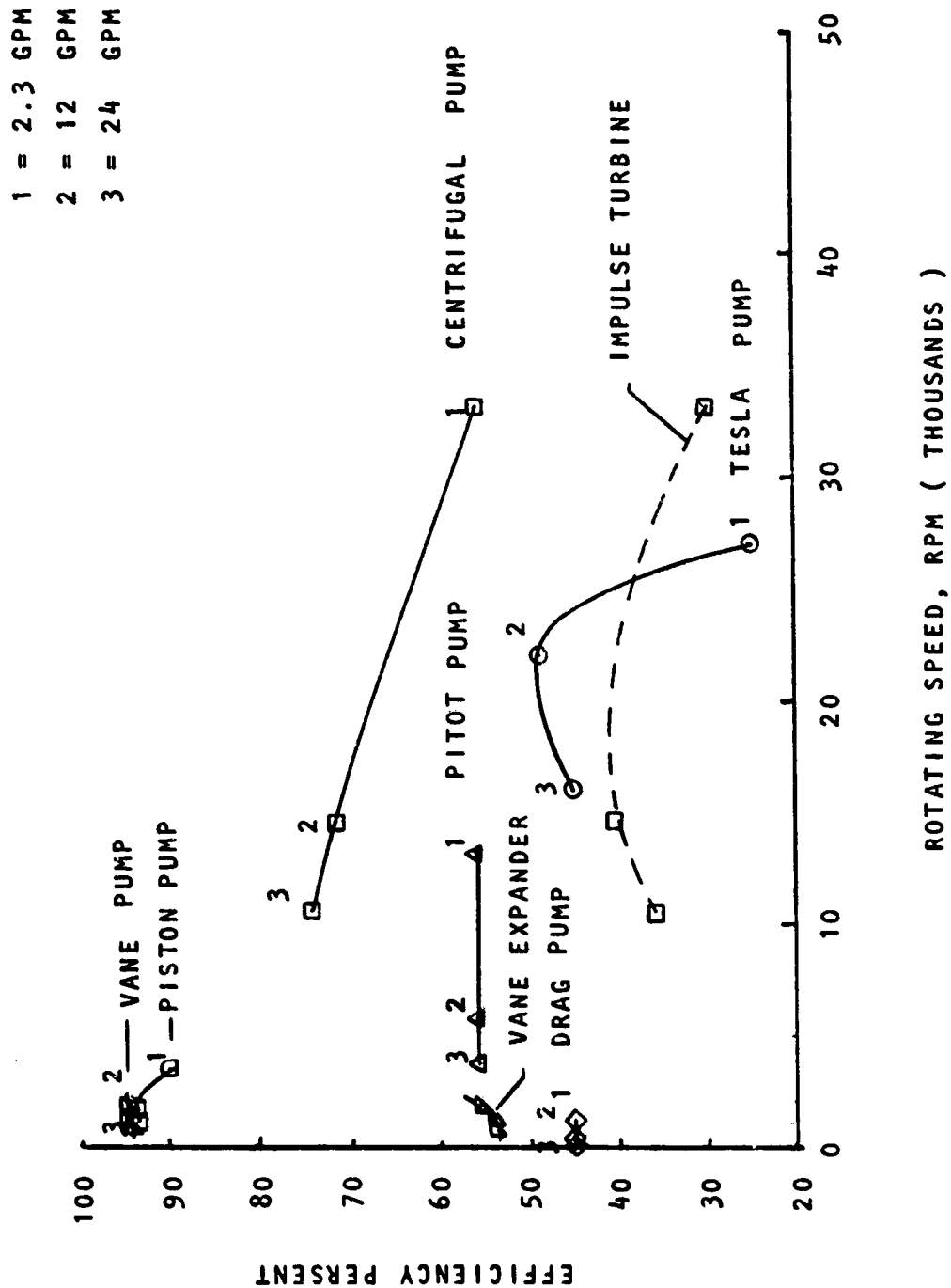


Figure 31. Liquid Oxygen Pump and Drive Performance

NPSH = 2 FT HIGH - HEAD

1 = 2.3 GPM
2 = 12 GPM
3 = 24 GPM

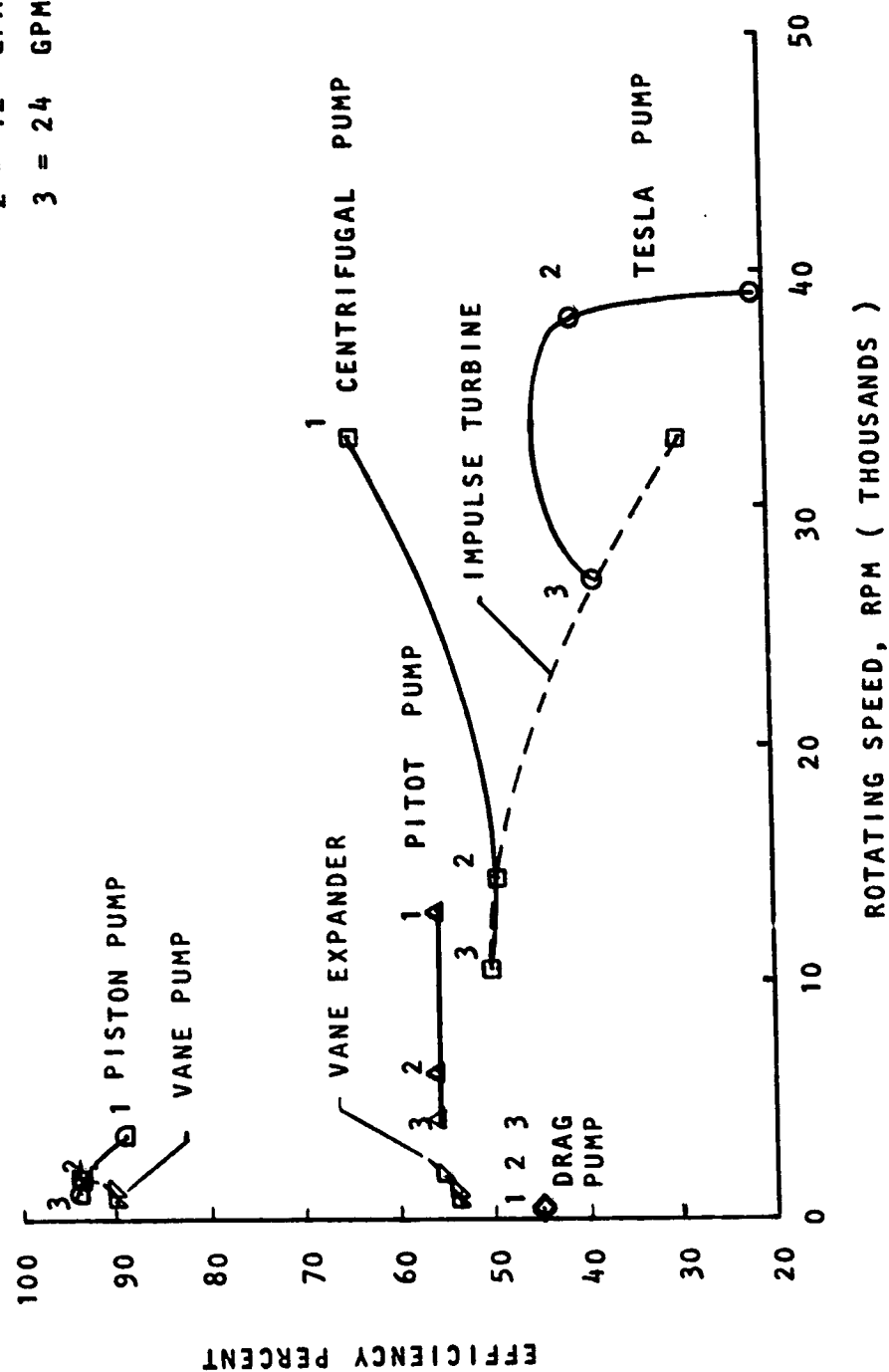


Figure 32. Liquid Oxygen Pump and Drive Performance

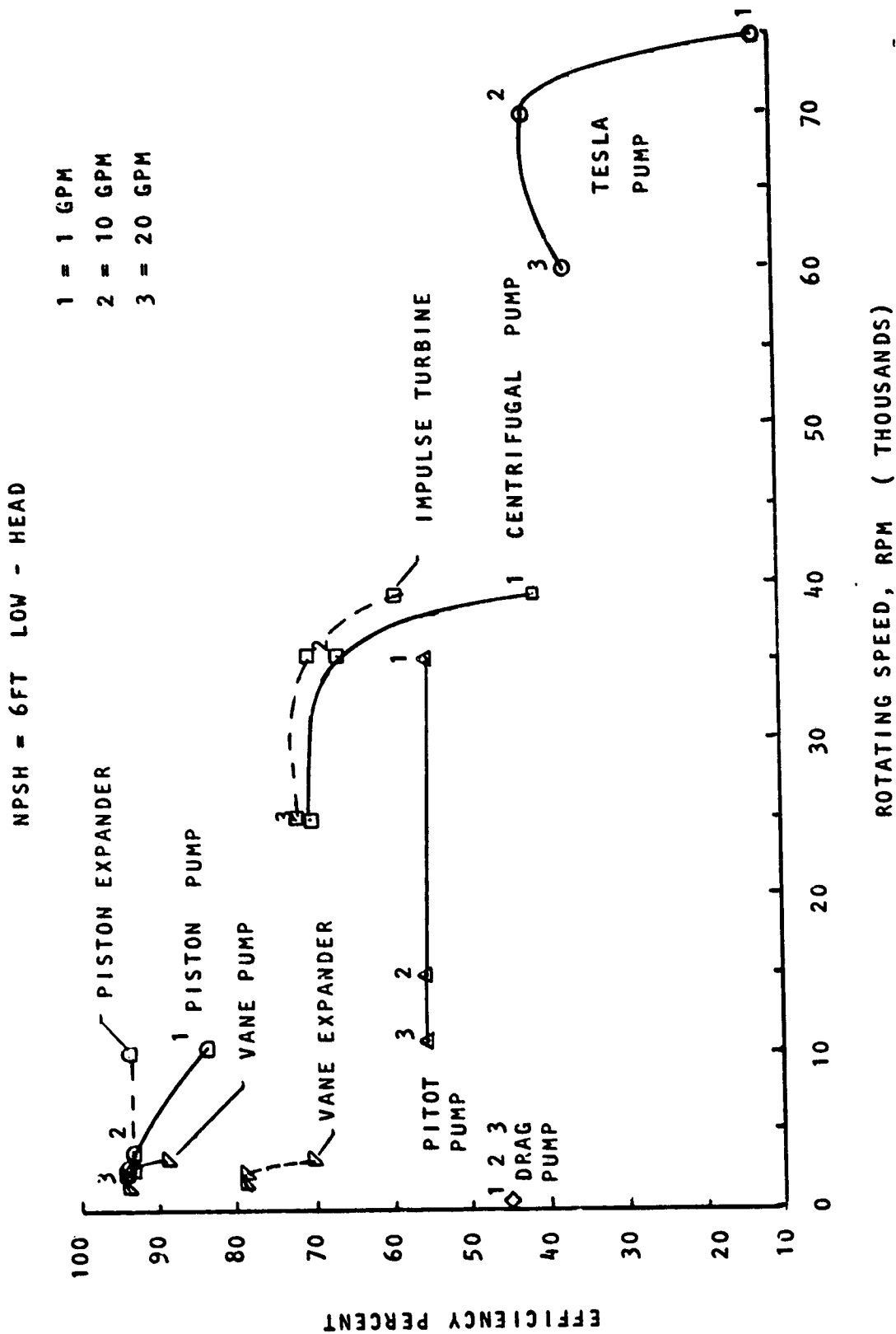


Figure 33. Liquid Methane Drive and Pump Performance

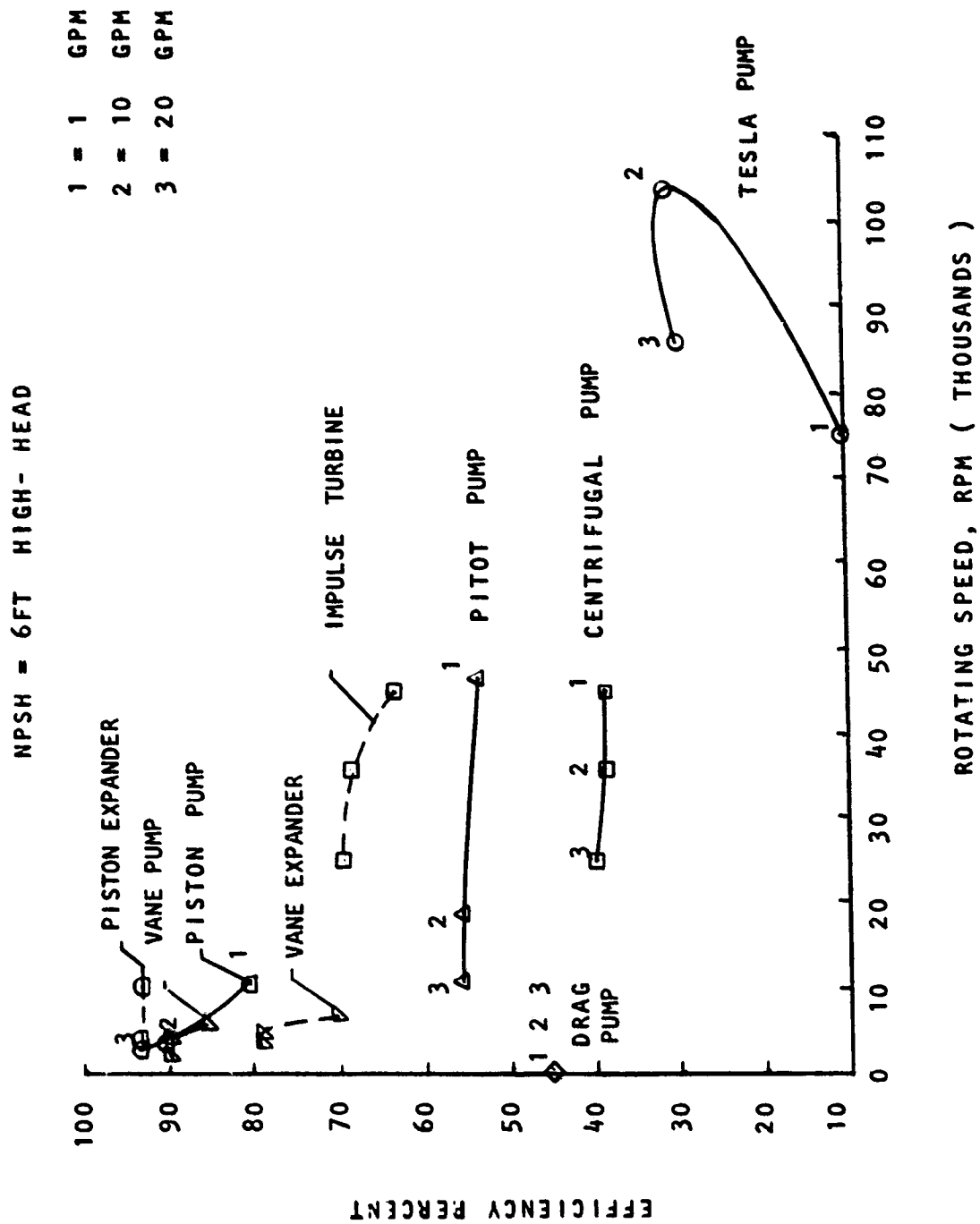


Figure 34. Liquid Methane Pump and Drive Performance

NPSH = 15FT LOW - HEAD

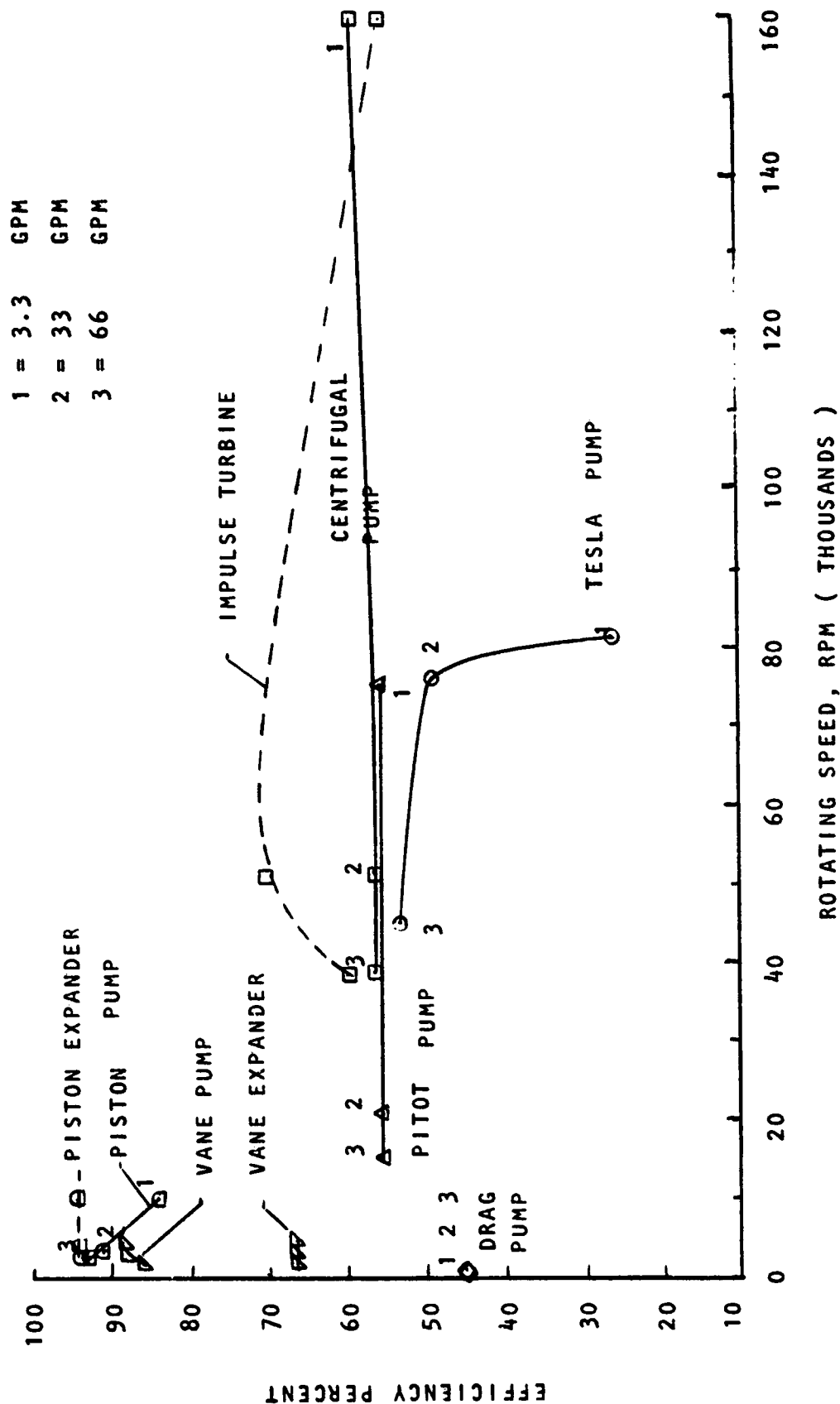


Figure 35. Liquid Hydrogen Pump and Drive Performance

NPSH = 15FT HIGH - HEAD

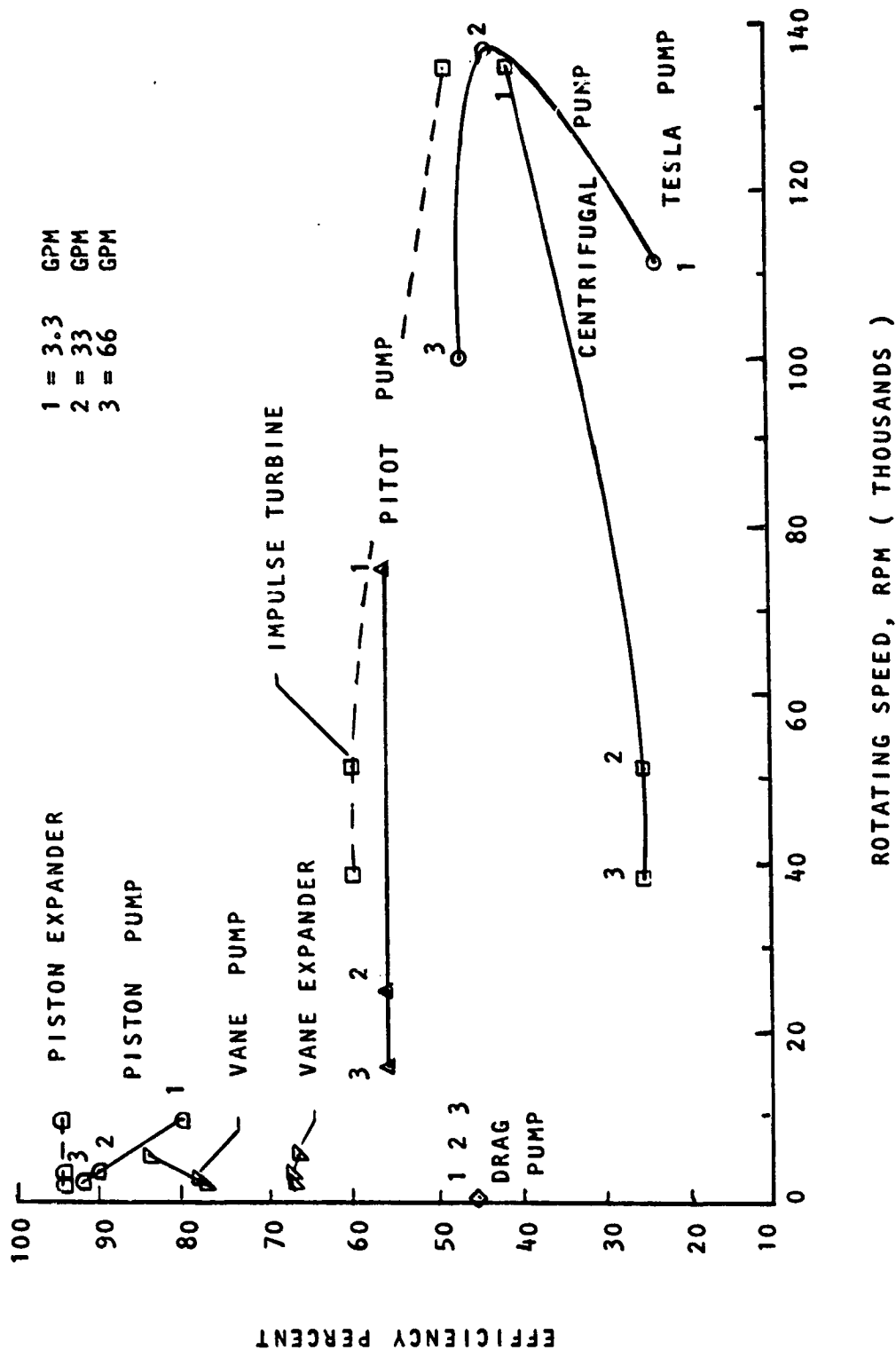


Figure 36. Liquid Hydrogen Pump and Drive Performance

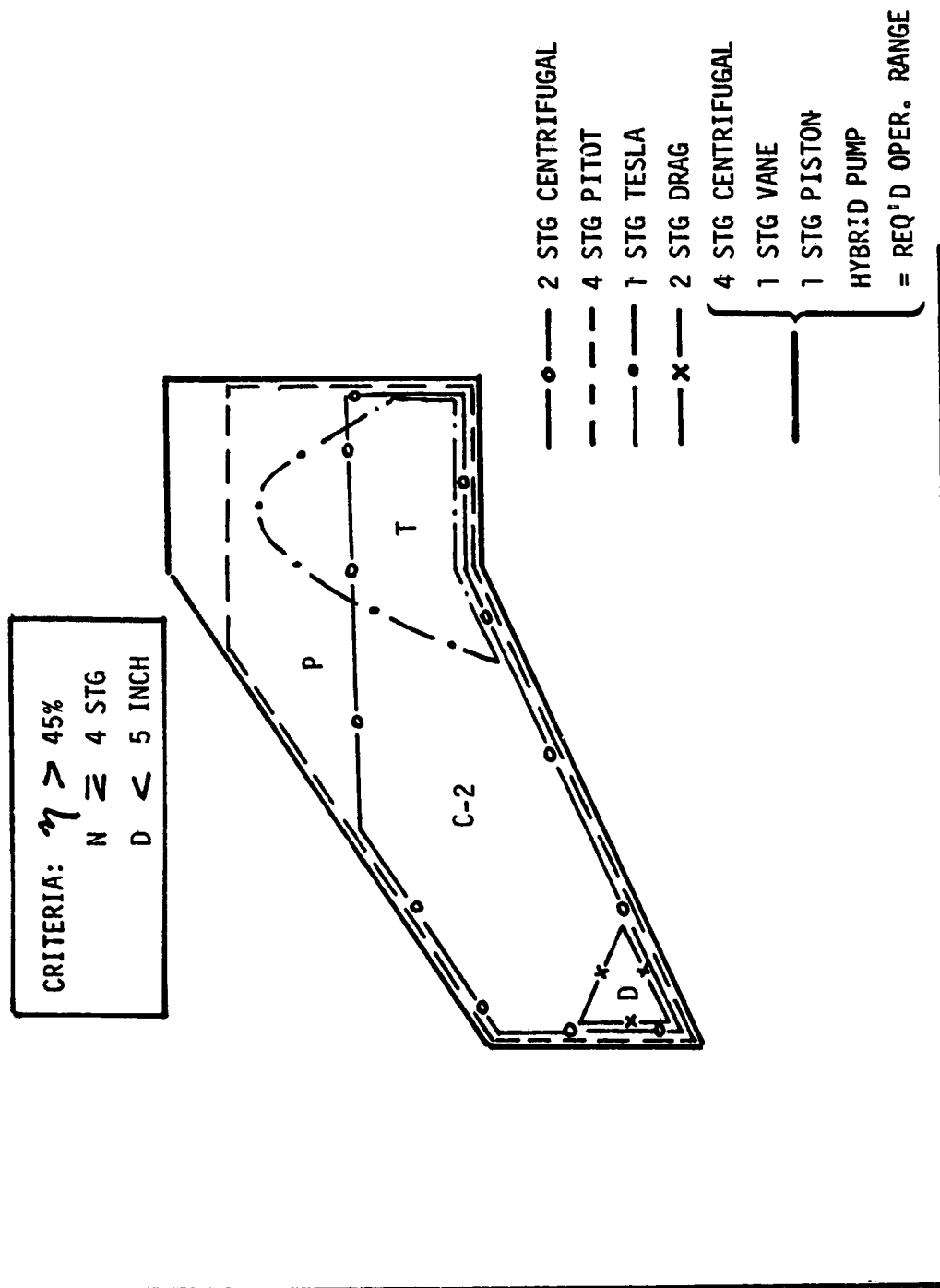


Figure 37. LOX Pump Operating Ranges

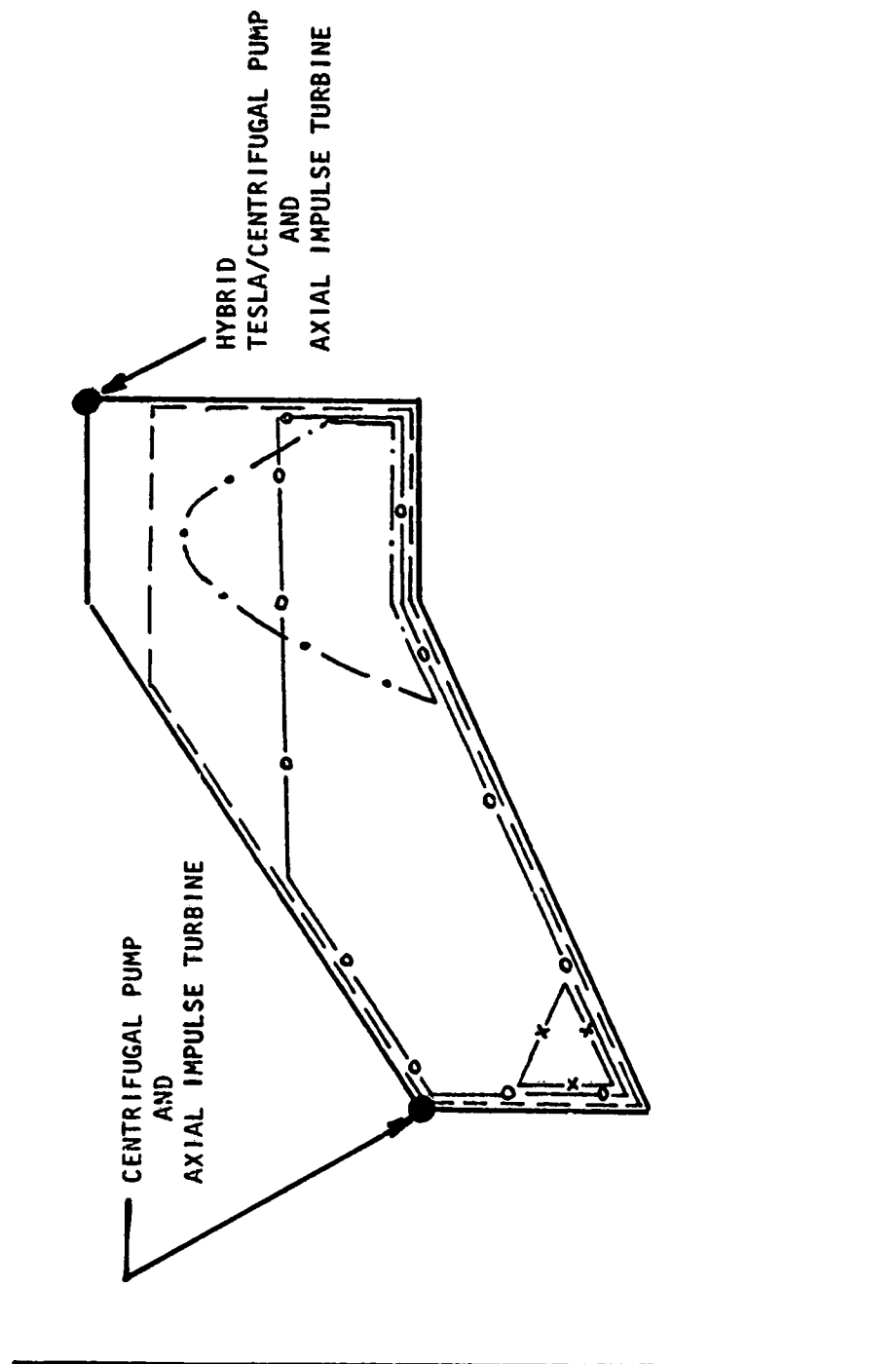


Figure 38. Recommended LOX Preliminary Design Points

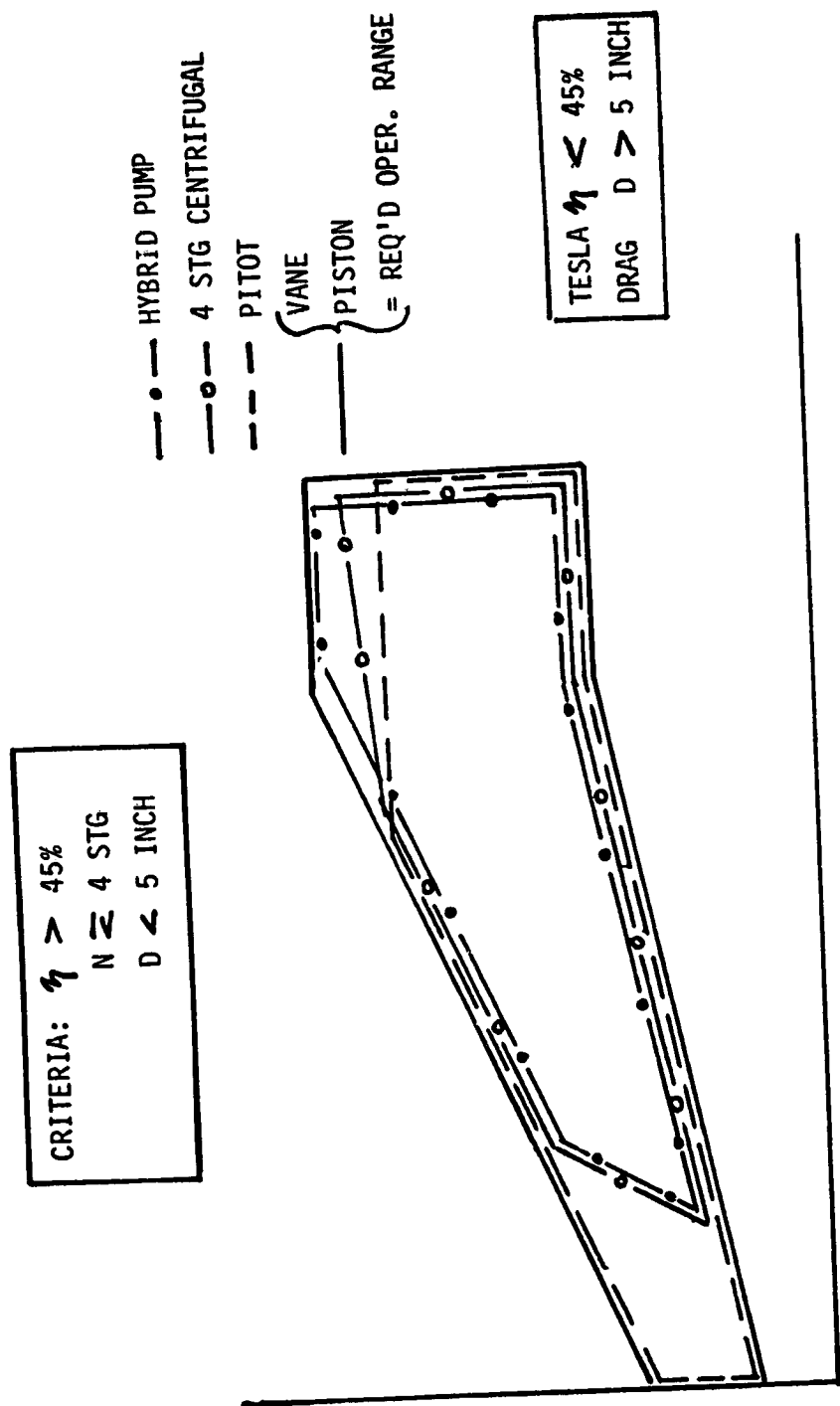


Figure 39. Liquid Methane Pump Operating Ranges

CRITERIA: $\eta > 45\%$

D < 5 IN

N ≤ 4 STG

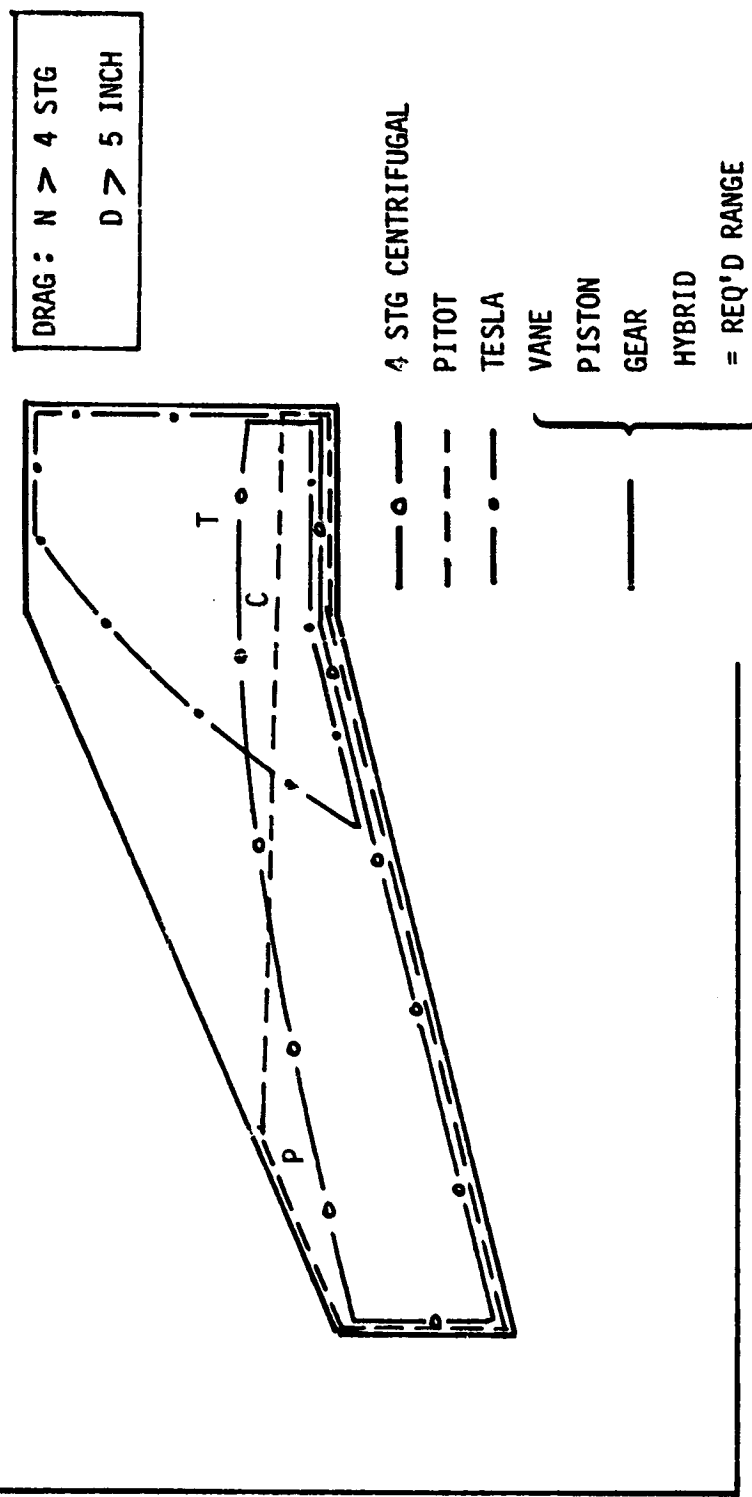


Figure 41. Liquid Hydrogen Pump Operating Range

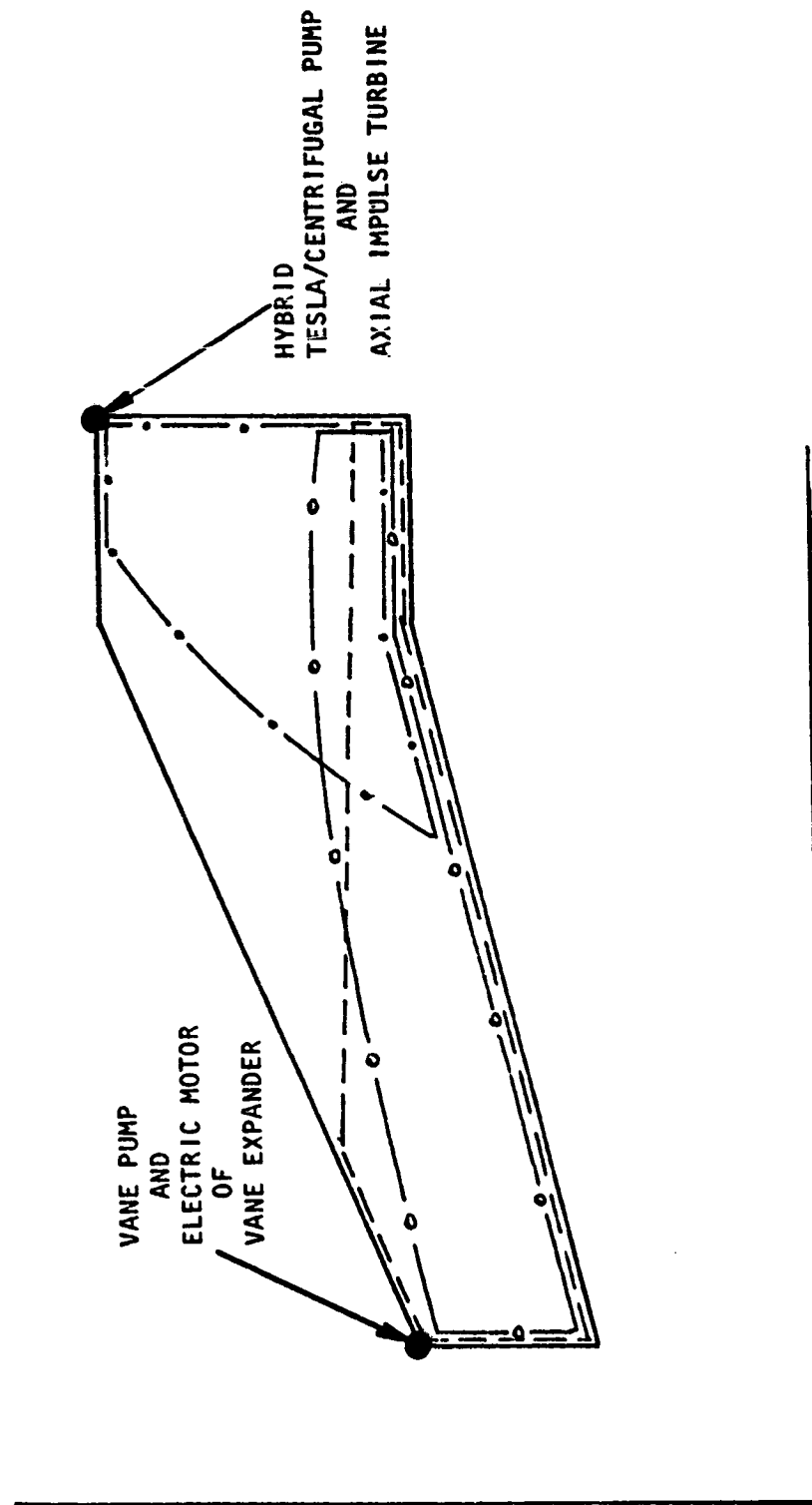


Figure 42. Recommended Liquid Hydrogen Pump Preliminary Design Points

DISCUSSION: TASK II, TRADE STUDIES

This task was originally established to evaluate the effect of varying three parameters: NPSH, head rise and mounting location. During Task I, the effects of various head rise and NPSH values were evaluated. During the Task I review at NASA-LeRC it was agreed that no further effort would be expended on head rise effects. The effects were clearly evident in the curves produced as part of the task (Appendix A). The effects of increased NPSH were also covered in Task I. The Statement-of-Work (SOW), 2 psi higher and unlimited values were examined. The results are also part of Appendix A. It was agreed that the six pumps selected for preliminary design in Task III would be evaluated to determine what would be necessary to operate at very low NPSH values.

Mounting the pumps at various locations on the engine affects the engine weight, size, performance and propellant management. Typically, pumps are mounted on the engine. This tends to lower the net positive suction head (NPSH) at the pump inlets. The results can be pump cavitation and overspeed with catastrophic consequences. To prevent this from happening, the pump can be designed for lower NPSH forcing it to be larger, slower and less efficient or the propellant tank pressure can be increased (to provide higher NPSH) resulting in heavier vehicle weight and reduced payload. Another solution to the problem is to move the propellant pumps to the tanks. This makes pump and tank design easier but increases the ducting length and resultant losses. This reduces the pressure available at the combustion chamber and, therefore, reduces PC and ISP, thus, reducing overall system performance. To select the optimum location for pumps, the specific system must be analyzed. This is necessary because the effect of pump mounting location will be dependent upon engine PC, thrust level, tank pressure, engine type and propellants used.

PRECEDING PAGE BLANK NOT FILMED

DISCUSSION: TASK III, PRELIMINARY DESIGN

This task was performed from March through September 1980. The purpose was to hydrodynamically, aerodynamically and mechanically design six pump-drives applicable to specific low thrust engines. The designs are considered preliminary but are detailed enough to address all significant development and production problems. Following the mechanical design, weight, cost, performance and manufacturing risk and life assessment efforts were performed. A complete set of the final drawings for the selected pump-drive design points are included in Appendix B.

CONCEPT SELECTIONS AND OVERVIEW

Following the Oral Review of Task I, NASA selected the design operating points and propellants for six preliminary designs. The selected design points for the designs (numbered 1 through 6) are shown in Fig. 43 through Fig. 48. Note that design points 1 and 3 are outside the original study envelopes. Both are centrifugal pumps powered by axial impulse turbines. They are selected to be compatible with a 300-pound (1335 n) thrust oxygen-hydrogen engine. Designs 2 and 4 are compatible with a 1,515-pound (6742 n) thrust oxygen-hydrogen engine. They are Tesla-centrifugal hybrid pumps powered by axial impulse turbines. The flow range limit for these pumps is expected to be $0.65 Q/N$ to $1.3 Q/N$, where Q/N is the design flow-speed ratio. By maintaining the speed and flow within these limits, the pump operating range is defined. Figure 49 shows that the operating ranges for designs 1 and 2 cover most of the original study envelope for liquid hydrogen. Figure 50 shows that design 3 and 4 operating range cover most of the envelope for liquid oxygen. Designs 5 and 6 are positive displacement pumps selected for 1,000-pound (4450 N) thrust engines. They are fuel pumps, design 5 being a hydrogen vane pump-motor and design 6 being a methane piston pump-drive. Being positive displacement the flowrate is directly proportional to the speed. The pump discharge pressure is a direct function of the pump back pressure. Positive displacement pumps (5 and 6) are capable (within structural limits) of covering the entire study envelope. Their optimum operating point, however, is their design point (highest combined efficiency).

In the following sections, the results of the preliminary design effort will be covered in detail. To avoid repetition, some discussion of the topics is in order. Hydrodynamic and aerodynamic analyses were performed to zero in on the primary hydrodynamic and aerodynamic geometry for each machine. The analysis was significantly more detailed than that performed in Task I, where trends in performance and gross dimensions were of most interest. For the six design points, the exact diameters, number of stages, speed, number of blades and efficiencies were determined. However, this does not mean that a complete analysis was performed. The exact blade shape, blade loading and hydro-aero contours and many other detail items still have to be established before actual fabrication begins. The objective of a preliminary design in which all significant fabrication and performance problems are identified has been thoroughly met. Mechanical design was accomplished with the same objective in mind. The layouts shown in subsequent sections have included many hours of analysis, in addition to the effort required to actually draw them. The first four were created and drawn using a Computer Aided Design (CAD) system. This

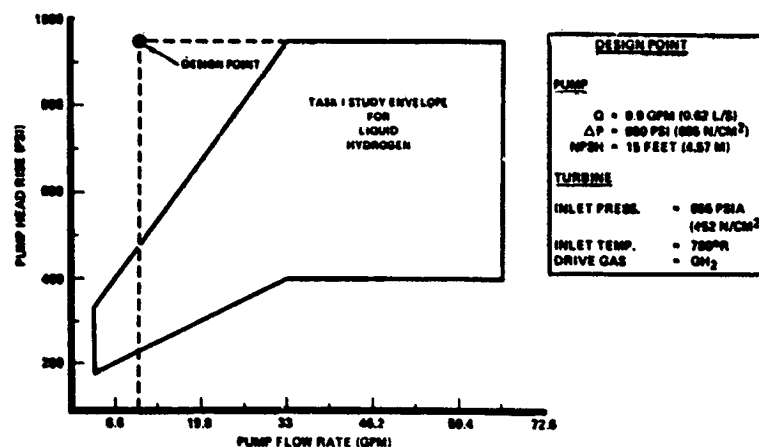


Figure 43. LTCPSPT Design No. 1 Centrifugal Pump-Axial Turbine

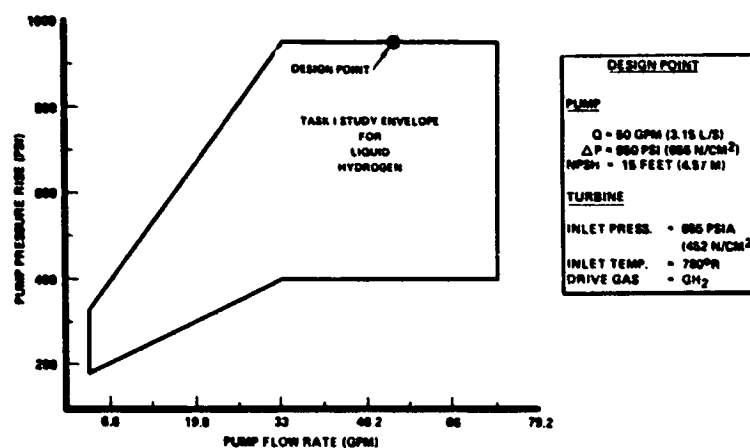


Figure 44. LTCPSPT Design No. 2 Tesla-Centrifugal Pump-Axial Turbine

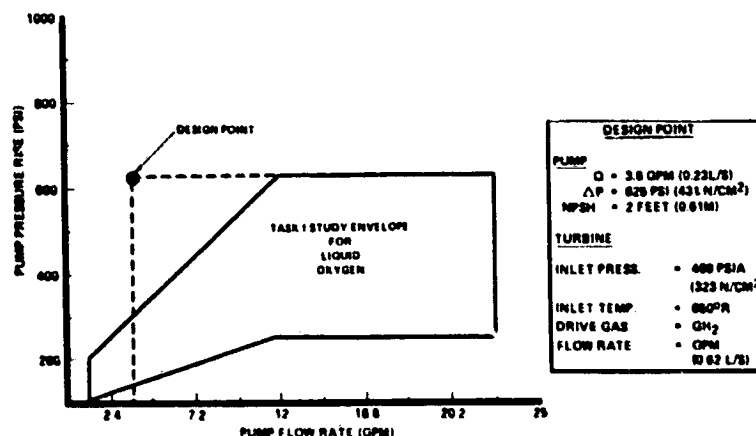


Figure 45. LTCPSPT Design No. 3 Centrifugal Pump-Axial Turbine

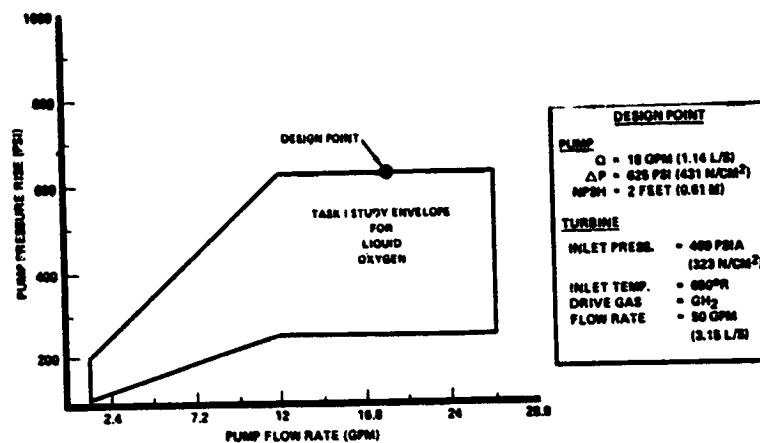


Figure 46. LTCPSPT Design No. 4 Tesla-Centrifugal Pump-Axial Turbine

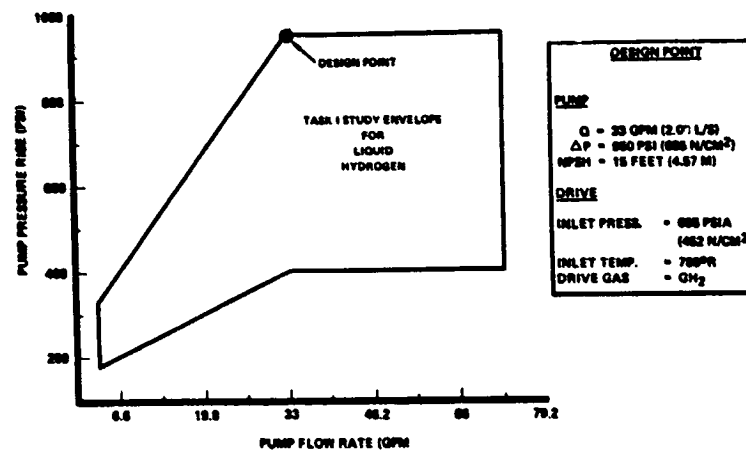


Figure 47. LTCPSPT Design No. 5 Vane Pump-Vane Expander

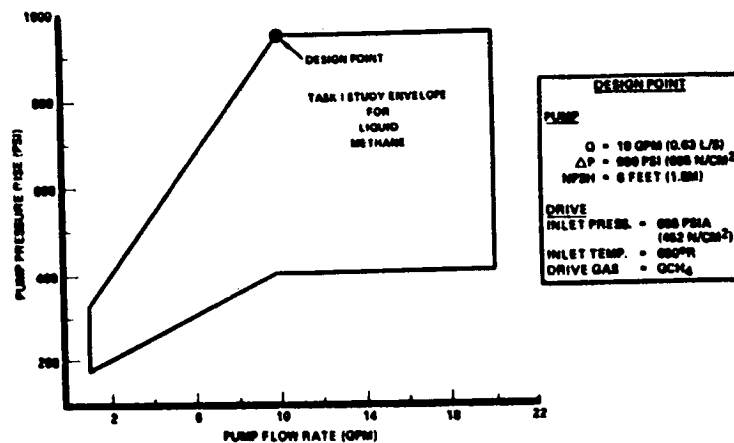


Figure 48. LTCPSPT Design No. 6 Piston Pump-Piston Drive

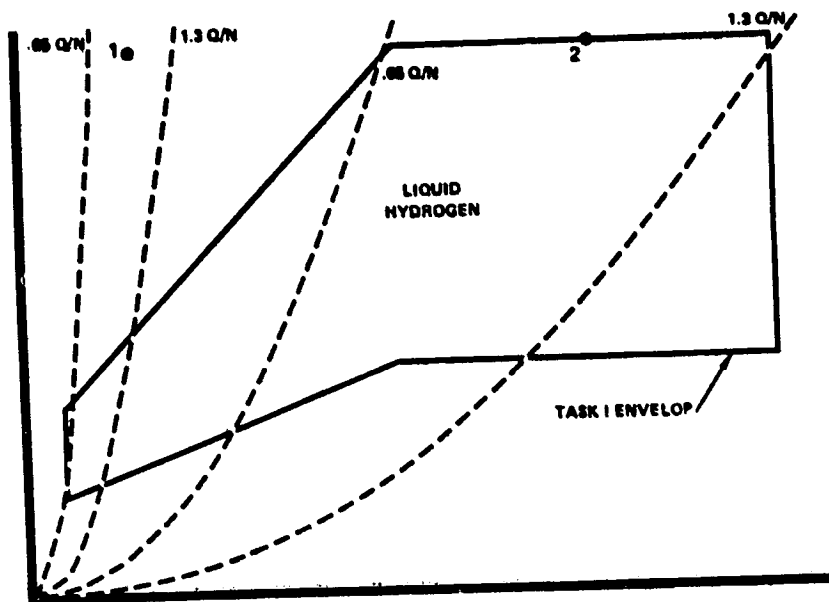


Figure 49. Designs 1 and 2 Cover Task I Envelope

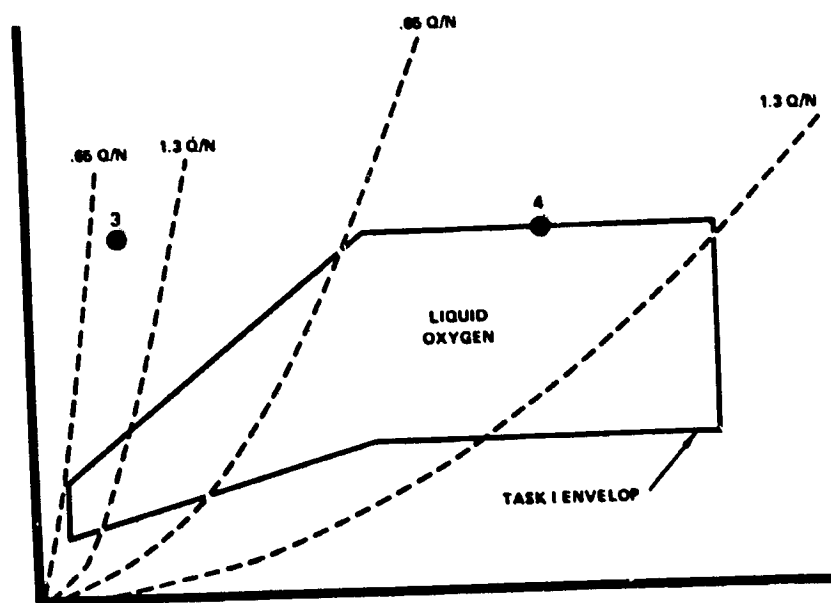


Figure 50. Designs 3 and 4 Cover Task I Envelope

system allows increased flexibility in the way drawings can be formed and utilized. As a result, it may appear that the design effort expended on designs 1 through 4 is more extensive than that for the hand drawn designs 5 and 6; however, this is not the case. Approximately the same effort was expended on each of the six pump-drive designs. Stress analysis was performed in a overview or survey fashion. The impeller and turbine tip speeds were compared with similar turbopumps on the Space Shuttle Main Engine (SSME). This is a standard technique for establishing a feel for the stress levels in the rotating parts. Another indicator is the P/A blade stress in the turbine wheels. The adequacy of wall thicknesses was determined by pressure vessel calculations. Torque and thermal stresses were also examined to ensure no major problems exist in the designs. The weight of each part was calculated using techniques developed at Rocketdyne. The weights are dry in that the propellant and purge fluid weights are not included. The weight of fasteners required to attach the unit to inlet and outlet lines and to structural supports (if required) is also omitted. The life capability of each unit was assessed to determine the issues associated with life. The requirement for each design is 5,000 pounds/hour divided by the thrust in pounds force. This results in the following life requirements for the six design:

<u>Design</u>	<u>Life Requirement, Hours</u>	<u>Engine Thrust, Pounds</u>
1	16.66	300
2	3.30	1515
3	16.66	300
4	3.30	1515
5	5.0	1000
6	5.0	1000

The risk in regard to meeting performance requirements and being able to overcome fabrication problems was assessed. The cost of fabrication was estimated on a rough-order-of-magnitude (ROM) basis.

The estimates are for fabrication, assembly, inspection and proof pressure testing only and are in September 1980 dollars. The cost of a program that would detail design, fabricate and test a selected pump-drive would be very difficult to estimate because schedule, test objectives and other requirements could vary greatly. The estimates are divided into two major categories: recurring and tooling costs. The recurring cost is that cost associated with each unit. The tooling cost is all monies required to prepare to fabricate the first unit. This includes special tools, templates, measurement and assembly jigs and casting pattern fabrication and special handling equipment. The first unit cost is the sum of the tooling and recurring costs.

DESIGN 1, HYDROGEN TURBOPUMP

As mentioned above, Fig. 43 shows the design point for the fuel turbopump on a 300-pound (1335 N) thrust engine. The figure also shows the pump requirements for flow, head rise and minimum NPSH. In addition, the turbine inlet pressure, temperature and drive gas are included. The engine is an expander type with

series turbines (fuel first). In the case of this design, the turbine inlet pressure of 655 psi (452 N/Cm²) was not compatible with the required power. As a result, the pressure was adjusted to provide adequate power to the turbine.

Hydrodynamic Design and Performance

A layout of Design 1 is shown in Fig. 51. This unit consists of an inducer and a four-stage centrifugal pump driven by a partial admission (7%) impulse turbine. The pump is designed to handle 9.9 gpm ($62.5 \times 10^{-5} \text{ m}^3/\text{sec}$) of liquid hydrogen with a pressure rise of 950 psi (655 N/Cm³) at a speed of 140,000 rpm (14,661 rad/sec).

As can be seen from the layout, the inducer and first stage of the pump are overhung beyond the 10 mm pump end bearing. The second, third and fourth stage of the pump are supported between the bearings while the turbine is overhung beyond the 10 mm turbine end bearing. A single seal is required to prevent leakage of liquid hydrogen from the pump into the turbine.

The inducer has four blades with the capability of operating at an NPSH of 15 feet (4.57 m). The four centrifugal impellers have similar passages with backward curved blades and with shrouds both front and rear. In the crossover networks approximately 75% of the diffusion is accomplished in the outward radial portion of the diffuser. The impeller tip speed at 140,000 rpm will be 745 ft/sec (227 m/sec). The head coefficient per stage is 0.45.

Figure 52 shows the calculated design and off-design performance of the four-stage pump. As can be seen from the figure, the calculated efficiency at the design speed of 140,000 rpm, design flow of 9.9 gpm and design pressure rise of 950 psi is 32.5%.

The overall layout of the turbopump has been completed but the details remain to be done. These include the inducer blade shapes, the centrifugal impeller blades and shrouds, the blading in the crossover network and the balance piston and end thrust calculations. The pump discharge volute must also be designed.

Aerodynamic Design and Performance

The turbine was designed for optimum performance and minimum weight. The analysis was performed using Rocketdyne's partial admission gas-turbine hydrogen turbine analysis computer program. The program includes all hydrogen turbine analysis computer program. The program includes all gas path losses due to friction, turning, and secondary flows as well as partial admission losses due to the blade pumping and windage, end sector losses, stage losses, and a size effect based on experimental results.

The turbine design parameters are presented in Table 5. Inlet conditions were considered specified at the turbine inlet manifold. Turbine outlet total pressure and temperature are specified in the turbine outlet pipe just downstream of the turbine outlet collector.

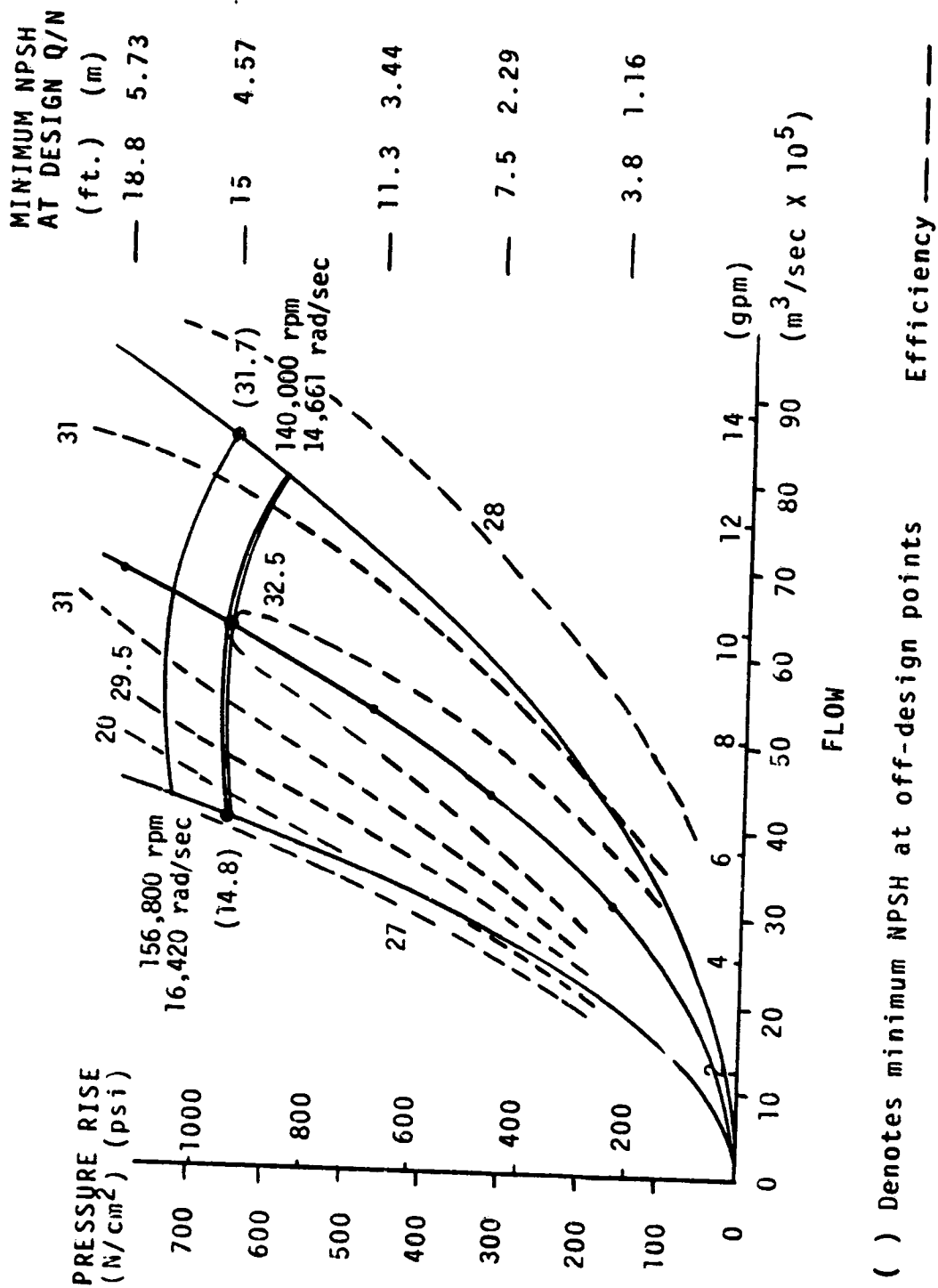


Figure 52. Calculated Design and Off-Design Performance of the Four-Stage Pump

TABLE 5. DESIGN 1, LOW THRUST PROPULSION SYSTEM
HPFTP TURBINE PERFORMANCE PARAMETERS

WORKING FLUID	GASEOUS HYDROGEN	GASEOUS HYDROGEN
OUTPUT POWER	12.682 kW	17 hp
SPEED	140,000 rpm	140,000 rpm
FLOWRATE	0.042 kg/sec	0.0926 lb/sec
INLET TOTAL TEMPERATURE	433.33 K	780 R
INLET TOTAL PRESSURE	51.02 BAR ABSOLUTE	740 psia
OUTLET TOTAL PRESSURE	33.03 BAR ABSOLUTE	479 psia
TOTAL PRESSURE RATIO	1.545	1.545
AVAILABLE ENERGY	178.1 kcal/kg	320.6 Btu/lb
ISENTROPIC VELOCITY	1221 m/sec	4007 ft/sec
MEAN DIAMETER	4.699 cm	1.85 inch
MEAN BLADE SPEED	372 m/sec	1222 ft/sec
VELOCITY RATIO	0.	0.
TOTAL PRESSURE ISEUTROPIC EFFICIENCY %	42.0	42.0
ROTOR TYPE	SHROUDED	SHROUDED

Turbine geometry parameters were optimized for high performance. The selected turbine mean diameter is shown in Fig. 53. The shrouded motor design minimizes the end wall and tip-clearance losses, thereby improving the stage efficiency.

The turbine predicted power losses are tabulated in Table 6. Primary losses are due to friction and turning in the nozzle and rotor profiles as shown by the expansion and kinetic energy losses. The inlet manifold loss was for a manifold with a radial inlet on a torus to the axial inlet nozzle. The velocity out of the stage was assumed lost in the exhaust manifold, and the total pressure at the turbine outlet flange was assumed to be equal to the static pressure at the rotor discharge. Partial admission losses and disk friction are also shown.

The velocity vector diagrams are shown in Fig. 54 for the design condition. Velocities out of the element include losses due to friction and turning but not the losses due to disk friction, size effects, or partial admission. Nozzle discharge Mach numbers are less than 0.6. It was conservatively assumed that all of the absolute leaving kinetic energy of the rotor discharge (equal to 353 m/sec) was lost.

The total and static pressures and temperatures in the blade path are shown in Fig. 56. The static pressure across the rotor is constant for the impulse

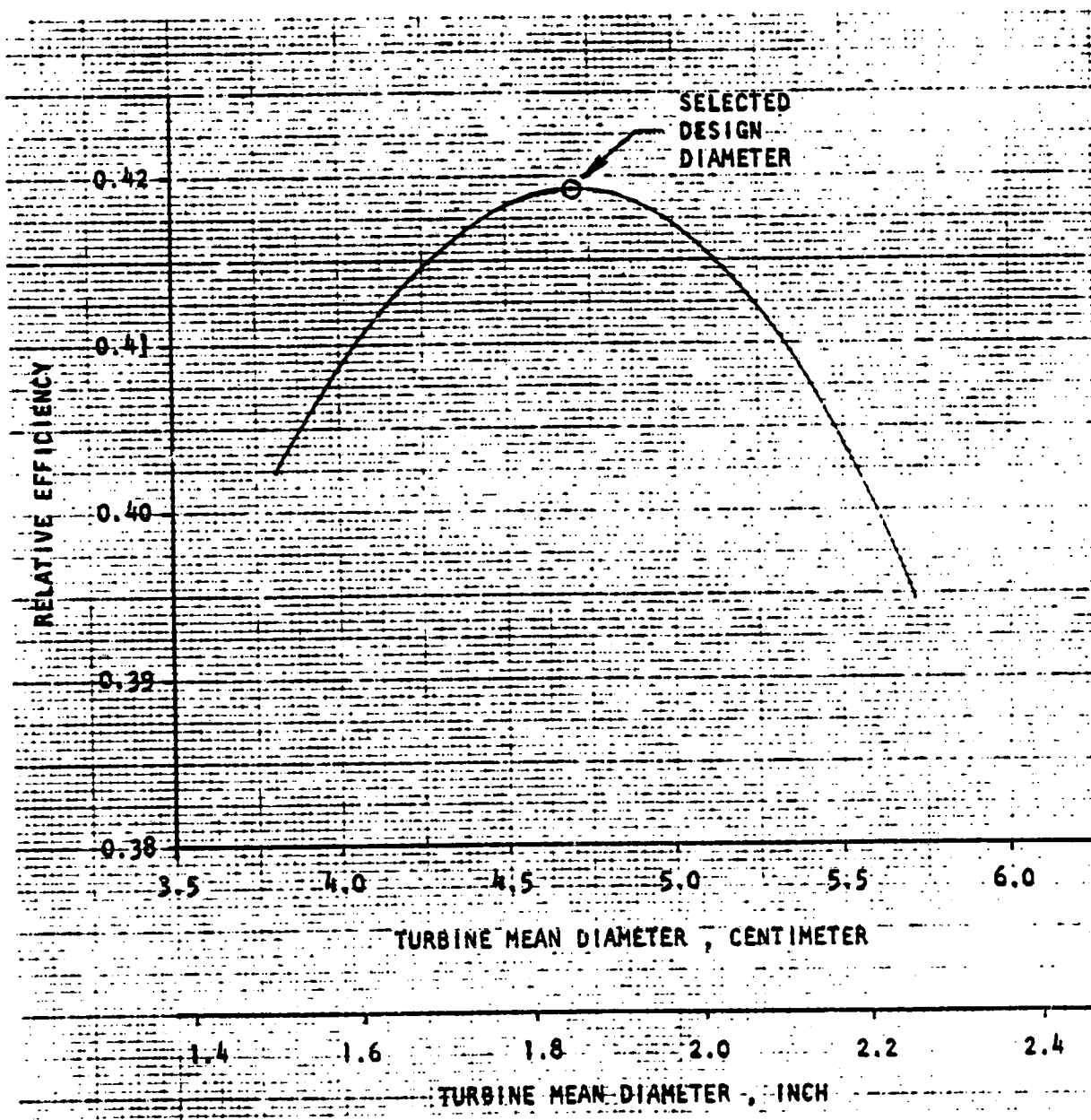


Figure 53. HPFTP Turbine Low Thrust Propulsion System, Mean Diameter Optimization, Design 1

TABLE 6. DESIGN 1, LOW THRUST-PROPULSION SYSTEM HPFTP TURBINE
FLANGE-TO-FLANGE EFFICIENCY AND PERFORMANCE

	FLOWRATE		ENTHALPY		POWR LOSS	
	Kg/S	Lb/sec	KCAL/Kg	Btu/LB	Kw	Hp
1. <u>POWER LOSSES</u>						
INLET MANIFOLD	0.0420	0.0926	5.928	10.671	1.00306	1.3982
I-R U/S SHAFT SEAL	0.0236	0.052	108.9972	196.195	1.08401	1.4531
I-N INLET INCIDENCE	0.0381	0.0874	0	0.000	0	0
I-N INLET KINETIC ENERGY	0.0381	0.0874	0	0.000	0	0
I-N EXPANSION ENERGY	0.0381	0.0874	15.076	27.1377	2.6526	3.5558
I-R INLET INCIDENCE	10381	0.0874	0	0.000	0	0
I-R INLET KINETIC ENERGY	10381	0.0874	32.7535	58.9564	5.4404	7.2928
I-R EXPANSION ENERGY	10381	0.0874	0	0.000	0	0
I-R WINDAGE					1.5990	2.1434
I-R END SECTOR MIXING					1.1206	1.5022
I-R RIM FRICTION					0.2523	.3383
I-R DISK FRICTION					0.06251	0.0838
I-P END CLEARANCE	0.0381	0.0874	0.8161	1.4689	0.1355	0.1817
S-1 DIAGRAM FACTOR ADJUSTMENT	0.0381	0.0874	14.0555	25.2999	2.3346	3.1295
I-R LEAVING ENERGY	0.0381	0.0874	14.9088	26.8358	2.4763	3.3195
TOTAL POWER LOSSES					18.2012	24.3984
2. <u>AVAILABLE POWER</u>						
WDOT INLET FLANGE	0.042 kg/sec		0.0926 lb/sec			
DHA T-S F-F	178.1 KCAL/Kg		320.6 BTU/Lb			
POWER AVAILABLE T-S F-F	31.33 Kw		42.00 Hp			
DHA T-T F-F	163.2 KCAL/Kg		293.8 BTU/lb			
POWER AVAILABLE T-T F-F	28.71 Kw		38.49 Hp			
3. <u>SHAFT POWER ETC. OVERALL</u>						
			POWER			
			Kw		Hp	
POWER AVAILABLE T-T F-F	31.33				42.00	
TOTAL POWER LOSSES	18.20				24.40	
SHAFT BRAKE POWER	13.14				17.61	
OVERALL EFFICIENCY T-T F-F			0.4196			
OVERALL U/C T-T			0.282			
OVERALL U/C T-T SQRT(2)			0.294			

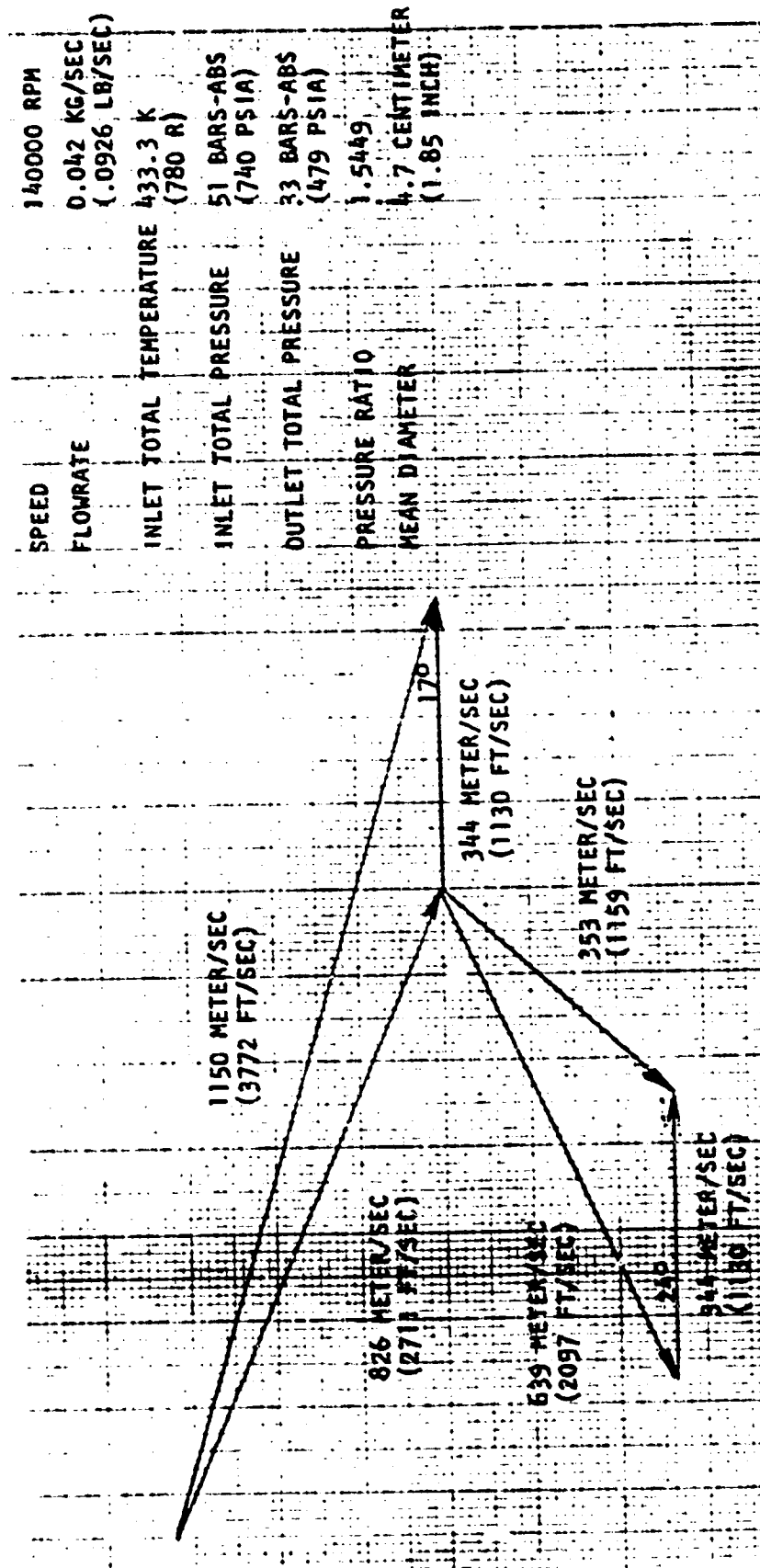
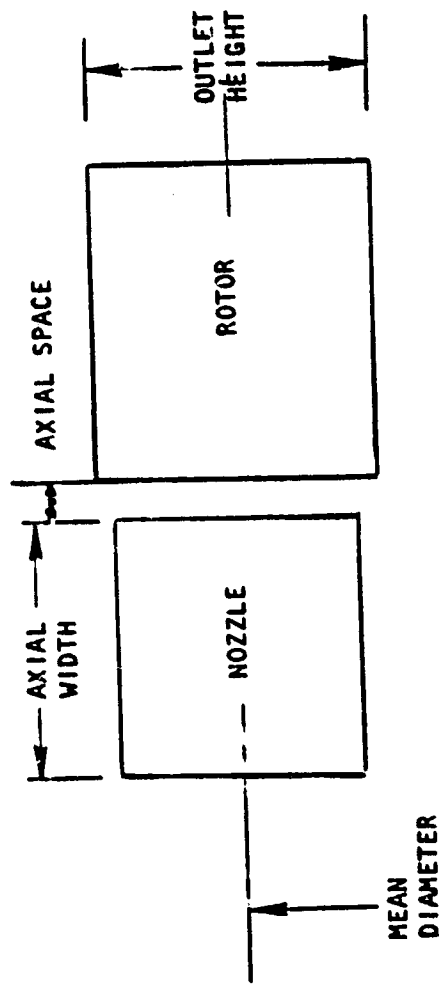


Figure 54. HPFTP Turbine Low Thrust Propulsion System Velocity Vector Diagram, Design 1



ELEMENT	NOZZLE	ROTOR
MEAN DIAMETER	4.7 CENTIMETER (1.85 IN)	4.7 CENTIMETER (1.85 IN)
OUTLET HEIGHT	0.61 CENTIMETER (0.24 IN)	0.76 CENTIMETER (0.30 IN)
INLET HEIGHT	0.61 CENTIMETER (0.24 IN)	0.76 CENTIMETER (0.30 IN)
AXIAL WIDTH	0.7 CENTIMETER (0.275 IN)	0.86 CENTIMETER (0.338 IN)
AXIAL SPACE	0.051 CENTIMETER (0.02 IN)	
PERCENT ADMISSION	7.6 %	
ADMISSION SECTORS	1	

Figure 55. HPFTP Turbine Low Thrust Propulsion System Preliminary Turbine Blade Path Data, Design 1

design to minimize pumping losses in the inactive rotor blades with partial admission. All of the expansion and acceleration of the flow occurs across the nozzles at the design condition. Since the rotor is pressure balanced, there will be no significant rotor axial thrust at the design condition.

Turbine sizing is shown in Fig. 55. The mean diameter is 4.699 centimeters (1.85 inches). The axial space between the nozzles and rotors should be minimized to reduce spillage loss at the ends of the axes of admission. Use of two nozzle sectors would be desirable from the standpoint of providing the structural and dynamic symmetry, but a single sector improves turbine efficiency approximately 2 to 3%. This turbine is required to deliver a high power per unit of mass flow rate. The turbine only has 7.6% partial admission and delivers 12.68 Kw. The optimum way to achieve this power is to maximize the efficiency by using the single sector nozzle design.

The rotor blades were shrouded for improving performance with a radia tip clearance of 0.005 cm (0.002 inch). The leakage past the rotor upstream side of the shaft seal was into the blading. The leakage was assumed to do no work in the turbine. The flow area sizing included the leakage.

The design predicted performance is 42% efficiency with a delivered power of 13.13 Kw (17.6 Hp), about 0.45 Kw higher than the required design power. The flange-to-flange efficiency and performance are presented in Table 6.

Mechanical Design

Design 1 is a four-stage centrifugal pump plus an inducer in front of the first stage impeller powered by a partical admission single stage axial flow turbine. The pump has an axial inlet and a radial discharge. The turbine has a radial inlet and an axial discharge. A full-size drawing is shown in Fig. B-1.

The rotating assembly consists of the turbine wheel with an integrally fabricated draw bar on which are mounted the four impellers and two bearings. Tension in the draw bar is applied by a nut in front of the first stage impeller. The bearings are mounted on the first and fourth stage impellers and the compressive load from the draw bar passes through the bearing inner races. The torque applied by the turbine is transmitted to the fourth stage impeller by a spline. The torque is then transferred between the impellers by tangs and slots machined integrally in each impeller. The use of a through hole in the impellers is possible because of the low tip speed of the impellers. The inducer is threaded on to the draw bar. The tab lock between the inducer and the impeller retaining nut allows the nut to be locked in an infinite number of positions when tensioning the draw bar. The torque required to drive the inducer will be transmitted by the lock tab washer.

Positioning of the impellers is provided by a pilot diameter and a normal bearing surface on each end. Repositioning error when the rotor is disassembled and reassembled is reduced by allowing that the impellers can be assembled in only in one angular rotation position.

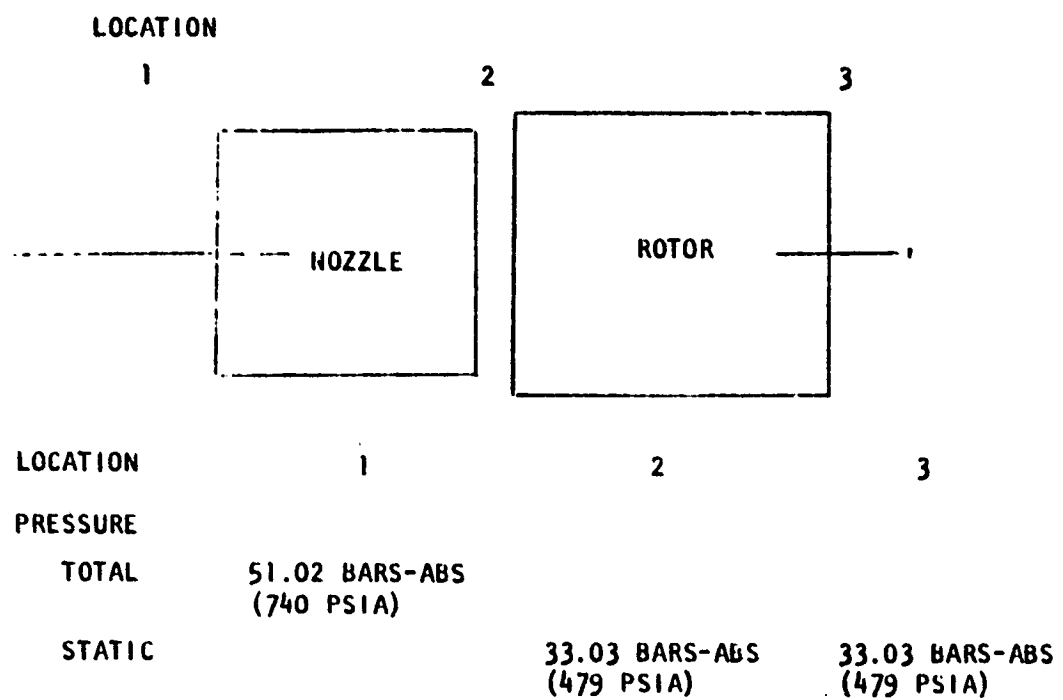


Figure 56. HPFTP Turbine Low Thrust Propulsion System Blade Path State Condition, Design 1

The pump housing assembly consist of three major components. The pump inlet contains a cast diffuser passage for the first stage impeller and provides a tunnel for the inducer. The pump bearing carrier contains the cast down comer which completes the crossover for the first stage impeller. It also provides a precision diameter for accepting the foreward pump bearing. The main pump housing contains the cast fourth stage impeller diffuser, the volute collector and discharge diffuser plus the turbine inlet, manifold and nozzle blades. The second and third stage impeller crossovers are cast and are buried in the assembly (i.e., no external flanges). They are piloted fore and aft and are pinned for angular radial positioning. The pins also carry the reaction torque from the crossovers. The turbine end bearing and turbine pump seal are located in the turbine end of the main pump housing.

The bearings are preloaded against each other at assembly by tension in the draw bar. The seal is retained in the main housing by a nut and cup lock washer.

Static seals are provided for all external flanges. An inner row of static seals seal the crossover at the impeller discharge diameter. Leakage past the seals will be united to the pump inlet aft of the inducer. The result is that the flange seals will see inducer discharge pressure, except the inlet flange static seal will see first stage impeller diffuser discharge pressure.

The bearings are of the angular contact type designed to run in LH_2 . The turbine/pump seal is of the controlled gap type and is internally pressurized. The pressurizing flow comes from the pump discharge. The leakage flow toward the pump provides the coolant flow for the turbine end bearing. The pump end bearing coolant flow is provided by the pressure rise of the first stage crossover.

The rotor thrust loads are balanced out by a balance piston that is an intergal part of the fourth stage impeller. The high pressure orifice is provided by a lip on the pump housing and a lip on the impeller outside diameter. The low pressure orifice is provided by matching surface on the impeller and housing. Balance piston flow is ducted to the ID of the fourth stage impeller and delivered to the inlet of the same impeller. The flow from the balance piston is mixed with the bearing coolant flow in the balance piston sump prior to returning to the fourth stage impeller inlet.

The impeller's eyes are sealed by stepped labyrinth wear rings. The rear shroud leakage is controlled by close fitting diameters between the crossovers and the impeller hubs. This close fitting diameter also forms a squeeze film damper for controlling the shaft excursions experienced during times that the pump rpm passes through a critical speed range.

The materials chosen for use in the pump and turbine are those that have been proven in previous turbopump designs. The impeller and crossovers will be fabricated from cast Inconel 718. The pump inlet and main pump housing will be fabricated from cast and wrought Inconel 718. The turbine wheel will have intergally machined blades and be made from Inconel 718. The bearings are 440C corrosion resistant steel.

Protection of the structural parts from hydrogen environment embrittlement is provided by plating the exposed surfaces with a suitable material that stops the embrittlement process.

As part of the mechanical design a preliminary stress survey was performed. The impeller tip speed is 745 ft/sec (227 m/s). This is well within the current technology. For example, the Space Shuttle Main Engine (SSME) fuel pump has an impeller tip speed of 1800 ft/sec (549 m/s). The turbine tip speed is 1466 ft/sec (447 m/s) which is also below the SSME tip speed of 1800 ft/sec (227 m/s). In addition, the P/A stress in the blades is 57,600 psi (39,727 n/Cm²). This is only slightly higher than the corresponding SSME stress of 56,000 psi (3862 n/Cm²). Inco 718 is the primary material from which the pumps are fabricated. It has properties of $F_{Ty} = 145,000$ psi (100,000 n/Cm²) and $F_{Ty} = 170,000$ psi (117,250 n/Cm²). These values are approximately 18% higher than those for the material used in the SSME (MAR-M-246 DS). Pressure vessel, torque and thermal stress are all well below safe limits. As a result, of the fore-going, no significant stress problems are anticipated when detail stress analysis is performed.

Rotordynamics analysis was performed to assure a 20% margin above and below the operating speed. The rotating assembly is modeled as shown in Fig. 57. Originally, the inducer was overhung further to the left (-X). Analysis showed a potential problem in that the first critical speed was less than one-half the operating speed. This condition is conducive to synchronous and subsynchronous whir and is, therefore, avoided. The design was modified and the results shown in Figure 58 were obtained. The first three mode shapes and critical speeds are shown. In addition, the estimated bearing spring rates of 100,000 lb/in. each are also shown as K1 and K2. Figure 59 shows the first four critical speeds plotted as a function of bearing spring rate. The turbo pump operates between the third and fourth critical speeds.

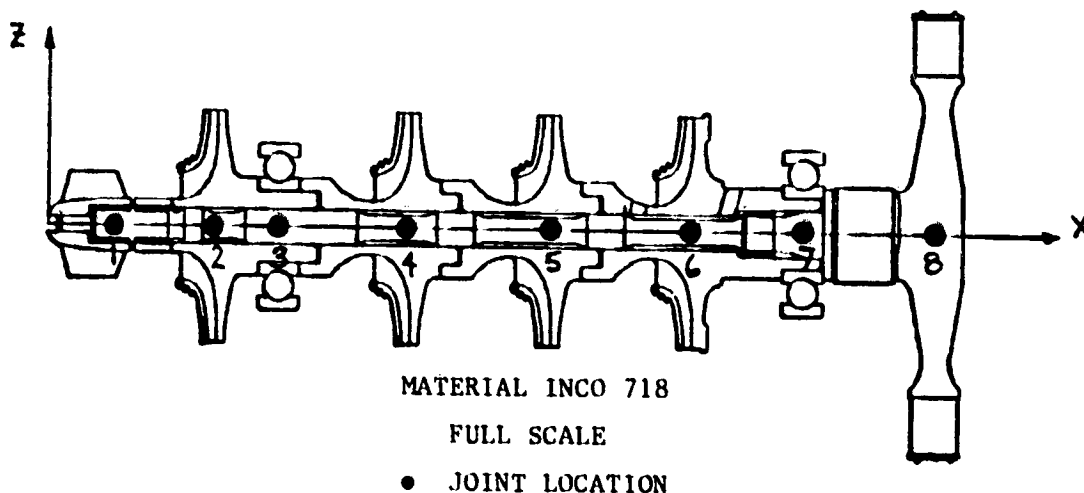
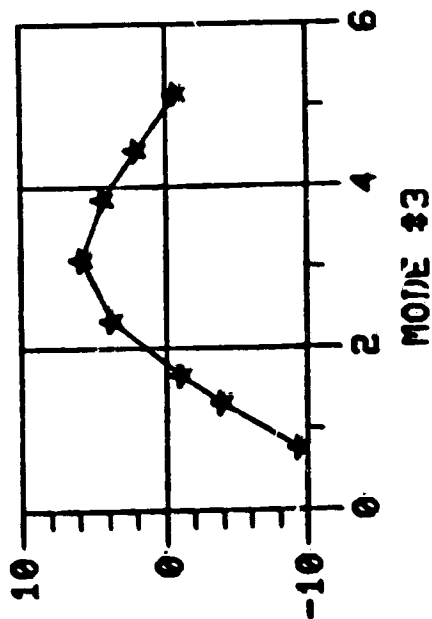
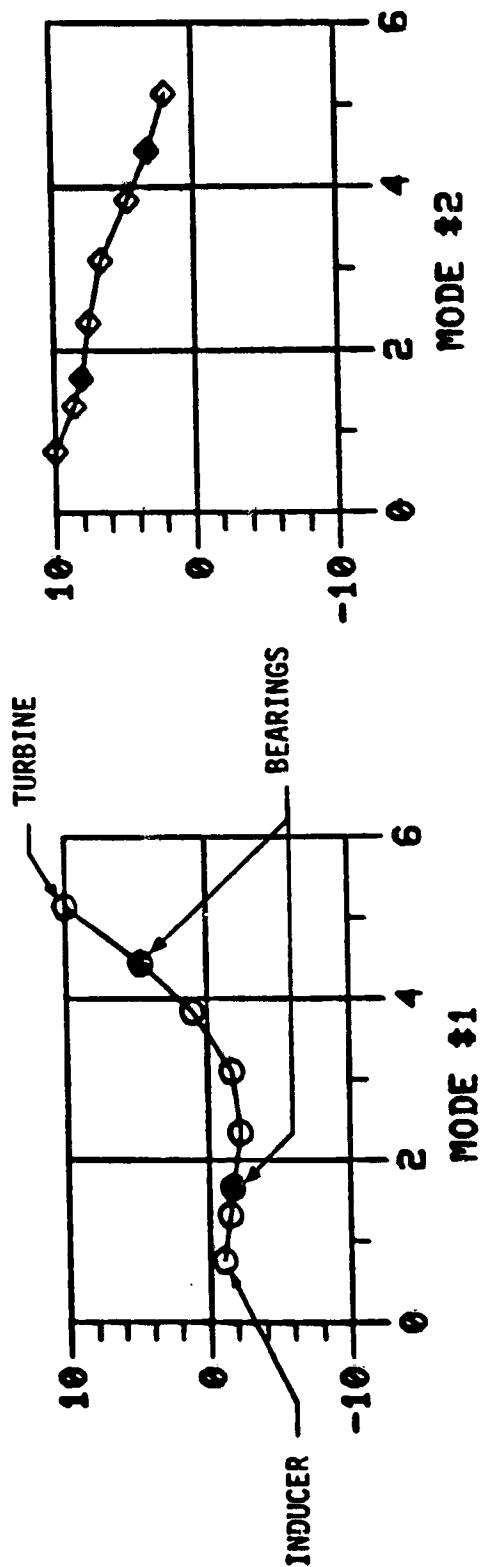


Figure 57. Design 1, Fuel Turbopump
(N = 140,000 rpm)



MODE	HZ	RPM
1	1214.800	72887.
2	1547.900	92874.
3	1854.300	111260.

K1 =	100000.	LB/IN
K2 =	100000.	LB/IN

Figure 58. Low Thrust Engine Turbopump Design No. 1 Critical Speed

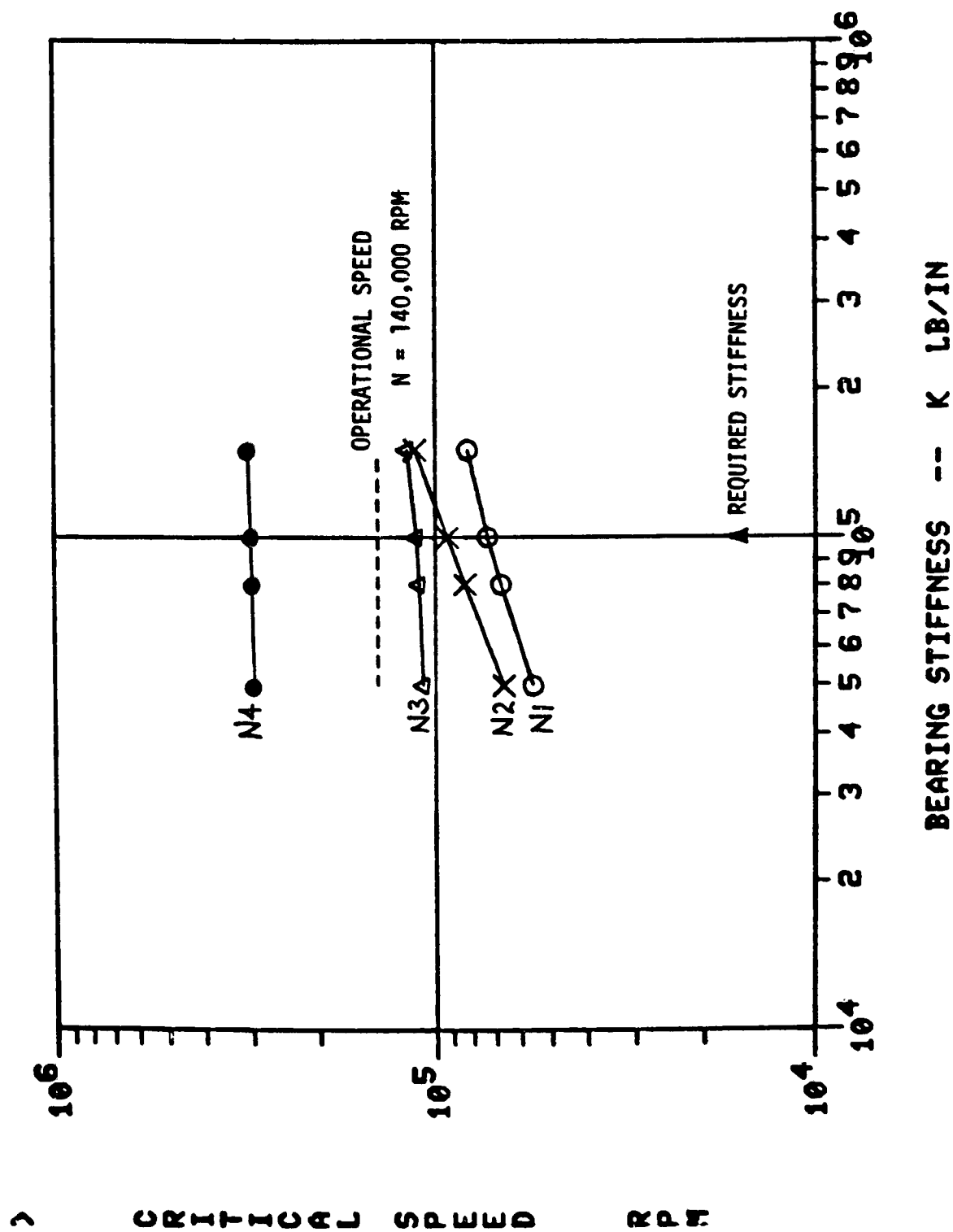


Figure 59. Low Thrust Engine Turbopump Design No. 1 Critical Speed
Critical Speed vs Bearing Stiffness

Weight Analysis

The weight of turbopump design 1 was estimated using proven techniques developed by Rocketdyne over the past 30 years. The total dry weight is 5.5 pounds (2.49 kg). The rotating assembly weighs 0.77 pound (0.35 kg) and the housing weighs 4.73 pounds (2.15 kg). Figure 60 shows the weight of each part of the turbopump. As a point of comparison, the inducer weighs 0.02 pound (9 grams), less than the weight of a penny.

Life Assessment

The pump tip speed and the turbine pitch line velocity are relatively low and therefore the stresses in all parts will be moderate. The Stress Group can predict blade frequencies so that proper blades thicknesses can be used to avoid any damaging blade vibrations.

Recently designed Rocketdyne inducers for waterjets and centrifugal pumps have been run for thousands of hours in sea water and liquid sodium without suffering any cavitation damage at design and higher flows. Damage can occur at low flows, however, cavitation damage over the entire range of flows in liquid hydrogen has been extremely rare in all of Rocketdyne experience with the fuel.

Bearing DN is 1,400,000 for both pump and turbine end bearings. This is high but not beyond the state of the art. Adequate bearing life is predicted. Seals are within current experience and are not expected to limit the life of the machine.

Performance and Manufacturing Risk

LOX turbopump had a fully-shrouded centrifugal impeller that was 2.55 inches in diameter with the turbine and other parts in proportion. Rocketdyne also manufactured and tested a centrifugal unit to pump liquid fluorine. The impeller in this pump was only 1.3 inches in diameter.

Pump component tests should be conducted to verify the predicted performance of a small partial emission pump stage. The tests may be conducted with water as the test fluid. The performance differences between water and liquid hydrogen may be analytically determined.

Finally, to verify the overall performance, the turbopump should be tested over a range of speeds, flows and inlet pressures to determine its H-Q and suction performance and its isentropic efficiency. The turbine performance in gaseous hydrogen can also be measured at the same time.

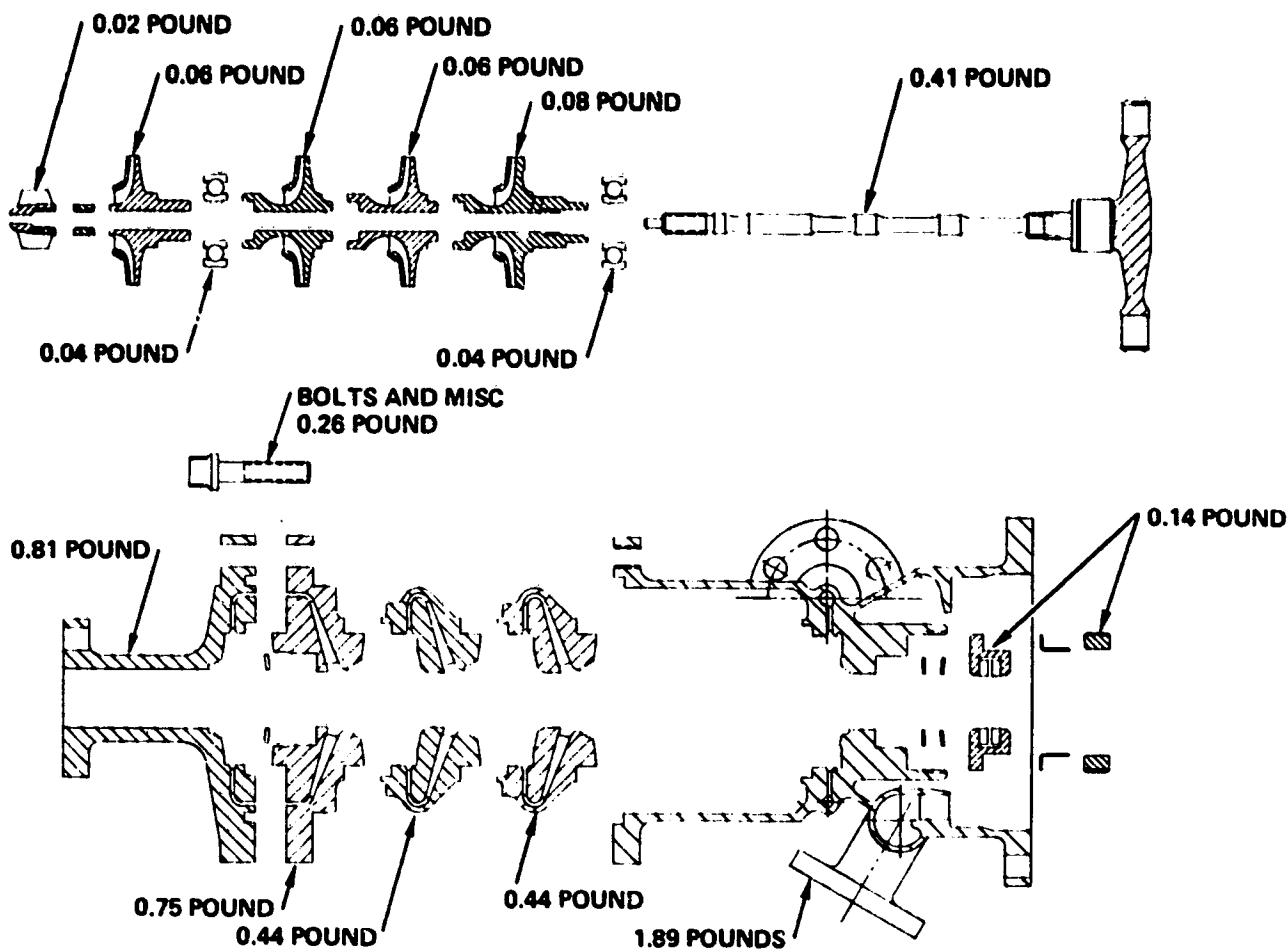


Figure 60. Design 1 Weighs 24.5 N (5.5 pounds)

Cost Analysis

This estimate of manufacturing cost is considered to be rough-order-of-magnitude (ROM) and includes the cost of actual fabrication and assembly in September 1980 dollars. The estimated cost of the fabrication is divided into two categories, tooling and recurring costs. The tooling cost is all the monies required to make the first part (minus the recurring cost). This includes the patterns required for castings, templates, special inspection tools and other specially made or purchased items required to fabricate the unit. The estimated cost for tooling is \$139,799. \$85,000 of which is for casting tooling, \$29,100 for purchased parts and raw material and \$25,600 for machining. The recurring cost of fabrication is estimated to be \$51,200, \$3,500 of which is for castings, \$700 for raw material and \$47,000 for machining. By combining the tooling and recurring costs, the first-unit cost is obtained - \$190,900.

DESIGN 2, HYDROGEN TURBOPUMP

Figure 44 shows the required operating point for Design 2. The pump AP, NPSH and flow are 950 psi (655 N/Cm²), 15 feet (4.57 M) and 50 gpm (3.15 L/S), respectively. The turbine inlet pressure, temperature and drive gas are 655 psi (452 N/Cm²), 780 R and CH₂, respectively.

Hydrodynamic Design and Performance

Design 2, Liquid hydrogen pump, is shown in Fig. 61. In order to maximize efficiency, it is desired to operate at the highest possible rotating speed to maximize the specific speed ($N \sqrt{Q}/H^{0.75}$) where N is rotating speed, Q is flowrate and H is head rise. For maximum simplicity, it is desired to accomplish this without the use of a low pressure or boost pump. In order to operate at high speed, an inlet pumping stage capable of operating at a very high suction specific speed ($N \sqrt{Q}/\text{NPSH}^{0.75} = 102,000$ (N, rpm; Q, gpm; NPSH, ft.) is required where NPSH is inlet total head above vapor pressure. Therefore, the Tesla or disk pump type was selected for its predicted high suction performance capability.

The second centrifugal stage incorporates an integral balance piston for axial thrust balance. The flow is directed between stages by a crossover diffusing system. The first stage of diffusion reduces the velocity to approximately one half the diffuser entering value. The in-flow diffusing passages reduce the velocity to match the impeller inlet requirement. The second centrifugal impeller discharges through vaned diffusers into a volute. The diffusion system allows full flow at the impeller discharge with an impeller tip width 1.143 mm (0.045 inch) adequate for manufacturing. The impellers are of the fully shrouded type with backwardly curved blades. The Tesla or disk pump incorporates a rotating housing configured to increase the radial velocity prior to entering its diffusing system. The rotating housing reduces hydraulic losses in the flowing fluid to maximize head rise. The fluid flow losses are traded for outer shroud friction drag resulting from interaction with the fixed housing.

The predicted pump head, flow, efficiency curve is presented in Fig. 62. The performance was calculated using Rocketdyne developed computer programs for both the Tesla and centrifugal stages. The Tesla pump performance analysis procedures are based on the preliminary results of tests performed at the David W. Taylor Naval Ship R&D Center, Annapolis, Maryland and reported by Mr. Joseph Morris.

Additional work is required to determine the Tesla pump disk spacing and number and to define the centrifugal impeller blade angle distributions and detailed shroud shapes. The detailed diffuser flow passage geometry must be determined. The axial thrust capability as a function of balance piston travel must be determined over the operating range. In order to finalize performance, the influence of internal flow leakage and the resultant fluid heating must be evaluated. The suction performance and head rise capability of the Tesla pump must be verified by tests pumping water.

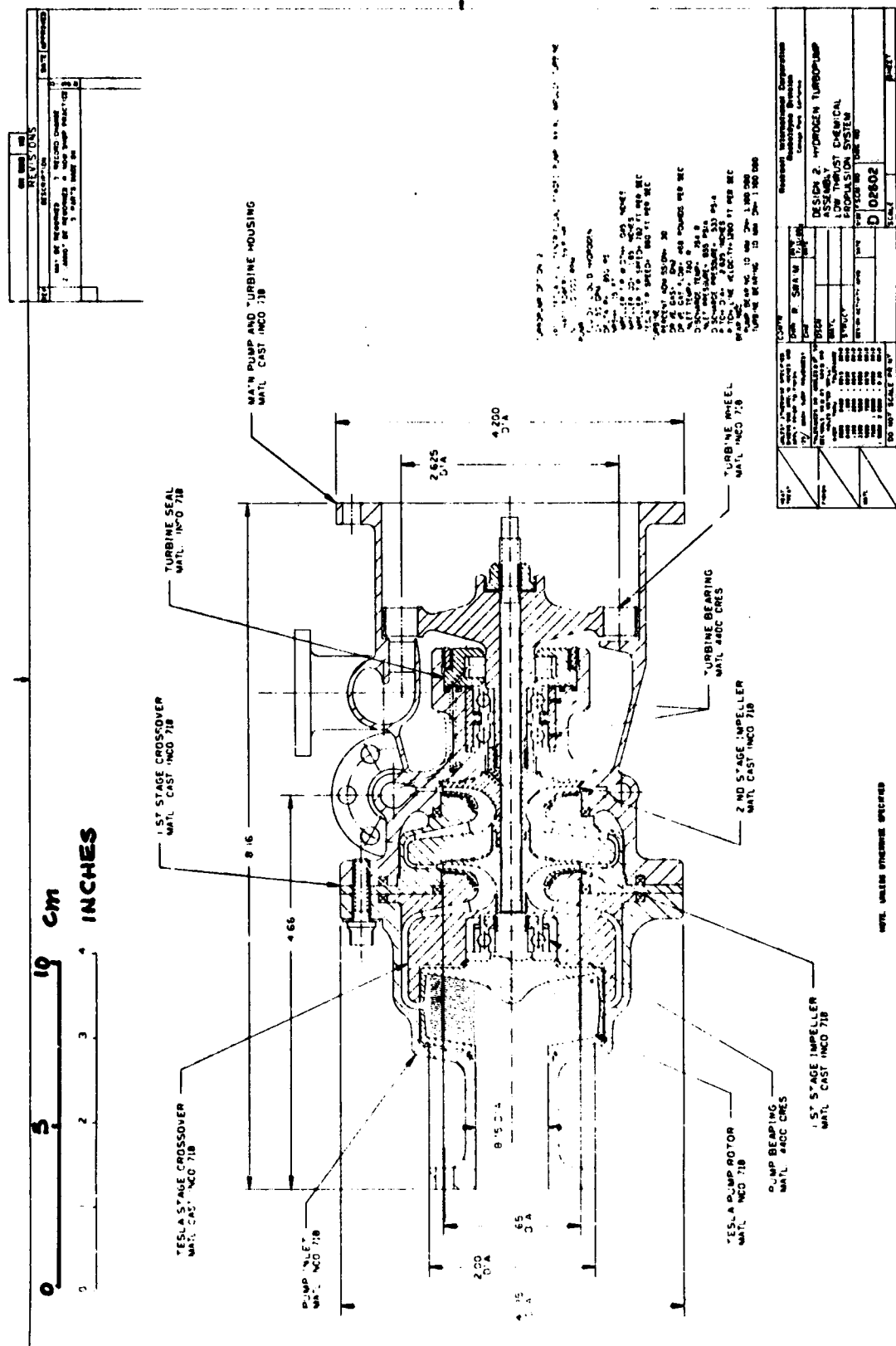


Figure 6l. Operating Point for Design 2.



Figure 62. Predicted Pumphead, Flow, Efficiency Curve.

Aerodynamic Design and Performance

The turbine for optimum performance was selected using Rocketdyne's partial admission, gaseous hydrogen turbine analysis computer program. The program considers all gas path losses due to turning, friction and secondary flows as well as partial admission losses due to blade pumping and windage, end sector losses and staging losses. The program also includes the losses due to size effects based on empirical results.

Turbine design parameters are listed in Table 7. Turbine power and speed were derived from studies of pump requirements and engine balances.

Inlet conditions were considered specified at the turbine inlet flange just upstream of the turbine inlet manifold. Turbine outlet pressure was assumed to exist in the discharge pipe just downstream of the turbine outlet collector.

The turbine geometry is based on blade heights and angles selected to achieve the higher efficiency (Fig. 63). At the highest efficiency point, the other turbine geometry parameters were also optimized. The shrouded rotor design provides higher turbine efficiency by minimizing the end and tip clearance losses.

TABLE 7. DESIGN 2, LOW-THRUST PROPULSION SYSTEM
HPFTP TURBINE PERFORMANCE PARAMETERS

WORKING FLUID	GASEOUS HYDROGEN	GASEOUS HYDROGEN
OUTPUT POWER	43.89 kW	58.63 hp
SPEED	110,000 rpm	110,000 rpm
FLOWRATE	0.212 kg/sec	0.468 lb/sec
INLET TOTAL TEMPERATURE	433.33 K	780 R
INLET TOTAL PRESSURE	45.16 BARS ABSOLUTE	655 psia
OUTLET TOTAL TEMPERATURE	418.89 K	755 R
OUTLET TOTAL PRESSURE	36.75 BAR ABSOLUTE	533 psia
TOTAL PRESSURE RATIO	1.229	1.229
AVAILABLE ENERGY	87.02 kcal/kg	156.63 Btu/lb
ISENTROPIC VELOCITY	854 m/sec	2801 ft/sec
MEAN DIAMETER	6.096 cm	2.40 inch
MEAN BLADE SPEED	351. m/sec	1152. ft/sec
VELOCITY RATIO	0.411	0.411
TOTAL PRESSURE ISENTROPIC EFFICIENCY, %	57.22	57.22
ROTOR TYPE	SHROUDED	SHROUDED

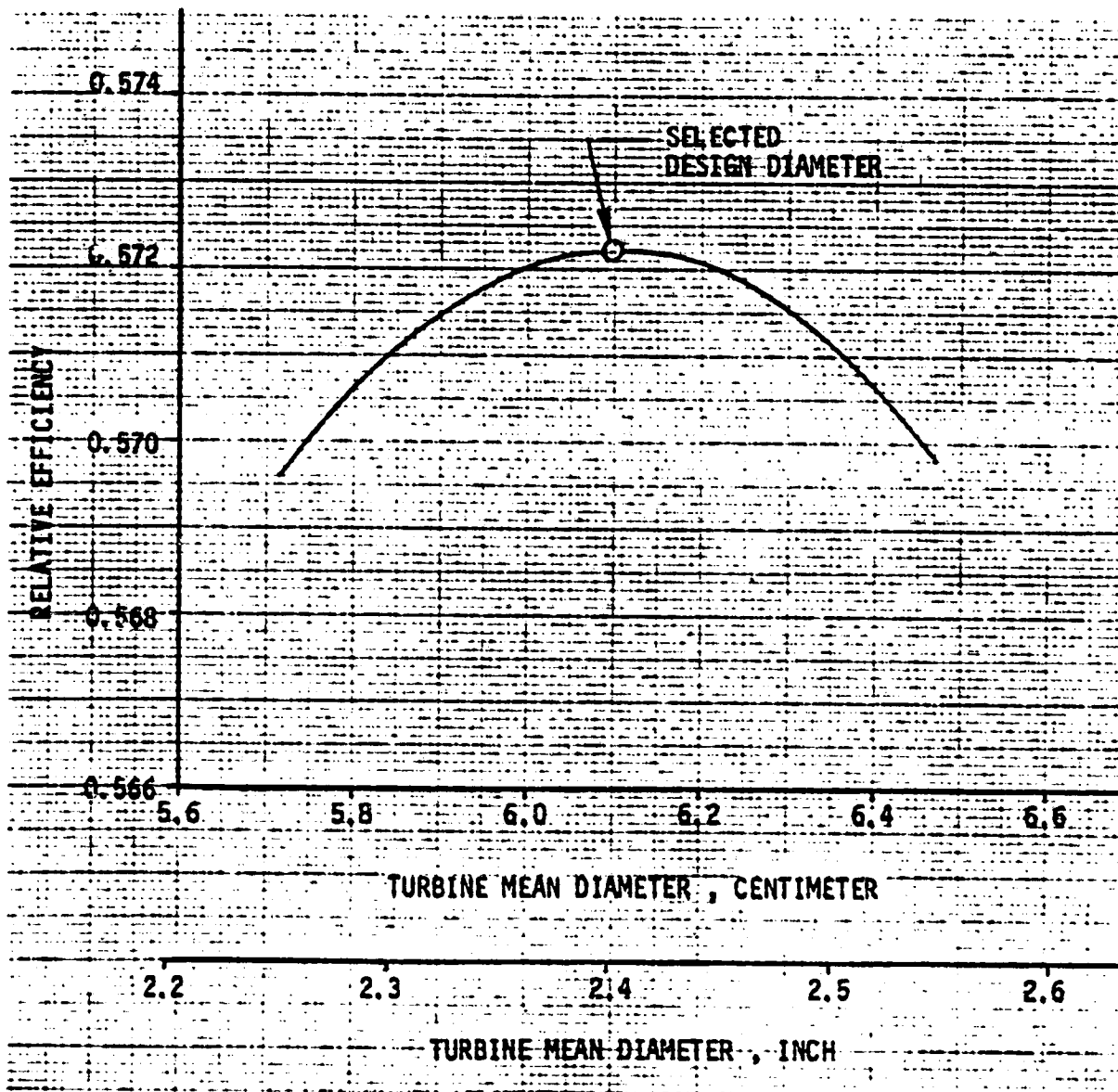


Figure 63. HPFTP Turbine Low Thrust Propulsion System, Mean Diameter Optimization, Design 2

The program predicted power losses for the turbine are tabulated to Table 8. The major losses are contributed by friction and turning in the nozzle and rotor profiles shown as the expansion and kinetic energy losses. The inlet manifold is assumed to have a radial inlet on a bifurcated torus to each sector of axial inlet nozzle. The velocity leaving the rotor was assumed to be unrecoverable, and the total pressure at the turbine outlet flange was set equal to the static pressure at the rotor discharge. Partial admission and disk friction losses are also shown.

The velocity vector diagrams are shown in Fig. 64 for the design condition. Velocities passing each element include losses due to skin friction and turning, but not losses contributed by disk friction, size effects, or partial admission. The nozzle discharge mach number is less than 0.35. The total and static pressures and temperatures in the blade path are presented in Fig. 66. Designing for 100% impulse at the design points results in constant static pressure across the rotor blades and minimizes the rotor pumping losses in the inactive part of the partial admission rotor blades. All gas expansion and flow acceleration are accomplished in the nozzles at the design condition. Because there is no static pressure gradient across the rotor in the axial direction, the axial thrust component for the rotor is eliminated.

The 6.007 cm (2.365 inch) mean turbine diameter is the basis for turbine sizing, and the results are shown in Fig. 65. The minimum spillage loss at the ends of the area of admission can be achieved by reducing the space between the nozzle and rotor. The double sector nozzle provides the structural and dynamic symmetry, but the efficiency is lower than for a single nozzle sector design by about 2 to 3%. The double sector nozzle design still delivers 2% more power than required at design, thus use of a double sector nozzle is preferable.

The rotor blades are shrouded to improve performance with a radial clearance of 0.005 cm (0.002 inch). The leakage past the rotor upstream side of the shaft seal was into the blading, but the leakage contributes no work in the turbine. The flow area sizing includes the leakage flow.

The design predicted performance is 57.2% with a delivered power of 44.28 Kw (59.35Hp), about 0.4 Kw higher than required. The flange-to-flange efficiency and performance are presented in Table 8.

Mechanical Design

Design 2 is a Tesla stage followed by two centrifugal stages pump powered by a partial admission single stage axial flow turbine. The pump has an axial inlet and a radial discharge. The turbine has a radial inlet and an axial discharge. A full-size drawing is shown in Fig. B-3 (Appendix B).

The rotating assembly consists of Tesla stage rotor with an integrally fabricated draw bar on which are mounted the two impellers, the turbine wheel plus the bearings. Tension in the draw bar is applied by the turbine wheel retaining nut. The pump end bearing is mounted on the Tesla rotor and retained by a nut and lock. The turbine end bearings are mounted on the turbine wheel and the compressure load imposed by the draw bar passes through their inner races. The torque applied

TABLE 8. DESIGN 2, LOW THRUST-PROPULSION SYSTEM
TURBINE FLANGE-TO-FLANGE EFFICIENCY AND PERFORMANCE

1. POWER LOSSES

INLET MANIFOLD
I-R U/S SHAFT SEAL
I-N INLET INCIDENCE
I-N INLET KINETIC ENERGY
I-N EXPANSION ENERGY
I-R INLET INCIDENCE
I-R INLET KINETIC ENERGY
I-R EXPANSION ENERGY
I-R WINDAGE
I-R END SECTOR MIXING
I-R RIM FRICTION
I-R DISK FRICTION
I-R END CLEARANCE
S-1 DIAGRAM FACTOR ADJUSTMENT
I-R LEAVING ENERGY
TOTAL POWER LOSSES

FLOWRATE		ENTHALPY		POWER LOSS	
Kg/sec	Lb/sec	KCAL/Kg	BTU/Lb	Kw	Hp
0.212	0.468	6.6844	12.032	5.9439	7.9678
0.0030	0.0067	60.7882	109.4188	0.7760	1.0403
0.209	0.4613	0	0	0	0
0.209	0.4613	0	0	0	0
0.209	0.4613	6.8744	12.3614	6.5763	8.8154
0.209	0.4613	0	0	0	0
0.209	0.4613	8.8353	15.9036	7.7438	10.3804
0.209	0.4613	0	0	0	0
		0		2.1003	2.8154
		0		1.1632	1.5592
		0		0.3581	0.4800
		0		0.1180	0.1582
0.209	0.4613	0.3014	0.5425	0.2641	0.3541
0.209	1.4613	5.5353	9.9636	4.8515	6.5033
0.209	0.4613	4.1964	7.5575	3.6780	4.9303
				33.1038	44.3751

2. AVAILABLE POWER

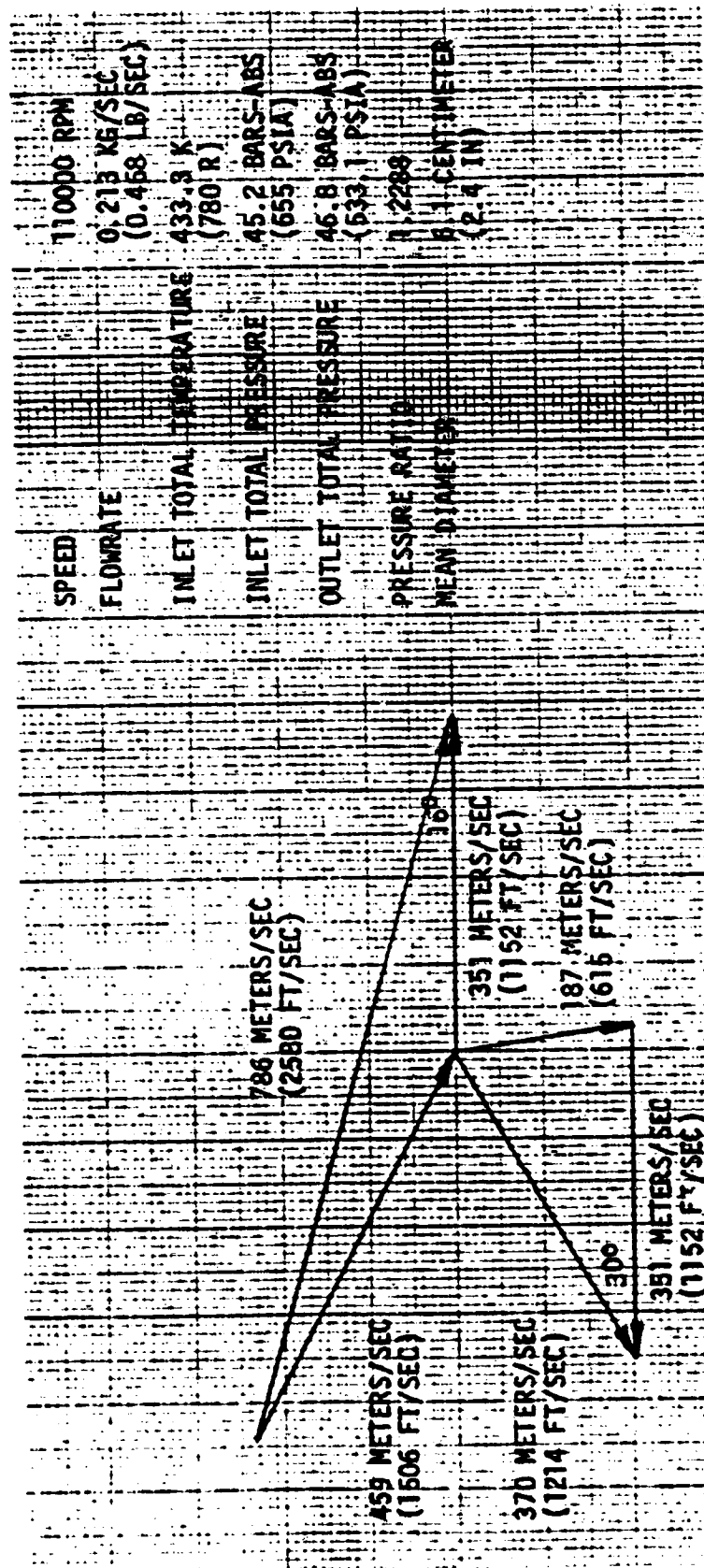
WDOT INLET FLANGE
DHA T-S F-F
POWER AVAILABLE T-S F-F
DHA T-T F-F
POWER AVAILABLE T-T F-F

0.212 Kg/sec	.468 lb/sec
87 KCAL/Kg	156.6 BTU/lb
77.38	103.73 Hp
82.82	149.08
73.65 Kw	98.72 Hp

3. SHAFT POWER ETC. OVERALL

POWER AVAILABLE T-T F-F
TOTAL POWER LOSSES
SHAFT BRAKE POWER
OVERALL EFFICIENCY T-T F-F
OVERALL U/C T-T
OVERALL U/C T-T SQRT(2)

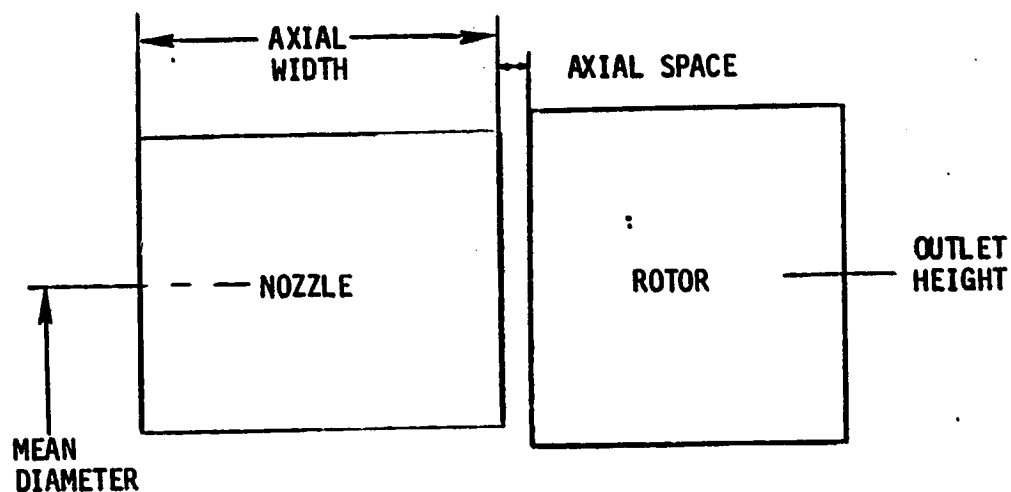
POWER	
Kw	Hp
77.38	103.73
33.10	44.375
44.28	59.35
0.572	
0.411	
0.421	



SPEED	110000 RPM
FLOWRATE	0.215 KG/SEC (0.468 LB/SEC)
INLET TOTAL TEMPERATURE	433.3 K (780 R)
INLET TOTAL PRESSURE	45.2 BARS-ABS (655 PSIA)
OUTLET TOTAL PRESSURE	46.8 BARS-ABS (683.1 PSIA)
PRESSURE RATIO	1.2289
MEAN DIAMETER	8.1 CENTIMETER (2.4 IN)

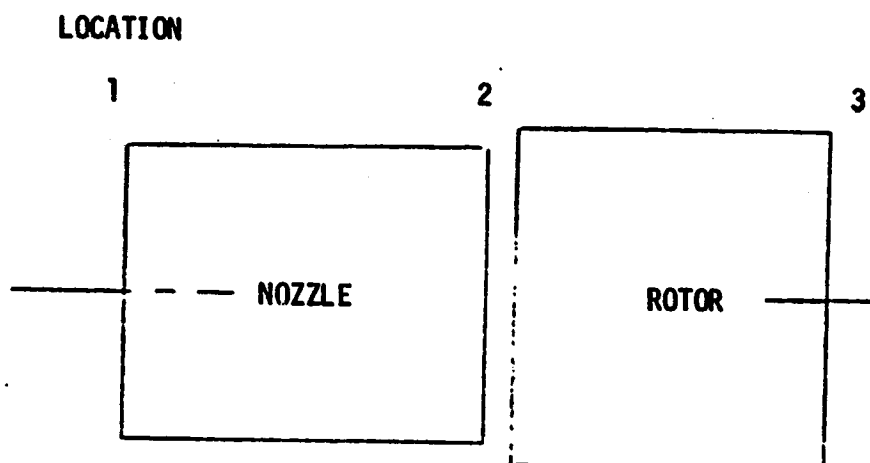
Figure 64. HPFTP Turbine -Low Thrust Propulsion System, Velocity Vector Diagram, Design 2

ORIGINAL PAGE IS
OF POOR QUALITY



ELEMENT	NOZZLE	ROTOR
MEAN DIAMETER	6.1 CENTIMETER (2.4 IN)	6.1 CENTIMETER (2.4 IN)
OUTLET HEIGHT	0.79 CENTIMETER (0.31 IN)	0.91 CENTIMETER (0.36 IN)
INLET HEIGHT	0.79 CENTIMETER (0.31 IN)	0.91 CENTIMETER (0.36 IN)
AXIAL WIDTH	0.98 CENTIMETER (0.385 IN)	0.85 CENTIMETER (0.335 IN)
AXIAL SPACE	0.076 CENTIMETER (0.03 IN)	
PERCENT ADMISSION	32 %	
ADMISSION SECTORS	2	

Figure 65. HPFTP Turbine Low Thrust Propulsion System,
Preliminary Turbine Blade Path Data, Design 2



LOCATION

PRESSURE

TOTAL

STATIC

1
45.16 BARS-ABS
(655 PSIA)

2
36.75 BARS-ABS
(533 PSIA)

3
36.75 BARS-ABS
(533 PSIA)

Figure 66. HPFTP Turbine Low Thrust Propulsion System,
Blade Path State Condition, Design 2

by the turbine wheel is transmitted to the second stage centrifugal impeller by a spline. The torque is then transferred to the first stage impeller by intergrally machined slots and tangs on the two impellers. The Tesla impeller torque is transmitted by the locked turbine wheel retaining nut.

The use of through holes through the turbine wheel and the two centrifugal impellers is possible because of the low tip speed of the impellers and turbine wheel.

Positioning of the impellers is provided by a pilot diameter and a normal bearing surface on each end. Repositioning error when the rotor is disassembled and reassembled is reduced by allowing the impellers and turbine wheel to assemble in only one angular rotation position.

The pump housing assembly consists of four major components. The pump inlet provides a tunnel for the Tesla pump inlet and a precision diameter to provide a seal between the pump inlet and the Tesla pump discharge. The pump bearing carrier contains the cast down comer which takes the Tesla pump discharge flow and brings it in to the eye of the first centrifugal stage impeller. It also provides a precision diameter for accepting the forward pump bearing mounting sleeve. The bearing sleeve is designed to be a radial spring with a low spring-rate to allow the OD of the Tesla pump to act as a squeeze film damper. The centrifugal pump crossover contain the cast diffuser and down comer passages. The main pump housing contains the cast second centrifugal stage impeller diffuser, the volute collector and discharge diffuser plus the turbine inlet, manifold and nozzle blades.

The arc of admission for the turbine is split into two equal arcs 180 degrees apart to eliminate an imposed moment that would result from a single admission arc. This reduces the radial load that the pump and turbine end-bearings are subjected to.

The turbine end bearings are preloaded against each other by selectively machining the preload spacer to the proper spacer to the proper thickness. The pump end bearing is preloaded to a lower preload than the turbine end bearings.

Static seals are provided for all external flanges. Static seals are also placed at the impeller discharge diameters so that the area between the inner and outer row of seals can be vented to the Tesla stage discharge pressure to keep the delta pressure on the external seals to a minimum.

The bearings are of the angular contact type designed to run in LH₂. The turbine/pump seal is of the controlled gap type and is internally pressurized. The pressurizing flow comes from the pump discharge and the leakage flow towards the pump provides the coolant flow for the turbine end bearings. The pump end bearing coolant flow is provided by the pressure difference across the Tesla stage down comer.

The rotor thrust loads are balanced out by a balance piston that is an intergal part of the second stage impeller. The high pressure orifice is provided by a lip on the pump housing and a lip on the impeller out side diameter. The low pressure orifice is provided by matching surfaces on the impeller and housing.

Balance piston leakage flow is ducted to the ID of the second stage impeller and delivered to the inlet of the same impeller. The flow from the balance piston is mixed with the bearing coolant flow in the balance piston sump prior to returning to the second stage impeller inlet.

The impeller eyes are sealed by stepped labyrinth wear rings. The rear shroud leakage from the Tesla pump are controlled by close fitting diameters between the housings and rotor parts. These close fitting diameters also form a series of squeeze film dampers for controlling the shaft excursions experienced during times that the pump rpm passes through a critical speed range.

The materials chosen for use in the pump and turbine are those that have been proven in previous turbopump designs. The impellers and crossover will be fabricated from cast Inconel 718. The pump inlet and main pump housing will be fabricated from cast and wrought Inconel 718. The turbine wheel will have intergally machined blades and be made from Inconel 718. The bearings are 440C corrosion resistant steel.

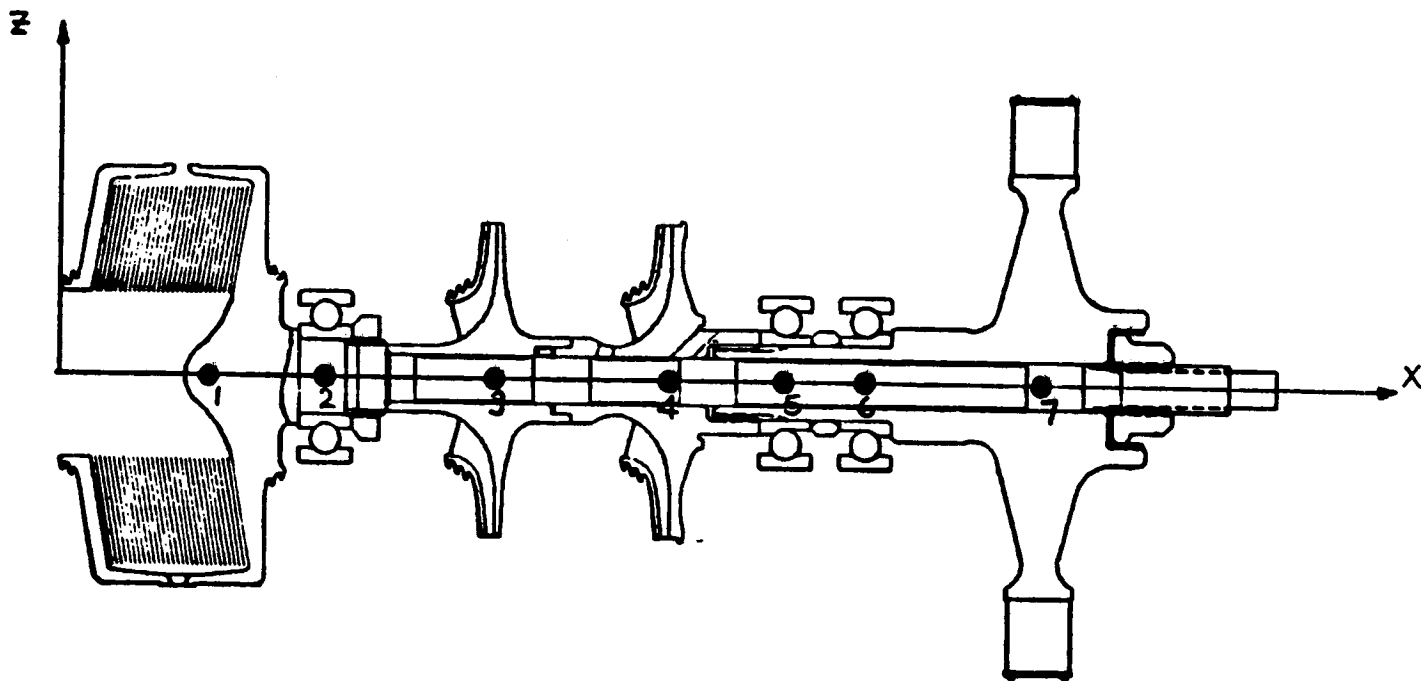
Protection of the structural parts from hydrogen environment embrittlement is provided by plating the exposed surfaces with a suitable material that stops the embrittlement process.

As part of the mechanical design, a preliminary stress survey was performed. The impeller tip speed is 792 ft/sec (241 M/S). This is less than half the impeller tip speed of the SSME fuel pump at 1800 ft/sec (549 M/S). The turbine tip speed is 1260 ft/sec (384 M/S) also below comparable SSME turbine tip speed at 1800 ft/sec (549 M/S). The P/A blade stress is 61600 psi (42486 N/Cm²) which is slightly higher than the stress in the SSME fuel turbine but still well below the strength of Inco 718. Pressure, torque and thermal stresses are all well below the strength of Inco 718. No problems of a significant nature are anticipated during detail stress analysis.

Rotordynamic analysis was performed to assure a 20% margin (from resonant speeds) above and below the operating speed. The rotating assembly was modeled as shown in Fig. 67. With a springrate of 100,000 lb/in. the first critical speed was less than one-half the operating speed (110,000 rpm). The solution was to modify the bearing springrate by preloading the bearings. With this modification all three critical speeds were increased so that the first was slightly higher than one-half the operating speed. Figure 68 shows the final mode shapes with a 150,000 lb/in. springrate. Figure 69 shows the critical speeds as a function of bearing springrate.

Weight Analysis

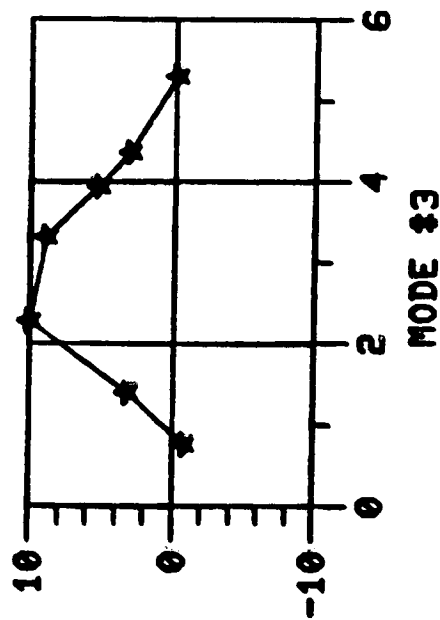
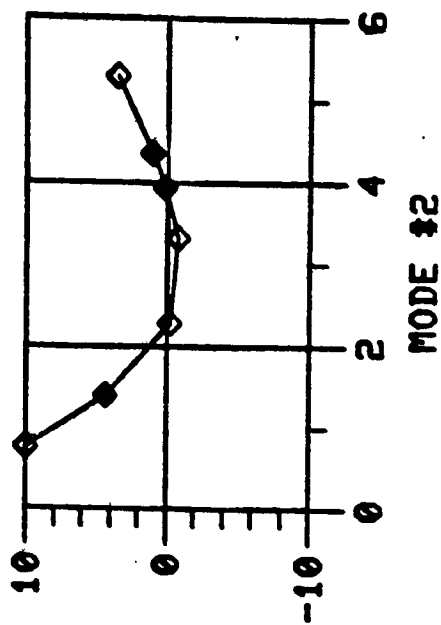
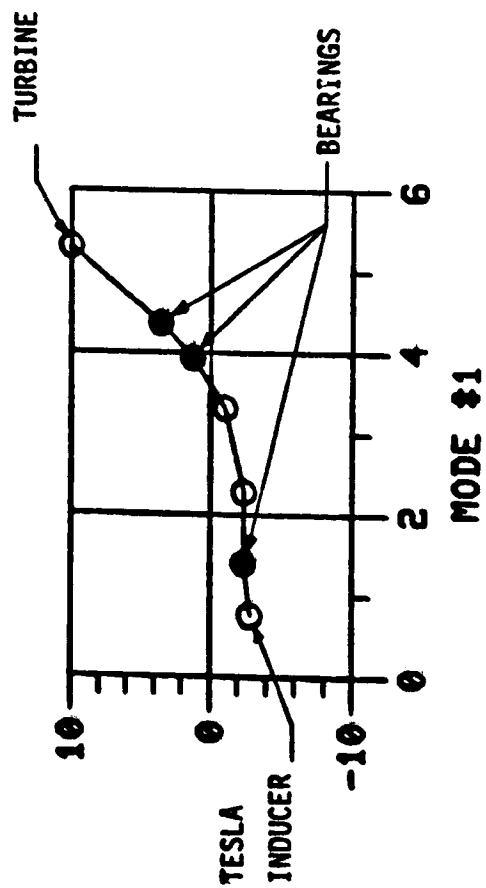
The weight of turbopump 2 (dry) is 10.0 lb (4.54 kg). The rotating assembly weighs 1.70 lb (0.77 kg) and the housing weighs 8.30 lb (3.76 kg). Figure 70 is a part by part breakdown of weights.



MATERIAL INCO 718
FULL SCALE

● JOINT LOCATION

Figure 67. Design 2, Fuel Turbopump Tesla Inducer ($N = 110,000$ RPM)



MODE	HZ	RPM
1	921.690	55301.
2	967.730	58064.
3	3051.700	183100.

K1	-	150000.	LB/IN
K2	-	150000.	LB/IN
K3	-	150000.	LB/IN

MODE SHAPES

Figure 68. Low Thrust Engine Design No. 2 Critical Speed

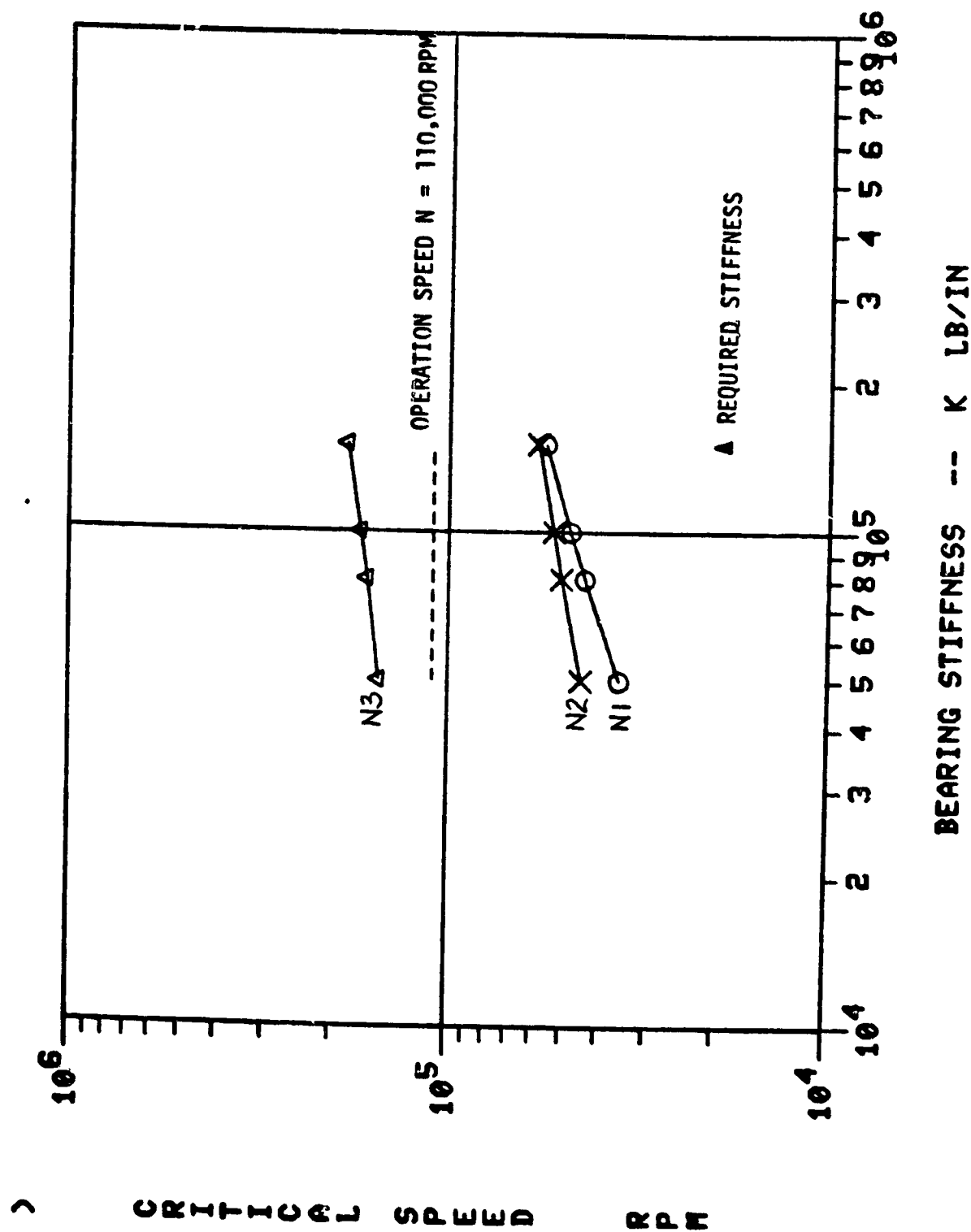


Figure 69. Low Thrust Engine Design No. 2 Critical Speed
Critical Speed vs Bearing Stiffness

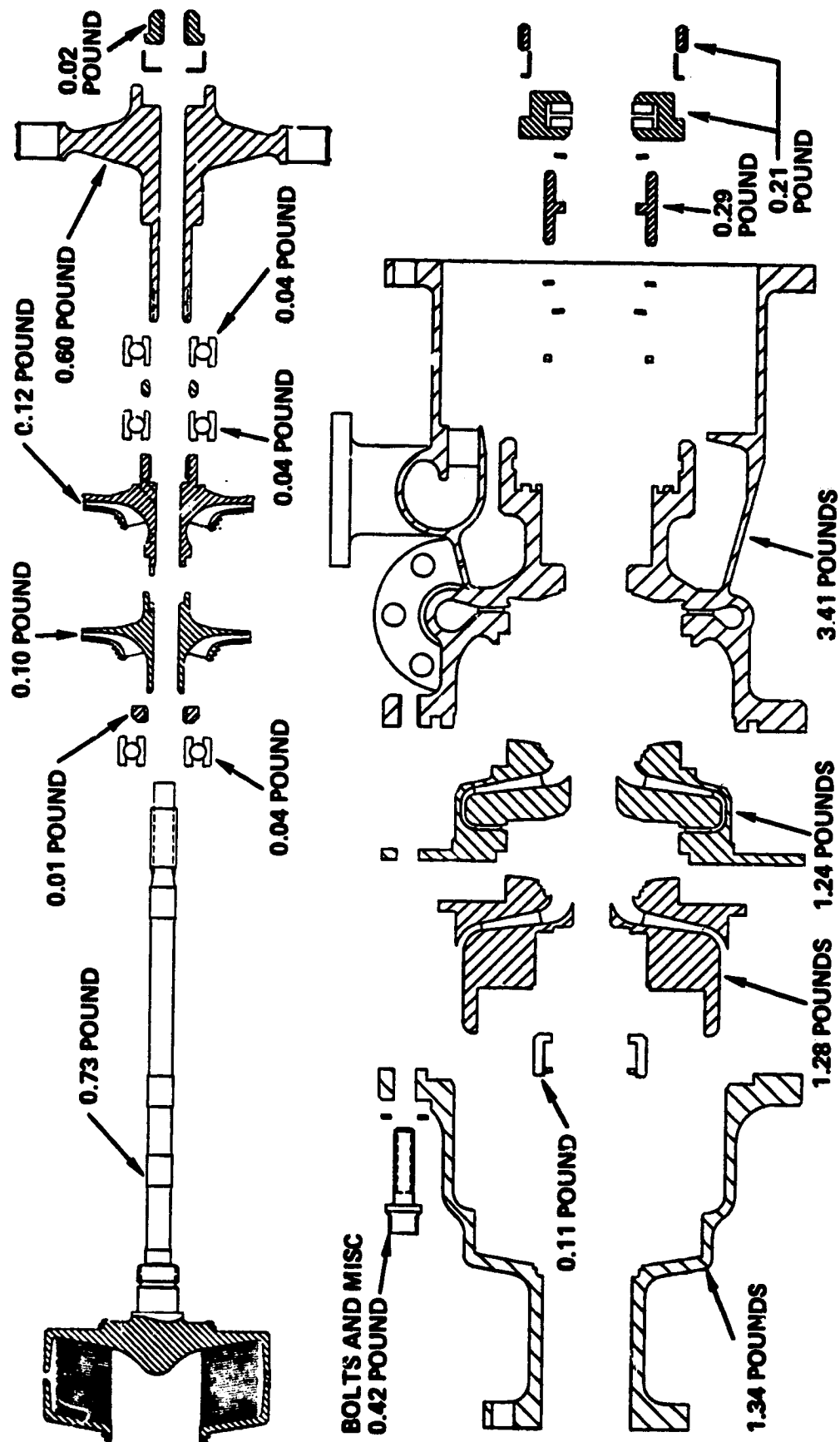


Figure 70. Design 2 Weighs 44.5 N (10.0 pounds)

Life Assessment

The tip speeds are well within Rocketdyne experience for both small and large size hydrogen pumps. Therefore long life is anticipated for the hydrodynamic components with respect to cavitation damage, fluid erosion and fluid force induced fatigue. Bearing DN is 1,100,000 and bearings are predicted to provide the required life. Seals are also predicted to perform satisfactorily.

Performance and Manufacturing Risk

The impeller tip diameter 0.042m (1.65 inch) and tip width 1.143mm (0.045 inch) are within industry experience for small pumps. The Mark 36 oxidizer pump which was successfully operated had an impeller tip diameter of 0.0330m (1.3 inch) with a tip width of 1.12mm (0.044 inch). The Mark 48-F liquid hydrogen pump which demonstrated meeting performance goals had an impeller tip diameter of 0.1031m (4.06 inch) and a tip width of 3.81mm (0.15 inch). The Mark 36 impeller was cast of Inconel 718 and operated at 75,000 rpm pumping liquid fluorine. The Mark 48-F impeller was machined from a titanium forging with integral shrouds. Rocketdyne specific speed experience with liquid hydrogen pumps at design point is below 700 ($N = \text{rpm}$, Q_{gpm} , $H \text{ ft}$).

Industry experience, therefore, from both the standpoint of small pump manufacture and performance leads to the conclusion that the risk of meeting both goals is small. Test programs for the 50 gpm pump should therefore be directed to verify the test pump performance and optimize and verify the centrifugal pump performance as well as to investigate design concepts which simplify small pump manufacture as well as insure part-to-part repeatability.

Cost Analysis

The ROM cost of fabricating design 2 estimated \$135,700 for tooling, \$81,000 of which is for casting tooling, \$29,100 for raw material and purchased parts, and \$25,600 for machining. Recurring cost is estimated to be \$52,500; \$2,600 for cast parts, \$700 for raw material, and \$49,200 for machining. The first unit cost is the sum of tooling and recurring costs or \$188,200.

DESIGN 3, OXYGEN TURBOPUMP

The operating requirements for Design 3 are shown in Fig. 45. The pump requirements are 625 psi (431 n/cm²), 3.6 gpm (0.23 L/S), with 2 FT (0.61m) NPSH. The LOX turbine follows the fuel turbine. The inlet pressure is relatively low (compared to fuel pump discharge pressure) at 469 psi (323 n/cm²). This creates a pressure ratio of 1.4 from fuel turbine inlet to LOX turbine inlet. The temperature at the turbine inlet is 650R.

Hydrodynamic Design and Performance

A layout of Design 3 is shown on Fig. 71. It consists of an inducer and a two-stage centrifugal pump powered by a 5.6% partial admission turbine. The design flow rate of the pump is 3.6 gpm (22.7×10^{-5} m³/sec) of liquid oxygen at a speed of 26,500 rpm (2775 rad/sec). The pressure rise at this point is 625 psi (431 n/cm²).

The layout shows that the inducer and first stage of the pump are overhung beyond the 0.375 inch (approximately 9.5mm) pump end bearing. The second stage and a positive separation seal package are supported between the bearings; the turbine and a single seal are overhung beyond the 15mm turbine end bearing. The seal package has the same concept as that used on the Space Shuttle Main Engine High Pressure LOX Turbopump.

The inducer has four blades with the capability of operating at an NPSH of 2 feet (0.61m). The two fully-shrouded centrifugal impellers have similar passages with backward curved blades and a head coefficient of 0.495 per stage. The impeller tip speed at 26,500 rpm will be 206 ft/sec (62.8 m/sec). The radially outward diffusers will also have similar passages with the absolute velocity leaving each impeller being reduced by approximately one half. The crossover passage will remove rotation and prepare the fluid for entry into the second impeller while the flow leaving the second impeller will be collected in a volute.

Figure 72 shows the calculated design and off-design performance of the two-stage pump. The figure shows that at the design speed of 26,500 rpm, the design flow of 3.6 gpm and the design pressure rise of 625 psi the efficiency was calculated to be 23%.

The over-all layout of the turbopump has been completed but the pump details remain to be done. These include the inducer blades, the centrifugal impeller blades and shrouds, the blading in the crossover network, the pump discharge volute and the end thrust and balance piston calculations.

Aerodynamic Design and Performance

The turbine performance optimization was performed using Rocketdyne's partial admission gaseous Hydrogen turbine analysis computer program. The program includes all gas path losses contributed by turning, friction, and secondary flows, as well as partial admission losses due to blade pumping and windage, end sector losses and staging losses. Empirical data accounting for the size effect is also included in the program.

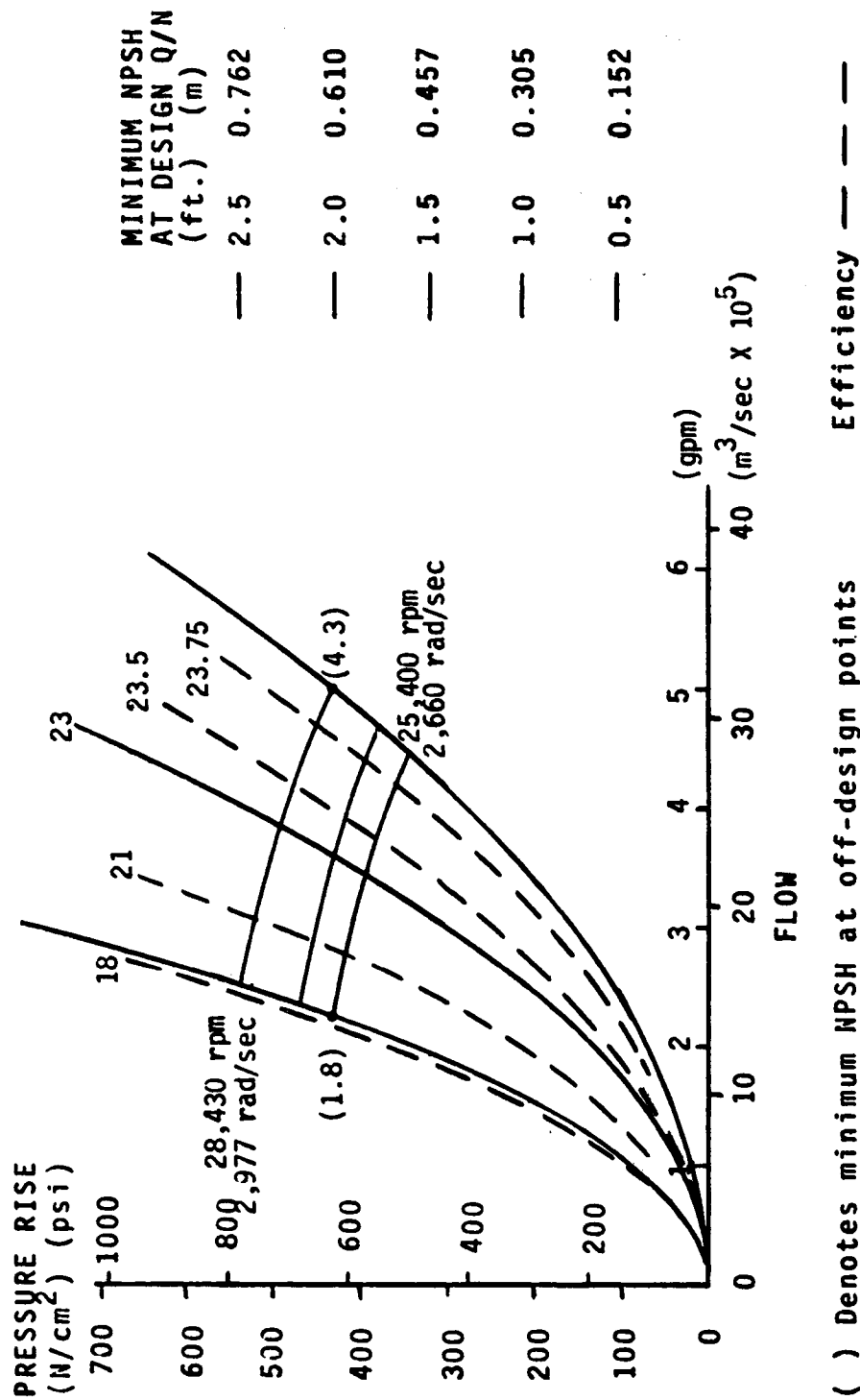


Figure 72. Calculated Design and Off-Design Performance of the Two-Stage Pump

Turbine design parameters are listed in Table 9. Inlet conditions were considered specified at the turbine inlet flange which is just upstream of the turbine inlet manifold. Turbine discharge conditions are specified at the inlet to the pipe just downstream of the turbine outlet collector.

The selected turbine mean diameter is based on Fig. 73. Turbine geometry parameters were optimized for high performance and minimum weight. The selected turbine mean diameter is for optimized blade heights and angles. On the expanded relative efficiency scale, the selected diameter of 12.7 centimeters (5 inches) is shown to be within 0.02 points of the peak efficiency, but is 2.3% smaller than the diameter at peak efficiency. The smaller size was selected resulting in a lower weight of the turbine. At this selected 12.7 cm mean diameter, the delivered power is almost equal to the rated power requirement (4.30 kw), thus a smaller size cannot be used.

The turbine predicted power losses are tabulated in Table 10. Primary losses are due to skin friction and turning in the nozzle and rotor profiles as shown by the expansion and Kinetic energy losses. The inlet manifold loss was for a manifold with a radial inlet on a torus to the axial inlet nozzle. The velocity out of the stage was assumed lost in the exhaust manifold, and the total pressure at the turbine outlet flange was assumed to be equal to the static pressure at the rotor discharge. Partial admission losses and disk friction are also shown.

The velocity vector diagrams are shown in Fig. 74 for the design condition. Velocities out of the element include losses contributed by friction and turning but not losses due to the disk friction, size affect, or partial admission. Nozzle discharge Mach numbers are as low as 0.35. It was conservatively assumed that all the absolute leaving kinetic energy of the rotor discharge was not recoverable.

The total and static pressures, as well as temperature in the blade path, are shown in Fig. 76. The constant pressure across the rotor for the impulse design minimizes pumping losses in the inactive rotor blade with partial admission. All expansion and acceleration of the flow is accomplished across the nozzles at the design condition. Because there is static pressure gradient across the rotor blade in the axial direction, there will be no rotor axial thrust at the design operating condition.

The turbine sizing is summarized in Fig. 75. The rotor mean diameter is 12.7 cm (5 inches) with shrouded blade design. The shrouded rotor minimizes the end wall losses and tip clearance losses resulting in a higher performance efficiency. The axial space between the nozzle and rotor should be minimized to reduce the spillage loss at the ends of the arcs of admission. The use of double sector nozzles for providing structural and dynamic symmetry is normally recommended, but a single sector nozzle gives higher turbine efficiency by 2 to 3%. The maximum efficiency of the double sector nozzle design is 31.48% with power 4.17 kw. This is not enough power for design operating conditions. Thus, a single sector nozzle design is required. With only 5.6% admission, a single sector nozzle design is more practical.

TABLE 9. DESIGN 3, LOW THRUST PROPULSION SYSTEM
HPOTP TURBINE PERFORMANCE PARAMETERS

WORKING FLUID	GASEOUS HYDROGEN	GASEOUS HYDROGEN
OUTPUT POWER	4.24 kW	5.68 hp
SPEED	26,500 rpm	26,500 rpm
FLOWRATE	0.042 kg/sec	0.0926 lb/sec
INLET TOTAL TEMPERATURE	408.336 K	735 R
INLET TOTAL PRESSURE	33.03 BARS ABSOLUTE	479 psia
OUTLET TOTAL PRESSURE	27.65 BARS ABSOLUTE	401 psia
TOTAL PRESSURE RATIO	1.1945	1.1945
AVAILABLE ENERGY	70.9 kcal/kg	127.6 Btu/lb
ISENTROPIC VELOCITY	771 m/sec	2528 ft/sec
MEAN DIAMETER	12.7 cm	5.0 inches
MEAN BLADE SPEED	176 m/sec	578 ft/sec
VELOCITY RATIO	0.229	0.229
TOTAL PRESSURE ISENTROPIC EFFICIENCY, %	34.46	34.46
ROTOR TYPE	SHROUD	SHROUD

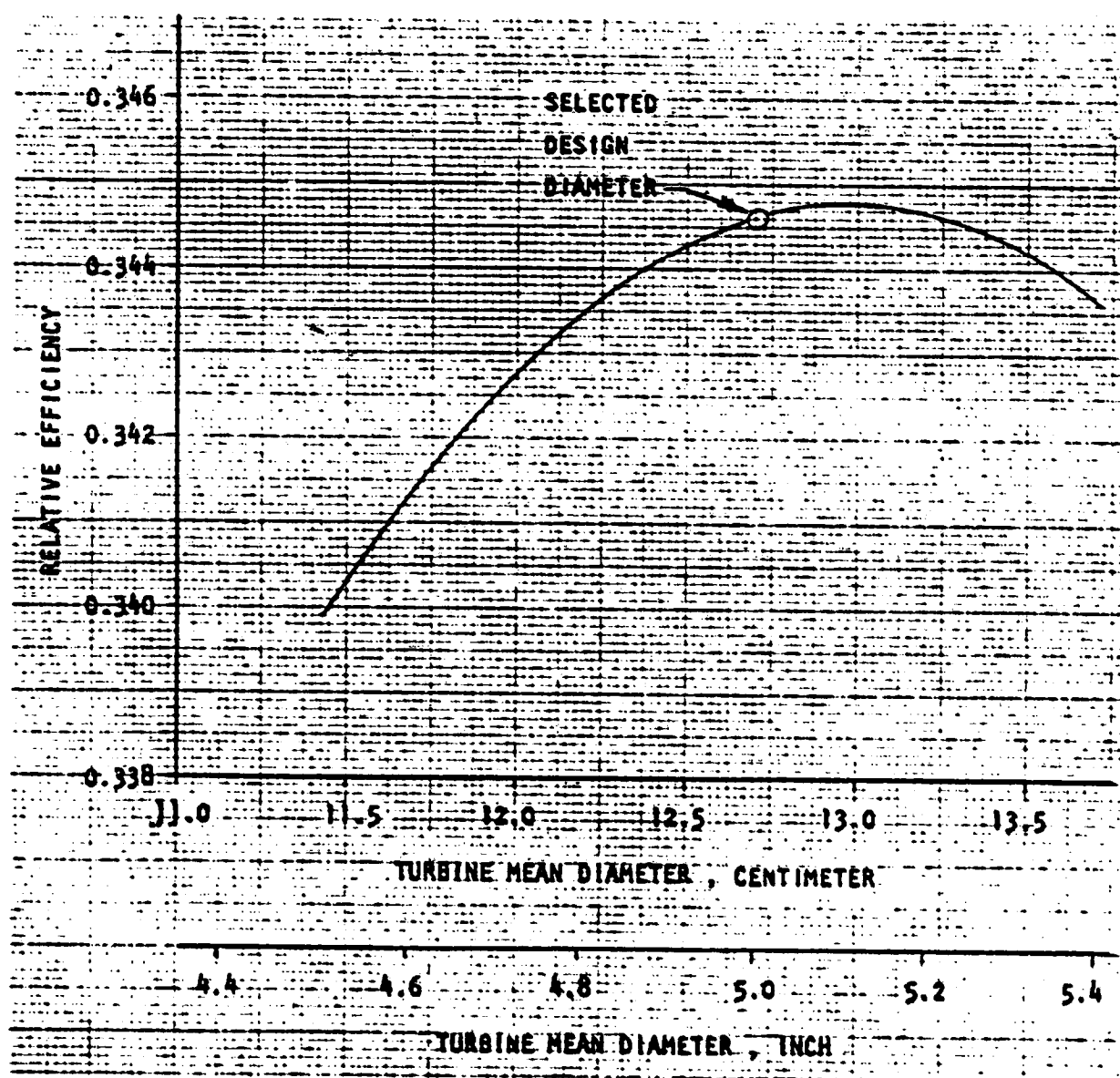


Figure 73. HPOTP Turbine Low Thrust Propulsion System, Mean Diameter Optimization, Design 3

TABLE 10. DESIGN 3, LOW THRUST-PROPULSION SYSTEM HPOTP
TURBINE FLANGE-TO-FLANGE EFFICIENCY AND PERFORMANCE

1. POWER LOSSES

INLET MANIFOLD
I-R U/S SHAFT SEAL
I-N INLET INCIDENCE
I-N INLET KINETIC ENERGY
I-N EXPANSION ENERGY
I-R INLET INCIDENCE
I-R INLET KINETIC ENERGY
I-R EXPANSION ENERGY
I-R WINDAGE
I-R END SECTOR MIXING
I-R RIM FRICTION
I-R DISK FRICTION
I-R END CLEARANCE
S-1 DIAGRAM FACTOR ADJUSTMENT
I-R LEAVING ENERGY
TOTAL POWER LOSSES

FLOWRATE		ENTHALPY		POWER LOSS	
Kg/sec	Lb/sec	KCAL/Kg	BTU/Lb	Kw	Hp
0.0420	0.0926	8.5941	15.4694	1.5121	2.0269
0.0049	0.0108	36.3458	65.4224	0.7455	0.9493
0.0371	0.0818				
0.0371	0.0818	5.4672	9.8410	0.6920	1.2895
0.0371	0.0818				
0.0371	0.0818				
0.0371	0.0818	13.2212	23.7982	2.0550	2.7547
0.0371	0.0818				
				0.2992	0.4011
				0.5005	0.6709
				0.05916	0.0793
				0.09049	0.1213
0.0371	0.0818	0.2694	0.4849	0.04185	0.0561
0.0371	0.0818	4.6396	8.3513	0.7216	0.9667
0.0371	0.0818	7.6456	13.7620	1.1884	1.5930
					10.9589
0.0420 Kg/sec			0.0926 lb/sec		
70.897 KCAL/Kg			127.62 BTU/lb		
12.474 Kw			16.7213 Hp		
63.251 KCAL/Kg			113.85 BTU/lb		
11.129 Kw			14.918 Hp		

2. AVAILABLE POWER

WDOT INLET FLANGE
DHA T-S F-F
POWER AVAILABLE T-S F-F
DHA T-T F-F
POWER AVAILABLE T-T F-F

3. SHAFT POWER ETC. OVERALL

POWER AVAILABLE T-T F-F
TOTAL POWER LOSSES
SHAFT BRAKE POWER
OVERALL EFFICIENCY T-T F-F
OVERALL U/C T-T
OVERALL U/C T-T SQRT(2)

POWER	
Kw	Hp
12.409	16.7213
8.175	10.9589
4.298	5.7624
0.3446	
0.2287	
0.2419	

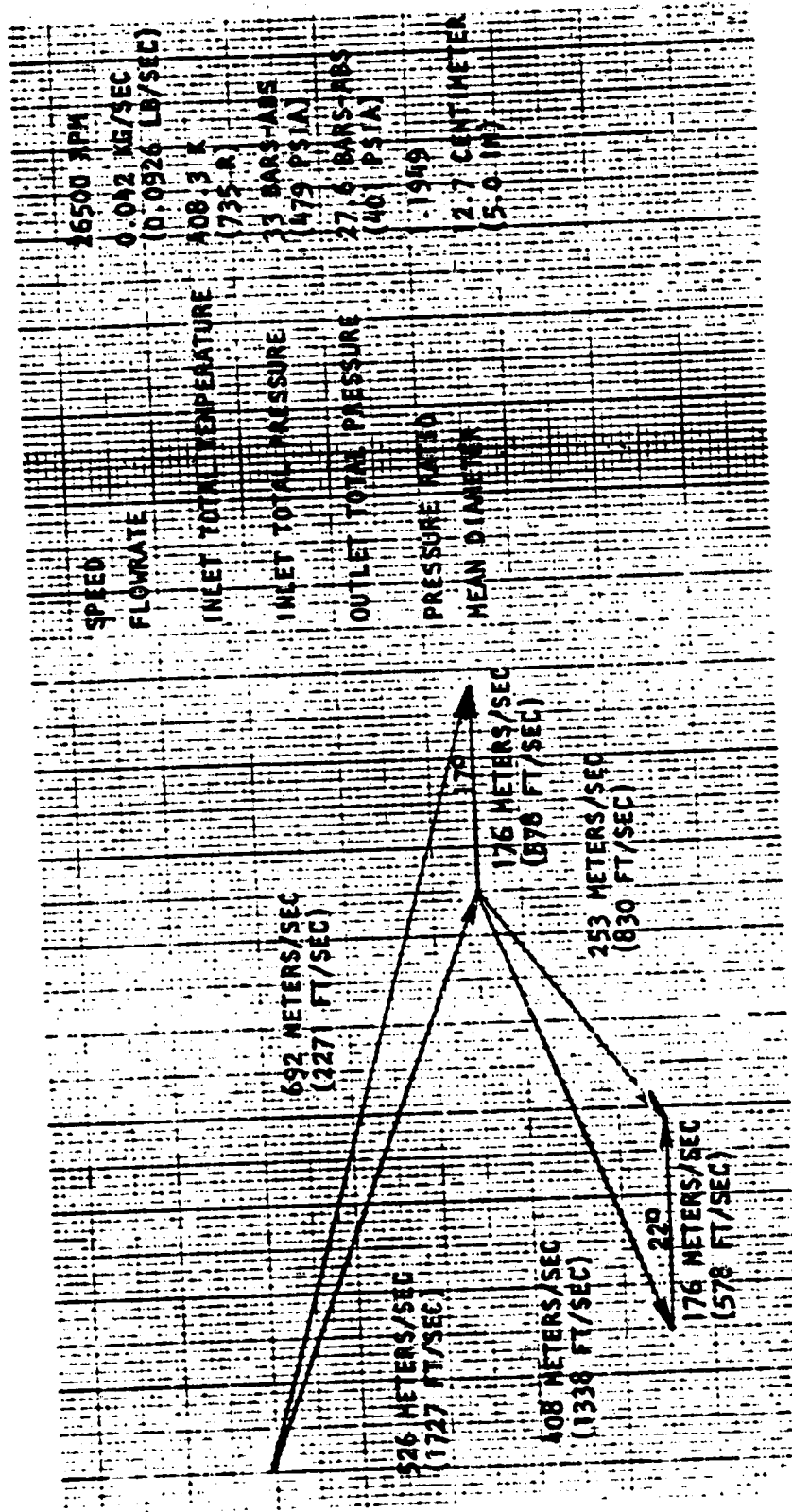
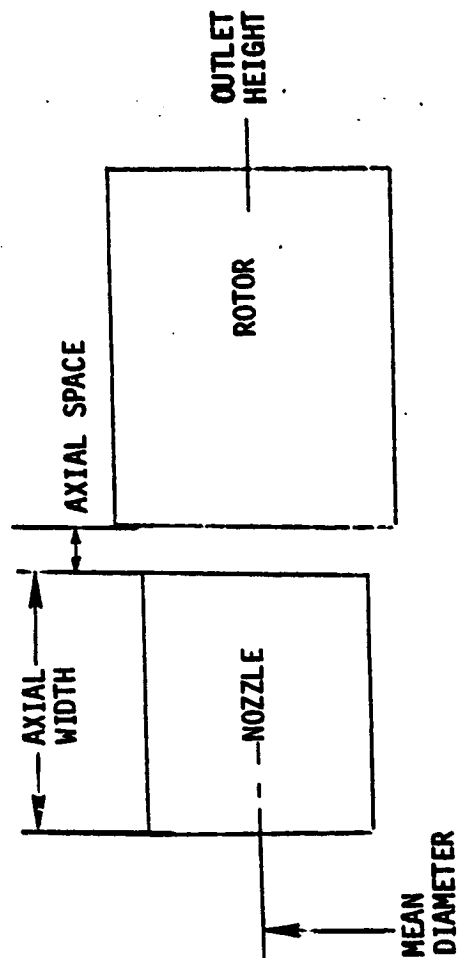
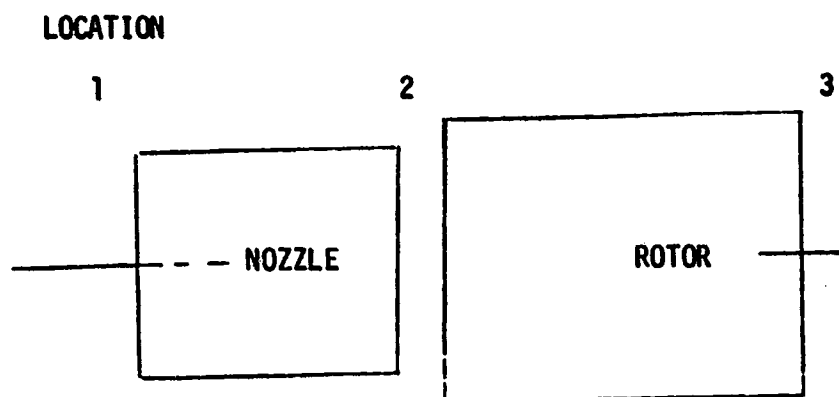


Figure 74. HPOTP Turbine Low Thrust Propulsion System, Velocity Vector Diagram, Design 3



ELEMENT	NOZZLE	ROTOR
MEAN DIAMETER	12.7 CENTIMETER (5.0 IN)	12.7 CENTIMETER (5.0 IN)
OUTLET HEIGHT	0.61 CENTIMETER (0.24 IN)	0.76 CENTIMETER (0.30 IN)
INLET HEIGHT	0.61 CENTIMETER (0.24 IN)	0.76 CENTIMETER (0.30 IN)
AXIAL WIDTH	0.70 CENTIMETER (0.275 IN)	0.97 CENTIMETER (0.38 IN)
AXIAL SPACE	0.127 CENTIMETER (0.05 IN)	
PERCENT ADMISSION	5.6 %	
ADMISSION SECTORS	1	

Figure 75. HPOTP Turbine Low Thrust Propulsion System, Preliminary Turbine Blade Path Data, Design 3



LOCATION	1	2	3
PRESSURE			
TOTAL	33.0 BARS-ABS (479 PSIA)		
STATIC		27.6 BARS-ABS (401 PSIA)	27.6 BARS-ABS (401 PSIA)

Figure 76. HPOTP Turbine Low Thrust Propulsion System,
Blade Path State Condition, Design 3

The rotor blades were shrouded to improve performance with a tip clearance of 0.005 cm (0.002 inch). The leakage past the rotor upstream side of the shaft seal was dumped into the blading, but the leakage was assumed to be not recoverable work for the turbine. The flow area sizing includes the leadage.

The design predicted performance is 34.46% isentropic efficiency based on total-to-total pressure and delivers 4.24 Kw at 26,500 rpm. The flange-to-flange efficiency and performance are presented in Table 10.

Mechanical Design

Design 3 is a 2 stage centrifugal pump plus an inducer in front of the first stage impeller powered by a partial admission single stage axial flow turbine. The pump has an axial inlet and a radial discharge. The turbine has a radial inlet and an axial discharge.

The rotating assembly consist of the turbine wheel, pump shaft, two centrifugal impellers and an inducer plus the pump and turbine bearings. The pump end of the shaft is functionally a draw bar upon which the two impellers and the inducer are mounted. Tension in the draw bar is applied by a nut in front of the first stage impeller. The pump bearing is mounted on the first stage impeller and the compressive load from the draw bar passes thru the bearing inner rack. The turbine end bearing is mounted on the pump shaft and is retained along with the turbine wheel by the turbine wheel retaining nut. The torque applied by the turbine is transmitted to the pump shaft by keys which is in turn transmitted to the second stage impeller by a spline. The torque transfer between the second and first stage impellers is accomplished by slots and tangs machined integrally in each impeller. The use of a thru hole in the impellers and the turbine wheel is possible because of the low tip speeds. The inducer is threaded on to the draw bar. The tab lock between the inducer and the impeller retaining nut allows the nut to be locked in an infinite number of positions when tensioning the draw bar. The torque required to drive the inducer will be transmitted by the lock tab washer.

Positioning of the impellers is provided by a pilot diameter and a normal bearing surface on each end. Repositioning error when the rotor is disassembled and reassembled is reduced by allowing that the rotating elements can be assembled in only one angular rotation position.

The pump housing assembly consists of three major components. The pump inlet forms the inducer tunnel and provides the wear ring seal for the first stage impeller.

The crossover and pump bearing carrier provides a cast diffuser for the first stage impeller and the down comer for the second stage impeller. The main pump housing contains the cast diffuser for the second stage impeller, the volute collector and discharge diffuser. The turbine housing contains the turbine inlet, manifold and nozzle blades.

The bearings are preloaded against each other at assembly. The turbine seal is mounted to the turbine housing by bolts.

Static seals are provided for all external flanges. An inner static seal seals the second stage impeller discharge pressure and leakage past it is vented to inlet pressure thereby reducing the pressure seen by the external seal.

The seals that separate the pumped fluid from the turbine bearing coolant fluid are all of the controlled gap type. The pump seal has two sealing elements and leakage past this seal flows into the area between the pump seal and the intermediate seal. The intermediate seal is internally pressurized by an inert gas that forms the high pressure barrier between the two working fluids. Inert gas that leaks toward the pump is mixed with the pump fluid that leaked past the pump seal and is vented over board. The bearing coolant seal has two bearing elements and leakage past them mixes the the leakage flow of the inert gas past the intermediate seal that leaked towards the turbines. This mixed gas is then vented over board. The turbine gas seal is of the controlled gap type and the chamber that contains the turbine end bearing is pressurized to a higher pressure than the turbine nozzle exit pressure so that the bearing coolant leakage flow goes into the turbine.

The rotor thrust loads are balanced out by a balance piston that is an integral part of the second stage impeller. The high pressure orifice is provided by a lip on the pump housing and a lip on the impeller outside diameter. The low pressure orifice is provided by matching surfaces on the impeller and housing. Balance piston leakage flow is ducted to the ID of the second stage impeller and delivered to the inlet of the same impeller.

The impeller eyes are sealed by stepped labyrinth wear rings. The rear shroud leakage is controlled by a close fitting diameter between the cross overs and the impeller hubs. This close fitting diameter also forms a squeeze film damper for controlling the shaft excursions experienced during times that the pump rpm passes thru a critical speed range.

The materials chosen for use in the pump and turbine are those that have been proven in previous turbopump designs. The impellers and cross overs will be fabricated from cast Inconel 718. The pump inlet and main pump housing will be fabricated from cast and wrought Inconel 718. The turbine wheel will have integrally machined blades and be made from Inconel 718. The bearings are 440C corrosion resistant steel.

Protection of the structural parts from hydrogen embrittlement environment is provided by plating the exposed surfaces with a suitable material that stops the embrittlement process.

As part of the Mechanical Design, a preliminary stress survey was performed. The impeller tip speed is 206 ft/sec (62.8 M/S) which is much less than the 1000 ft/sec (304.8 M/S) seen at the tip of the SSME LOX pump impeller. The turbine tip speed is 624 ft/sec (190.2 M/S) which is also much less than the corresponding SSME turbine tip speed of 1500 ft/sec (457 M/S). The P/A blade stress is an

order of magnitude less than that in the comparable SSME turbine. Pressure vessel, torque, and thermal stresses are low compared to the strength of Inco 718. A detailed stress analysis is not expected to uncover any significant stress problems.

Rotordynamic analysis was performed on Design 3. Figure 77 shows the rotor as modeled. The analysis showed that the first resonant speed was above the operating speed of 26,500 rpm, Fig. 78. A minimum bearing springrate of 150,000 lb/in. (263,000 N/cm) was established to maintain the required 20% margin on speed, Fig. 79. The increase in spring rate from 100,000 to 150,000 lb/in. was accomplished by increasing the preload.

Weight Analysis

The weight of turbopump 3 is 12.0 lb (5.44 kg) dry. The rotating assembly weighs 2.13 lb (0.97 kg) and the housing weighs 9.87 (4.48 kg). A part by part weight break down is shown in Fig. 80.

Life Assessment

The stresses in all parts of the turbopump are moderate to low because the rotating speed is low. Blading resonant frequencies will be avoided to provide long life capability. Bearing DN's are 255,000 and 397,000 for pump and turbine bearings respectively. No problem with bearings or seals is anticipated.

Rocketdyne inducers for waterjets and centrifugal pumps have been run for thousands of hours in sea water and potentially more damaging liquid sodium without showing any cavitation damage at design and higher flows. So if the inducer is not run at high speed for extended periods at low flows it should have a long life.

The hydrodynamic design will also result in lower than normal blade loads giving confidence of long life for the entire turbopump.

Performance and Manufacturing Risk

There is industry experience in the fabrication of similar pumps. Rocketdyne's Mark 48 LOX turbopump has a fully-shrouded centrifugal impeller that is 2.55 inches in diameter with other components in proportion. Rocketdyne has also manufactured and tested a pump containing a fully shrouded centrifugal impeller with a diameter of 1.3 inches. This unit was successfully tested in both Freon and liquid fluorine.

To verify predicted performance, the component pump should first be tested in water as the performance differences between water and LOX can be determined analytically. Then, to verify the over-all performance, the turbopump should be tested over a range of speeds, flows and inlet pressures to determine its H-Q and suction performance. The turbine performance in gaseous hydrogen can also be measured at the same time and from the input and output power measurements the over-all efficiency can be calculated.

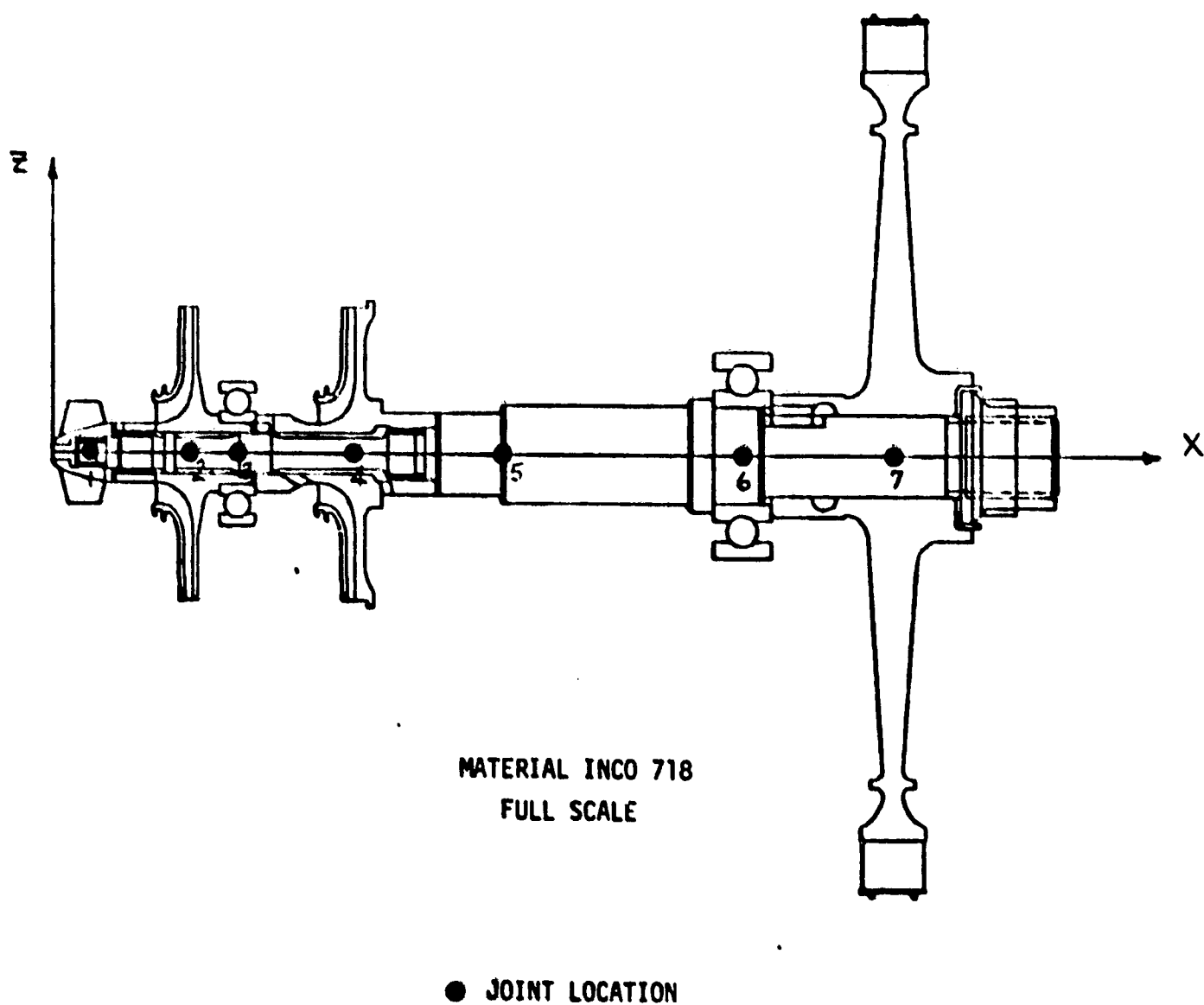
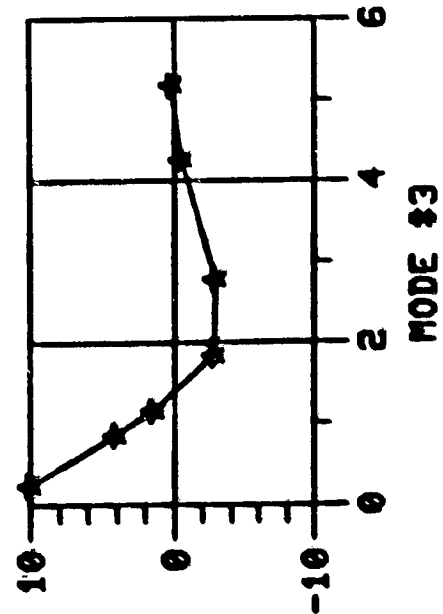
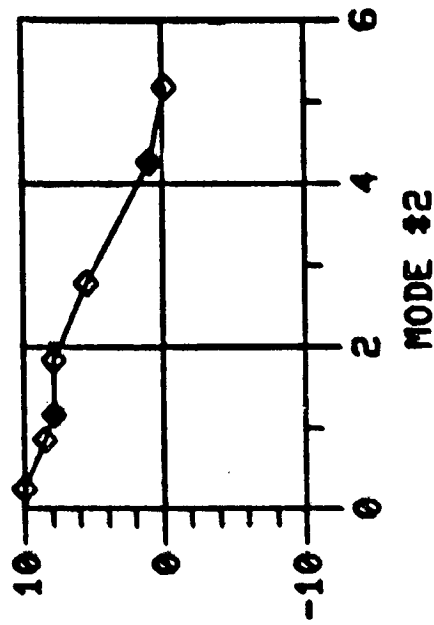
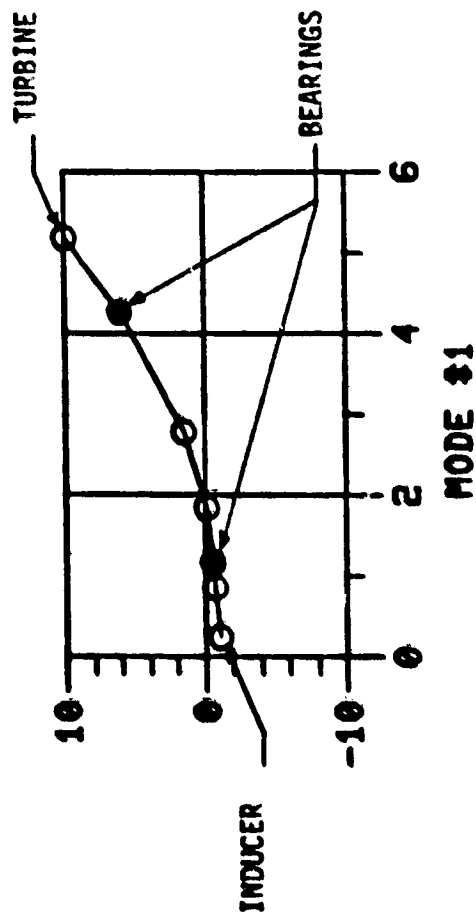


Figure 77. Design 3, LOX Turbopump ($N = 26,500$ RPM)



MODE	HZ	RPM
1	697.410	41845.
2	2498.600	149920.
3	3209.600	192580.

K1	=	150000.	LB/IN
K2	=	150000.	LB/IN

MODE SHAPES

Figure 78. Low Thrust Engine Turbopump Design 3 Critical Speed

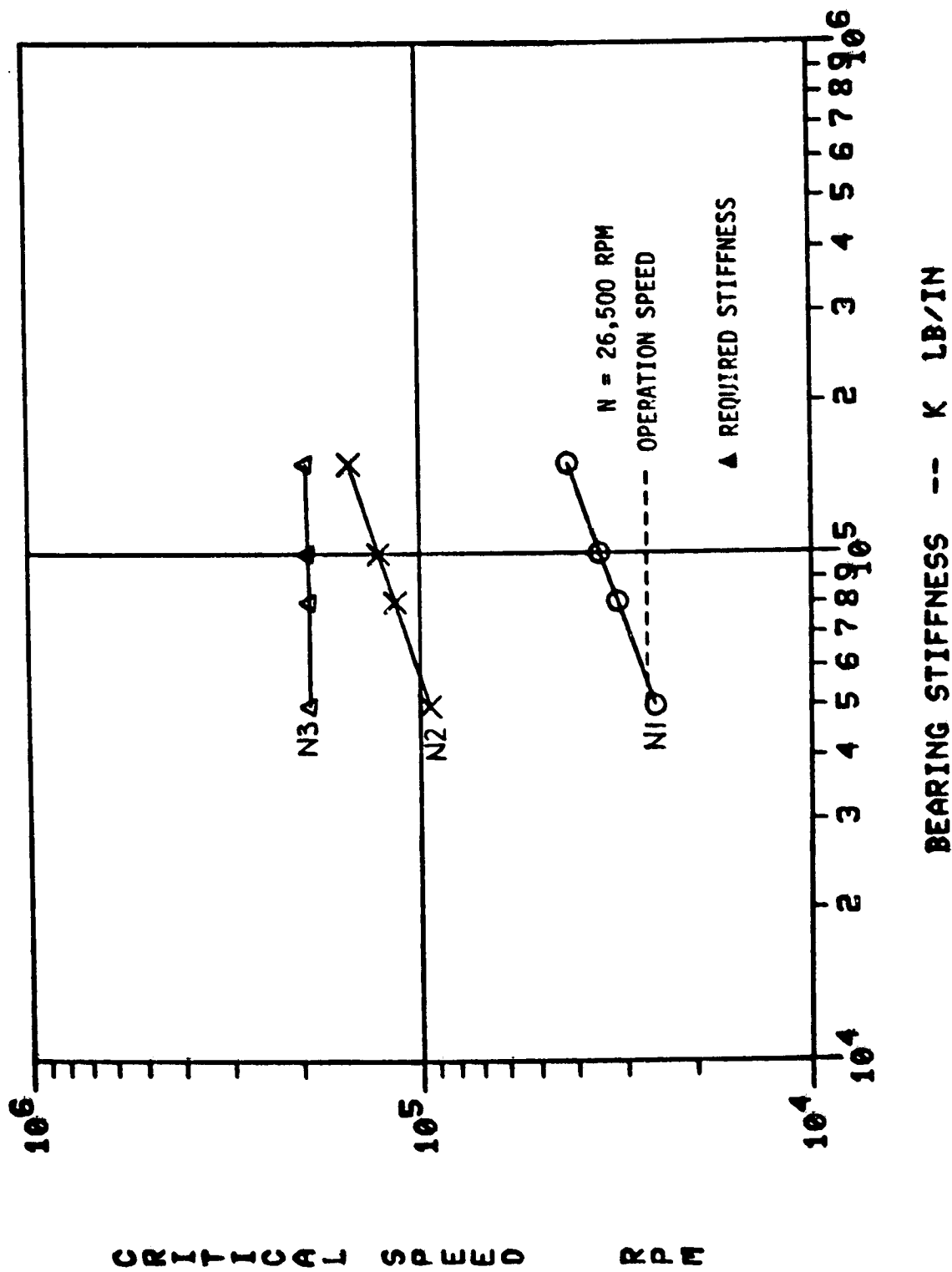


Figure 79. Low Thrust Engine Turbopump Design 3 Critical Speed
Critical Speed vs Bearing Stiffness

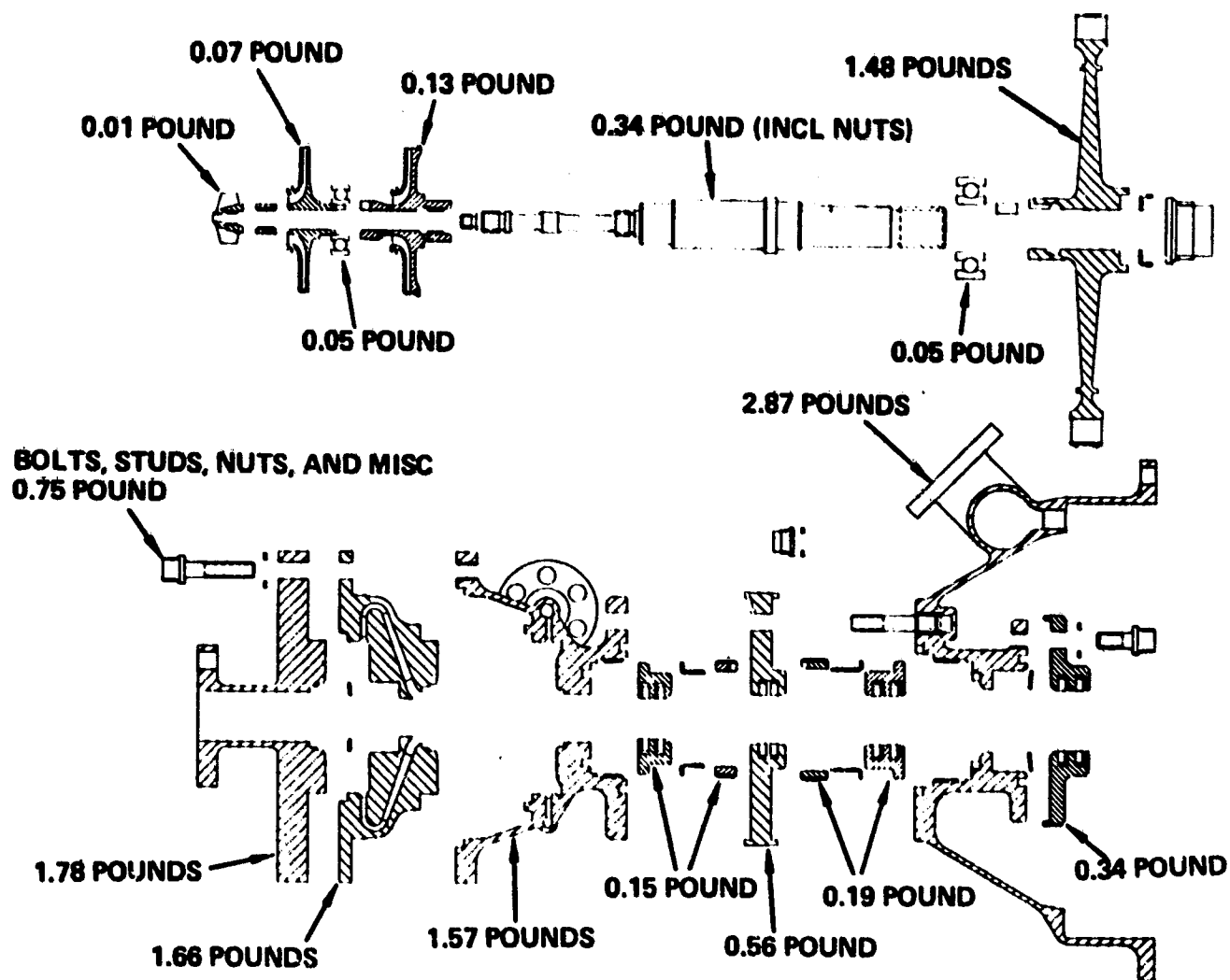


Figure 80. Design 3 Weighs 53.4 N (12.0 Pounds)

Cost Analysis

The ROM cost for fabrication of Design 3 is \$132,800 for tooling and \$54,700 recurring cost. The tooling consists of \$80,000 for casting patterns, \$29,200 for raw materials and purchased parts, and \$25,600 for machining. The recurring cost consists of \$2,500 for castings, \$600 for raw material, and \$51,600 for machining. The first unit cost (the sum of tooling and recurring costs) is \$189,500.

DESIGN 4, OXYGEN TURBOPUMP

The operating requirements for Design 4 are shown in Fig. 46. It is required to pump 18 gpm (1.14 L/S) of liquid oxygen to 625 psia (431 N/cm²) while drawing in propellant at 2 ft (0.61m) NPSH. The turbine operates on gaseous hydrogen entering at 469 psia (323 N/cm²), and 650 R.

Hydrodynamic Design and Performance

The Design 4 liquid oxygen pump is shown in Fig. 81. The pump efficiency is maximized when the specific speed ($N\sqrt{Q}/H^{0.75}$) is near a value of 2000 with N = rotating speed rpm, Q flow rate in gpm and H head rise in feet. The simplest system is produced when a low speed boost pump is not required. In order to operate at high speed the inlet stage must be capable of operating at a very high suction specific speed ($N\sqrt{Q}/\text{NPSH}^{0.75}$) = 70,600 where N is rotating speed in rpm, Q flow rate in gpm and NPSH is inlet total head above vapor pressure in feet. The Tesla or disk pump was therefore selected for its high suction performance capability. The following centrifugal stage incorporates an integral balance piston for axial thrust balance. The flow is directed from the Tesla stage by a cross-over diffusing system. The first stage of diffusion reduces the velocity to approximately one-half the diffuser entering velocity. The inflow diffusing passages reduce the velocity to match the impeller inlet velocity. The centrifugal impeller discharges through a vaned diffuser into a volute. The high rotating speed permitted by the Tesla first stage permits a full emission pump design with an impeller tip width of 14.22 mm (0.056 inch) which is adequate for manufacturing. The centrifugal impeller is fully shrouded with backwardly curved blades. The Tesla pump incorporates a rotating housing designed to increase the meridional velocity prior to entering its diffusing system. The rotating housing reduces hydraulic losses in the flowing fluid to maximize head rise. The fluid flow losses are traded for outer shroud friction drag resulting from interaction with the fixed housing.

The predicted pump head, flow, efficiency curve is presented as Fig. 82. The performance was calculated using Rocketdyne developed computer programs for both the Tesla and centrifugal stages. The Tesla pump performance analysis procedures are based on the preliminary results of tests performed at the David W. Taylor Naval Ship R&D Center, Annapolis Maryland and reported by Mr. Joseph Morris.

Additional work is required to determine the Tesla pump disk spacing and number as well as to define the centrifugal impeller blade angle distribution and detailed shroud shapes. The diffuser passage shapes must be analyzed in detail. Axial thrust capability as a function of balance piston travel must be determined over the pump operating range. The suction performance and head rise capability of the Tesla pump must be verified by tests pumping water. The water suction performance will be analytically corrected to liquid oxygen values.

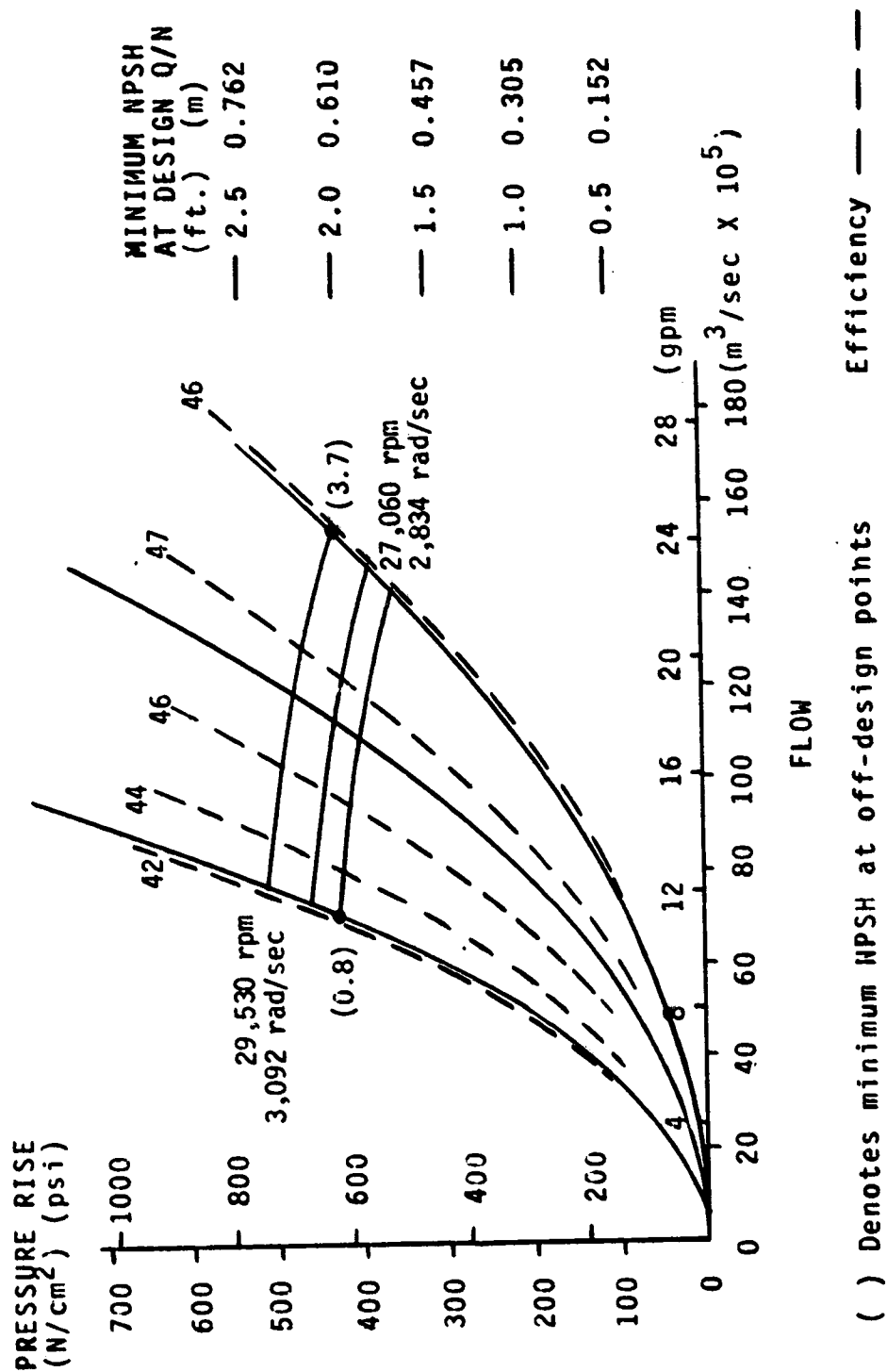


Figure 82. Predicted Pump Head, Flow, Efficiency Curve

Aerodynamic Design and Performance

The turbine performance was optimized by Rocketdyne's partial admission gaseous Hydrogen turbine analysis computer program. The program includes all the gas path losses contributed by turning, friction and secondary flows as well as partial admission losses due to inactive blade pumping and windage, end sector and staging losses. An experimental correlation to include size effect is also built into the program.

Table 11 is the listing for the required design parameters. Inlet conditions were considered as specified at the turbine inlet flange which is in the inlet pipe just upstream of the inlet manifold. The turbine discharge pipe is just downstream of the turbine discharge collector.

The selected turbine mean diameter is based on Fig. 83 where turbine geometry parameters were optimized for high performance. The selected turbine mean diameter is 11.557 cm (4.55 inch) and was based on optimized blade heights and angles. The shrouded rotor design can minimize the end wall and tip clearance losses with resulting higher rotor efficiency.

TABLE 11. DESIGN 4, LOW THRUST PROPULSION SYSTEM
TURBINE PERFORMANCE PARAMETERS

WORKING FLUID	GASEOUS HYDROGEN	GASEOUS HYDROGEN
OUTPUT POWER	10.459 kW	14.02 hp
SPEED	28,000 rpm	28,000 rpm
FLOWRATE	0.212 kg/sec	0.468 lb/sec
INLET TOTAL TEMPERATURE	418.84 K	754 R
INLET TOTAL PRESSURE	36.750 BARS ABSOLUTE	533 psia
OUTLET TOTAL PRESSURE	34.474 BARS ABSOLUTE	500 psia
TOTAL PRESSURE RATIO	1.0660	1.0660
AVAILABLE ENERGY	25.568 kcal/kg	47.8225 Btu/lb
ISENTROPIC VELOCITY	472 m/sec	1548 ft/sec
MEAN DIAMETER	11.557 cm	4.55 inch
MEAN BLADE SPEED	169 m/sec	556 ft/sec
VELOCITY RATIO	0.359	0.359
TOTAL PRESSURE ISENTROPIC EFFICIENCY, %	46.82	46.82
ROTOR TYPE	SHROUD	SHROUD

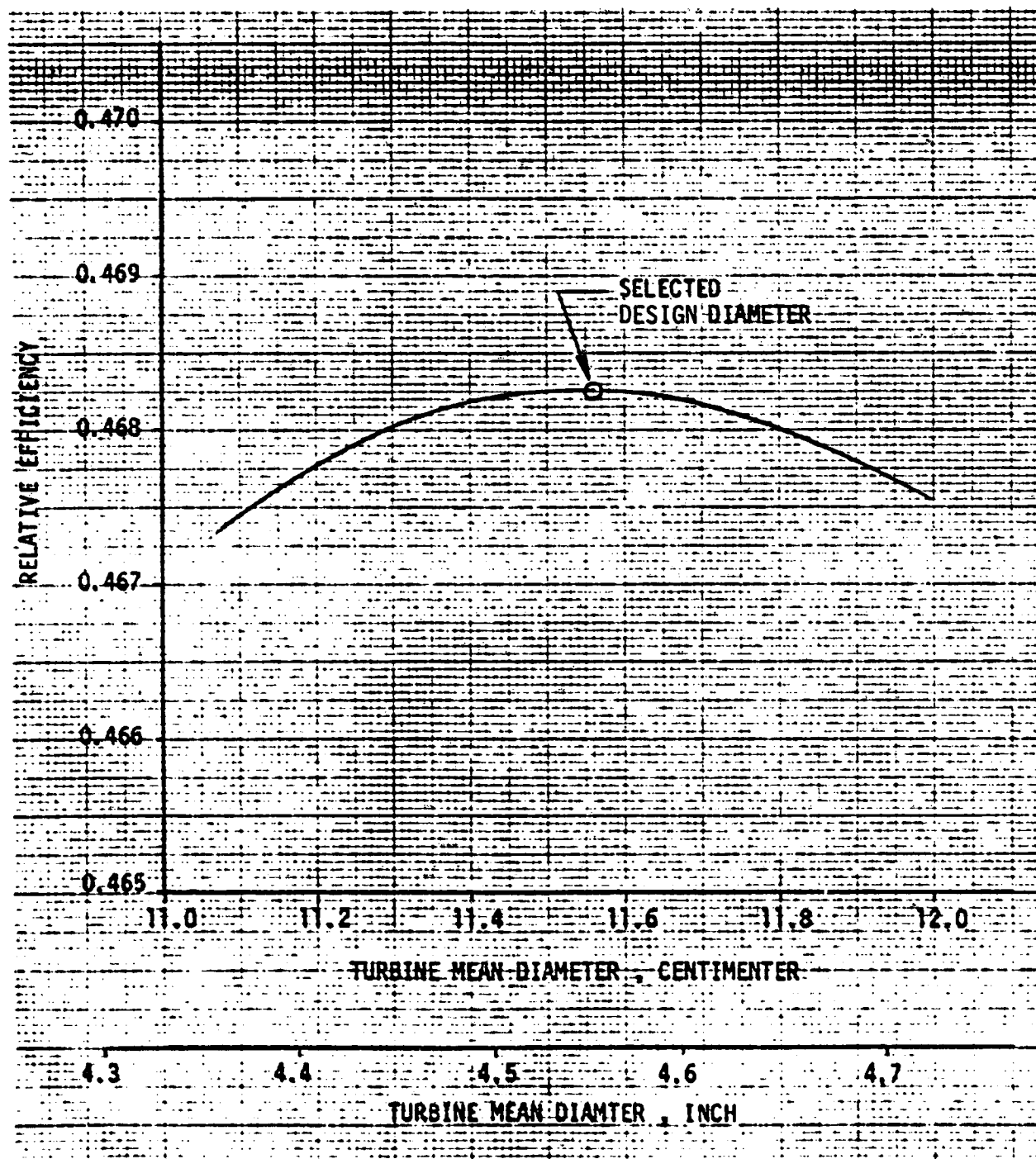


Figure 83. HPOTP Turbine Low Thrust Propulsion System, Mean Diameter Optimization, Design 4

Table 12 is the tabulation for the predicted power losses. The major losses are contributed by friction and turning in the nozzle and rotor profiles known as the expansion and kinetic energy losses. The inlet manifold loss was for a manifold with a radial inlet on a torus to the axial inlet nozzle. The absolute velocity leaving the nozzle was assumed not recoverable, and the total pressure at the turbine discharge flange was assumed to be equal to the static pressure at the rotor discharge. Pastral admission losses and disk friction are also considered.

The velocity vector diagrams are shown in Fig. 84 for the design operating condition. Velocities out of the element include losses contributed by friction and turning, but not disk friction losses, size effects or pastral admission losses. Nozzle discharge mach number is a low value of 0.15. It is conservatively assumed that all the absolute leaving kinetic energy of the rotor discharge (equal to 75 M/sec) was not recoverable.

The total and static pressure, as well as temperature in the blade path are shown in Fig. 86. The static pressure is constant across the rotor for the impulse design to minimize pumping losses in the inactive rotor blade with partial admission. All of the flow expansion and acceleration is accomplished in the nozzle at the design operating condition. Because there is no static pressure gradient across the rotor blade axial direction, there will be no rotor axial thrust at design.

The turbine sizing is summarized in Fig. 85. The rotor mean diameter is 11.557 centimeter (4.55 inch) with a shrouded blade design. The shrouded rotor minimizes the end wall losses and tip clearance losses, resulting in a higher overall rotor efficiency.

The axial space between the nozzles and rotors should be minimized to reduce the spillage loss at the end of the arcs of admission. The potential of a single sector nozzle providing 2 to 3% higher performance efficiency is well known, but a double sector nozzle gives structural and dynamic symmetry. The available pressure ratio from Design 2 to 4 is large enough to afford a double sector nozzle design. The 34% partial admission also lends itself readily to a double sector nozzle design.

The rotor blades were shrouded for improving performance with a tip clearance of 0.005 cm (0.002 inch). The leakage past the rotor upstream side of the shaft seal was into the blading, but the leakage was considered not to be recoverable for the turbine. The flow area sizing includes the leakage.

The design has a predicted performance of 46.82% total pressure Isentropic efficiency and delivers 10.46 kw of power at 28,000 rpm. The flange-to-flange performance is presented in Table 12.

Mechanical Design

Design 4 is a Tesla stage followed by a single stage centrifugal pump powered by a partial admission single stage axial flow turbine. The pump has an axial inlet and a radial discharge. The turbine has a radial inlet and an axial discharge.

TABLE 12. DESIGN 4, LOW THRUST-PROPULSION SYSTEM TURBINE
FLANGE-TO-FLANGE EFFICIENCY AND PERFORMANCE

1. POWER LOSSES

INLET MANIFOLD
I-R U/S SHAFT SEAL
I-N INLET INCIDENCE
I-N INLET KINETIC ENERGY
I-N EXPANSION ENERGY
I-R INLET INCIDENCE
I-R INLET KINETIC ENERGY
I-R EXPANSION ENERGY
I-R WINDAGE
I-R END SECTOR MIXING
I-R RIM FRICTION
I-R DISK FRICTION
I-R END CLEARANCE
S-1 DIAGRAM FACTOR ADJUSTMENT
I-R LEAVING ENERGY
TOTAL POWER LOSSES

FLOWRATE		ENTHALPY		POWER LOSS	
Kg/sec	Lb/sec	KCAL/Kg	BTU/Lb	Kw	Hp
0.2123	0.408	7.9249	14.2749	7.0471	9.4465
0.0060	0.0131	12.467	26.4406	0.3658	0.4903
0.2063	0.4549				
0.2063	0.4549				
0.2063	0.4549	1.5257	2.7463	1.3567	1.8187
0.2063	0.4549				
0.2063	0.4549	1.8612	3.3501	1.6087	2.1564
0.2063	0.4549				
				0.4721	0.6328
				0.2683	0.3597
				0.09631	0.1291
				0.05975	0.0801
0.2063	0.4549	0.04356	0.0784	0.03767	0.0505
0.2063	0.4549	0.7821	1.4078	0.6760	0.9062
0.2063	0.4549	0.6644	1.1959	0.5743	0.7698
					16.8401

2. AVAILABLE POWER

WDOT INLET FLANGE
DHA T-S F-F
POWER AVAILABLE T-S F-F
DHA T-T F-F
POWER AVAILABLE T-T F-F

0.2123 Kg/sec	0.4680 lb/sec
26.568 Kcal/Kg	47.8225 Btu/lb
23.626 Kw	31.6696 Hp
25.904 Kcal/Kg	46.6266 Btu/lb
23.034 Kw	30.877 Hp

3. SHAFT POWER ETC. OVERALL

POWER AVAILABLE T-T F-F
TOTAL POWER LOSSES
SHAFT BRAKE POWER
OVERALL EFFICIENCY T-T F-F
OVERALL U/C T-T
OVERALL U/C T-T SQRT(2)

POWER	
Kw	Hp
23.625 Kw	31.669 Hp
12.563	16.840
11.624	14.829
0.4682	
0.3592	
0.3634	

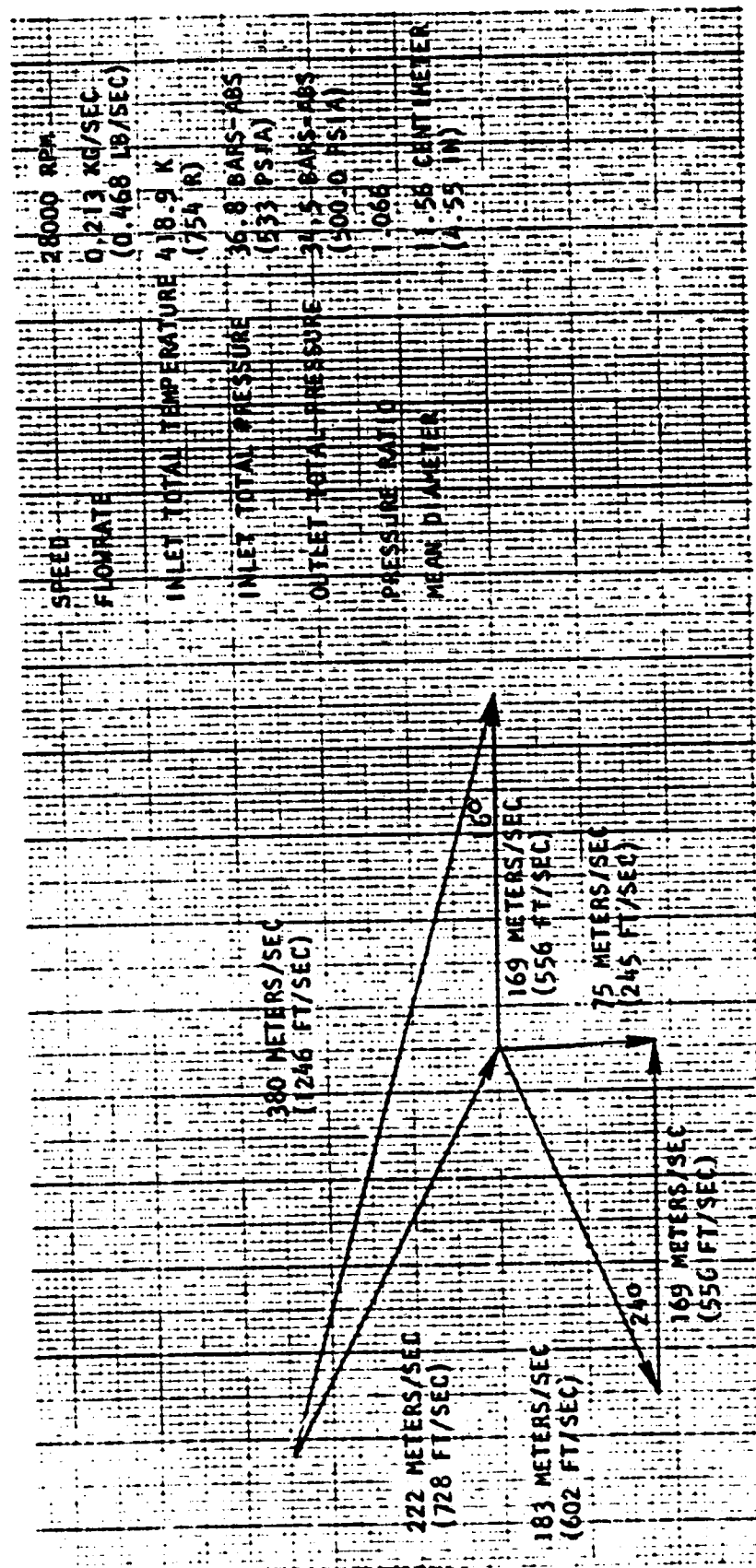
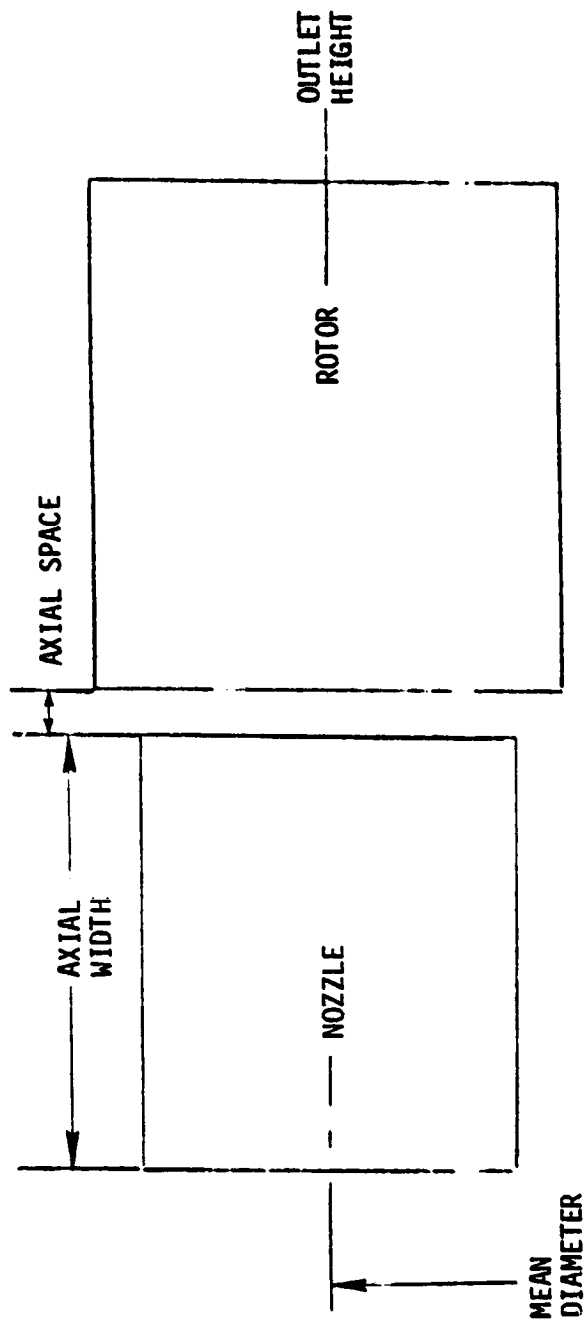


Figure 84. HPOTP Turbine Low Thrust Propulsion System, Velocity Vector Diagram, Design 4



ELEMENT	NOZZLE	ROTOR
MEAN DIAMETER	11.56 CENTIMETER (4.55 IN)	11.56 CENTIMETER (4.55 IN)
OUTLET HEIGHT	1.02 CENTIMETER (0.40 IN)	1.27 CENTIMETER (0.50 IN)
INLET HEIGHT	1.02 CENTIMETER (0.40 IN)	1.27 CENTIMETER (0.50 IN)
AXIAL WIDTH	1.17 CENTIMETER (0.46 IN)	1.37 CENTIMETER (0.54 IN)
AXIAL SPACE	0.127 CENTIMETER (0.05 IN)	
PERCENT ADMISSION	34 %	
ADMISSION SECTORS	2	

Figure 85. HPOTP Turbine Low Thrust Propulsion System, Preliminary Turbine Blade Path Data, Design 4

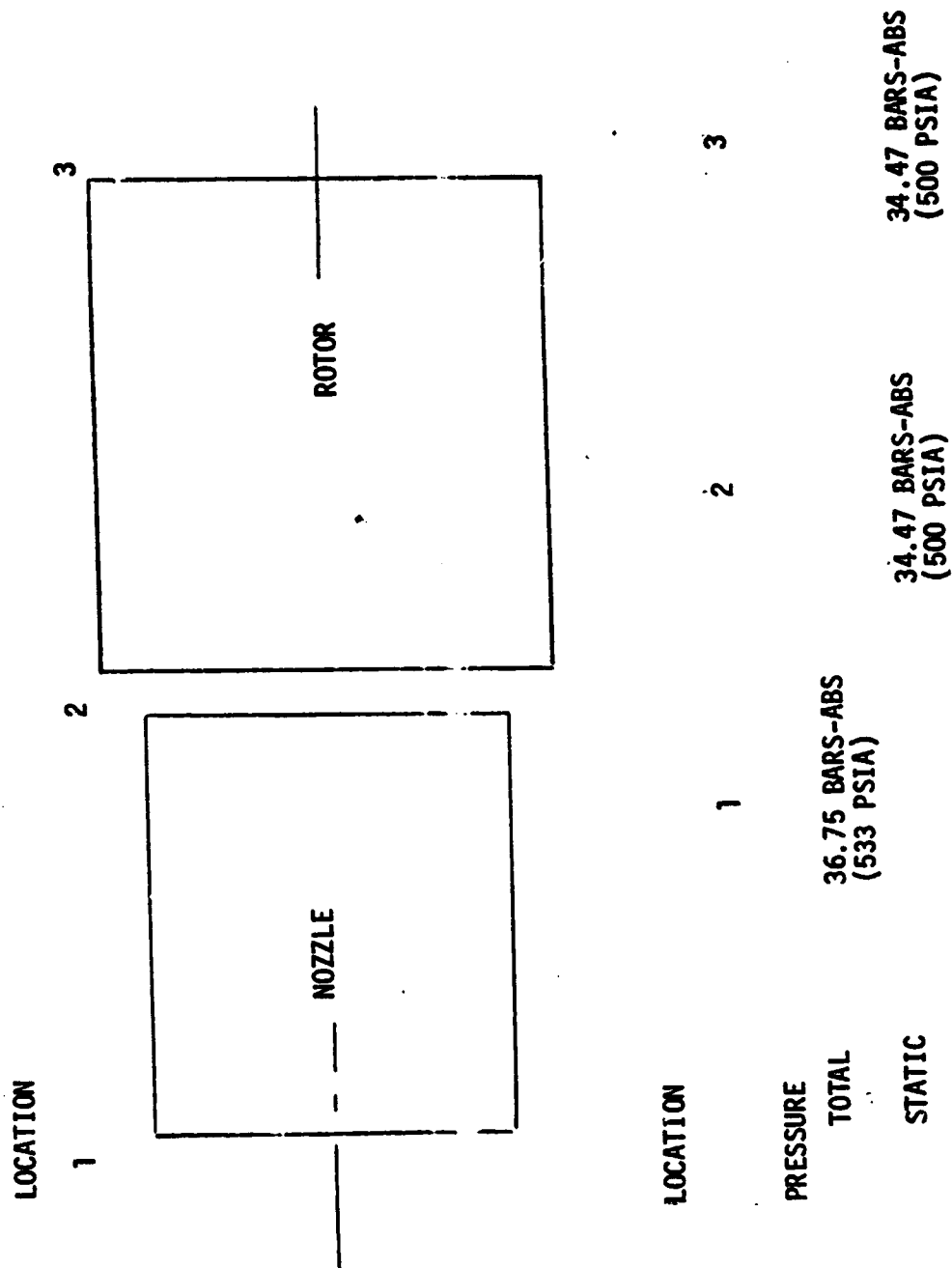


Figure 86. HPOTP Turbine Low Thrust Propulsion System,
Blade Path State Condition, Design 4

The rotating assembly consists of the turbine wheel, pump shaft, one centrifugal impeller and the Tesla pump rotor plus the pump and turbine bearings. The pump end of the shaft is functionally a draw bar upon which the impeller and the Tesla rotor are mounted. Tension in the draw bar is applied by a nut in front of the Tesla stage rotor. The pump bearing is mounted on the Tesla stage rotor and the compressive load from the draw bar passes through the bearing inner rack. The turbine end bearing is mounted on the pump shaft and is retained along with the turbine whereby the turbine wheel retaining nut. The torque applied by the turbine is transmitted to the pump shaft by keys which in turn is transmitted to the second stage impeller by a spline. The torque transfer between the impeller and the Tesla pump rotor is accomplished by slots and tangs machined integrally in each rotor. The use of a through hole in the pump rotors and the turbine wheel is possible because of the low tip speeds.

Positioning of the rotors is provided by a pilot diameter and a normal bearing surface on each end. Repositioning error when the rotor is disassembled and reassembled is reduced by allowing that the rotating elements can be assembled in only one angular rotation position.

The pump housing assembly consists of four major components. The pump inlet provides a tunnel for the Tesla pump inlet and a precision diameter to provide a seal between the pump inlet and the Tesla pump discharge. The pump bearing carrier contains the cast down comer which takes the Tesla pump discharge flow and brings it in to the eye of the centrifugal stage impeller. It also provides a precision diameter for accepting the forward pump bearing. The bearing support diameter is designed to be a radial spring with a low spring rate to allow the OD of the Tesla pump to act as a squeeze film damper. The main pump housing contains the cast centrifugal stage impeller diffuser, the volute collector and discharge diffuser. The turbine housing contains the turbine inlet, manifold and nozzle blades.

The arc of admission for the turbine is split into two equal arcs 180 degrees apart to eliminate an imposed moment that would result from a single arc of admission. This reduces the radial load that the pump and turbine end bearings are subjected to.

The bearings are preloaded against each other at assembly. The turbine seal is mounted to the main housing by bolts.

Static seals are provided for all external flanges. An inner static seal seals the centrifugal impeller discharge pressure and leakage past it is vented to inlet pressure, thereby reducing the pressure seen by the external seal.

The seals that separate the pumped fluid from the turbine bearing coolant fluid are all of the controlled gap type. The pump seal has 2 sealing elements and leakage past this seal flows into the area between the pump seal and the intermediate seal. The intermediate seal is internally pressurized by an inert gas that forms the high pressure barrier between the two working fluids. Inert gas that leaks toward the pump is mixed with the pump fluid that leaked past the pump seal and is vented over board. The bearing coolant

seal has two sealing elements and leakage past them mixes with the leakage flow of the inert gas past the intermediate seal that leaked towards the turbine. This mixed gas is then vented over board. The turbine gas seal is of the controlled gap type and the chamber that contains the turbine end bearing is pressurized to a higher pressure than the turbine nozzle exit pressure so the bearing coolant leakage flow goes into the turbine.

Coolant flow for the turbine end bearings is brought in from an outside source. The pump end bearing coolant flow is provided by the pressure difference across the Tesla stage down comer.

The rotor thrust loads are balanced out by a balance piston that is an integral part of the second stage impeller. The high pressure orifice is provided by a lip on the pump housing and a lip on the impeller outside diameter. The low pressure orifice is provided by matching surfaces on the impeller and housing. Balance piston leakage flow is ducted to the ID of the second stage impeller and delivered to the inlet of the same impeller.

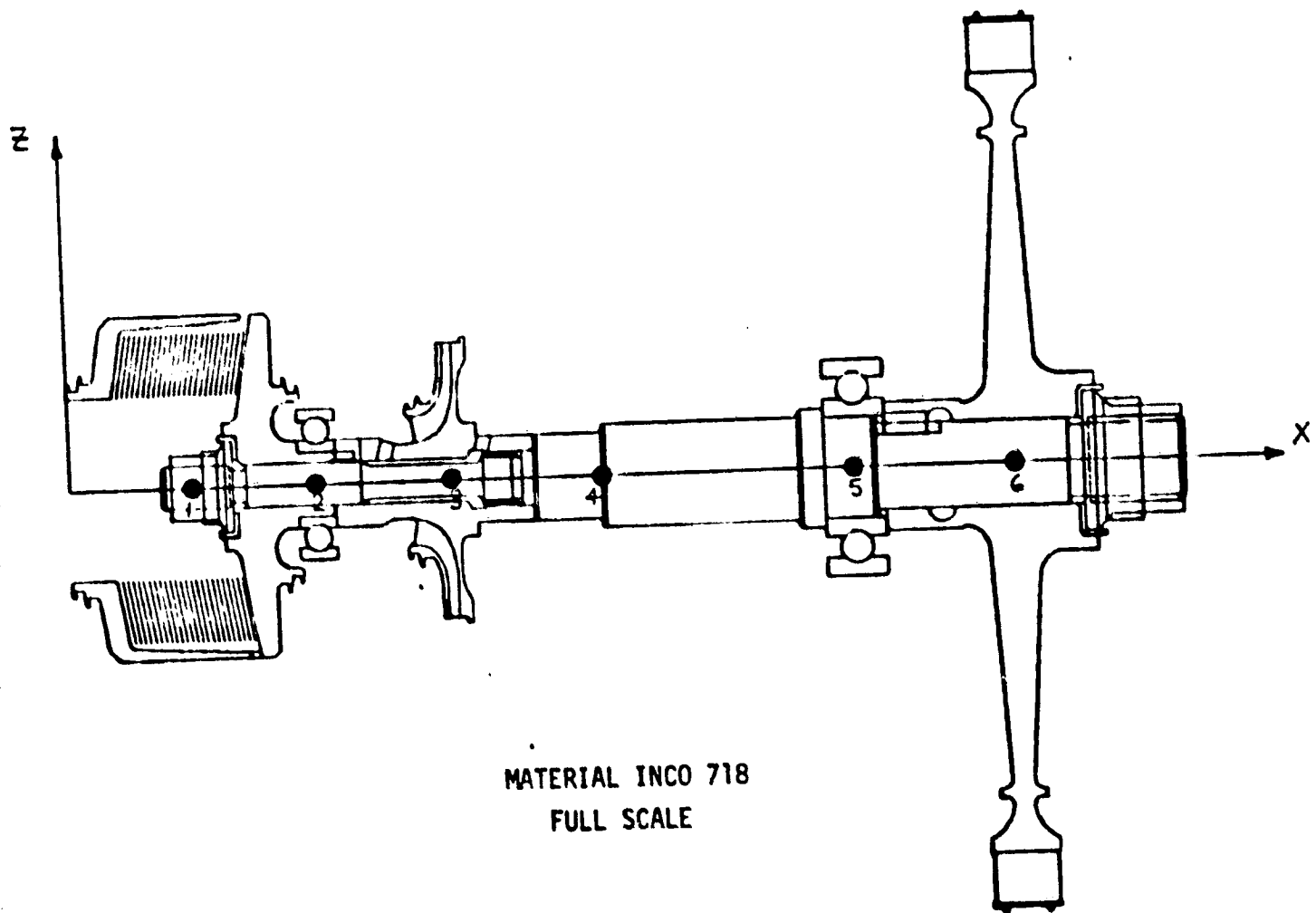
The impeller eyes are sealed by stepped labyrinth wear rings. The rear shroud leakage and the leakage from the Tesla pump are controlled by close fitting diameters between the housings and rotor parts. These close fitting diameters also form a series of squeeze film dampers for controlling the shaft excursions experienced during times that the pump rpm passes through a critical speed range.

The materials chosen for use in the pump and turbine are those that have been proven in previous turbopump designs. The impellers and cross overs will be fabricated from cast Inconel 718. The pump inlet and main pump housing will be fabricated from cast and wrought Inconel 718. The pump inlet and main pump housing will be fabricated from cast and wrought Inconel 718. The turbine wheel will have integrally machined blades and be made from Inconel 718. The bearings are 440C corrosion resistant steel.

Protection of the structural parts from hydrogen embrittlement environment is provided by plating the exposed surfaces with a suitable material that stops the embrittlement process.

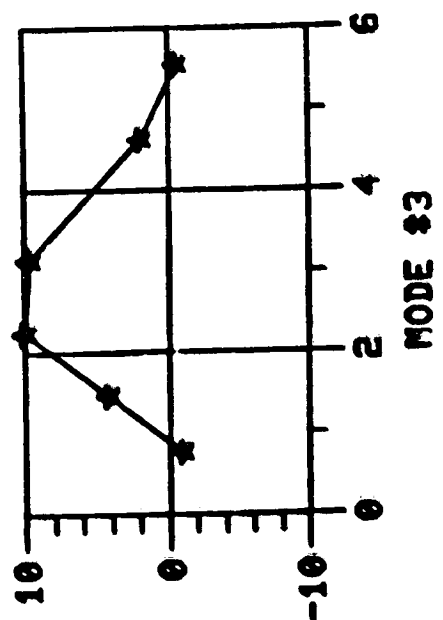
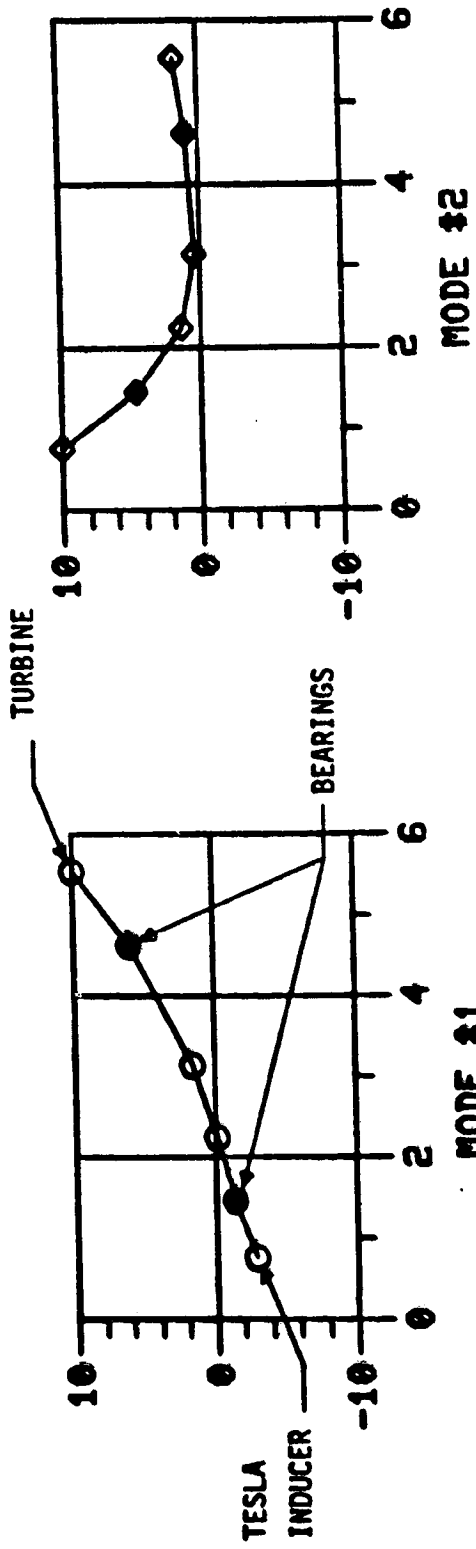
As part of the mechanical design a preliminary stress survey was performed. The impeller tip speed is 195 ft/sec (59.4 M/S) which is less than one-fifth the comparable SSME speed (1000 F/S). The turbine speed is 635 ft/sec (194 M/S) which is less than half the SSME speed (1500 F/S). As with Design 3 the P/A blade stress is an order of magnitude less than the comparable SSME blade stress. Pressure vessel, torque, and thermal stresses are also low. Detailed stress analysis is not expected to reveal any significant stress problems.

Rotordynamic analysis was performed to determine the resonant frequencies and to assure that there is a 20% margin between the operating speed and any resonant speeds. The rotor was modeled as shown in Fig. 87. The first three mode shapes and their resonant frequencies and speeds are shown in Fig. 88. Note the first resonance is 42,613 rpm when the bearing springrate (k_1 , k_2) is 150,000 lb/in (263,000 N/cm). This is 52% above the operating speed, 28,000 rpm as shown in Fig. 89.



● JOINT LOCATION

Figure 87. Design 4 LOX Turbopump (Tesla Inducer
N = 28,000 rpm)



MODE	HZ	RPM
1	710.210	42613.
2	915.110	54907.
3	3210.000	192600.

K1	=	150000.	LB/IN
K2	=	150000.	LB/IN

Figure 88. Low Thrust Engine Turbopump Design 4 Critical Speed

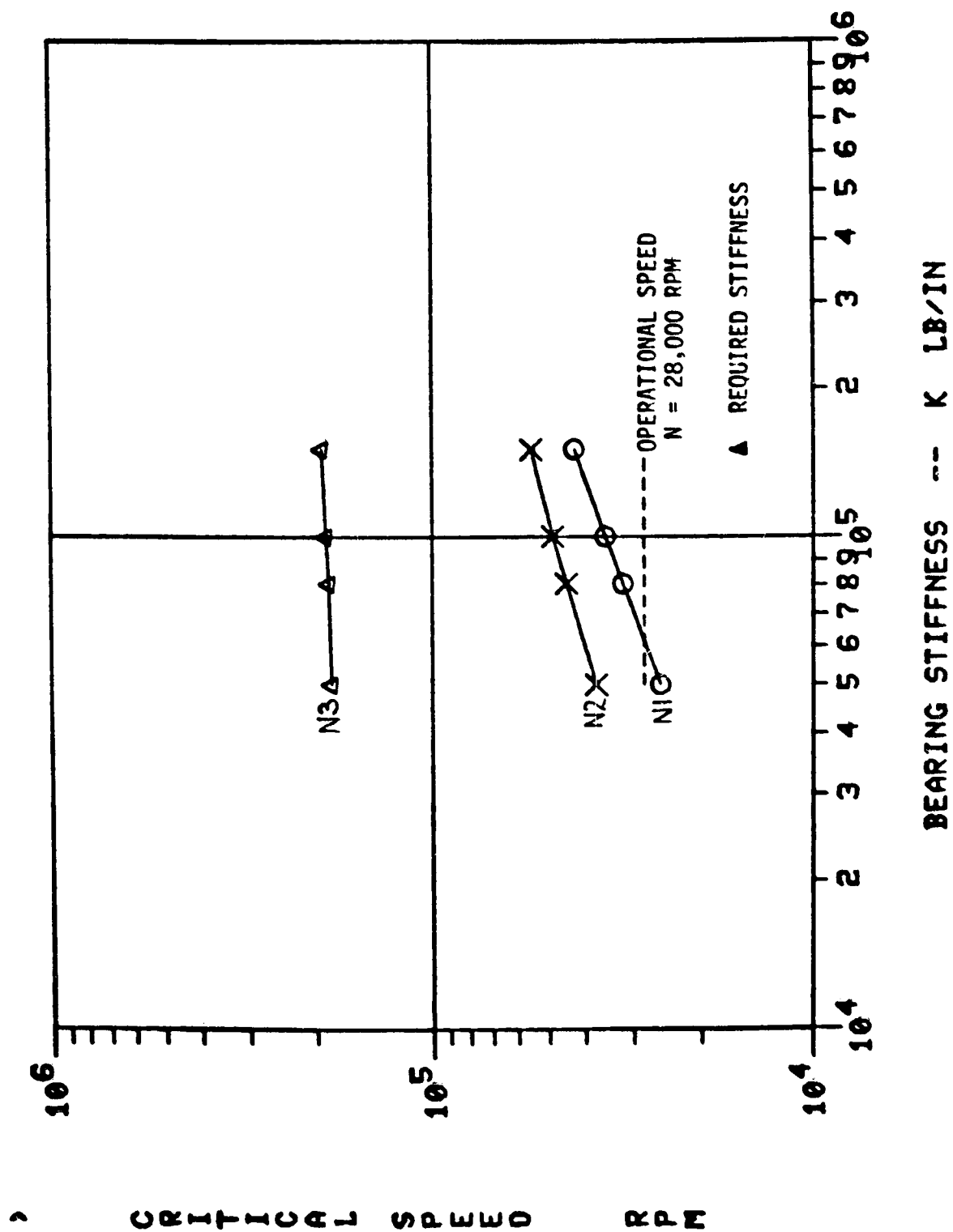


Figure 89. Low Thrust Engine Turbopump Design 4 Critical Speed, Critical Speed vs Bearing Stiffness

Weight Analysis

The dry weight of Design 4 is 10.5 lb (4.76 kg). The rotor weighs 2.5 lb (1.13 kg) and the housing weighs 8.0 lb (3.63 kg). A part by part weight breakdown is shown in Fig. 90.

Life Assessment

The tip speeds are well within industry experience for both small and large size oxygen pumps. Therefore a high confidence level of meeting life requirements for the hydrodynamic components exists with respect to cavitation damage, fluid erosion and fluid force induced vibration. Bearing DN's are 269,000 and 390,000 for pump and turbine bearings respectively. No problem is anticipated with bearings or seals. Adequate life for the turbopump is predicted.

Performance and Manufacturing Risk

The impeller tip diameter 0.0406 m (1.60 inch) and tip width 1.422 mm (0.056 inch) are within the experience of industry for small pumps. Rocketdyne's Mark 36 oxidizer pump which was successfully operated pumping refrigerant and fluorine had an impeller tip diameter of 0.0330 m (1.3 inch) with a tip width of 1.12 mm (0.044 inch). It was an Inconel 718 investment casting which operated at a tip speed of 130 m/s (426 fms).

Rocketdyne's Mark 48-0 LOX pump which demonstrated performance had an impeller tip diameter of 0.0648 m (2.55 inch) and a tip width of 3.84 mm (0.151 inch). The impeller was machined from an Inconel 718 forging and operated at a tip speed of 245 m/s (835 fps). The centrifugal stage specific speed of 950 using $N = \text{rpm}$, $Q = \text{gpm}$ and $H = \text{feet}$ is well within industry experience for high confidence of meeting performance goals. The pump size and passage dimensions are within industry experience for confidence in meeting manufacturing requirements. Test programs for the 18 gpm oxygen pump should therefore be directed to verify the Tesla pump performance and optimize the centrifugal pump performance as well as to investigate the performance implications of pump design concepts which lead to simplified manufacture and improved part-to-part consistency.

Cost Analysis

The ROM cost of Design 4 was assessed. Tooling cost is estimated to be \$124,900. \$70,000 of which is casting pattern tooling, \$29,300 for raw material and purchased parts, and \$25,600 for machining. The recurring cost is \$56,700, \$2,100 for castings, \$500 for raw material, and \$54,100 for machining. The first unit cost is, therefore, estimated to be \$179,000.

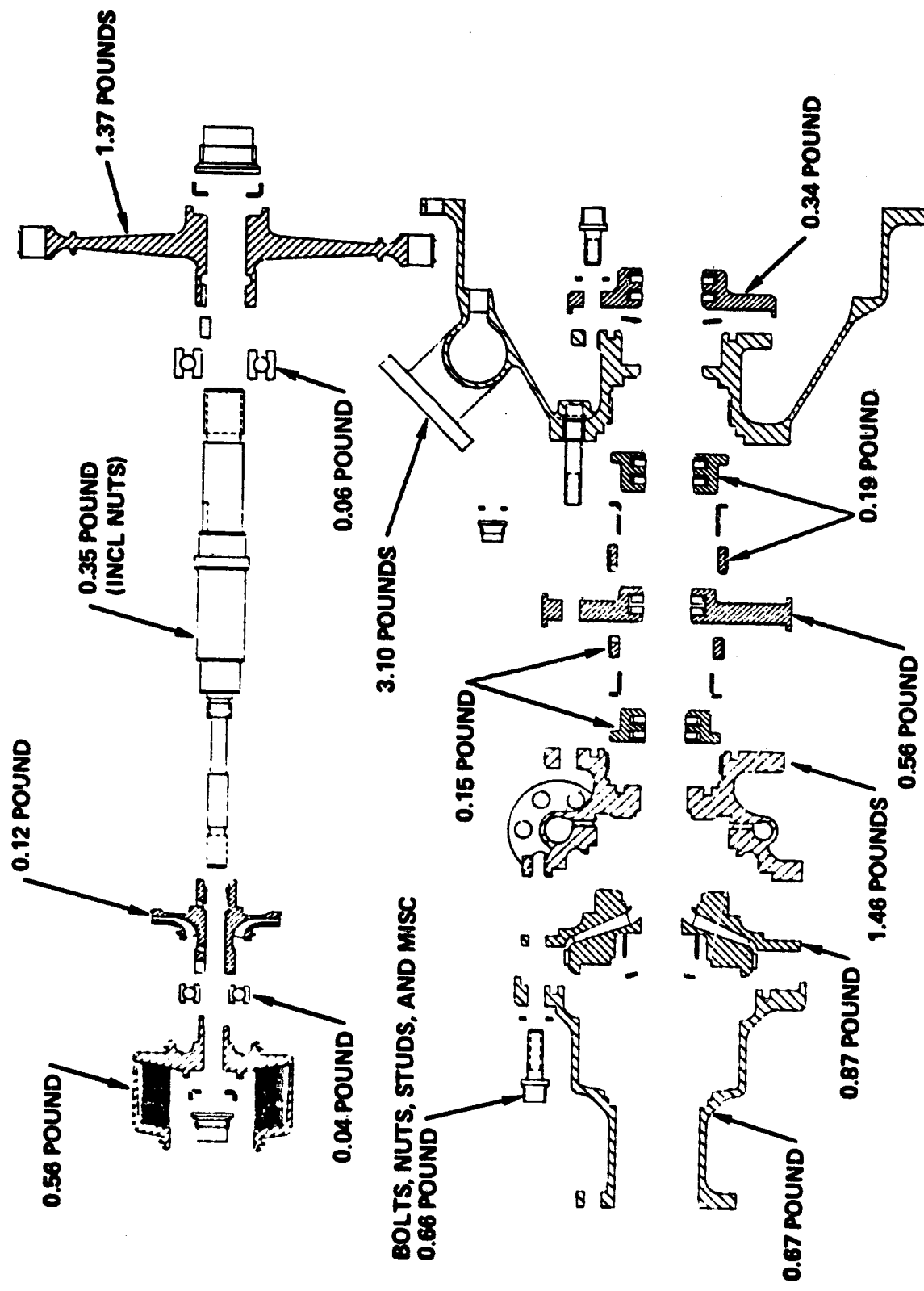


Figure 90. Design 4 Weighs 46.7 N (10.5 Pounds)

DESIGN 5, HYDROGEN VANE PUMP-MOTOR

The operating requirements for the vane pump-motor are shown in Fig. 47. The pump is required to draw flow at 15 ft (4.57 m) NPSH and discharge it at 950 psi (655 N/cm²). The required flow rate is 33 gpm (2.08 L/S). The motor inlet pressure is 655 psi (452 N/cm²) at 780 R.

Hydrodynamic and Aerodynamic Design and Performance

The pump is driven by gaseous hydrogen where the available pressure is 655 psi. The gas inlet temperature is 780 R. Observing that the pump and motor rotate at the same speed and must pass the same quantity of propellant, design performance diagram is calculated by showing the efficiency product as function of rotative speed for different values of the pump clearance to diameter ratio (s/D) and eccentricity ratio (e/D). Typical data are shown in Fig. 91 which in addition shows the required NPSH values. The general trend is that the efficiency product increases with increasing eccentricity ratios and increasing speeds, whereas NPSH requirements increase with increasing speed and decreasing eccentricity ratios. A limiting factor is the available NPSH of 15 feet. It is shown in Fig. 91 that for this constraint, clearance to diameter ratios of 0.0005 will give extremely low efficiency products, and that clearance to diameter ratios of 0.0001 must be selected to obtain the desired efficiency products. All data shown in Fig. 91 are calculated for a rotor length to diameter ratio of $l/D = 1$. The required pump diameters are shown in Fig. 92.

To avoid excessive vane sliding velocities in the guiding slots, an eccentricity ratio of $e/D = 0.05$ is selected which yields a design with the following significant dimensions:

$$\begin{aligned}D_p &= 2.6 \text{ inch} \\D_M &= 7.66 \text{ inch} \\N &= 1950 \text{ rpm} \\\eta_M \times \eta_p &= 0.864\end{aligned}$$

A brief examination of the structural problems indicated excessive radial loads. To avoid this a double flooded arrangement shown in Fig. 93 was designed. Due to the additional leakage at the cross over point between the two pumping and expanding passages, lower volumetric efficiencies than for the single flooded arrangements are calculated. Retaining a NPSH value of 15 feet for the design point, the following dimensions result:

$$\begin{aligned}D_p &= 2.02 \text{ inch} \\D_M &= 5.665 \text{ inch} \\N &= 2500 \text{ rpm} \\\eta_M \times \eta_p &= 0.743\end{aligned}$$

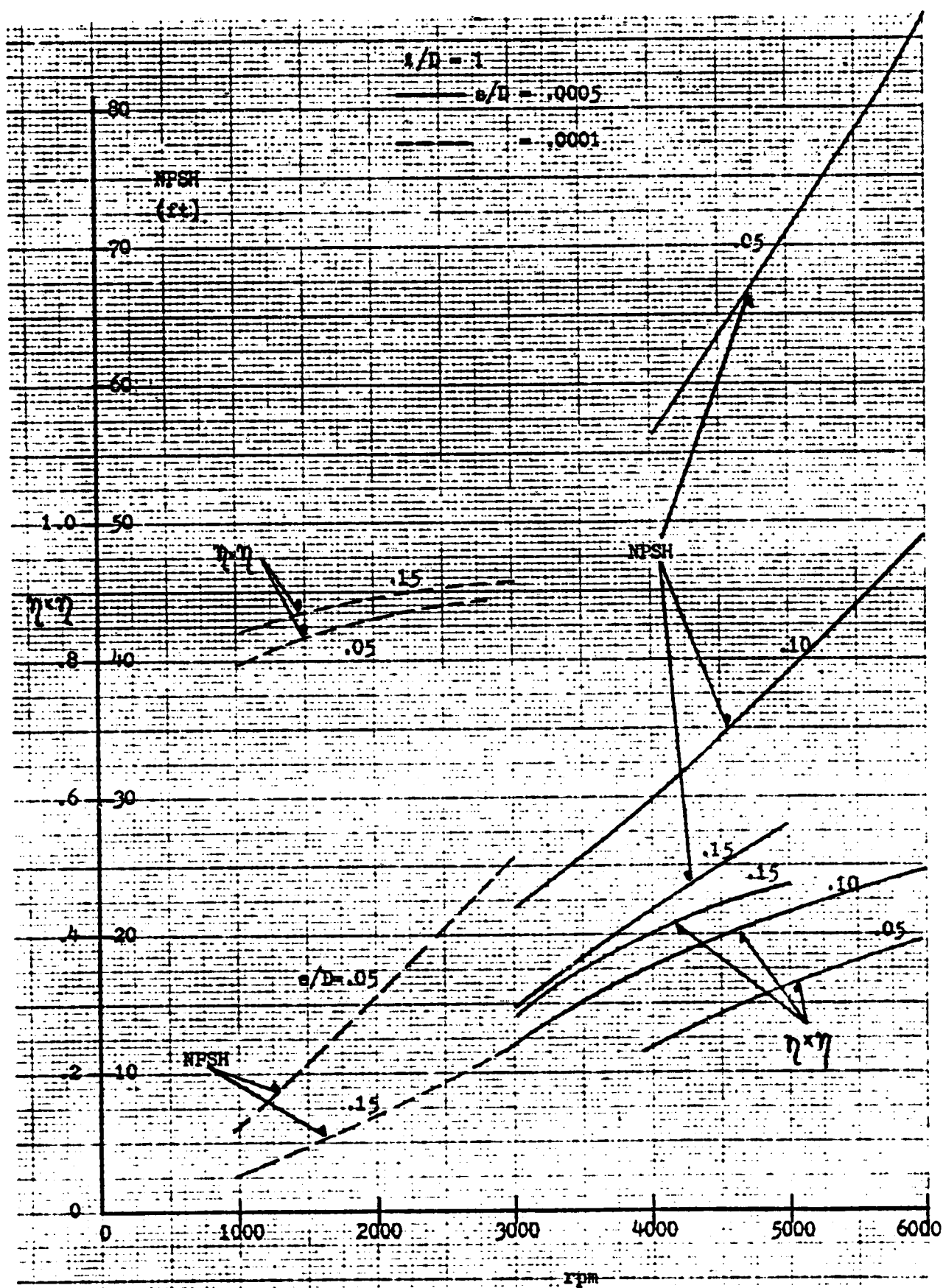


Figure 91. Vane Pump-Motor Design Data

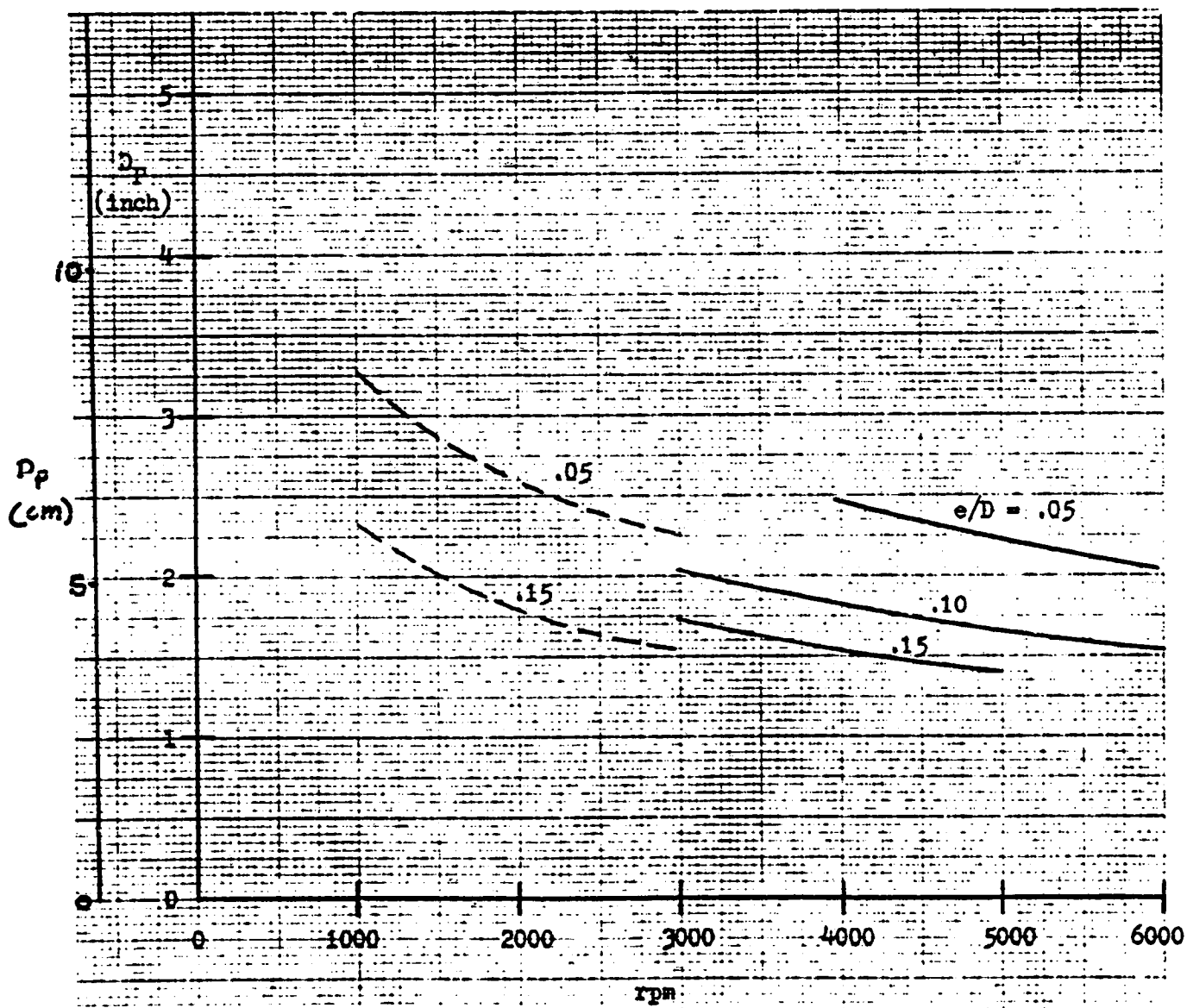


Figure 92. Vane Pump-Motor Design Data

THIS DATA IS
OF LOW QUALITY

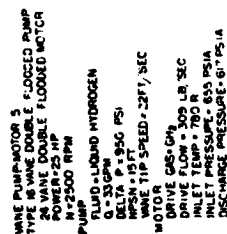


Figure 93. Design 5 Hydrogen Vane Pump-Motor

The desired operating envelope is shown in Fig. 94. Calculating for the above described unit, the off-design performance, it is again found that the ratio of the volumetric efficiencies of expander and pump changes with flow rate as shown in Fig. 94 by the lines of constant η_{V-M}/η_{V-P} values so that the unit becomes mismatched at off-design operation.

For the selected design, the pump efficiency decreases faster with decreasing flow rates than the expander efficiency. This is due mainly to the comparatively large carry over losses at the cross-over points A. They can be reduced by providing more vanes in the pump section. This, however, will aggravate the fabrication requirements. Another possible remedy is to allow the expander volumetric efficiency to drop faster with decreasing flow rates by reducing the number of vanes in the expander section. With this assumption and by varying the s/D ratios a configuration was determined where the volumetric efficiency ratio was nearly constant over the performance envelope. The desired s/D values are 0.0001 for the pump and 0.00014 for the expander. The design point efficiency product decreased to 0.70. This yields expander back pressures as shown in Fig. 95. The required rotative speed is again proportional to the flow rate so that NPSH values result as shown in Fig. 96.

Mechanical Design

Design 5 is a vane positive displacement pump powered by a vane positive displacement expander (motor). The rotating speed is 2500 rpm. The motor shaft is supported between a pair of roller bearings. The pump rotor floats on two keys which provide the torque from the motor shaft. End wear is compensated for by pressure loaded floating end plates. The pump is mounted to the main housing by eight bolts. There are 16 precision ground vanes in the pump which is double flooded. This means that the flow is split equally between two inlets and outlets and that the pumping takes place in half a revolution. The housing is also precision ground to produce the very close fit required at the vane ends, rotor ends, and OD. Pump end bearing lubrication is tapped from the pump discharge and routed through the pump end bearing and returned to the pump inlet. Motor end bearing lubrication is again tapped from pump discharge but is then routed to the backside of the pump floating end plate, ducted through the center of the shaft, through a tube sealed with O rings and discharged through the bearing to the backside of the motor floating end plate and is finally vented into the motor discharge. Extremely close tolerances are called for, some less than 0.0002 inches. The pump diameter is 2.02 inches (5.13 cm). Its 16 vanes rub the housing at 22 ft/sec. The motor is 5.65 inches (14.35 cm) in diameter and rubs 24 vanes against the motor housing at 61.6 ft/sec (18.78 m/s). The motor is also double flooded, having two separate sections functioning in one half the circumference. Because of the close fits required the wall thicknesses are substantial. This results in low stress levels. The main housing has a bending stress calculated to be 55,000 psi (37,933 n/cm^2), which is well within the capability of Inco 718. The pressure vessel stresses are below 10,000 psi (6,897 n/cm^2) also well below the strength of 718. No rotordynamic analysis was performed due to low rotating speed.

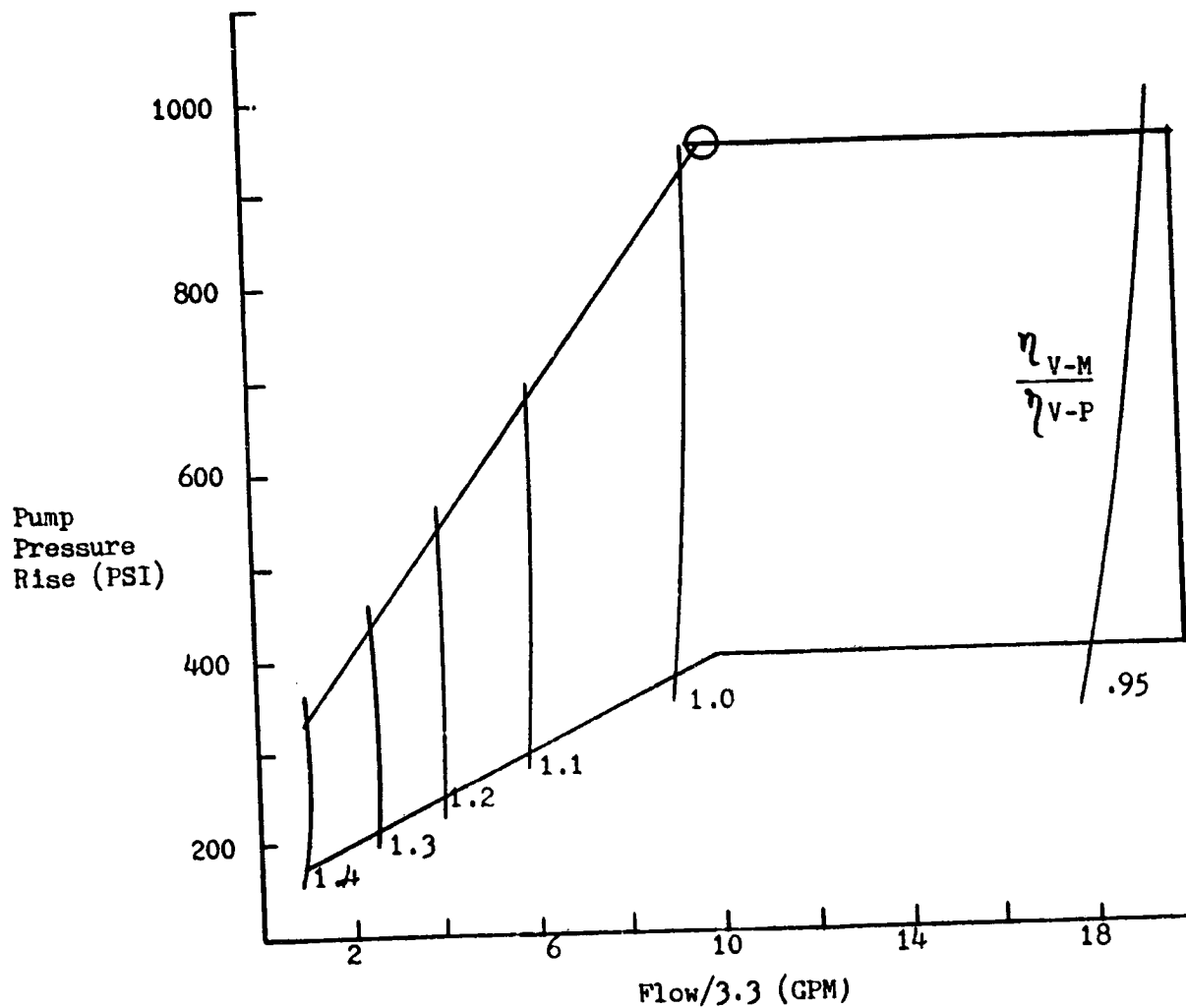


Figure 94. Vane Pump-Motor Part Load Data

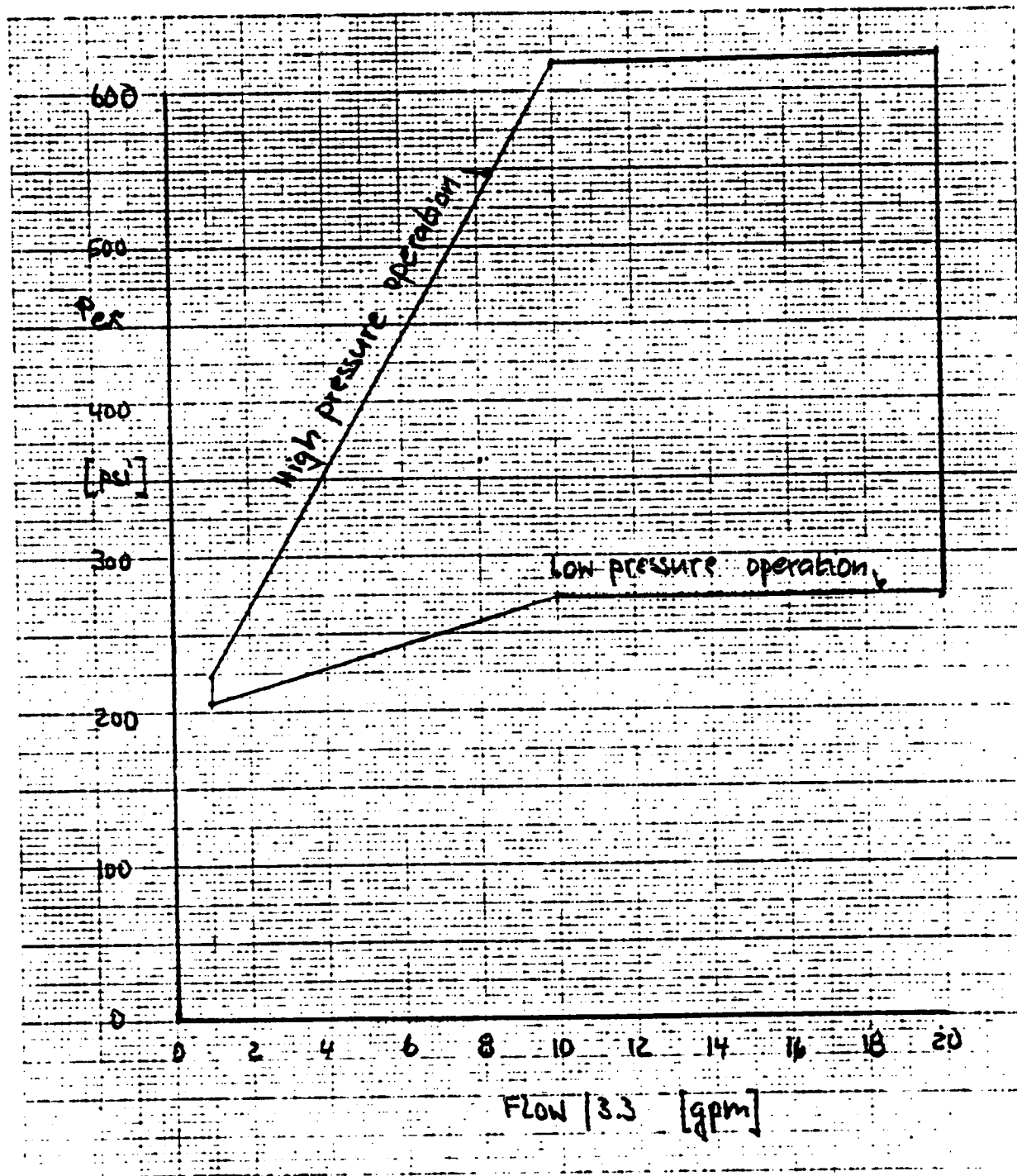


Figure 95. Vane Pump-Motor Back Pressures

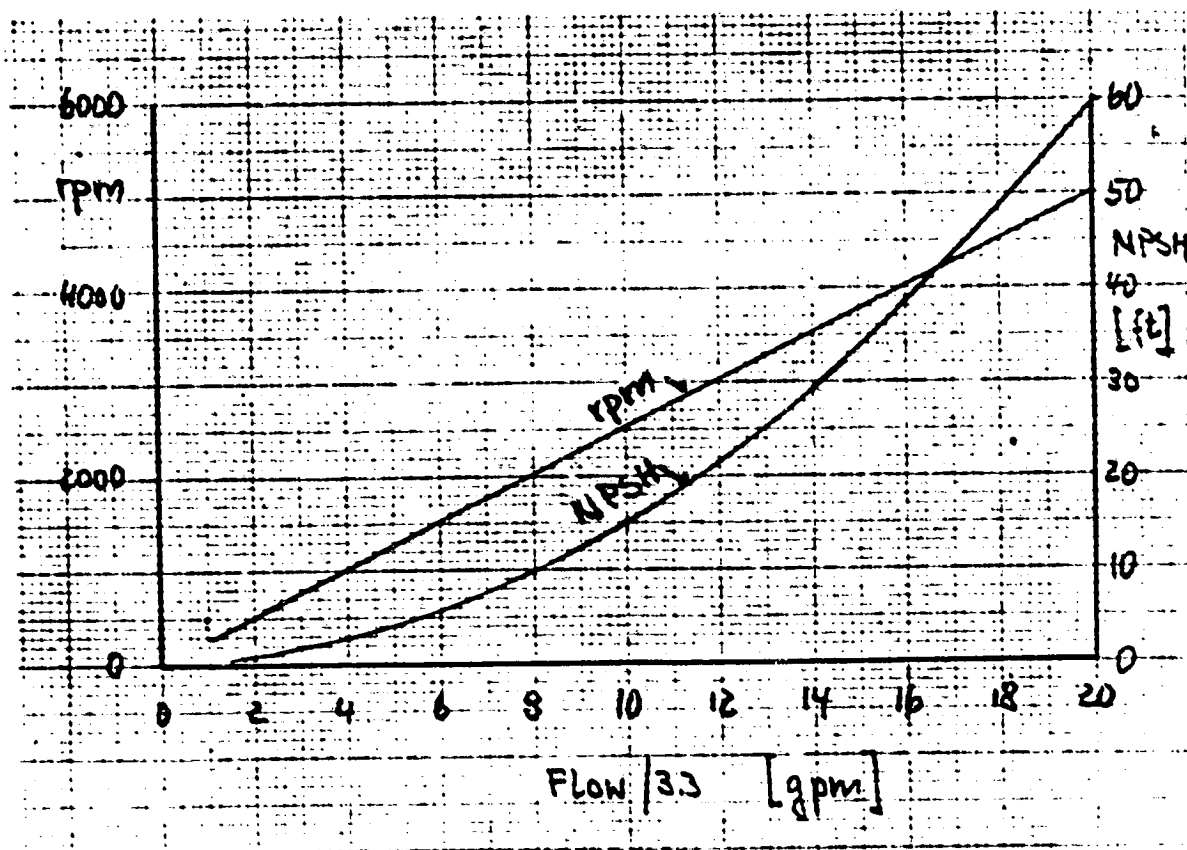


Figure 96. Speed and NPSH as Functions of Flow

Weight Analysis

The weight of Design 5 is quite high at 94 lb (42.6 kg). This is due to the size of the unit as well as the thick walls required for clearance and alignment control. The rotating parts weigh 39.61 lb (17.96 kg) and the housing weighs 54.39 lb (29.56 kg). A part by part weight breakdown is shown in Fig. 97.

Life Assessment

The life of both positive displacement pumps is less certain than the previous dynamic pumps. Large areas are constantly being rubbed, vane ends plus sides, rotor ends, side plate faces, and housing IDs. The life should be acceptable because of the low rotating speed and resultant low tip speeds. However, testing must be performed to establish the actual wear rates and characteristics under the proposed operating conditions before any definitive life predictions can be made. The bearing DN's are 62,500, which is very low and indicates that bearing life will not be a concern. Similarly the carbon nose seal should have no trouble meeting the life requirement.

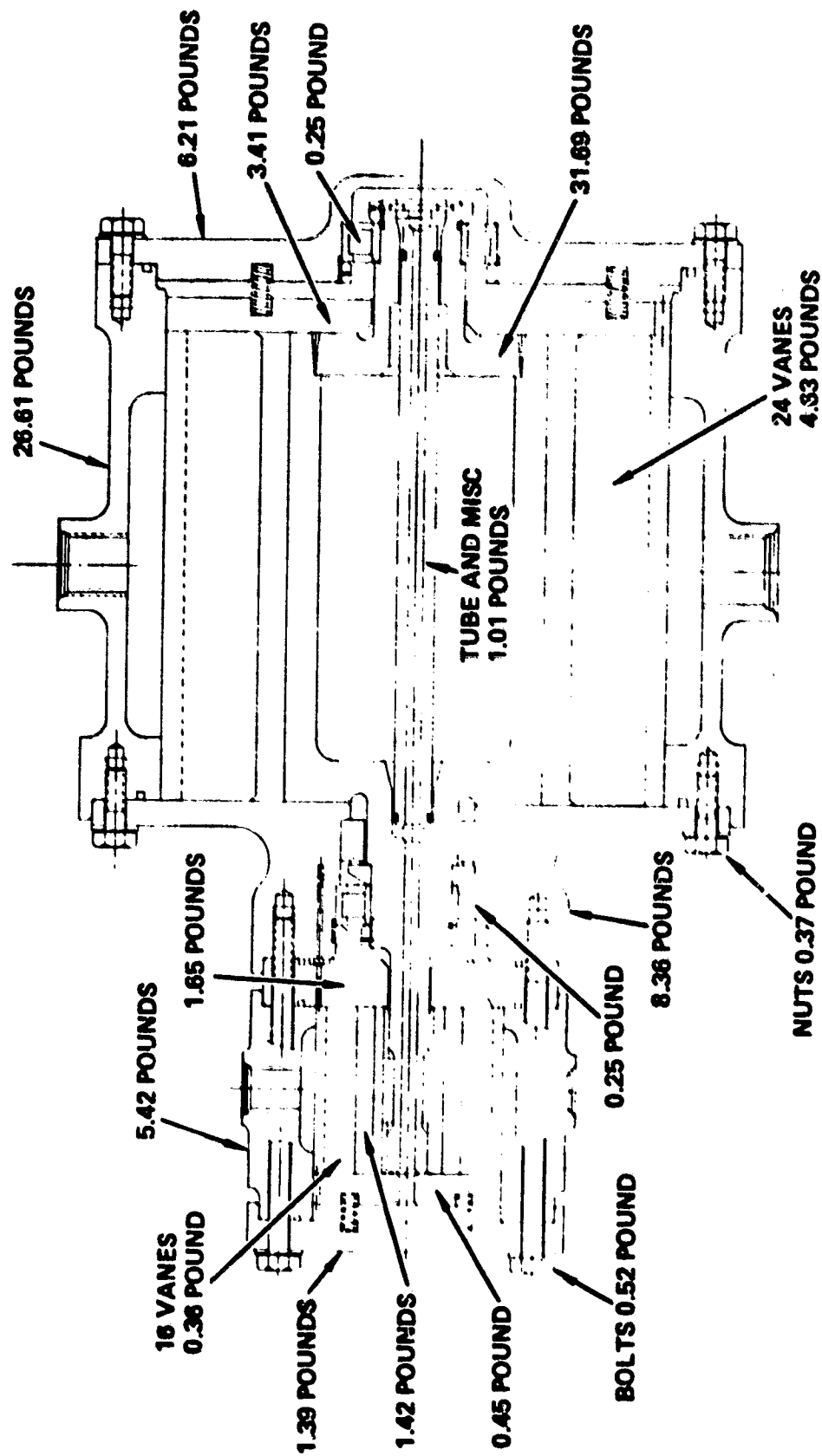


Figure 97. Design 5 Weighs 4.8 N (94.0 Pounds)

Performance and Manufacturing Risk

Performance risk is very low, assuming that the required clearances can be produced and maintained throughout the life of the unit. However, if the parts wear unevenly or in an uncompensated region, performance will fall dramatically as indicated in Task 1. Manufacturing risk is significant. The tolerances required are exacting and result in very difficult grinding of non-axial symmetrical shapes. Concentricity is of utmost concern because of the relatively long and close fits of the two rotors. Vane fit in the rotor grooves is another area of concern where precision machining of narrow, deep grooves with ± 0.0001 tolerance is required.

Cost Analysis

The estimated cost of the vane pump-motor is \$40,300 for tooling and \$112,000 recurring cost. The tooling consists of \$13,600 for raw material and purchased parts, and \$26,700 for machining. The recurring cost consists of \$11,100 for raw material and purchased parts and \$100,900 for machining. The first unit cost (the sum of tooling and recurring) is \$152,300.

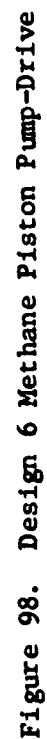
DESIGN 6, METHANE PISTON PUMP-DRIVE

The operating requirements for the piston pump-drive are shown in Fig. 48. The pump is required to draw flow at no more than 6 feet (1.83 m) NPSH and discharge it at 950 psi (655 n/cm²). The flow rate is 10 gpm (0.63 L/S). The drive inlet pressure is 655 psia (452 n/cm²) and the inlet temperature is 650 R. Originally the pump-drive was designed to have a minimum of 6 feet NPSH capability. This resulted in an average piston speed of 14.1 ft/sec (4.30 m/s) and a 0.538 inch (1.37 cm) pump diameter with a 1.0 inch (2.54 cm) stroke. The cyclic rate was 5,000 cpm. The pump and drive could both function satisfactorily under these conditions. When a gas cycling valve was designed it was determined that no valve could be designed that could pass the pump flow and cycle it from one side of the drive piston to the other 5,000 times a minute. This allowed only 0.006 second to vent, pressurize, and move the piston one-half stroke. The cyclic rate was reduced by a factor of eight by doubling the scale of the piston pump-drive. As a result the presently designed unit has a functioning valve and dramatically improved suction performance. The negative effect, however, is that the unit is now quite large and heavy.

Hydrodynamic and Aerodynamic Design and Performance

The pump is driven by gaseous methane. The available pressure (655 psia) is 68.9% of the pressure delivered by the pump and the temperature of the drive is 650 R. A linear axial piston pump, directly coupled with a linear piston expander as a drive element as shown in Fig. 98. The common element in this device is that the pump stroke must be equal to the expander stroke and that the mass flow rate delivered by the pump is equal to the mass flow rate fed to the expander (neglecting drive bypass flow). Observing these coupling conditions, the design relation for the pump and expander part can be evaluated numerically and yield a diagram as shown in Fig. 99 by plotting lines of constant efficiency products (pump efficiency times expander efficiency) as function of the stroke, S , and linear piston velocity, v , for different stroke to diameter ratios (S/D) of the pump and fixed values of the clearance to diameter ratio (s/D) and piston length to diameter ratio (L/D).

Because the required NPSH for the pump is proportional to the square of the linear piston velocity, a scale of NPSH values is superimposed over the linear speed scale. This diagram shows that in general the efficiency product increases with increasing piston velocities and increasing stroke values. Because the NPSH is limited to 6 feet, a large margin exists due to the low piston velocity. Approximate values for the desired pump piston diameter can also be shown as indicated by the righthand scale of Fig. 99. It should be added that the piston diameter of the expander tends to be larger by a factor of 4 to 5 due to the lower density of the gaseous methane. Selecting a clearance to diameter ratio of 0.0002 and a stroke of 2 inches, a pump piston diameter of 1.076 inches and an expander piston diameter of 4.41 inches results. The average piston speed is 3.47 ft/sec which corresponds to a cyclic speed of 625 cpm. The efficiency product is calculated to be 69.1%, the expander having a comparatively low efficiency value of 74.4% and the pump being 92.9%.



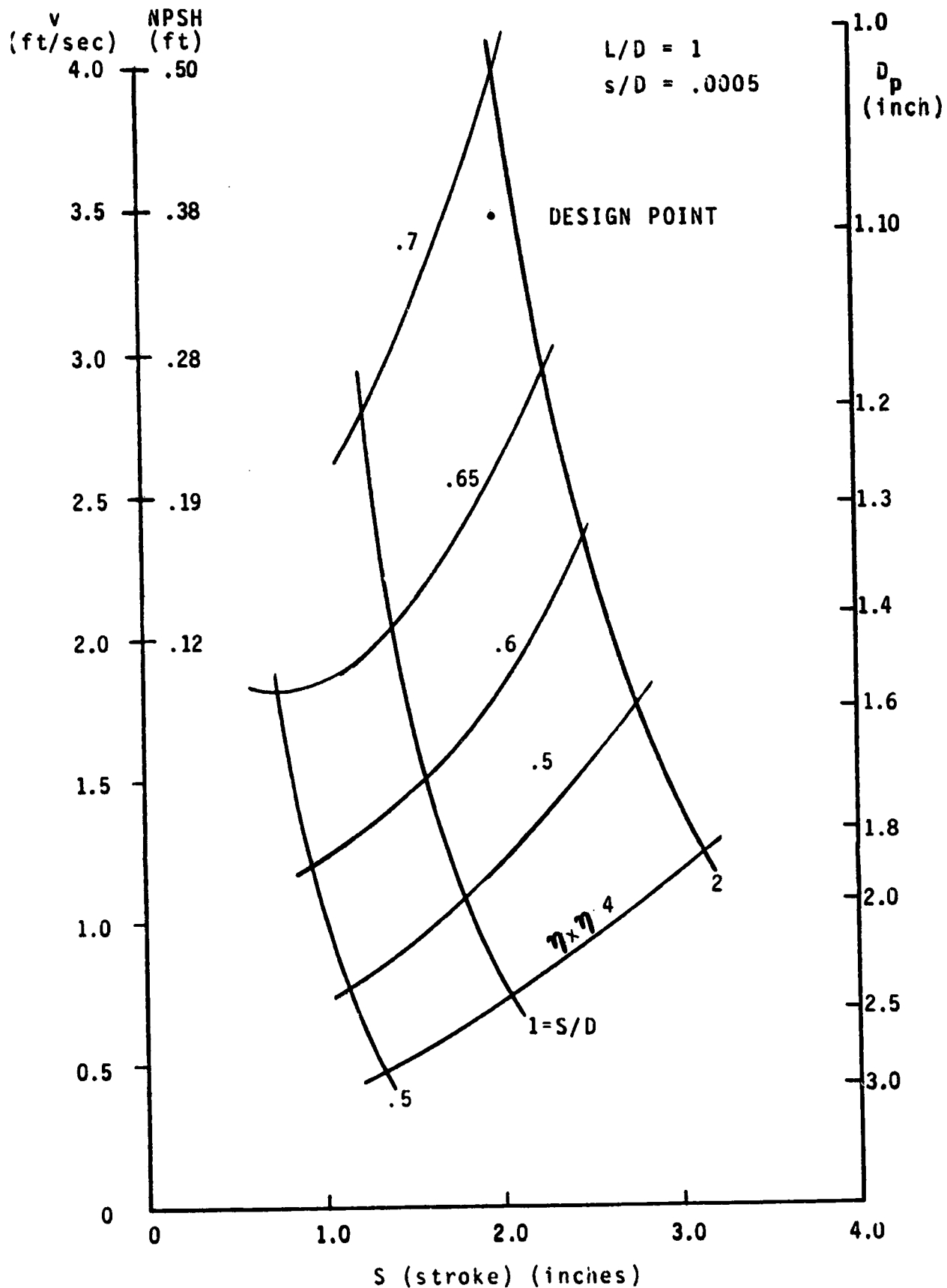


Figure 99. Design Relationship Methane Pump-Drive

The performance range to be covered is shown in Fig. 100 by plotting the desired performance envelope in terms of pressure ratio and flowrates. Calculating the volumetric efficiency of the pump and expander for this envelope it is found that for the assumed clearances the expander volumetric efficiency decreases at a faster rate than the pump volumetric efficiency with decreasing flow rates. This is indicated in Fig. 100 by showing lines of constant ratios of expander volumetric efficiency to pump volumetric efficiency. This means that a comparatively high portion of the flowrate delivered from the pump to the expander has already leaked out from the expander section before the stroke is completed, when operating at low flowrates whereas at design point operation the pump and expander leakage rates are matched over the stroke. Thus a mismatch occurs at low flowrates meaning that a somewhat complex control mechanism is required to keep the unit running properly over the desired envelope.

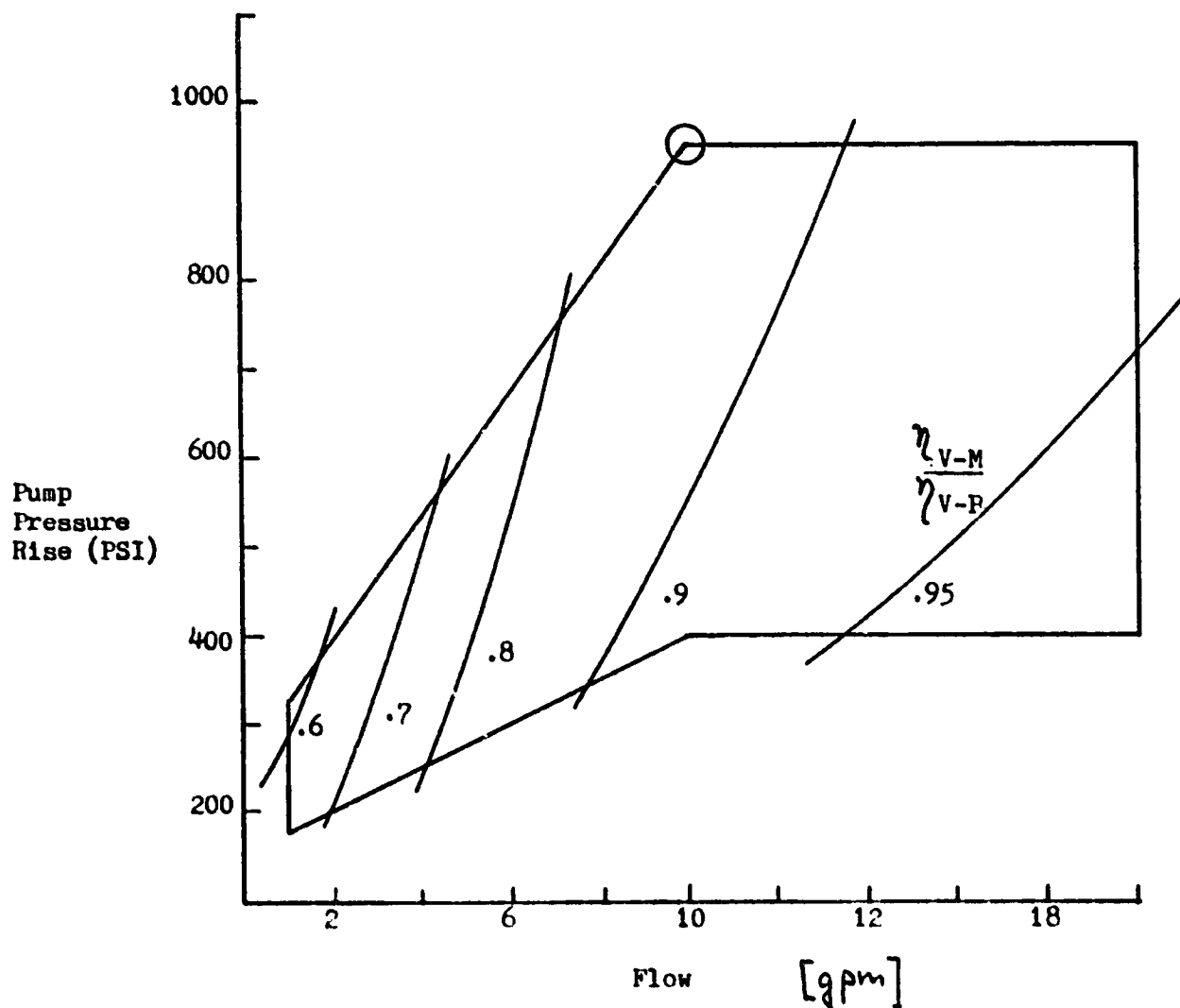


Figure 100. Methane Pump-Drive Part Load Data

A more convenient method would be to prevent the rapid decrease of the expander volumetric efficiency by decreasing the expander clearance. Retaining the clearance to diameter ratio of the pump portion at 0.0002 and reducing the clearance to diameter ratio of the expander portion to 0.00004, the volumetric efficiencies of both units, pump and expander, stay nearly constant over the desired operating range. Because the expander diameter is about 4-1/2 times the pump diameter, the same absolute values for the clearance will be desired to achieve a fair match over the performance range. This method will cause more stringent requirements for fabrication.

Another possibility is to retain the original s/D ratio (0.0002) for the expander piston and to increase the clearance of the pump piston to make the drop-off in the volumetric pump efficiency with decreasing flow rates similar to the expander. Preliminary calculations show that the selection of s/D = 0.0005 yields a fair match of pump and expander over the performance range. The design point efficiency product, however, decreases to 0.545.

Using the efficiency product data resulting for this design, the required expander back pressure is calculated and shown in Fig. 101 as function of the pump flow rate for high pressure and low pressure operation. The cyclic speed is proportional to the flowrate and the required NPSH value increases with the square of the speed as shown in Fig. 102.

Additional effort is required to establish the control system necessary to match the drive requirements to the pumping requirements. An excess drive capability is required to allow adjustment of the overall pump-drive operating point to match the design point required performance. Bypass of a small amount of drive flow with a control valve or orifice should provide this capability.

Mechanical Design

Design 6 is an in-line double acting piston drive with two pumps (one at each end) acting 180 degrees out of phase. There are three major moving parts, the main piston, servo valve, and solenoid valve. The piston has two inlet check valves, one in each pump end. The main pump housing has two discharge check valves corresponding to the two ends of the piston. The pumps operate in a very simple double check valve piston pump fashion. The drive is actuated by delta pressure alternated from side to side by the servo valve. The servo valve is, in turn, shuttled back and forth by alternating pressure from a solenoid valve which alternately pressurizes the ends of the servo valve, while allowing the other end to vent through an orifice to drive discharge pressure. The unit is machined from Inco 718 forgings. As with Design 5, the tolerances required to maintain the very close fits needed are very small (0.0002 inch). Alignment is critical for the main piston and will therefore require line-boring and precision line-grinding. The cylinder (sleeve) in which the pump operates is surrounded by incoming liquid methane. This will maintain a constant and uniform temperature in the sleeve and will help maintain the proper clearances. Sealing is performed by aluminum-bronze piston rings, three in each pump and

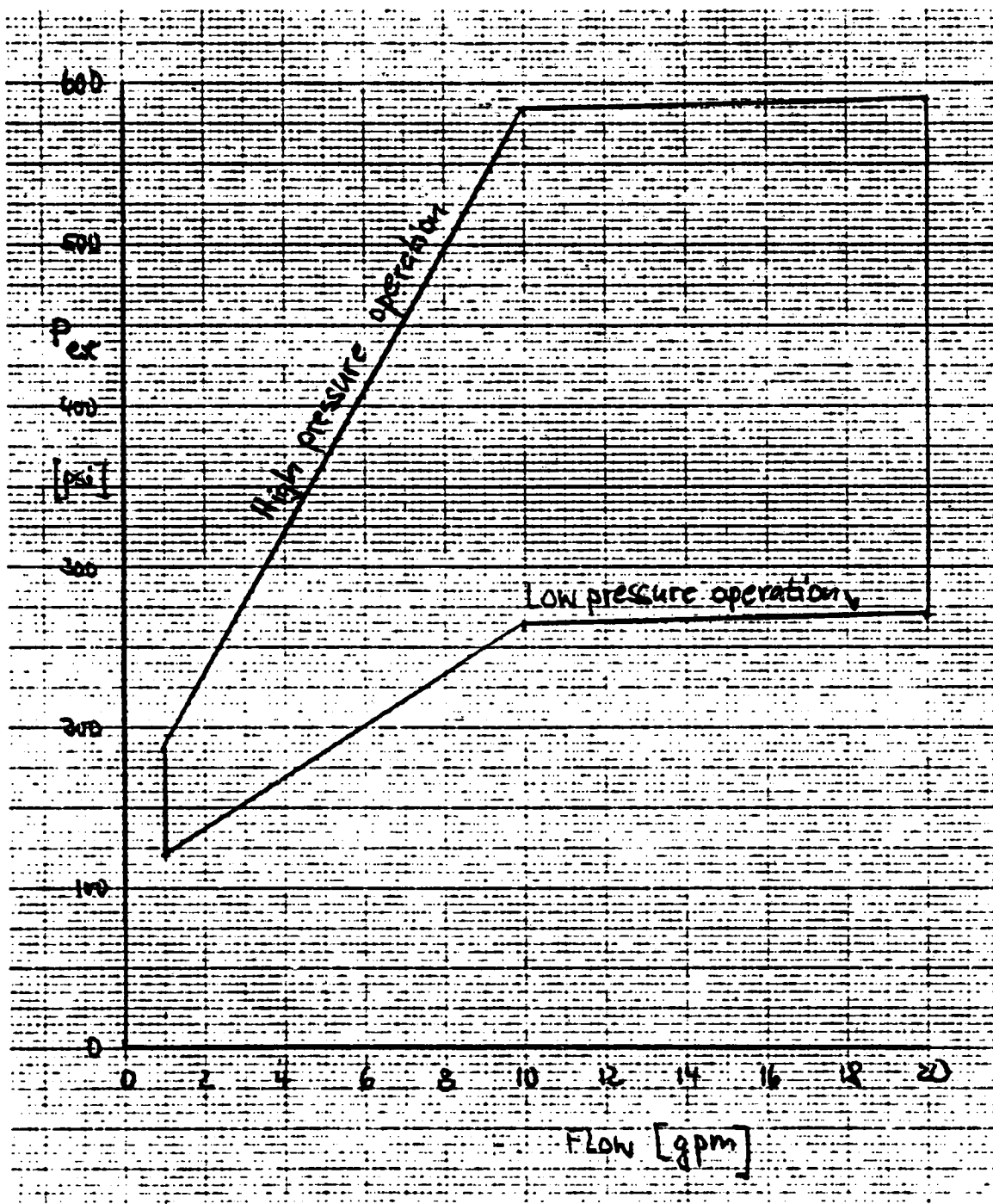


Figure 101. Methane Pump-Drive Back Pressures

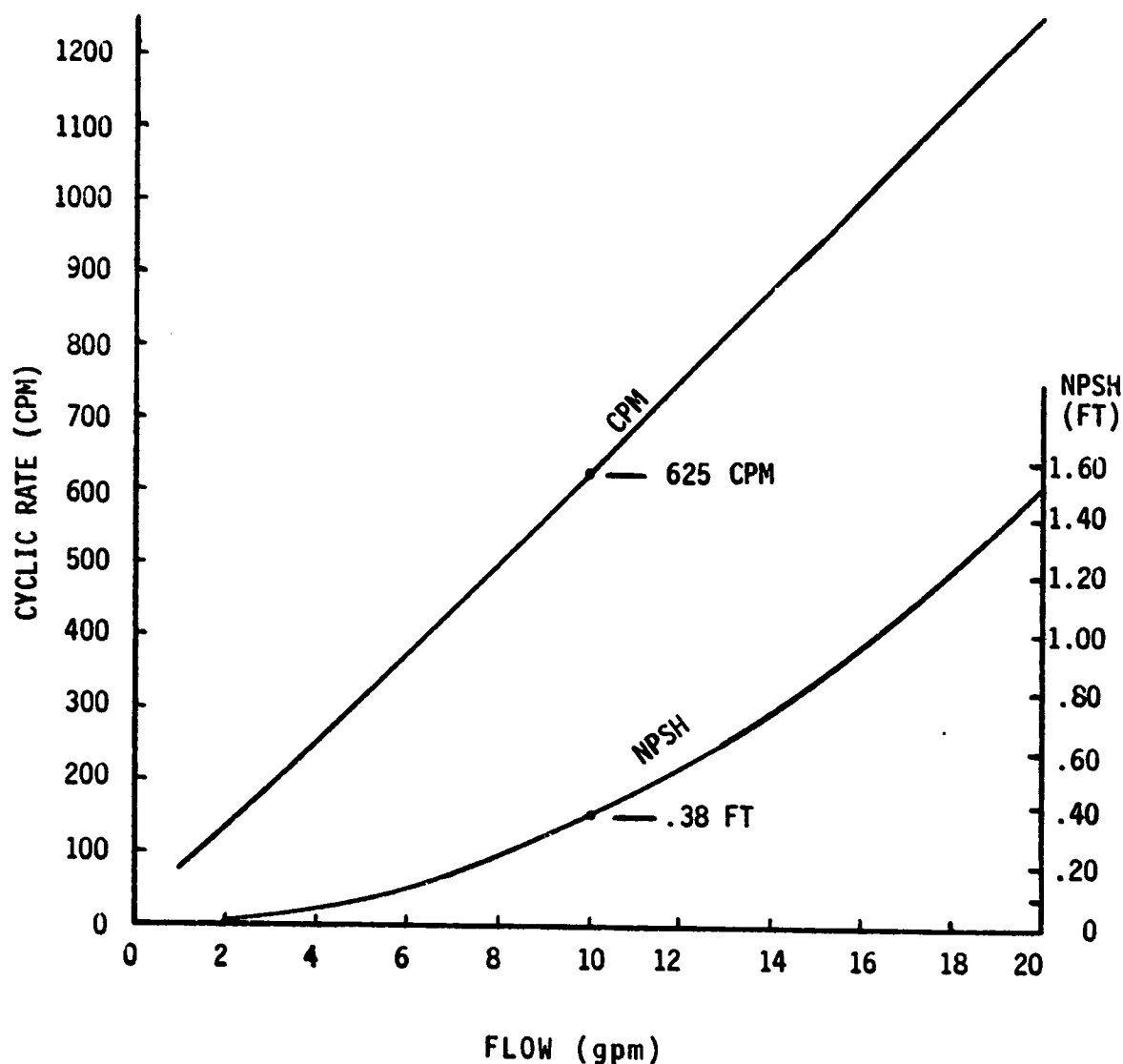


Figure 102. Cyclic Speed is Proportional to Flow Rate and Required NPSH Value Increases With the Square of Speed

three in the drive. No bearings are required. The average sliding velocity of the piston is 3.47 ft/sec. The timing of the solenoid valve will be such that the pressure difference on the drive will be vented just prior to the end of the stroke allowing the piston to be decelerated to even lower velocity by the pumping force. This will reduce the impact forces generated by the drive piston colliding with the housing. During the 5-hour life of the unit, 375,000 such collisions will take place. It is important that neither the piston nor housing yield (even locally) during these collisions. Stress analysis has shown that the bearing stresses are very low and no yielding is expected. Because of the low velocities, the inertial stresses are also very low. The thick walls required for alignment and clearance control result in very low pressure vessel stresses. As a result, no significant stress problems are expected.

Weight Analysis

The weight (dry) of Design 6 is 57.83 kg (127.5 lb). The main piston weights 3.93 kg (8.68 lb) and all others weight 64.69 kg (118.82 lb). A part by part weight breakdown is shown in Fig. 103.

Life Assessment

Life is sensitive to rubbing velocities and time. The velocity of the piston is low but over the planned life it will rub against the cylinder for 62,500 feet (19,050 m) or 11.8 miles (19.0 km). This is not a long distance for automobile pistons; they last 6 to 7 orders of magnitude longer. In an auto engine, however, the oil film lubricates the rubbing parts. Methane has a lubricity of nearly zero. This requires hydrostatic film separation of the parts to produce acceptable life. To establish the life of the piston pump-drive a development program must be performed. This will aid in establishing optimum clearance, configuration, and materials.

Performance and Manufacturing Risk

A low flow piston pump was successfully fabricated and tested in the late 1960's. No piston expander experience has been obtained at Rocketdyne. Rockwell International does have experience in the commercial application of piston expanders. This experience can be drawn upon if required. As mentioned above a development program is required to resolve the issues of performance and producibility. As with the vane pump-motor, the piston pumpdrive requires precision machining.

Cost Analysis

The cost of Design 6 is estimated at \$102,200 for tooling and \$149,400 recurring. The tooling consists of \$31,800 for raw material and \$70,400 for machining. The recurring cost consists of \$6,500 for raw material and purchased parts and \$142,900 for precision machining.

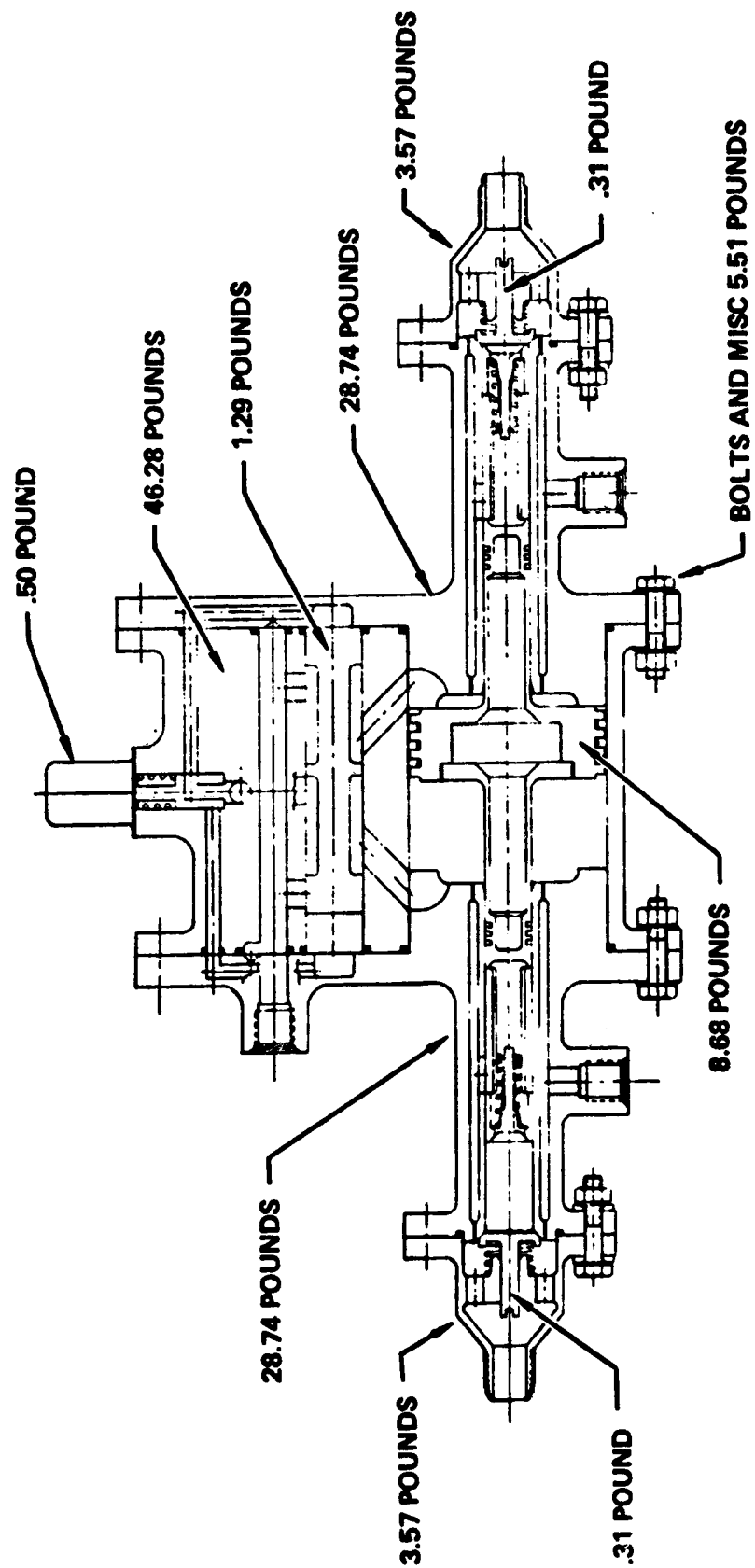


Figure 103. Design 6 Weighs 567 N (127.5 Pounds)

TASK IV DISCUSSION: TECHNOLOGY ASSESSMENT

Examination of the design parameters generated in the Analysis of Candidate Pumps (Task I) and Preliminary Design (Task II) phases of this contract indicate that several turbopump elements are required to function in operating regions or conditions where the empirical base is limited. Testing is needed to substantiate the performance predictions made on an analytical basis and to be able to select the optimum detail approach from a family of promising concepts. Technology validation is needed in the following areas:

- Pump Hydrodynamic Performance
- Turbine Gas Dynamic Performance
- Bearing Life
- Rotordynamics
- Dynamic Seal Efficiency

The above list is roughly in the order of decreasing importance. In the following sections, each of the above areas is discussed in some detail; the technology problems or unknowns are identified; an approach for obtaining the desired information is outlined; and a preliminary program plan and schedule are presented.

PUMP HYDRODYNAMIC PERFORMANCE

Figure 104 illustrates the design head-flow points of pumps designed and tested by Rocketdyne. Experience is most prevalent at high flowrates, e.g., over 1000 gpm, with fewer data points in the range of 100 to 1000 gpm and very limited exposure below 100 gpm. The pattern is believed to be representative of general experience in the industry as well. As noted in Fig. 104, the operating range of the pumps for a low-thrust chemical rocket engine falls in the range where empirical data are very limited.

The study conducted as part of this program has indicated that centrifugal pump types are the best candidates for low-thrust chemical rocket engine applications, when taking into account performance, weight, life, reliability, and producibility. The following discussion of pump technology requirements, therefore, addresses that pump concept.

Goals

To place the pump technology for this application on a firm basis, data are needed to substantiate the analytically predicted performance values at low specific speeds and small size. Anchoring of the performance maps in data should provide more accurate tradeoffs among the potentially applicable approaches; facilitate a more precise engine definition; and minimize the early development problems.

PRECEDING PAGE BLANK NOT FILMED

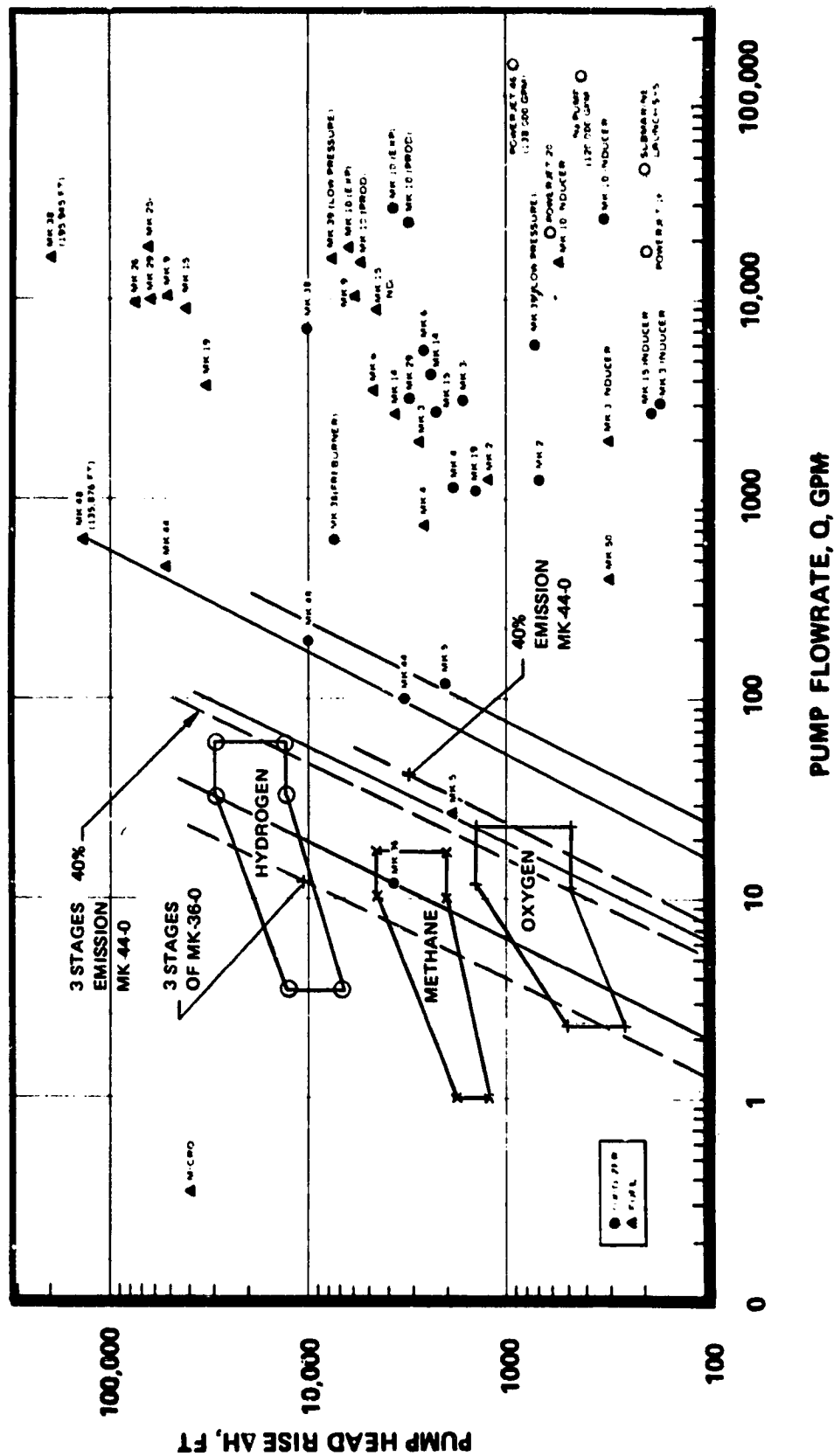


Figure 104. Flowrate vs Head for Pumps Manufactured by Rocketdyne

The technology effort should be directed toward obtaining generic information on the most effective approaches to attaining high pump performance in the low specific speed region. Increasing pump performance is of interest because it leads to lower turbine power requirement and, ultimately, to higher engine specific impulse. In certain cases, improved performance per stage could lead to a reduction in the number of stages required, with attendant mechanical and cost benefits.

Programs directed at establishing pump technology should have the parallel goal of confirming the producibility of the proposed concepts. This goal should have the dual function of defining the limits of producibility with current costing and manufacturing practices, and of eliminating procurement blind alleys during the development phase.

The study of candidate pump concepts has revealed that the shear force pumping concept (Tesla pump) may offer advantages in terms of suction performance capability, when used as an inducer stage. The benefit was primarily applicable for engines of >1000 pounds thrust. Improved suction capability would facilitate operating the rotor, which may include several centrifugal stages, at higher operating speed with attendant increase in efficiency and reduction in size.

Basic data should be generated with the shear force pump to define its performance and mechanical characteristics.

Approach

The recommended approach for obtaining the general technology data noted above is to use actual scale hardware in a pump tester in which the test articles of the various pump concepts can be installed interchangeably, tested, and removed on an economical basis. Testing should be initiated by screening several pump concepts in water at approximately 40,000 rpm. This should provide a comparison of the competing approaches at a comparatively low cost. Based on the water test results, the design that exhibits the most desirable performance characteristics should be tested in the propellants of interest, i.e., liquid hydrogen, liquid methane, or liquid oxygen. Cost savings can be realized if the tester designed for water testing can be constructed with sufficient flexibility to permit its use in the propellant test series as well.

Recommended Test Articles

Based on the defined operating regions for this program, the following specific test articles are recommended for evaluation in water:

1. Conventional Pumps - Full Emission
Specific Speeds - 250, 550

2. Partial Admission - Diffuser Controlled

Based on MK 36* - $N_s = 328, 465, 735$

New Pump - $N_s = 544, 769, 1216$

3. Partial Admission - Impeller Controlled

New Pump - $N_s = 544$

4. Open-Face Design

New Pump - $N_s = 544$

5. Tesla Inducer

Inducer and Housing Tested as a Pump

Program Schedule

The program elements involved in the pump technology effort are noted in Fig. 105, with an estimate of the time phasing of the various tasks.

TURBINE GAS DYNAMIC PERFORMANCE

The turbine designs that evolved to drive the centrifugal pumps from this study program have very low power requirements and, consequently, are characterized by low volume flowrates and low pressure ratios. Beyond a certain point, it is not practical to reduce blade and nozzle heights to match the flowrate in regard to area. The cases studied in this program required that the arc of admission of the nozzle be reduced to the range of 5.6 to 30%. Technology effort is needed to define the efficiency of these low-admission, low-pressure-ratio turbines. Rocketdyne has used axial-impulse turbines in the designs generated as part of this study. Other concepts, i.e., radial inflow, Terry, or re-entry staging, could be competitive and might be explored to advantage in a technology program.

Goals

The goals of the recommended turbine technology program are to define the performance of low-pressure-ratio, partial-admission, axial-impulse turbines in the power range of 10 to 50 bhp, and to explore design modifications that have the potential of improving performance. A further objective is to obtain comparative data on competing concepts.

Approach

To obtain the above information, full-scale hardware should be used and turbine efficiency as a function of gas spouting velocity ratio should be established using a tester in conjunction with a power-absorbing dynamometer or torque meter. Ambient-temperature GH_2 or air should be used as the propellant, and the turbine tip speed should be reduced to match the design velocity relationships.

*Rotating and Positive Displacement Pumps for Low-Thrust Rocket Engines, NASA CR-72965.

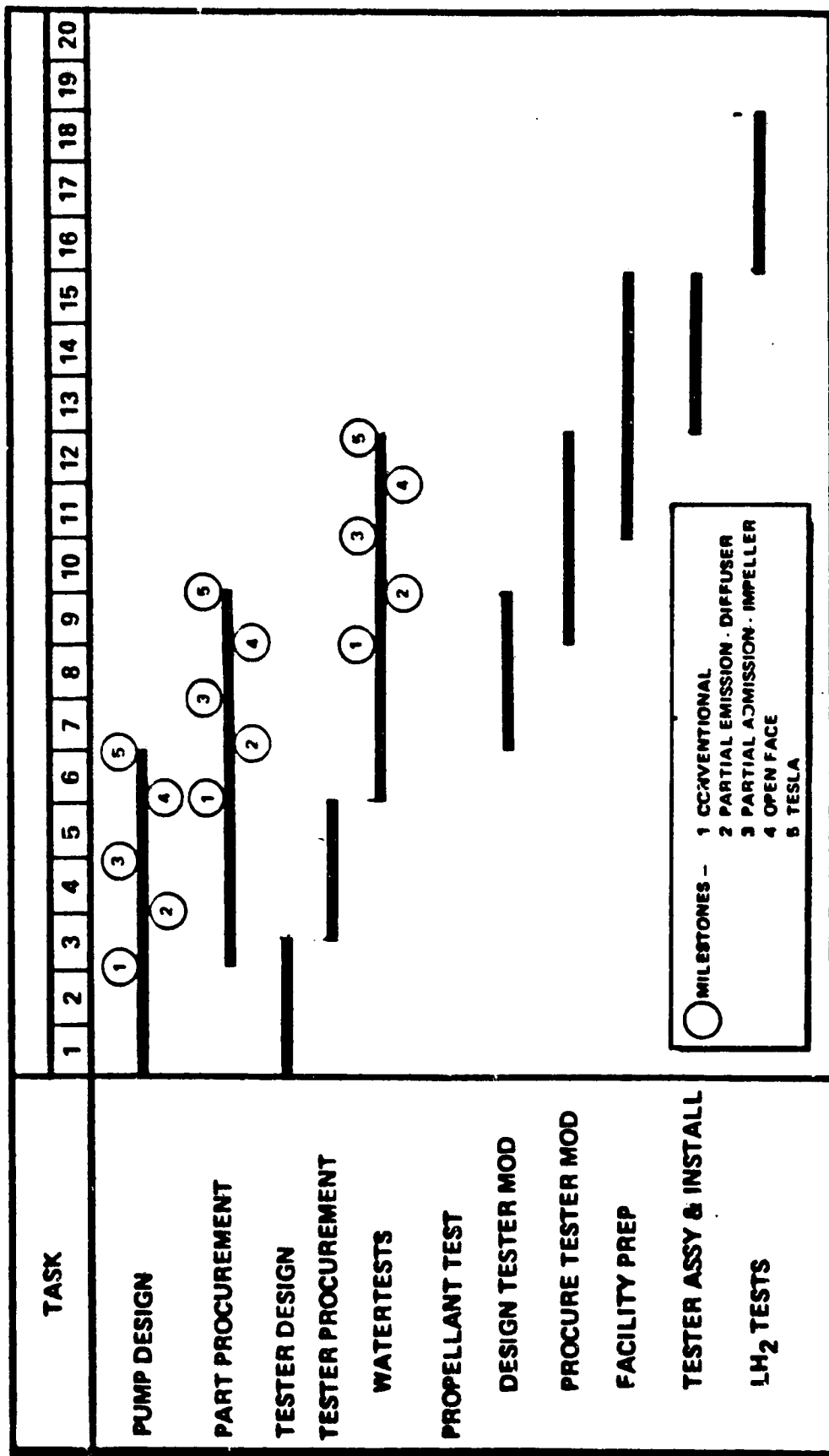


Figure 105. Pump Technology Advancement Schedule

Test Article

Testing is recommended to establish the performance characteristics of a low-specific-speed, low-admission, axial-impulse turbine with a blade height of 0.38 cm (0.150 inch), which is currently considered the lower limit from a performance standpoint. The efficiency of the turbine should be determined over a wide range of velocity ratios at approximately the following admission percentages: 5, 10, 25, 50, and 100%.

The second phase of the turbine technology effort should be devoted to determining if the turbine efficiency of the above concept can be improved by modifying some of the design parameters. Specifically, a lower blade height should be tested to determine if an improvement in efficiency can be realized with an increase in the arc of admission. The benefits of incorporating an axial seal over the inactive segment of the rotor should be assessed, and the relative advantages of the two-stage, partial-admission concept versus re-entry staging should be determined.

Potentially competitive alternate concepts for this application are the radial inflow and Terry turbines. Testing of these concepts would be worthwhile to explore the possibility of increasing performance or obtaining comparable performance with a more cost-effective concept.

Program Schedule

The anticipated schedule of a turbine technology program is outlined in Fig. 106.

BEARING LIFE

Speed limits (in terms of diameter x rpm) based on theoretical analysis are lower for the smaller-bore ball bearings utilized in small, high-rotational-speed, centrifugal pumps, but experimental data are needed to define these limits with more certainty, including the producibility of durable Armalon cages below the 15 mm bearing bore size in question. Testing should be conducted to provide data on both counts relative to current design concepts. In addition, improvements in the life and reliability of small ball bearings can be realized by applying recent material developments in the balls and races and possibly to the cage.

A potential alternate approach toward a significant increase in life and speed capability may be offered by hydrostatic bearings. Their feasibility has been demonstrated in liquid hydrogen in turbopump testing at Rocketdyne, and more recently in a tester at NASA-LeRC. The operating characteristics and design constraints of hydrostatic bearings need to be defined in cryogenic high-speed applications.

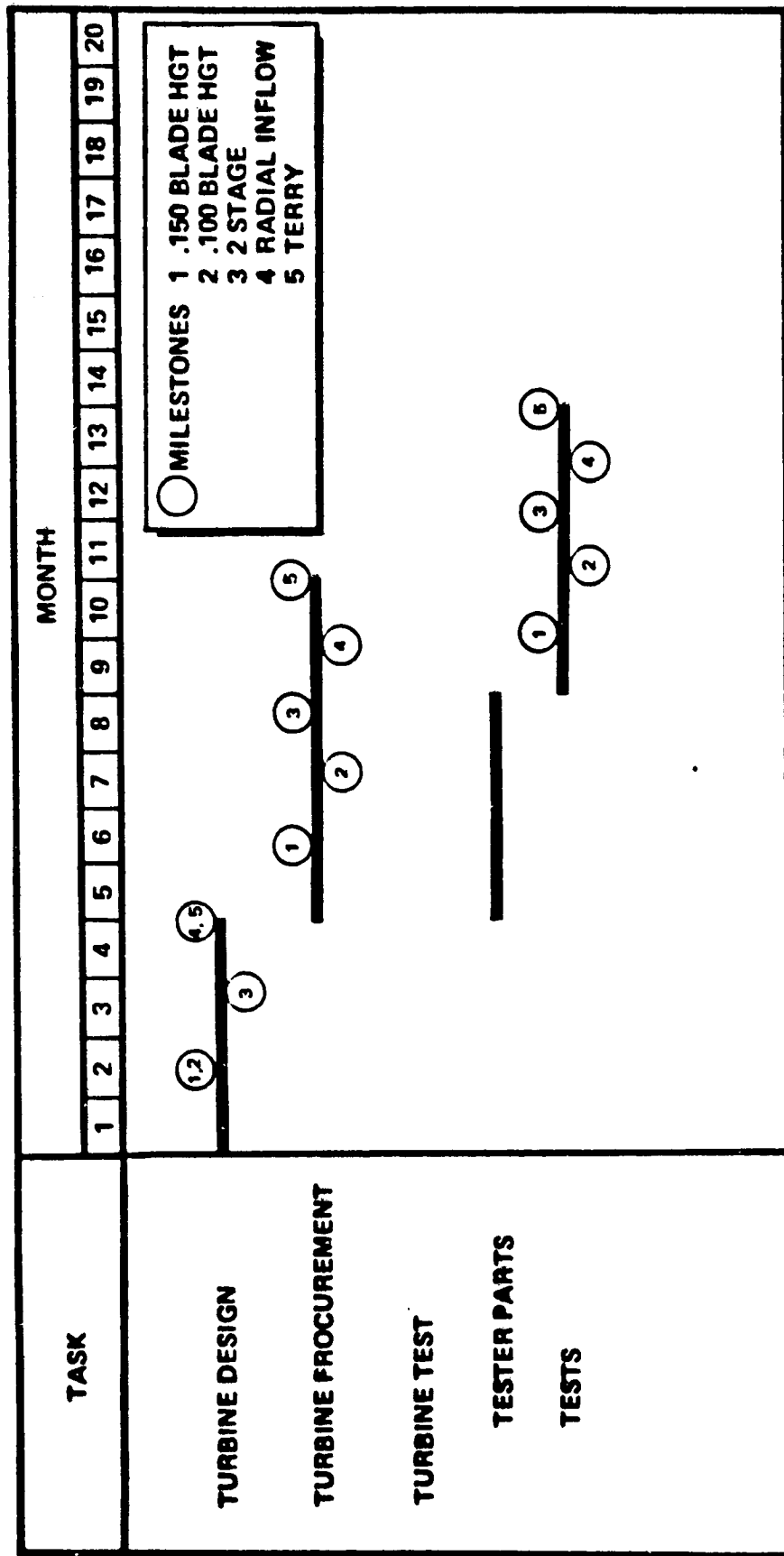


Figure 106. Turbine Technology Advancement Program

Approach and Test Articles

The specific recommendations are to procure both 440C and BG42 (AMS 5749) races and balls in the 10 mm size and attempt to produce cages in that size from Armalon. If Armalon cages of acceptable quality cannot be produced in the 10 mm size, an alternate material must be selected and evaluated. Potential candidates may be Rulon or nylon (LH₂).

Testing should be conducted in liquid hydrogen at turbopump operating speeds in a tester capable of applying radial and axial loads on the bearings. The length of test time and the corresponding test cost can be reduced by applying higher loads than predicted for the turbopumps and analytically converting the data to predict life with the lower loads.

Bearings made of 440C should be tested to establish a baseline with current materials in small sizes, followed by testing of newer materials to determine if an improvement in life can be realized.

Technology effort is currently in progress both at NASA-LeRC and Rocketdyne to demonstrate the applicability of hydrostatic bearings in a hybrid concept that also includes ball bearings to function during start and shutdown transient periods. Basic technology information will be obtained in these programs; follow-ons may be required to work out any problems in the concept.

Program Schedule

The program schedule of rolling-element bearings is dominated by procurement time requirements which, for special orders of this type, extend to a minimum of 1 year and possibly longer. In accordance, a 20-month schedule is outlined in Fig. 107 for a ball bearing technology program. In addition to the design and fabrication of test bearings, either an existing tester would have to be modified to accommodate smaller bore bearings or a new tester would need to be designed and fabricated. A minimum of 6 months should be allowed for the test activity with liquid hydrogen.

ROTORDYNAMICS

Because of the high speeds of low-thrust rocket engine turbomachinery, the rotors operate above one or more critical speeds. To achieve satisfactory operation under these conditions, the rotor, as assembled into the turbopump, must be precisely balanced. Current practice in which the rotating assembly is balanced at low speeds (≈ 2000 rpm), disassembled, and reassembled at pump build, may not yield an acceptable precision in the final assembled state. An assessment of the residual imbalance level is needed and the amount of imbalance that can be tolerated needs to be defined. If the repeatability with the current procedure is unacceptable, two approaches should be evaluated: a method of performing final balance measurements and corrections after the rotor is assembled in the housings should be explored ("in-place balancing"), or the concept of using integral rotors (i.e., rotors that are not disassembled after balancing) and split internal housings should be studied.

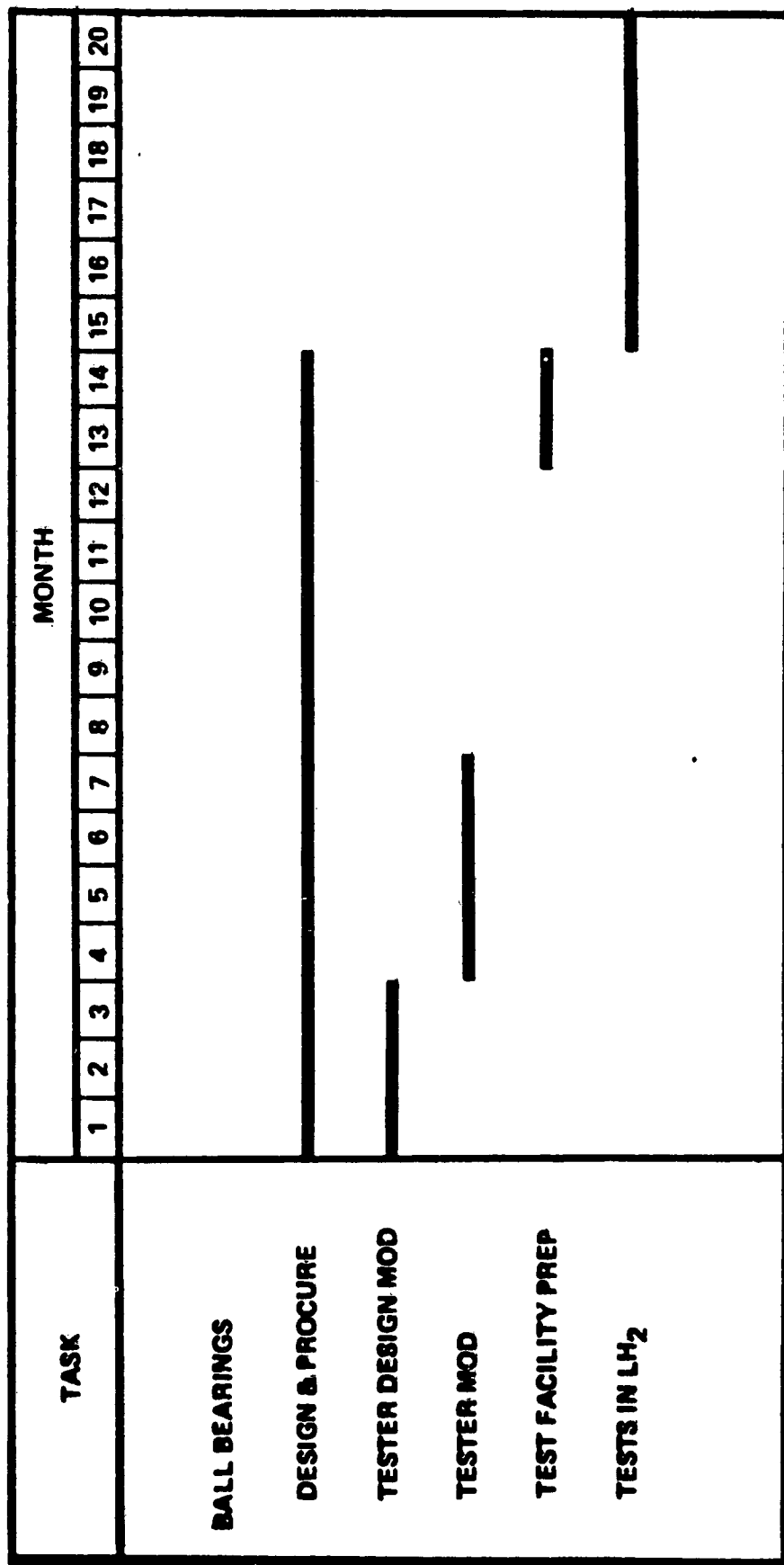


Figure 107. Bearing Technology Assessment Schedule

Empirical-based information is needed to improve rotordynamic analytical programs. Data are needed on the spring rate of small bearings, and the damping coefficients need to be determined for the sizes and speeds under consideration.

Approach and Test Articles

The information relative to rotordynamic behavior can best be obtained by utilizing a tester with actual turbopump bearings to support the test rotor, and with a small, ambient-temperature, air-driven turbine as the driver. Impeller masses, piloting, and general balancing and assembly procedures should duplicate proposed turbopump concepts. The tests can be run in air to determine critical speeds from which bearing radial spring rates can be derived. To measure damping coefficients, testing would have to be conducted in liquid hydrogen or other propellants of interest.

Testing should address the three considerations discussed above. First, a series of balance and rotor vibration tests should be conducted to document the rotor response to various balancing techniques. Rotors should be balanced at low speed (2000 rpm), high speed (>first critical), and after assembly in the housing. Residual imbalances should be established and the respective rotor responses documented. Second, small-bearing stiffness should be measured by comparing actual and predicted critical speeds. Finally, the rotors should be tested in liquid hydrogen and damping coefficients should be measured by monitoring rotor motion, housing vibration, and forces between simulated impellers and housings with strain gages on the housing members.

Program Schedule

The principal phases of the recommended rotordynamic technology program are presented in Fig. 108 with estimated time requirements.

DYNAMIC SEAL EFFICIENCY

Because of the low pump flowrates, low-thrust rocket engines must include shaft seals with low leakage rates. Although the shaft rotational speeds are high, the sizes are relatively small and, as a result, the surface speeds are in a range where conventional rubbing face seals may be applicable. The key issue with conventional face seals is whether they can meet the 10- to 50-hour life requirement. Testing needs to be conducted to determine this issue with authority. If rubbing seals prove impractical, hydrodynamic liftoff seals need to be developed.

Approach and Test Articles

The recommended program is to first determine the feasibility of applying conventional rubbing contact seal concepts by conducting a test program in which life, leakage, and power loss factors are established, then to develop hydrodynamic liftoff seals for application where conventional seals are not practical.

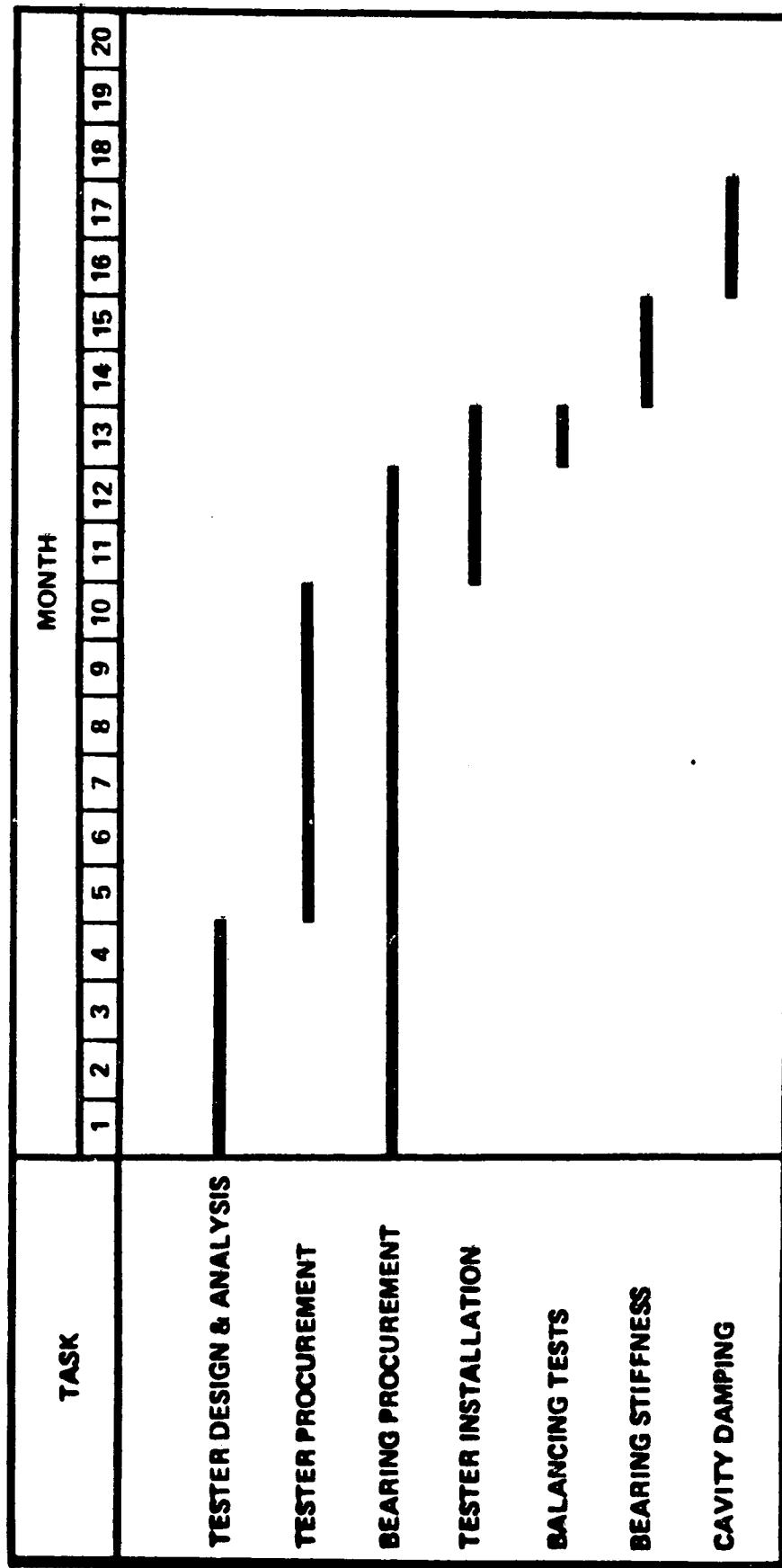


Figure 108. Shaft Dynamic Assessment Schedule

The specific concepts recommended are as follows. Moderate speeds of the liquid oxygen pumps should make conventional seals applicable; therefore, testing of an axial, face-rubbing, carbon-nose seal is recommended for the primary LOX seal and a segmented, carbon, shaft-riding seal for the intermediate seal. Lack of cooling and higher differential pressures would eliminate rubbing-contact types for the turbine seal. For this location, a floating-ring, controlled radial gap-type carbon seal is recommended.

The higher rotating speeds of liquid hydrogen pumps rule out rubbing-contact seals, which leaves the floating-ring type as the most attractive concept.

Should the face-type seal prove unacceptable from a life consideration for the primary LOX seal, a spiral-groove, hydrodynamic, liftoff seal should be developed by testing in a tester in which pump fluid conditions and mating ring motions can be accurately simulated.

Program Schedule

The principal components of a seal technology program and their time phasing are presented in Fig. 109.

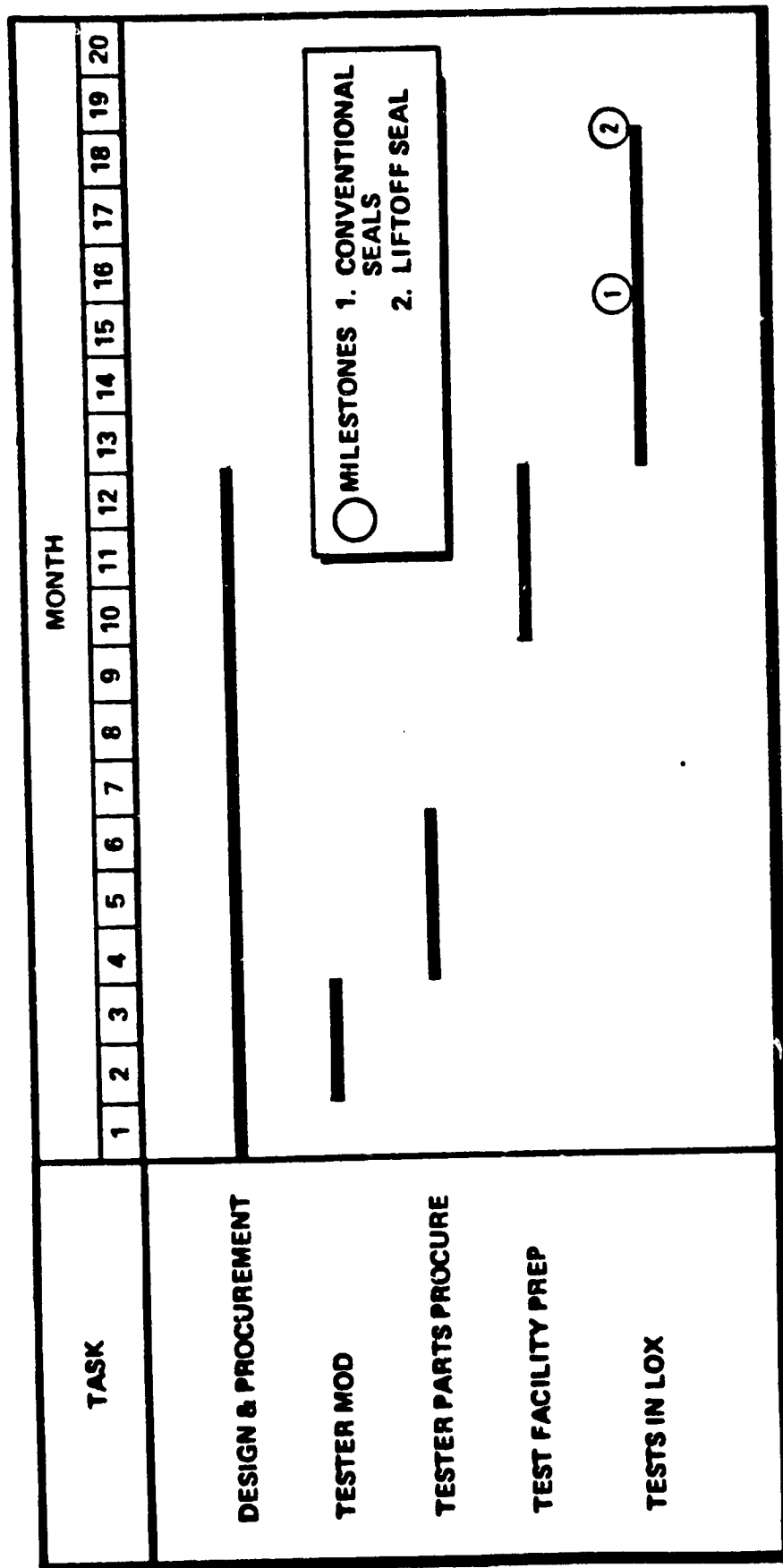


Figure i09. Seal Technology Assessment Schedule

APPENDIX A
TASK I CURVES

- Figure A-1. Centrifugal LOX Pump - NPSH = 2 Feet, Speed
- Figure A-2. Centrifugal LOX Pump - NPSH = 2 Feet, Efficiency (Two Stages Maximum)
- Figure A-3. Centrifugal LOX Pump - NPSH = 2 Feet, Efficiency (Four Stages Maximum)
- Figure A-4. Centrifugal LOX Pump - NPSH = 2 Feet, Diameter (Two Stages Maximum)
- Figure A-5. Centrifugal LOX Pump - NPSH = 2 Feet, Diameter (Four Stages Maximum)
- Figure A-6. Centrifugal LOX Pump - NPSH = 2 Feet, Discharge Width (Two Stages Maximum)
- Figure A-7. Centrifugal LOX Pump - NPSH = 2 Feet, Discharge Width (Four Stages Maximum)
- Figure A-8. Centrifugal LOX Pump - NPSH = 2 Feet, Power (Two Stages Maximum)
- Figure A-9. Centrifugal LOX Pump - NPSH = 2 Feet, Power (Four Stages Maximum)
- Figure A-10. Centrifugal LOX Pump - NPSH = 6.05 Feet, Speed
- Figure A-11. Centrifugal LOX Pump - NPSH = 6.5 Feet, Efficiency (Two Stages Maximum)
- Figure A-12. Centrifugal LOX Pump - NPSH = 6.05 Feet, Efficiency (Four Stages Maximum)
- Figure A-13. Centrifugal LOX Pump - NPSH = 6.05 Feet, Diameter (Two Stages Maximum)
- Figure A-14. Centrifugal LOX Pump - NPSH = 6.5 Feet, Diameter (Four Stages Maximum)
- Figure A-15. Centrifugal LOX Pump - NPSH = 6.05 Feet, Discharge Width (Two Stages Maximum)
- Figure A-16. Centrifugal LOX Pump - NPSH = 6.05 Feet, Discharge Width (Four Stages Maximum)
- Figure A-17. Centrifugal LOX Pump - NPSH = 6.05 Feet, Power (Two Stages Maximum)
- Figure A-18. Centrifugal LOX Pump - NPSH = 6.05 Feet, Power (Four Stages Maximum)
- Figure A-19. Centrifugal LOX Pump - NPSH Optimized
- Figure A-20. Centrifugal LOX Pump - NPSH Optimized, Speed ($N_s = 2000$)
- Figure A-21. Centrifugal LOX Pump - NPSH Optimized, Speed ($D_t = 0.7$ inch)
- Figure A-22. Centrifugal LOX Pump - NPSH Optimized, Efficiency ($N_s = 2000$)
- Figure A-23. Centrifugal LOX Pump - NPSH Optimized, Efficiency ($D_t \geq 0.7$ inch)

- Figure A-24. Centrifugal LOX Pump - NPSH Optimized, Diameter ($N_s = 2000$)
- Figure A-25. Centrifugal LOX Pump - NPSH Optimized, Diameter ($D_t \geq 0.7$ inch)
- Figure A-26. Centrifugal LOX Pump - NPSH Optimized, Discharge Width ($N_s = 2000$)
- Figure A-27. Centrifugal LOX Pump - NPSH Optimized, Discharge Width ($D_t \geq 0.7$ inch)
- Figure A-28. Centrifugal Methane Pump - NPSH = 6 Feet, Design Limitations
- Figure A-29. Centrifugal Methane Pump - NPSH = 6 Feet, Speed
- Figure A-30. Centrifugal Methane Pump - NPSH = 6 Feet, Speed ($S_s = 30,000$)
- Figure A-31. Centrifugal Methane Pump - NPSH = 6 Feet, Efficiency
- Figure A-32. Centrifugal Methane Pump - NPSH = 6 Feet, Diameter
- Figure A-33. Centrifugal Methane Pump - NPSH = 6 Feet, Discharge Width
- Figure A-34. Centrifugal Methane Pump - NPSH = 6 Feet, Power
- Figure A-35. Centrifugal Methane Pump - NPSH = 16.47 Feet, Speed
- Figure A-36. Centrifugal Methane Pump - NPSH = 16.47 Feet, ($S_s = 30,000$)
- Figure A-37. Centrifugal Methane Pump - NPSH = 16.47 Feet, Efficiency
- Figure A-38. Centrifugal Methane Pump - NPSH = 16.47 Feet, Diameter
- Figure A-39. Centrifugal Methane Pump - NPSH = 16.47 Feet, Discharge Width
- Figure A-40. Centrifugal Methane Pump - NPSH = 16.47 Feet, Power
- Figure A-41. Centrifugal Methane Pump - NPSH Optimized
- Figure A-42. Centrifugal Methane Pump - NPSH Optimized, Speed ($N_s = 1950$)
- Figure A-43. Centrifugal Methane Pump - NPSH Optimized, Speed ($D_t \geq 0.7$ inch)
- Figure A-44. Centrifugal Methane Pump - NPSH Optimized, Efficiency ($N_s = 1950$)
- Figure A-45. Centrifugal Methane Pump - NPSH Optimized, Efficiency ($D_t \geq 0.7$ inch)
- Figure A-46. Centrifugal Methane Pump - NPSH Optimized, Diameter ($N_s = 1950$)
- Figure A-47. Centrifugal Methane Pump - NPSH Optimized, Diameter ($D_t \geq 0.7$ inch)
- Figure A-48. Centrifugal Methane Pump - NPSH Optimized, Discharge Width ($N_s = 1950$)
- Figure A-49. Centrifugal Methane Pump - NPSH Optimized, Discharge Width ($D_t \geq 0.7$ inch)
- Figure A-50. Centrifugal Hydrogen Pump - NPSH = 15 Feet, Speed
- Figure A-51. Centrifugal Hydrogen Pump - NPSH = 15 Feet, Efficiency
- Figure A-52. Centrifugal Hydrogen Pump - NPSH = 15 Feet, Diameter
- Figure A-53. Centrifugal Hydrogen Pump - NPSH = 15 Feet, Discharge Width
- Figure A-54. Centrifugal Hydrogen Pump - NPSH = 15 Feet, Power

- Figure A-55. Centrifugal Hydrogen Pump - NPSH = 83.6 Feet, Limitations
- Figure A-56. Centrifugal Hydrogen Pump - NPSH = 83.6 Feet, Speed
- Figure A-57. Centrifugal Hydrogen Pump - NPSH = 83.6 Feet, Efficiency
- Figure A-58. Centrifugal Hydrogen Pump - NPSH = 83.6 Feet, Diameter
- Figure A-59. Centrifugal Hydrogen Pump - NPSH = 83.6 Feet, Discharge Width
- Figure A-60. Centrifugal Hydrogen Pump - NPSH = 83.6 Feet, Power
- Figure A-61. Centrifugal Hydrogen Pump - NPSH Optimized
- Figure A-62. Centrifugal Hydrogen Pump - NPSH Optimized, Speed
- Figure A-63. Centrifugal Hydrogen Pump - NPSH Optimized, Efficiency
($D_t \geq 0.7$ inch)
- Figure A-64. Centrifugal Hydrogen Pump - NPSH Optimized, Efficiency
($N = 190,000$ rpm)
- Figure A-65. Centrifugal Hydrogen Pump - NPSH Optimized, Diameter
($D_t \geq 0.7$ inch)
- Figure A-66. Centrifugal Hydrogen Pump - NPSH Optimized, Diameter
($N = 190,000$ rpm)
- Figure A-67. Centrifugal Hydrogen Pump - NPSH Optimized, Discharge Width
($D_t \geq 0.7$ inch)
- Figure A-68. Centrifugal Hydrogen Pump - NPSH Optimized, Discharge Width
($N = 190,000$ rpm)
- Figure A-69. Pitot Pump Performance Data
- Figure A-70. Pitot Pump Optimum D/σ as a Function of Specific Speed
- Figure A-71. Pitot LOX Pump - NPSH = 2 Feet, Speed
- Figure A-72. Pitot LOX Pump - NPSH = 2 Feet, Diameter
- Figure A-73. Pitot LOX Pump - NPSH = 2 Feet, Power
- Figure A-74. Pitot LOX Pump - NPSH = 6.05 Feet, Speed
- Figure A-75. Pitot LOX Pump - NPSH = 6.05 Feet, Diameter
- Figure A-76. Pitot Methane Pump - NPSH = 6 Feet, Speed
- Figure A-77. Pitot Methane Pump - NPSH = 6 Feet, Efficiency
- Figure A-78. Pitot Methane Pump - NPSH = 6 Feet, Diameter
- Figure A-79. Pitot Methane Pump - NPSH = 6 Feet, Power
- Figure A-80. Pitot Methane Pump - NPSH = 16.47 Feet, Speed (Two Stages)
- Figure A-81. Pitot Methane Pump - NPSH = 16.47 Feet, Speed
- Figure A-82. Pitot Methane Pump - NPSH = 16.47 Feet, Efficiency (Two Stages)
- Figure A-83. Pitot Methane Pump - NPSH = 16.47 Feet, Efficiency
- Figure A-84. Pitot Methane Pump - NPSH = 16.47 Feet, Diameter (Two Stages)

- Figure A-85. Pitot Methane Pump - NPSH = 16.47 Feet, Diameter
- Figure A-86. Pitot Methane Pump - NPSH = 16.47 Feet, Power (Two Stages)
- Figure A-87. Pitot Hydrogen Pump - NPSH = 15 Feet, Speed
- Figure A-88. Pitot Hydrogen Pump - NPSH = 15 Feet, Diameter
- Figure A-89. Pitot Hydrogen Pump - NPSH = 15 Feet, Power
- Figure A-90. Pitot Hydrogen Pump - NPSH = 83.57 Feet, Speed
- Figure A-91. Pitot Hydrogen Pump - NPSH = 83.57 Feet, Speed (Two Stages)
- Figure A-92. Pitot Hydrogen Pump - NPSH = 83.57 Feet, Efficiency
- Figure A-93. Pitot Hydrogen Pump - NPSH = 83.57 Feet, Diameter
- Figure A-94. Pitot Hydrogen Pump - NPSH = 83.57 Feet, Diameter (Two Stages)
- Figure A-95. Pitot Hydrogen Pump - NPSH = 83.57 Feet, Power
- Figure A-96. Tesla LOX Pump, Speed
- Figure A-97. Tesla LOX Pump, Efficiency
- Figure A-98. Tesla LOX Pump, Diameter
- Figure A-99. Tesla LOX Pump, Power
- Figure A-100. Tesla Methane Pump, Speed - NPSH = 6 Feet
- Figure A-101. Tesla Methane Pump, Efficiency - NPSH = 6 Feet
- Figure A-102. Tesla Methane Pump, Diameter - NPSH = 6 Feet
- Figure A-103. Tesla Methane Pump, Power - NPSH = 6 Feet
- Figure A-104. Tesla Hydrogen Pump, Speed
- Figure A-105. Tesla Hydrogen Pump, Efficiency
- Figure A-106. Tesla Hydrogen Pump, Diameter
- Figure A-107. Tesla Hydrogen Pump, Power
- Figure A-108. Drag LOX Pump, Optimum Stages - NPSH = 2 Feet
- Figure A-109. Drag LOX Pump, Speed vs Diameter
- Figure A-110. Drag LOX Pump, Diameter, NPSH = 2 Feet, (Six Stages)
- Figure A-111. Drag LOX Pump, Diameter, (15 Inch Maximum) NPSH = 2 Feet, Six Stages
- Figure A-112. Drag LOX Pump, Diameter (12 Inch Maximum) NPSH = 6.05 Feet, Six Stages
- Figure A-113. Drag Methane Pump, Speed vs Diameter
- Figure A-114. Drag Methane Pump, Diameter (12 Inch Maximum) NPSH = 6 Feet, Six Stages
- Figure A-115. Drag Methane Pump, Diameter (12 Inch Maximum) NPSH = 16.47 Feet, Six Stages
- Figure A-116. Drag Hydrogen Pump, Speed vs Diameter

- Figure A-117. Drag Hydrogen Pump, Diameter, NPSH = 15 Feet
- Figure A-118. Drag Hydrogen Pump, Diameter, NPSH = 83.57 Feet
- Figure A-119. Vane LOX Pump - C/D = 0.00025, Speed, NPSH = 2 Feet
- Figure A-120. Vane LOX Pump - C/D = 0.00025, Efficiency, NPSH = 2 Feet
- Figure A-121. Vane LOX Pump - C/D = 0.00025, Efficiency (Vane L/D \leq 1.5), NPSH = 2 Feet
- Figure A-122. Vane LOX Pump - C/D = 0.00050, Efficiency, NPSH = 2 Feet
- Figure A-123. Vane LOX Pump - C/D = 0.00075, Efficiency, NPSH = 2 Feet
- Figure A-124. Vane LOX Pump - C/D = 0.00025, Diameter, NPSH = 2 Feet
- Figure A-125. Vane LOX Pump - C/D = 0.00025, Diameter (Vane L/D \leq 1.5) NPSH = 2 Feet
- Figure A-126. Vane Methane Pump - C/D = 0.00025, Speed, NPSH = 6 Feet
- Figure A-127. Vane Methane Pump - C/D = 0.00025, Efficiency, NPSH = 6 Feet
- Figure A-128. Vane Methane Pump - C/D = 0.00025, Efficiency (Vane L/D \leq 1.5), NPSH = 6 Feet
- Figure A-129. Vane Methane Pump - C/D = 0.00050, Efficiency, NPSH = 6 Feet
- Figure A-130. Vane Methane Pump - C/D = 0.00075, Efficiency, NPSH = 6 Feet
- Figure A-131. Vane Methane Pump - C/D = 0.00025, Diameter, NPSH = 6 Feet
- Figure A-132. Vane Methane Pump - C/D = 0.00025, Diameter (Vane L/D \leq 1.5), NPSH = 6 Feet
- Figure A-133. Vane Hydrogen Pump - C/D = 0.00025, Speed
- Figure A-134. Vane Hydrogen Pump - C/D = 0.00025, Efficiency
- Figure A-135. Vane Hydrogen Pump - C/D = 0.00025, Efficiency (Vane L/D \leq 1.5)
- Figure A-136. Vane Hydrogen Pump - C/D = 0.00050, Efficiency
- Figure A-137. Vane Hydrogen Pump - C/D = 0.00075, Efficiency
- Figure A-138. Vane Hydrogen Pump - C/D = 0.00025, Diameter
- Figure A-139. Vane Hydrogen Pump - C/D = 0.00025, Diameter (Vane L/D \leq 1.5)
- Figure A-140. Piston LOX Pump, Speed, NPSH = 2 Feet
- Figure A-141. Piston LOX Pump, Efficiency, NPSH = 2 Feet
- Figure A-142. Piston LOX Pump, Diameter, NPSH = 2 Feet
- Figure A-143. Piston LOX Pump, Power, NPSH = 2 Feet
- Figure A-144. Piston Methane Pump, Speed, NPSH = 6 Feet
- Figure A-145. Piston Methane Pump, Efficiency, NPSH = 6 Feet
- Figure A-146. Piston Methane Pump, Diameter, NPSH = 6 Feet
- Figure A-147. Piston Methane Pump, Power, NPSH = 6 Feet

- Figure A-148. Piston Hydrogen Pump, Speed
- Figure A-149. Piston Hydrogen Pump, Efficiency
- Figure A-150. Piston Hydrogen Pump, Diameter
- Figure A-151. Piston Hydrogen Pump, Power
- Figure A-152. Piston Hydrogen Pump, Effect of Clearance on Efficiency
- Figure A-153. Gear Hydrogen Pump, Speed
- Figure A-154. Gear Hydrogen Pump, Efficiency
- Figure A-155. Gear Hydrogen Pump, Diameter
- Figure A-156. Impulse Turbine Drive for Centrifugal LOX Pump, Pressure Ratio
- Figure A-157. Impulse Turbine Drive for Centrifugal LOX Pump, Efficiency
- Figure A-158. Impulse Turbine Drive for Centrifugal LOX Pump, Diameter
- Figure A-159. Impulse Turbine Drive for Centrifugal LOX Pump, Blade Height
- Figure A-160. Impulse Turbine Drive for Centrifugal Methane Pump, Pressure Ratio, NPSH = 6 Feet
- Figure A-161. Impulse Turbine Drive for Centrifugal Methane Pump, Efficiency
- Figure A-162. Impulse Turbine Drive for Centrifugal Methane Pump, Diameter
- Figure A-163. Impulse Turbine Drive for Centrifugal Methane Pump, Blade Height
- Figure A-164. Impulse Turbine Drive for Centrifugal Methane Pump, Percent Admission
- Figure A-165. Impulse Turbine Drive for Centrifugal Hydrogen Pump, Pressure Ratio
- Figure A-166. Impulse Turbine Drive for Centrifugal Hydrogen Pump, Efficiency
- Figure A-167. Impulse Turbine Drive for Centrifugal Hydrogen Pump, Diameter
- Figure A-168. Impulse Turbine Drive for Centrifugal Hydrogen Pump, Blade Height
- Figure A-169. Impulse Turbine Drive for Centrifugal Hydrogen Pump, Percent Admission
- Figure A-170. Vane Expander for Vane LOX Pump, Efficiency
- Figure A-171. Vane Expander for Vane LOX Pump, Diameter
- Figure A-172. Vane Expander for Vane LOX Pump, Efficiency ($P_1/P_2 = 1.3$)
- Figure A-173. Vane Expander for Vane LOX Pump, Diameter ($P_1/P_2 = 1.3$)
- Figure A-174. Vane Expander for Vane LOX Pump, Through Flow ($P_1/P_2 = 1.3$)
- Figure A-175. Vane Expander for Vane Methane Pump, Efficiency
- Figure A-176. Vane Expander for Vane Methane Pump, Diameter
- Figure A-177. Vane Expander for Vane Methane Pump, Efficiency ($P_1/P_2 = 1.3$)
- Figure A-178. Vane Expander for Vane Methane Pump, Diameter ($P_1/P_2 = 1.3$)
- Figure A-179. Vane Expander for Vane Methane Pump, Through Flow ($P_1/P_2 = 1.3$)

- Figure A-180. Vane Expander for Vane Hydrogen Pump, Efficiency
- Figure A-181. Vane Expander for Vane Hydrogen Pump, Diameter
- Figure A-182. Vane Expander for Vane Hydrogen Pump, Efficiency ($P_1/P_2 = 1.3$)
- Figure A-183. Vane Expander for Vane Hydrogen Pump, Diameter ($P_1/P_2 = 1.3$)
- Figure A-184. Vane Expander for Vane Hydrogen Pump, Through Flow ($P_1/P_2 = 1.3$)
- Figure A-185. Piston Expander for Piston Methane Pump, Diameter
- Figure A-186. Piston Expander for Piston Hydrogen Pump, Diameter

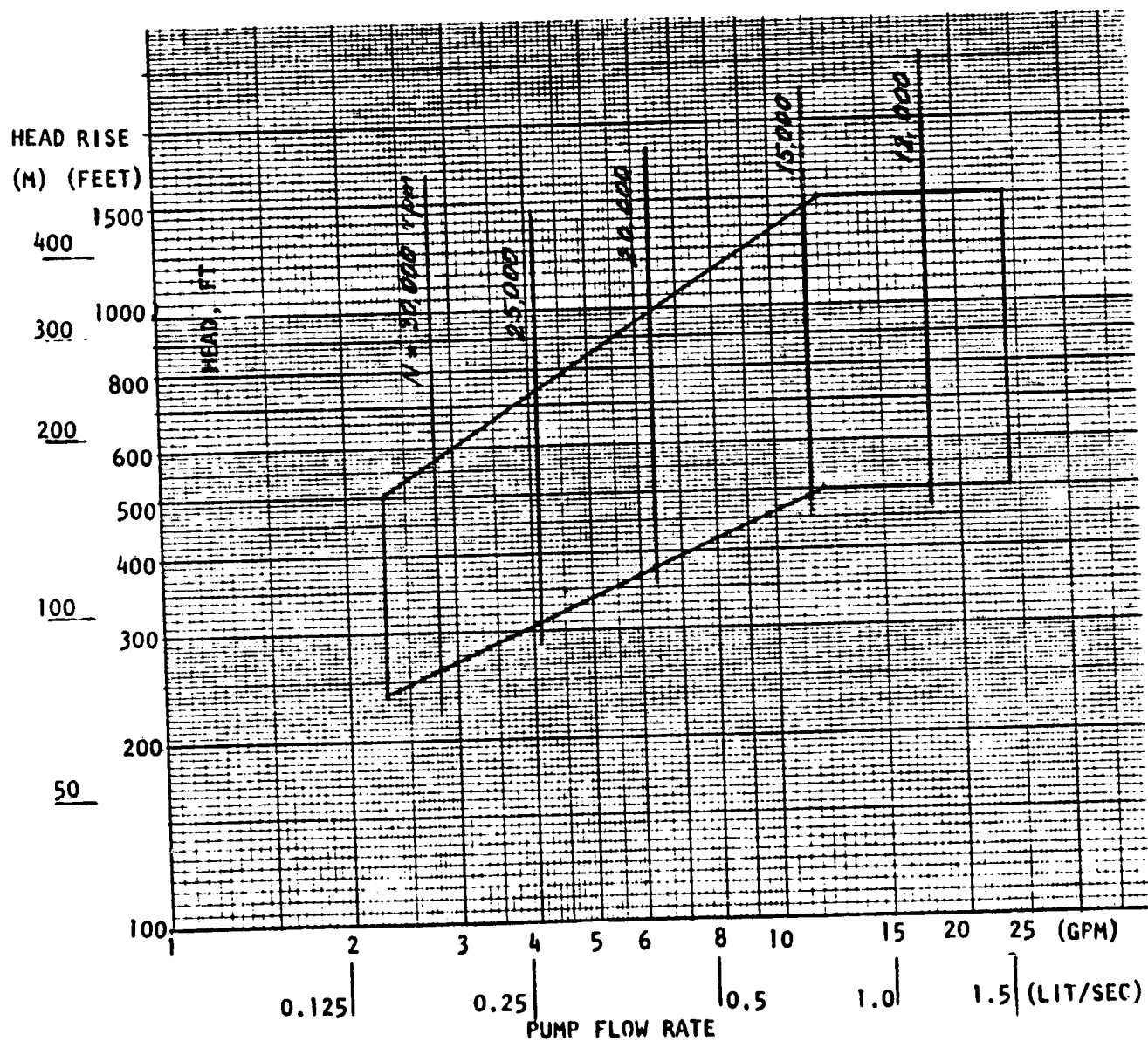


Figure A-1. Centrifugal LOX Pump - NPSH = 2 Feet, Speed

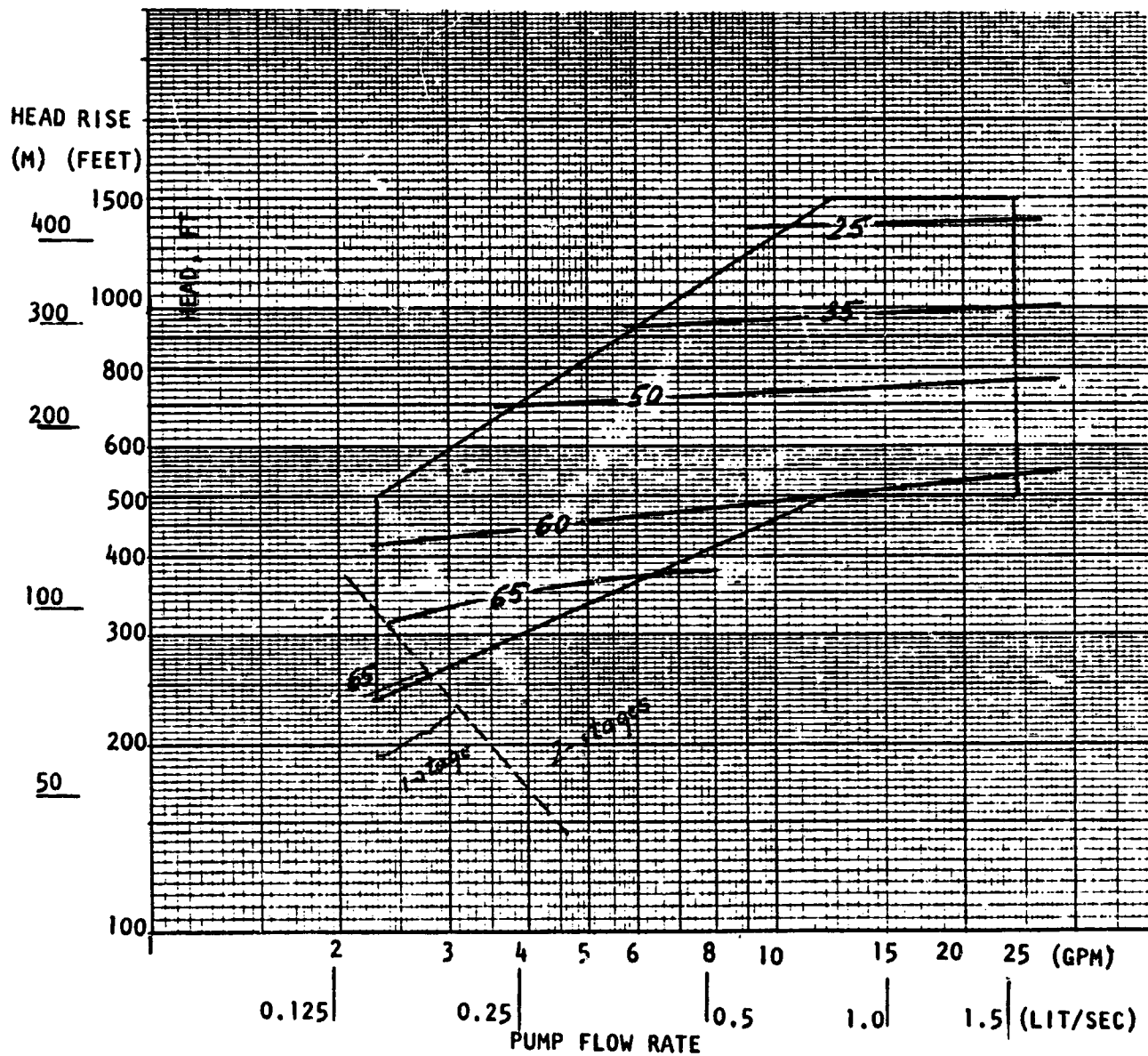


Figure A-2. Centrifugal LOX Pump - NPSH = 2 Feet, Efficiency (Two Stages Maximum)

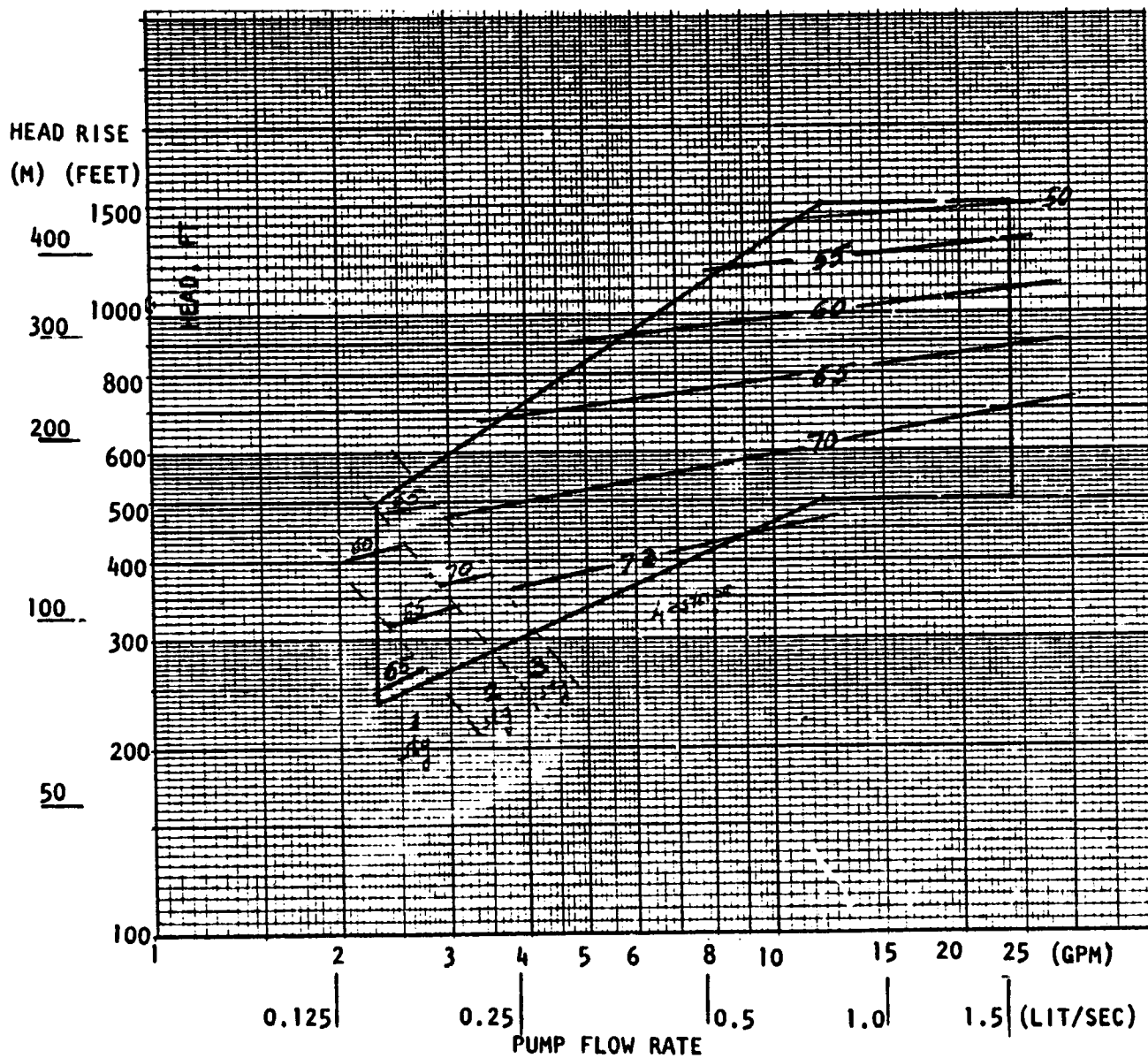


Figure A-3. Centrifugal LOX Pump - NPSH = 2 Feet, Efficiency (Four Stages Maximum)

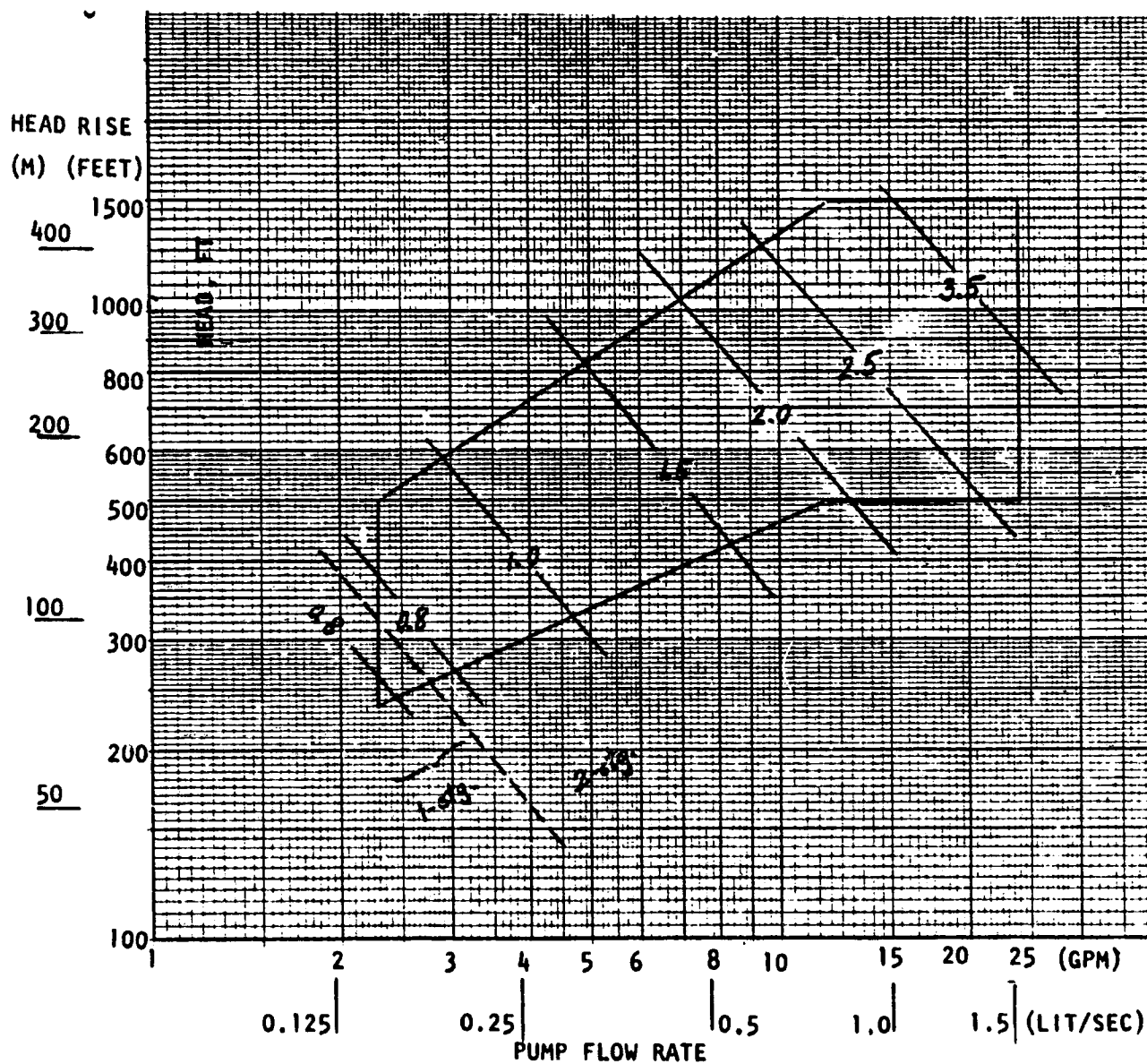


Figure A-4. Centrifugal LOX Pump - NPSH = 2 Feet, Diameter (Two Stages Maximum)

ORIGINAL PAGE IS
OF POOR QUALITY

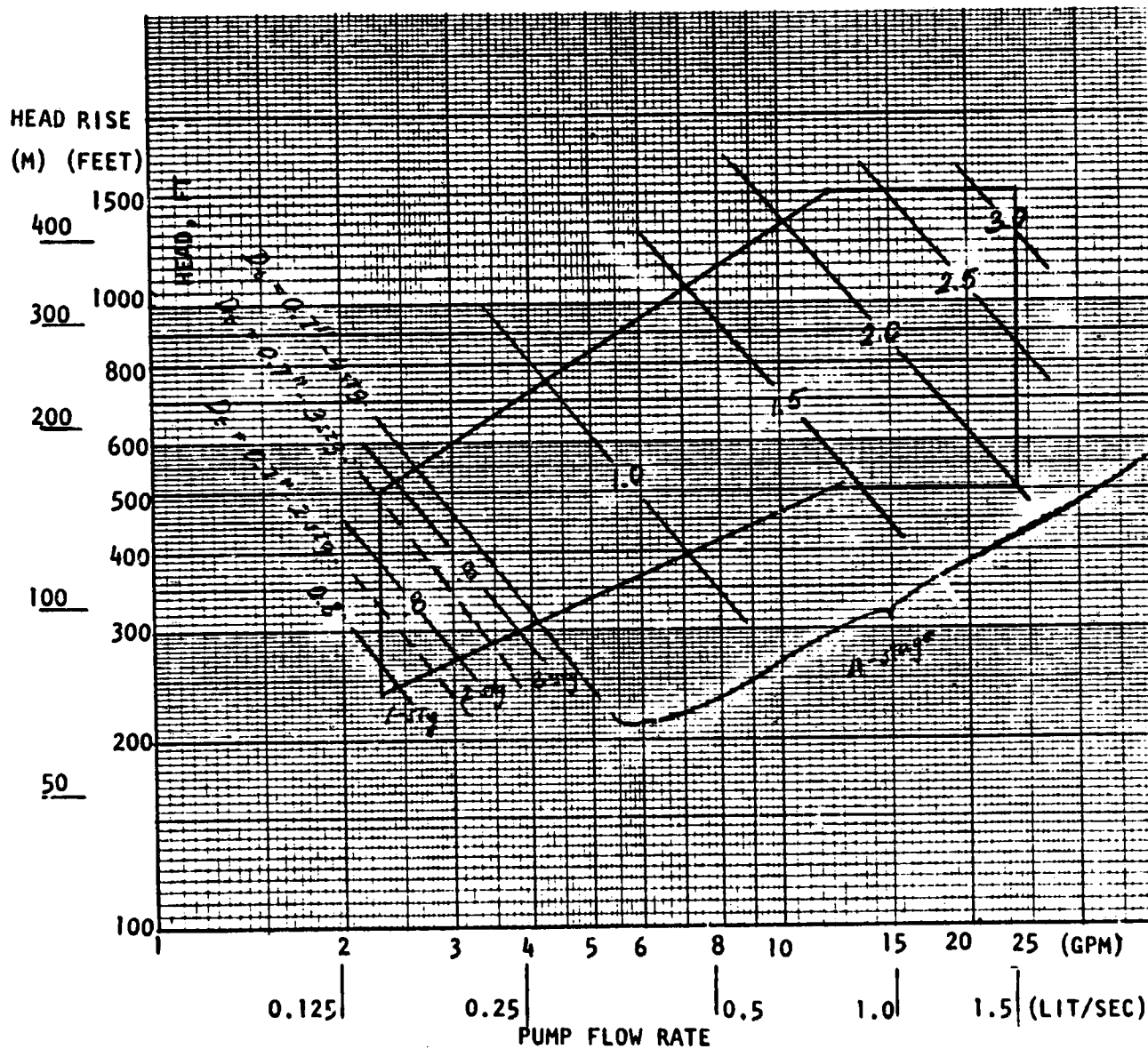


Figure A-5. Centrifugal LOX Pump - NPSH = 2 Feet, Diameter (Four Stages Maximum)

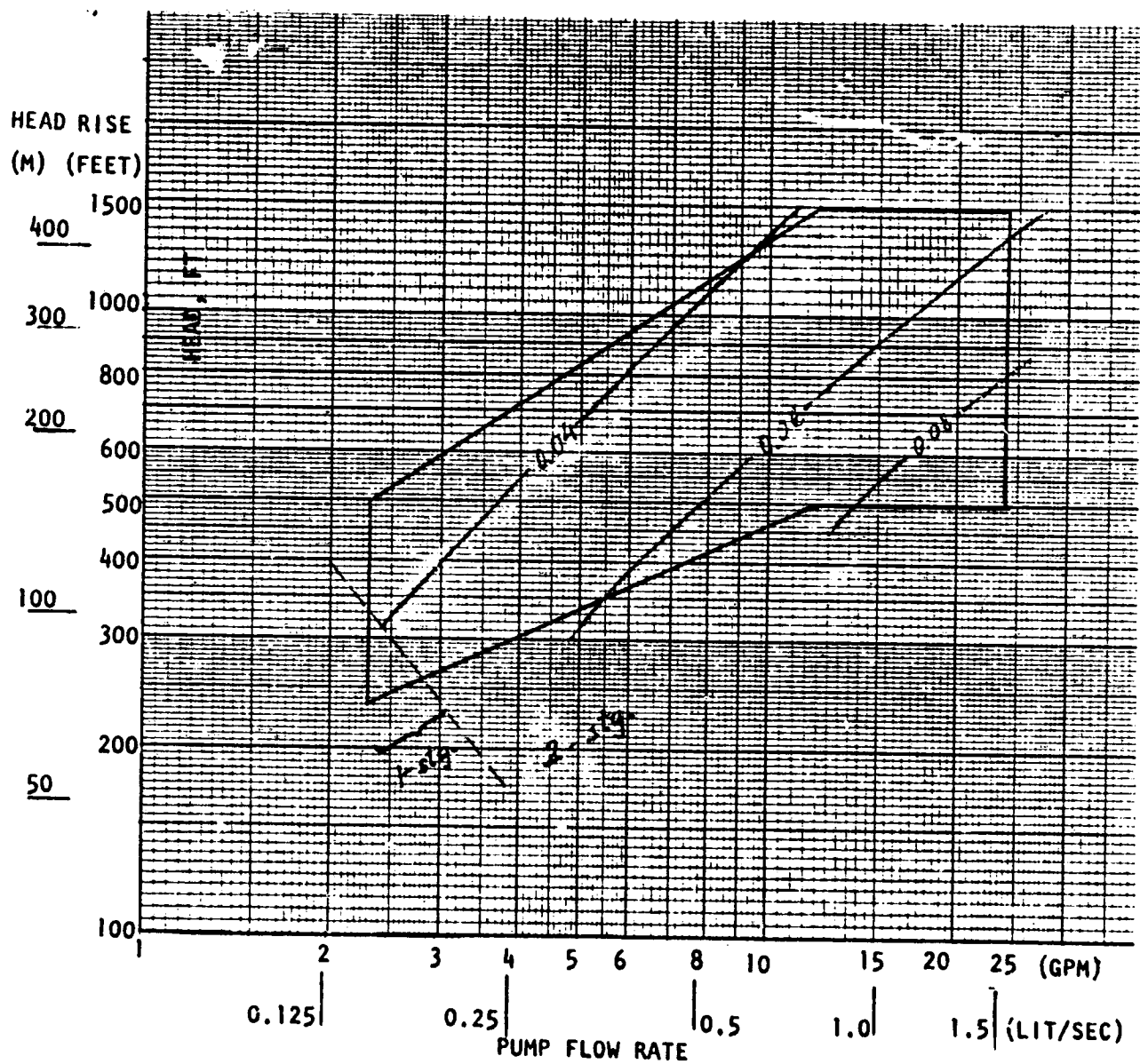


Figure A-6. Centrifugal LOX Pump - NPSH = 2 Feet, Discharge Width (Two Stages Maximum)

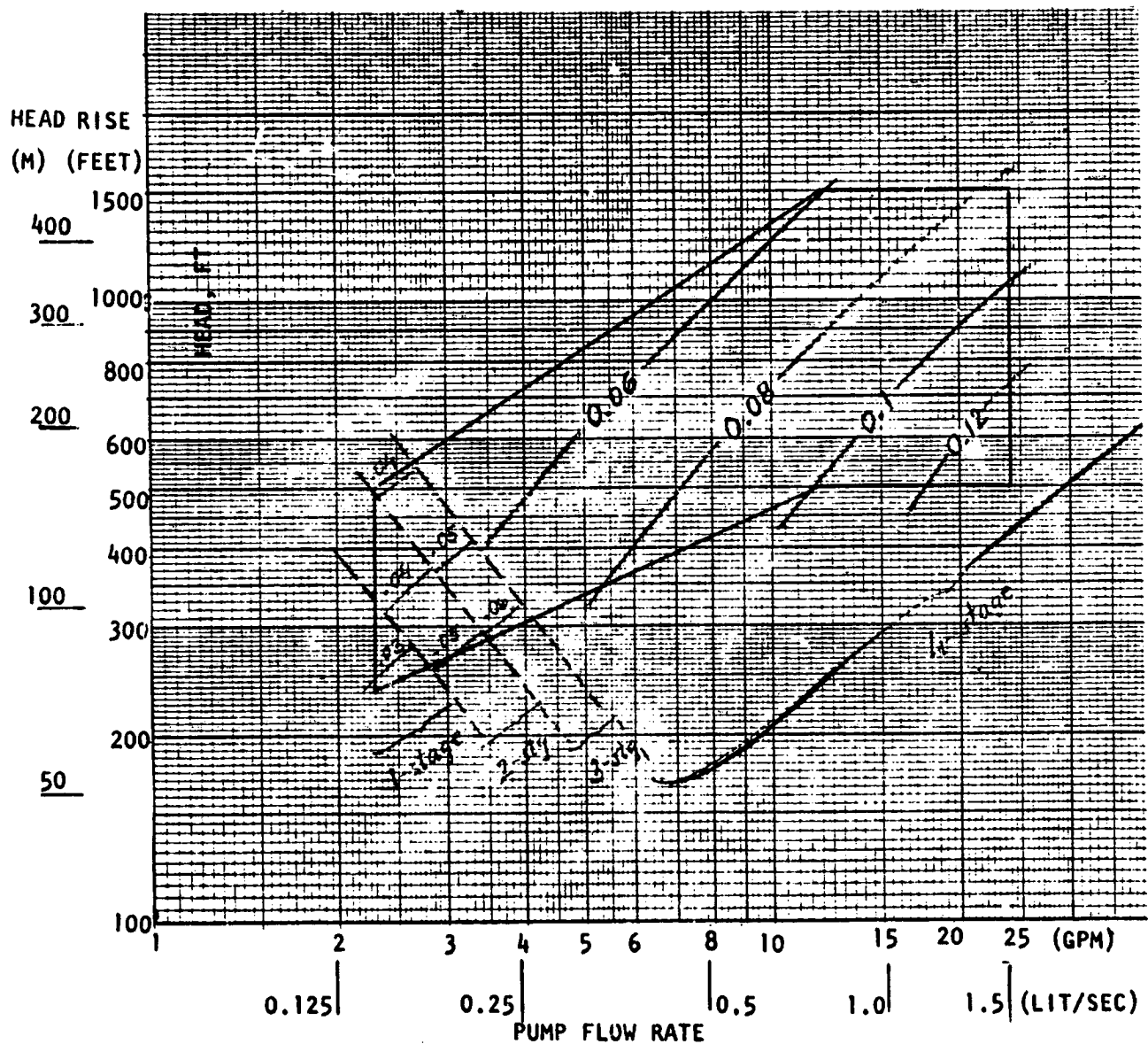


Figure A-7. Centrifugal LOX Pump - NPSH = 2 Feet, Discharge Width (Four Stages Maximum)

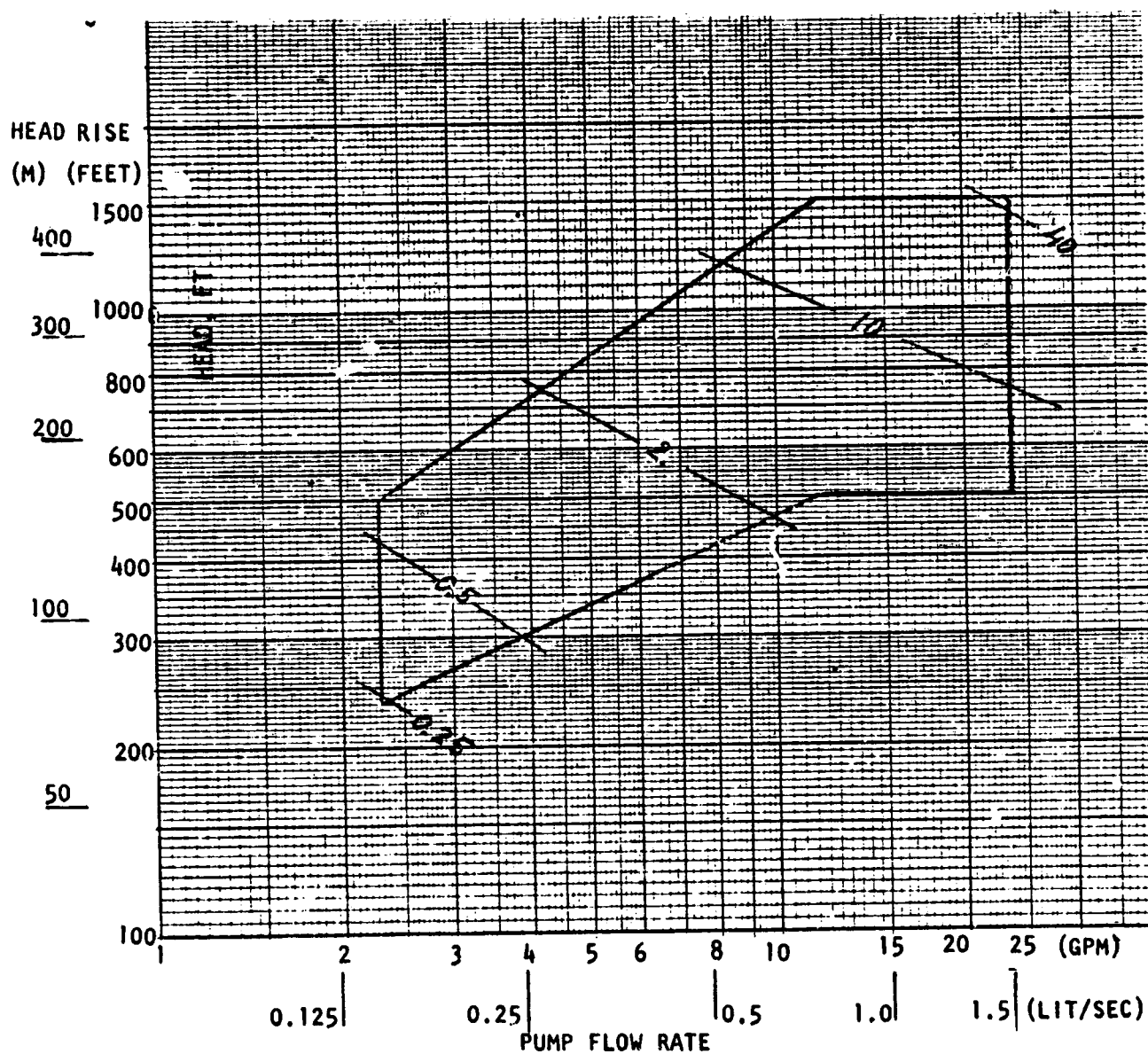


Figure A-8. Centrifugal LOX Pump - NPSH = 2 Feet, Power (Two Stages Maximum)

ORIGINAL PAGE IS
OF POOR QUALITY

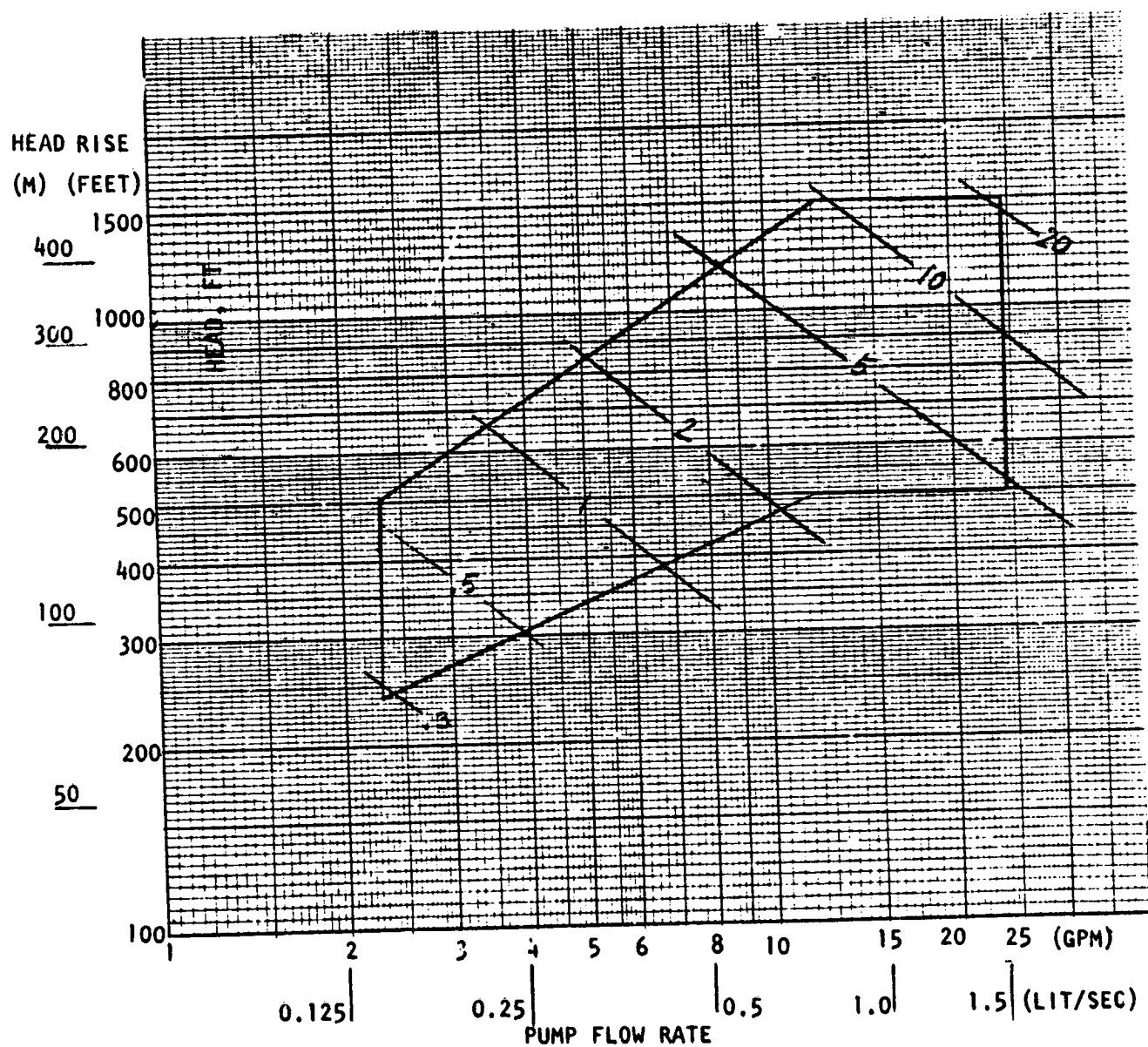


Figure A-9. Centrifugal LOX Pump - NPSH = 2 Feet, Power (Four Stages Maximum)

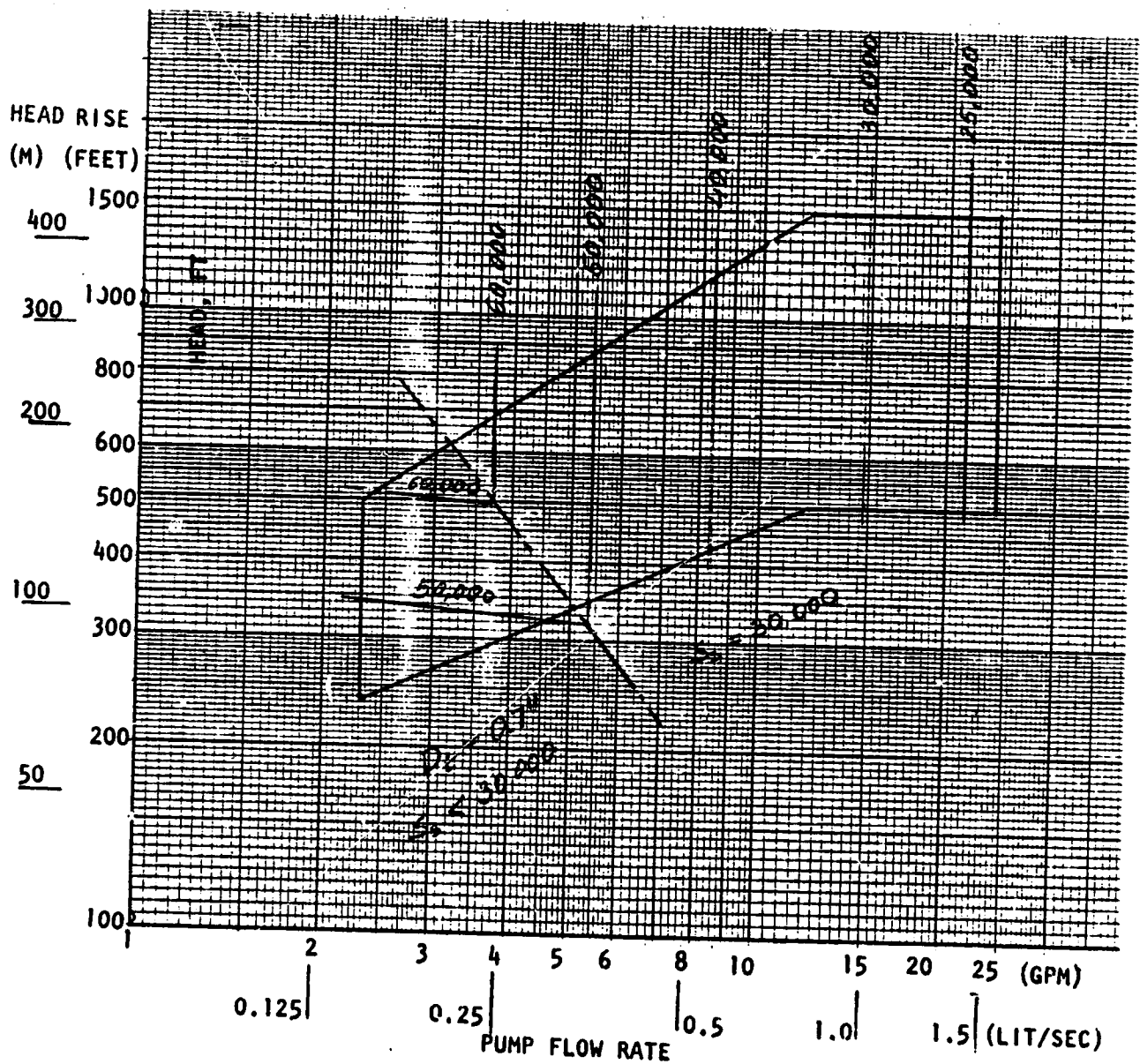


Figure A-10. Centrifugal LOX Pump - NPSH = 6.05 Feet, Speed

C-3

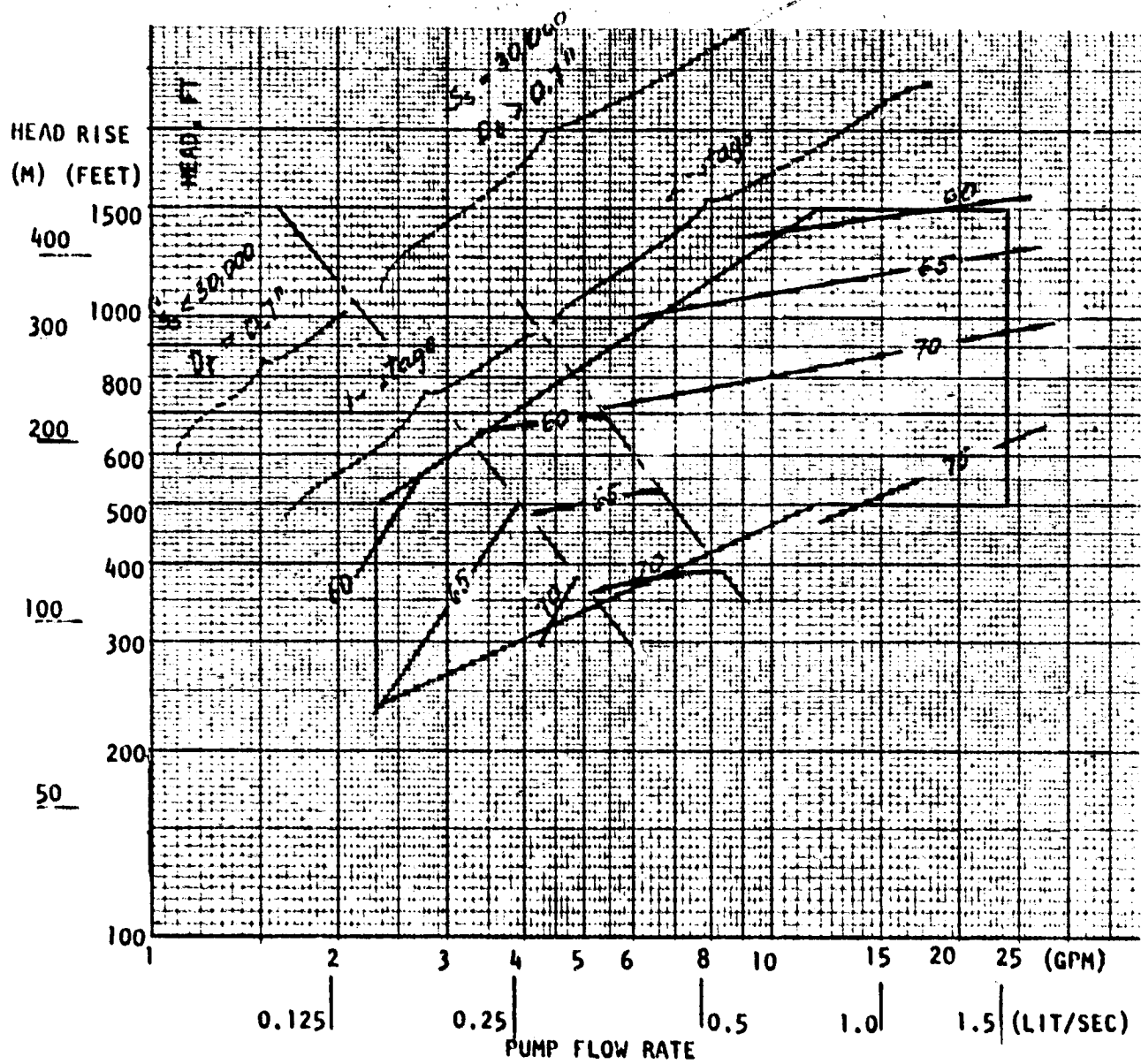
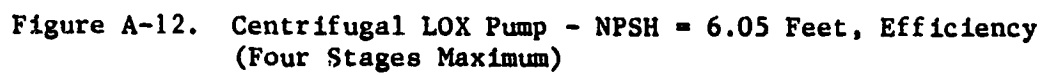


Figure A-11. Centrifugal LOX Pump - NPSH = 6.05 Feet, Efficiency (Two Stages Maximum)



191

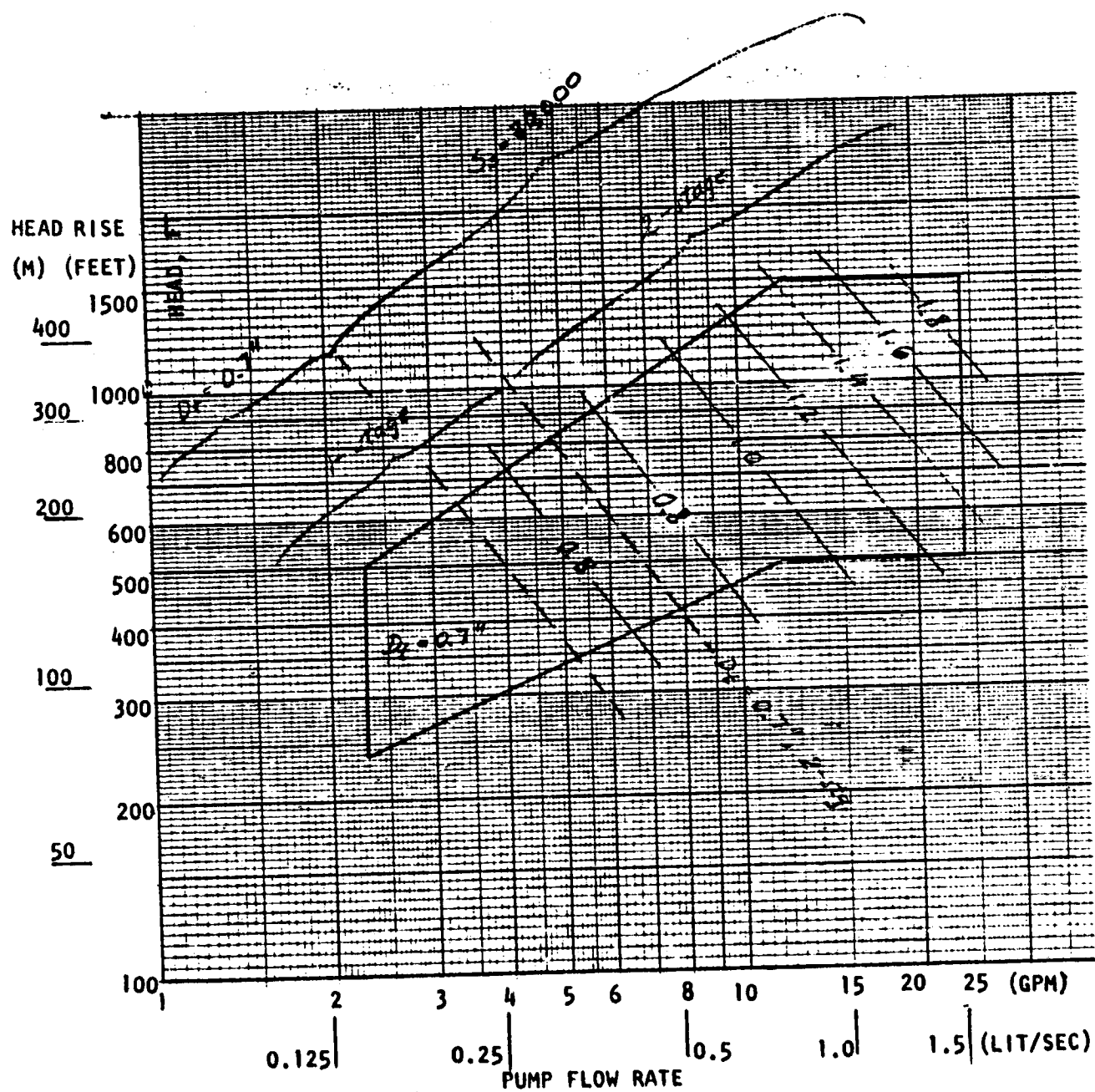
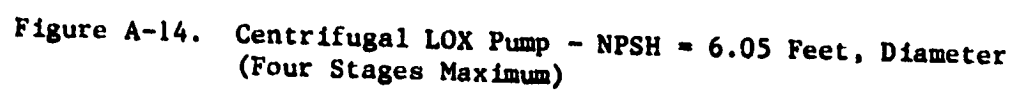


Figure A-13. Centrifugal LOX Pump - NPSH = 6.05 Feet, Diameter (Two Stages Maximum)



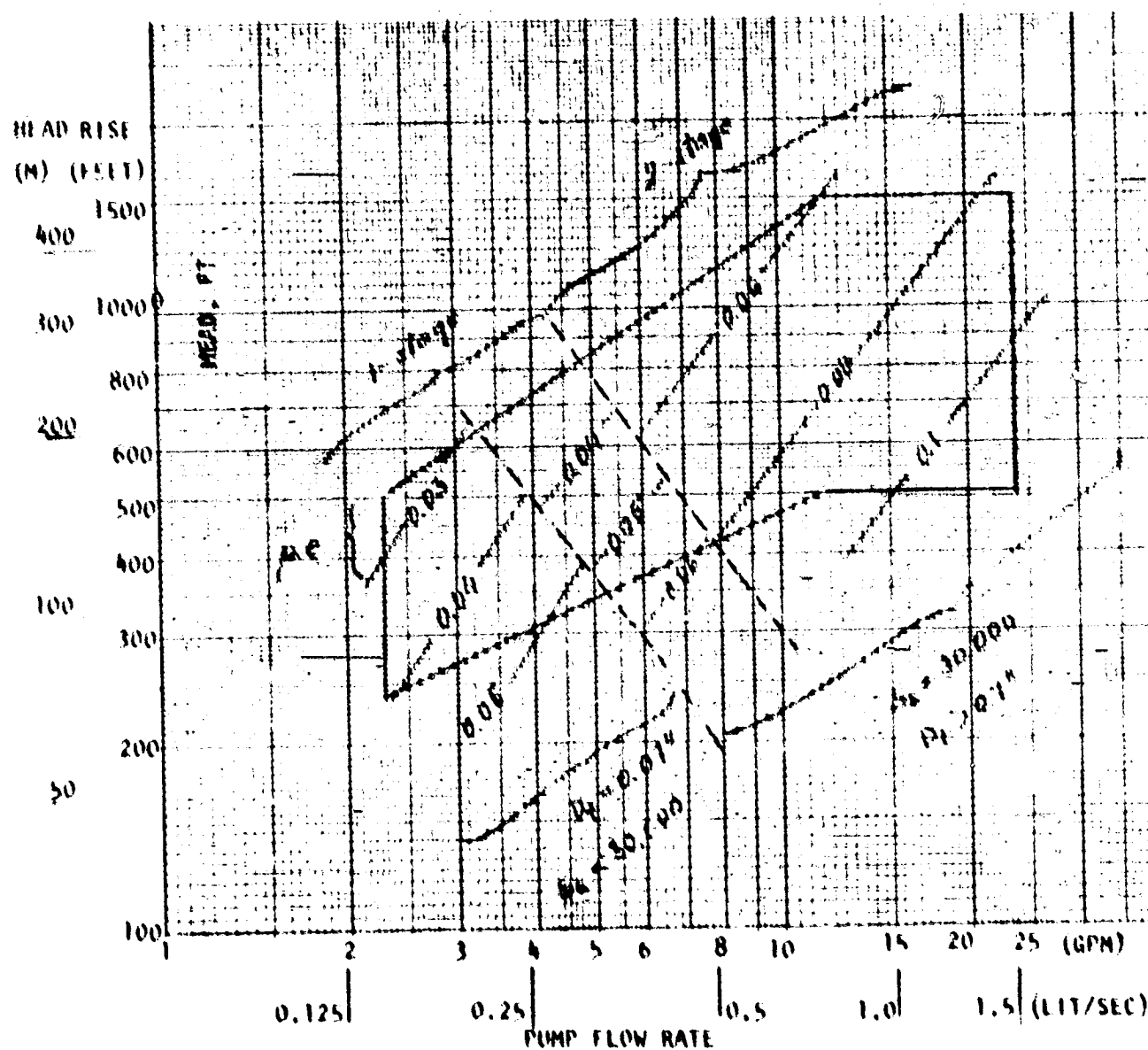


Figure A-15. Centrifugal 10X Pump - $NPSH = 6.05$ Feet, Discharge Width (Two Stages Maximum)

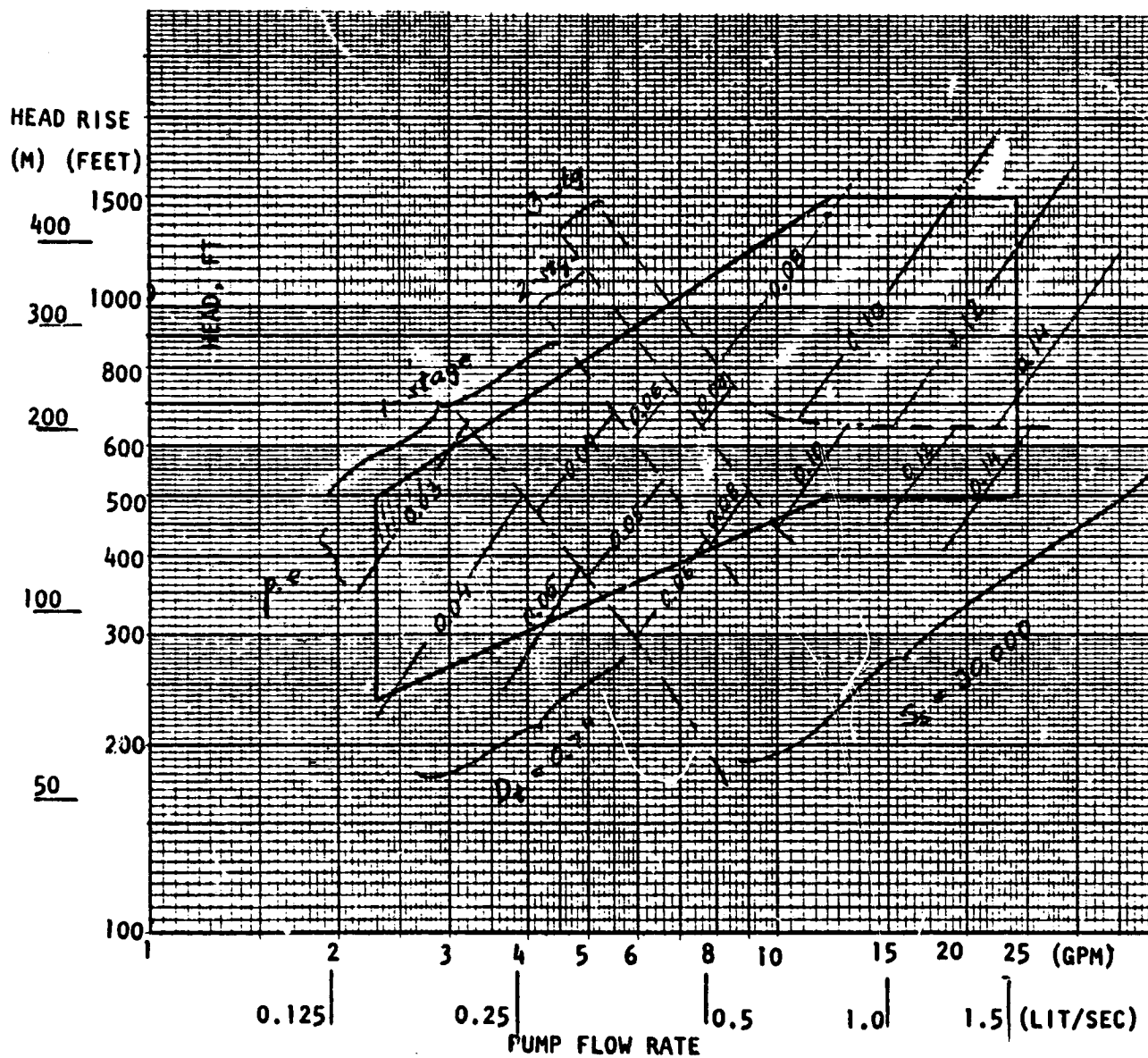


Figure A-16. Centrifugal LOX Pump - NPSH = 6.05 Feet, Discharge Width (Four Stages Maximum)

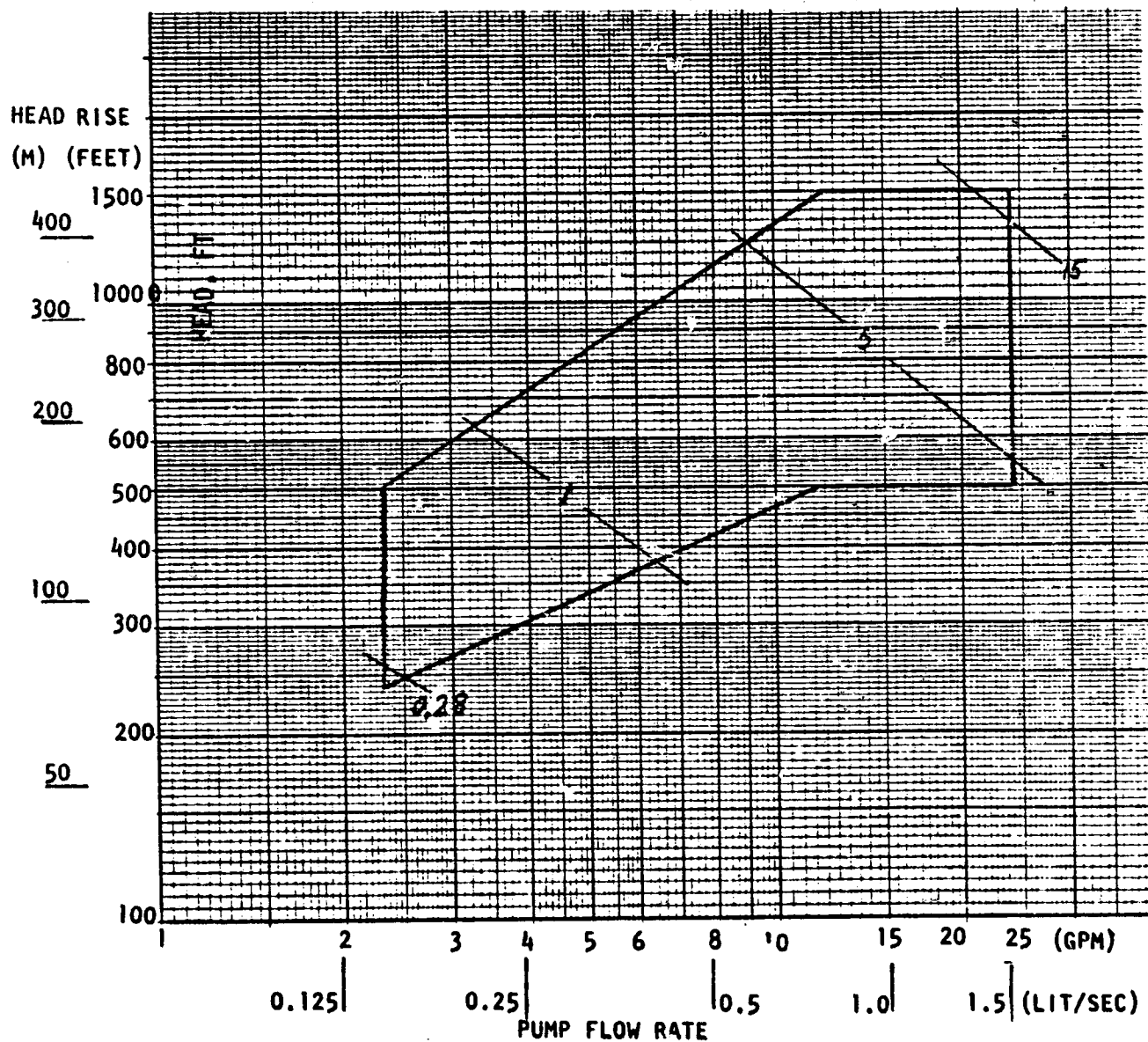


Figure A-17. Centrifugal LOX Pump - NPSH = 6.05 Feet, Power (Two Stages Maximum)

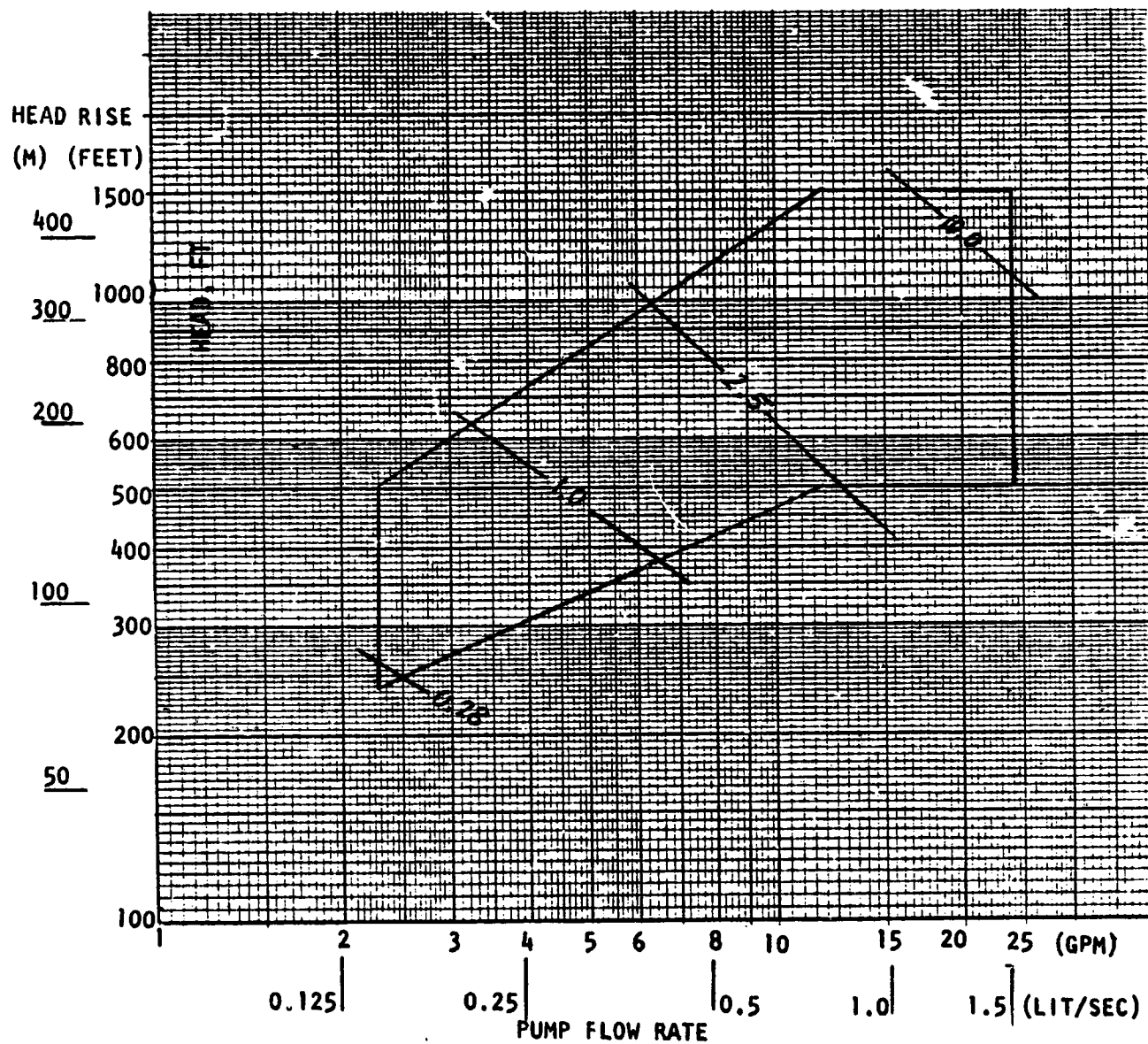


Figure A-18. Centrifugal LOX Pump - NPSH = 6.05 Feet, Power (Four Stages Maximum)

ORIGINAL PAGE IS
OF POOR QUALITY

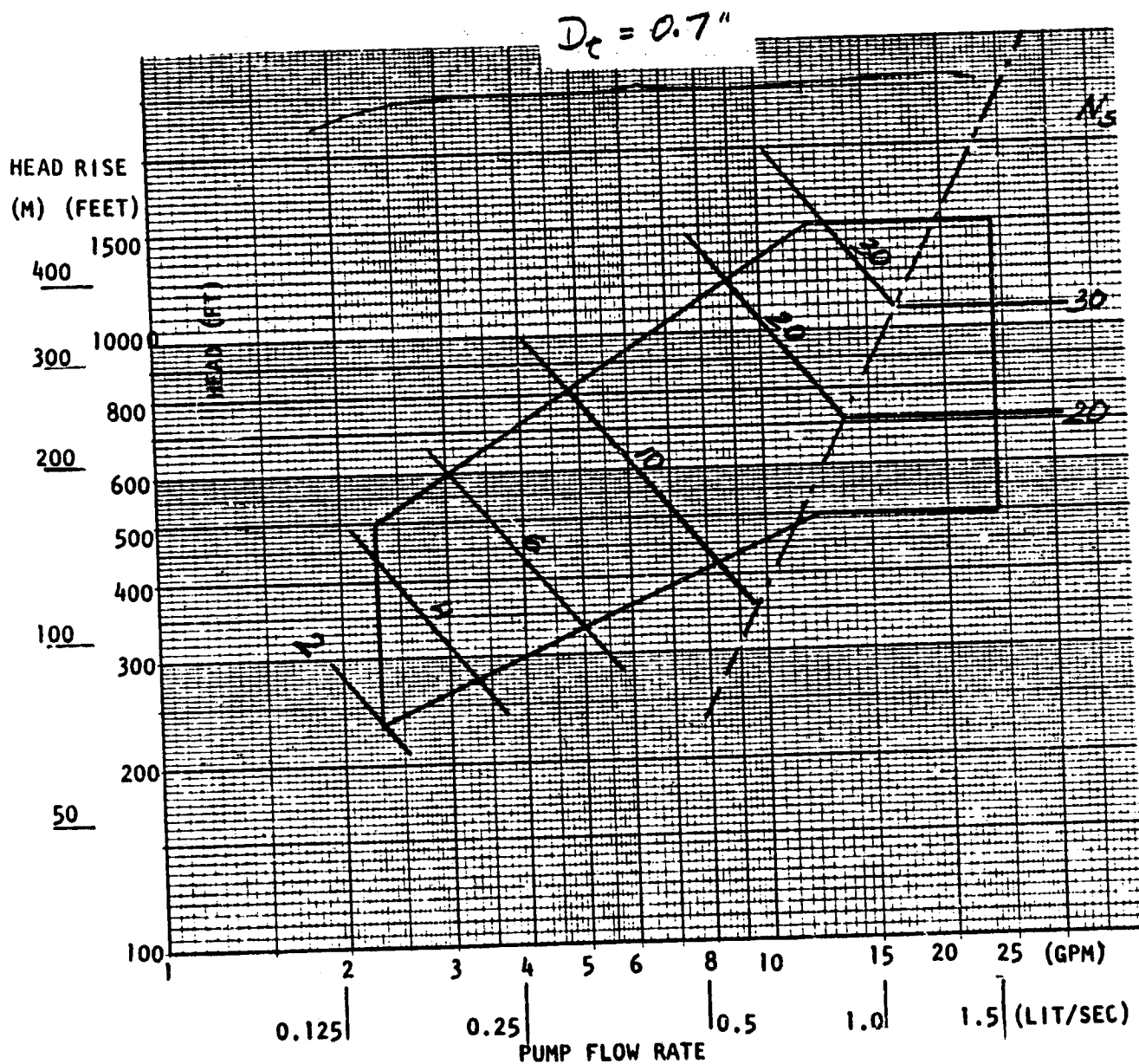


Figure A-19. Centrifugal LOX Pump - NPSH Optimized

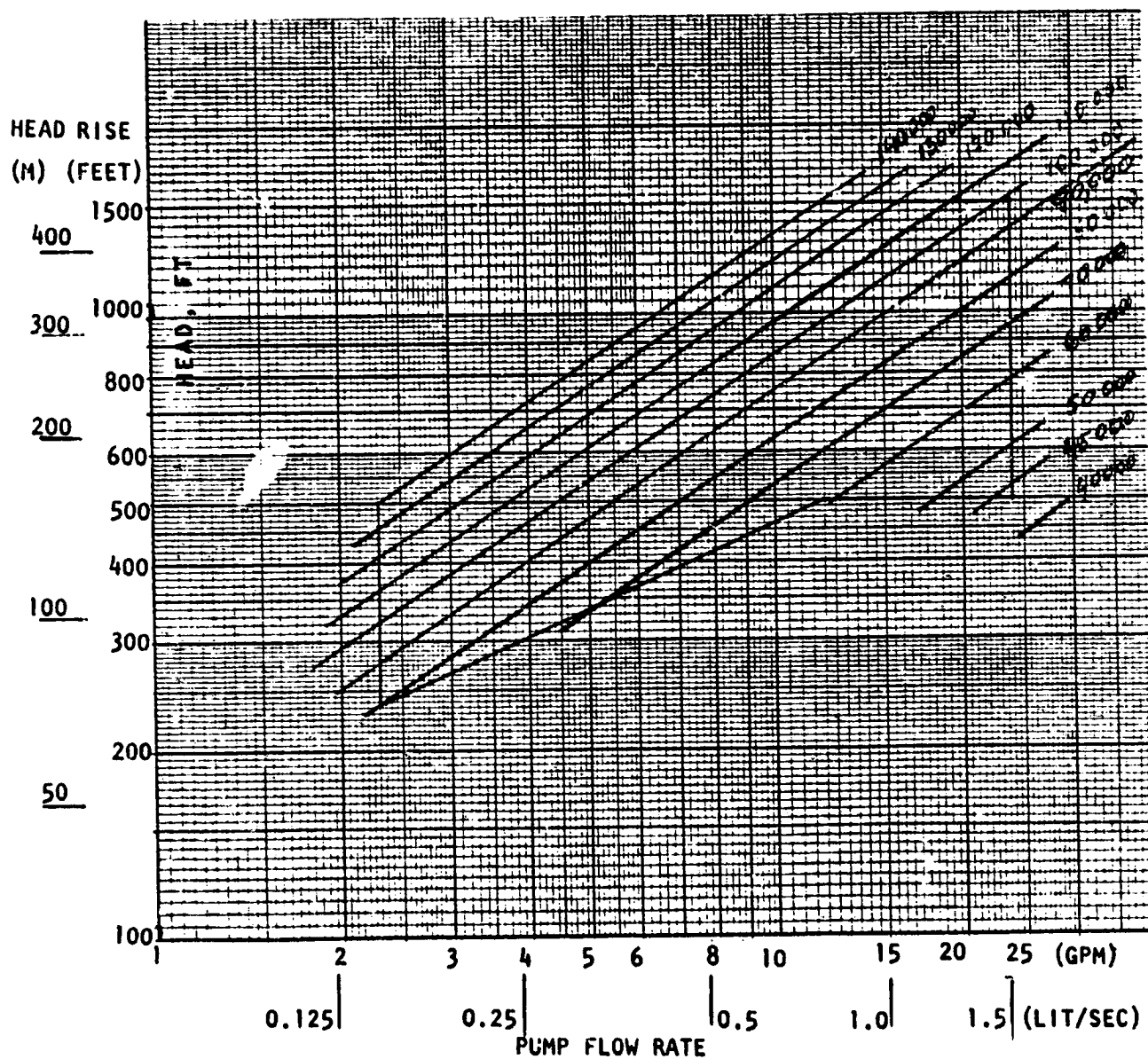


Figure A-20. Centrifugal LOX Pump - NPSH Optimized, Speed ($N_s = 2000$)

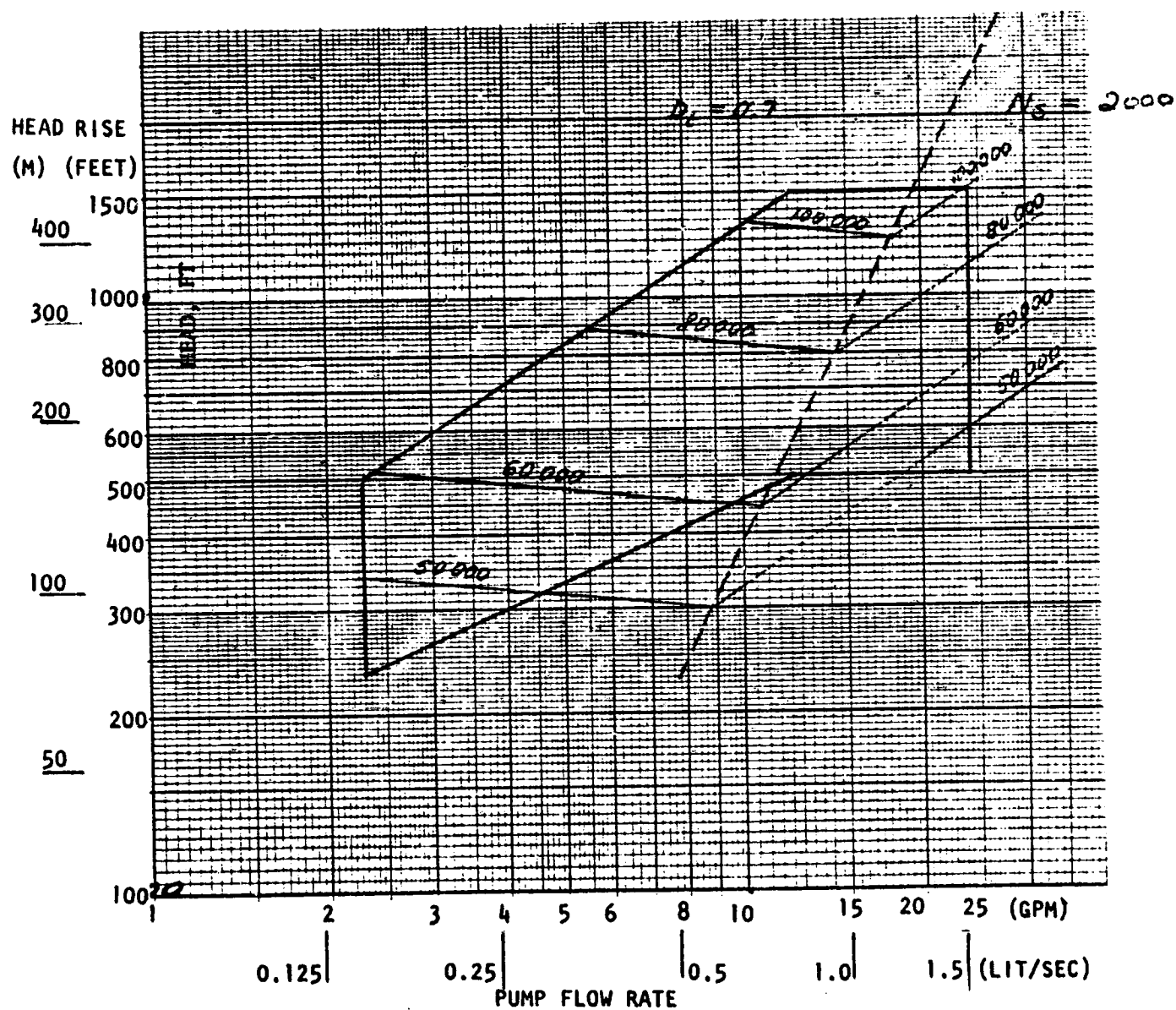


Figure A-21. Centrifugal LOX Pump - NPSH Optimized,
Speed ($D_t = 0.7$ inch)

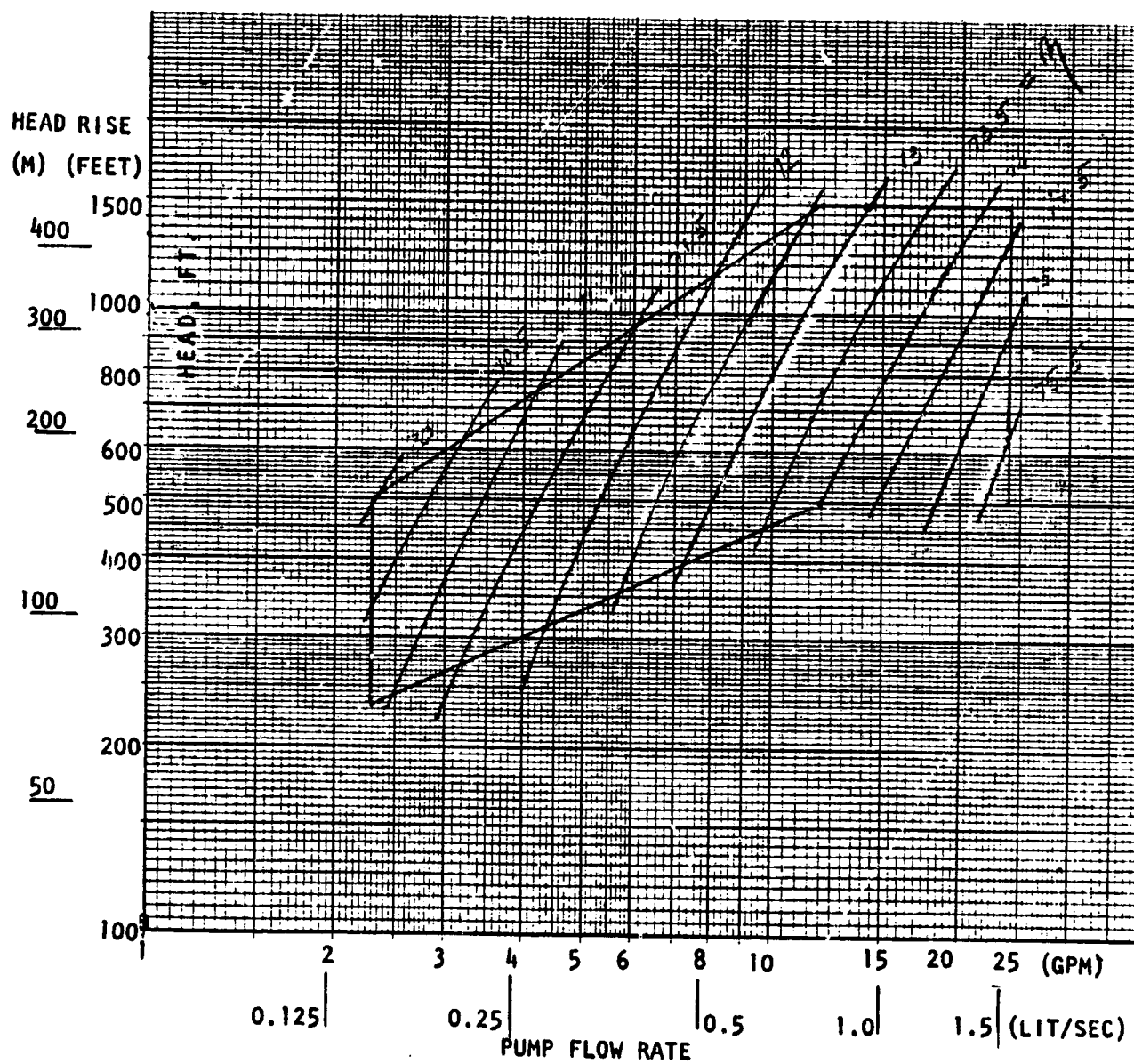


Figure A-22. Centrifugal LOX Pump - NPSH Optimized, Efficiency ($N_s = 2000$)

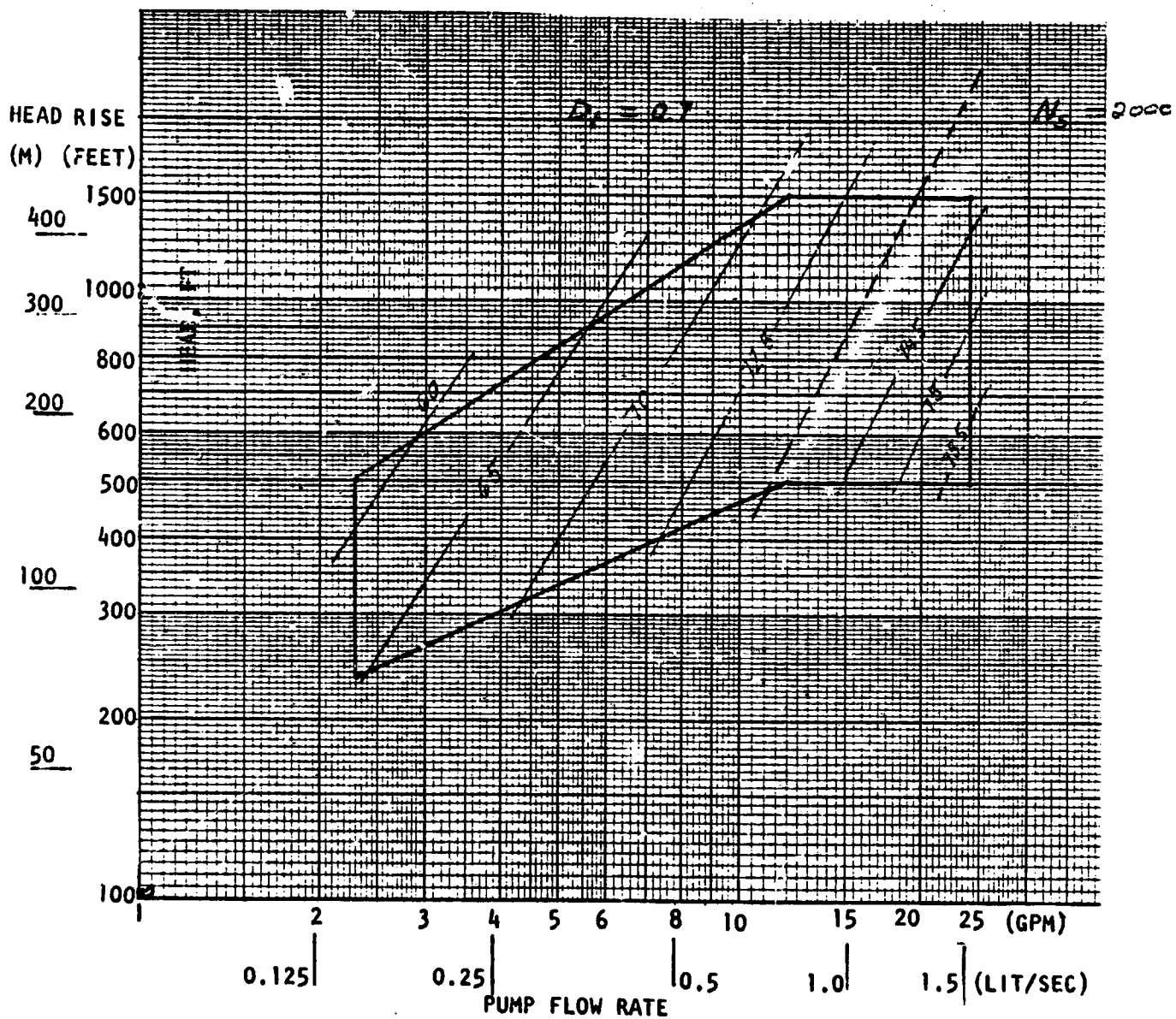


Figure A-23. Centrifugal LOX Pump - NPSH Optimized,
Efficiency ($D_t \geq 0.7$ inch)

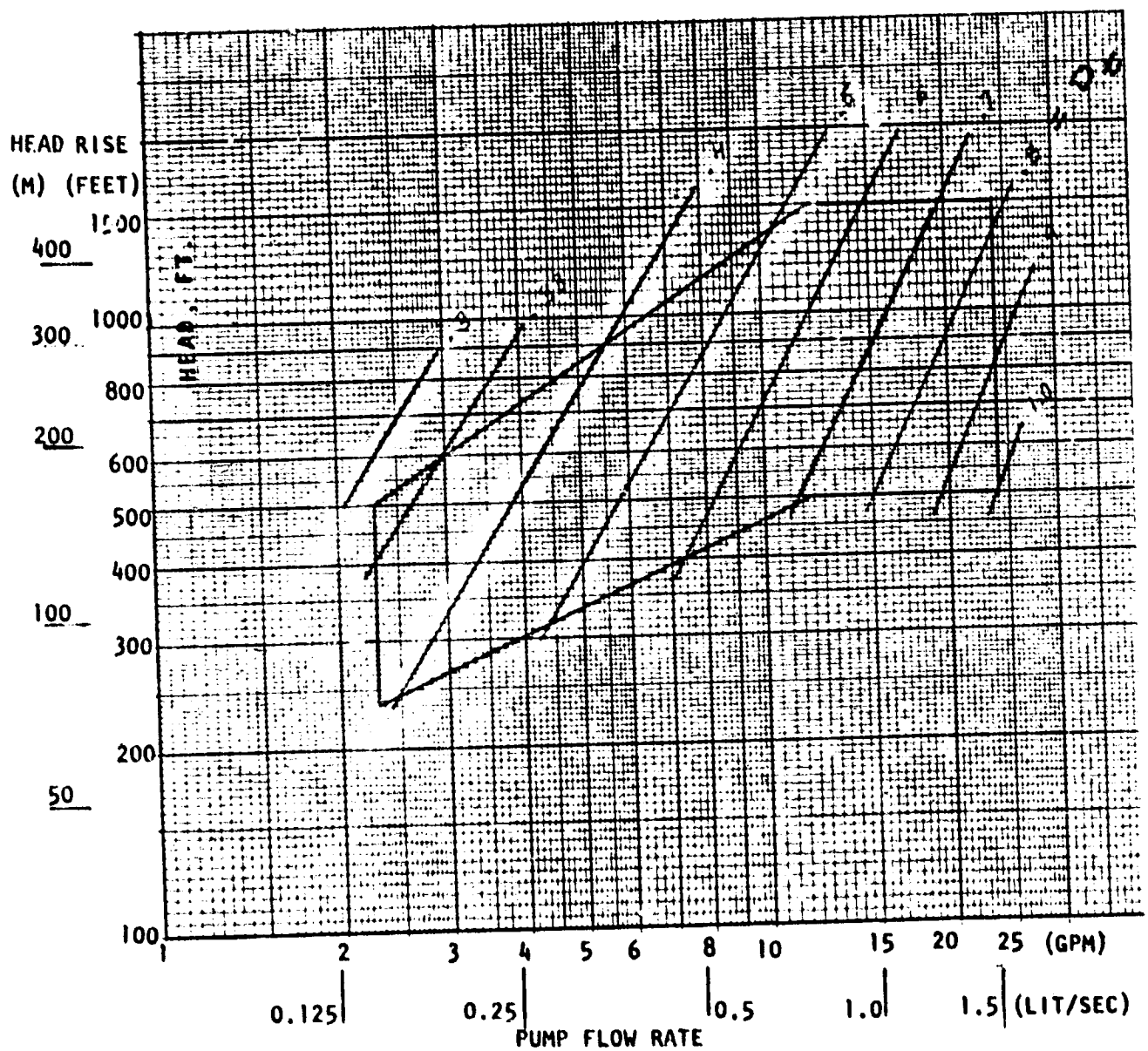


Figure A-24. Centrifugal LOX Pump - NPSH Optimized.
Diameter ($N_8 = 2000$)

ORIGINAL PAGE IS
OF POOR QUALITY

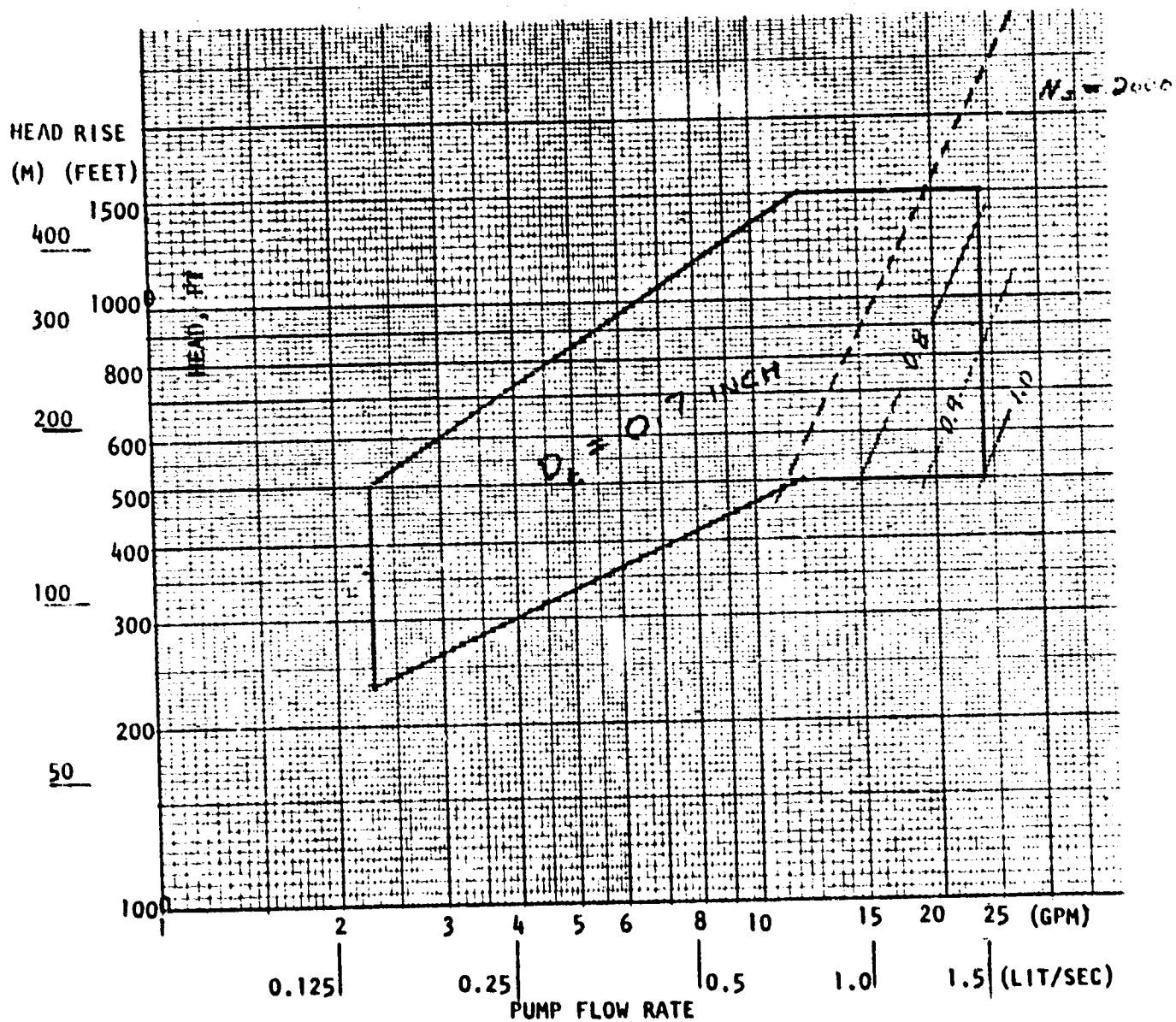
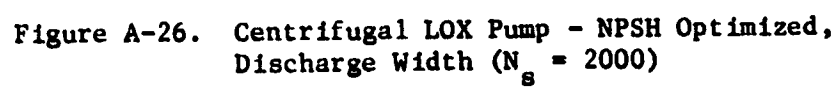
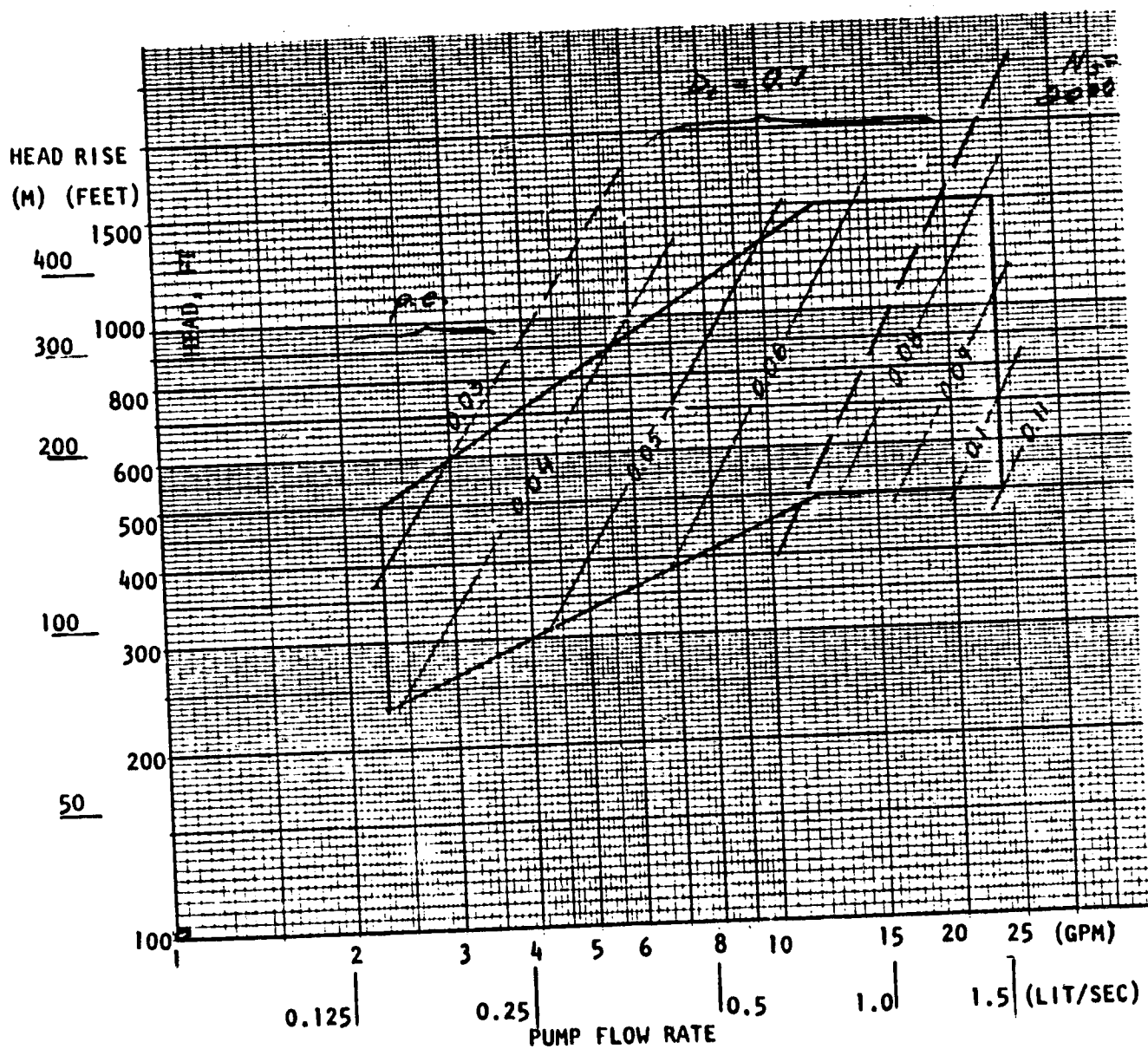


Figure A-25. Centrifugal LOX Pump - NPSH Optimized,
Diameter ($D_t \geq 0.7$ inch)





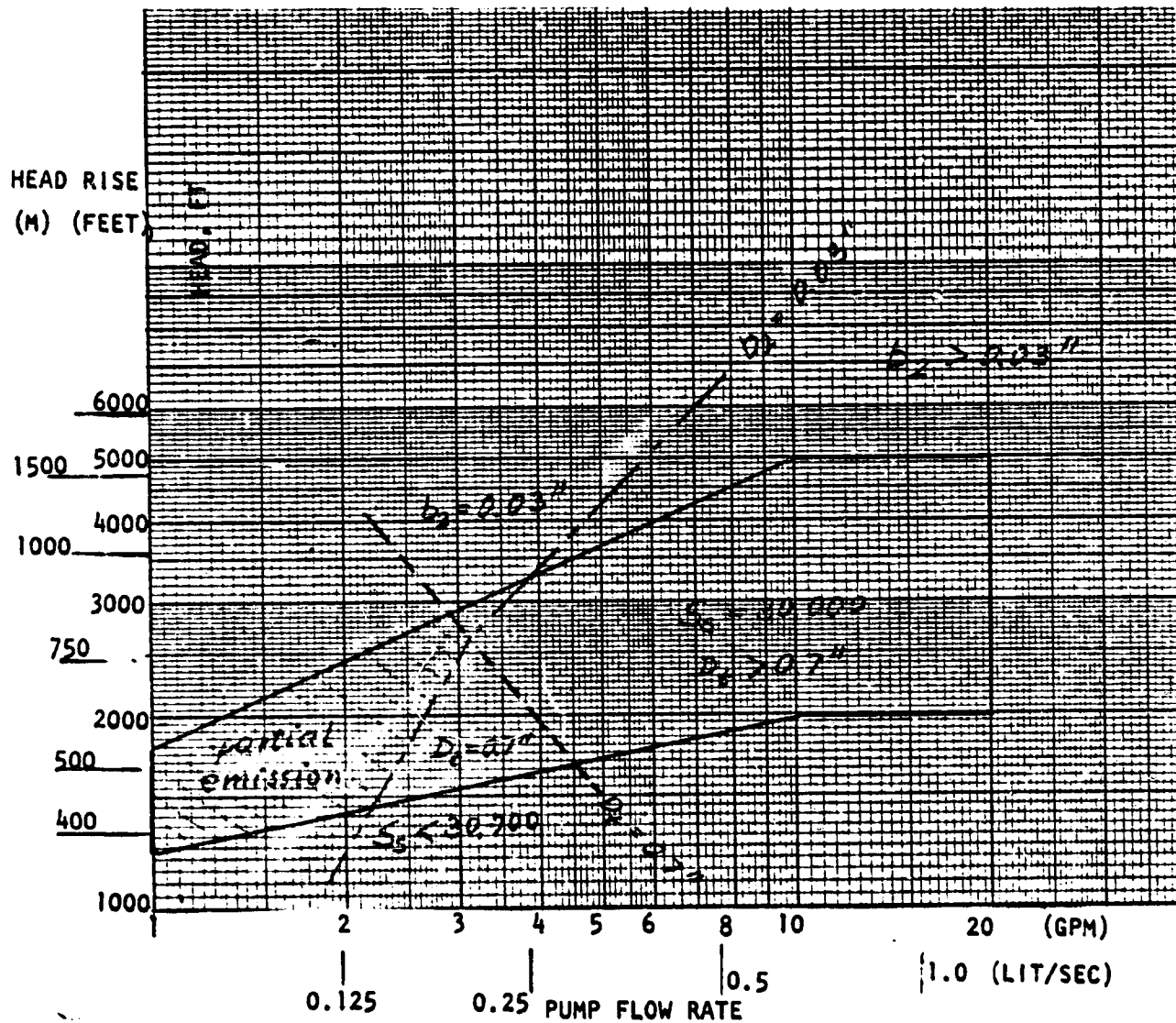


Figure A-28. Centrifugal Methane Pump - NPSH = 6 Feet,
Design Limitations

ORIGINAL PAGE IS
OF POOR QUALITY

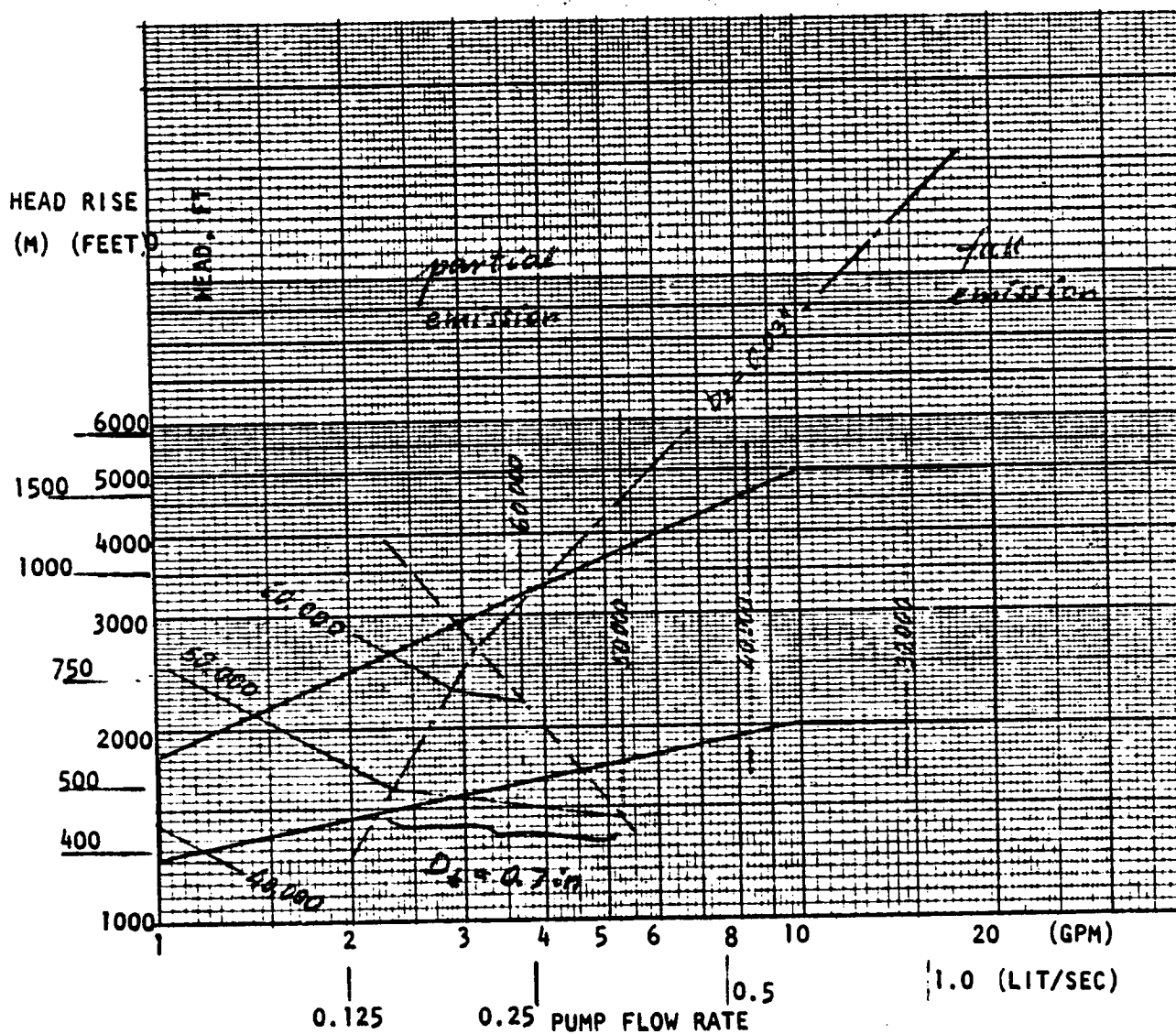


Figure A-29. Centrifugal Methane Pump - NPSH = 6 Feet, Speed

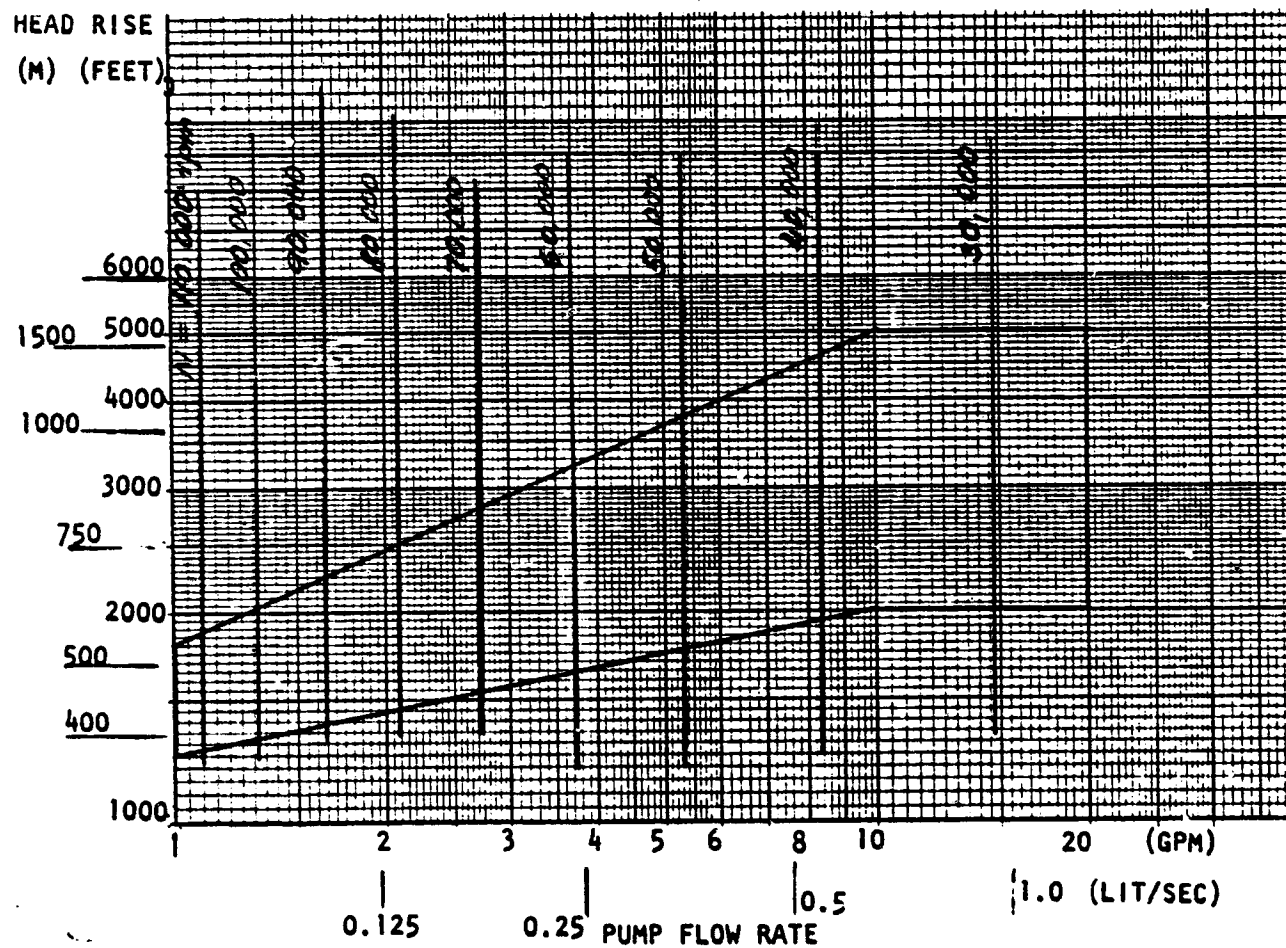


Figure A-30. Centrifugal Methane Pump - NPSH = 6 Feet,
Speed ($S_s = 30,000$)

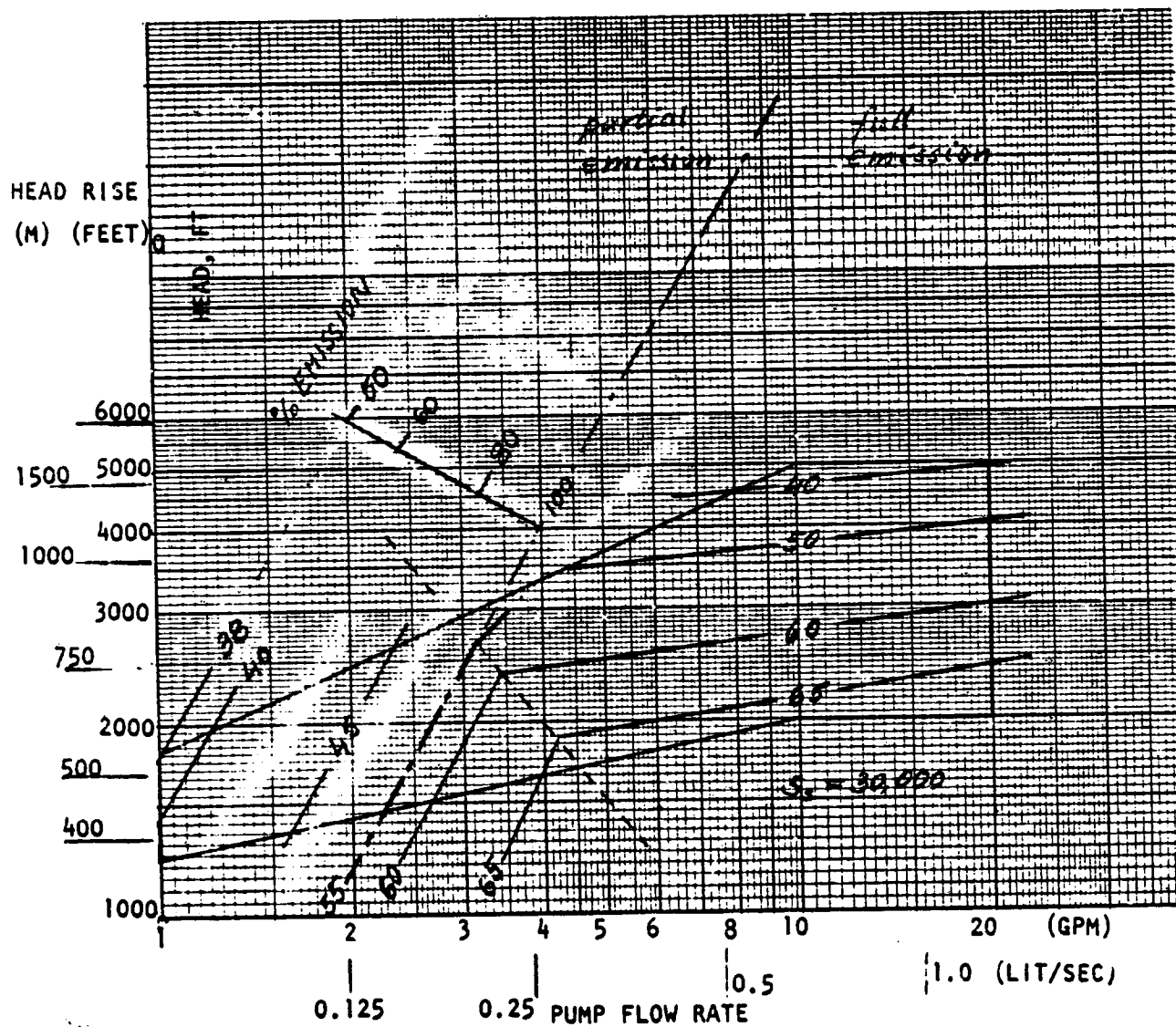


Figure A-31. Centrifugal Methane Pump - NPSH = 6 Feet, Efficiency

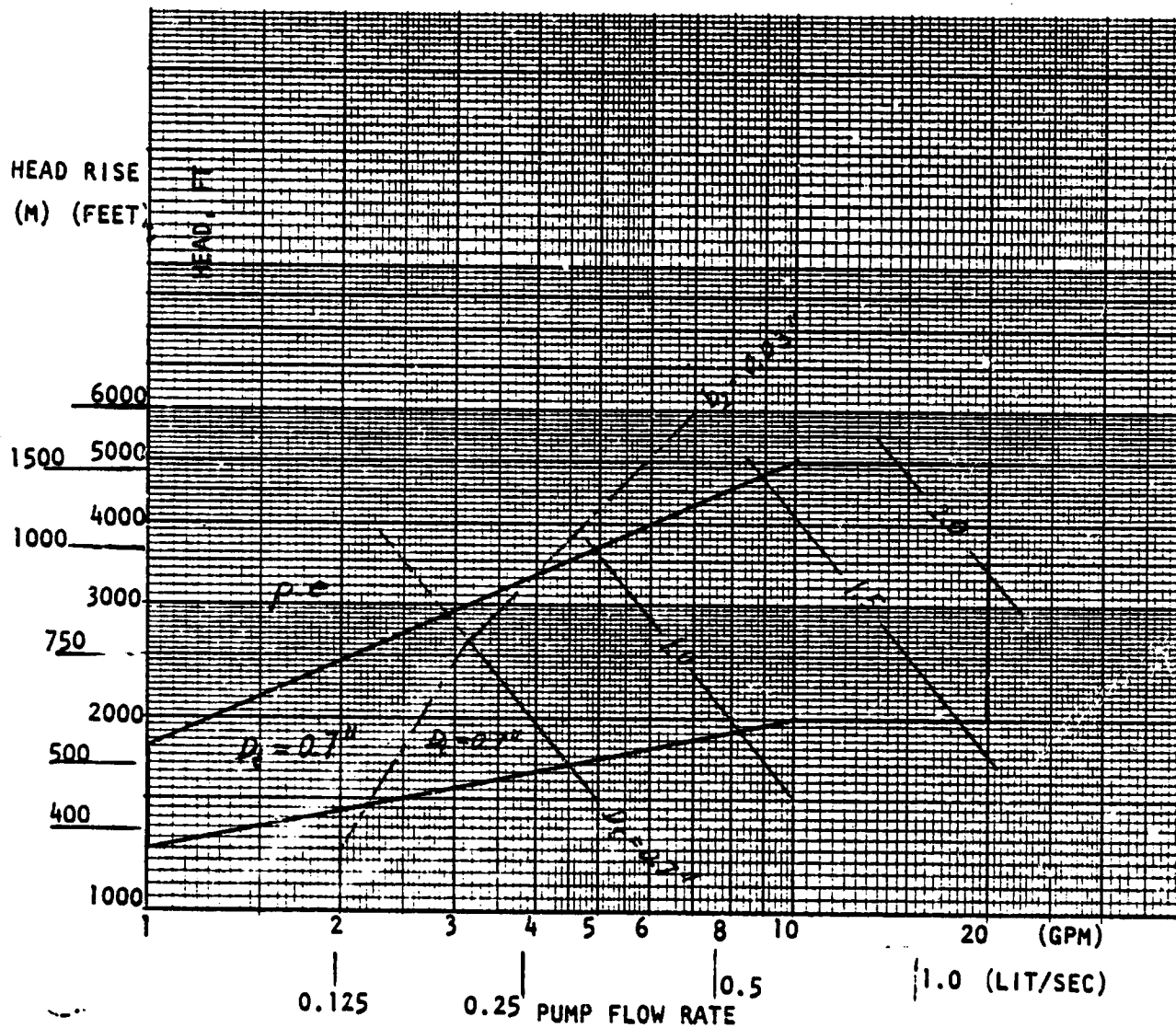


Figure A-32. Centrifugal Methane Pump - NPSH = 6 Feet, Diameter

ORIGINAL PAGE IS
OF POOR QUALITY

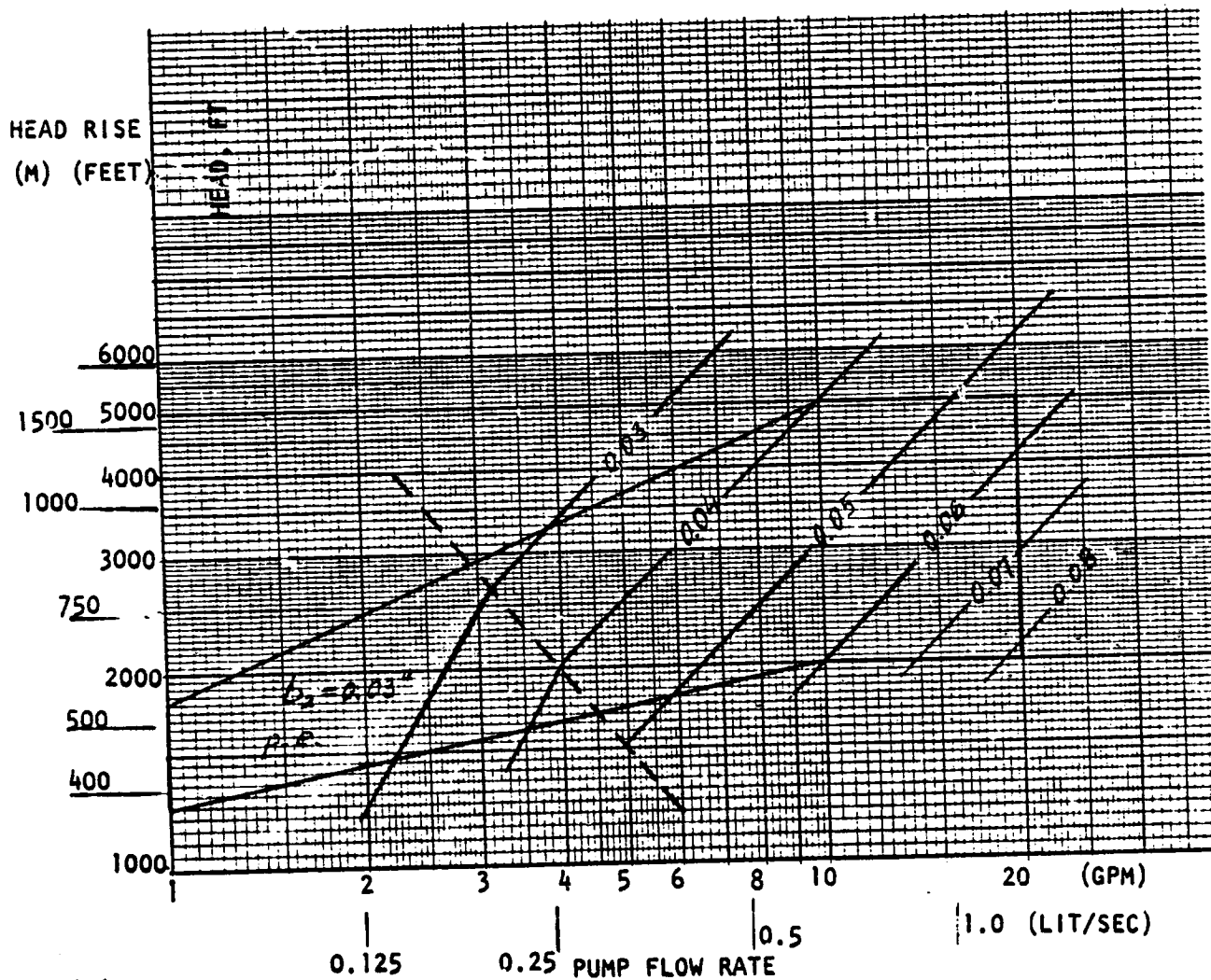


Figure A-33. Centrifugal Methane Pump - NPSH = 6 Feet, Discharge Width

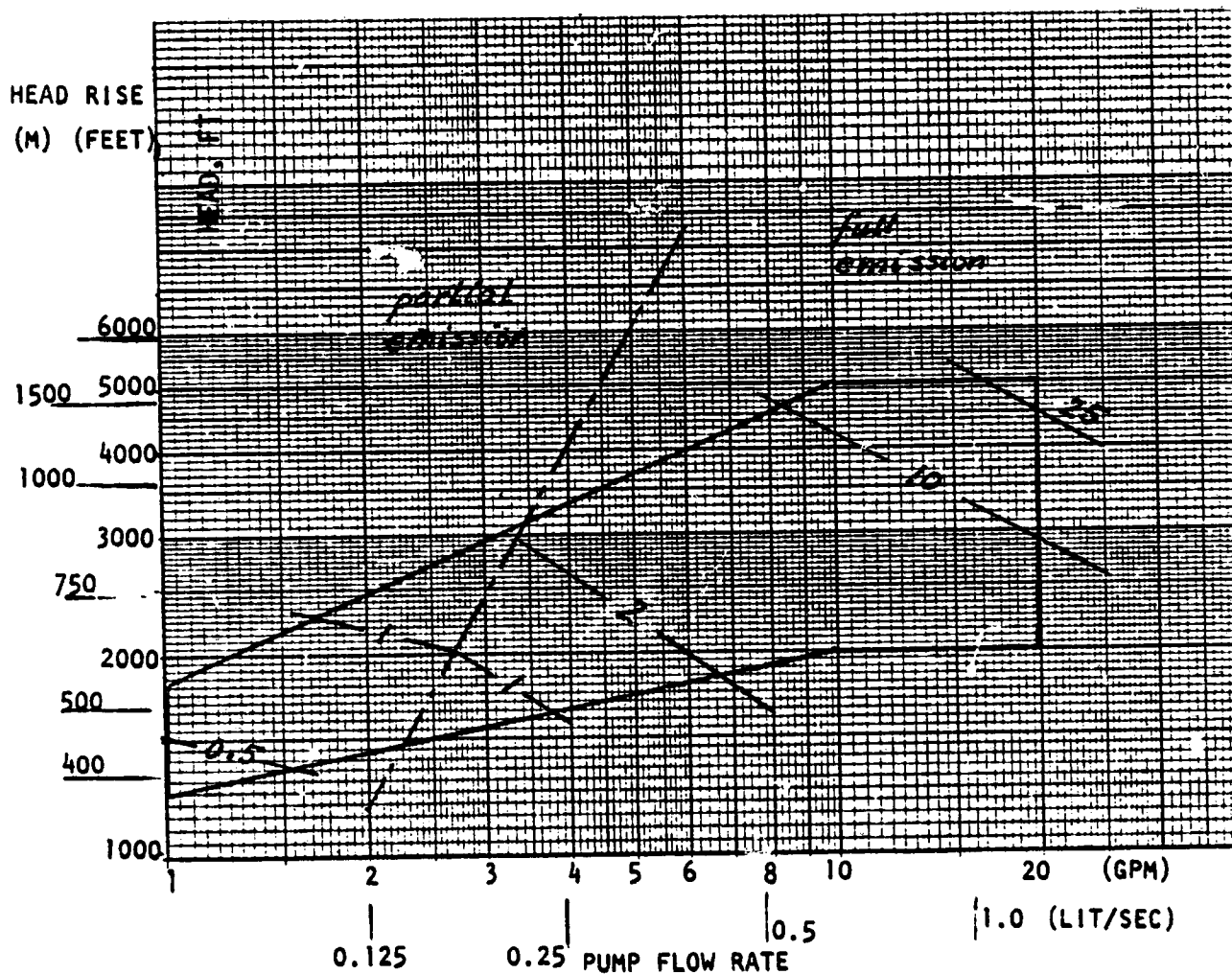


Figure A-34. Centrifugal Methane Pump - NPSH = 6 Feet, Power

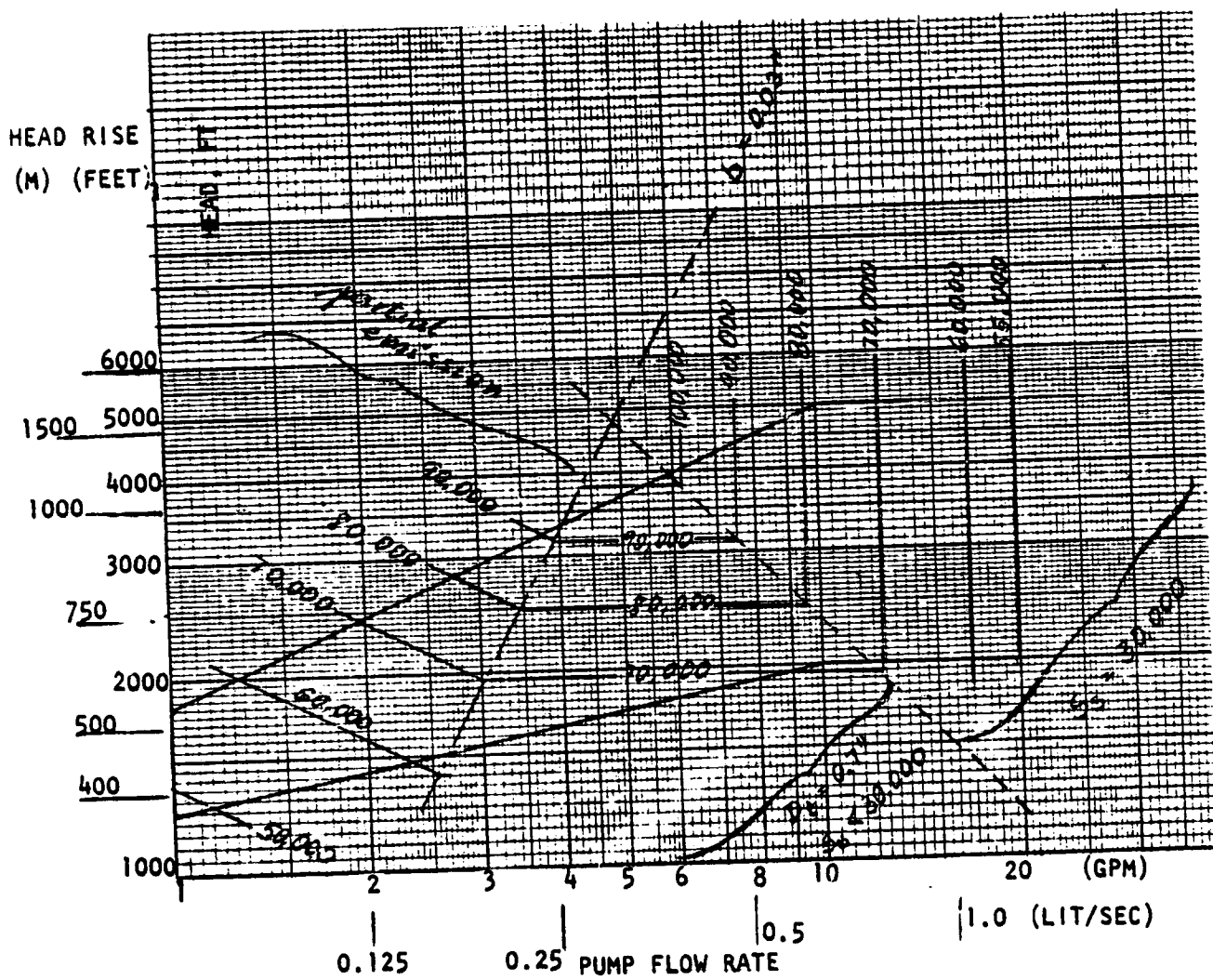


Figure A-35. Centrifugal Methane Pump - NPSH = 16.47 Feet, Speed

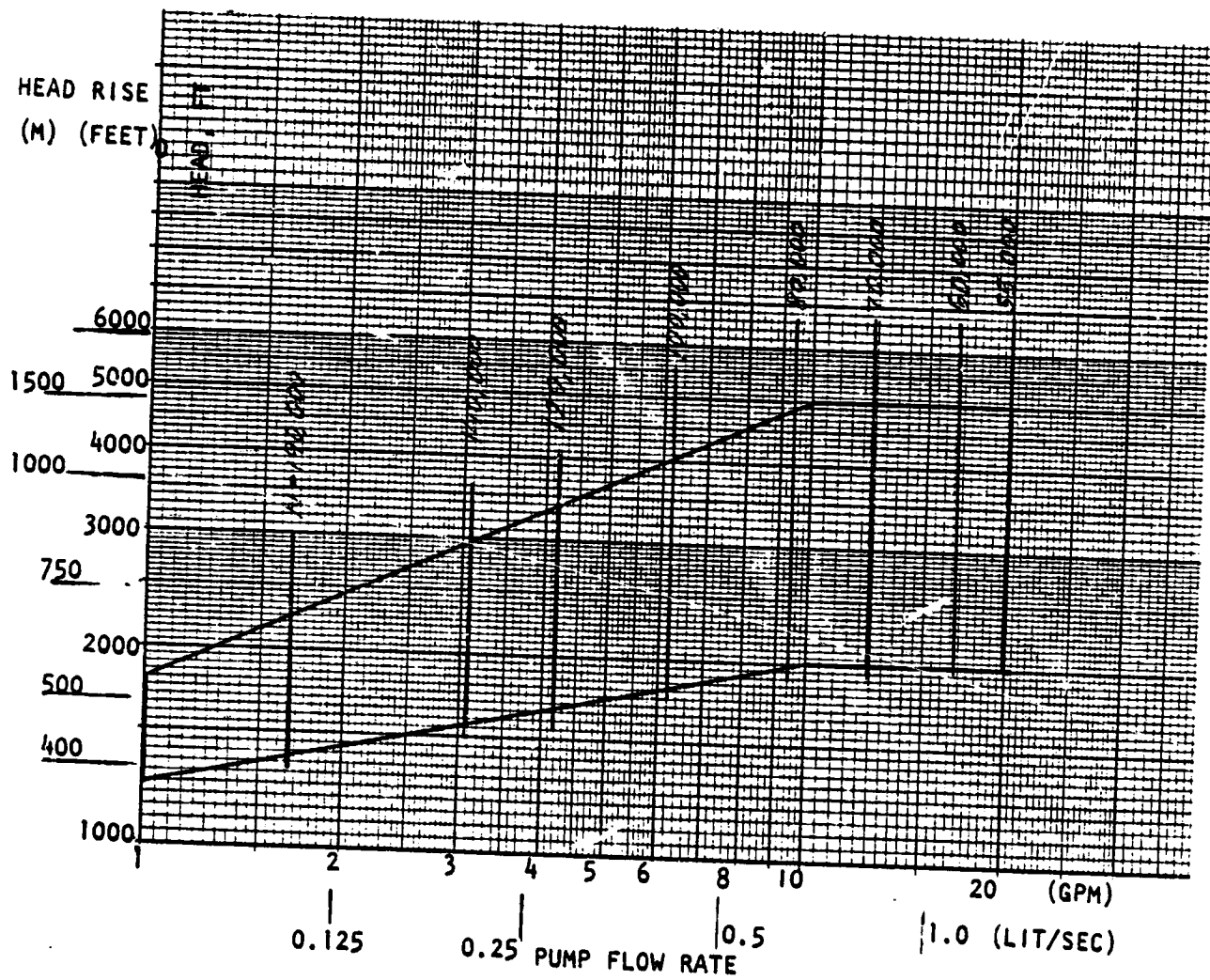


Figure A-36. Centrifugal Methane Pump - NPSH = 16.47 Feet, ($S_g = 30,000$)

ORIGINAL PAGE IS
OF POOR QUALITY

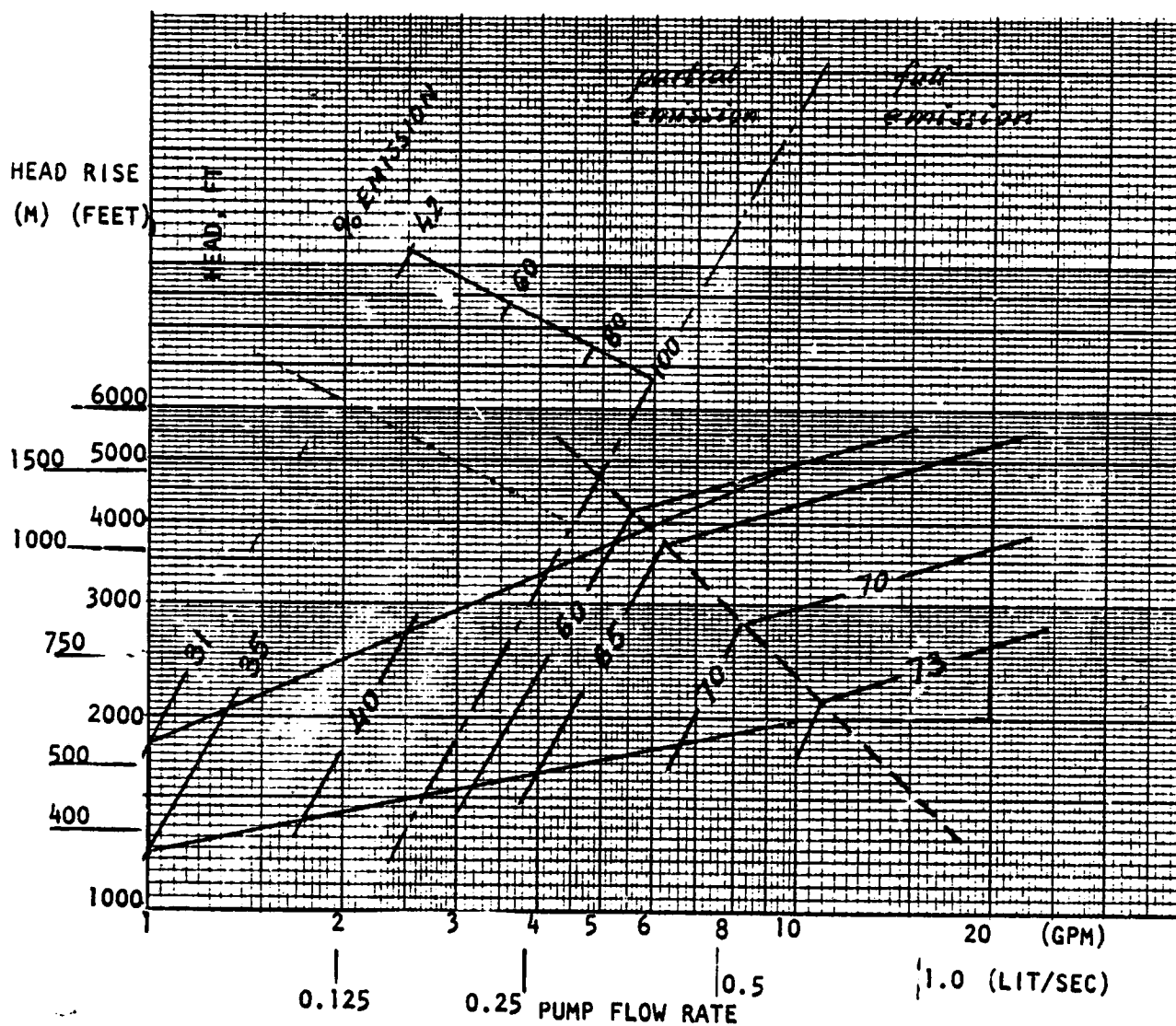


Figure A-37. Centrifugal Methane Pump - NPSH = 16.47 Feet, Efficiency

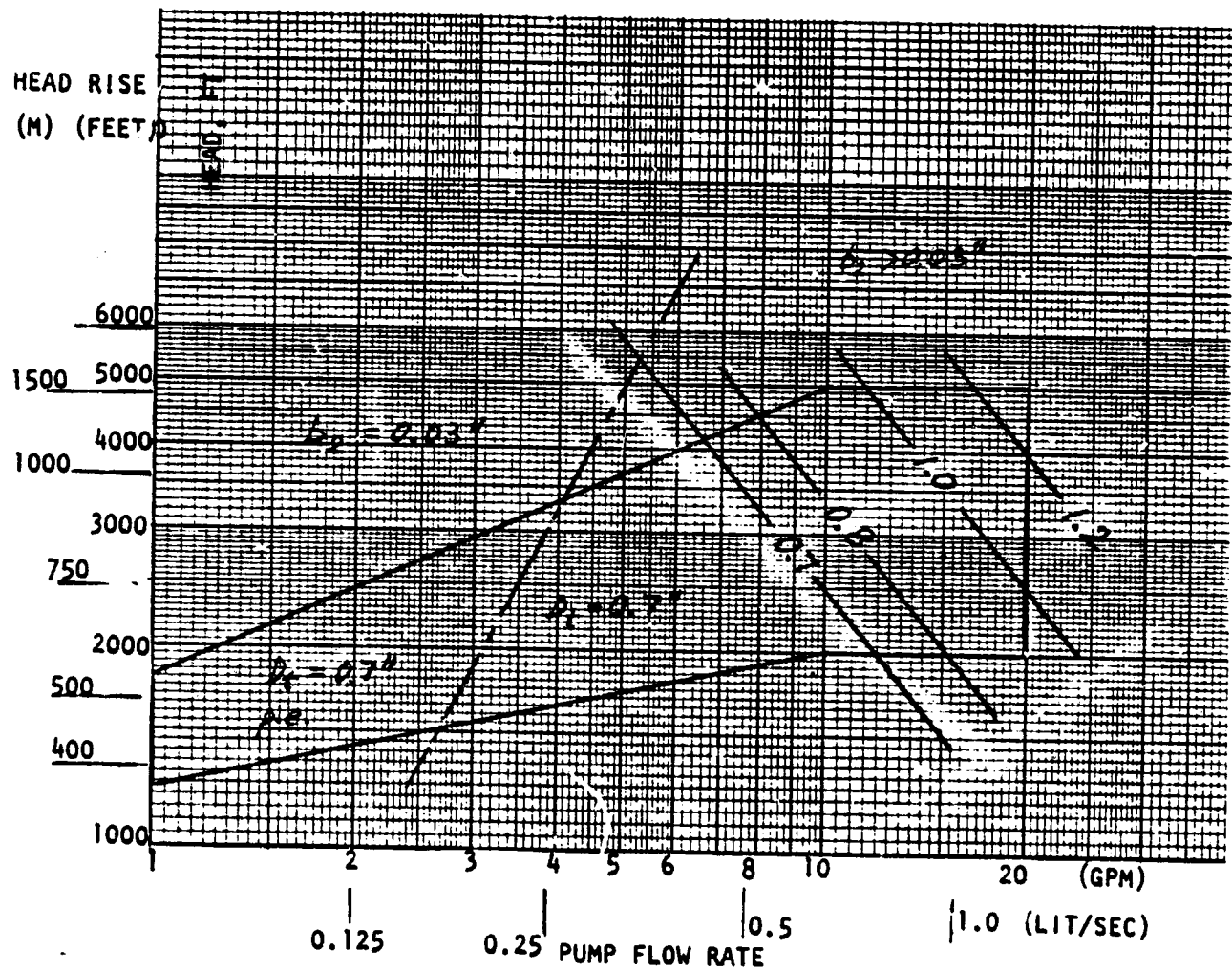


Figure A-38. Centrifugal Methane Pump - NPSH = 16.47 Feet, Diameter

ORIGINAL PAGE IS
OF POOR QUALITY

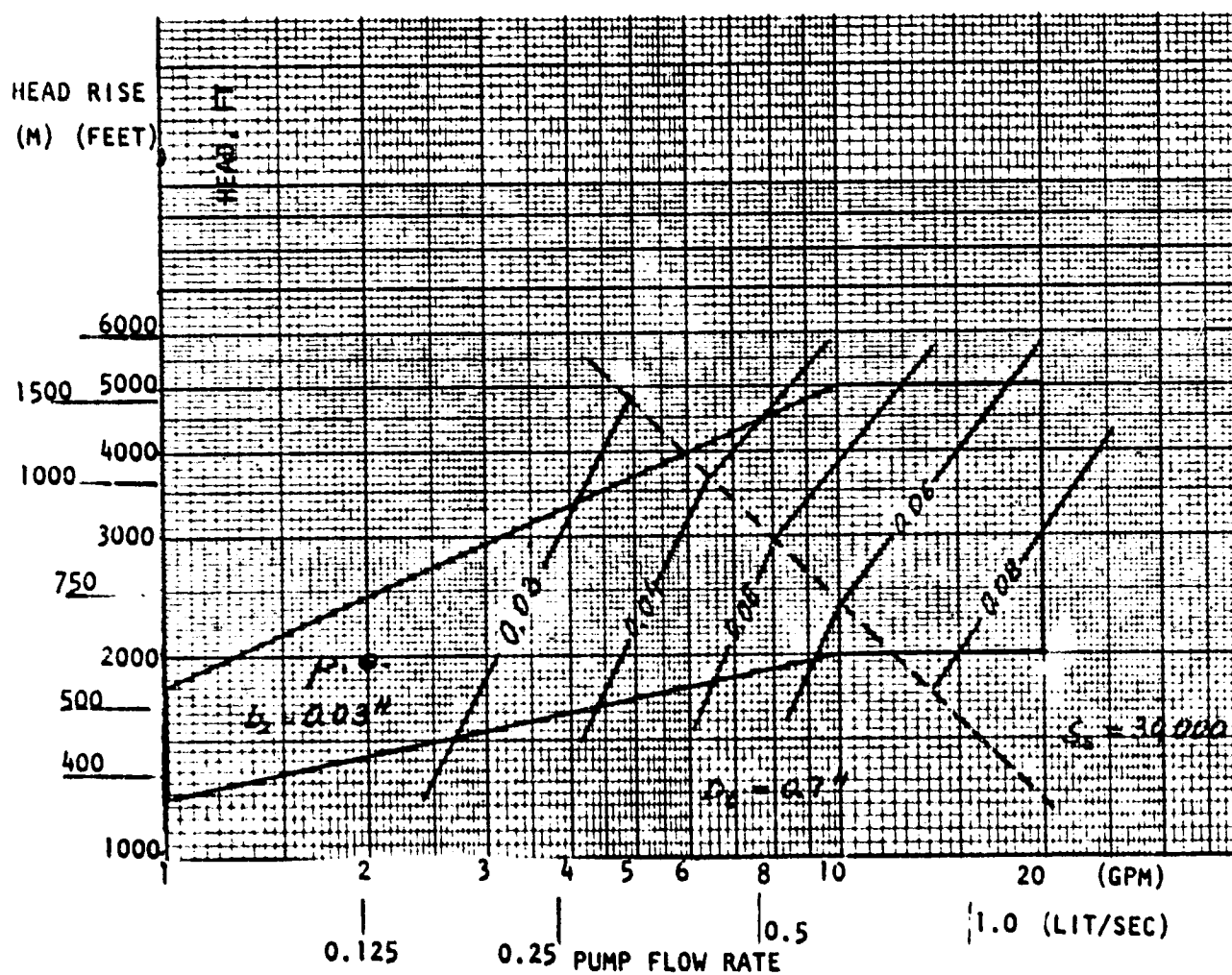


Figure A-39. Centrifugal Methane Pump - NPSH = 16.47 Feet,
Discharge Width

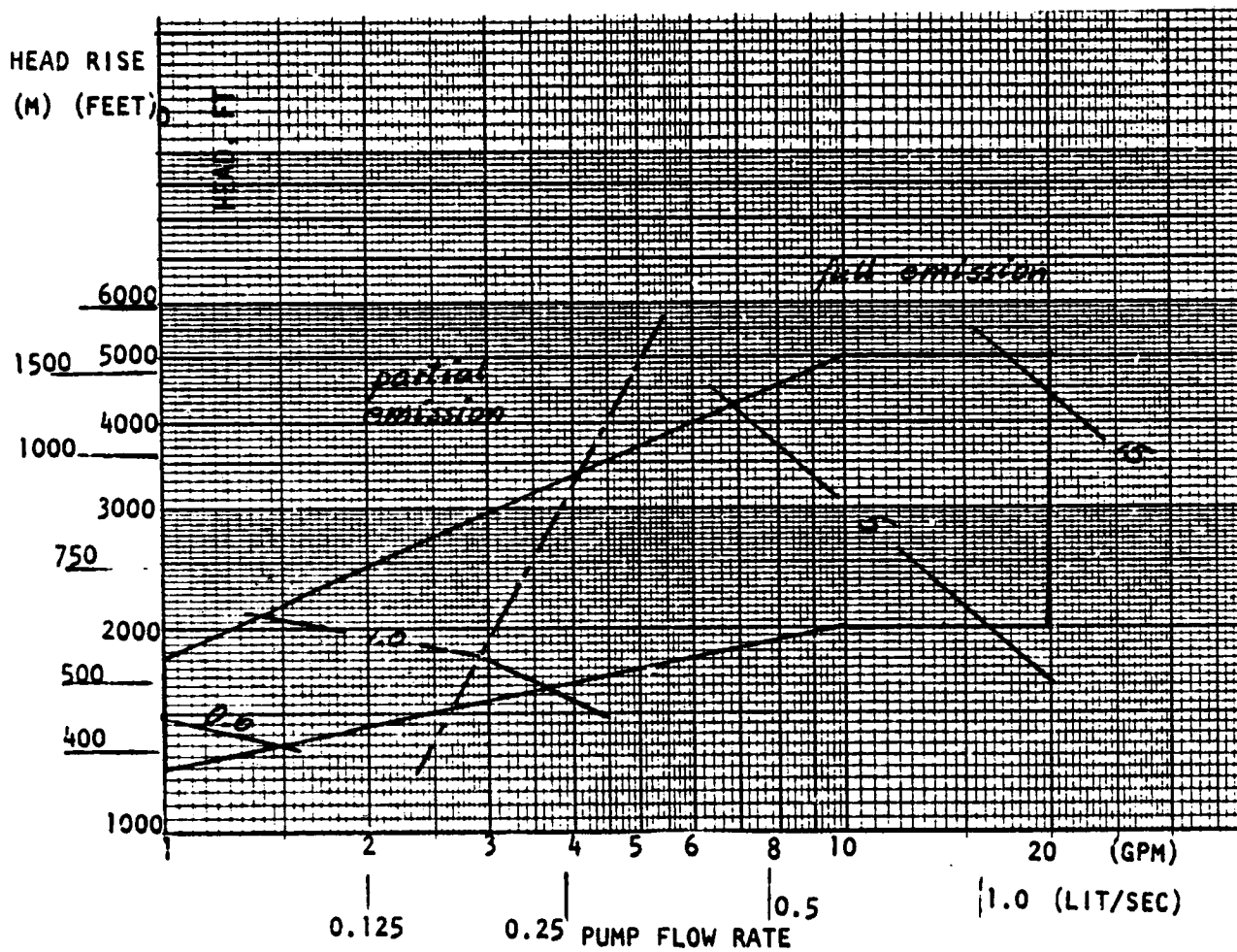


Figure A-40. Centrifugal Methane Pump - NPSH = 16.47 Feet, Power

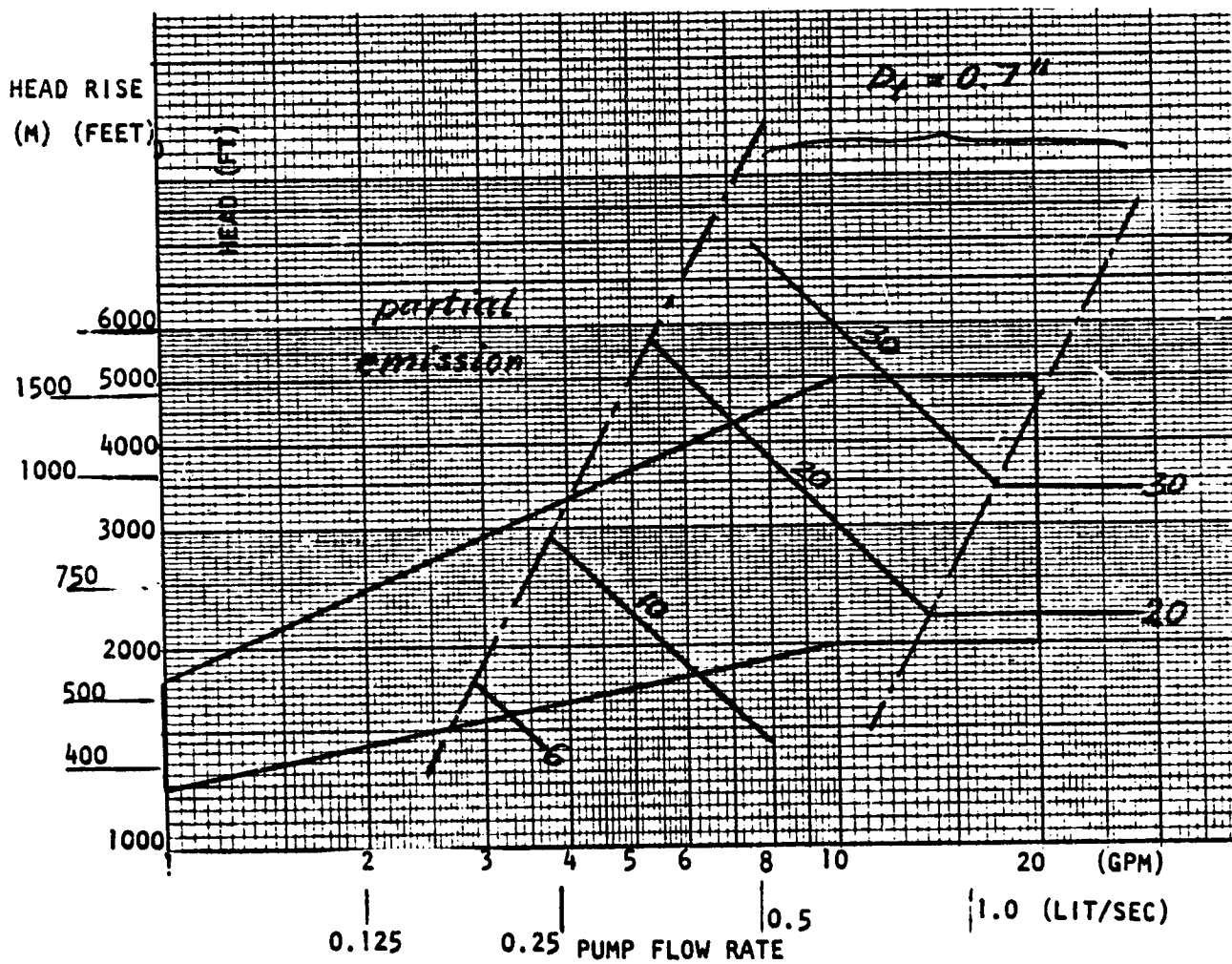


Figure A-41. Centrifugal Methane Pump - NPSH Optimized

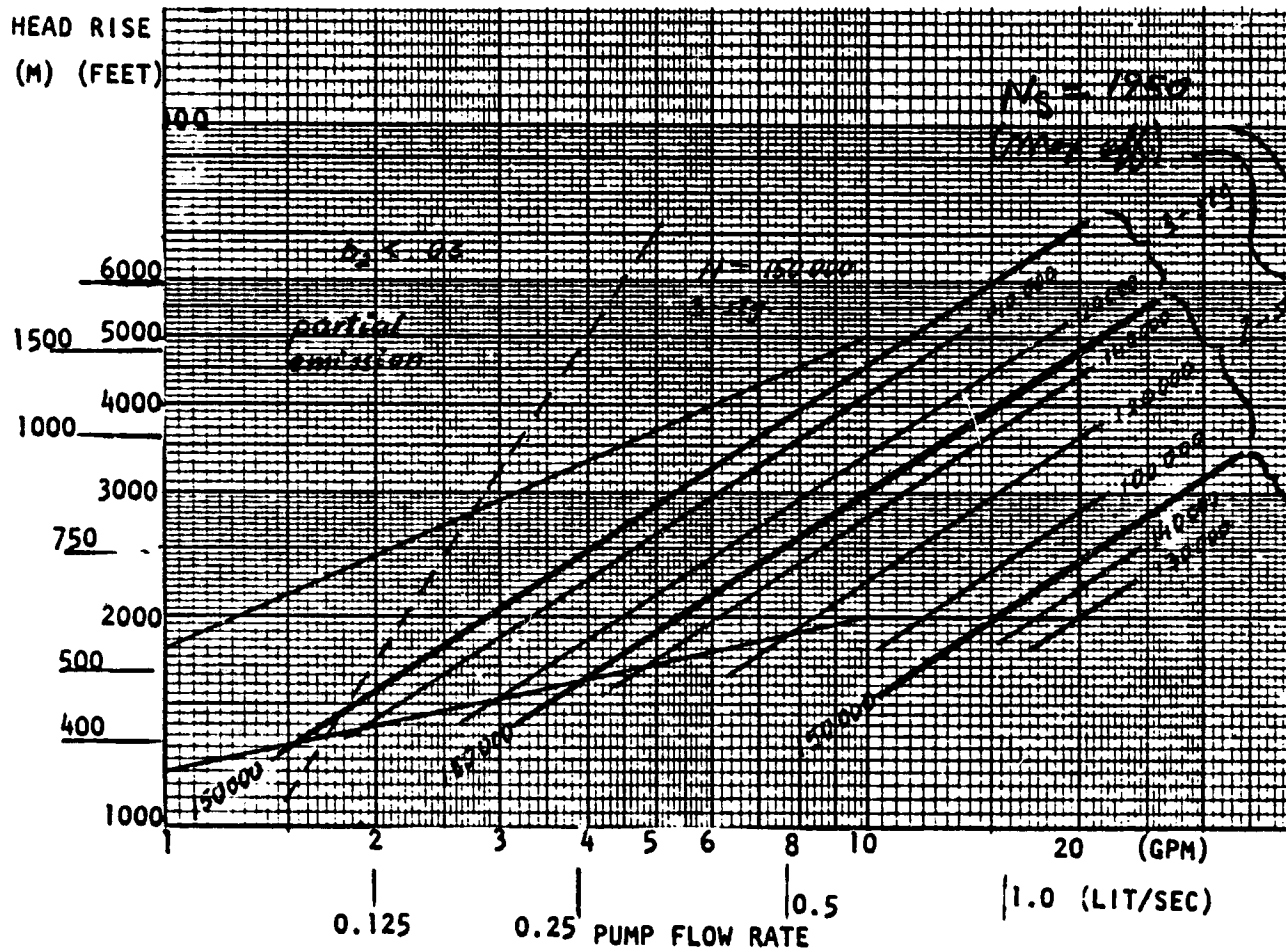


Figure A-42. Centrifugal Methane Pump - NPSH Optimized, Speed ($N_s = 1950$)

ORIGINAL PAGE IS
OF POOR QUALITY

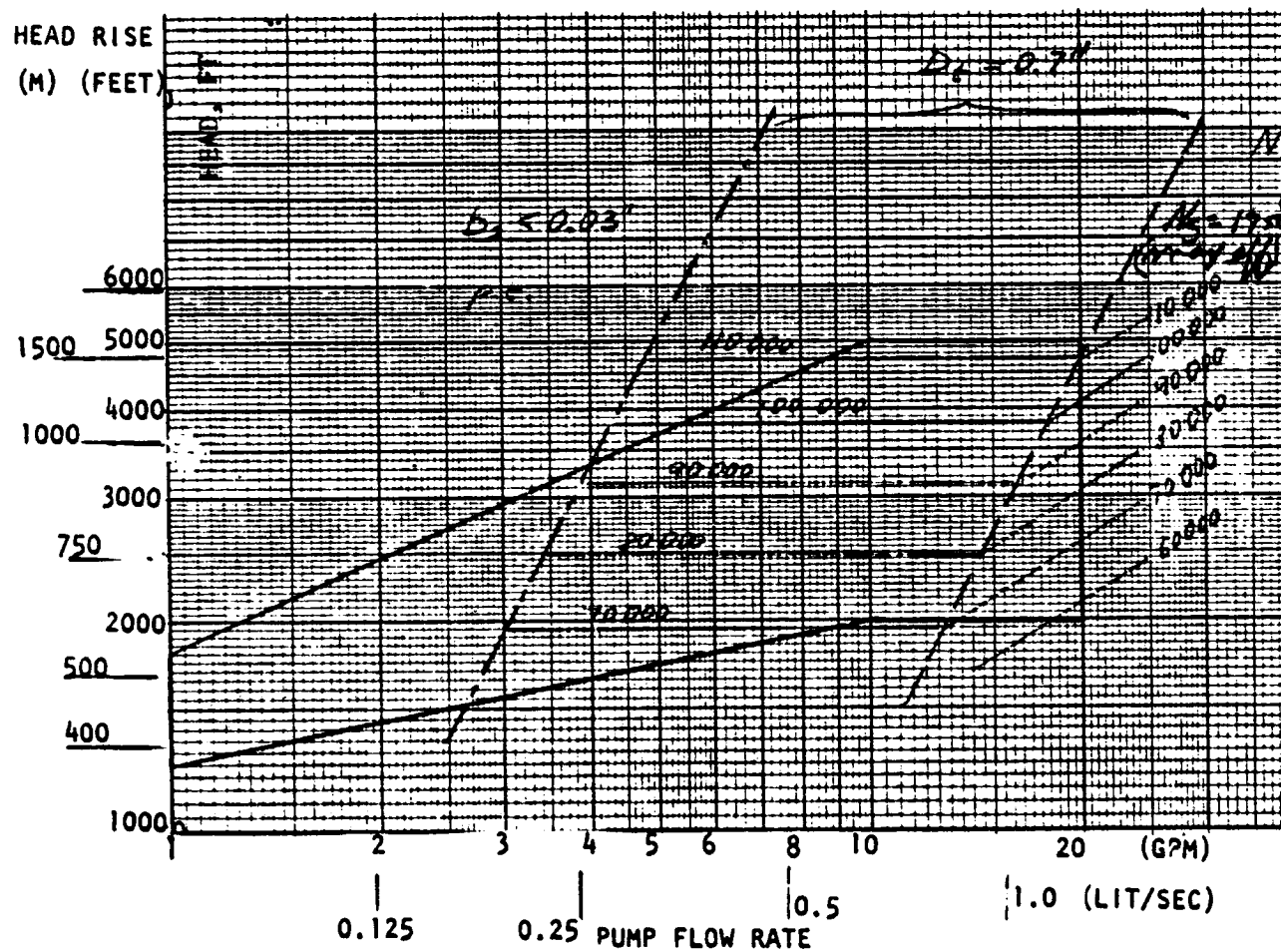


Figure A-43. Centrifugal Methane Pump - NPSH Optimized,
Speed ($D_t \geq 0.7$ inch)

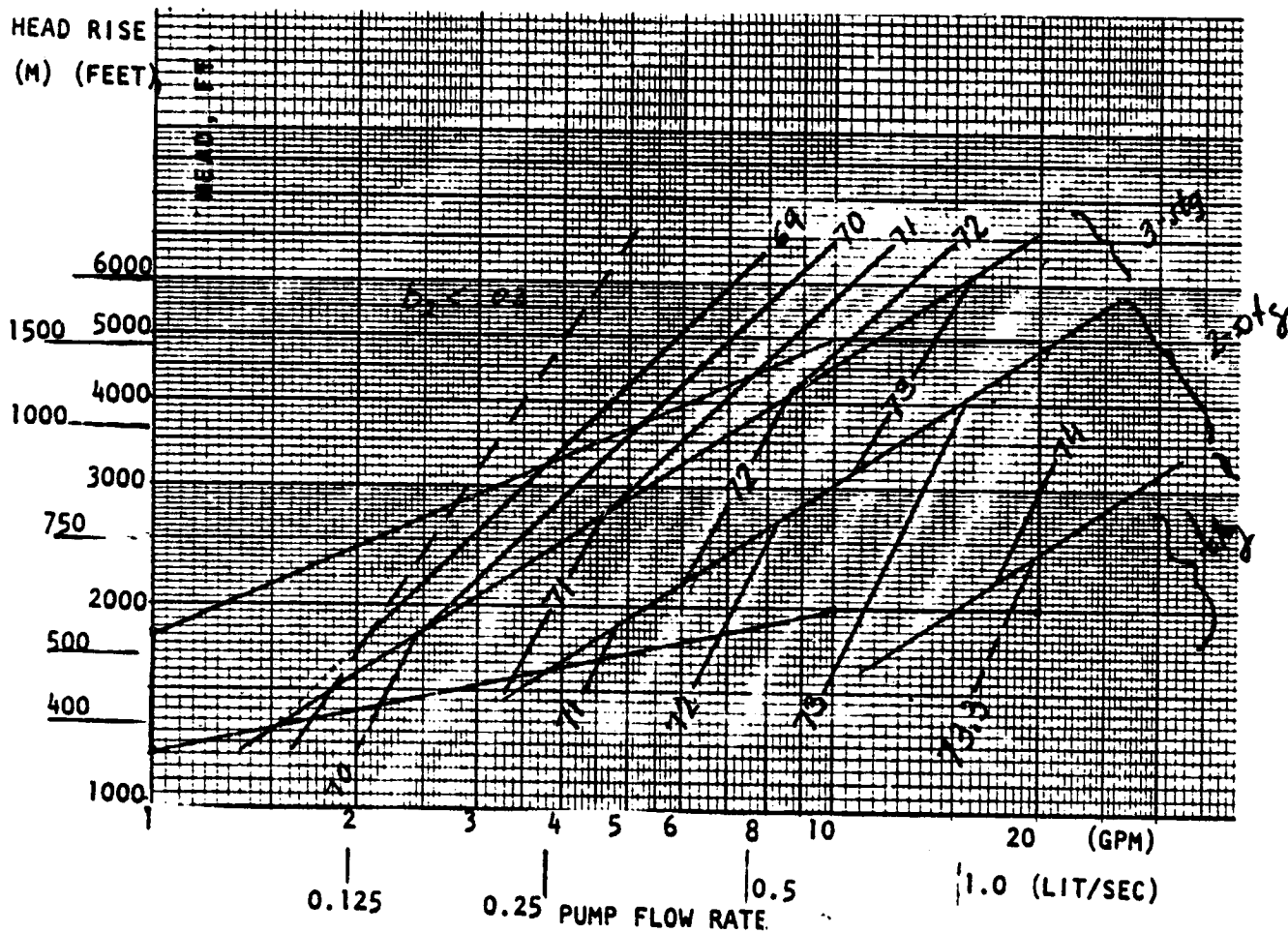


Figure A-44. Centrifugal Methane Pump - NPSH Optimized, Efficiency
($N_s = 1950$)

ORIGINAL PAGE IS
OF POOR QUALITY

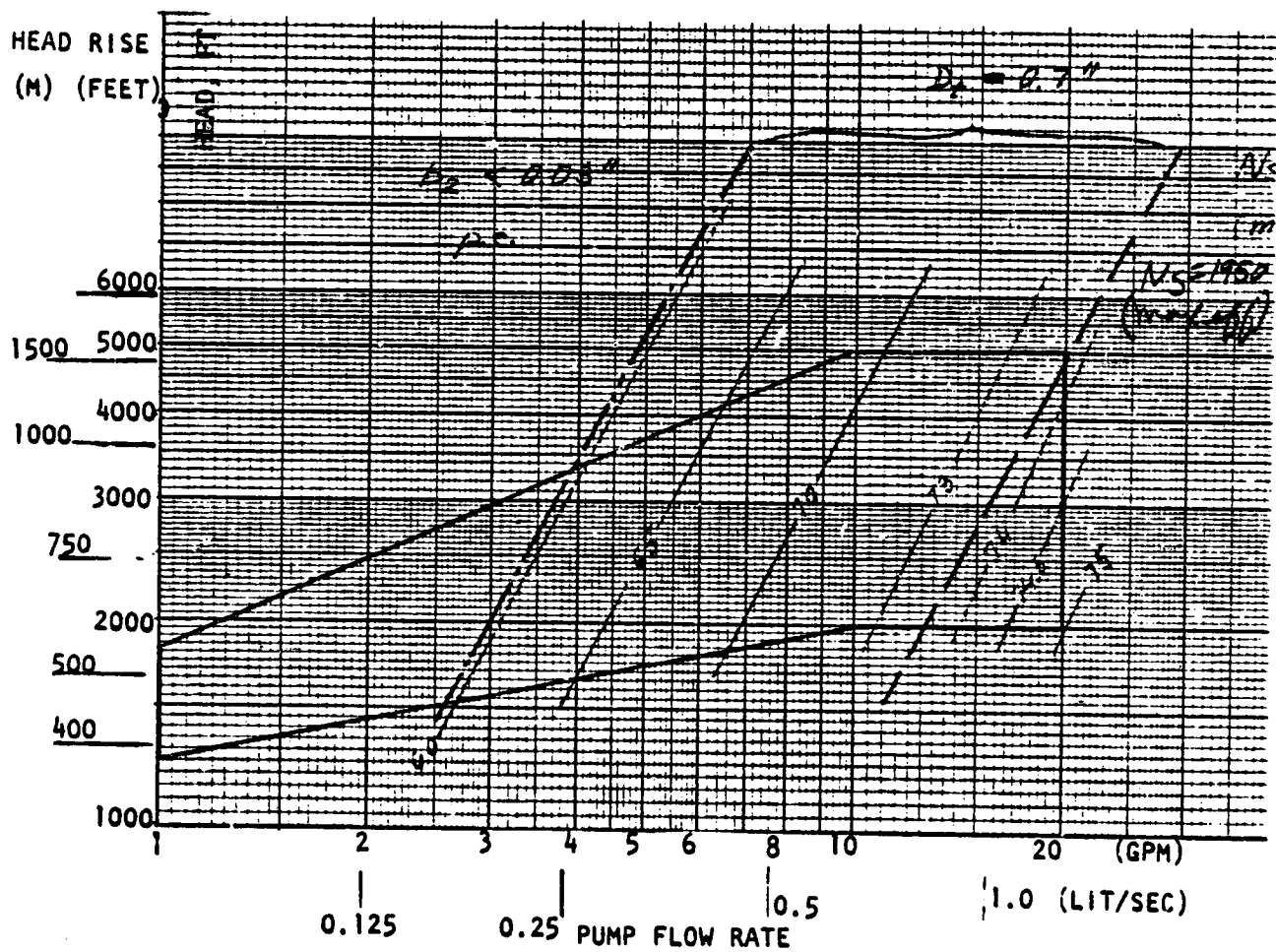


Figure A-45. Centrifugal Methane Pump - NPSH Optimized, Efficiency
 $(D_t \geq 0.7$ inch)

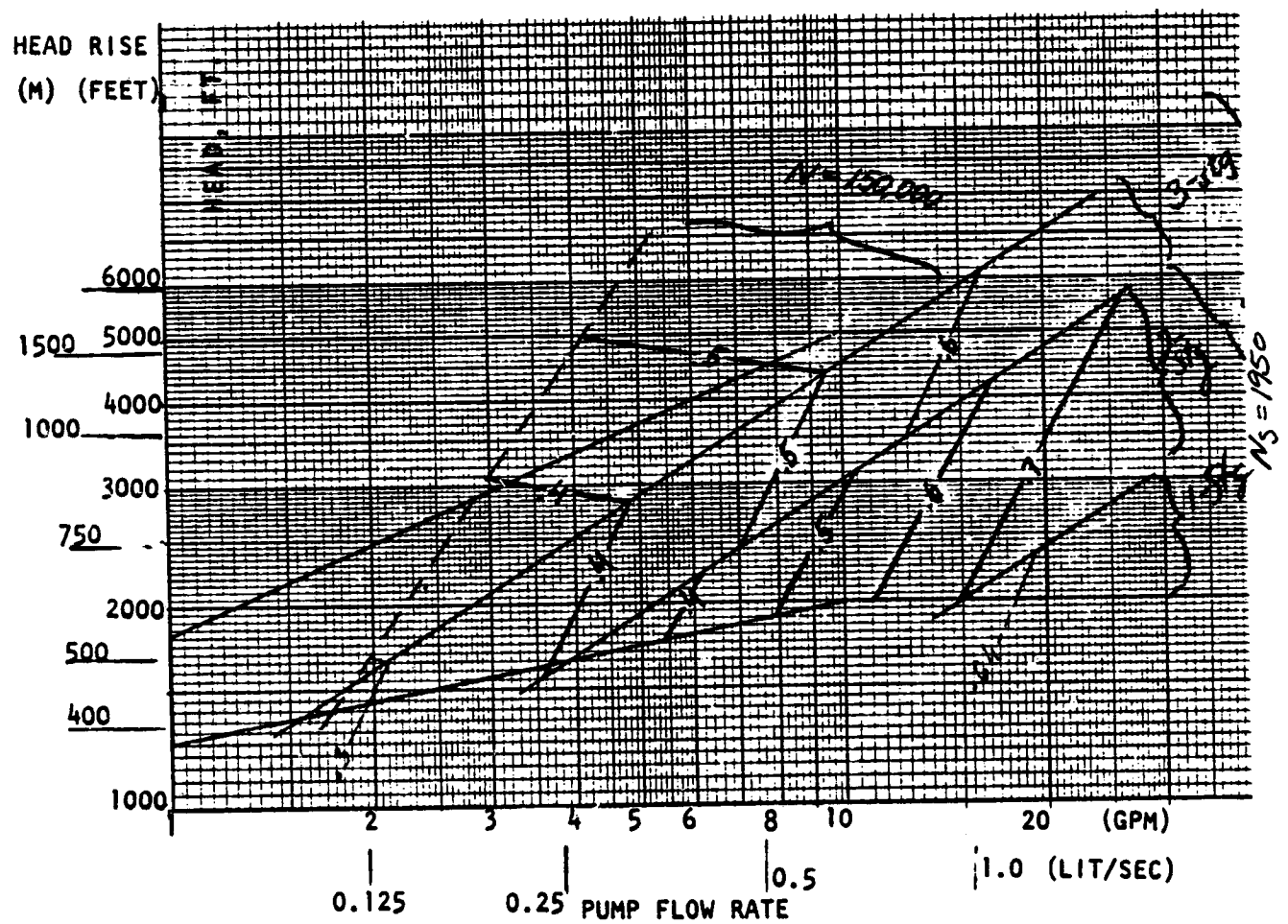


Figure A-46. Centrifugal Methane Pump - NPSH Optimized, Diameter
($N_s = 1950$)

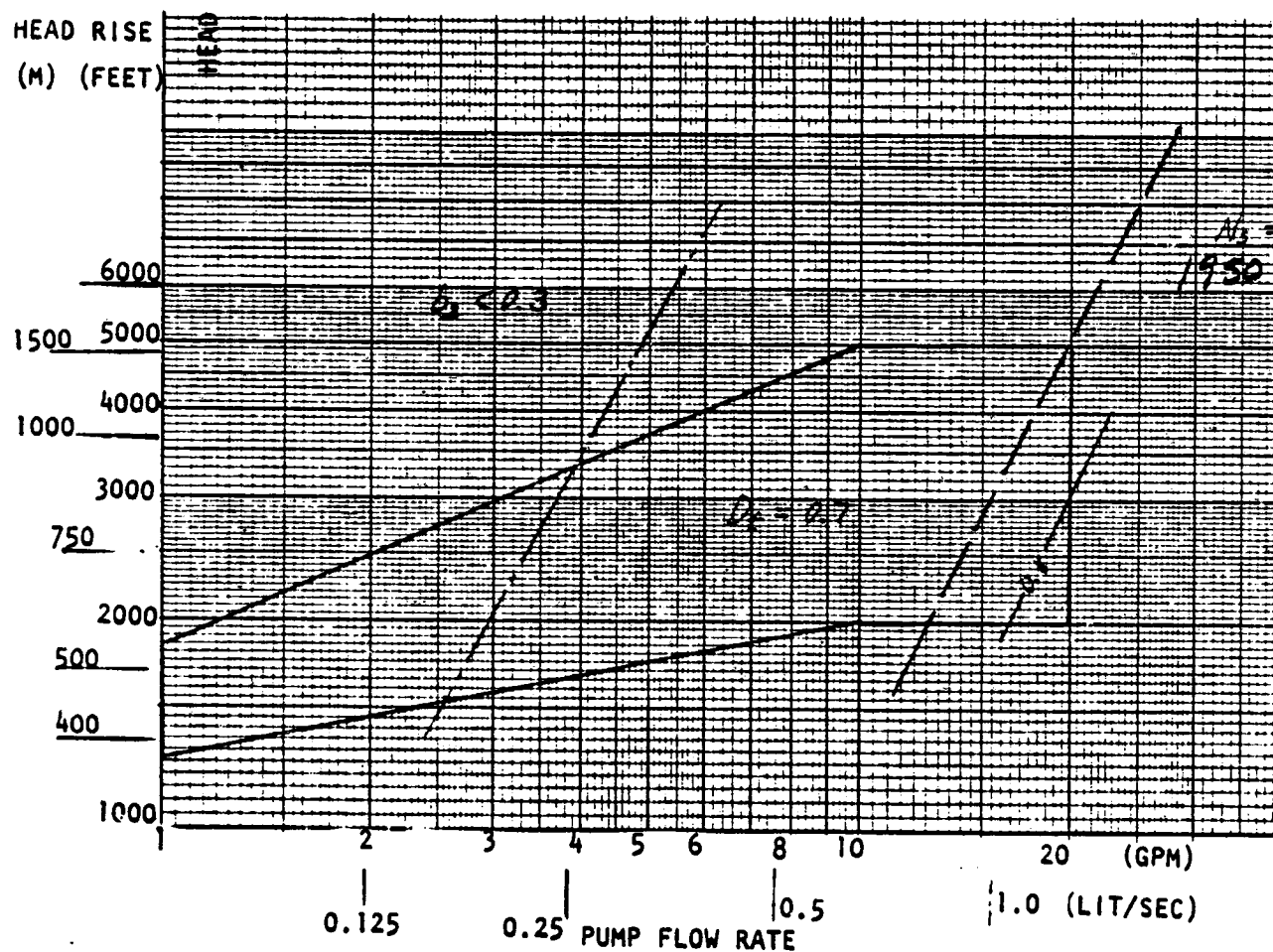


Figure A-47. Centrifugal Methane Pump - NPSH Optimized, Diameter ($D_t \geq 0.7$ inch)

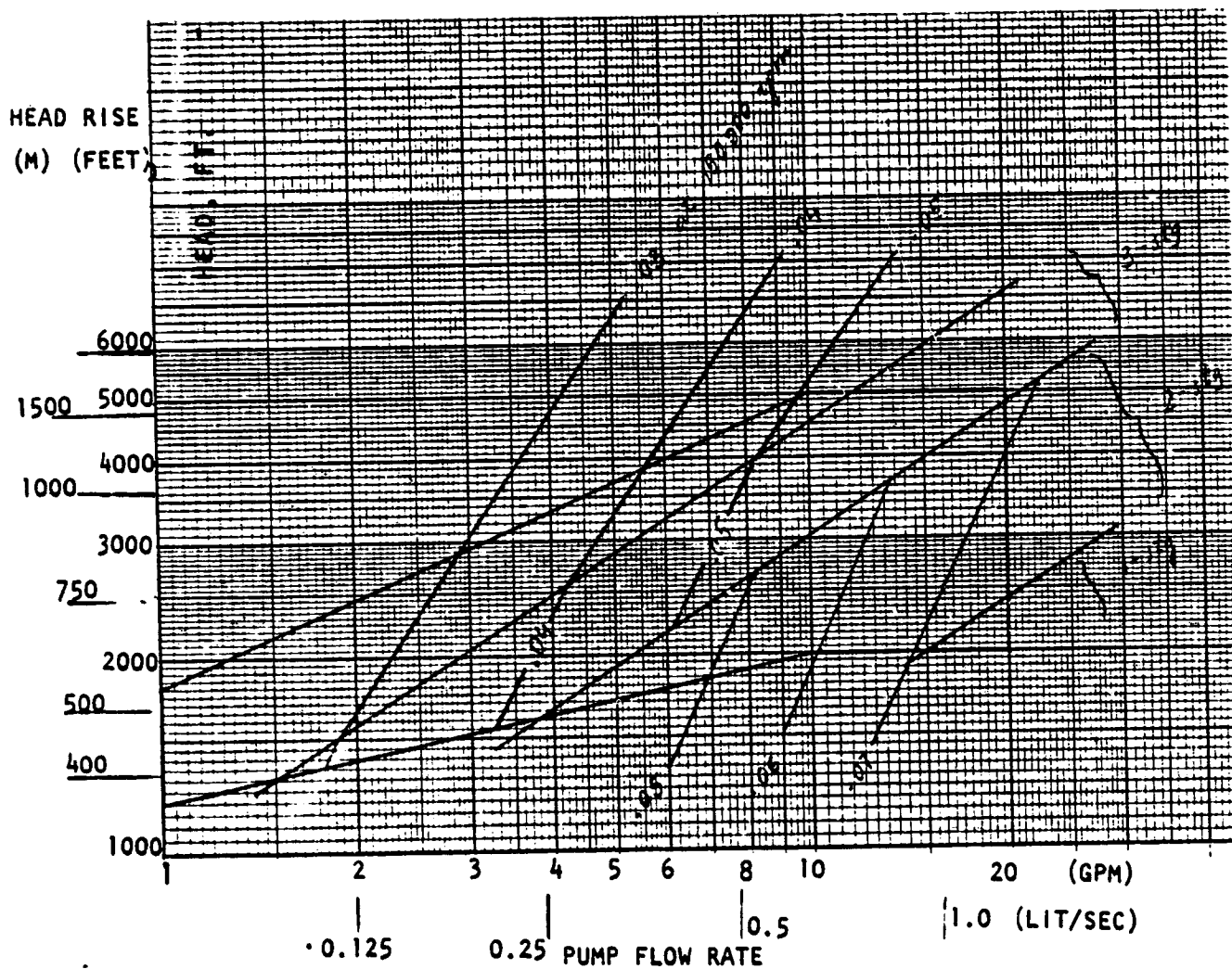


Figure A-48. Centrifugal Methane Pump - NPSH Optimized, Discharge Width ($N_s = 1950$)

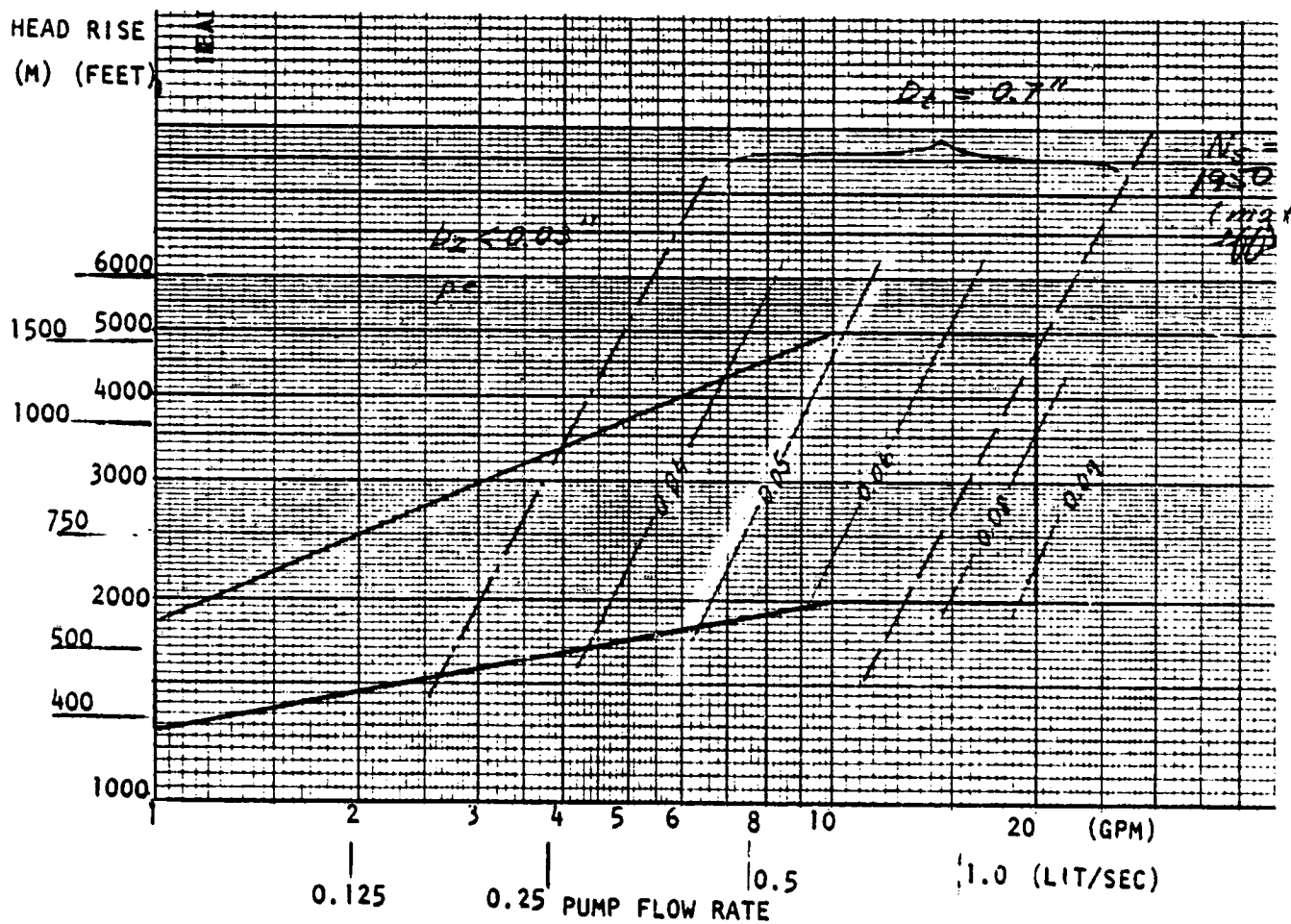


Figure A-49. Centrifugal Methane Pump - NPSH Optimized, Discharge Width ($D_t \geq 0.7$ inch)

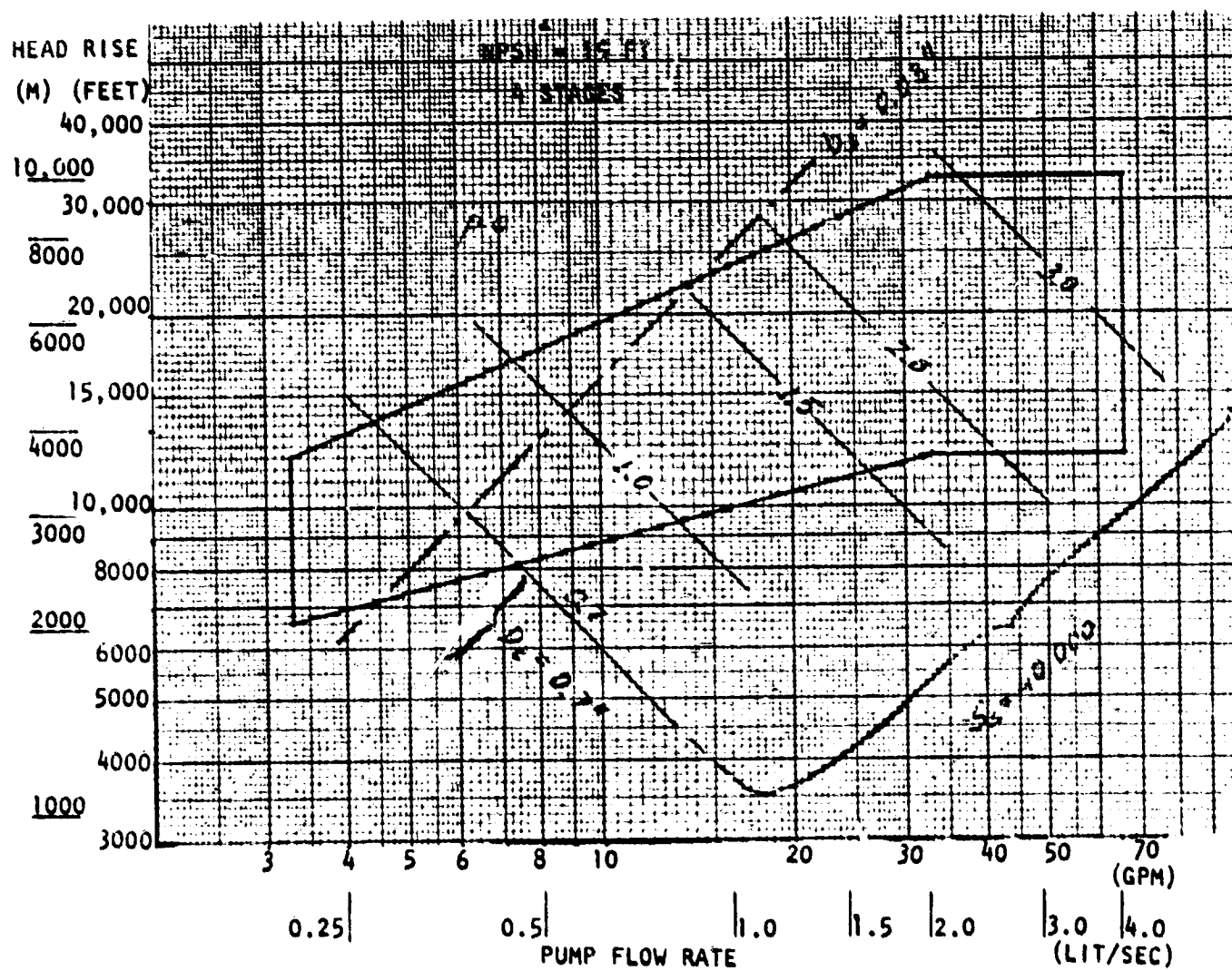


Figure A-52. Centrifugal Hydrogen Pump - NPSH = 15 Feet, Diameter

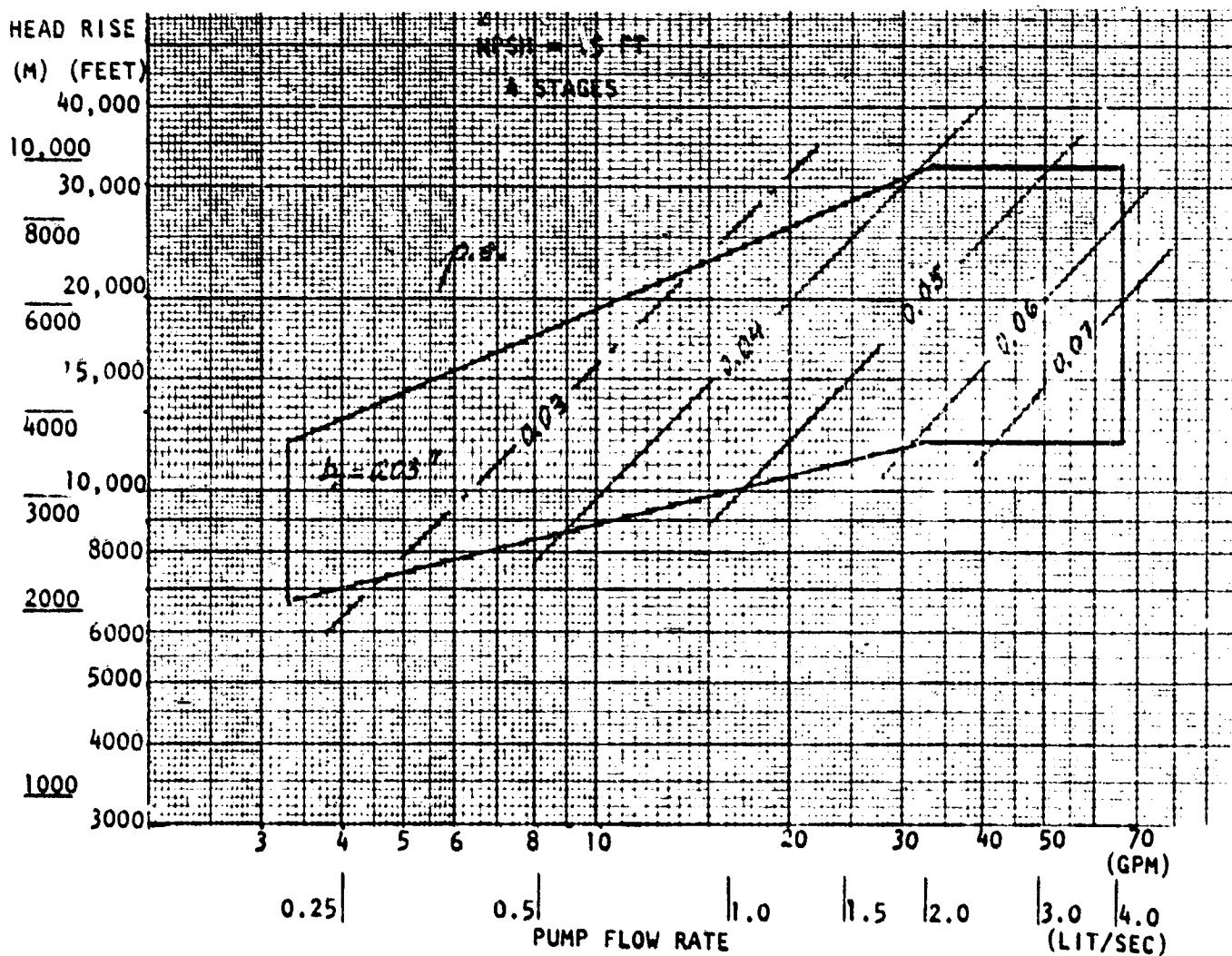


Figure A-53. Centrifugal Hydrogen Pump - NPSH = 15 Feet, Discharge Width

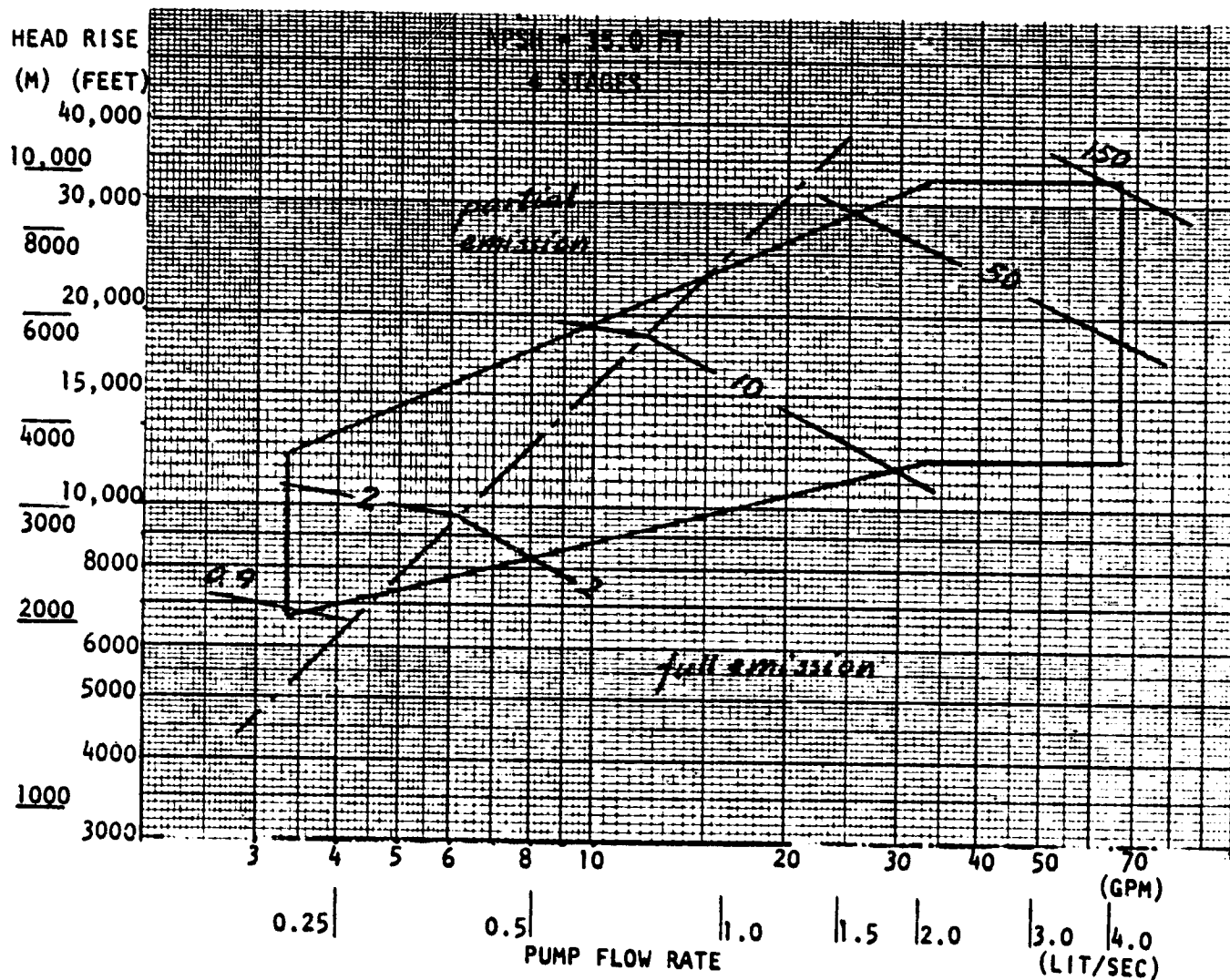


Figure A-54. Centrifugal Hydrogen Pump - NPSH = 15 Feet, Power

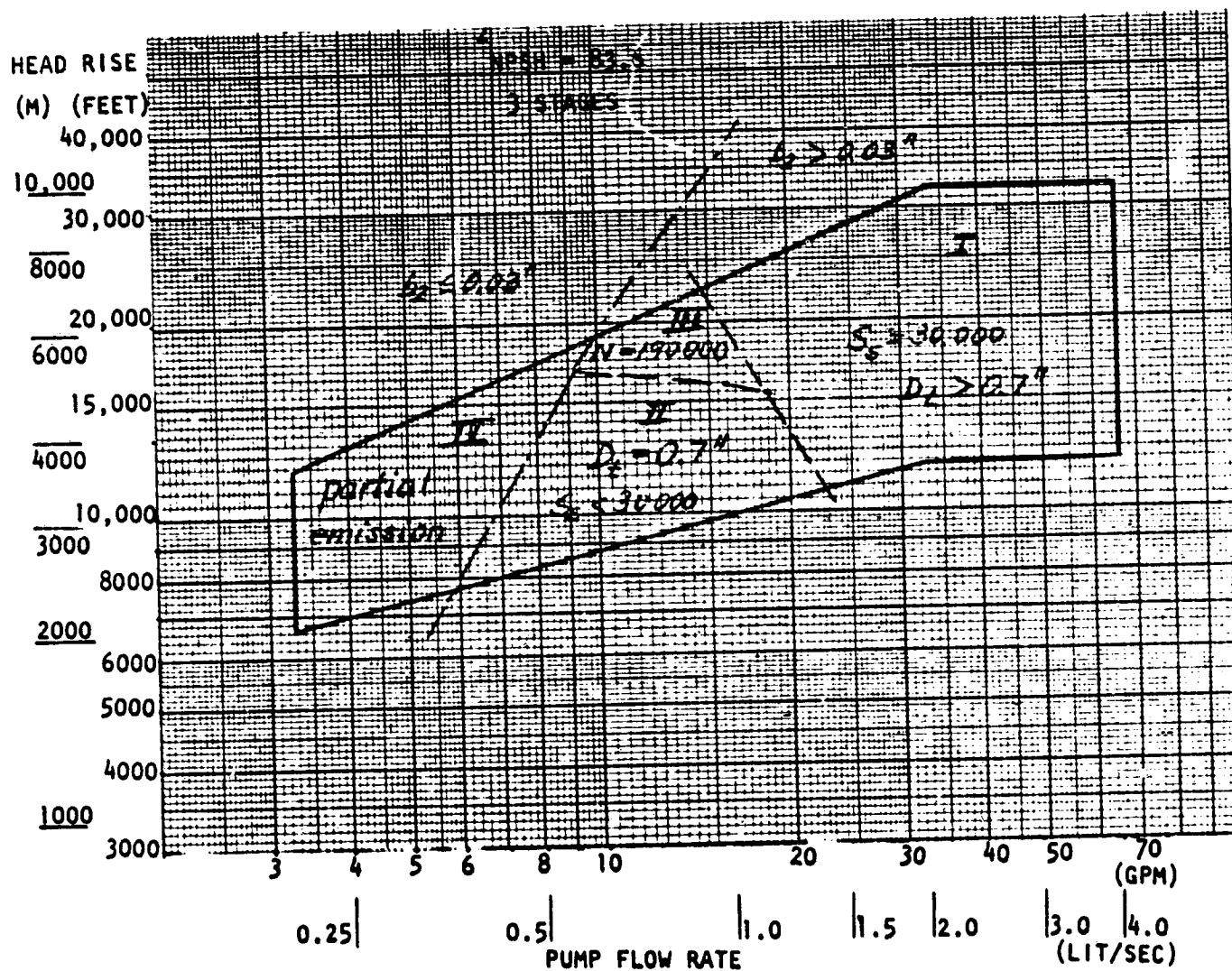


Figure A-55. Centrifugal Hydrogen Pump - NPSH = 83.6 Feet, Limitations

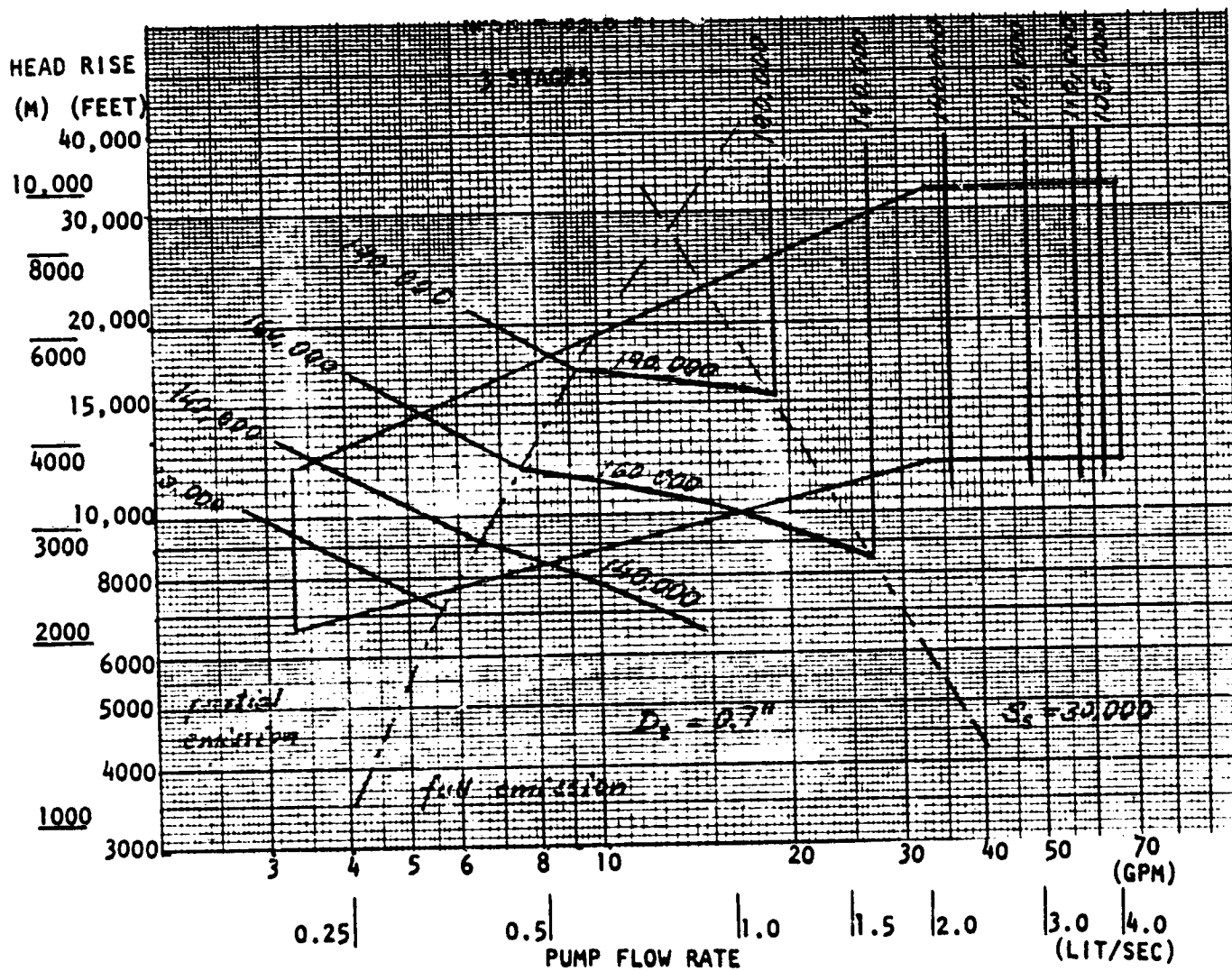


Figure A-56. Centrifugal Hydrogen Pump - NPSH = 83.6 Feet, Speed

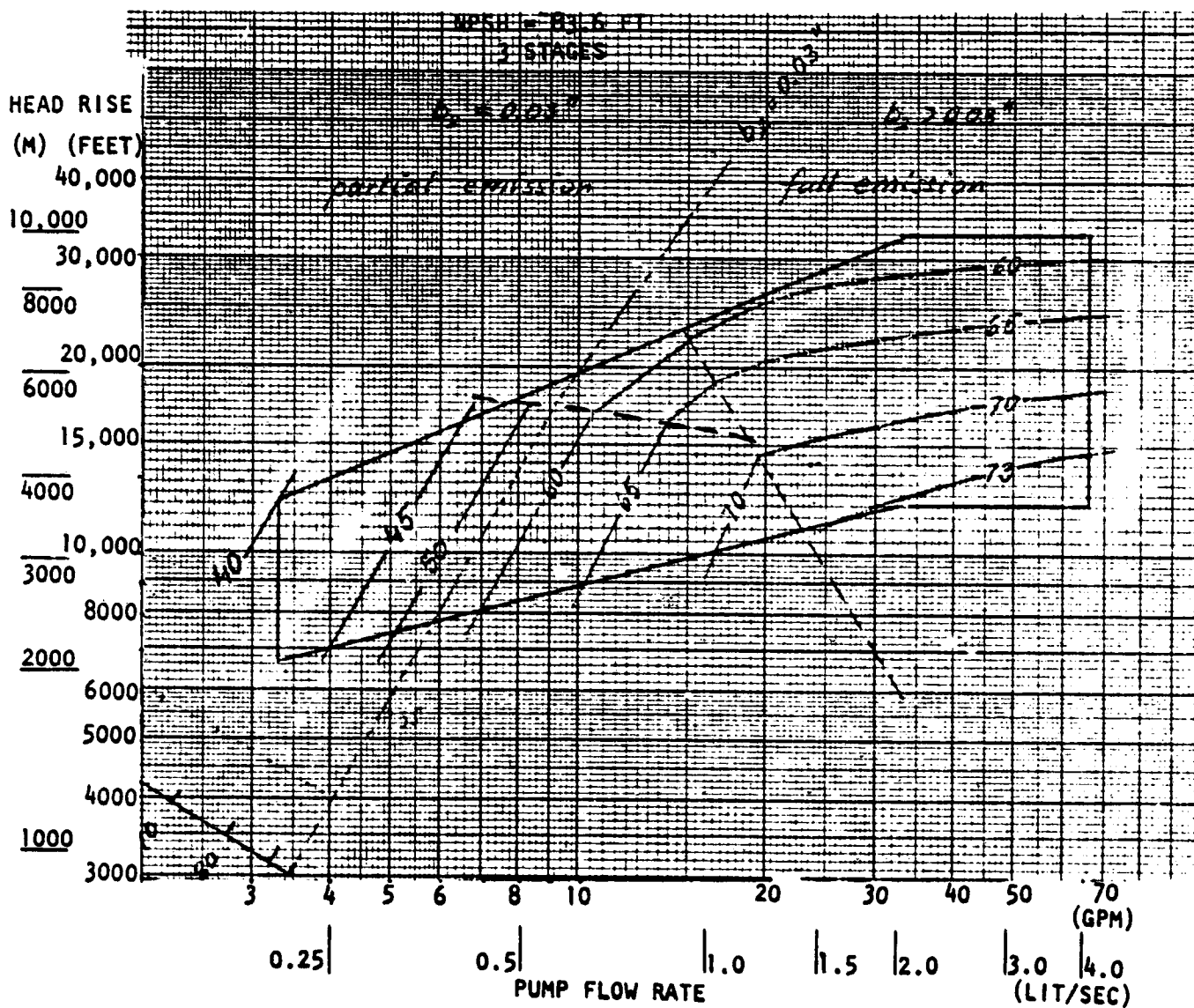


Figure A-57. Centrifugal Hydrogen Pump - NPSH = 83.6 Feet, Efficiency

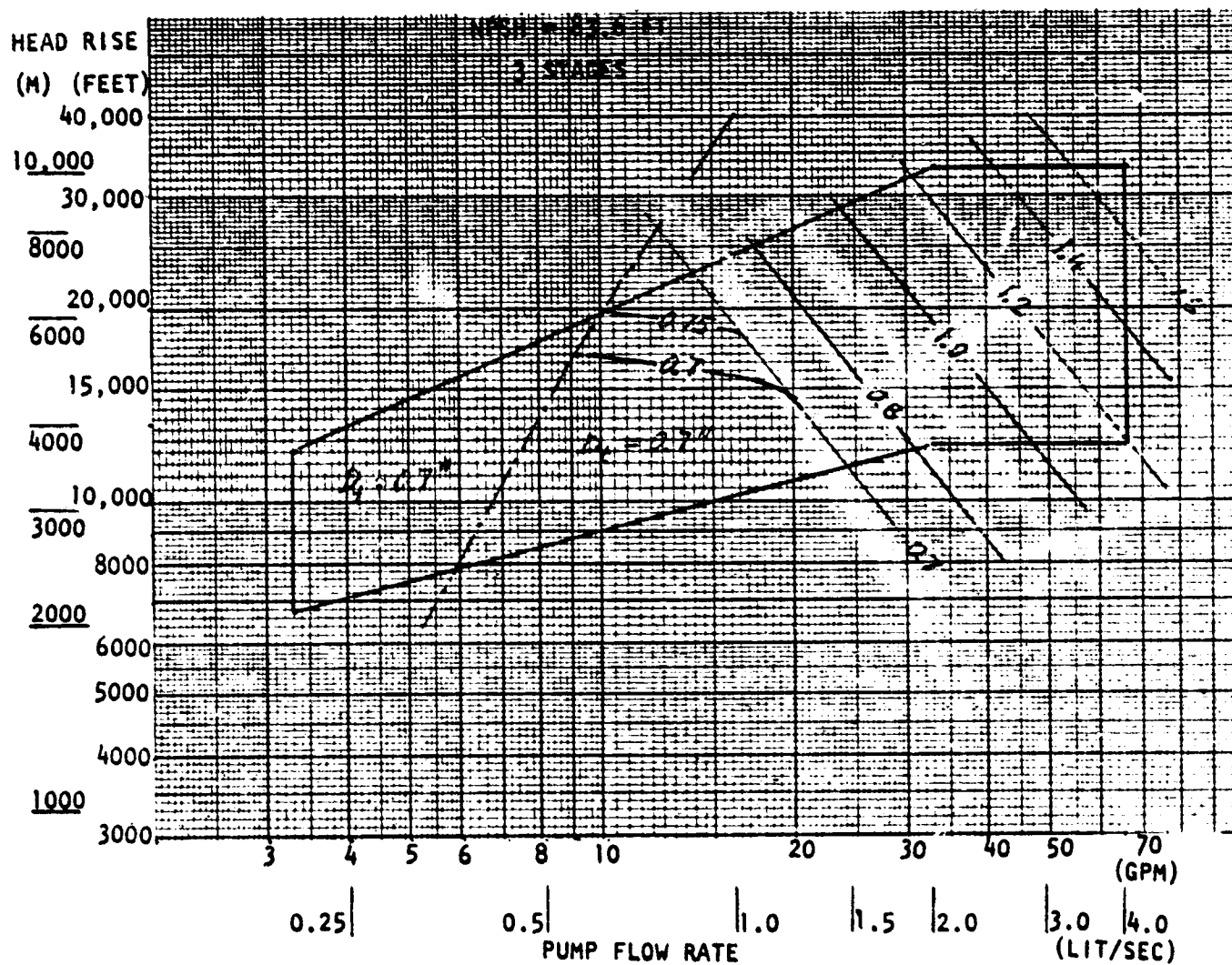


Figure A-58. Centrifugal Hydrogen Pump - NPSH = 83.6 Feet, Diameter

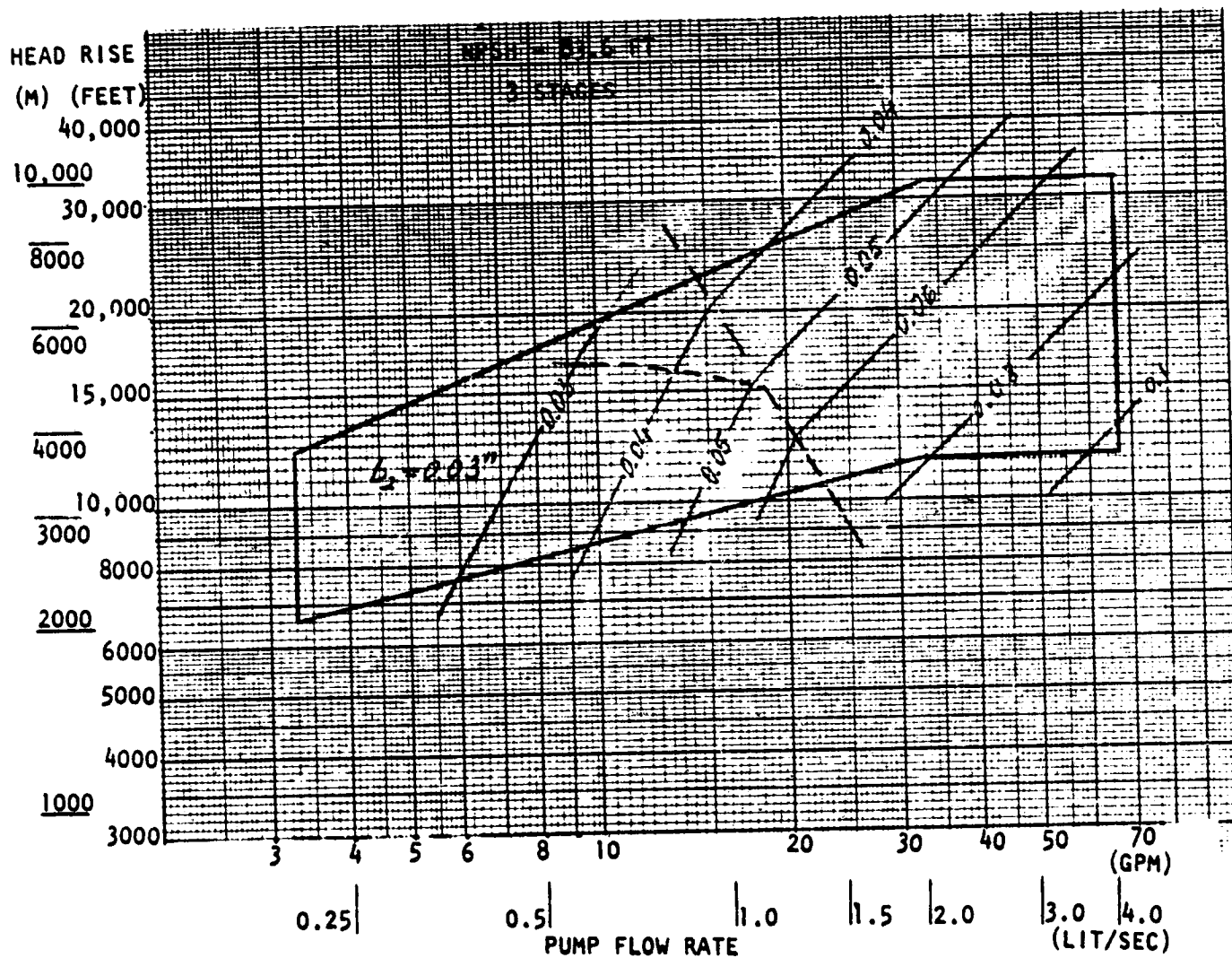


Figure A-59. Centrifugal Hydrogen Pump - NPSH = 83.6 Feet,
Discharge Width

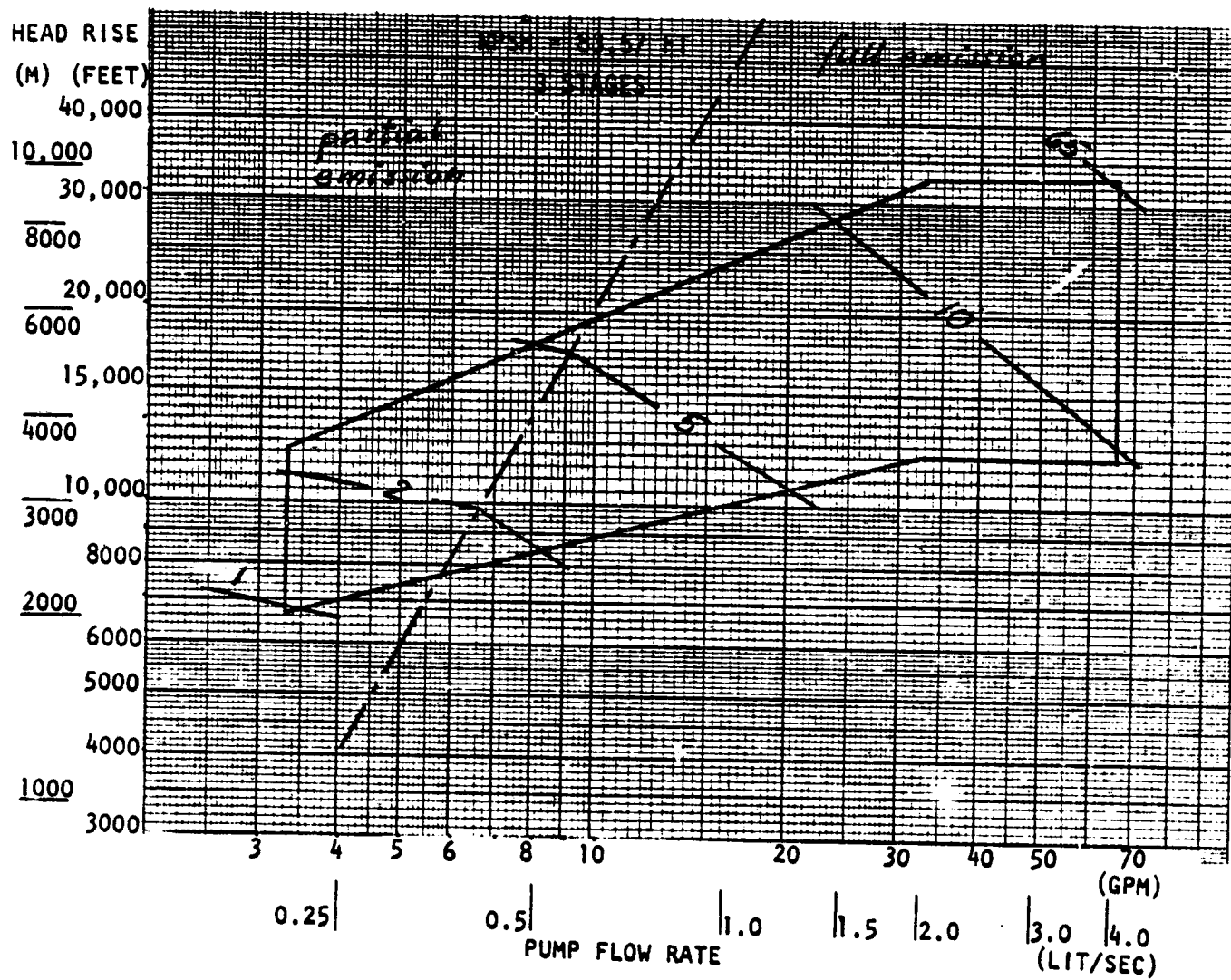


Figure A-60. Centrifugal Hydrogen Pump - NPSH = 83.6 Feet, Power

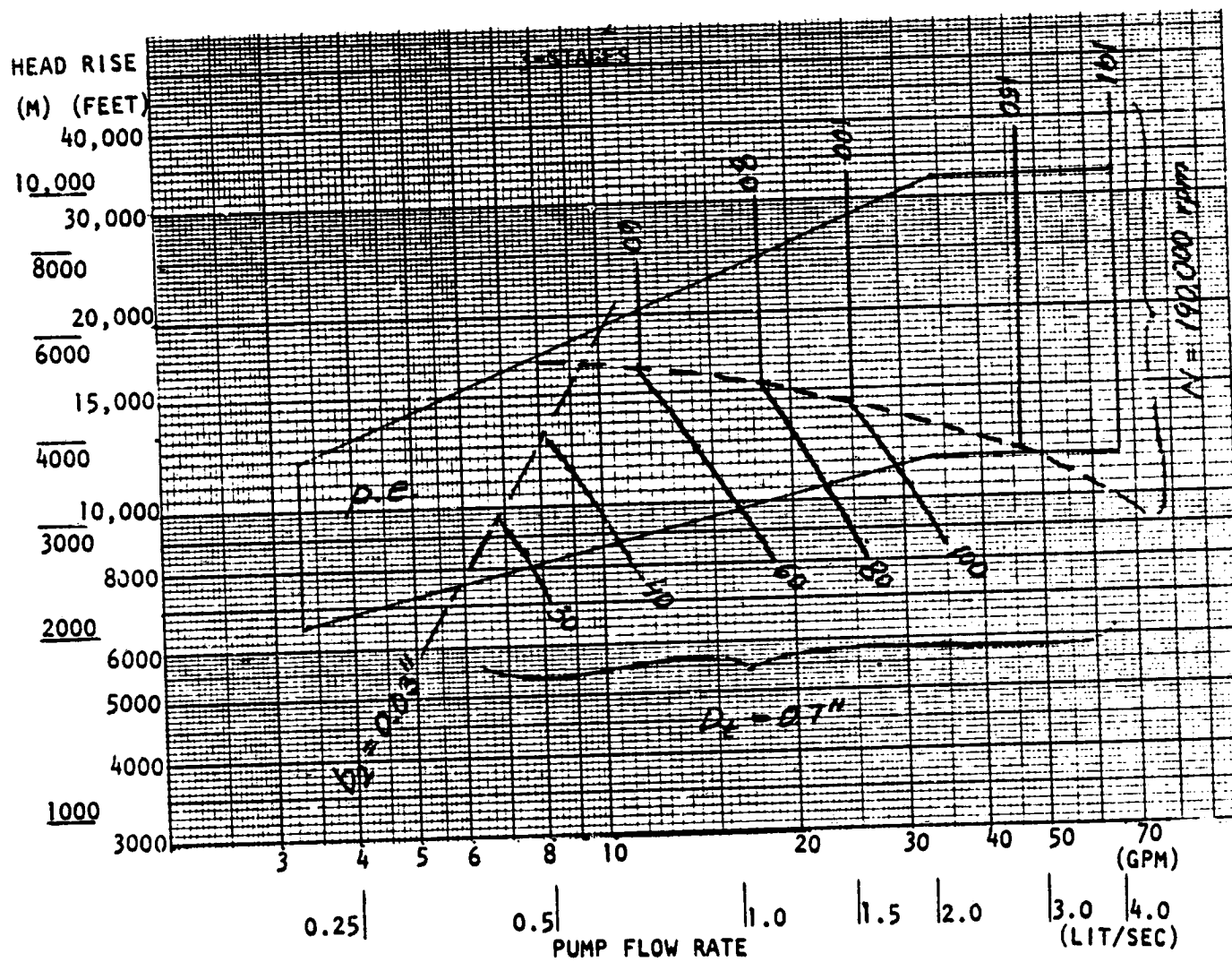


Figure A-61. Centrifugal Hydrogen Pump - NPSH Optimized

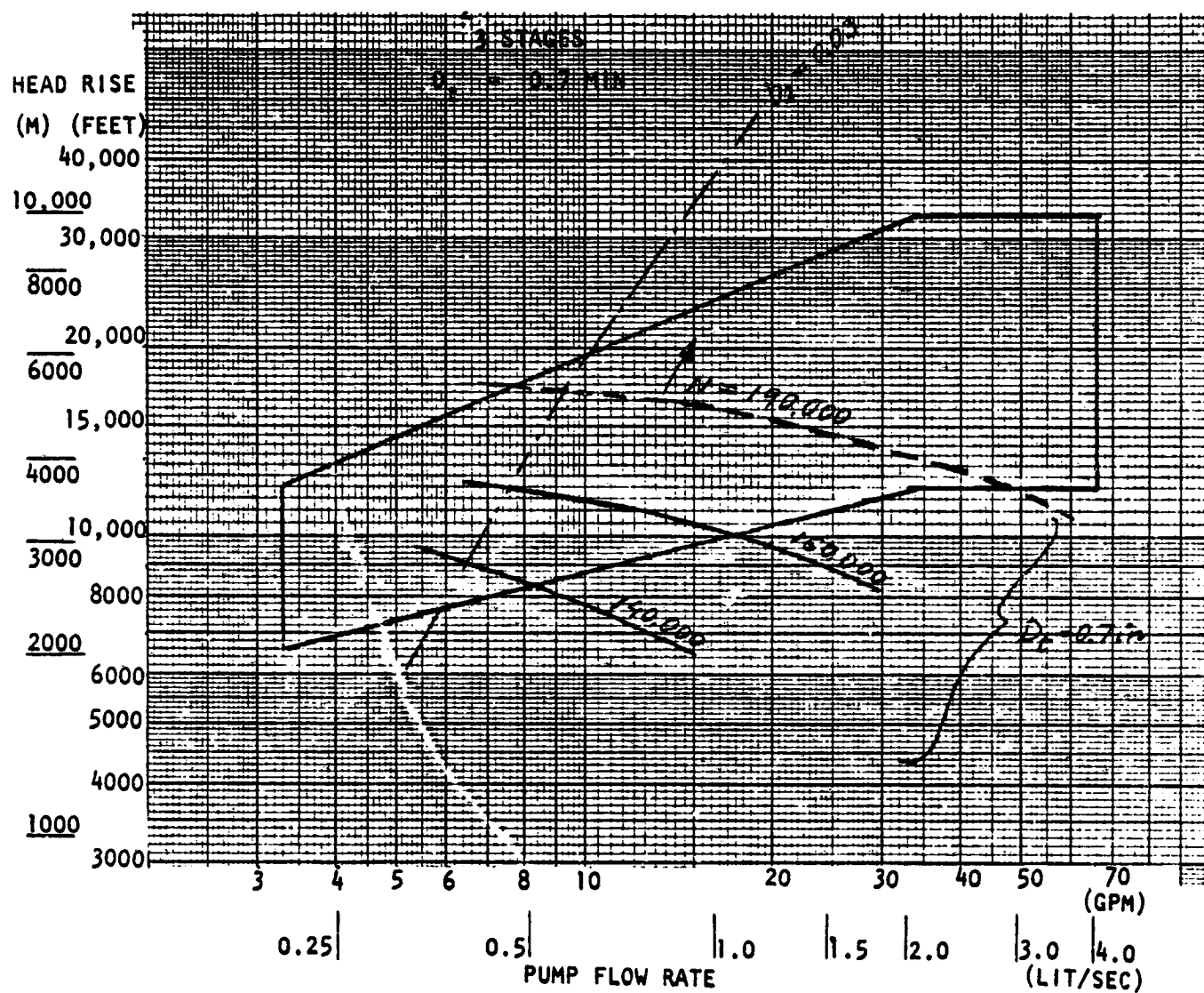


Figure A-62. Centrifugal Hydrogen Pump - NPSH Optimized, Speed

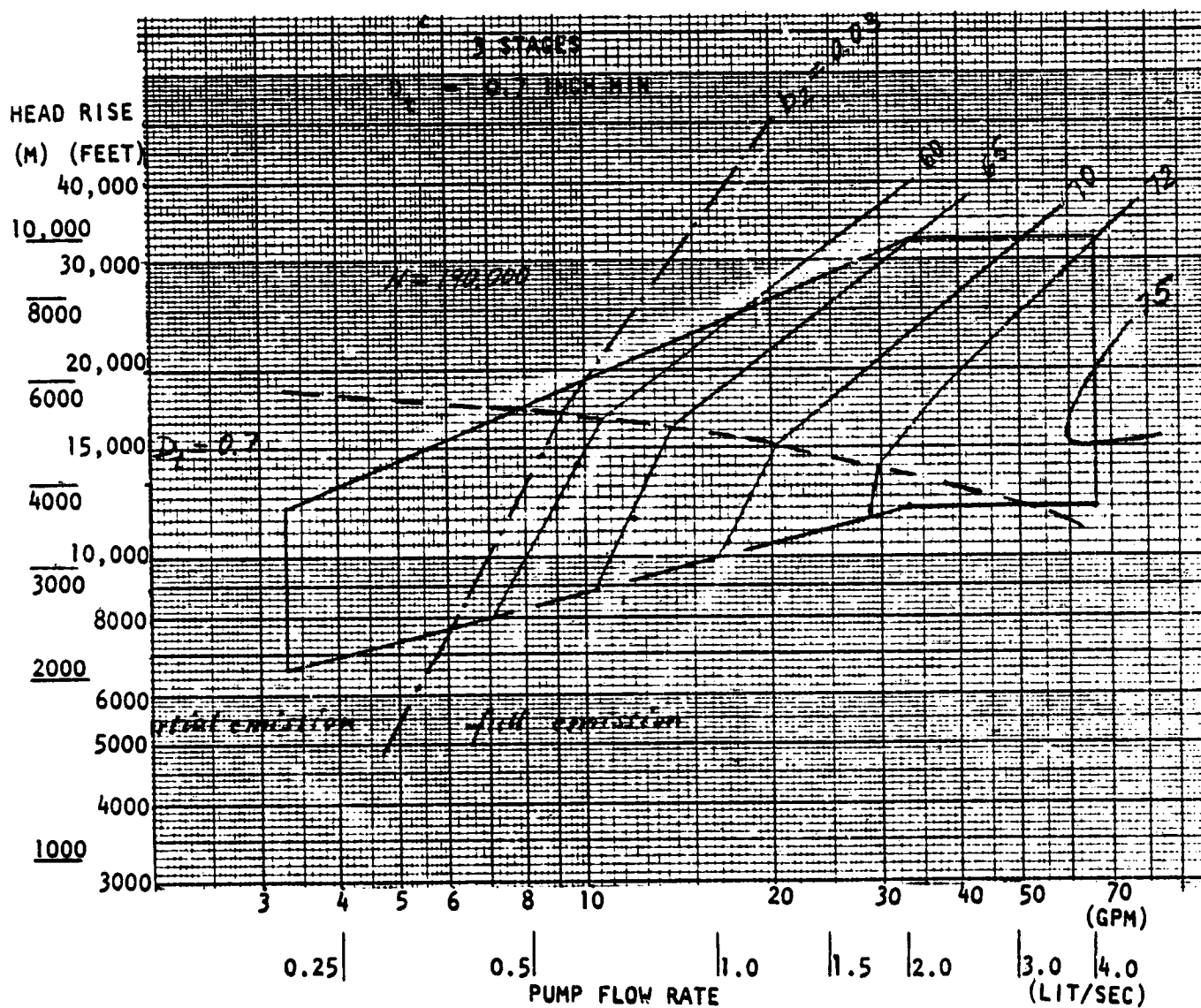


Figure A-63. Centrifugal Hydrogen Pump - NPSH Optimized, Efficiency ($D_t \geq 0.7$ inch)

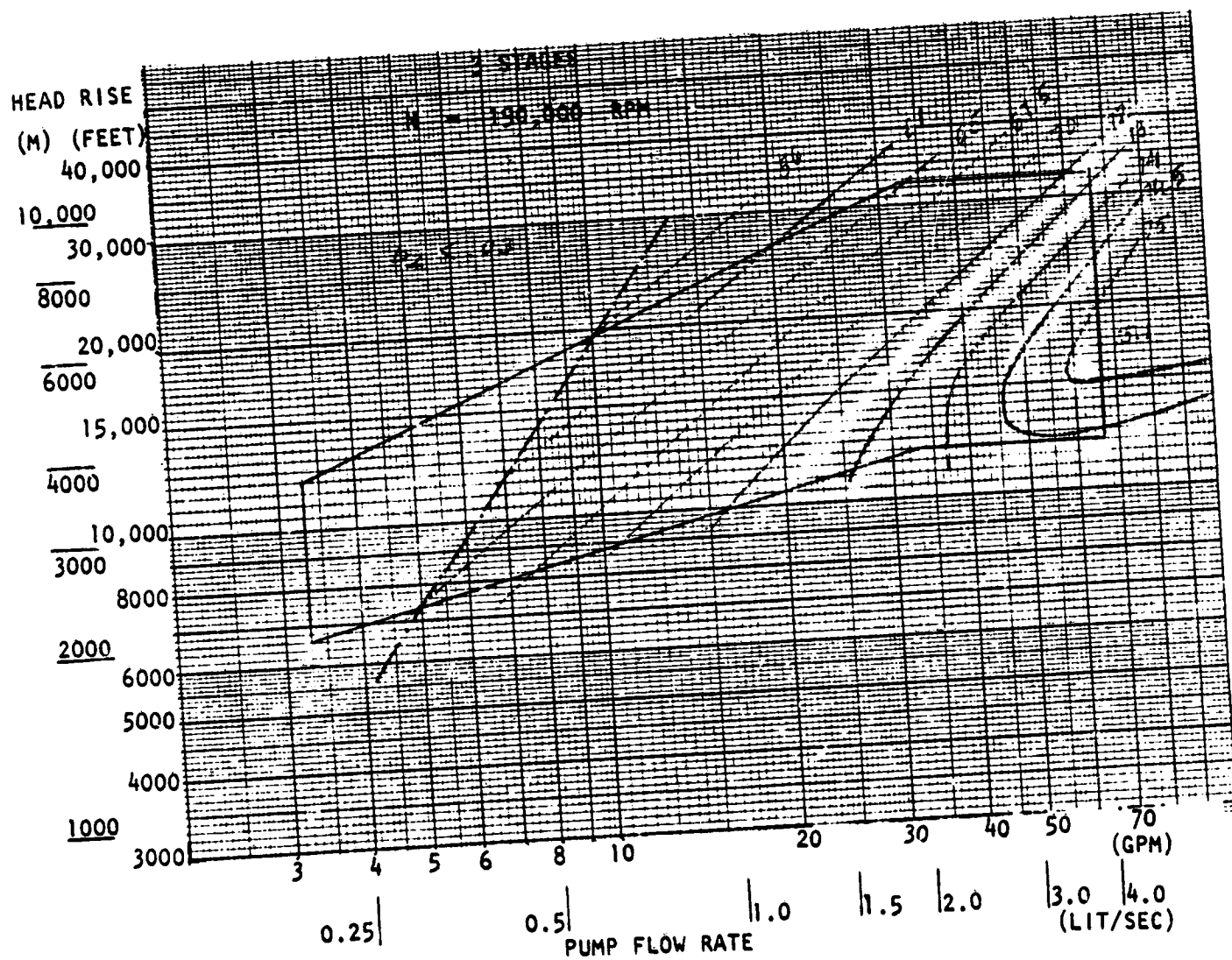


Figure A-64. Centrifugal Hydrogen Pump - NPSH Optimized, Efficiency
(N = 190,000 rpm)

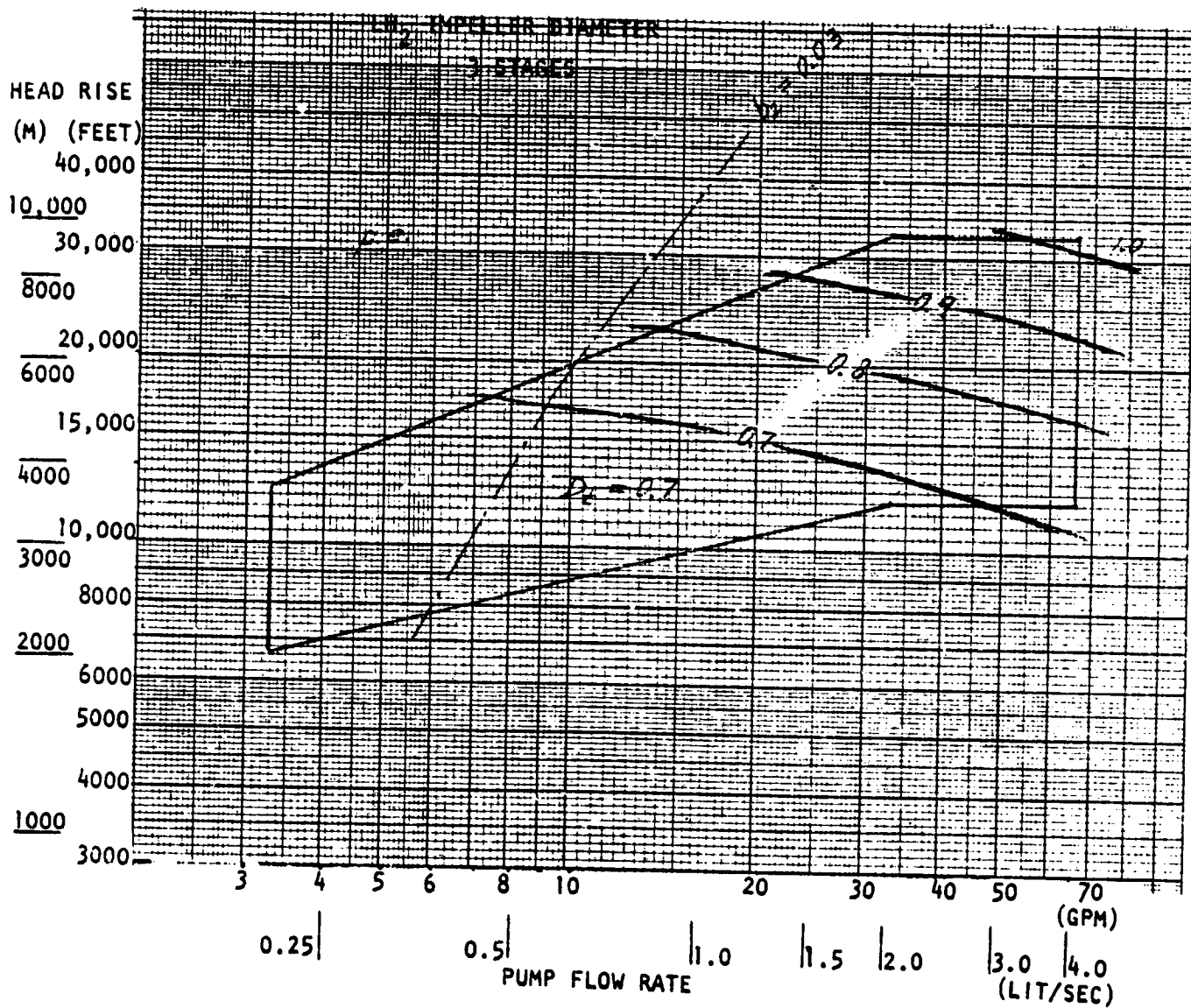


Figure A-65. Centrifugal Hydrogen Pump - NPSH Optimized,
Diameter ($D_t \geq 0.7$ inch)

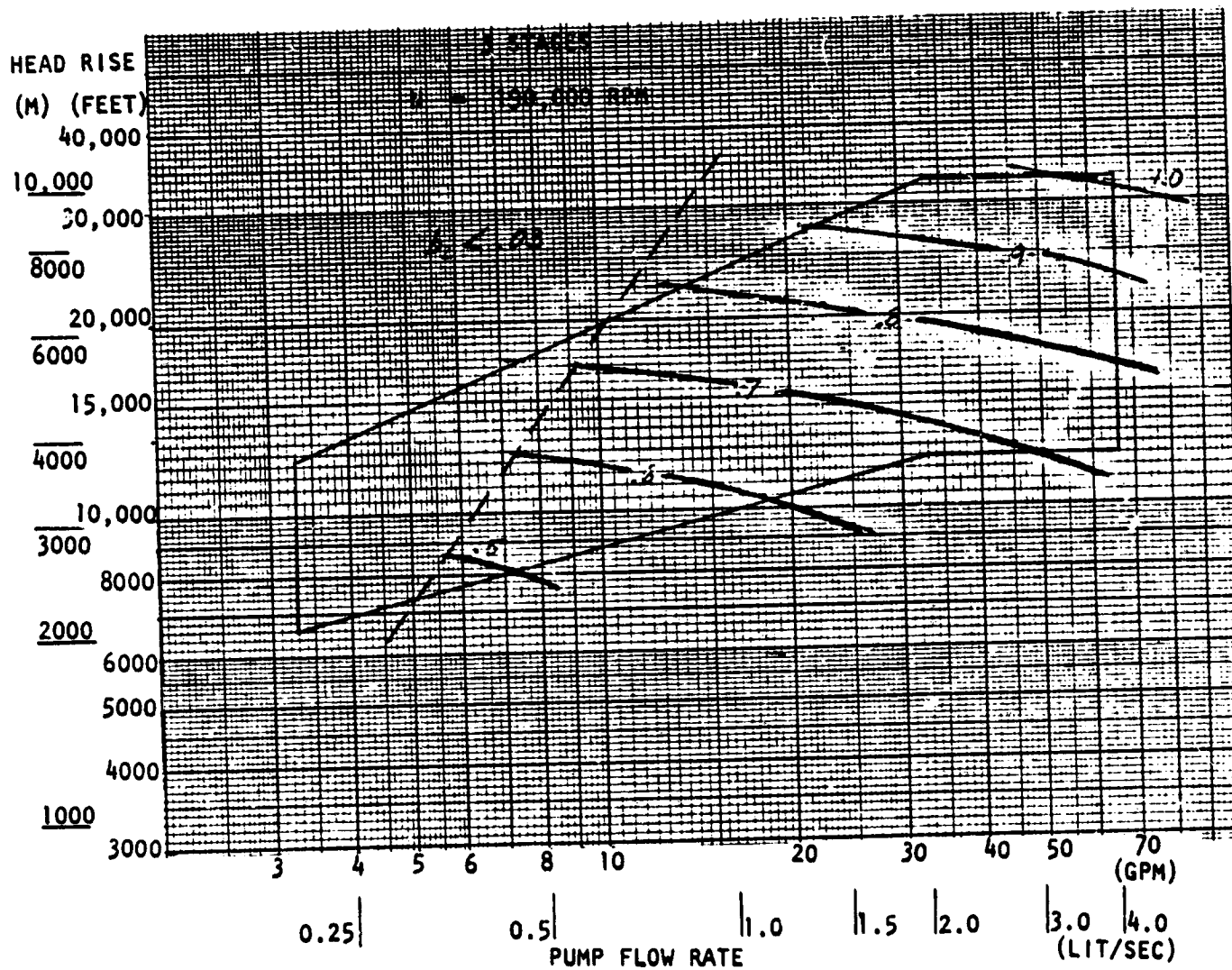


Figure A-66. Centrifugal Hydrogen Pump - NPSH Optimized, Diameter
(N = 190,000 rpm)

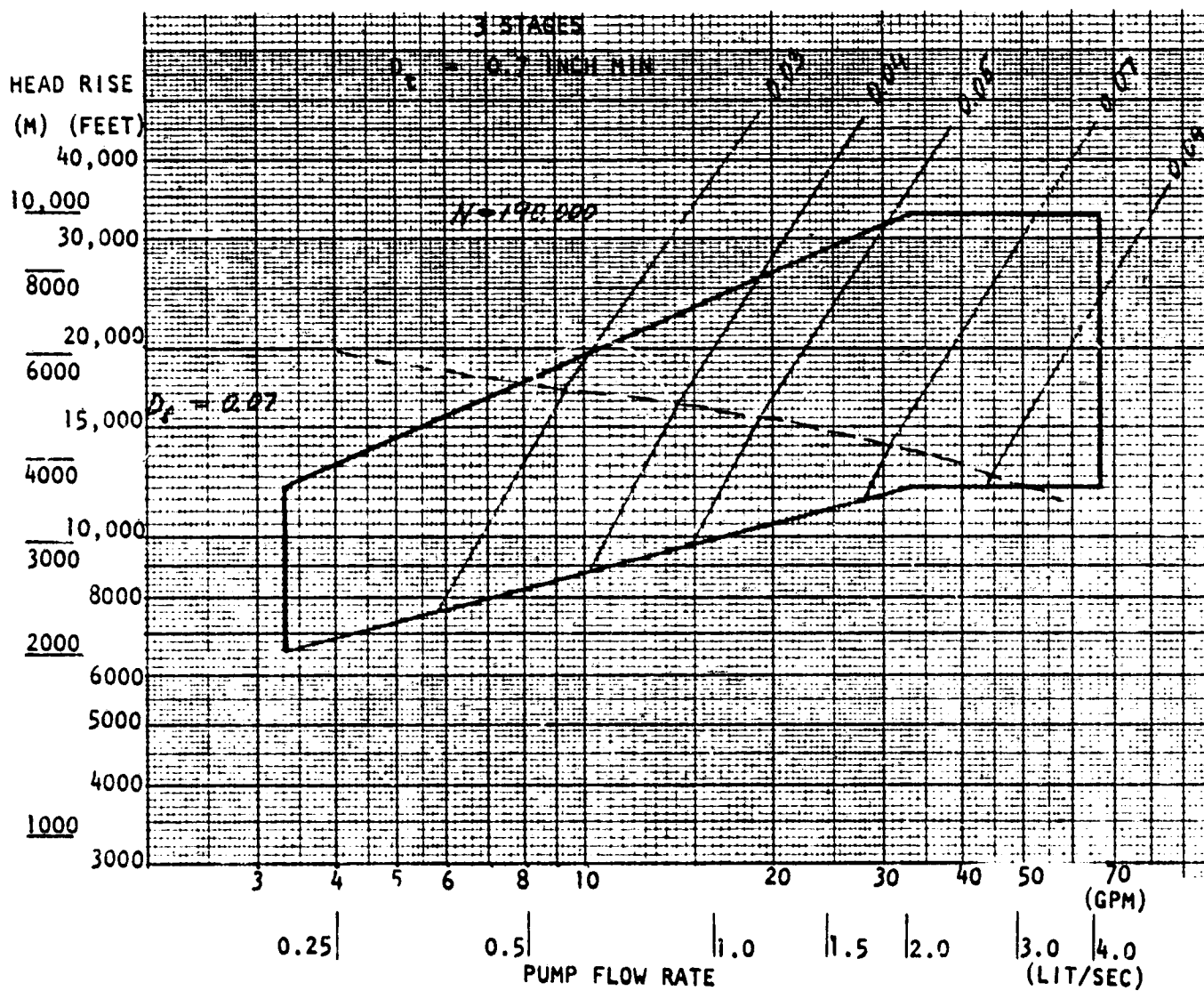


Figure A-67. Centrifugal Hydrogen Pump - NPSH Optimized, Discharge Width ($D_t \geq 0.7$ inch)

ORIGINAL PAGE IS
 OF POOR QUALITY

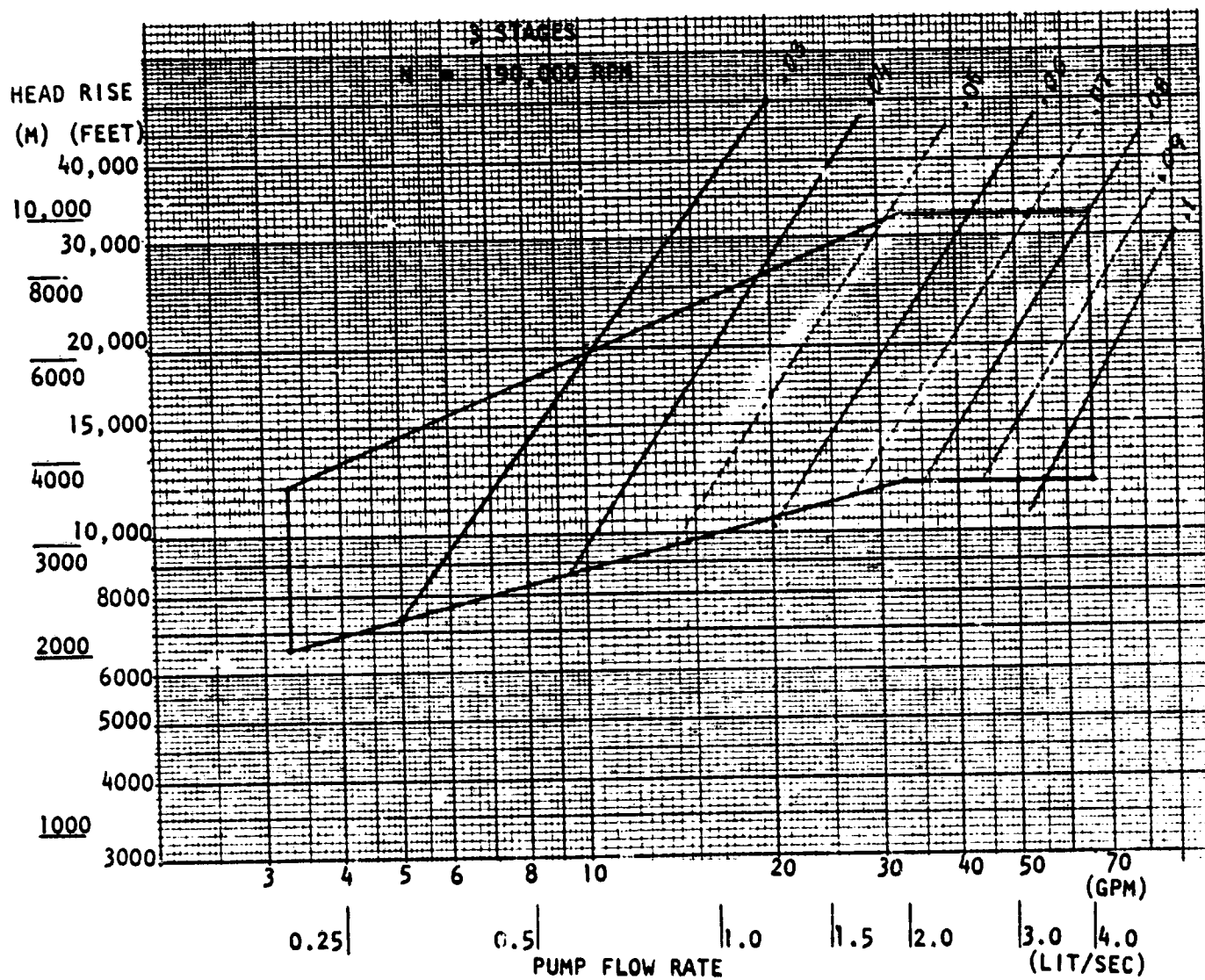


Figure A-68. Centrifugal Hydrogen Pump - NPSH Optimized, Discharge Width (N = 190,000 rpm)

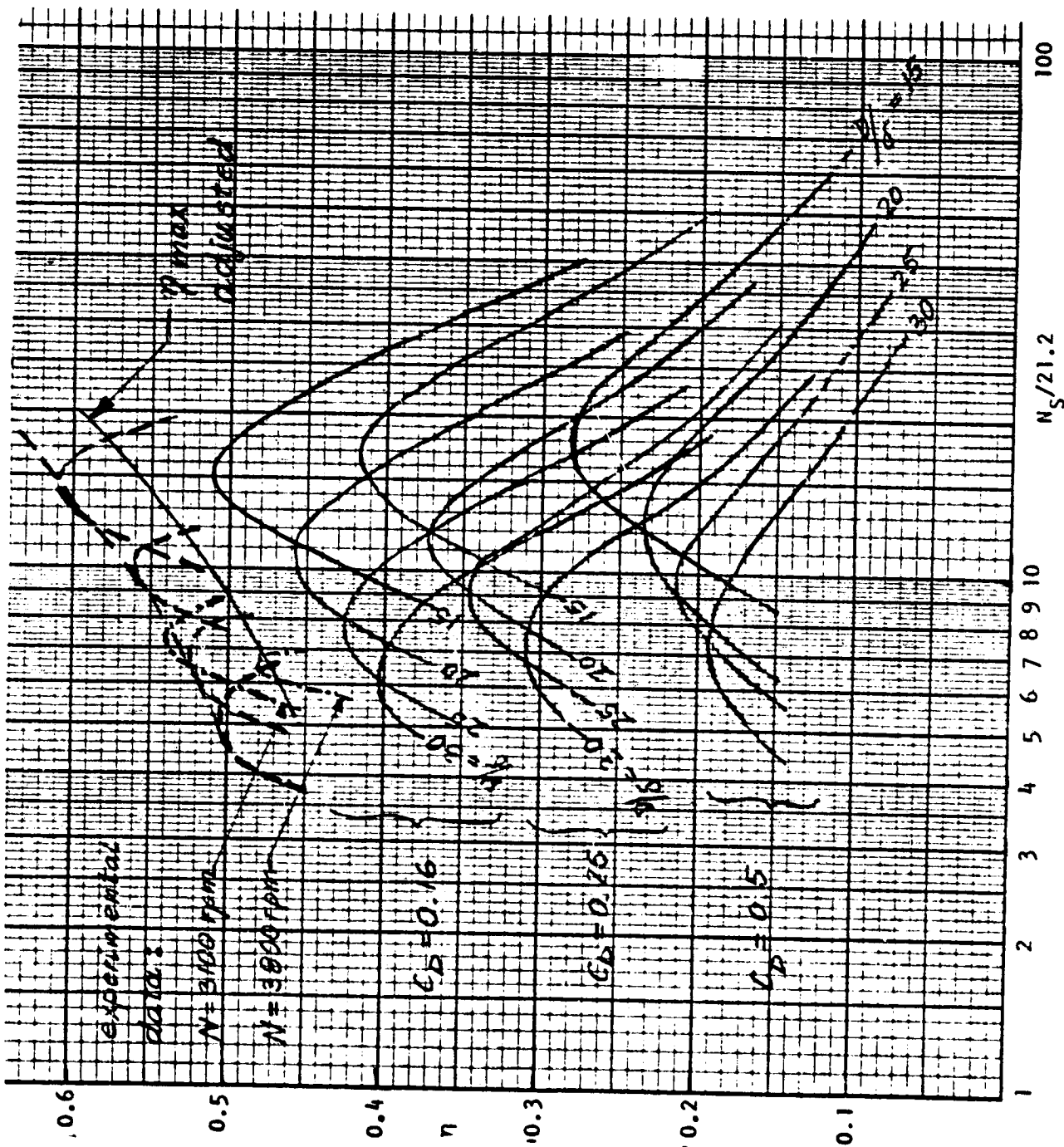


Figure A-69. Pitot Pump Performance Data

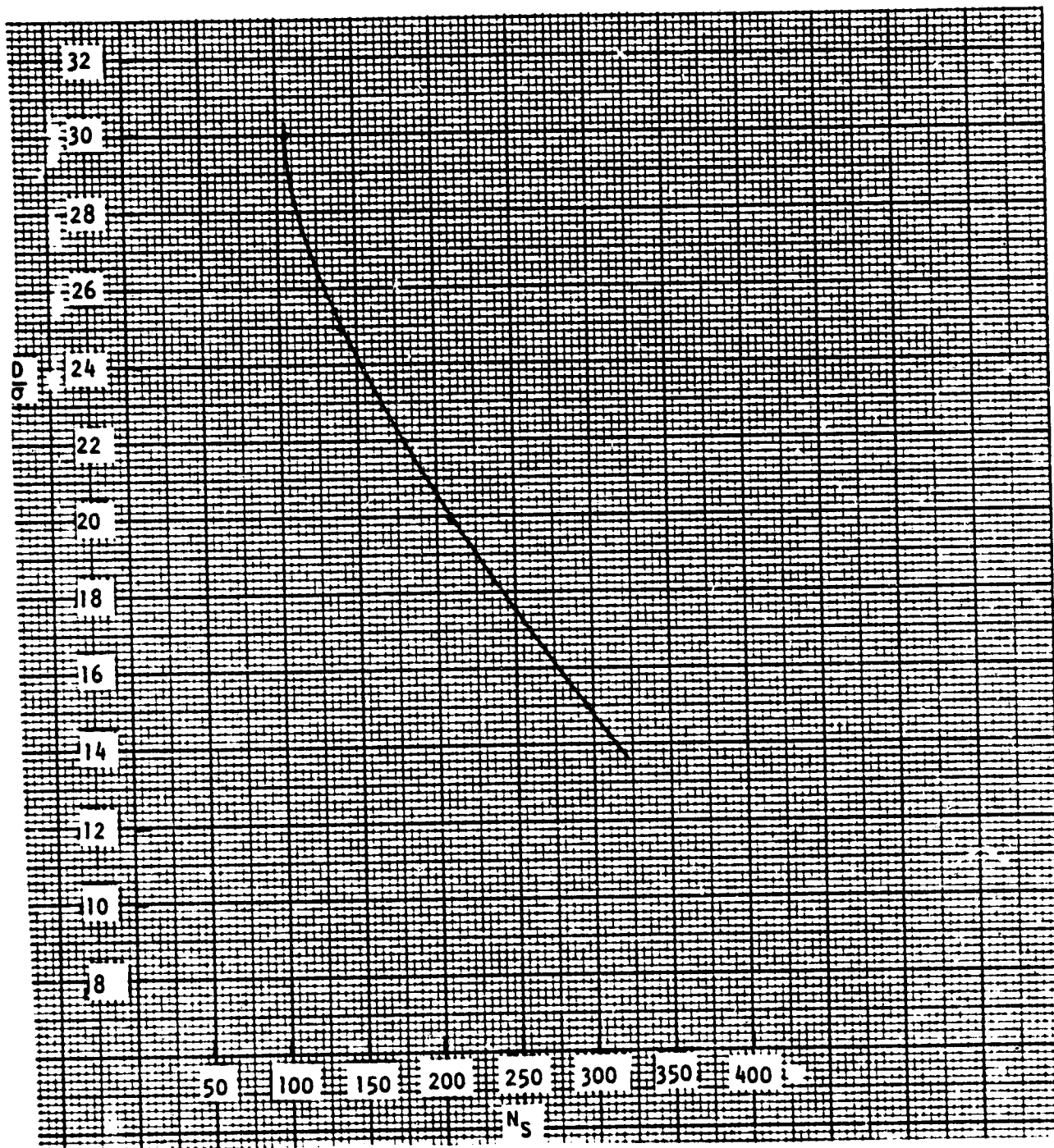


Figure A-70. Pitot Pump Optimum D/o as a Function of Specific Speed

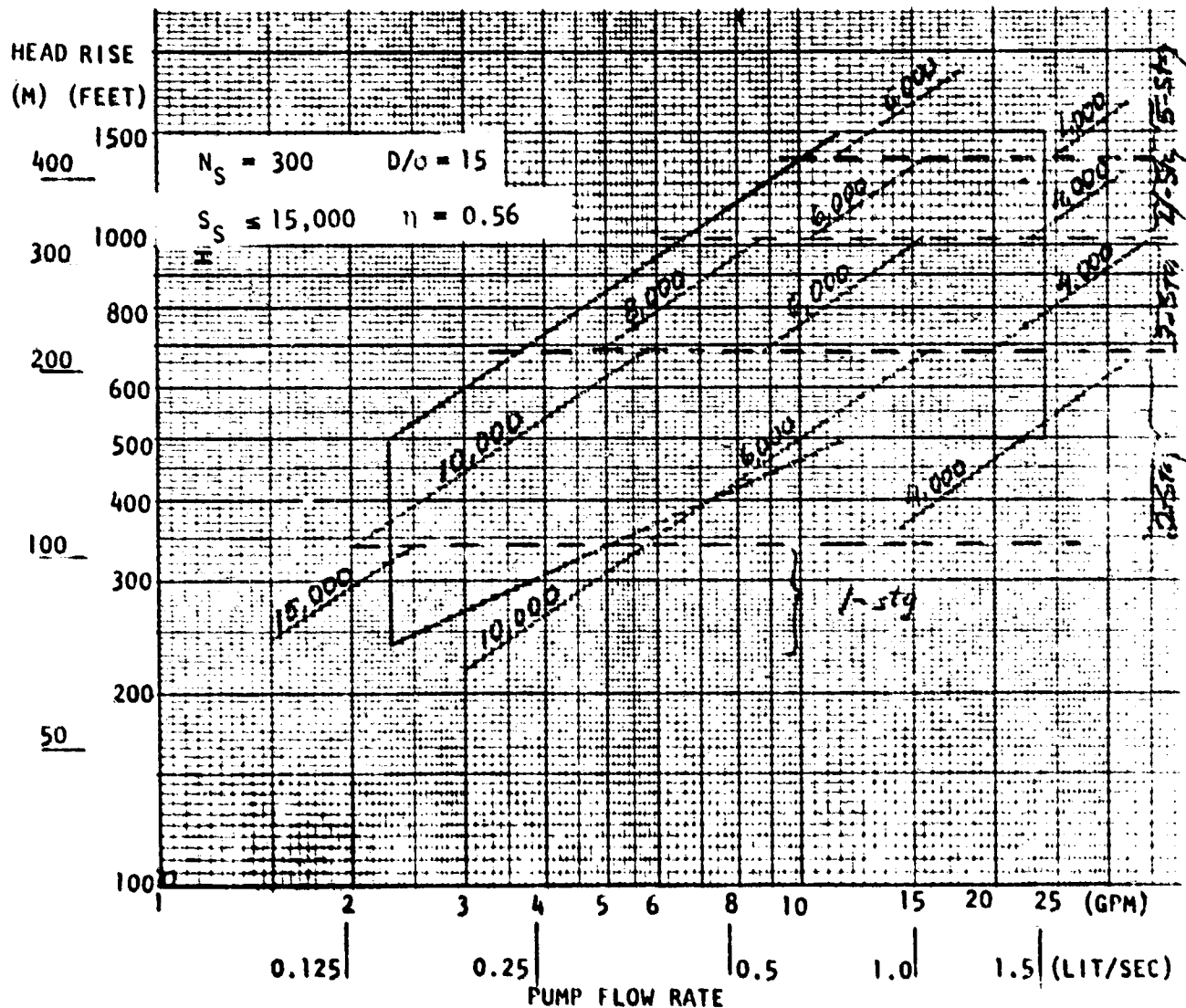


Figure A-71. Pitot LOX Pump - NPSH = 2 Feet, Speed

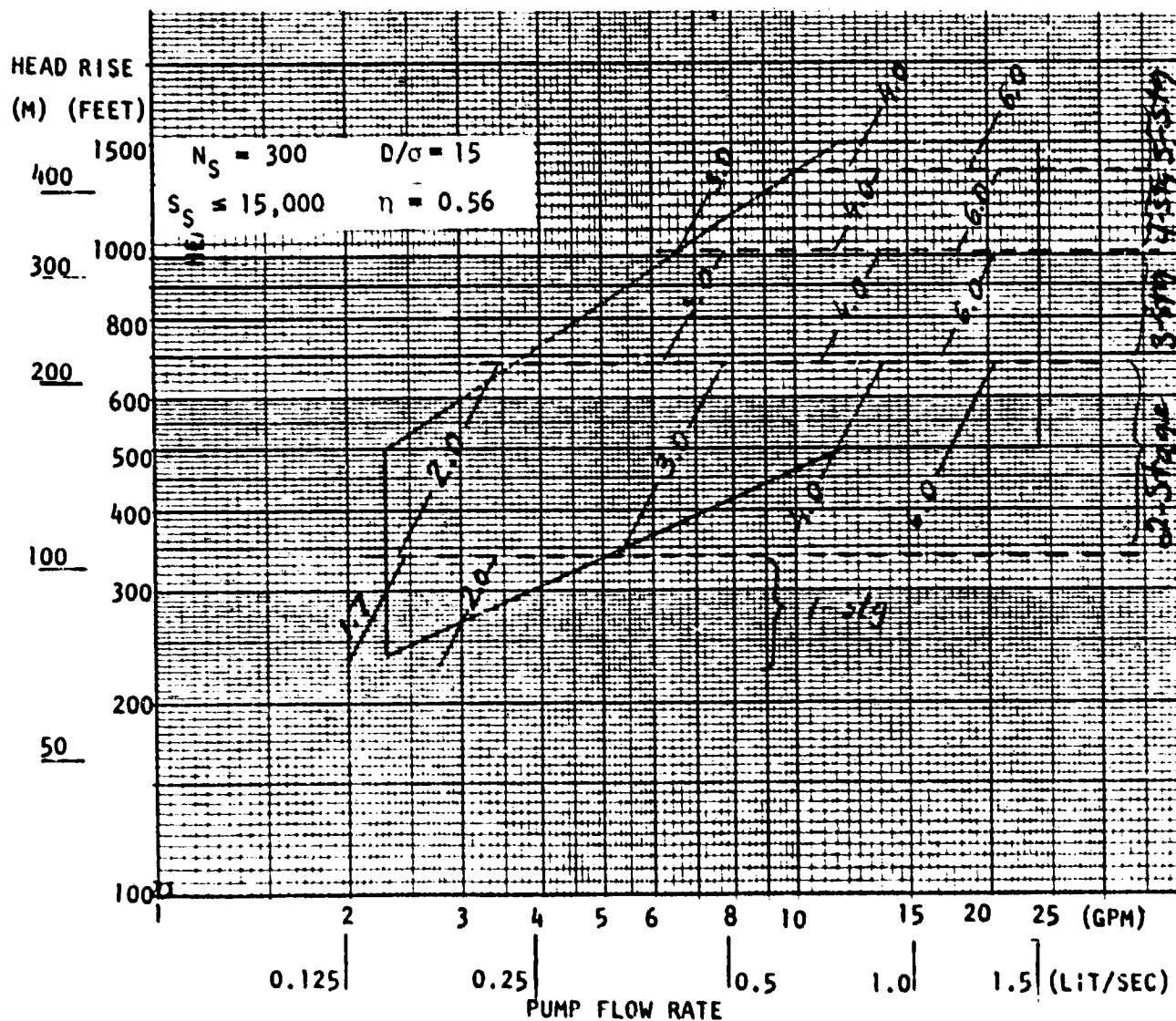


Figure A-72. Pitot LOX Pump - NPSH = 2 Feet, Diameter

ORIGINAL PAGE IS
 OF POOR QUALITY

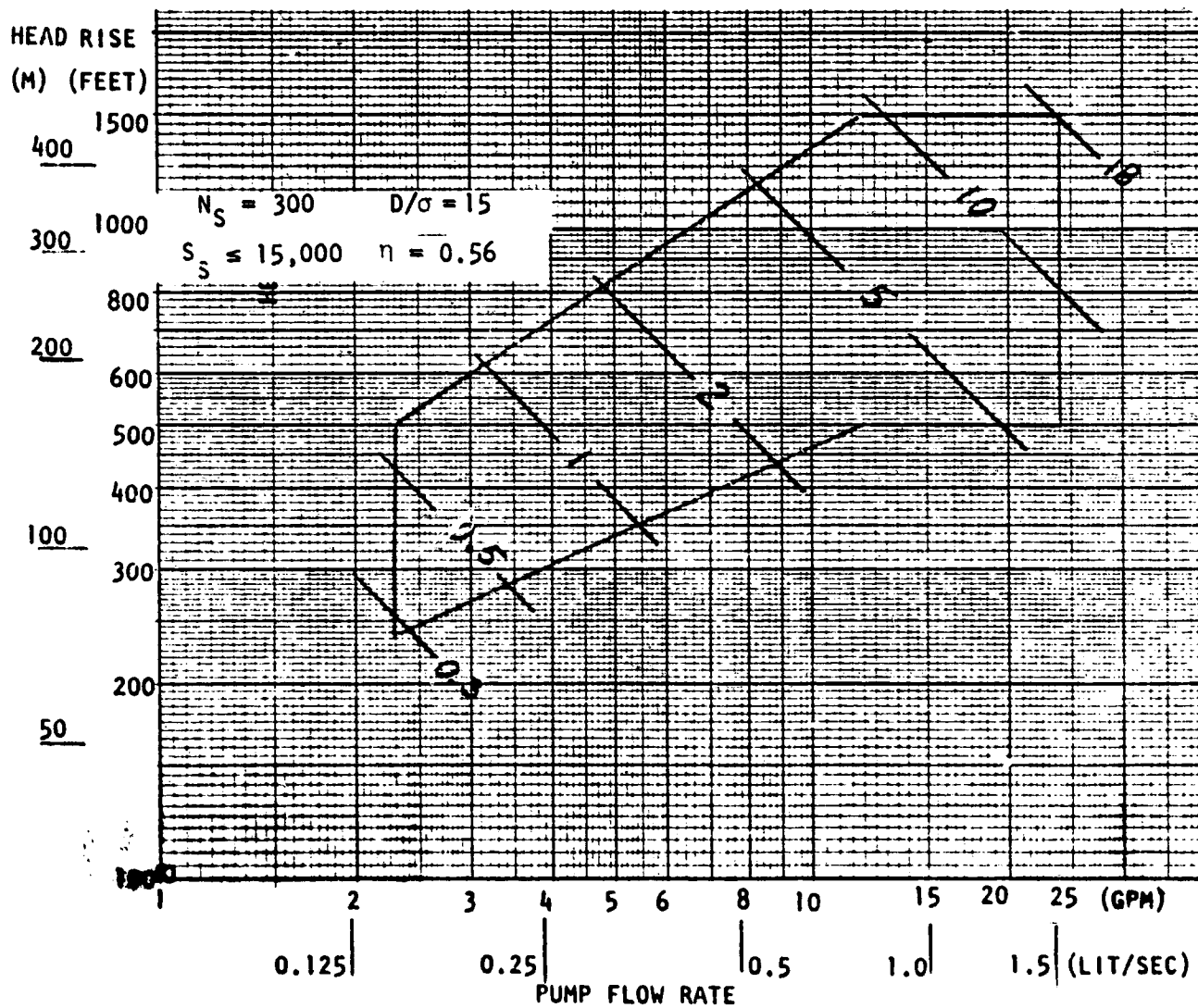


Figure A-73. Pitot LOX Pump - NPSH = 2 Feet, Power

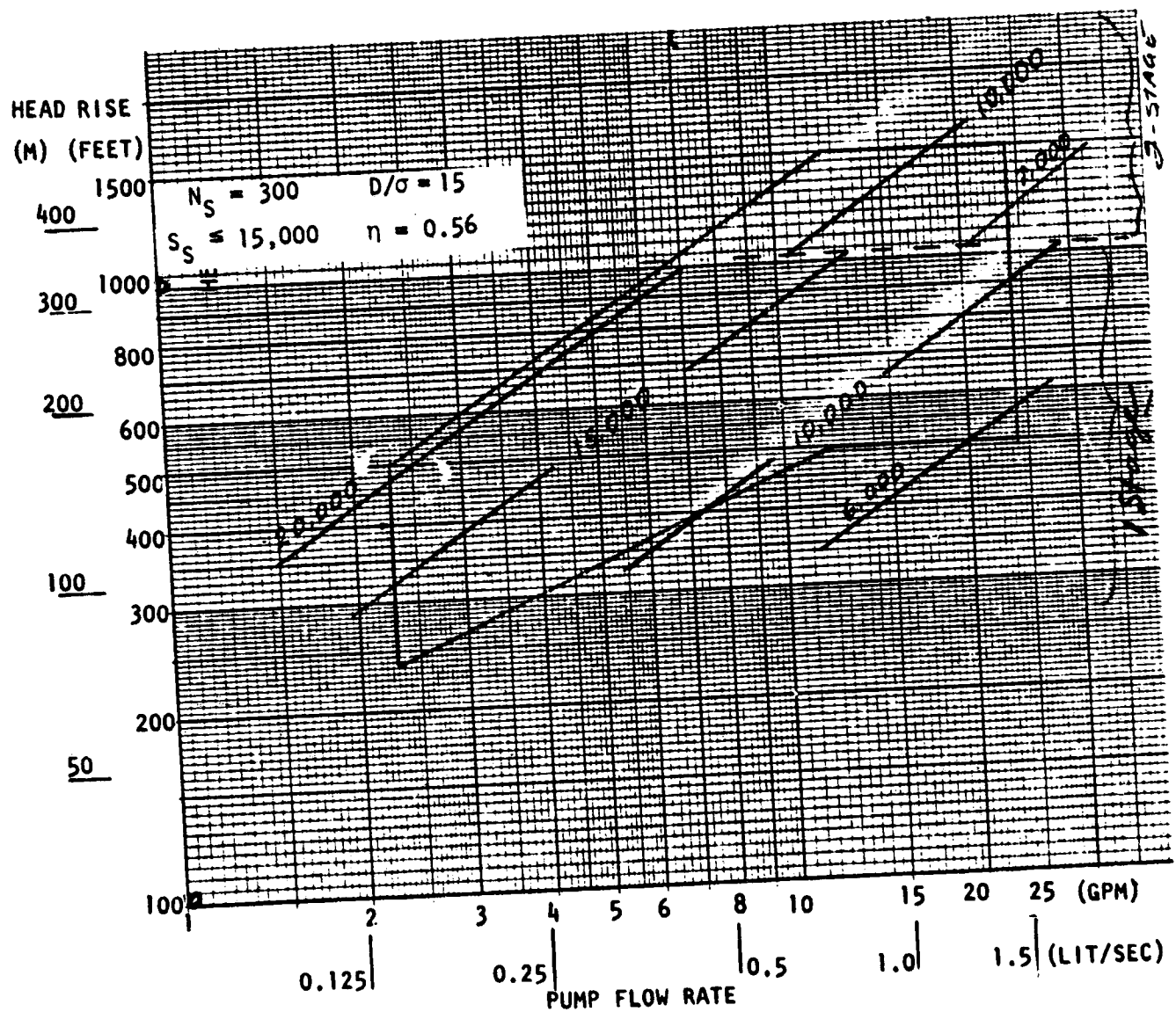


Figure A-74. Pitot LOX Pump - NPSH = 6.05 Feet, Speed

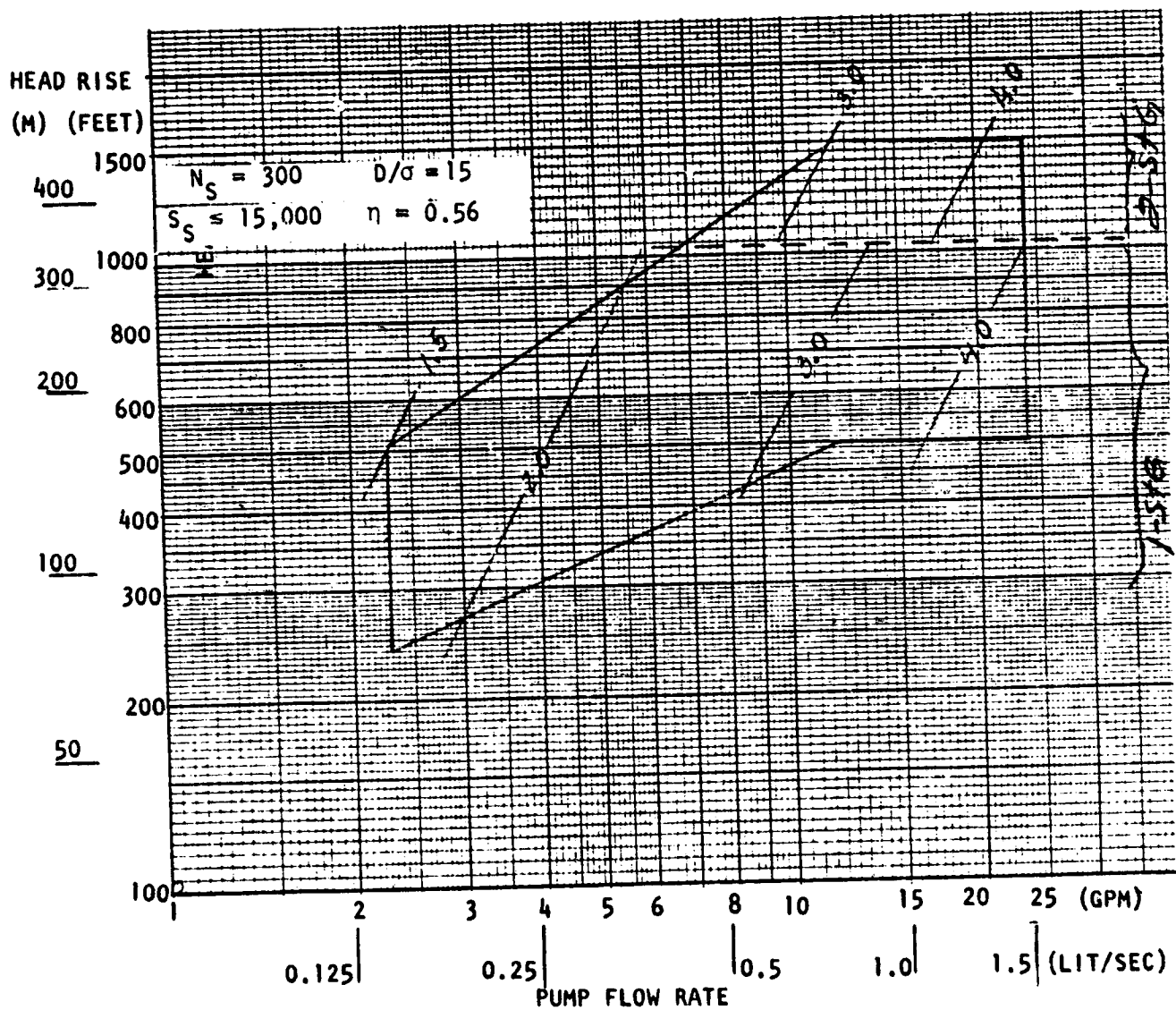


Figure A-75. Pitot LOX Pump - NPSH = 6.05 Feet, Diameter

ORIGINAL PAGE IS
OF POOR QUALITY

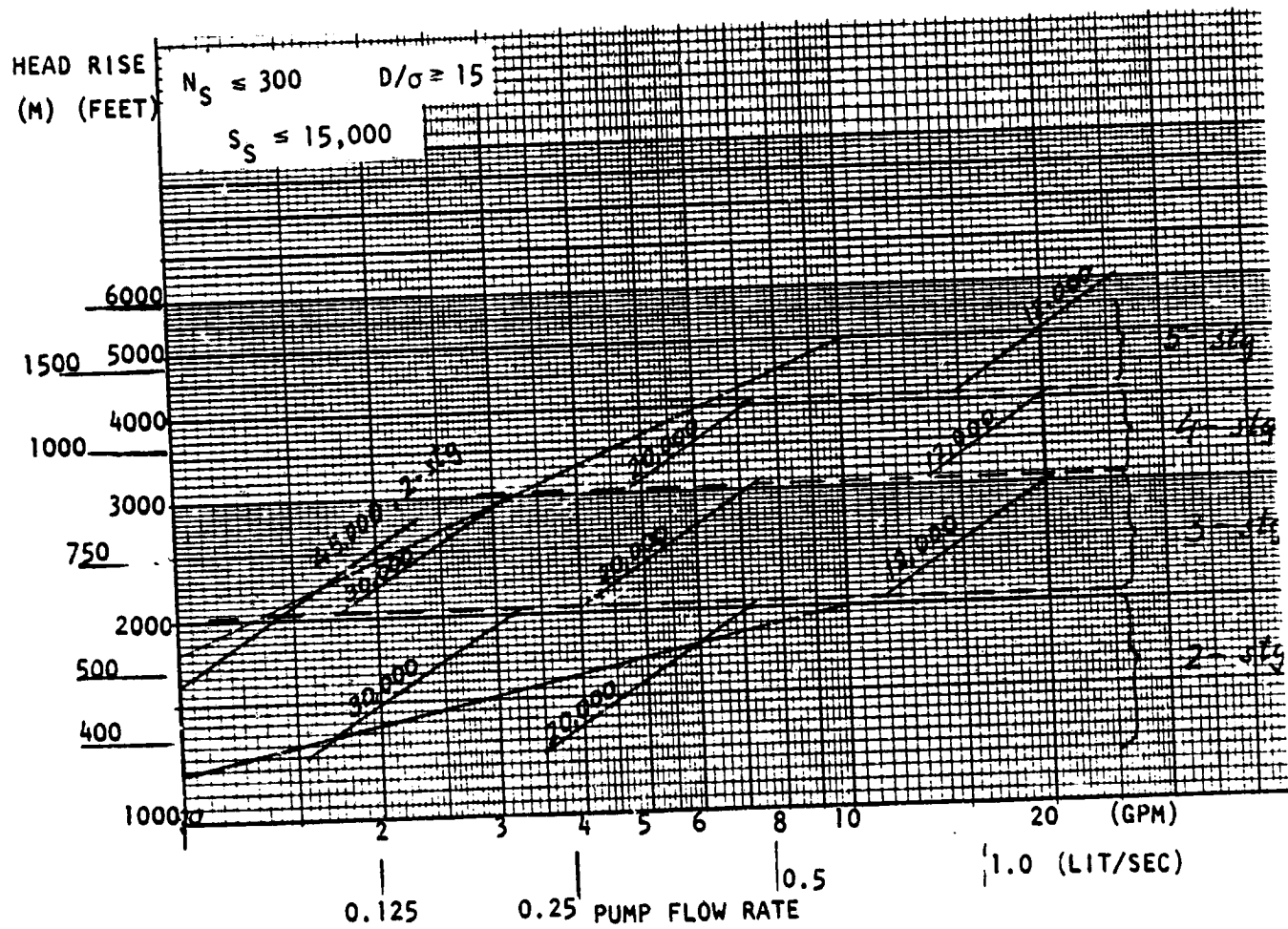


Figure A-76. Pitot Methane Pump - NPSH = 6 Feet, Speed

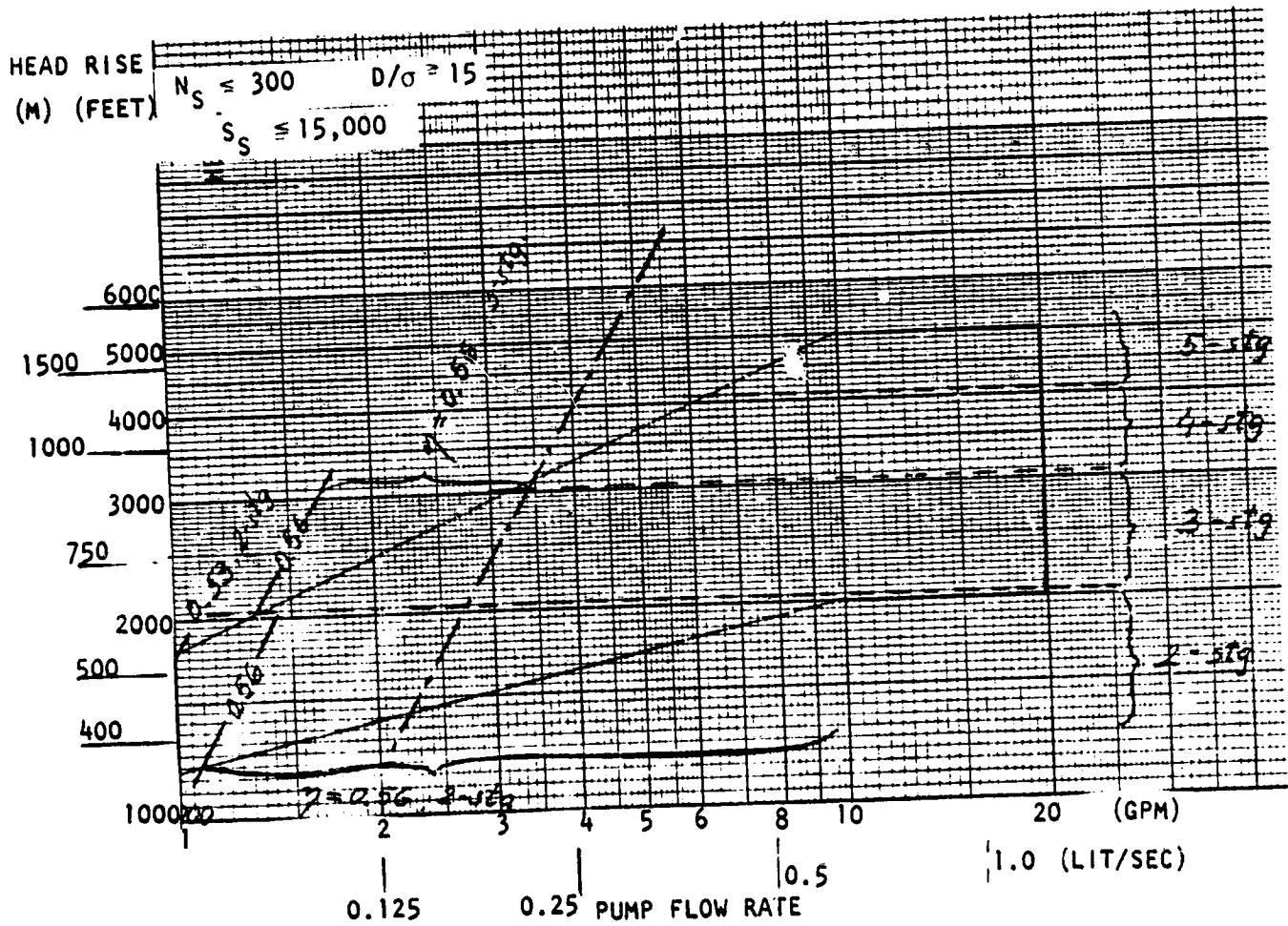


Figure A-77. Pitot Methane Pump - NPSH = 6 Feet, Efficiency

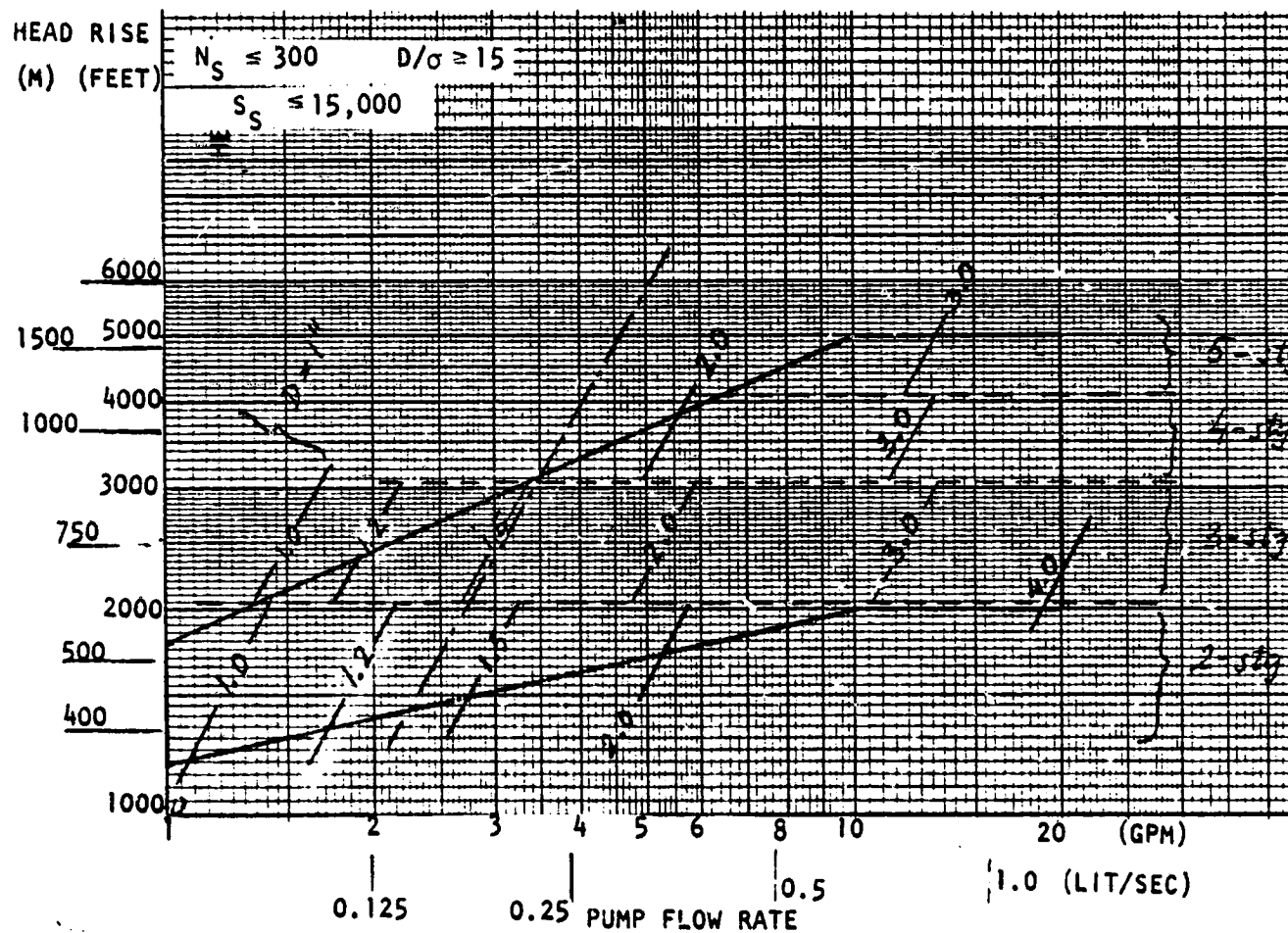


Figure A-78. Pitot Methane Pump - NPSH = 6 Feet, Diameter

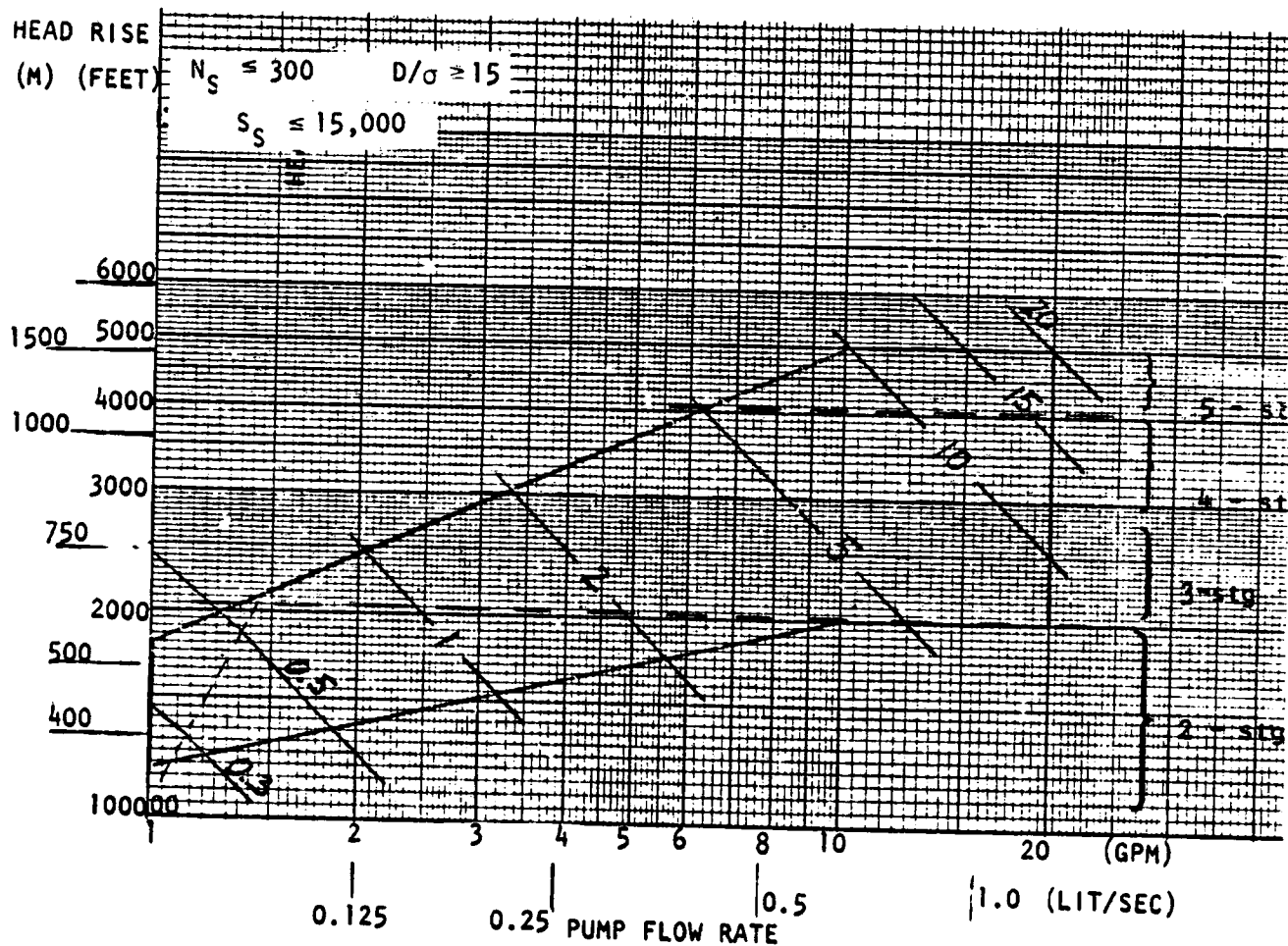


Figure A-79. Pitot Methane Pump - NPSH = 6 Feet, Power

ORIGINAL PAGE IS
OF POOR QUALITY

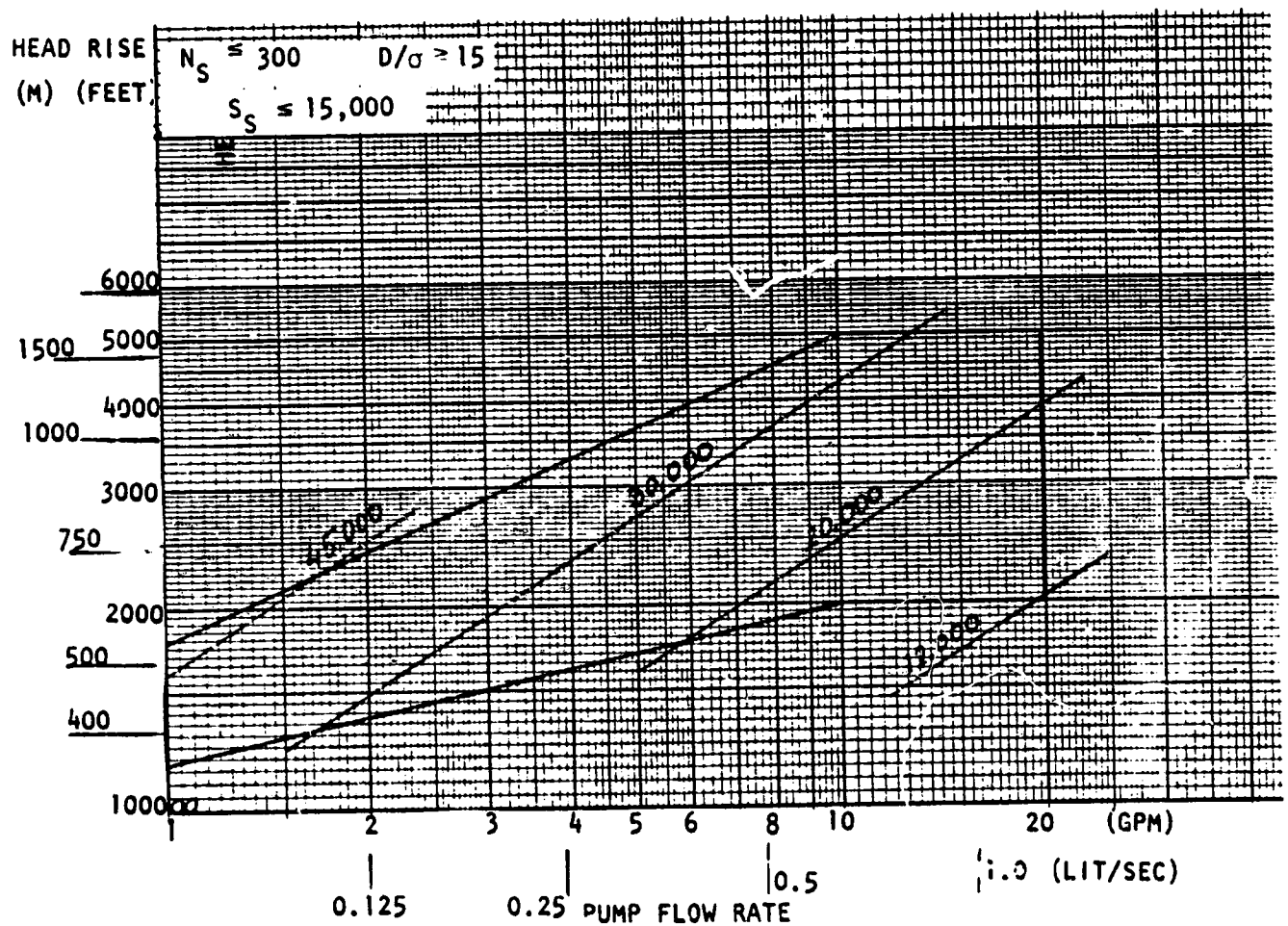


Figure A-80. Pitot Methane Pump - NPSH = 16.47 Feet, Speed (Two Stages)

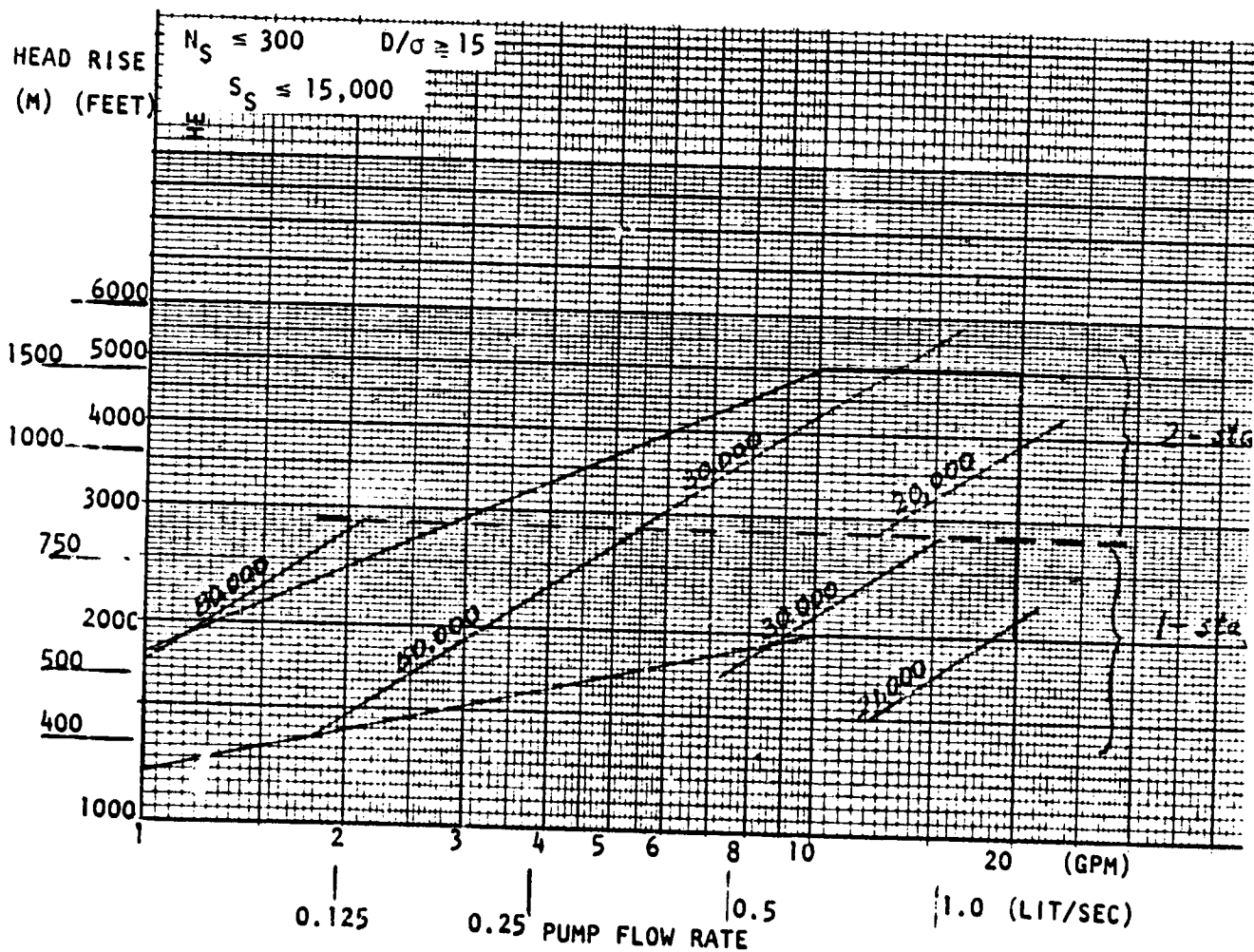


Figure A-81. Pitot Methane Pump - NPSH = 16.47 Feet, Speed

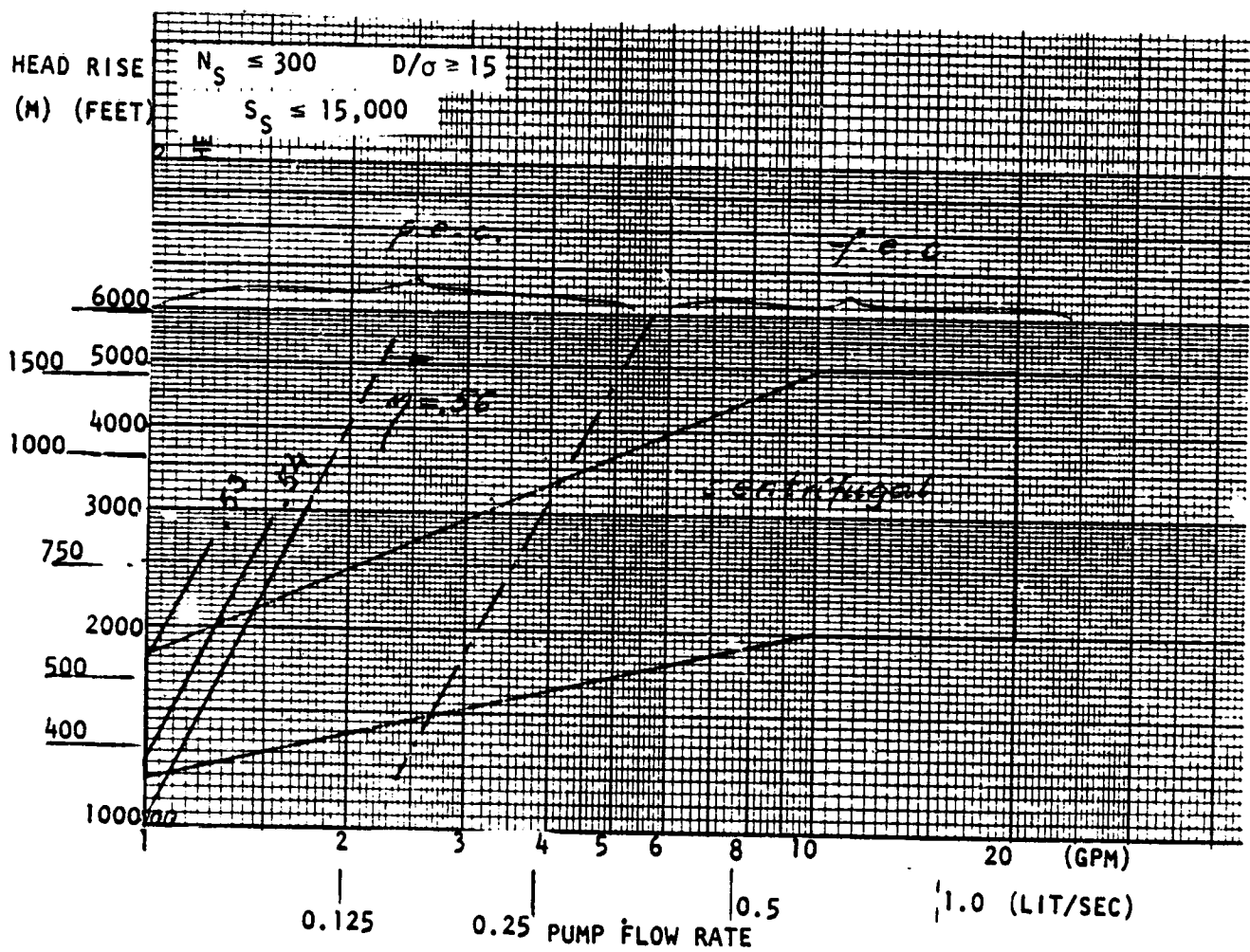


Figure A-82. Pitot Methane Pump - NPSH = 16.47 Feet, Efficiency (Two Stages)

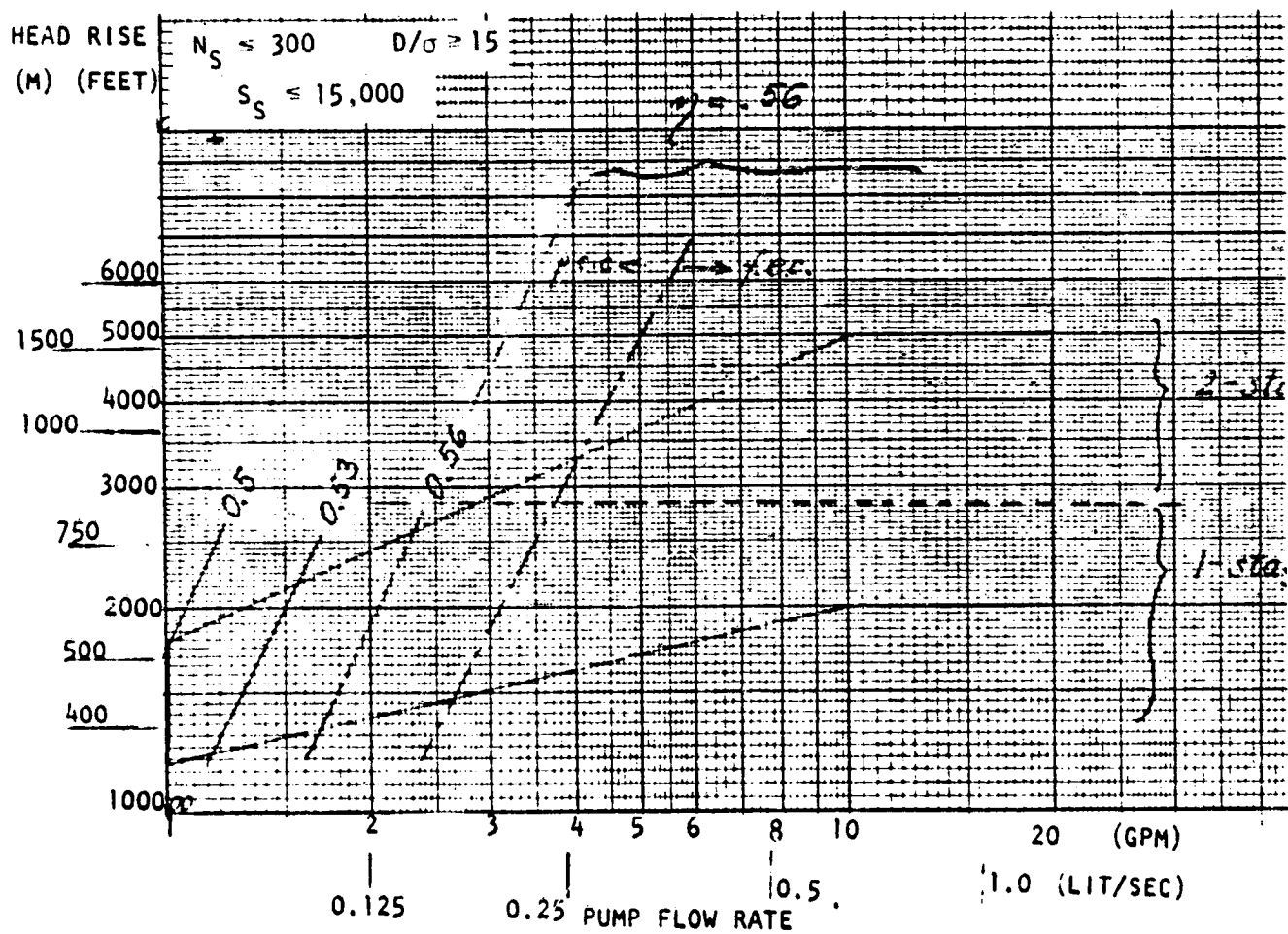


Figure A-83. Pitot Methane Pump - NPSH = 16.47 Feet, Efficiency

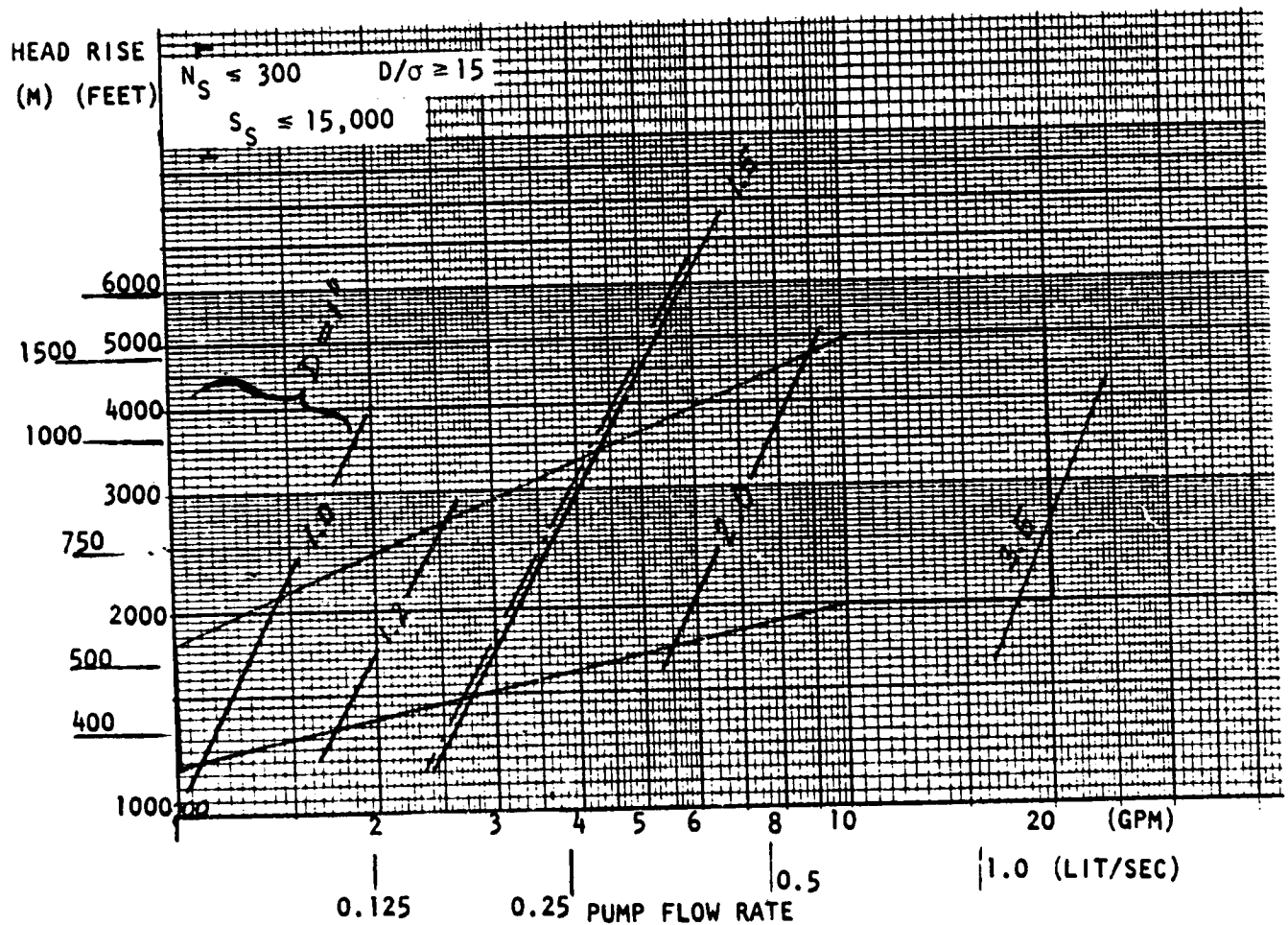


Figure A-84. Pitot Methane Pump - NPSH = 16.47 Feet,
Diameter (Two Stages)

ORIGINAL PAGE IS
OF POOR QUALITY

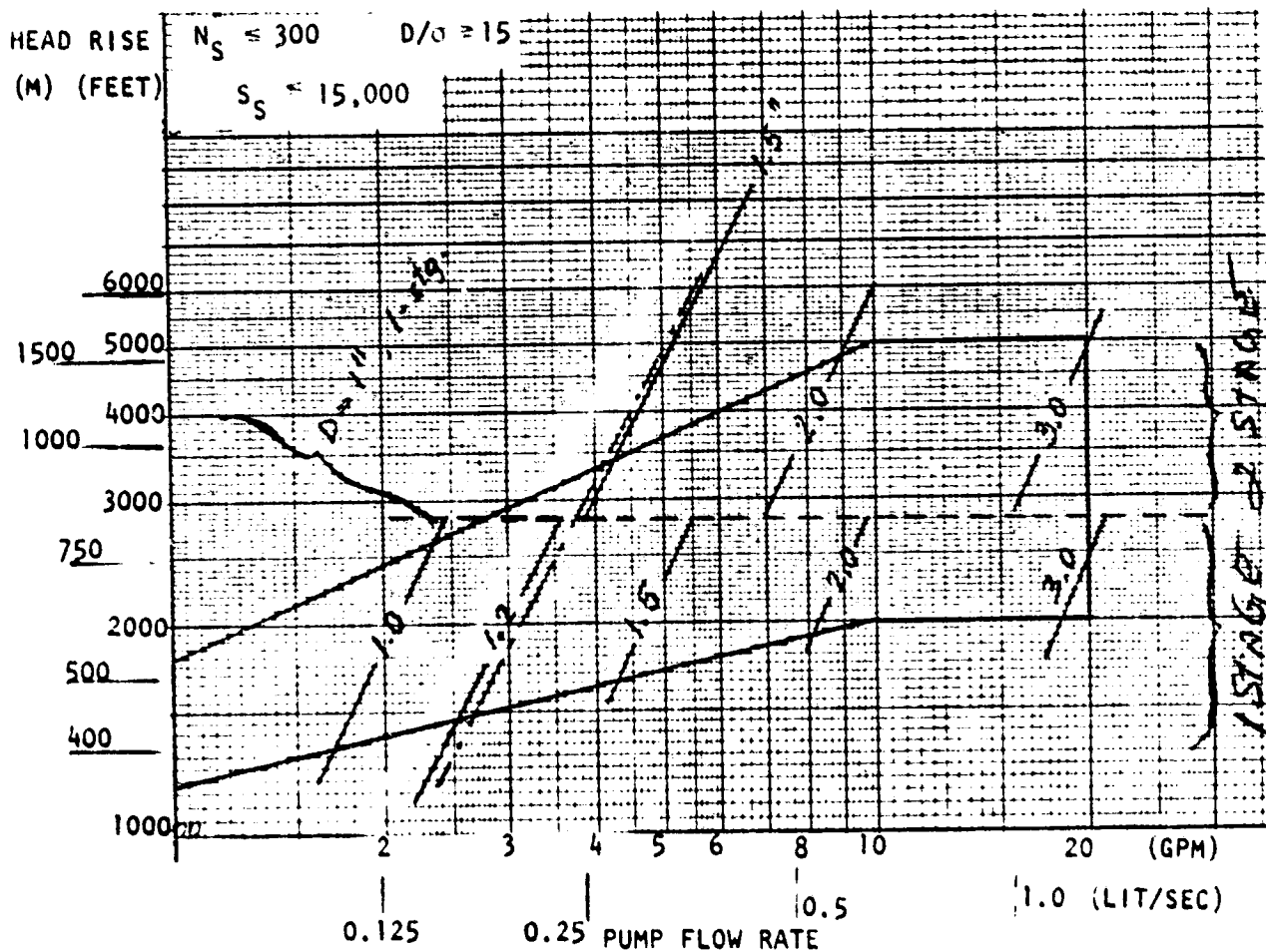


Figure A-85. Pitot Methane Pump - NPSH = 16.47 Feet, Diameter

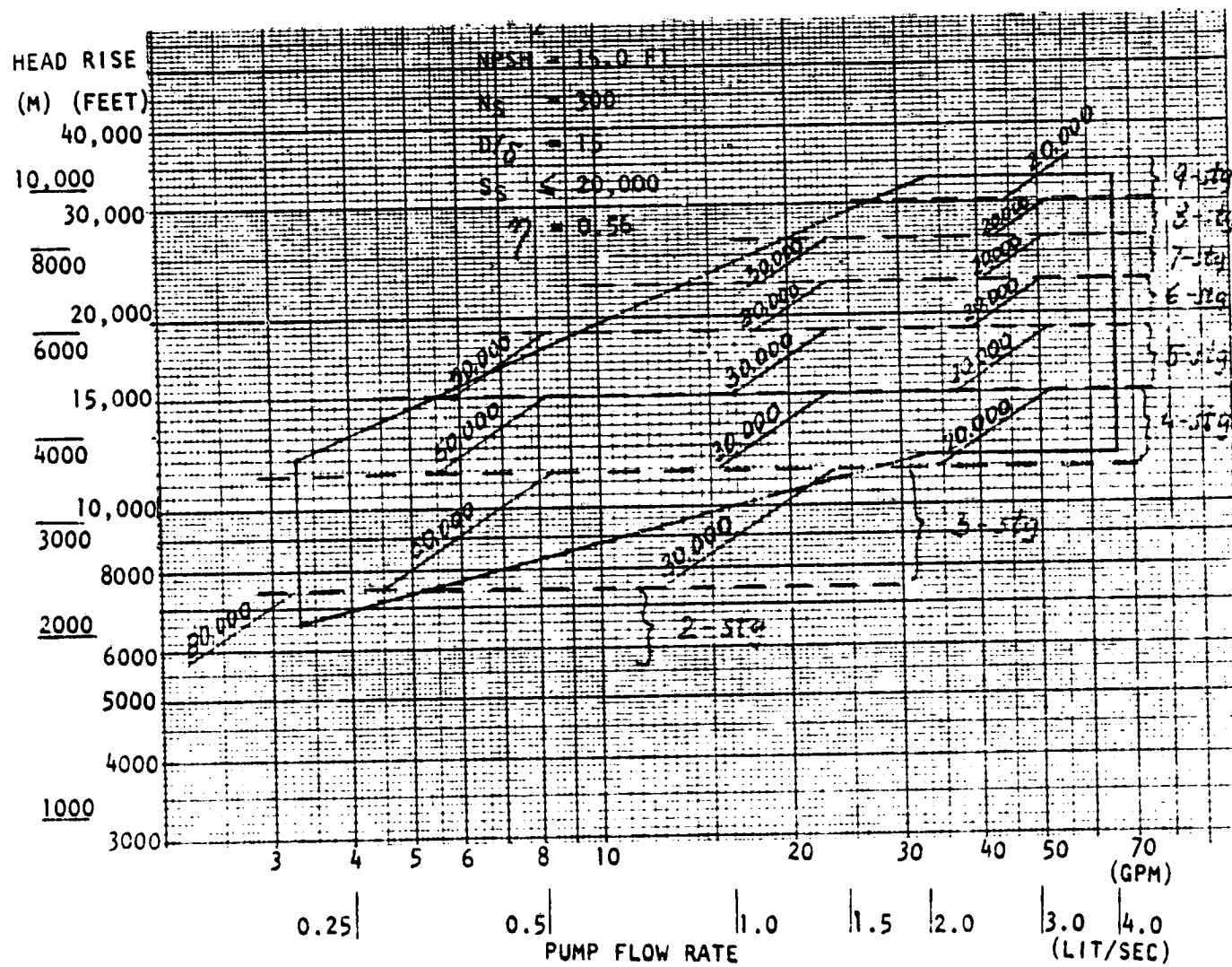


Figure A-87. Pitot Hydrogen Pump - NPSH = 15 Feet, Speed

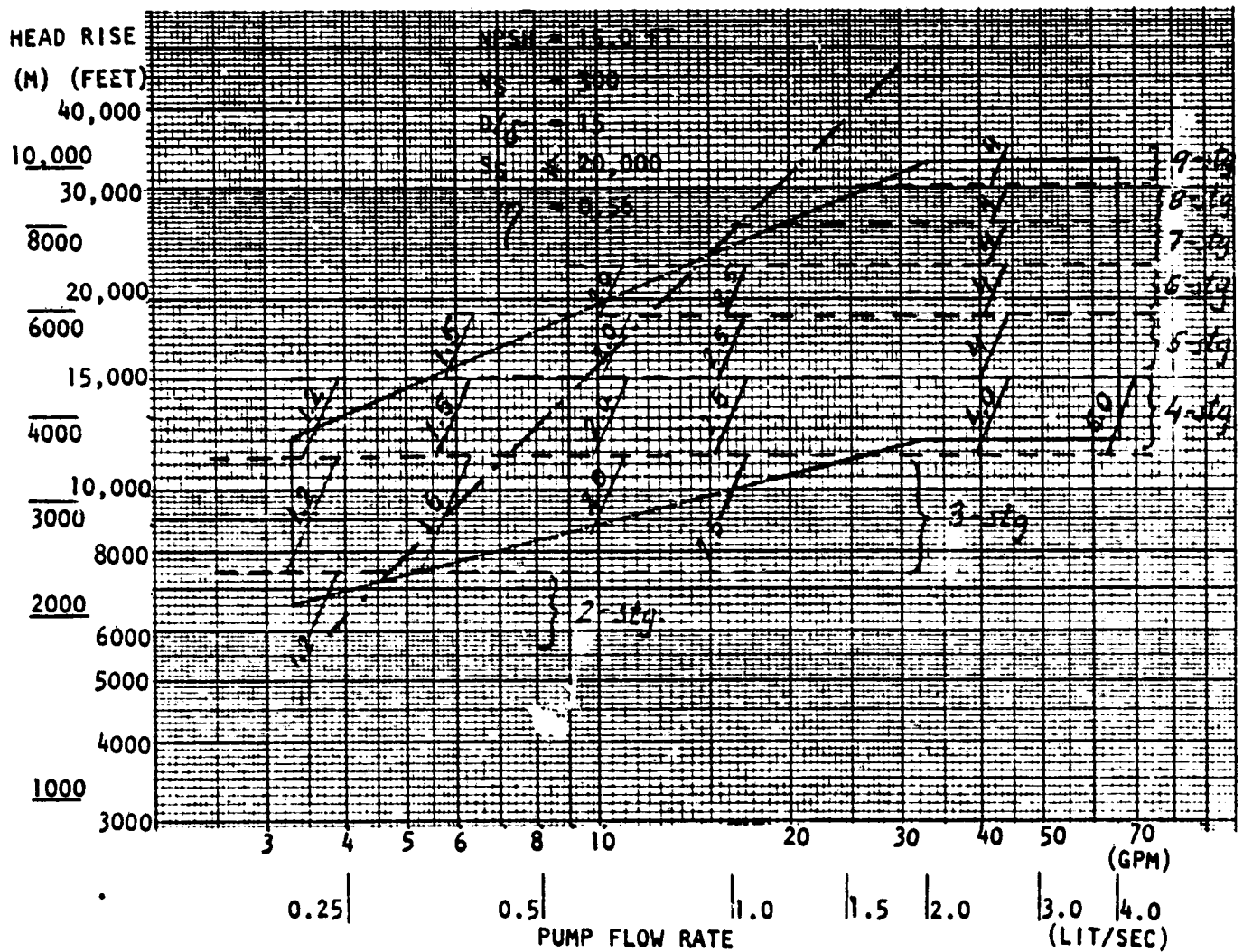


Figure A-88. Pitot Hydrogen Pump - NPSH = 15 Feet, Diameter

ORIGINAL PAGE IS
 OF POOR QUALITY

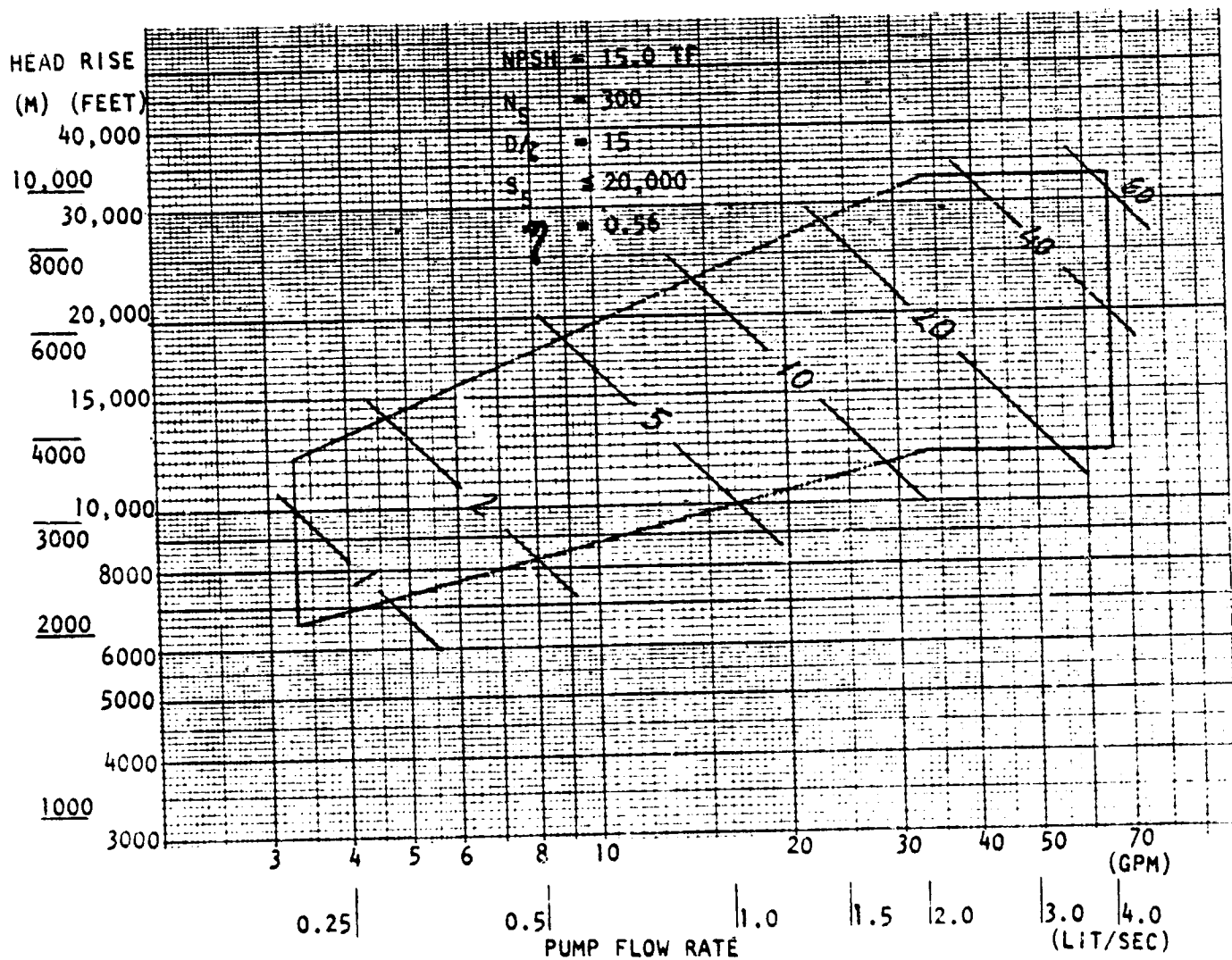


Figure A-89. Pitot Hydrogen Pump - NPSH = 15 Feet, Power

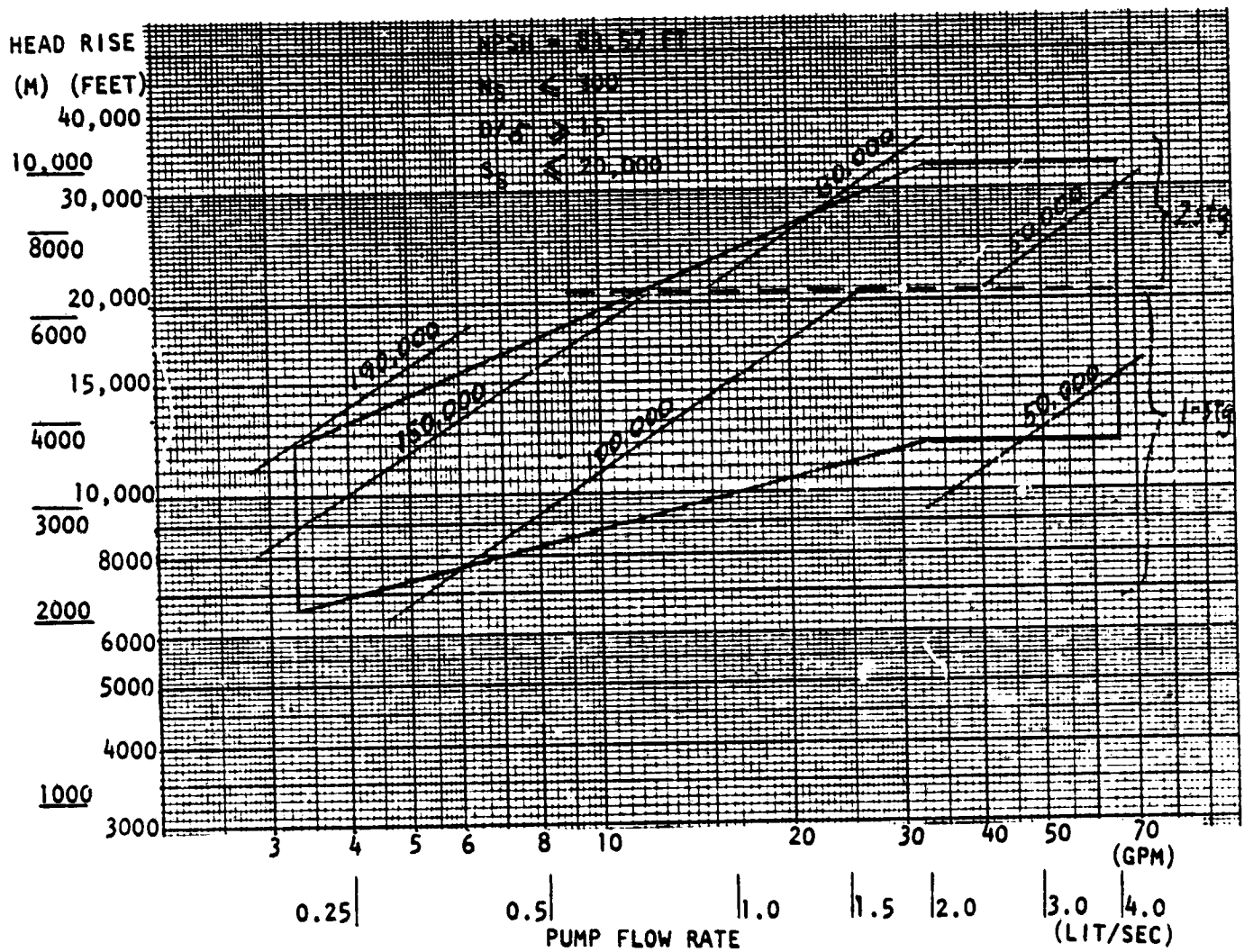


Figure A-90. Pitot Hydrogen Pump - NPSH = 83.57 Feet, Speed

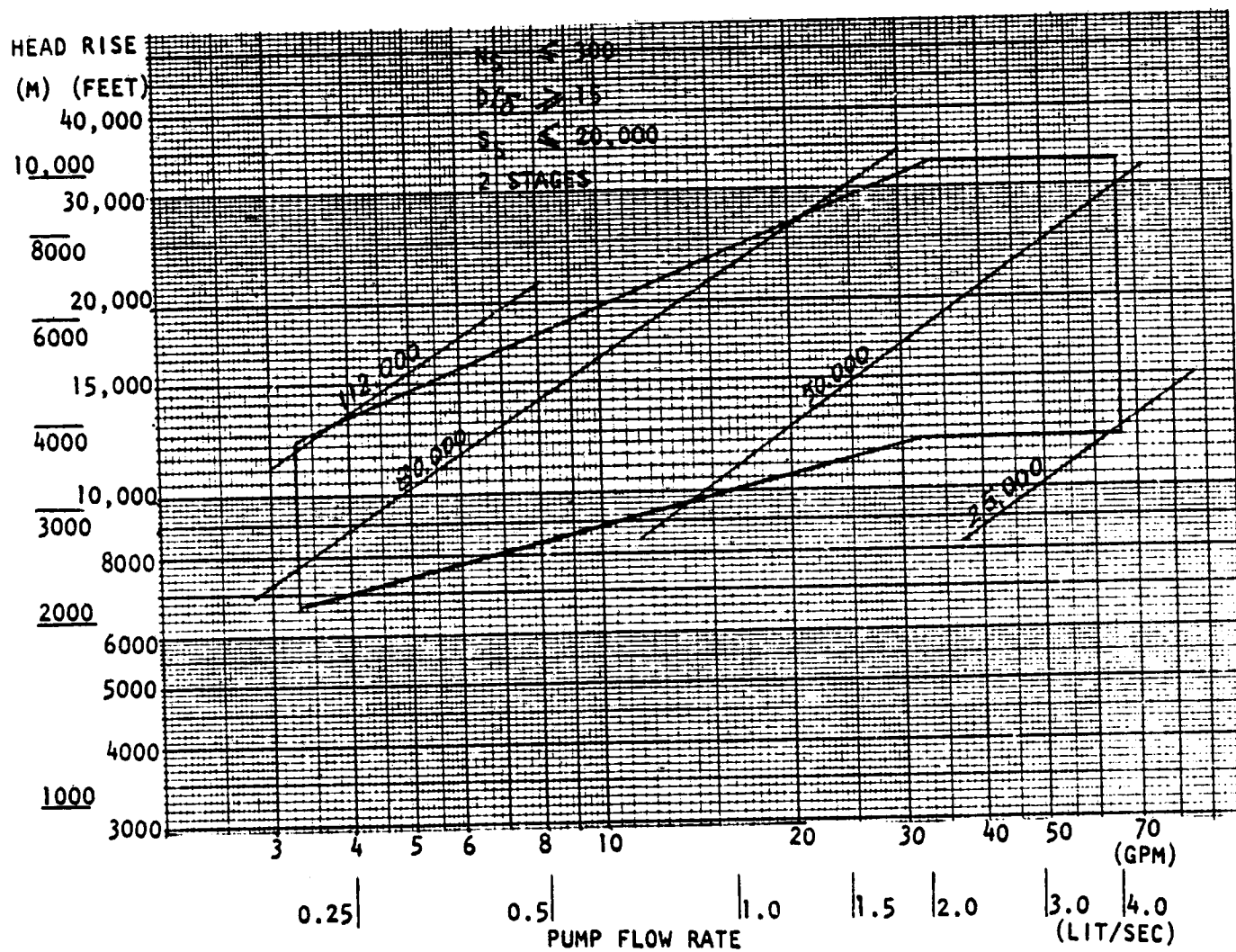


Figure A-91. Pitot Hydrogen Pump - NPSH = 83.57 Feet, Speed (Two Stages)



ORIGINAL PAGE IS
OF POOR QUALITY

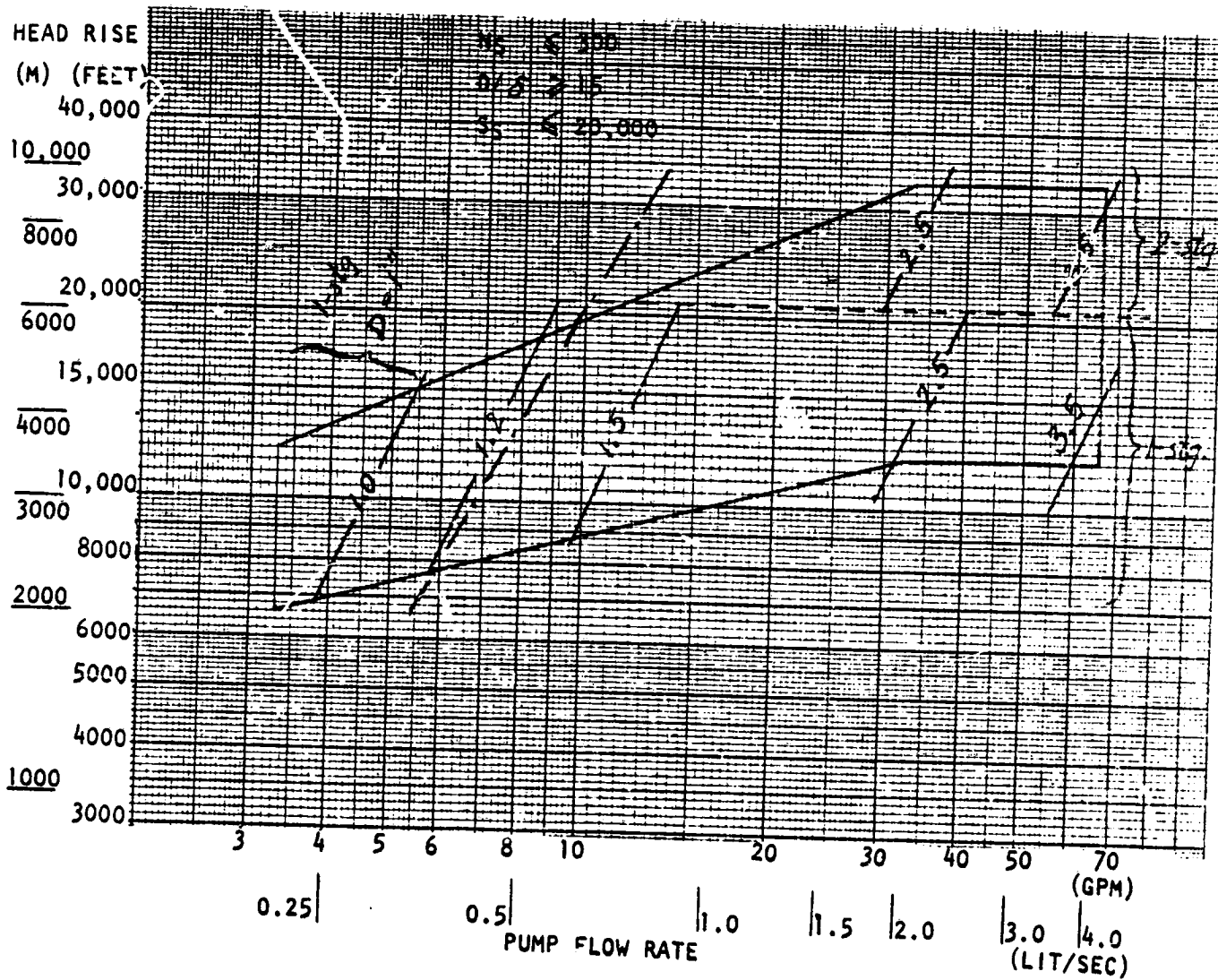


Figure A-93. Pitot Hydrogen Pump - NPSH = 83.57 Feet, Diameter

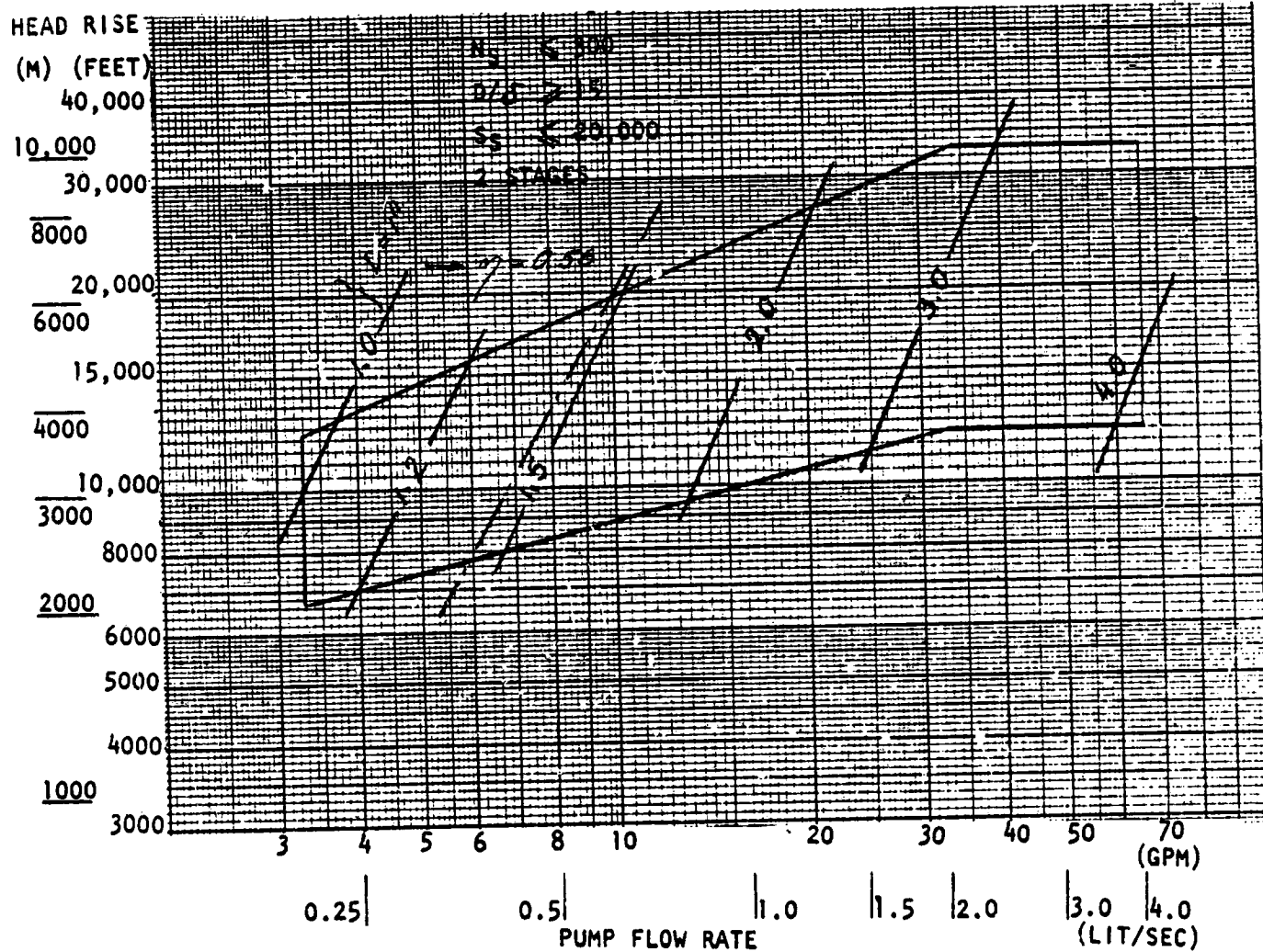


Figure A-94. Pitot Hydrogen Pump - NPSH = 83.57 Feet, Diameter (Two Stages)

ORIGINAL PAGE IS
OF POOR QUALITY

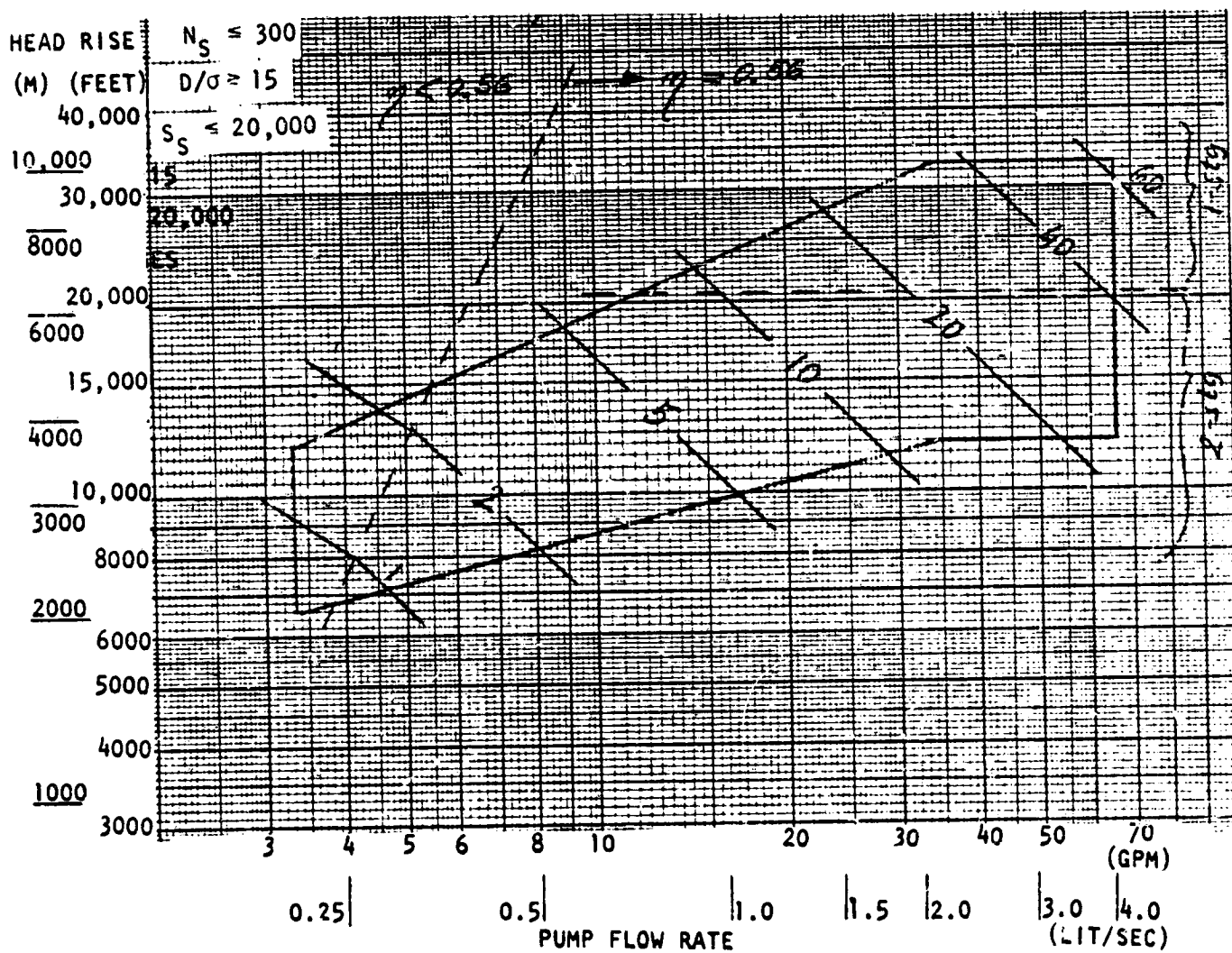


Figure A-95. Pitot Hydrogen Pump - NPSH = 83.57 Feet, Power

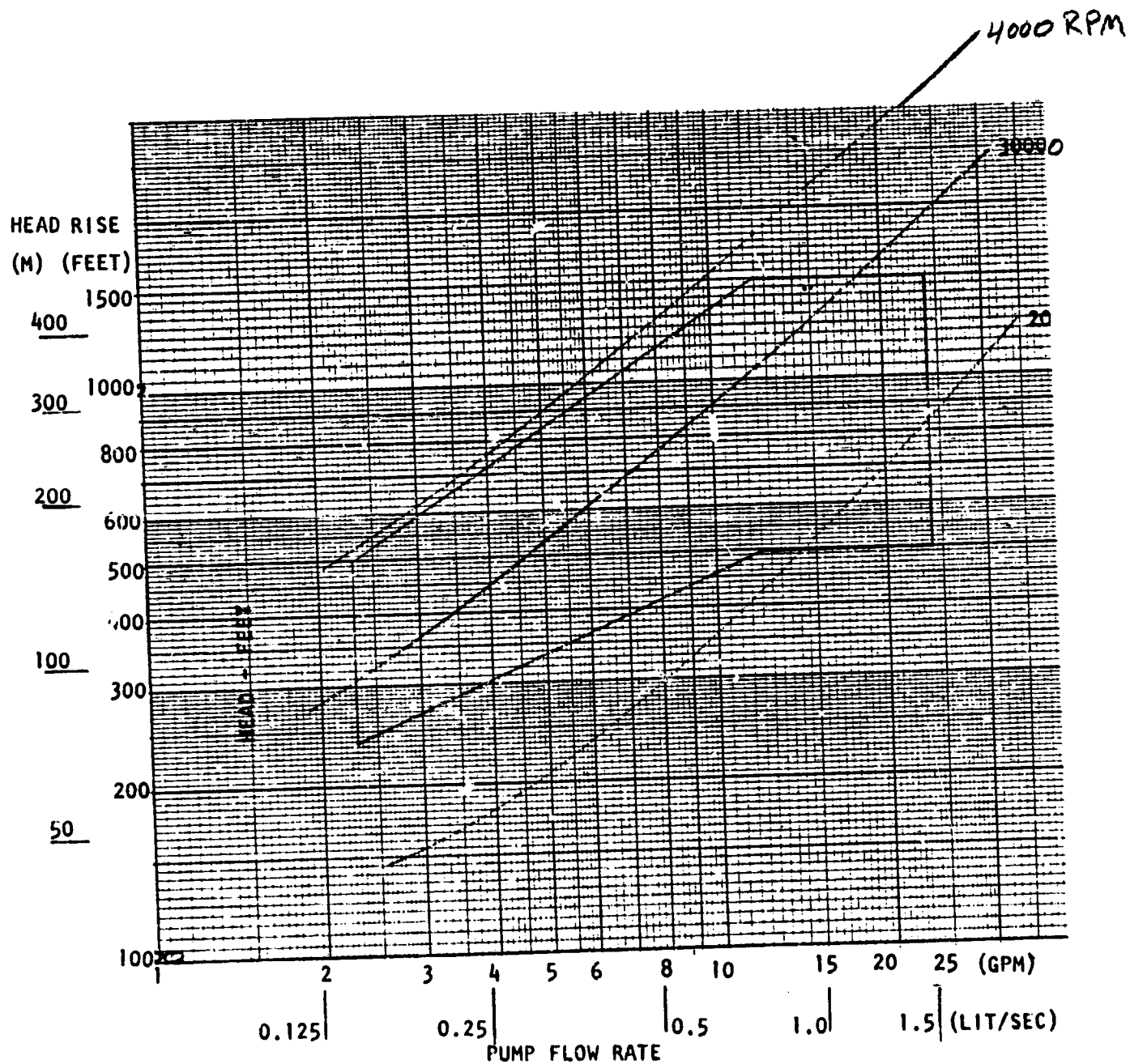


Figure A-96. Tesla LOX Pump, Speed

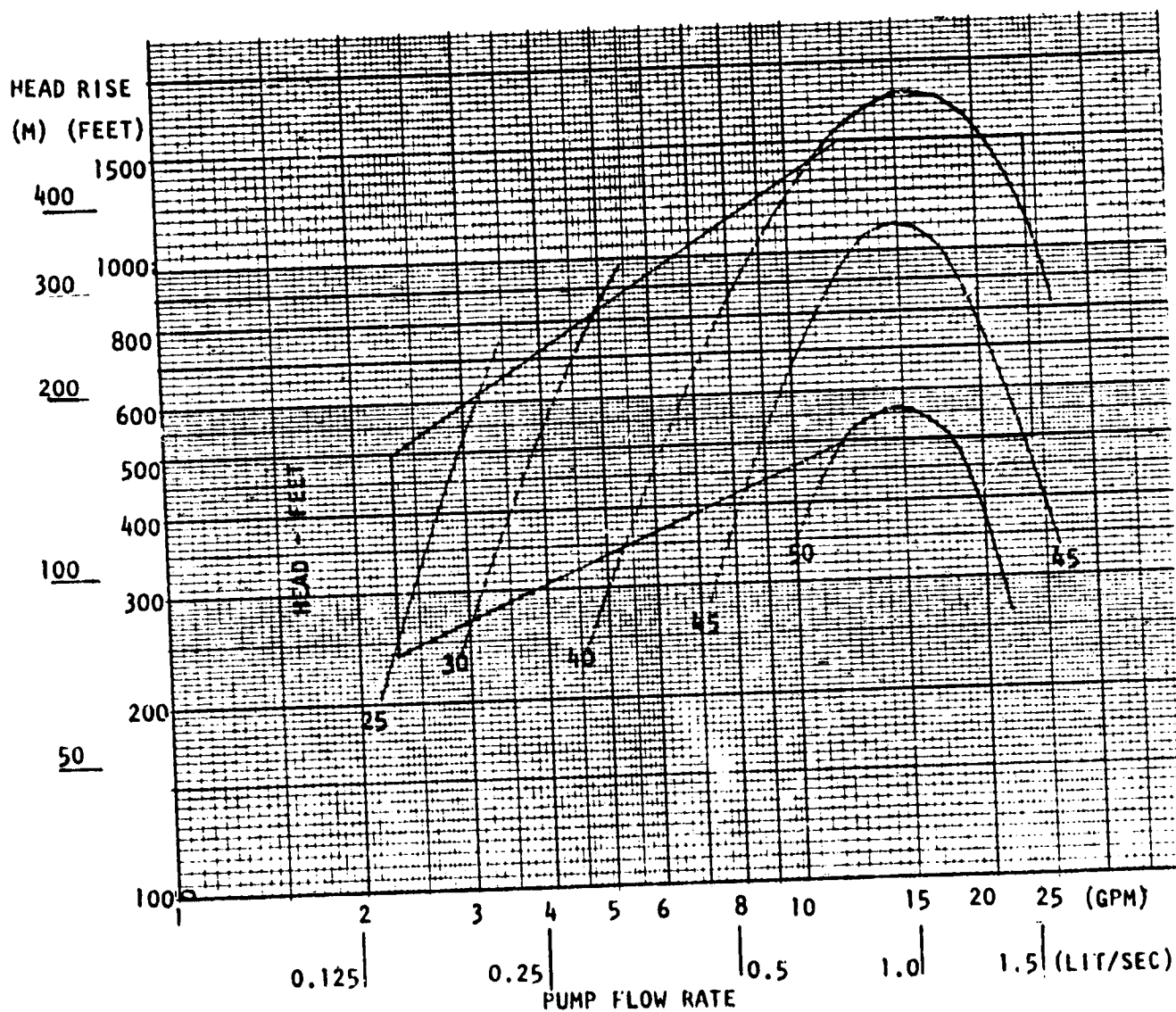


Figure A-97. Tesla LOX Pump, Efficiency

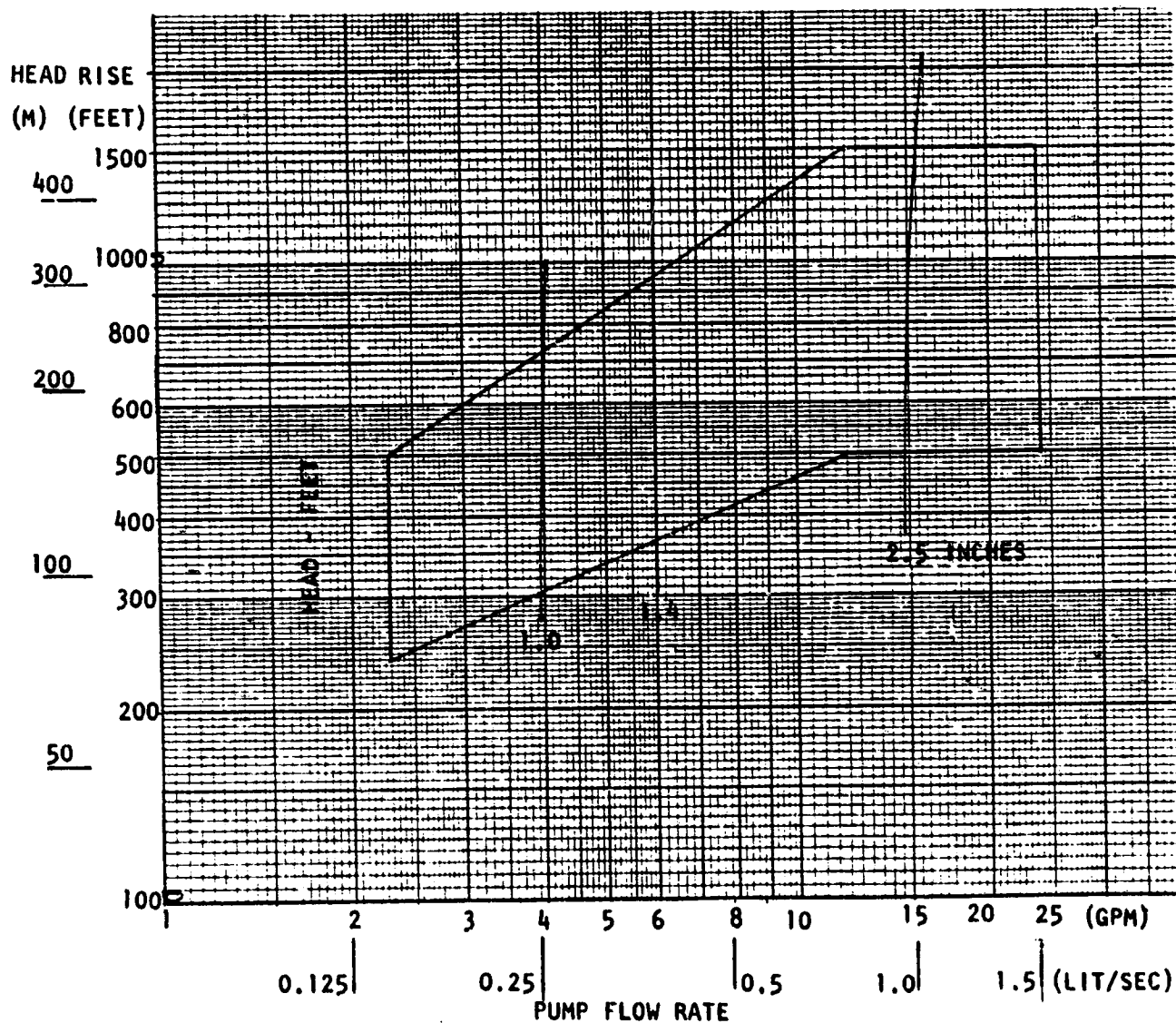


Figure A-98. Tesla LOX Pump, Diameter

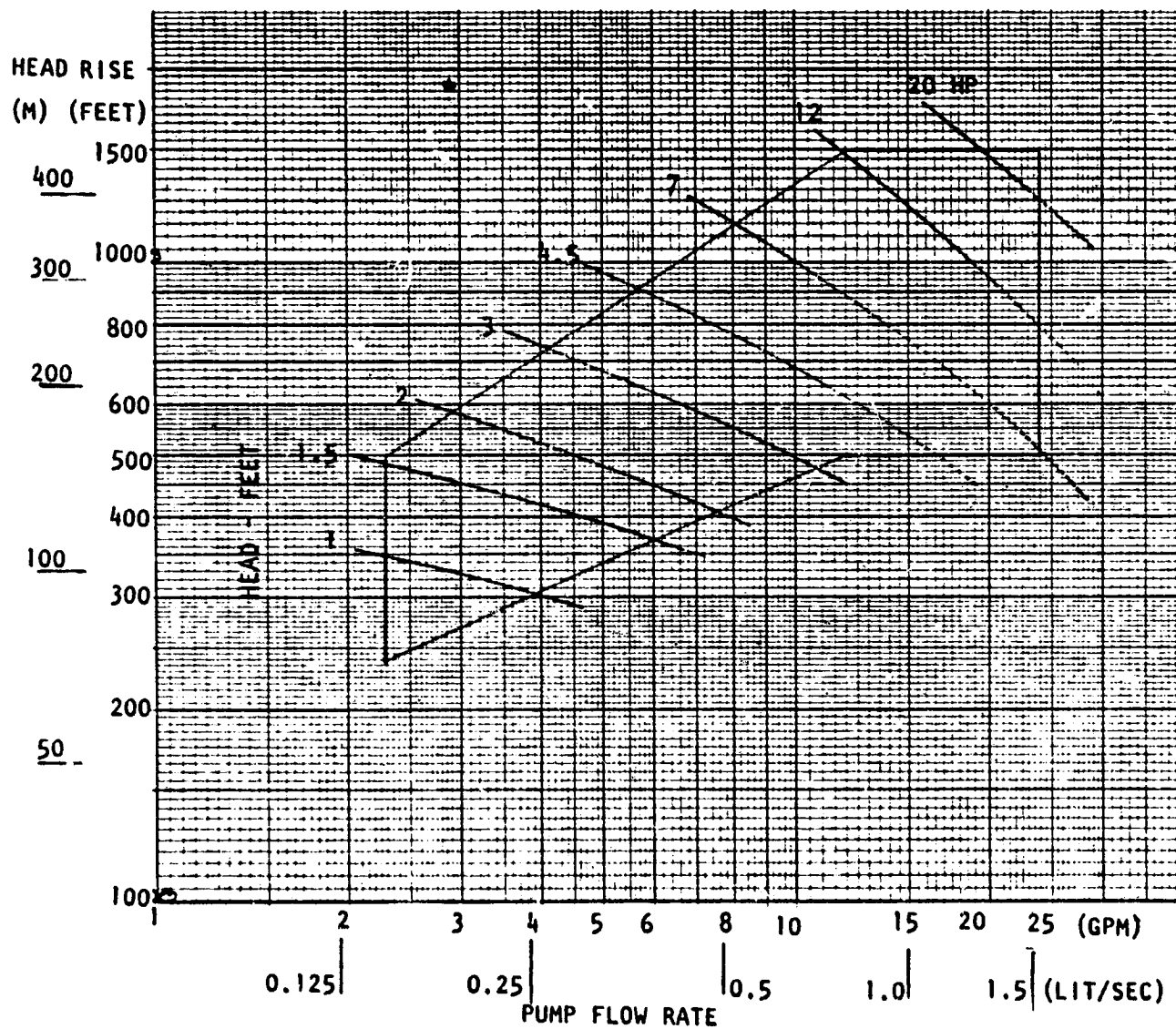


Figure A-99. Tesla LOX Pump, Power

ORIGINAL PAGE IS
OF POOR QUALITY

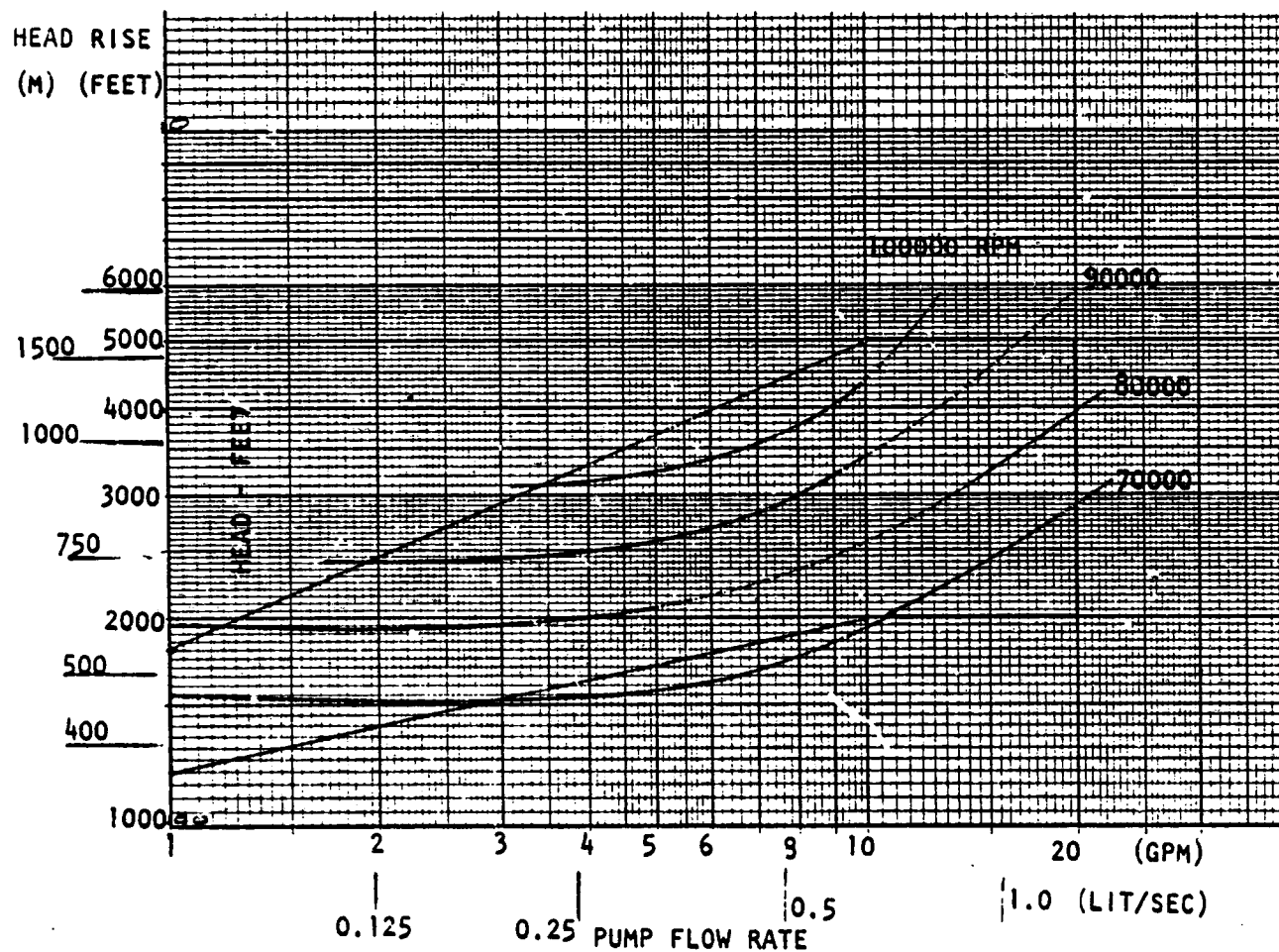


Figure A-100. Tesla Methane Pump, Speed - NPSH = 6 Feet

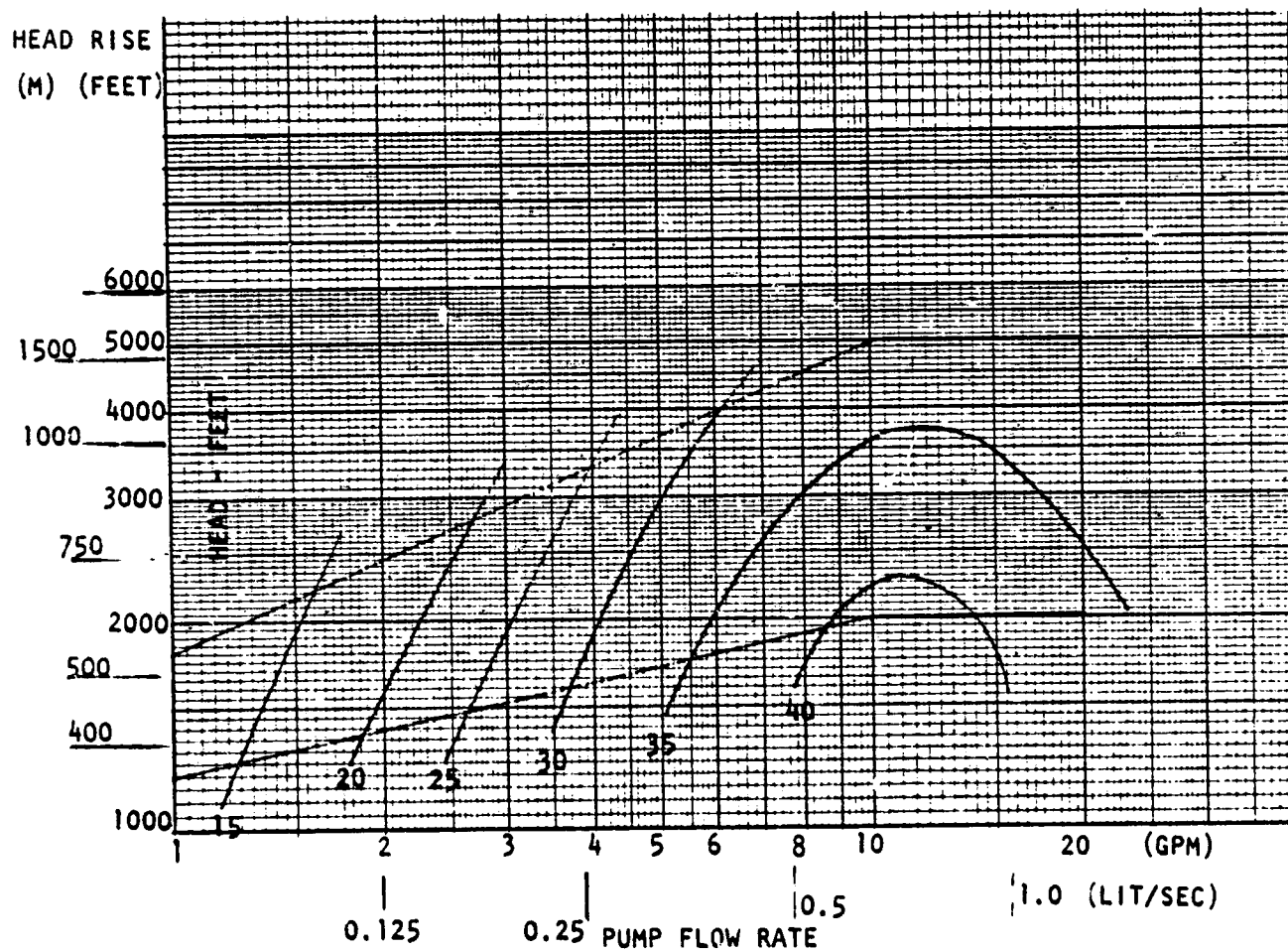


Figure A-101. Tesla Methane Pump, Efficiency - NPSH = 6 Feet

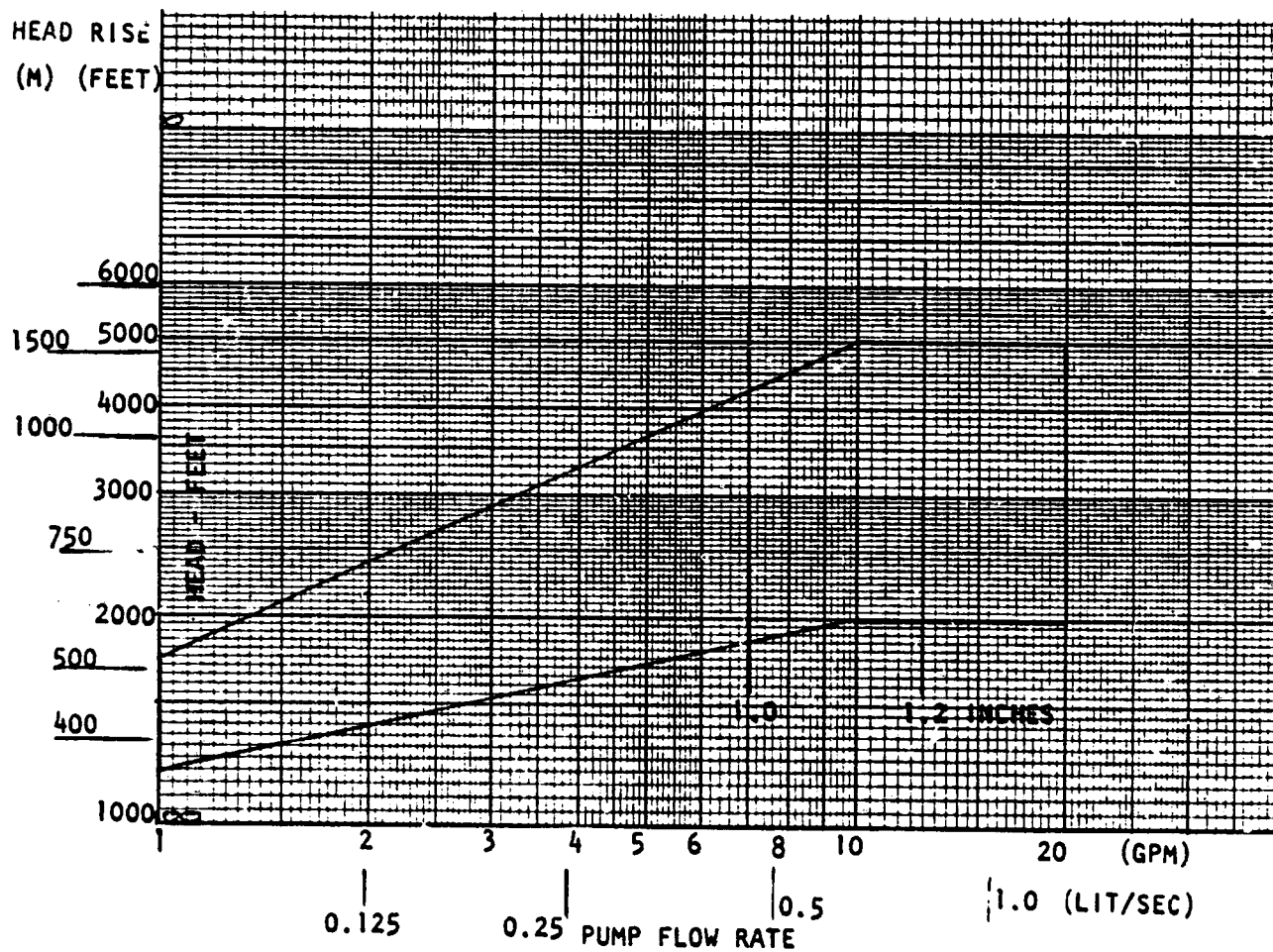


Figure A-102. Tesla Methane Pump, Diameter - NPSH = 6 Feet

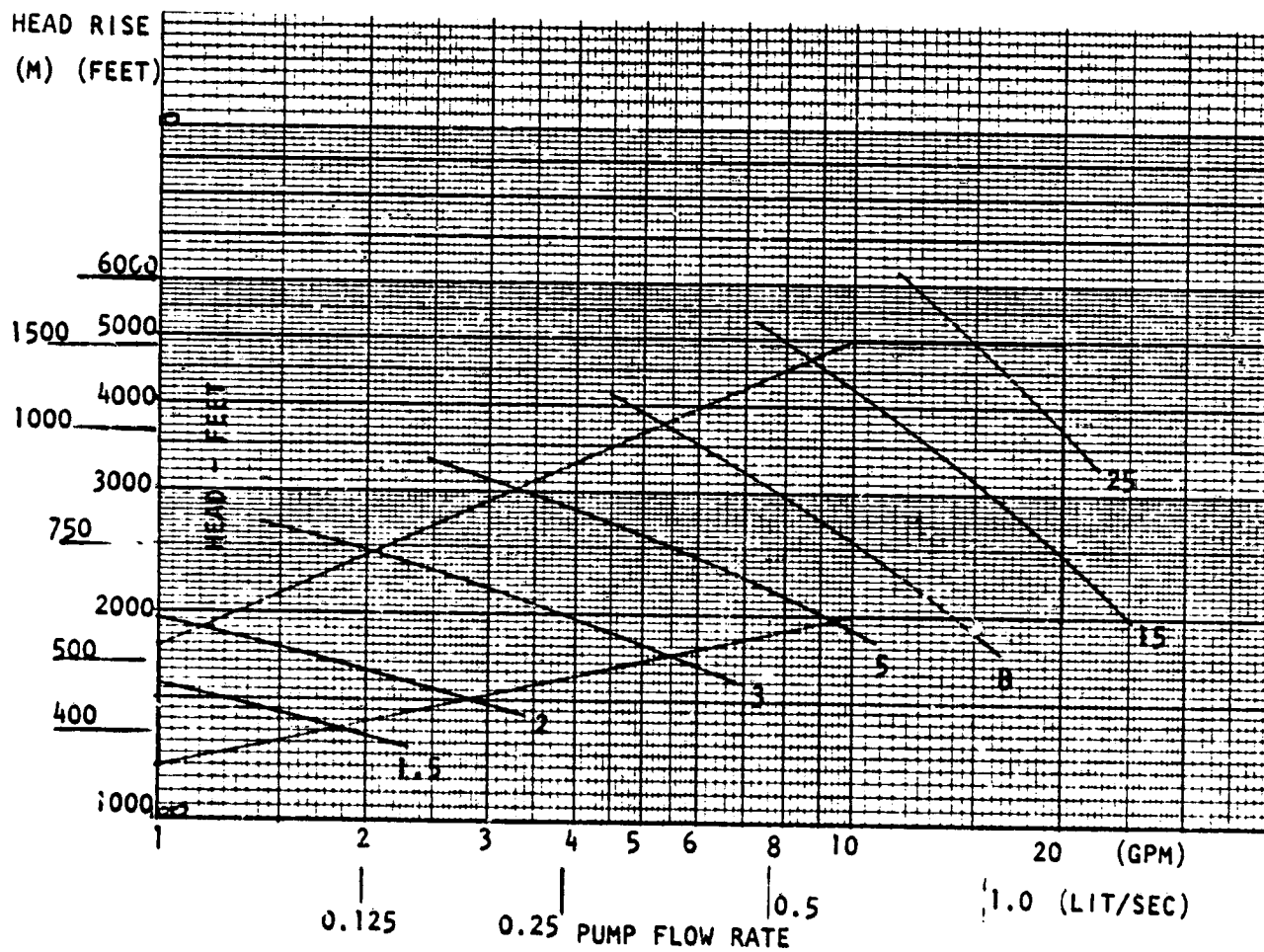


Figure A-103. Tesla Methane Pump. Power - NPSH = 6 Feet

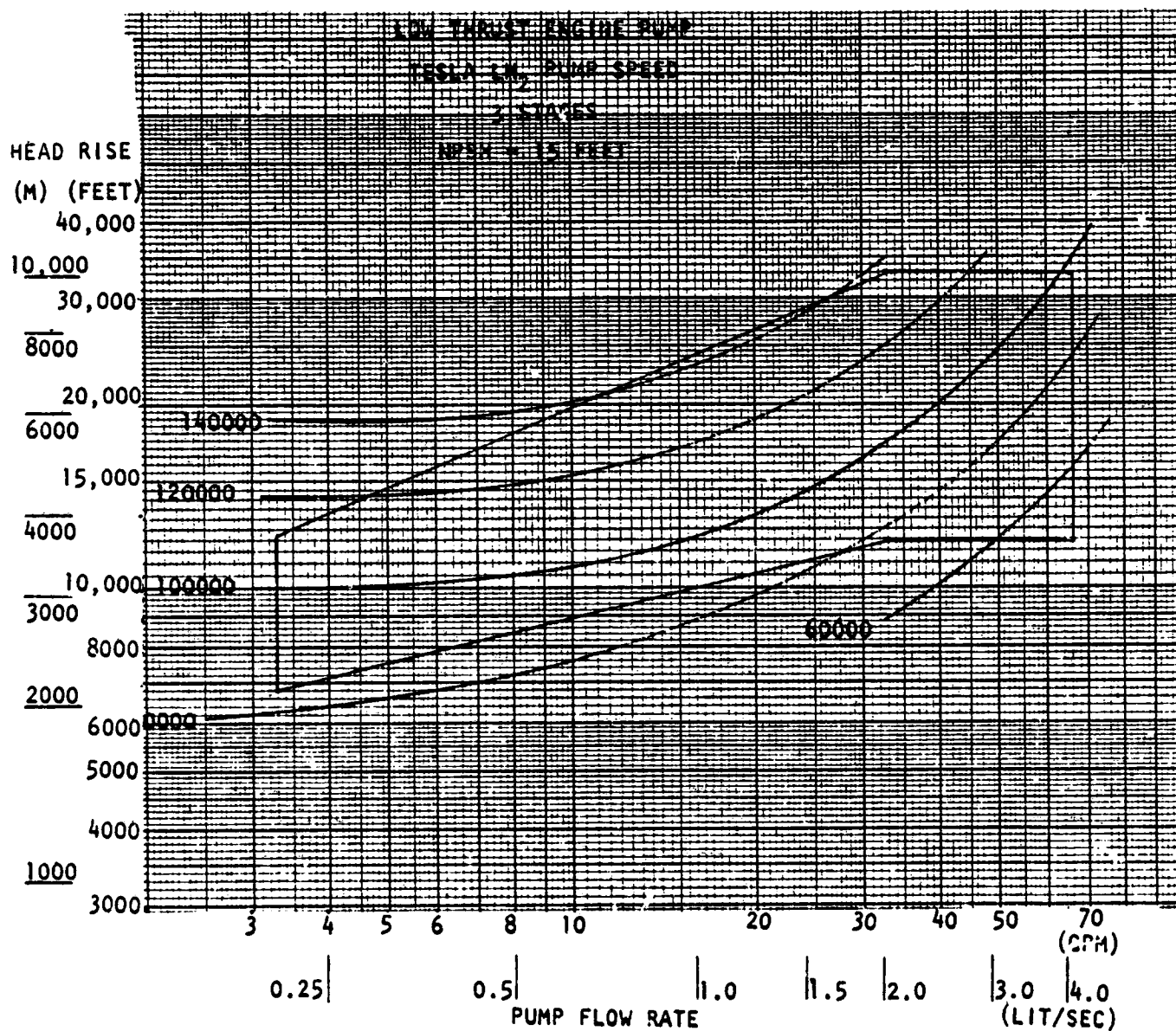


Figure A-104. Tesla Hydrogen Pump, Speed

ORIGINAL PAGE IS
OF POOR QUALITY

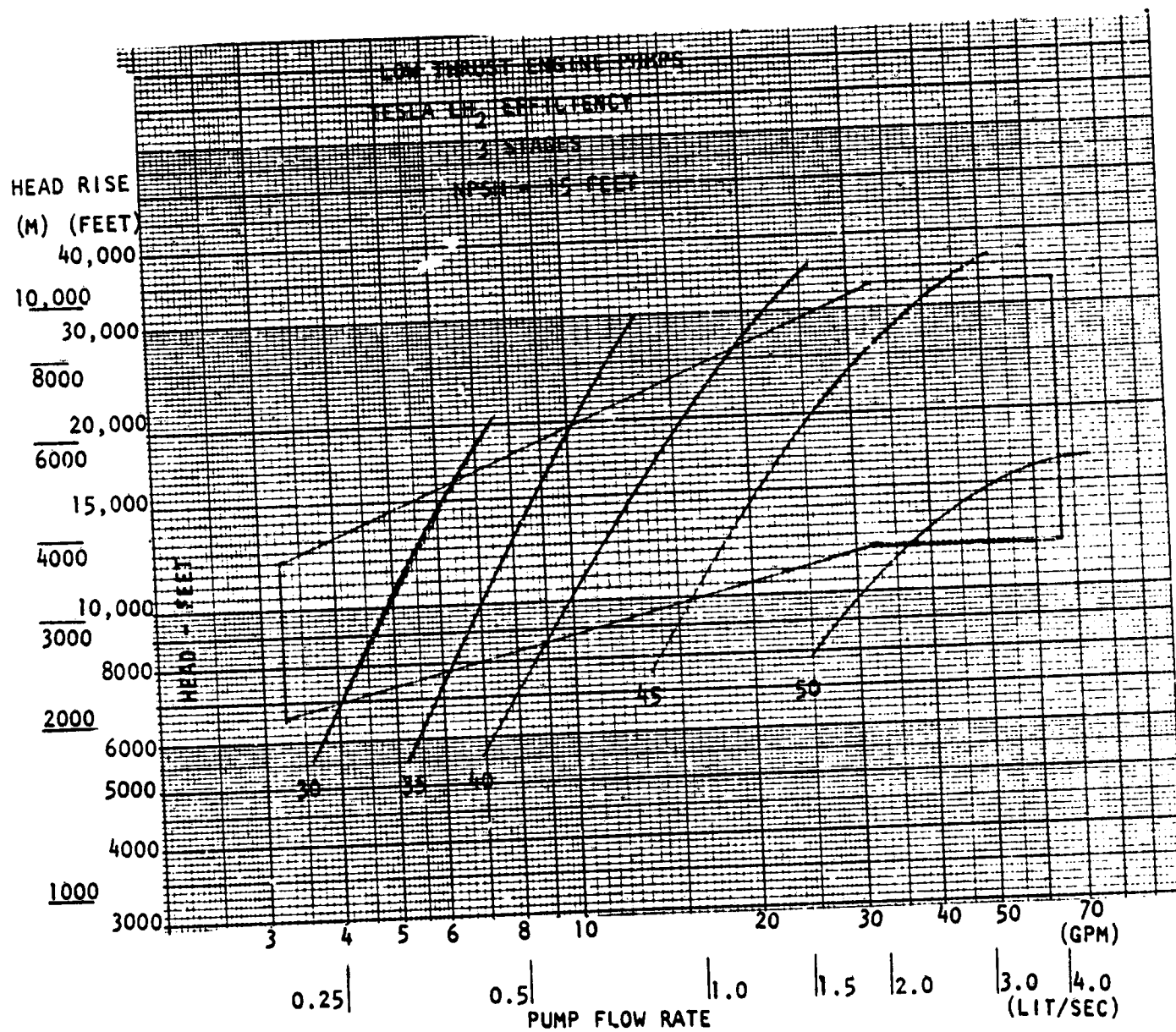


Figure A-105. Tesla Hydrogen Pump, Efficiency

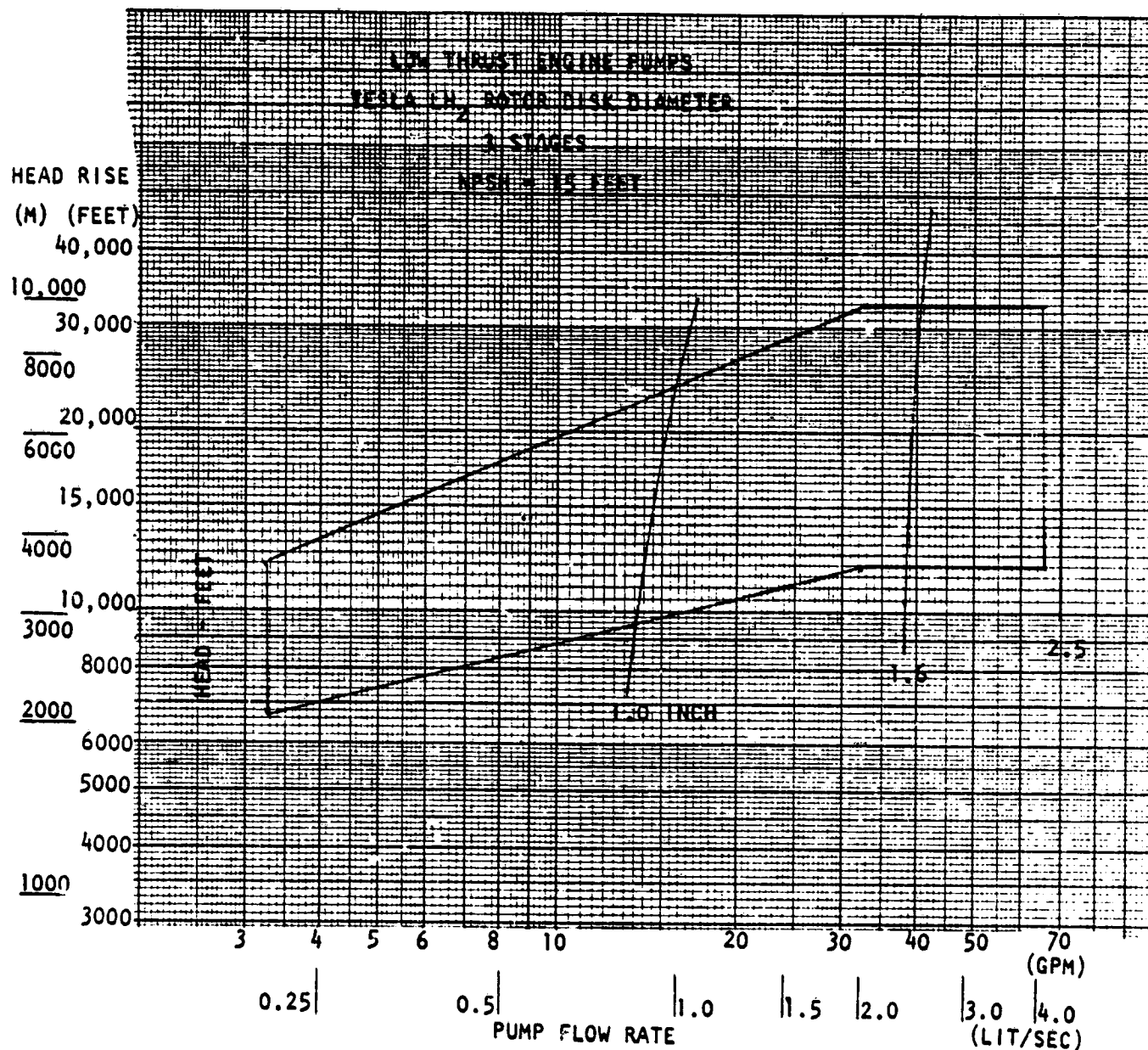


Figure A-106. Tesla Hydrogen Pump, Diameter

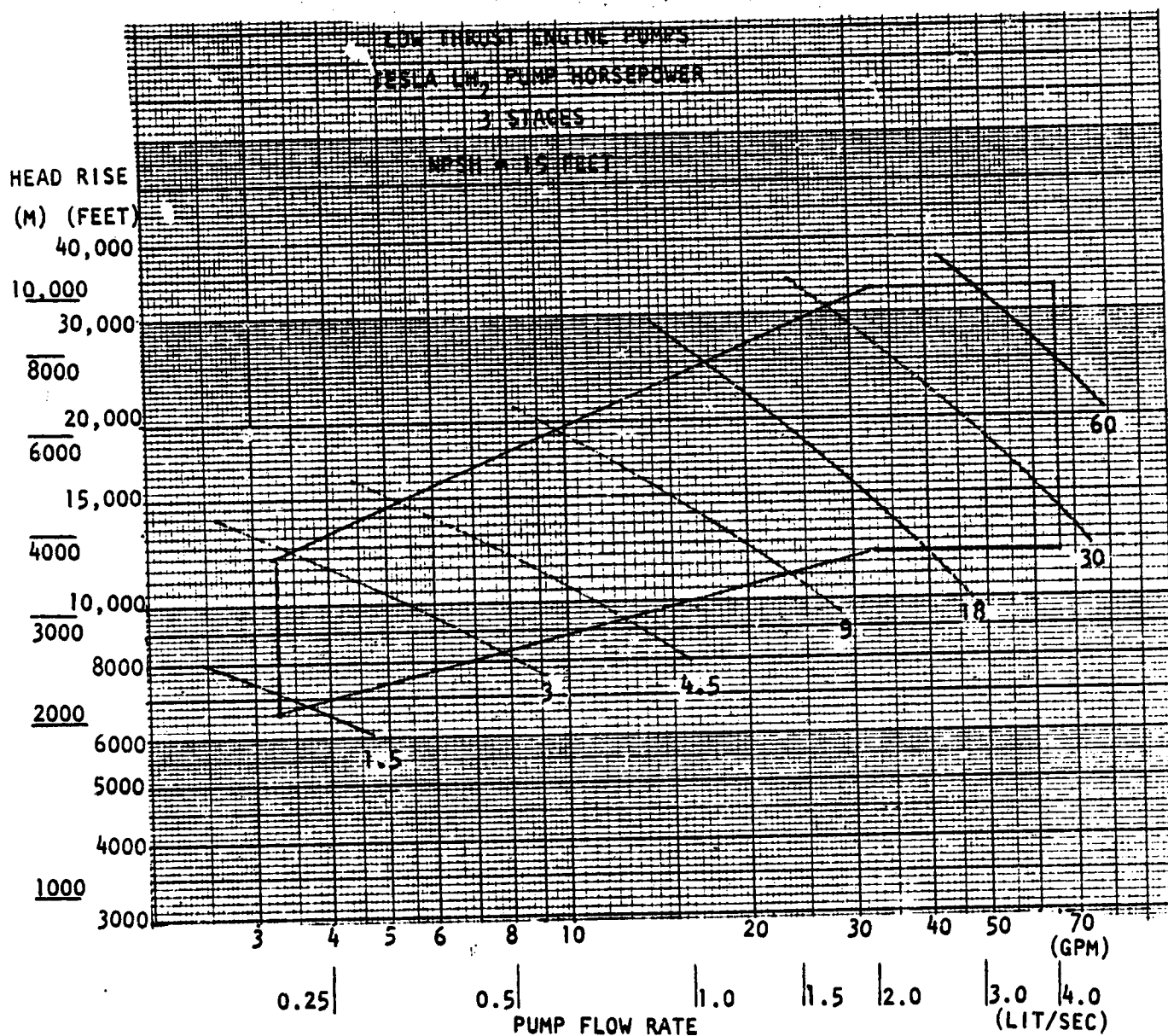


Figure A-107. Tesla Hydrogen Pump, Power

ORIGINAL PAGE IS
OF POOR QUALITY

C-4

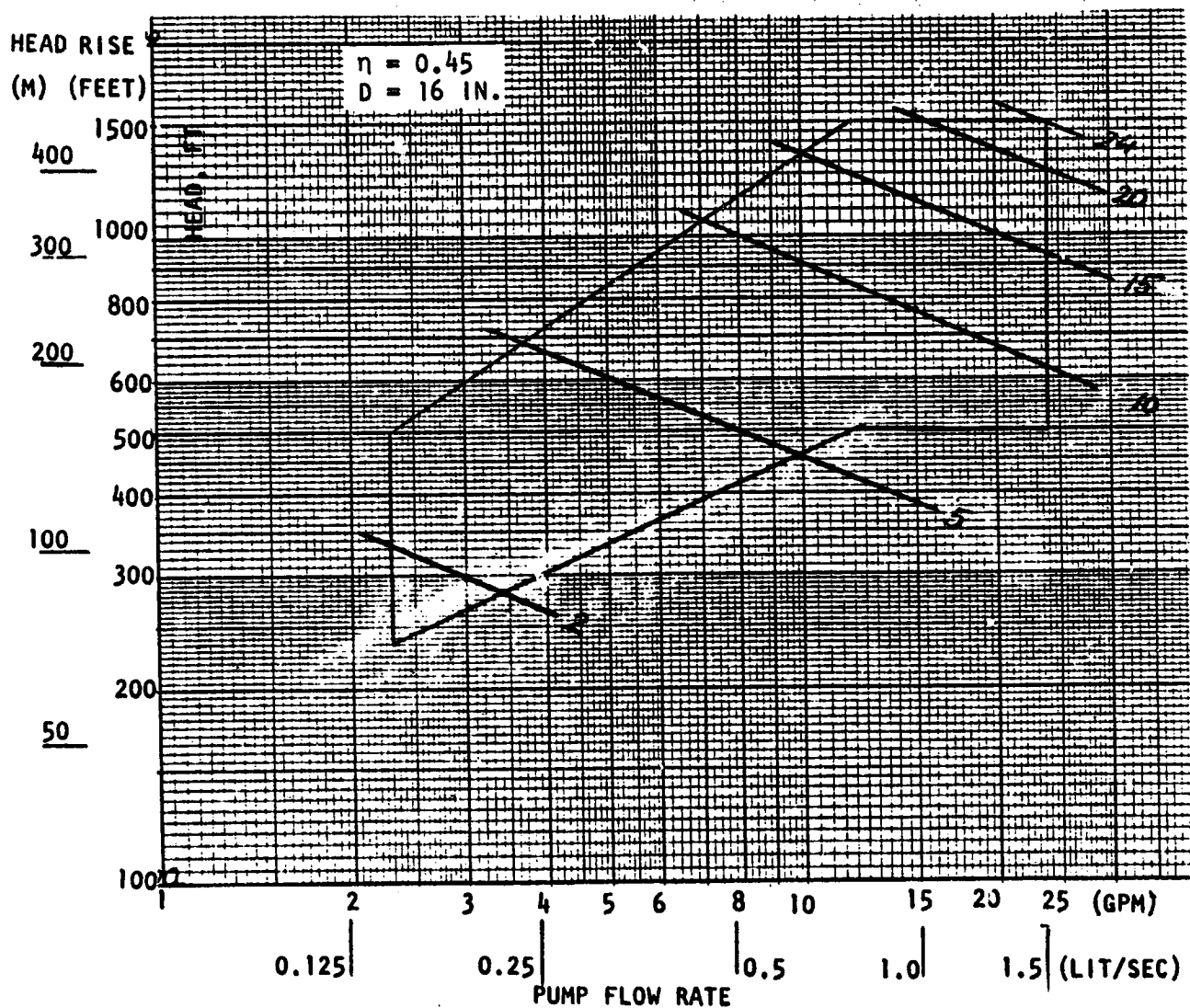


Figure A-108. Drag LOX Pump, Optimum Stages - NPSH = 2 Feet

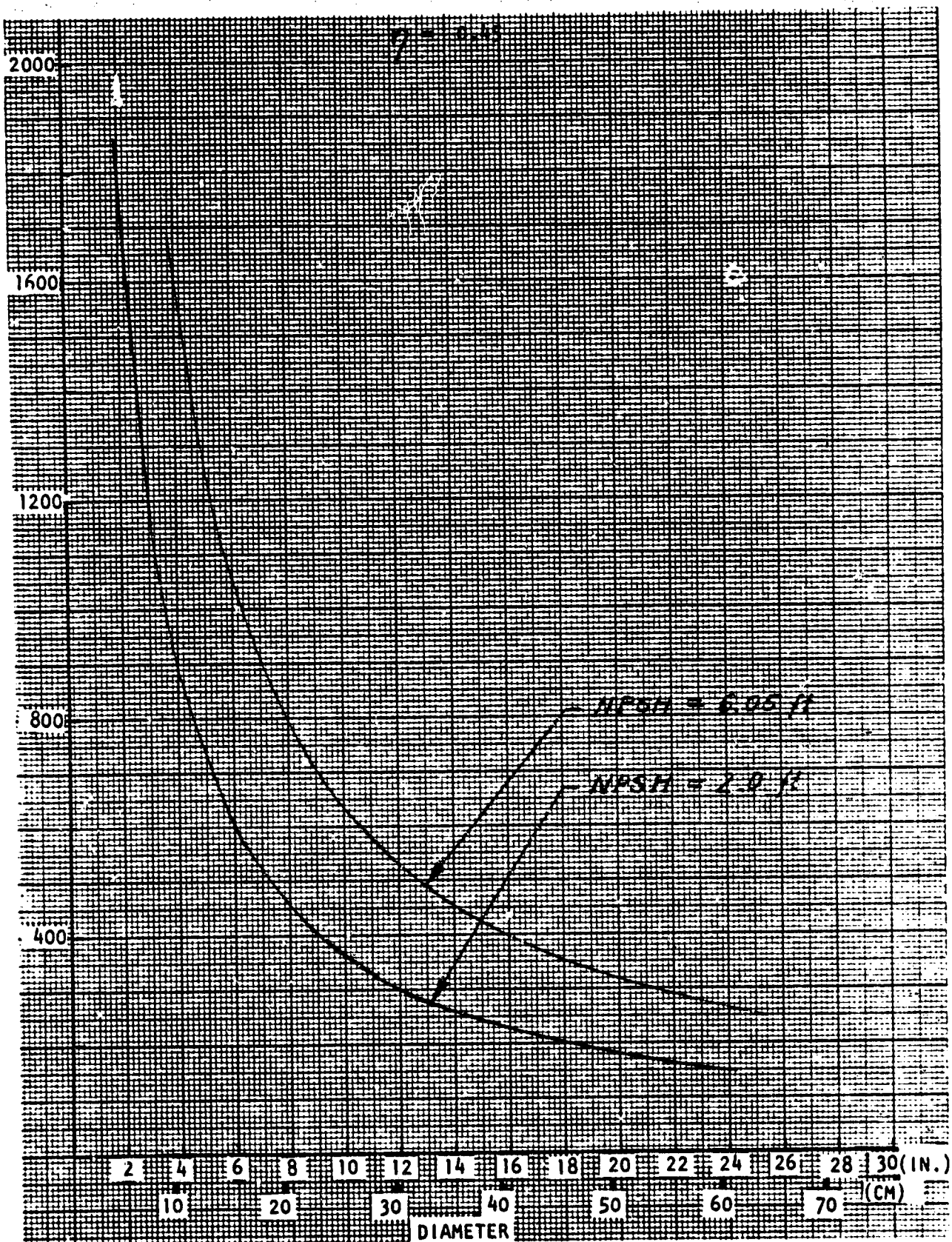


Figure A-109. Drag LOX Pump, Speed vs Diameter

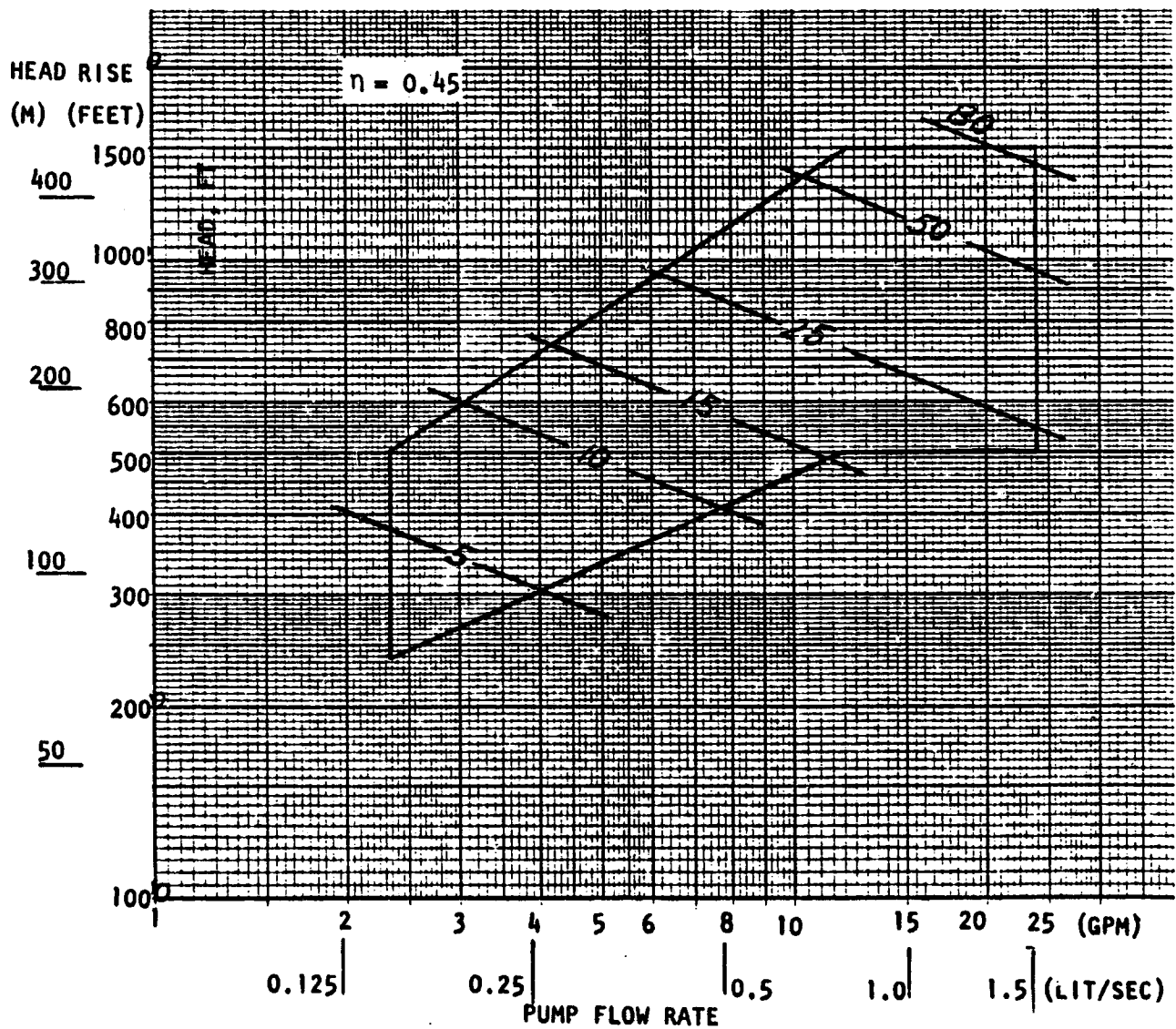


Figure A-110. Drag LOX Pump, Diameter, NPSH = 2 Feet, (Six Stages)

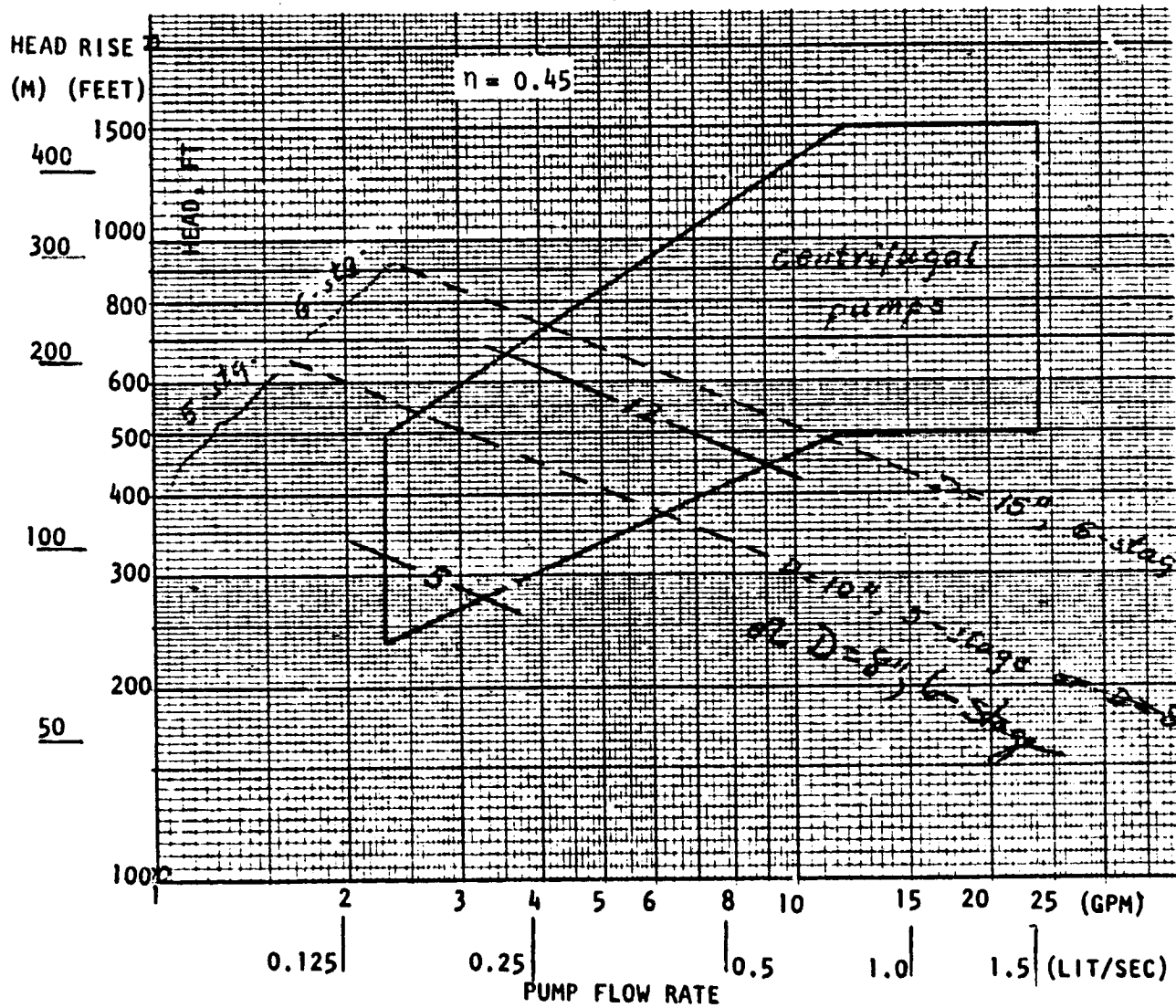


Figure A-111. Drag LOX Pump, Diameter, (15 Inch Maximum)
NPSH = 2 Feet, Six Stages

ORIGINAL PAGE IS
OF POOR QUALITY

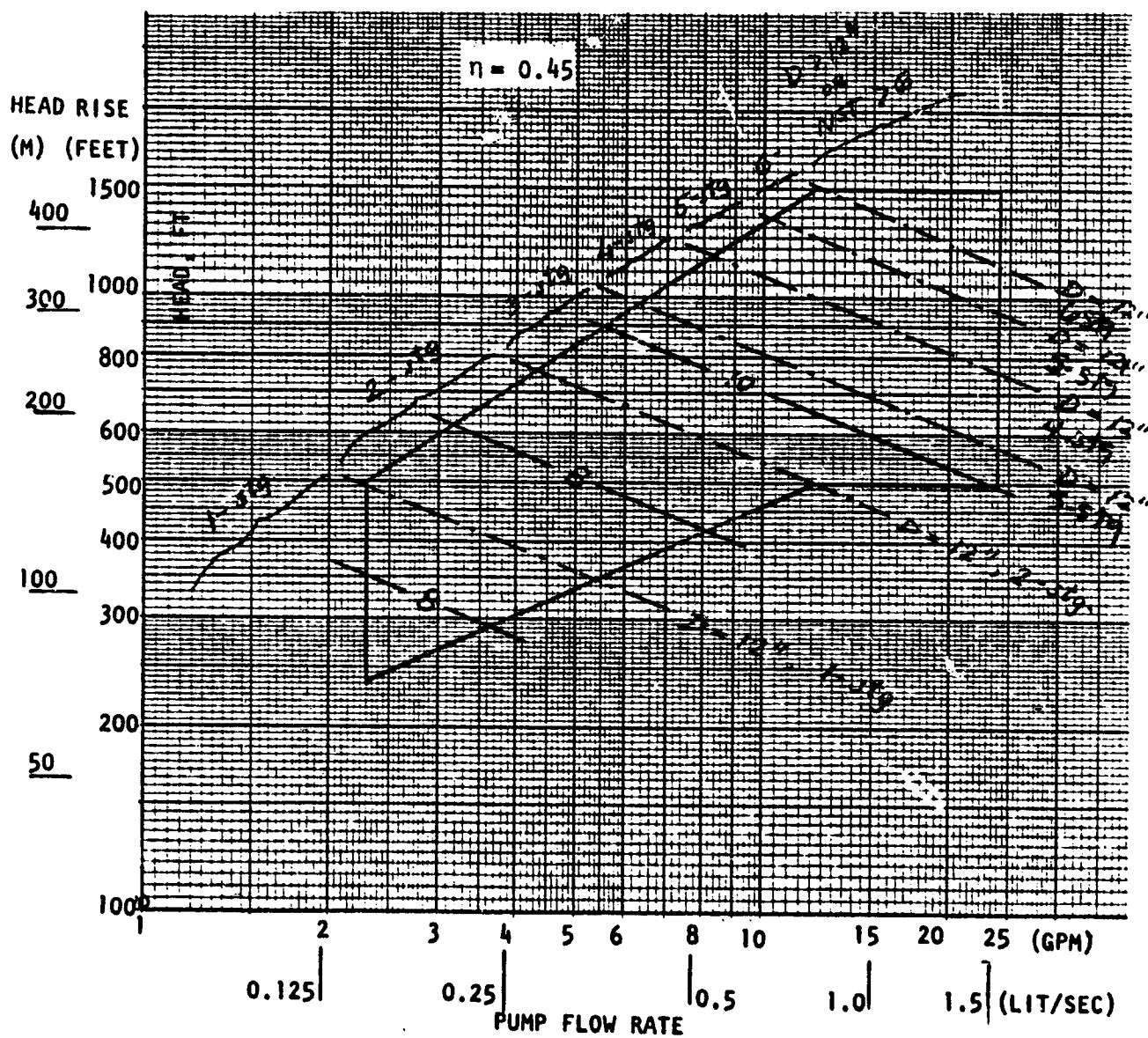


Figure A-112. Drag LOX Pump, Diameter (12 Inch Maximum)
NPSH = 6.05 Feet, Six Stages

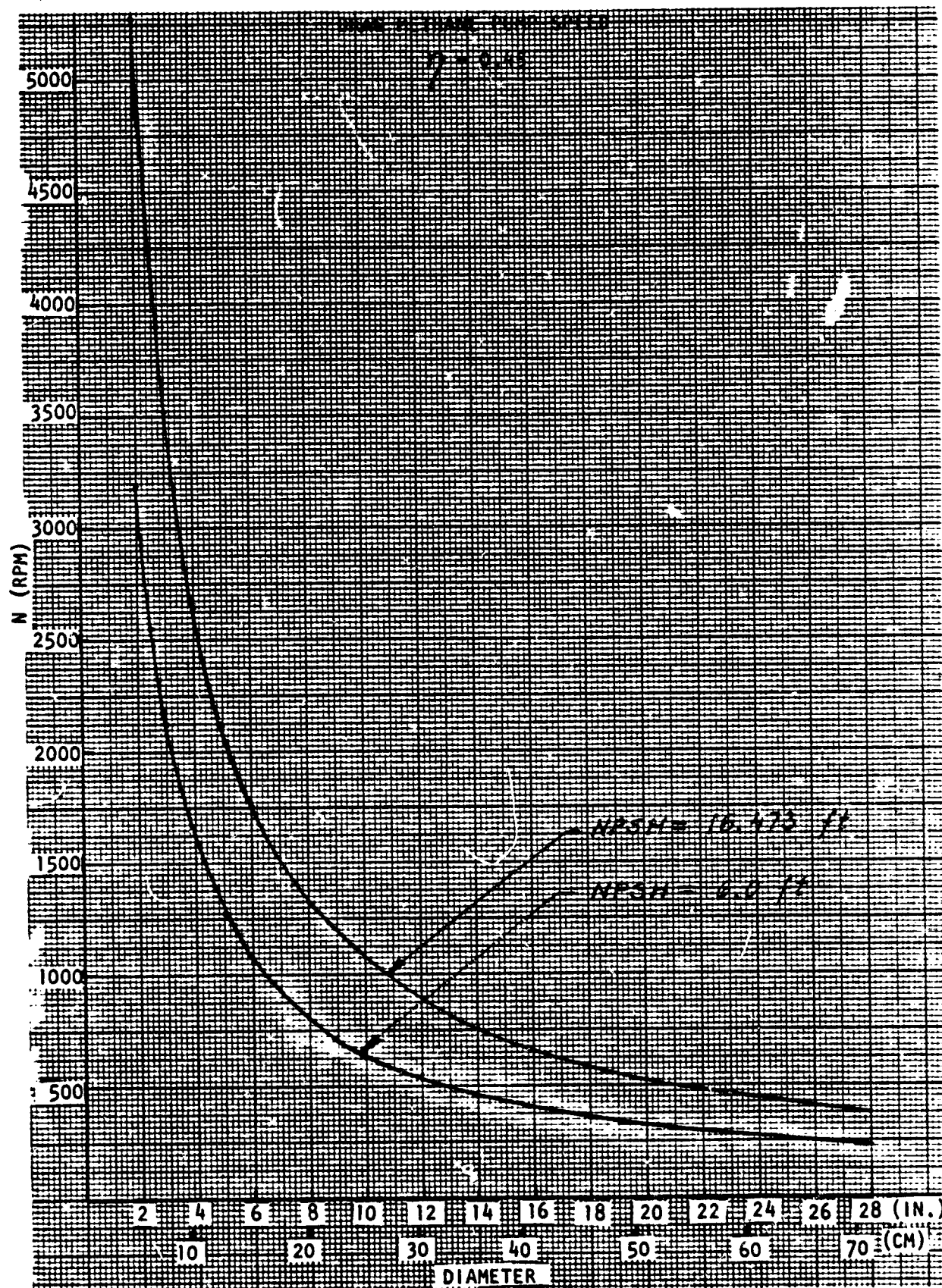


Figure A-113. Drag Methane Pump, Speed vs Diameter

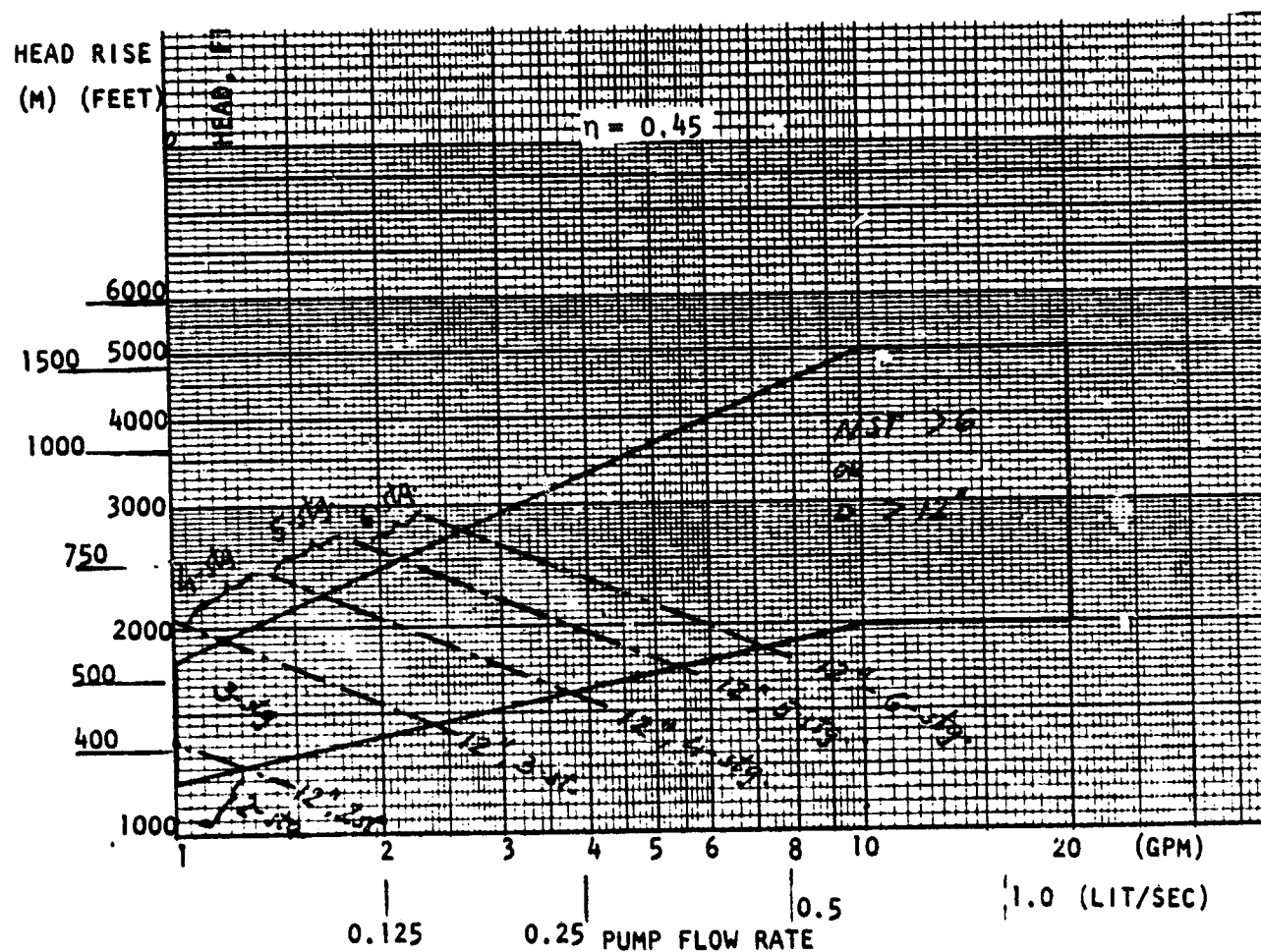


Figure A-114. Drag Methane Pump, Diameter (12 Inch Maximum)
NPSH = 6 Feet, Six Stages

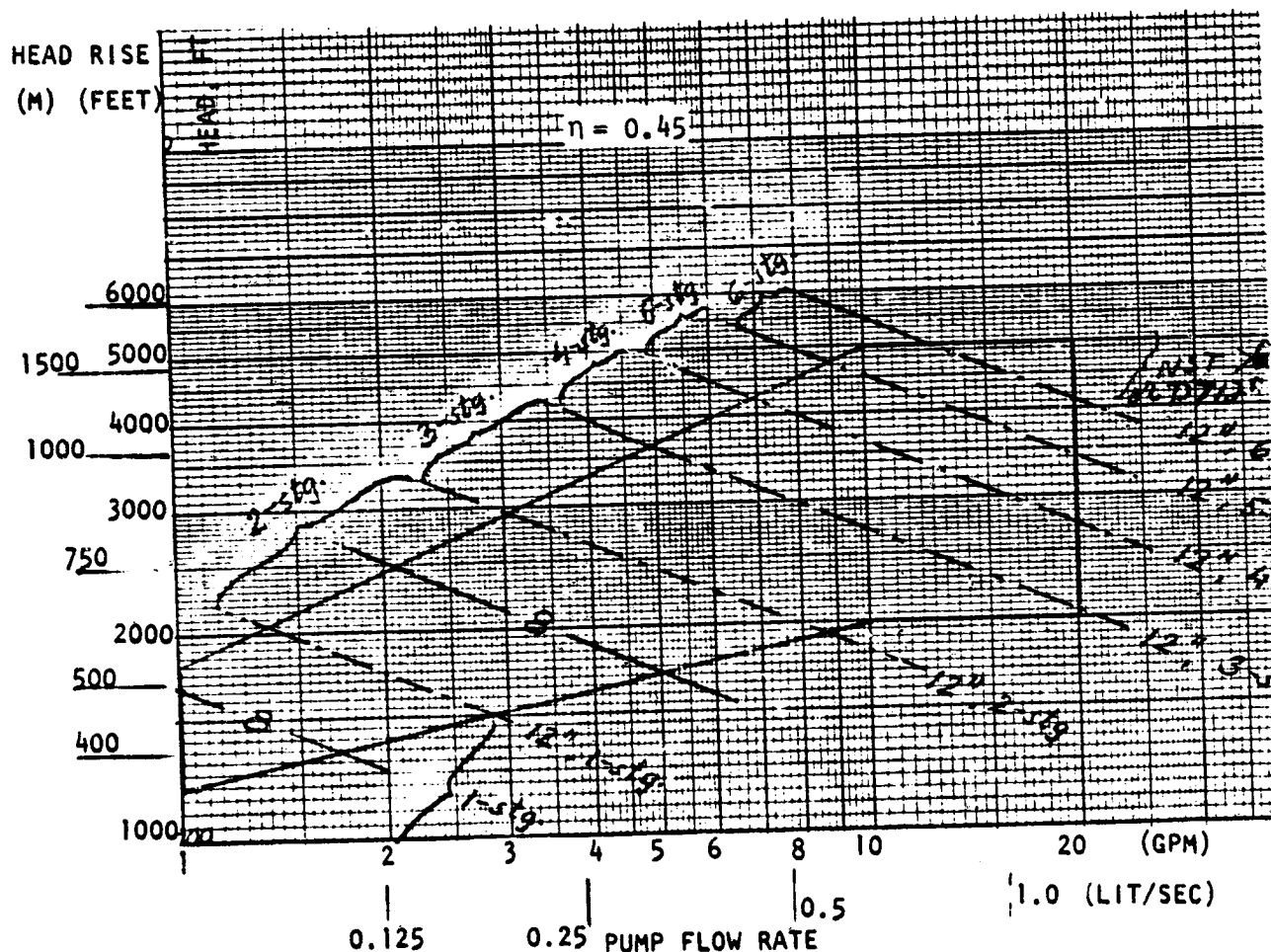


Figure A-115. Drag Methane Pump, Diameter (12 Inch Maximum)
NPSH = 16.47 Feet, Six Stages

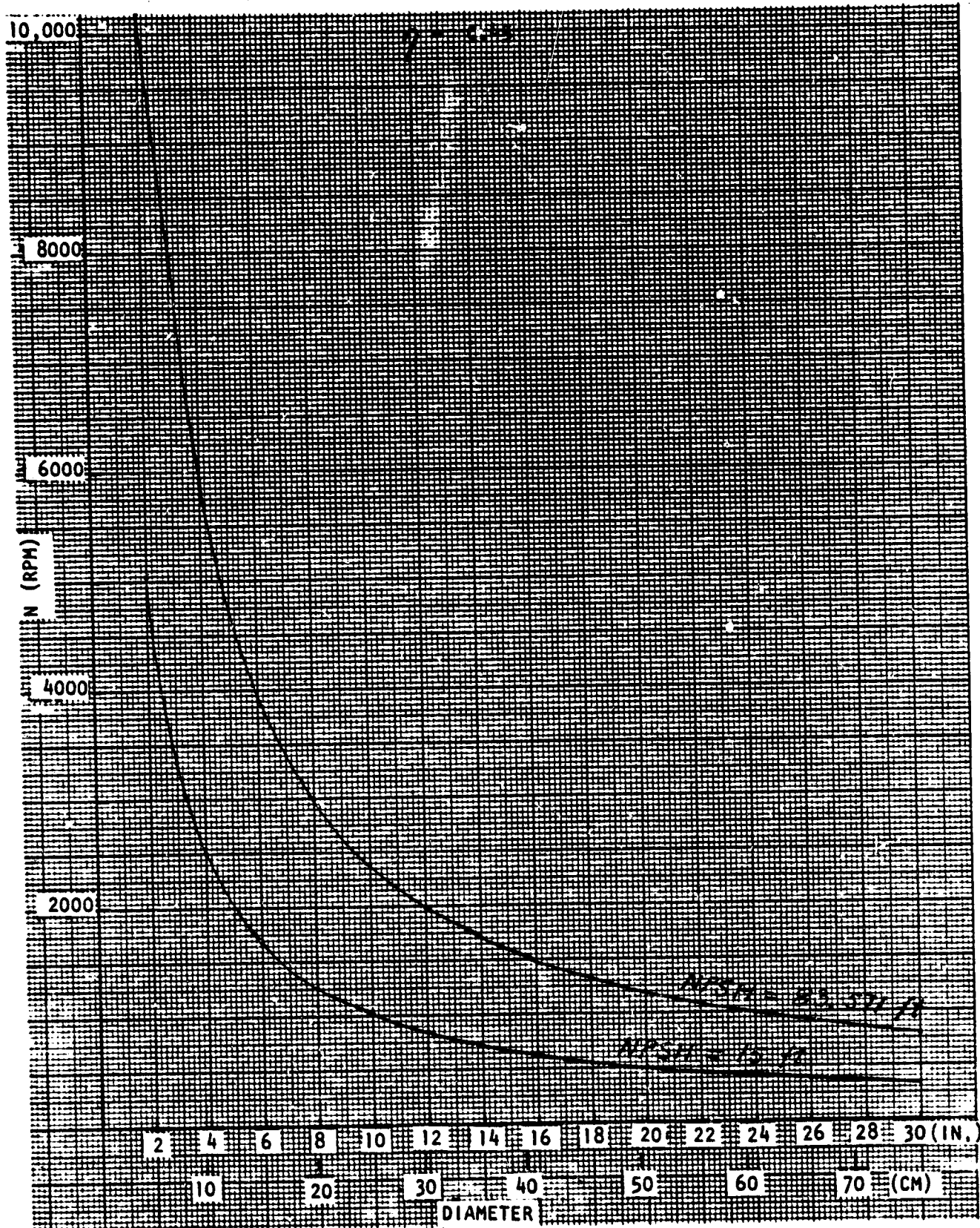


Figure A-116. Drag Hydrogen Pump, Speed vs Diameter

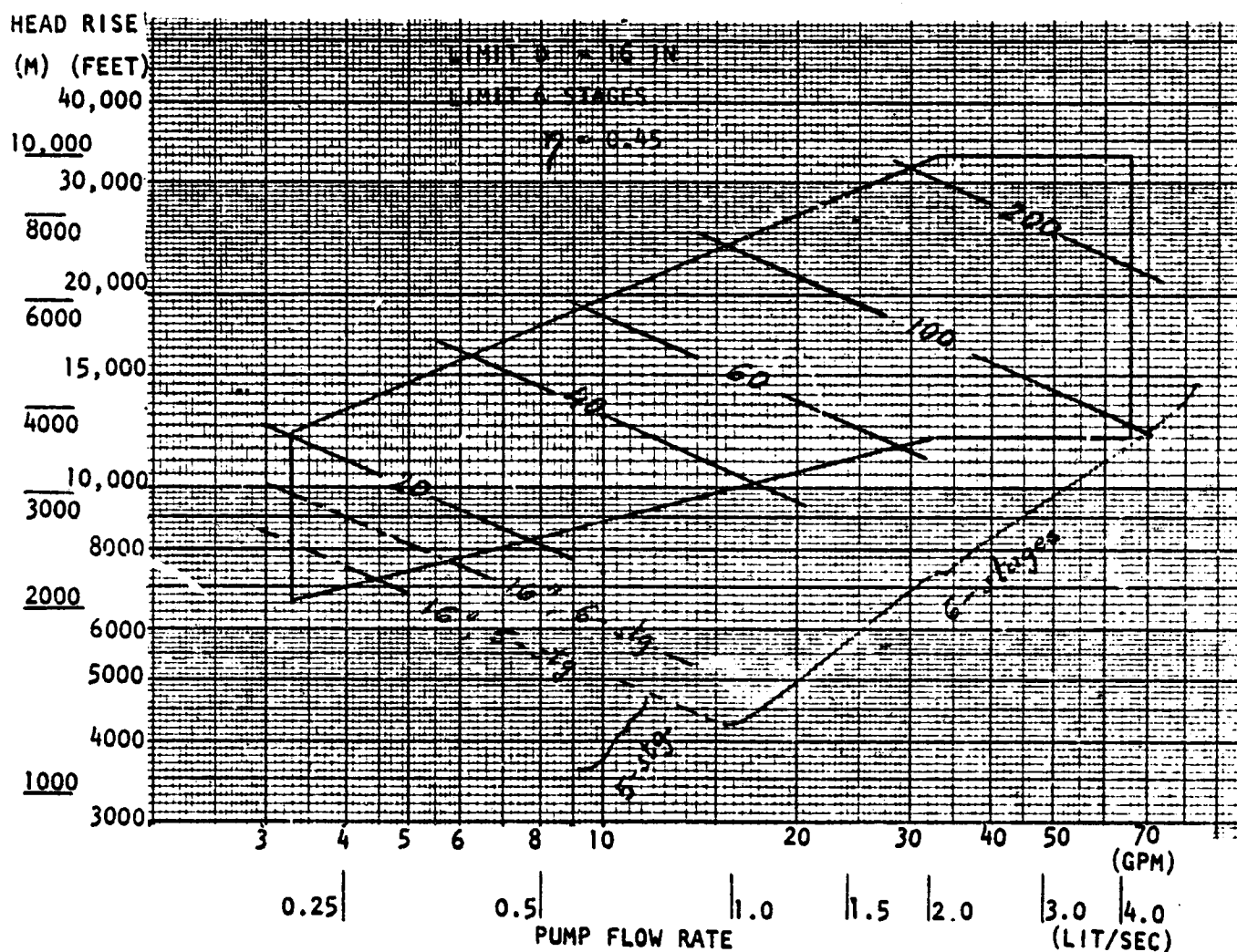


Figure A-117. Drag Hydrogen Pump, Diameter, NPSH = 15 Feet

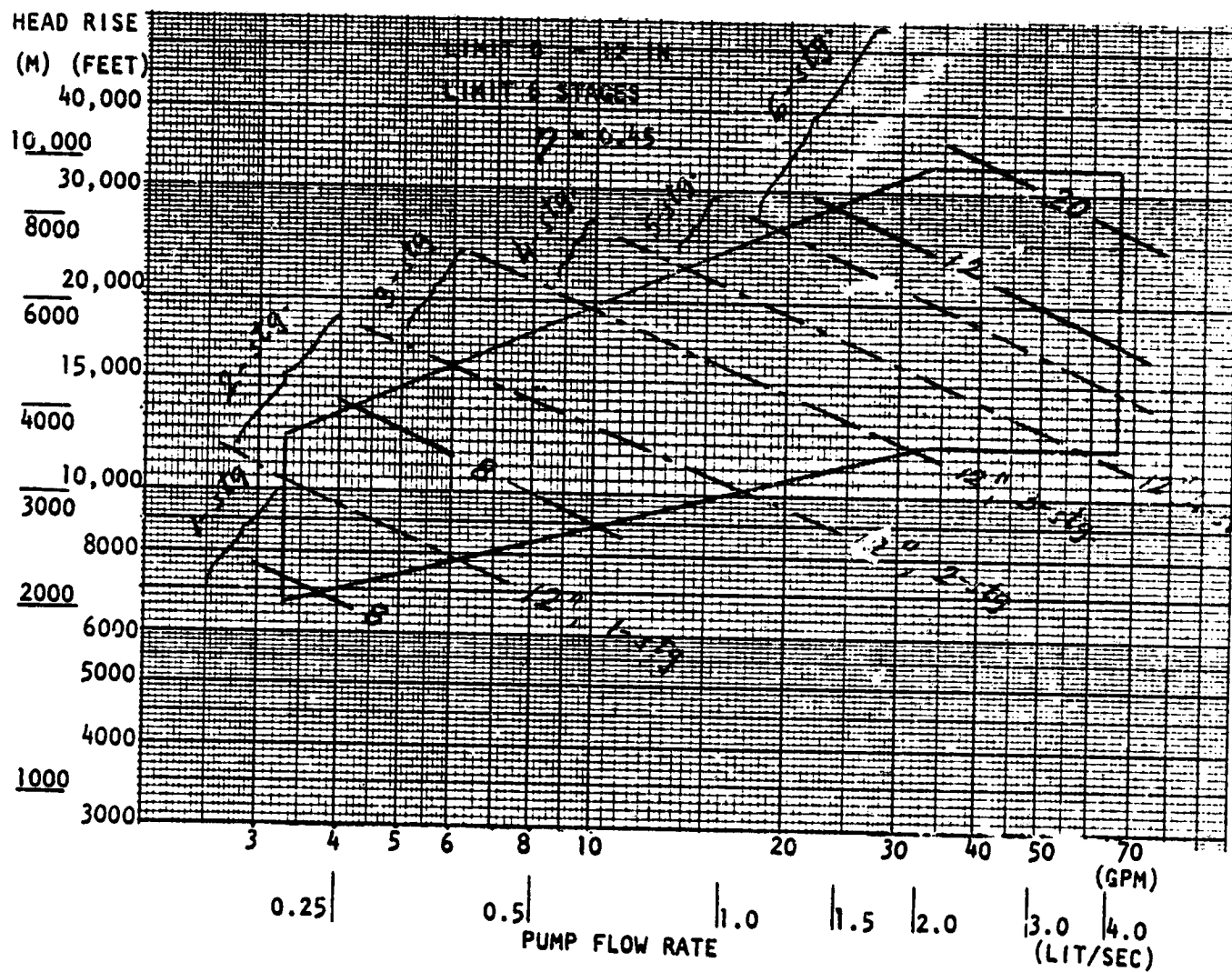


Figure A-118. Drag Hydrogen Pump, Diameter, NPSH = 83.57 Feet

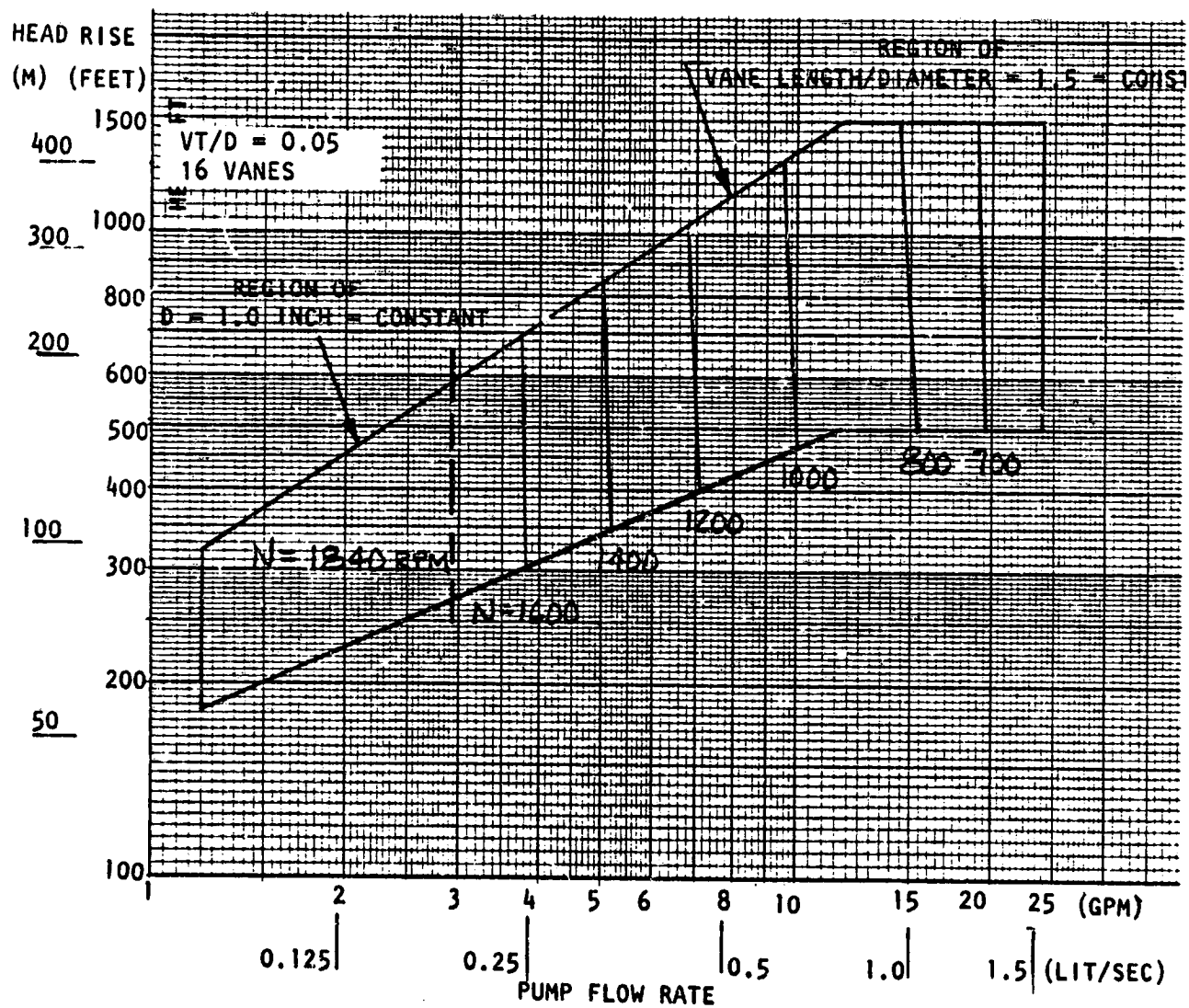


Figure A-119. Vane LOX Pump - C/D = 0.00025, Speed, NPSH = 2 Feet

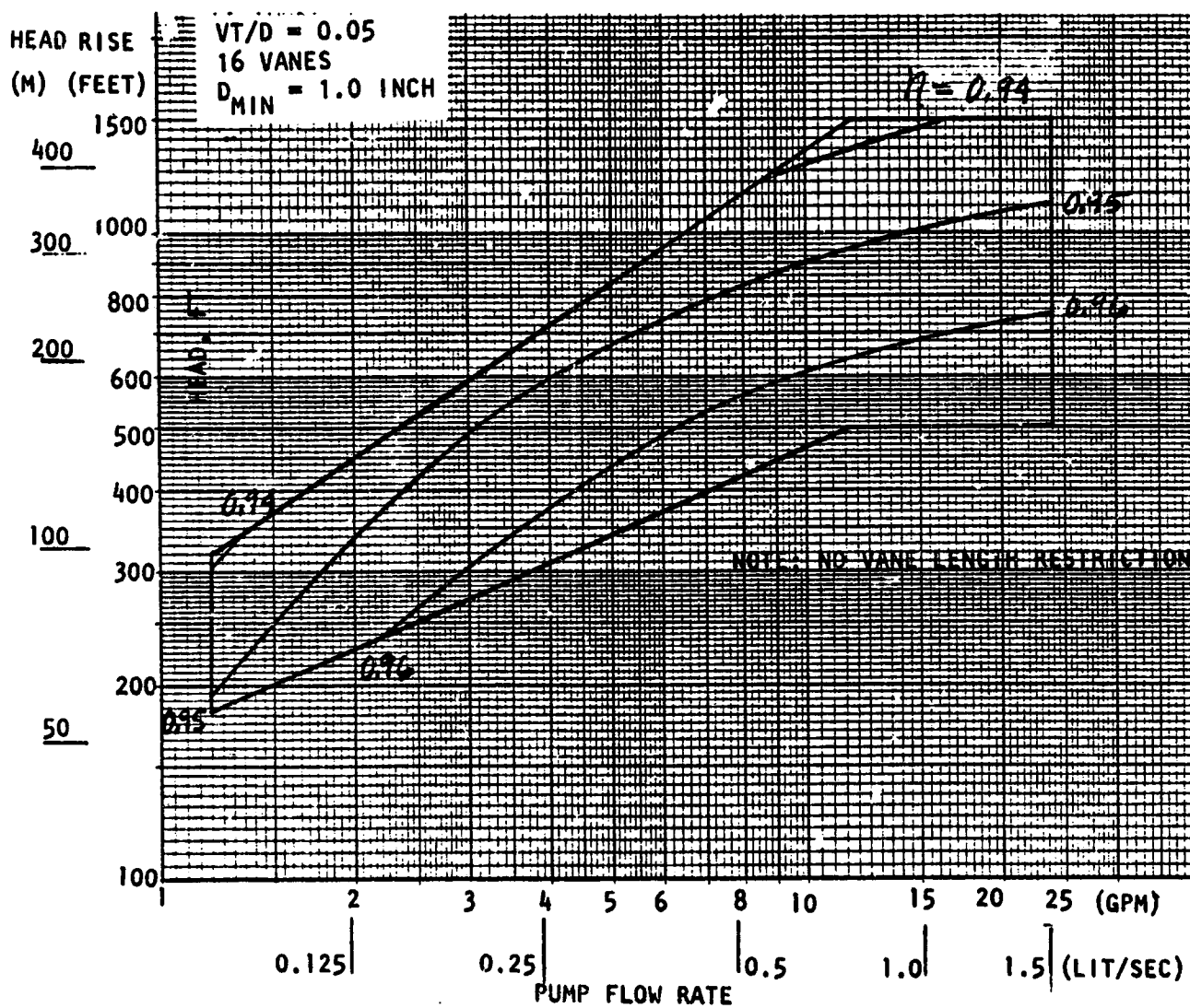


Figure A-120. Vane LOX Pump - C/D = 0.00025, Efficiency, NPSH = 2 Feet

ORIGINAL PAGE IS
OF TYPE 100X

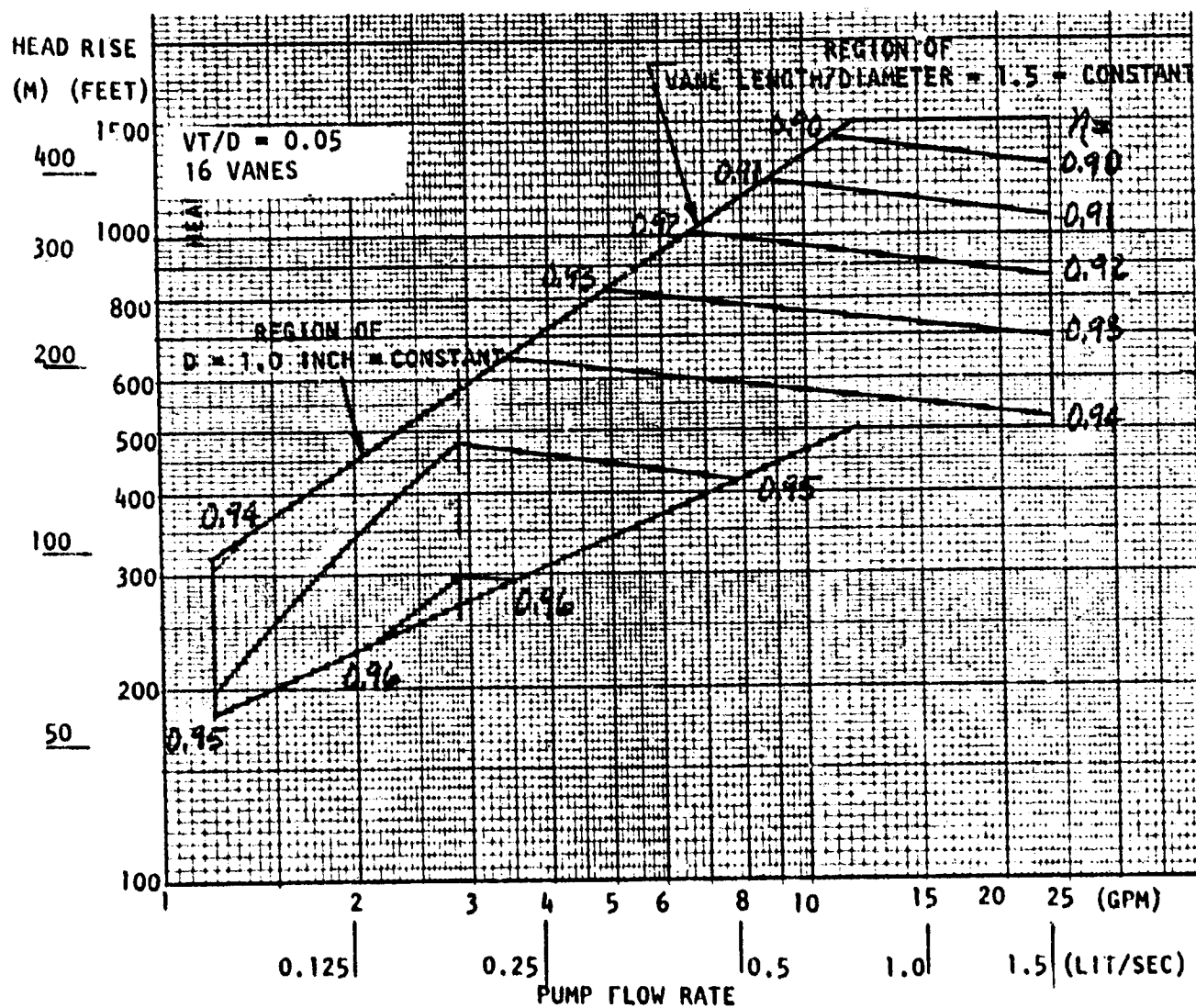


Figure A-121. Vane LOX Pump - $C/D = 0.00025$, Efficiency
(Vane $L/D \leq 1.5$), NPSH = 2 Feet

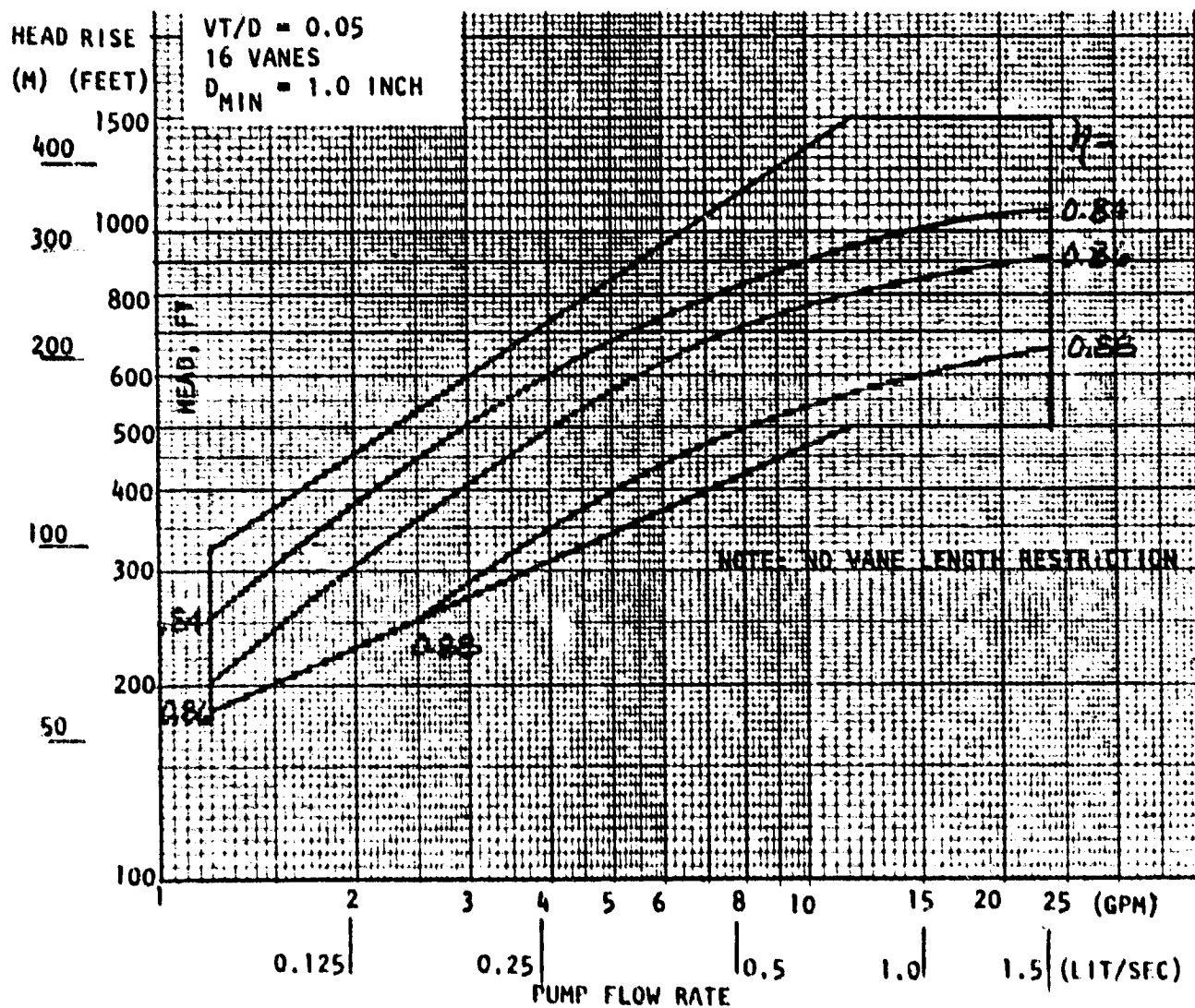


Figure A-122. Vane LOX Pump - C/D = 0.00050, Efficiency, NPSH = 2 Feet

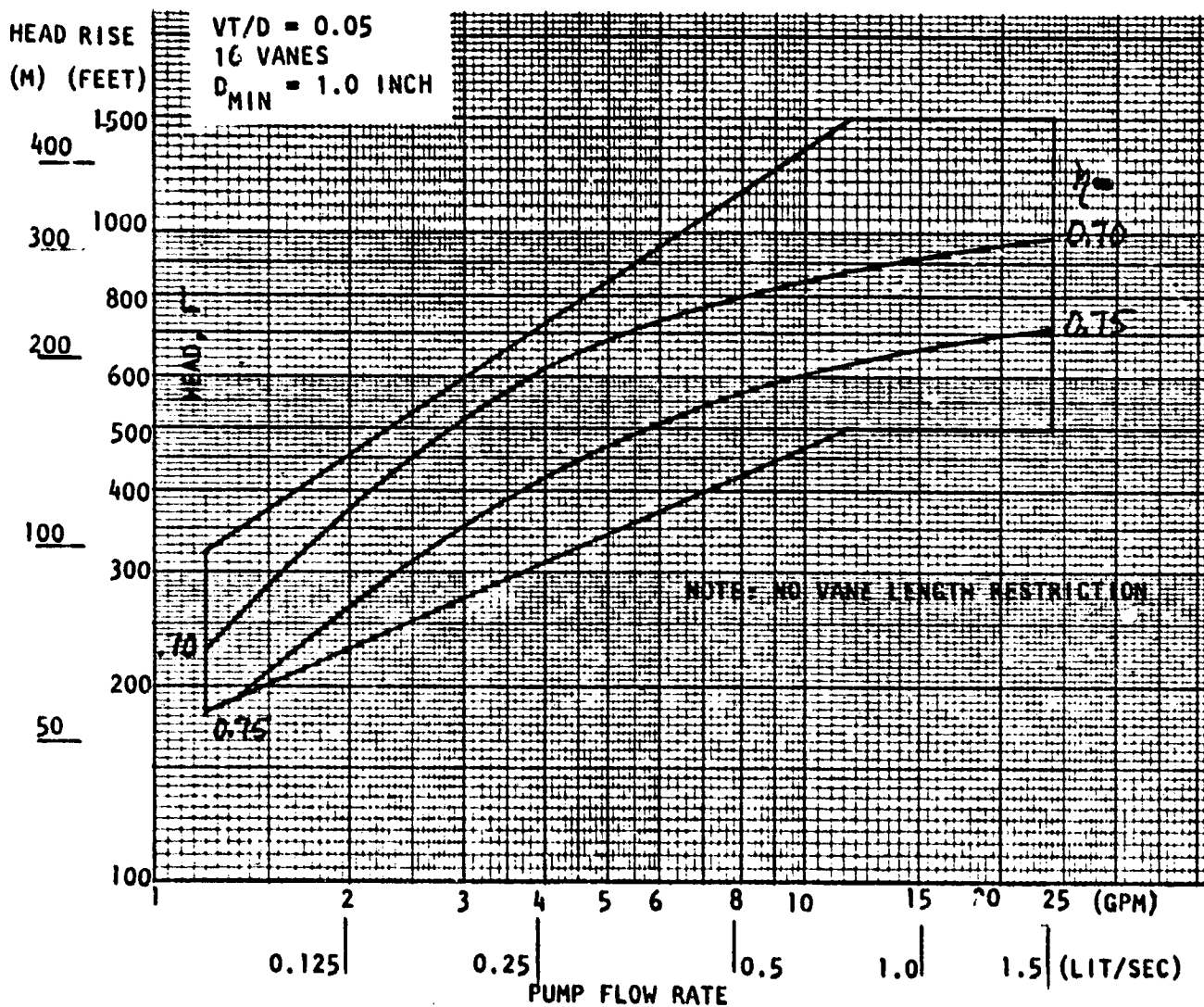


Figure A-123. Vane LOX Pump - C/D = 0.00075, Efficiency, NPSH = 2 Feet

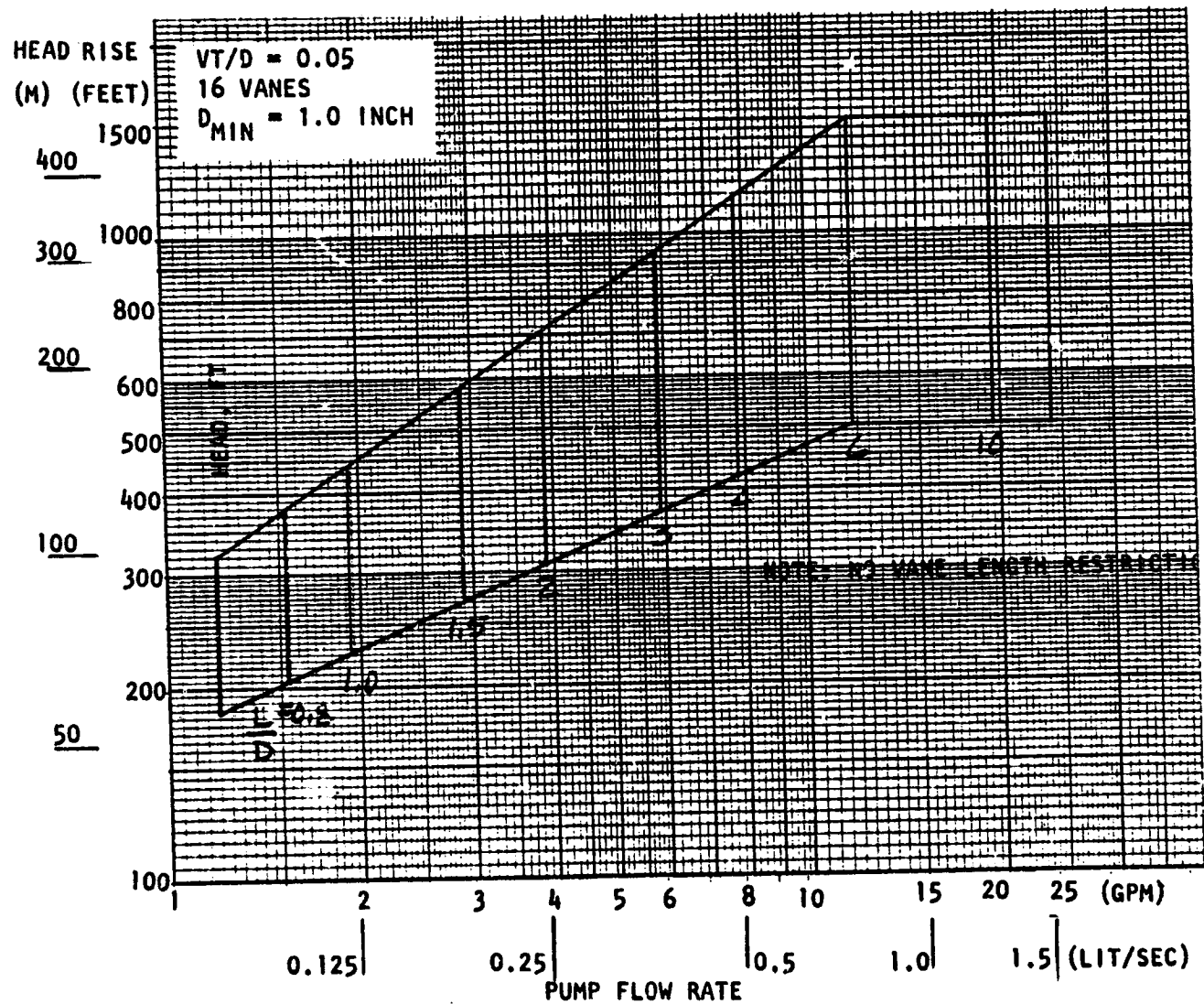


Figure A-124. Vane LOX Pump - C/D = 0.00025, Diameter, NPSH = 2 Feet

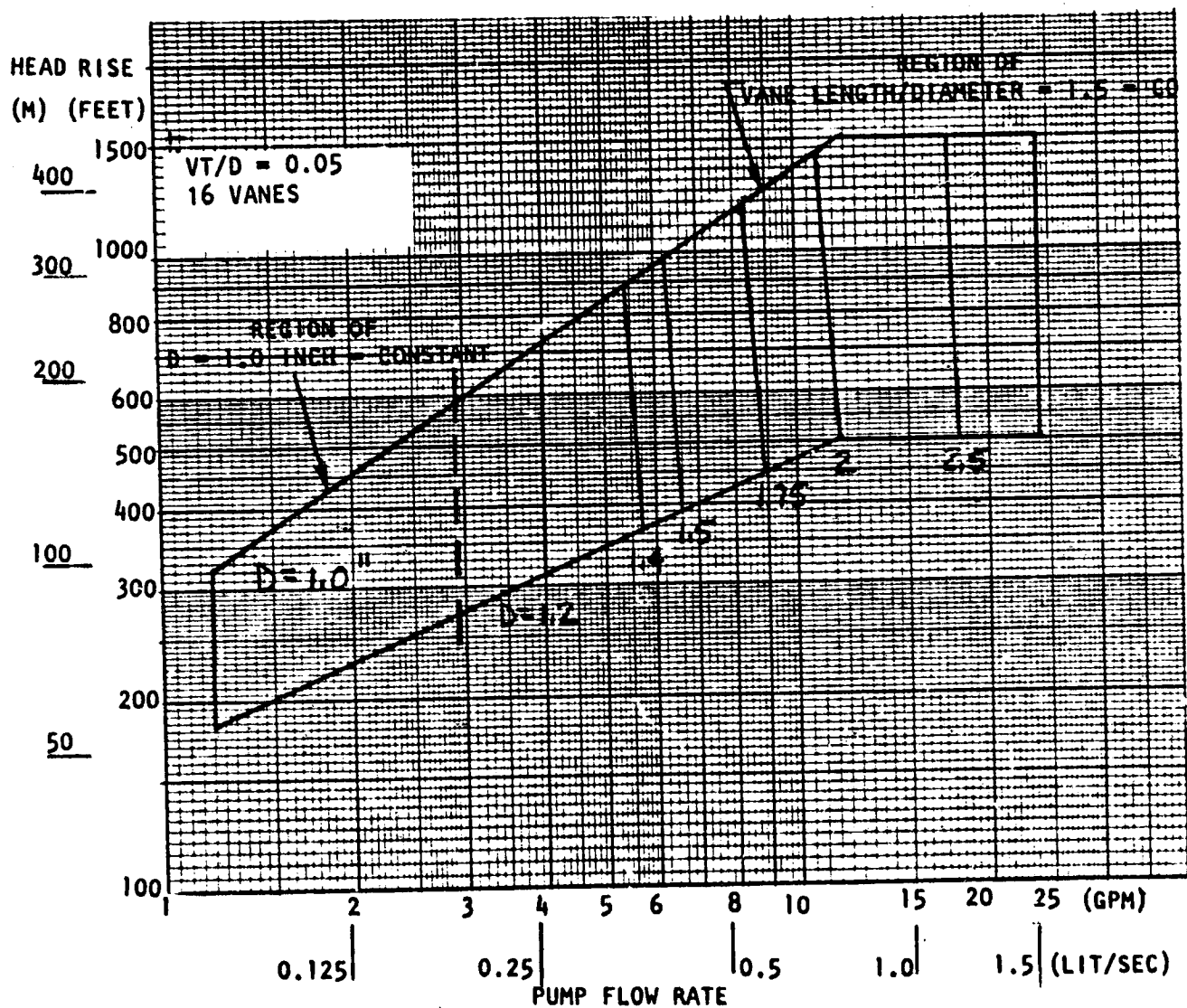


Figure A-125. Vane LOX Pump - $C/D = 0.00025$, Diameter
(Vane $L/D \leq 1.5$) NPSH = 2 Feet

HEAD RISE
(M) (FEET)

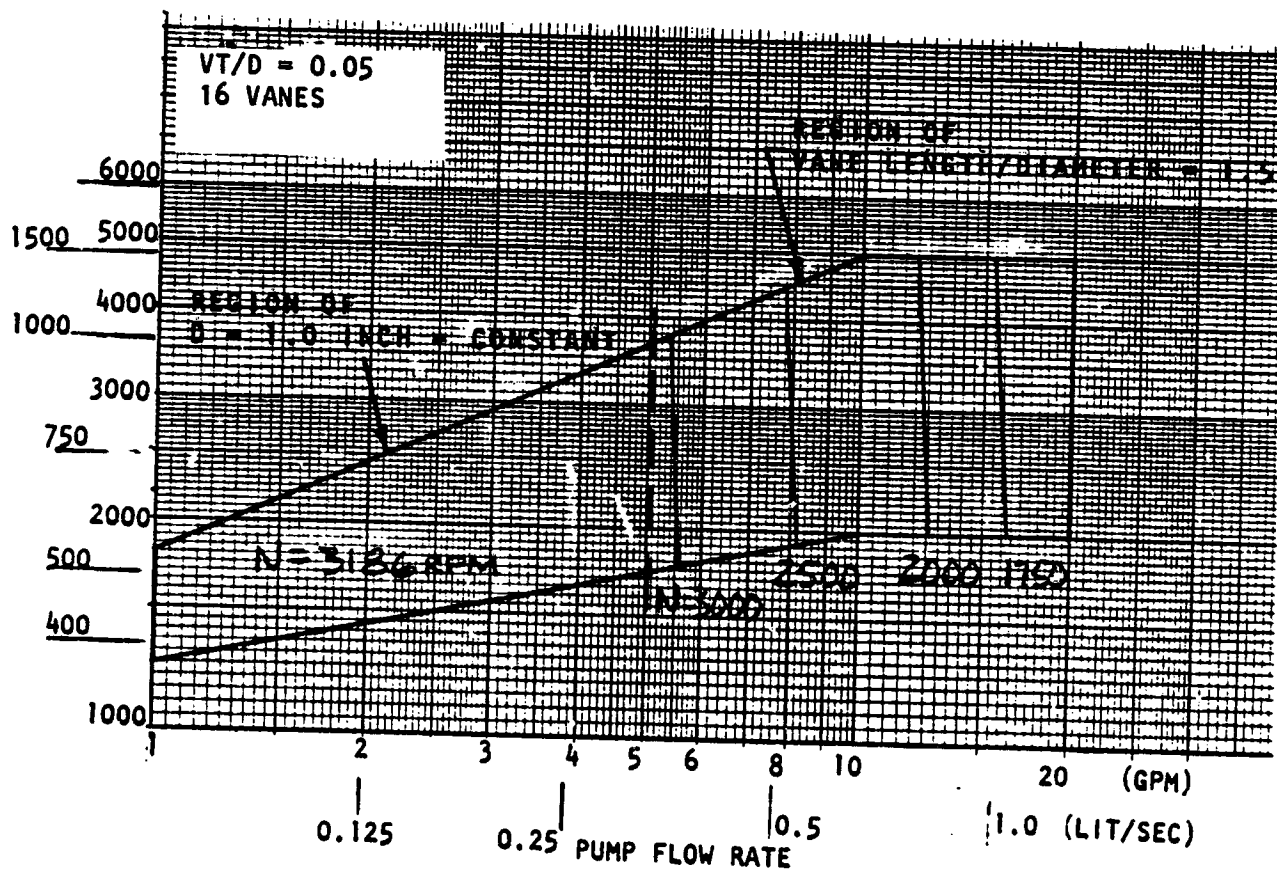


Figure A-126. Vane Methane Pump - C/D = 0.00025, Speed, NPSH = 6 Feet

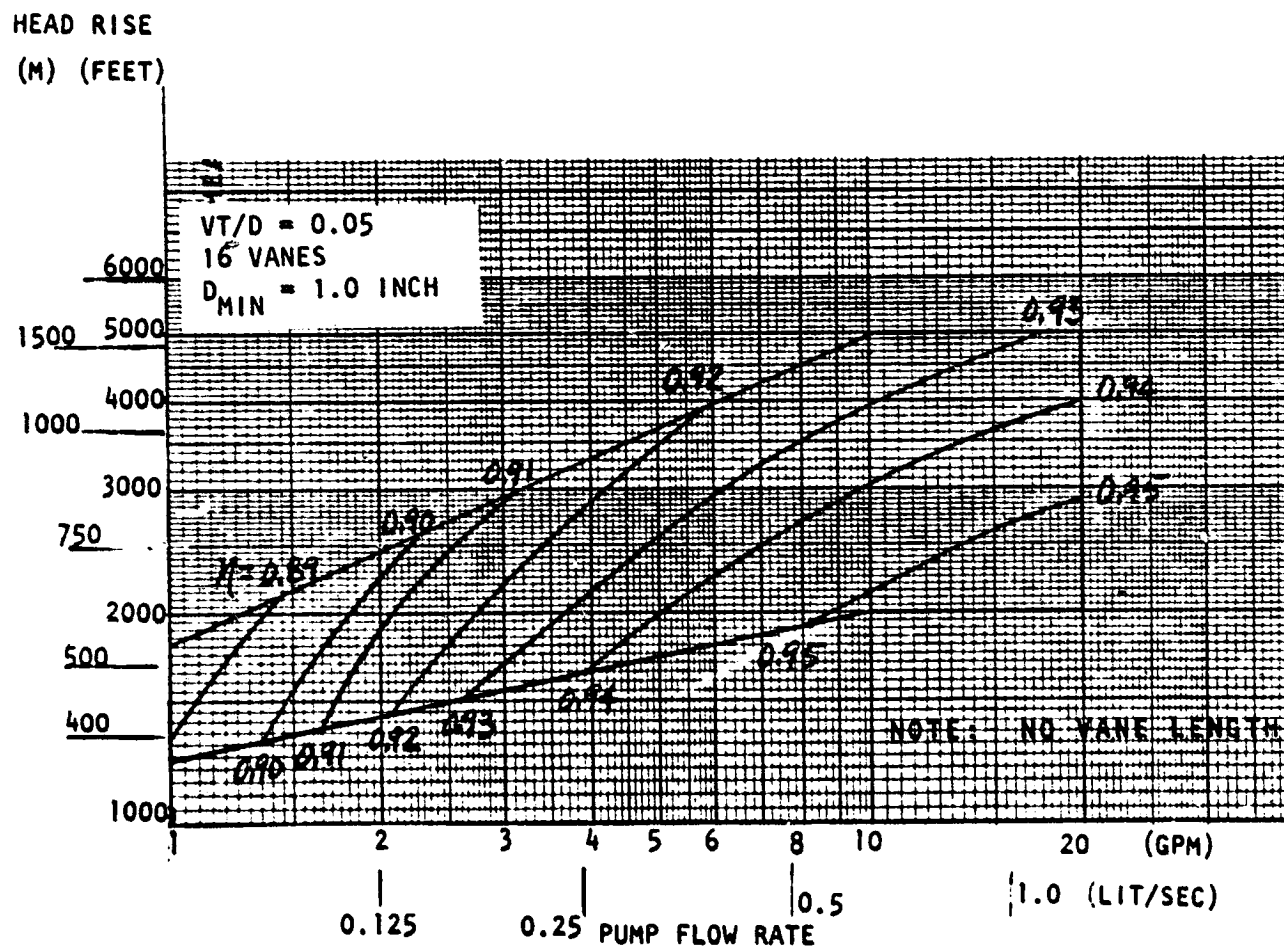


Figure A-127. Vane Methane Pump - C/D = 0.00025, Efficiency,
NPSH = 6 Feet

HEAD RISE
(M) (FEET)

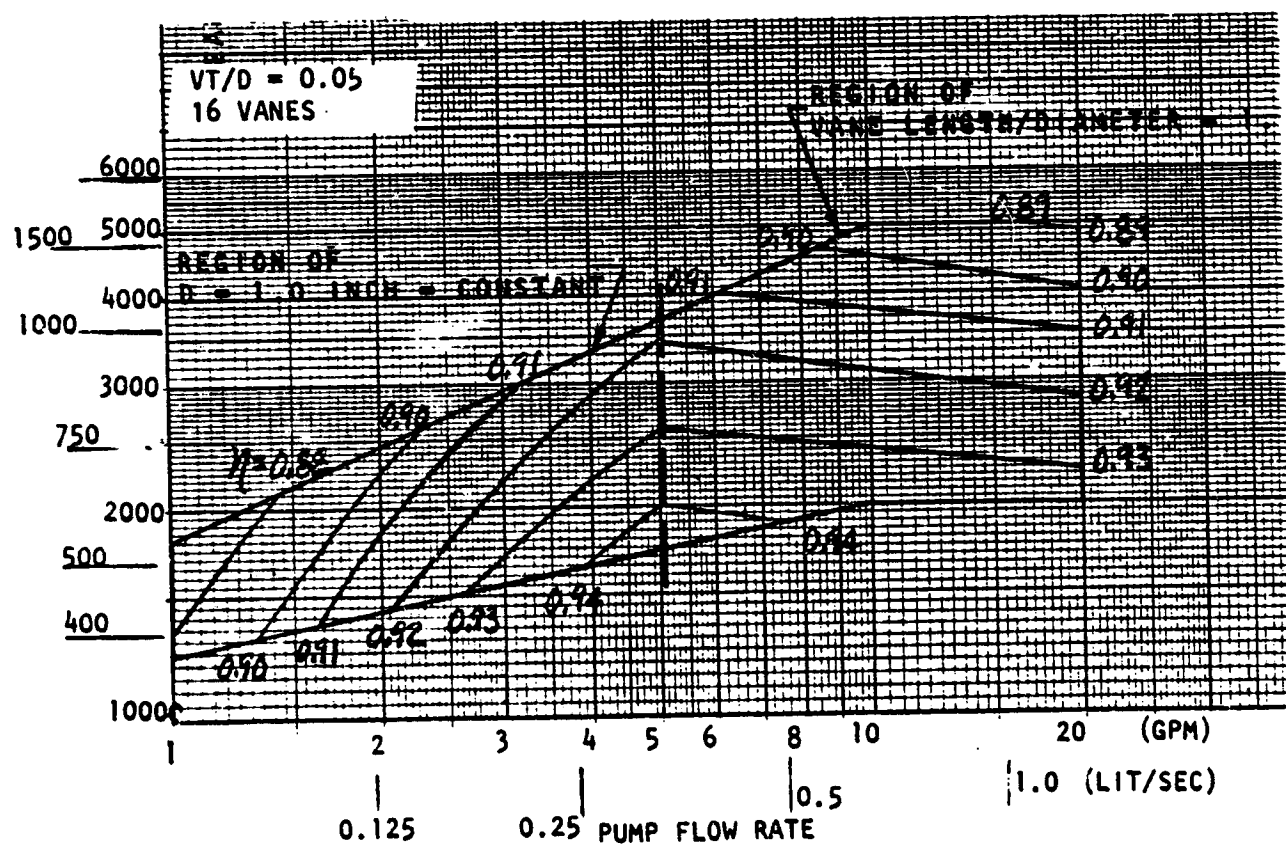


Figure A-128. Vane Methane Pump - $C/D = 0.00025$, Efficiency
(Vane $L/D \leq 1.5$), NPSH = 6 Feet

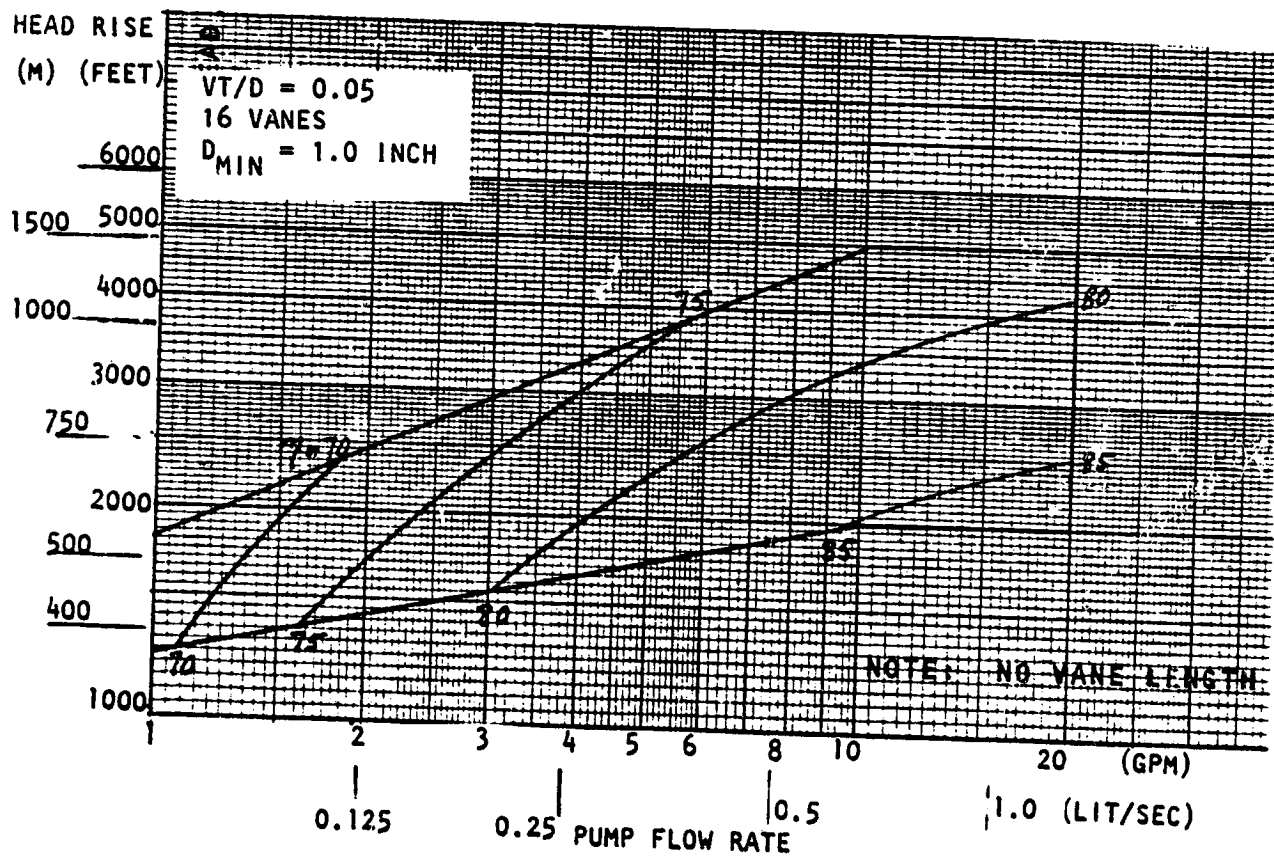


Figure A-129. Vane Methane Pump - C/D = 0.00050, Efficiency, NPSH = 6 Feet

HEAD RISE
(M) (FEET)

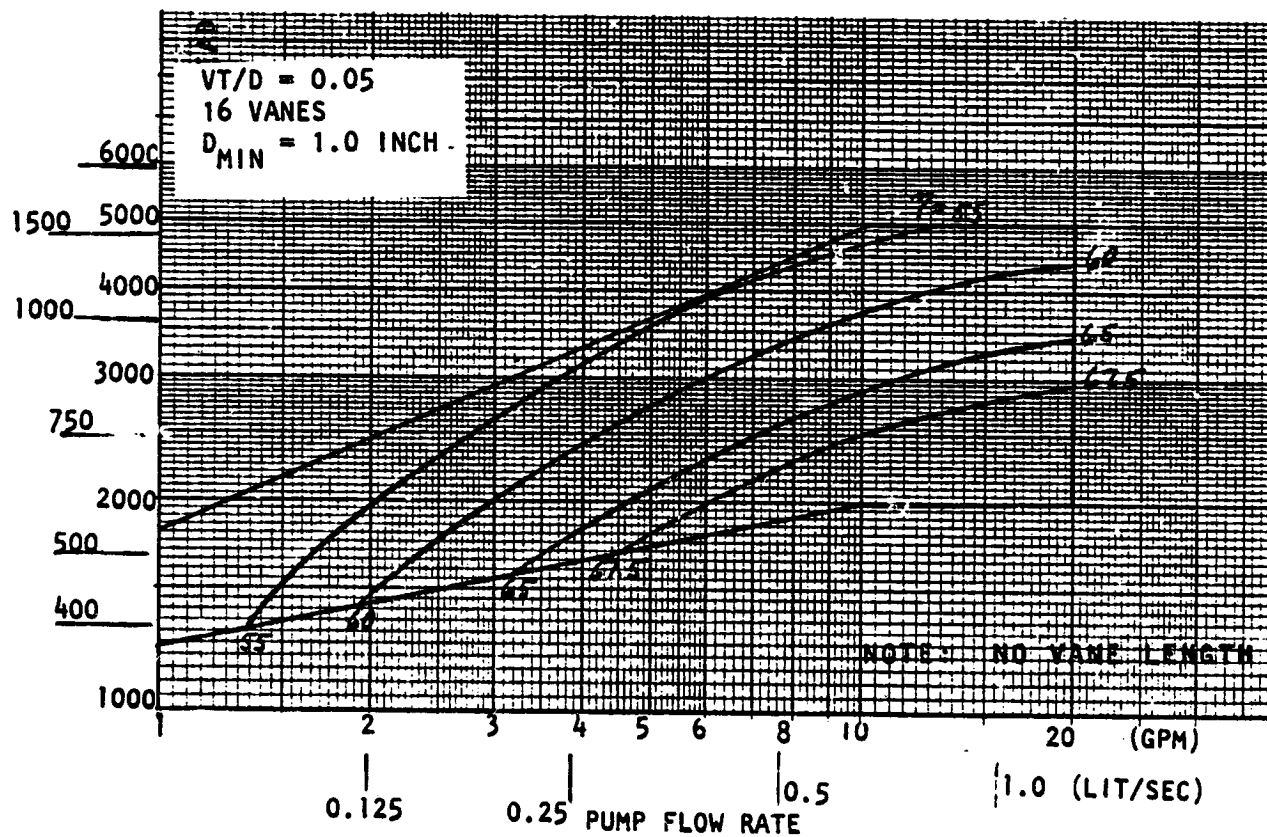


Figure A-130. Vane Methane Pump - C/D = 0.00075, Efficiency,
NPSH = 6 Feet

ORIGINAL PAGE IS
OF POOR QUALITY

HEAD RISE
(M) (FEET)

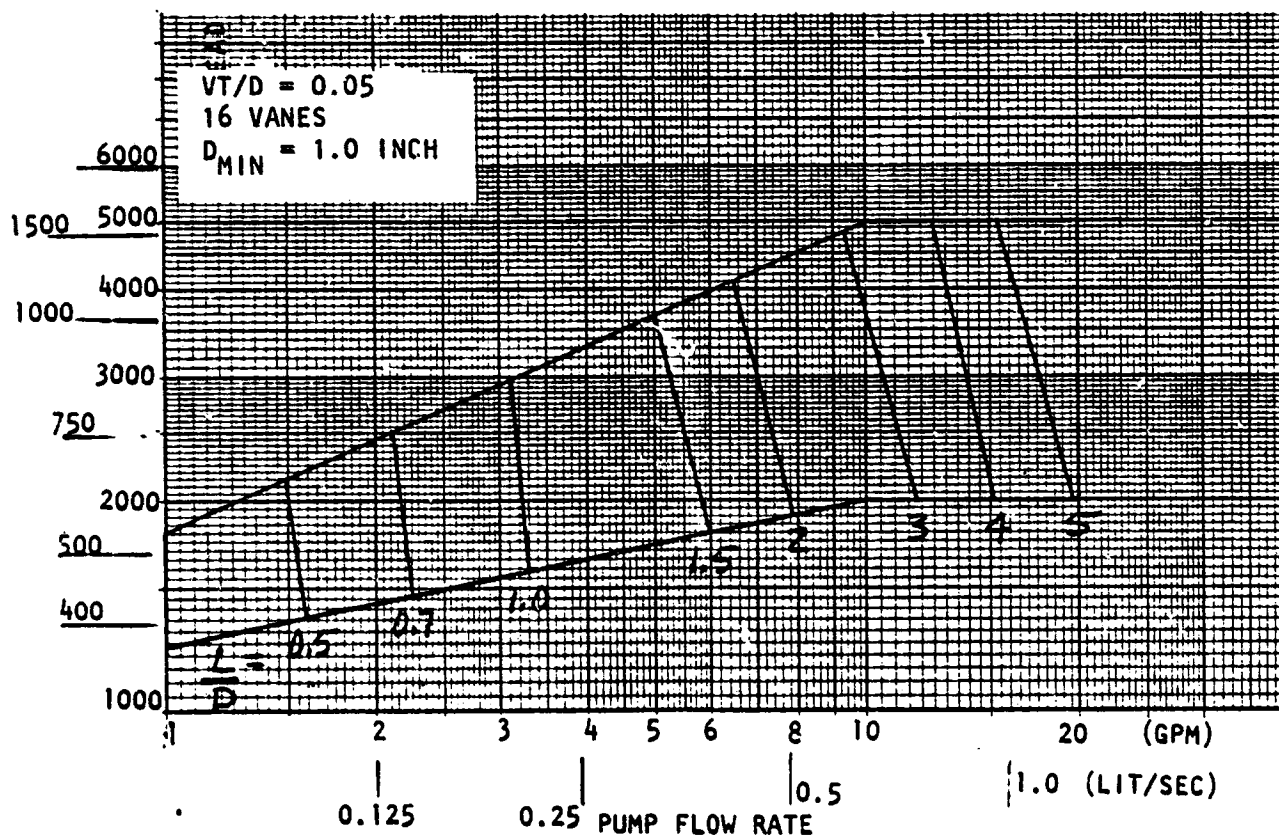


Figure A-131. Vane Methane Pump - C/D = 0.00025, Diameter,
NPSH = 6 Feet

HEAD RISE
(M) (FEET)

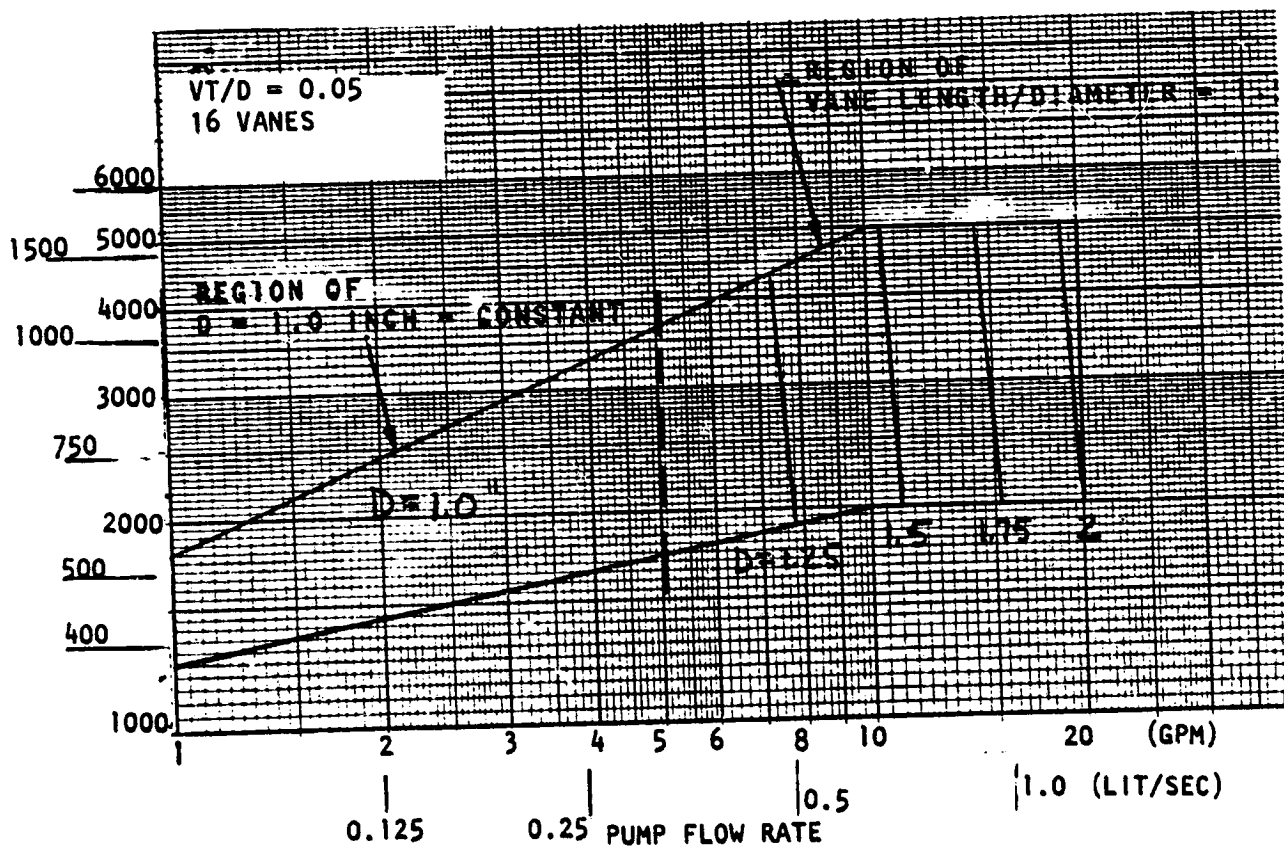


Figure A-132. Vane Methane Pump - C/D = 0.00025, Diameter
(Vane L/D ≤ 1.5), NPSH = 6 Feet

ORIGINAL PAGE IS
OF POOR QUALITY

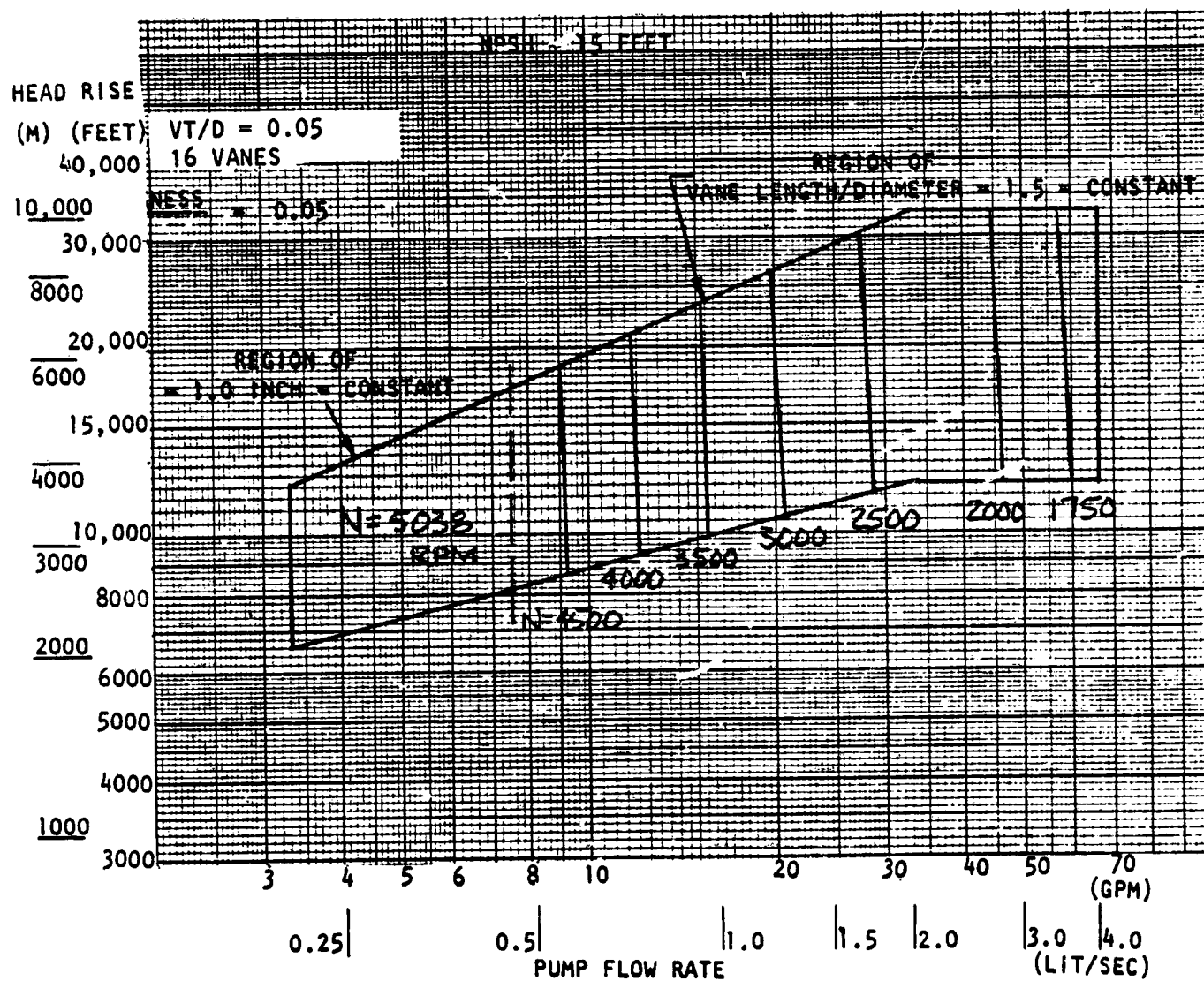


Figure A-133. Vane Hydrogen Pump - C/D = 0.00025, Speed

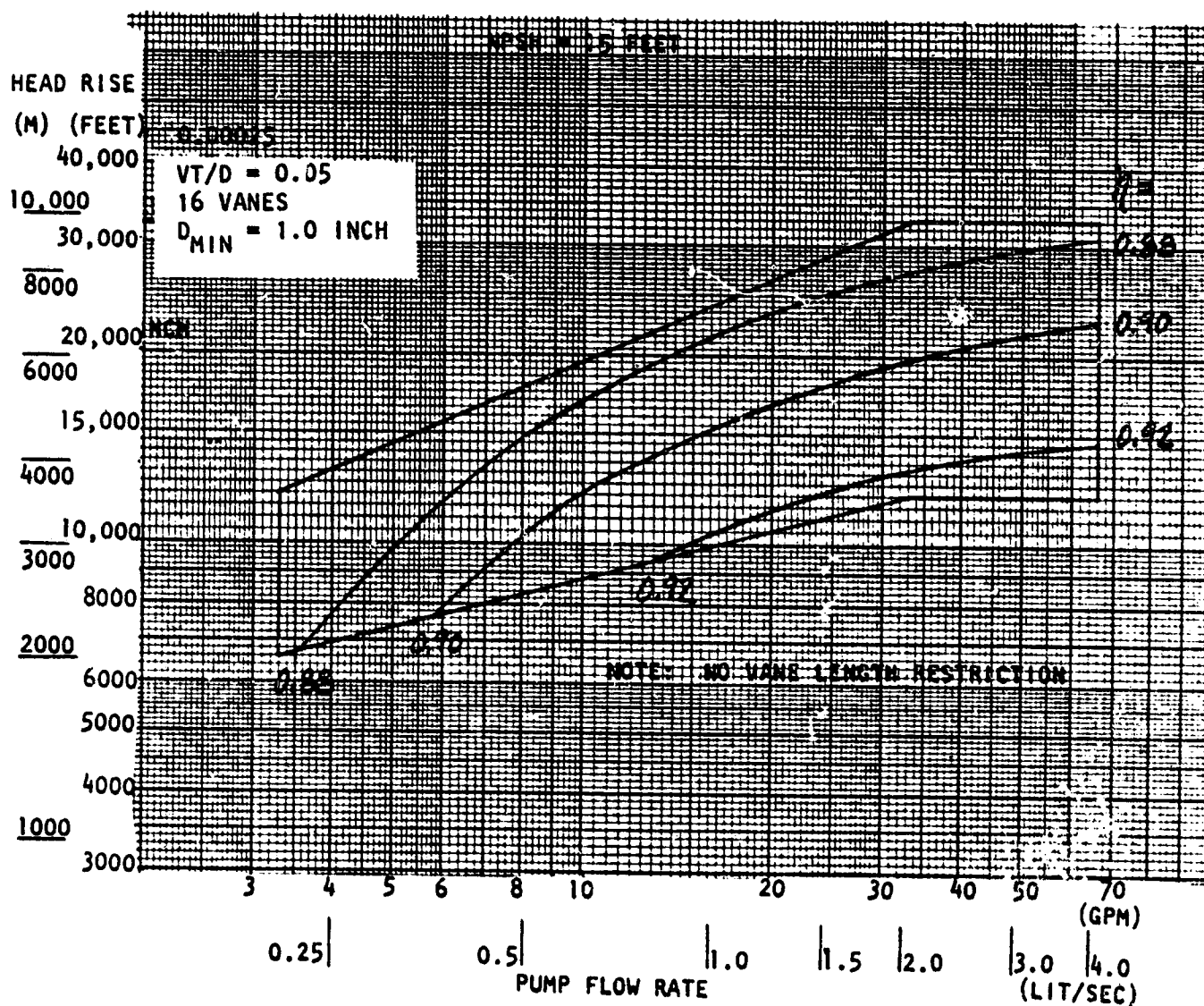


Figure A-134. Vane Hydrogen Pump - C/D = 0.00025, Efficiency

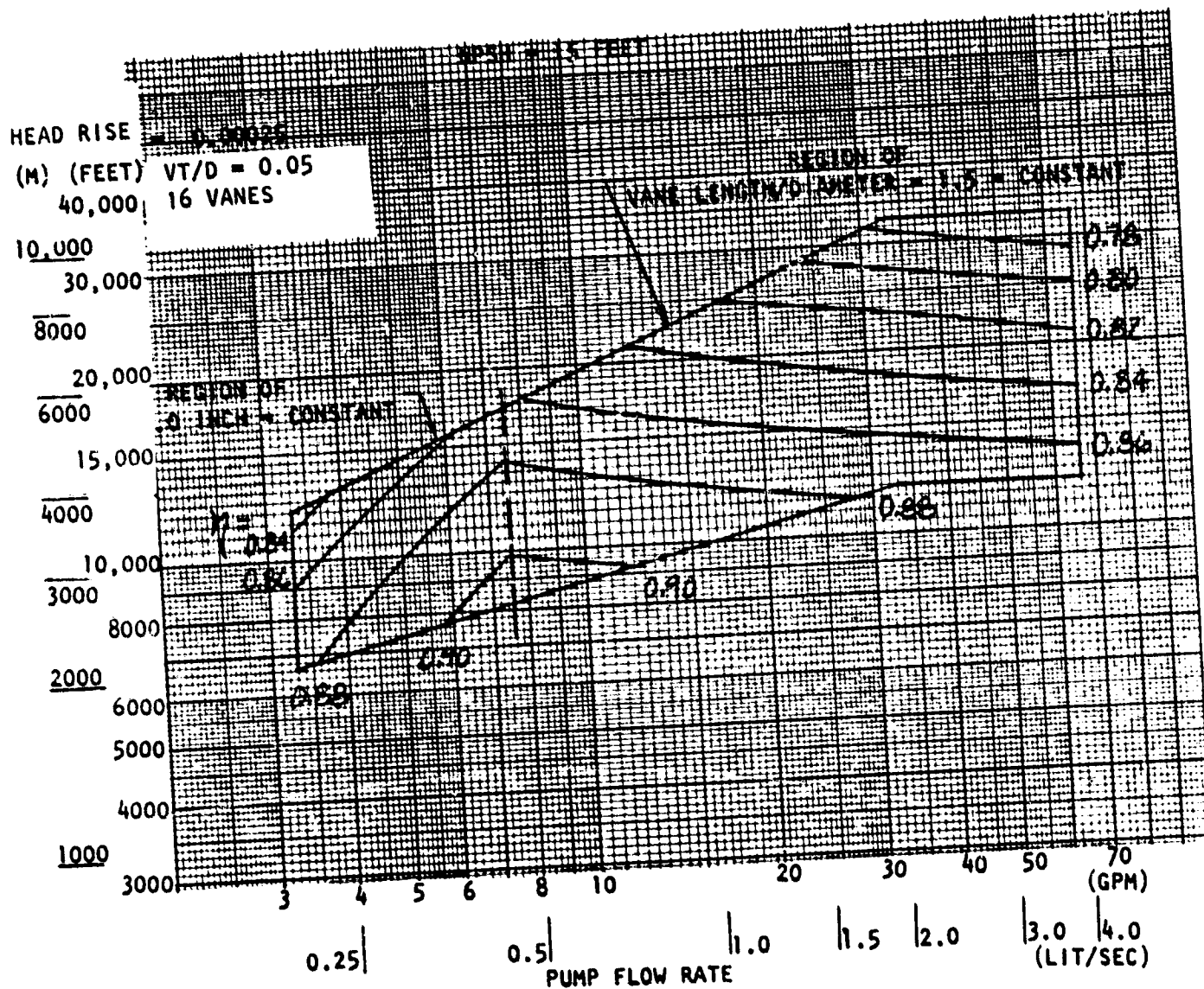


Figure A-135. Vane Hydrogen Pump - $C/D = 0.00025$, Efficiency
(Vane $L/D \leq 1.5$)

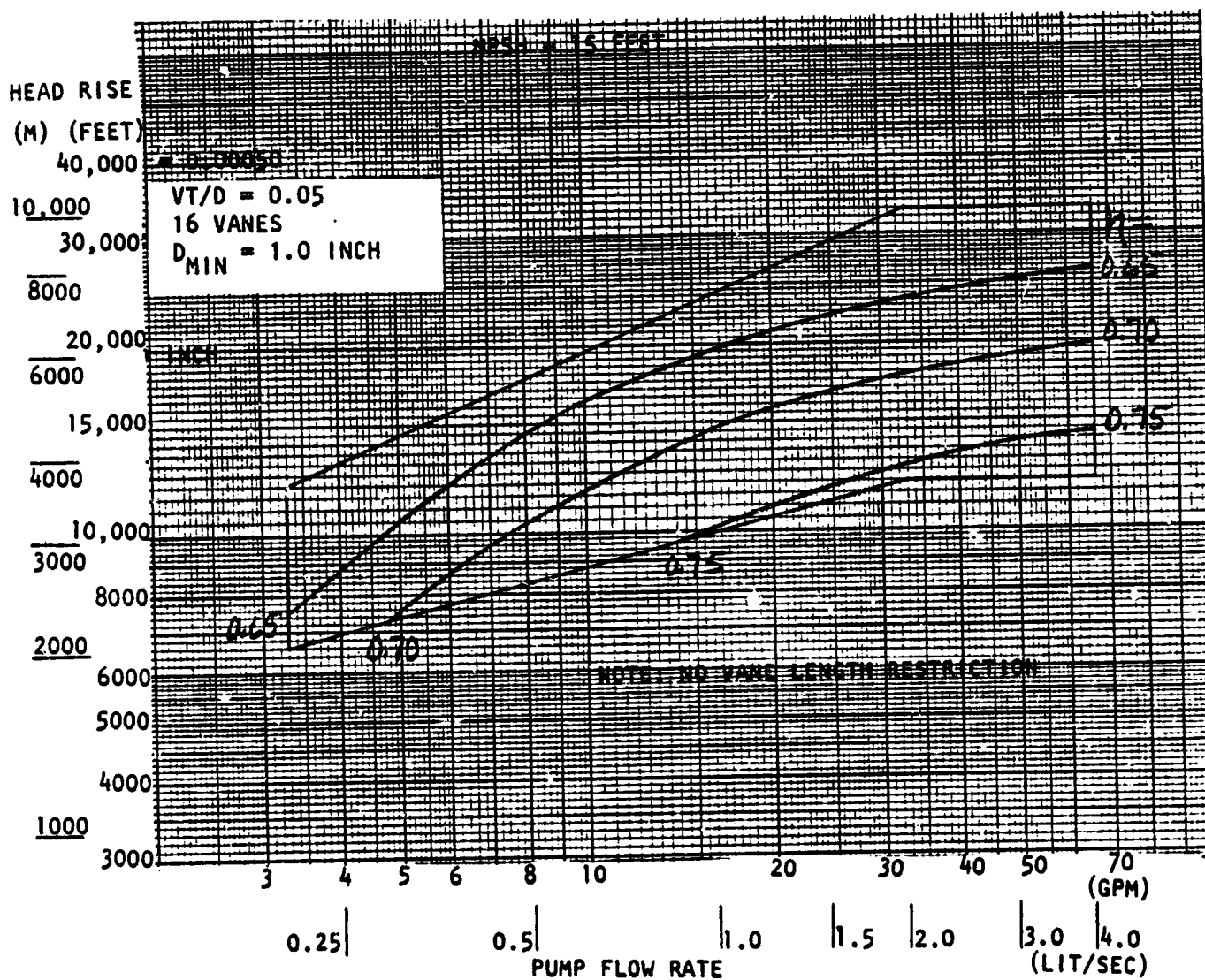


Figure A-136. Vane Hydrogen Pump - $C/D = 0.00050$, Efficiency

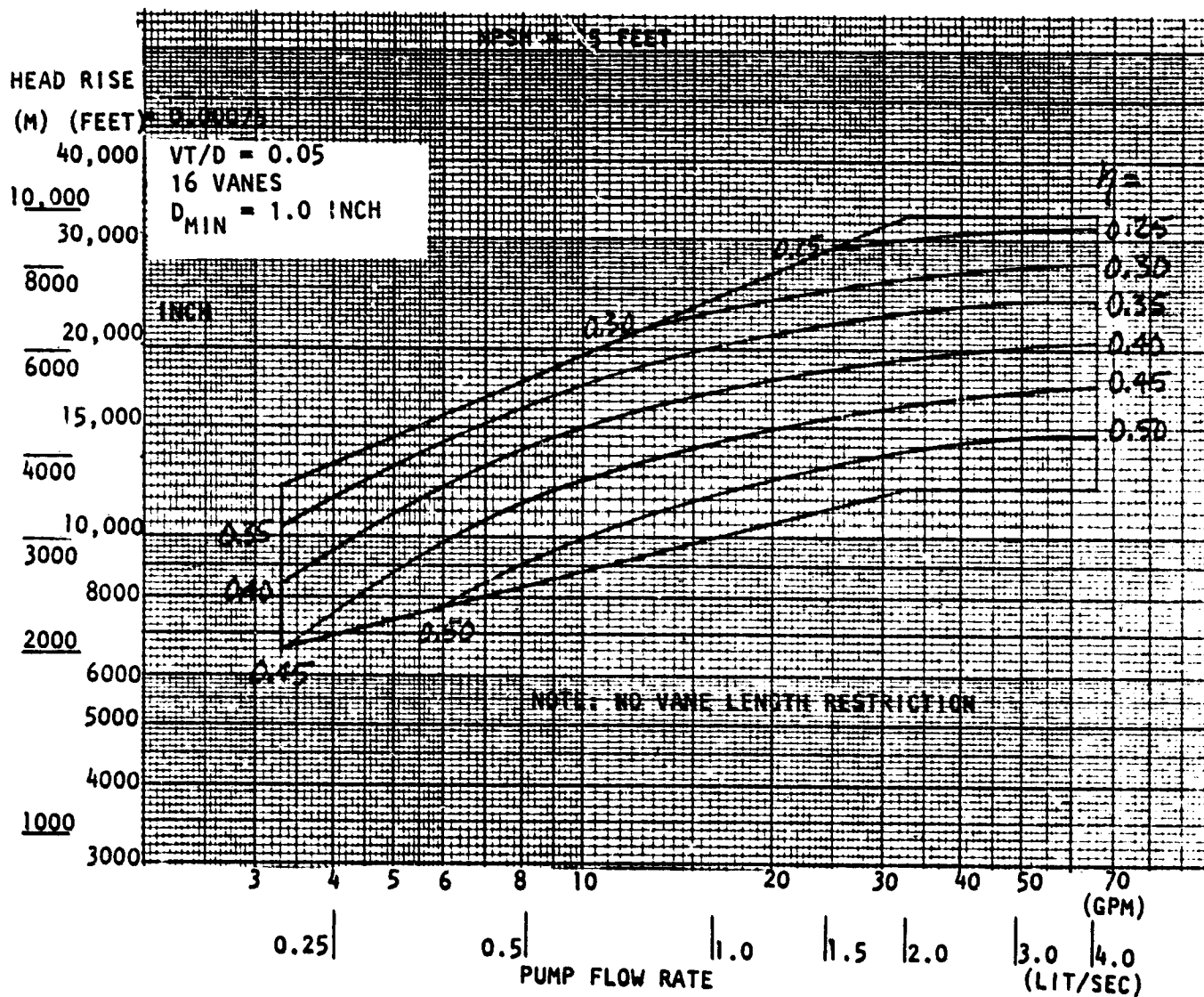


Figure A-137. Vane Hydrogen Pump - C/D = 0.00075, Efficiency

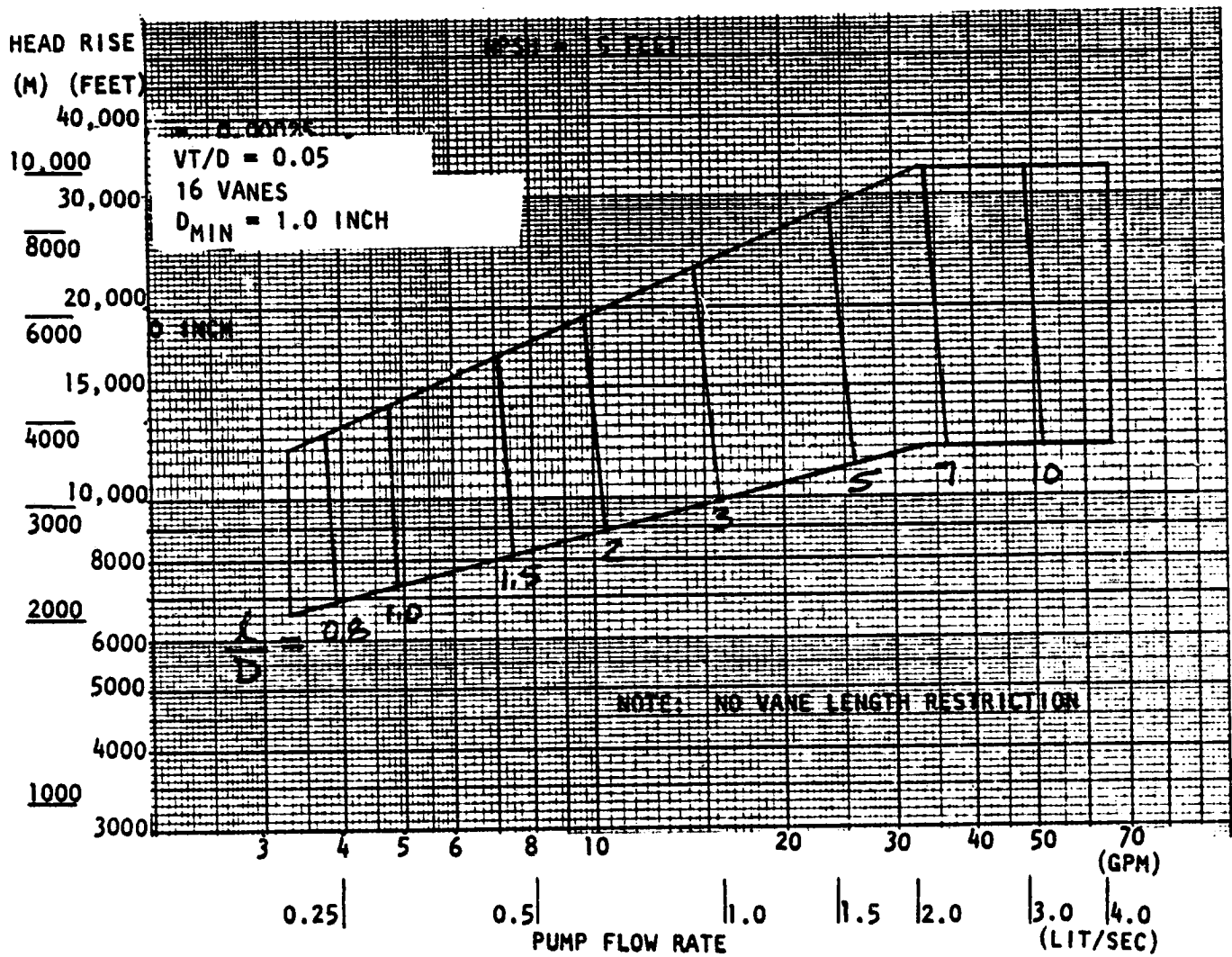


Figure A-138. Vane Hydrogen Pump - C/D = 0.00025, Diameter

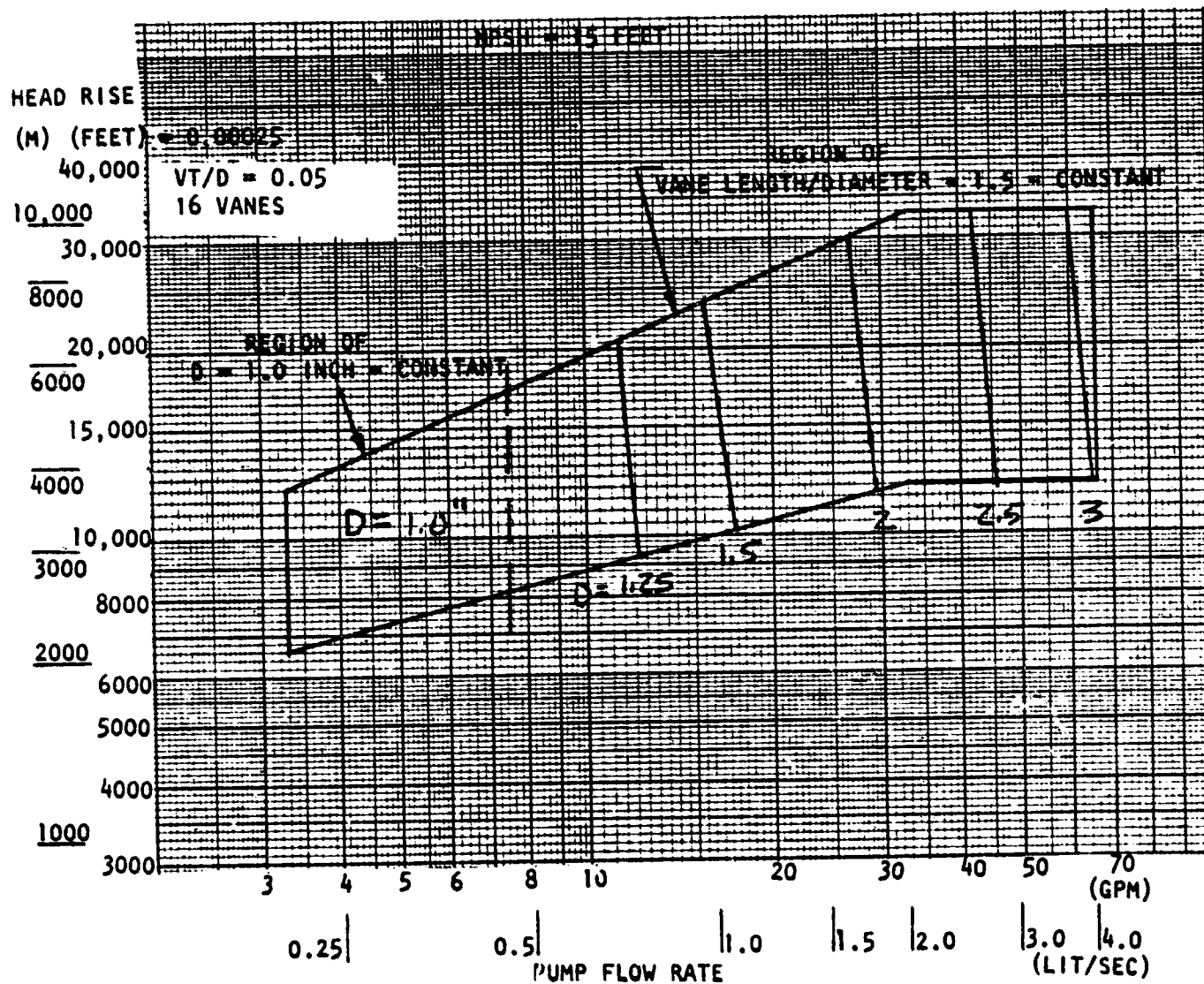


Figure A-139. Vane Hydrogen Pump - $C/D = 0.00025$, Diameter
(Vane $L/D \leq 1.5$)

HEAD RISE
(M) (FEET)

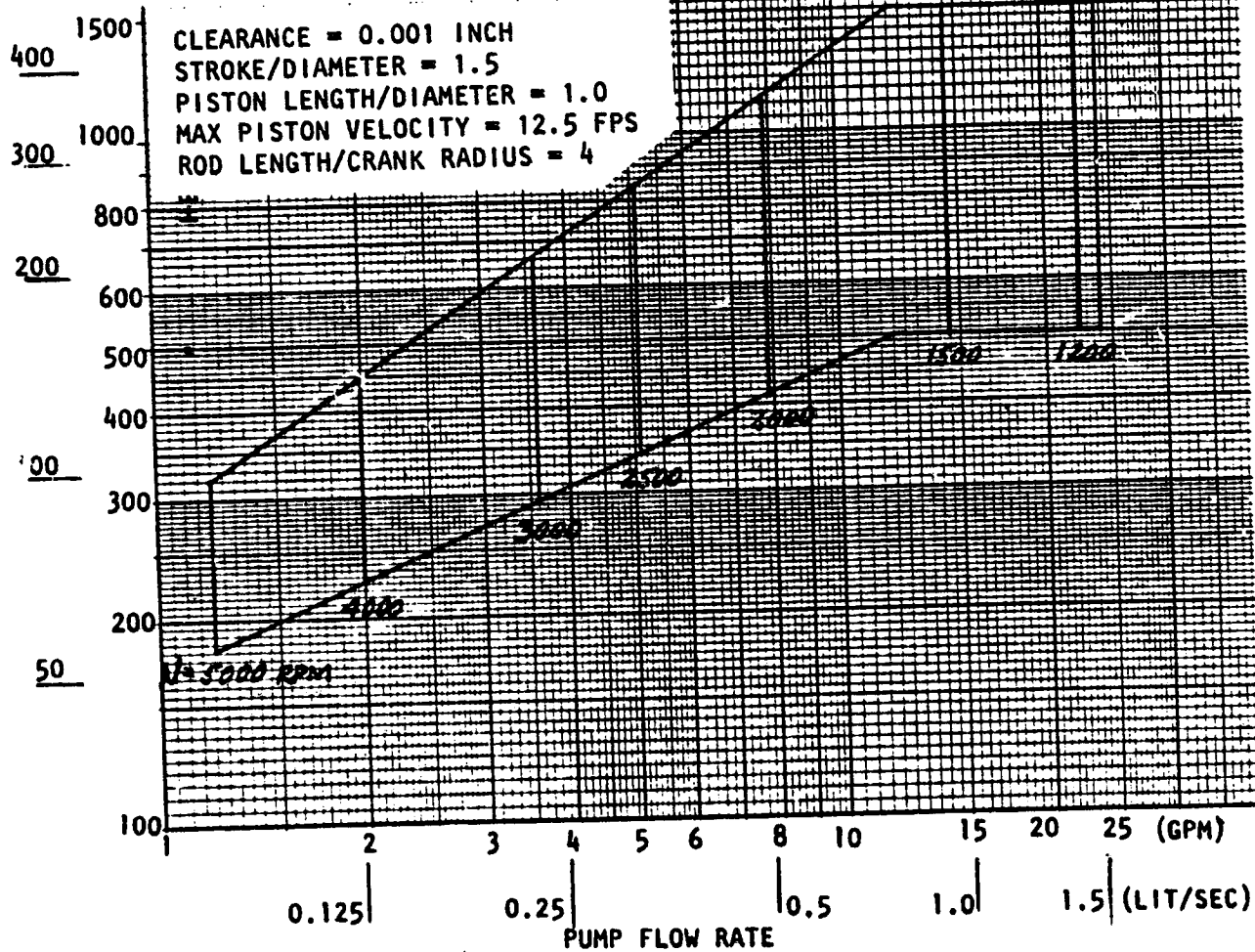


Figure A-140. Piston LOX Pump, Speed, NPSH = 2 Feet

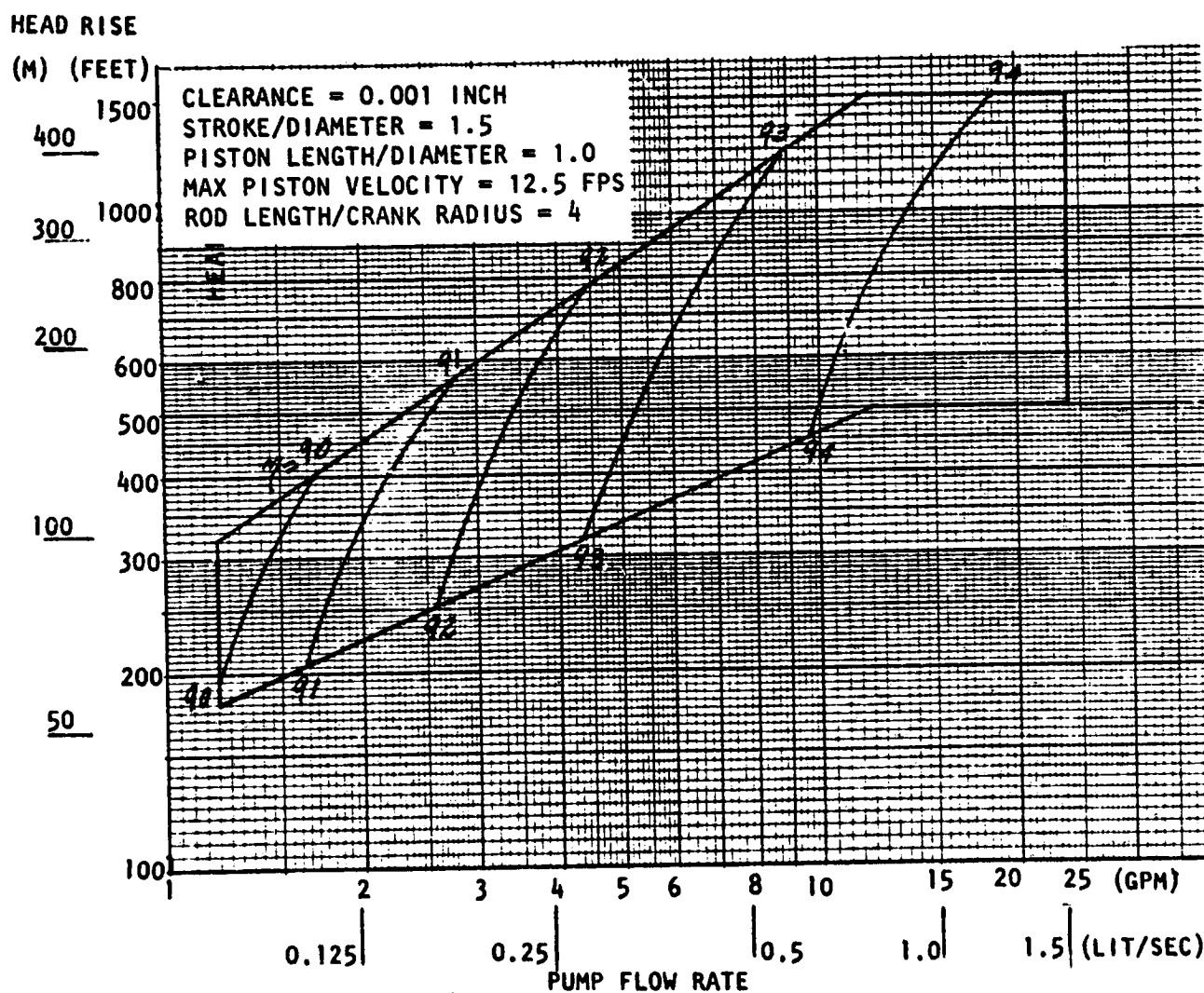


Figure A-141. Piston LOX Pump, Efficiency, NPSH = 2 Feet

ORIGINAL PAGE IS
OF POOR QUALITY

HEAD RISE

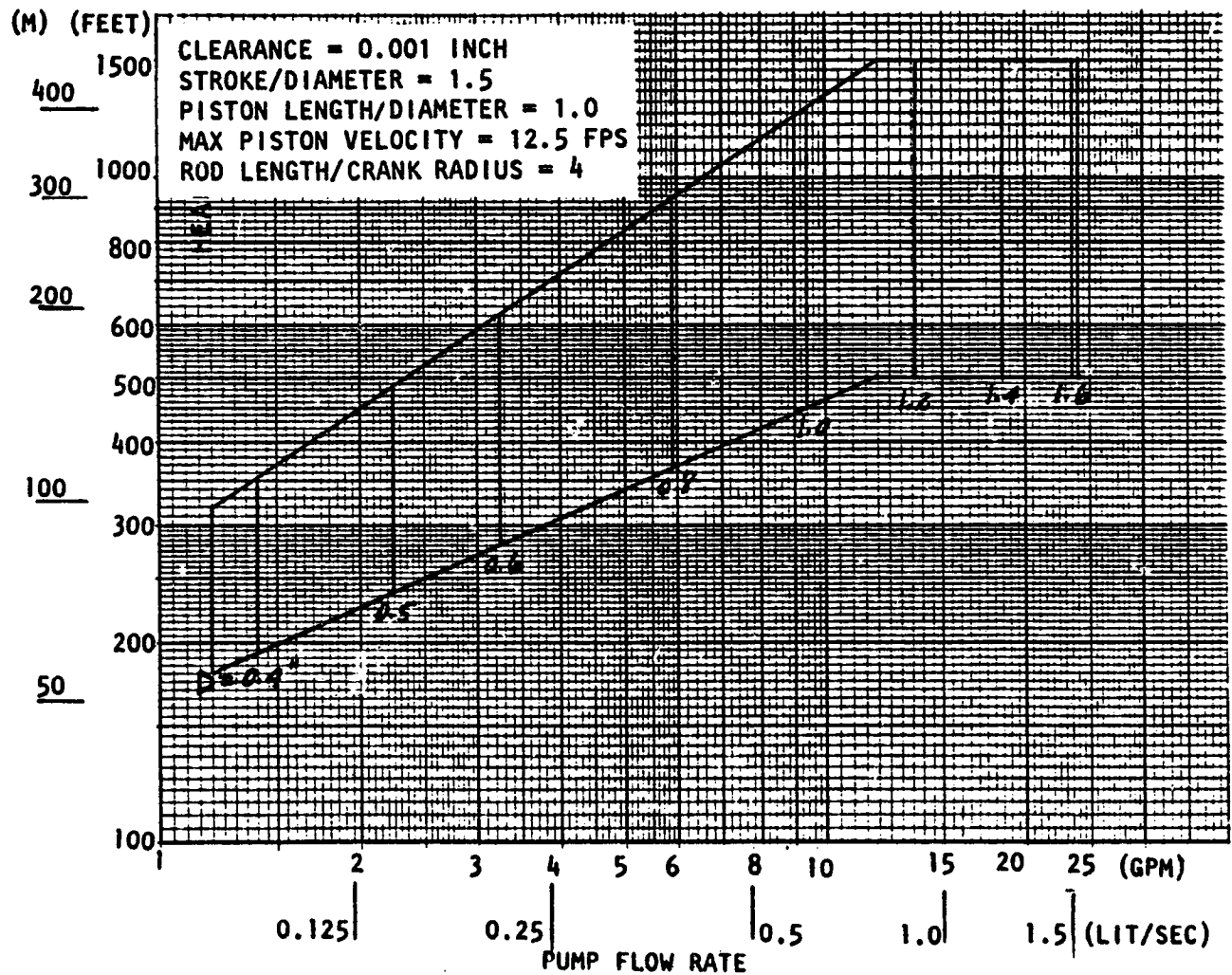


Figure A-142. Piston LOX Pump, Diameter, NPSH = 2 Feet

ORIGINAL PAGE IS
 OF POOR QUALITY

HEAD RISE

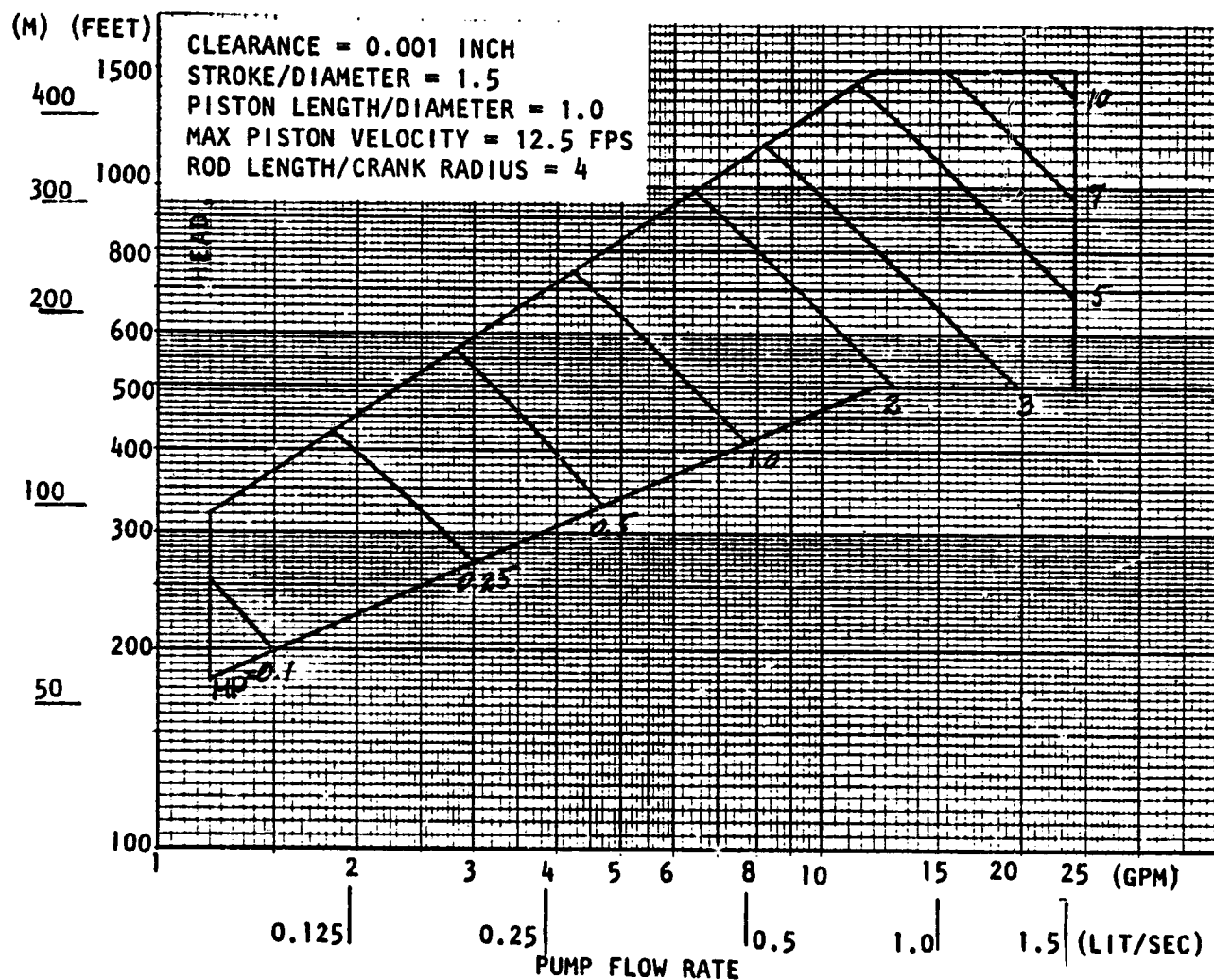


Figure A-143. Piston LOX Pump, Power, NPSH = 2 Feet

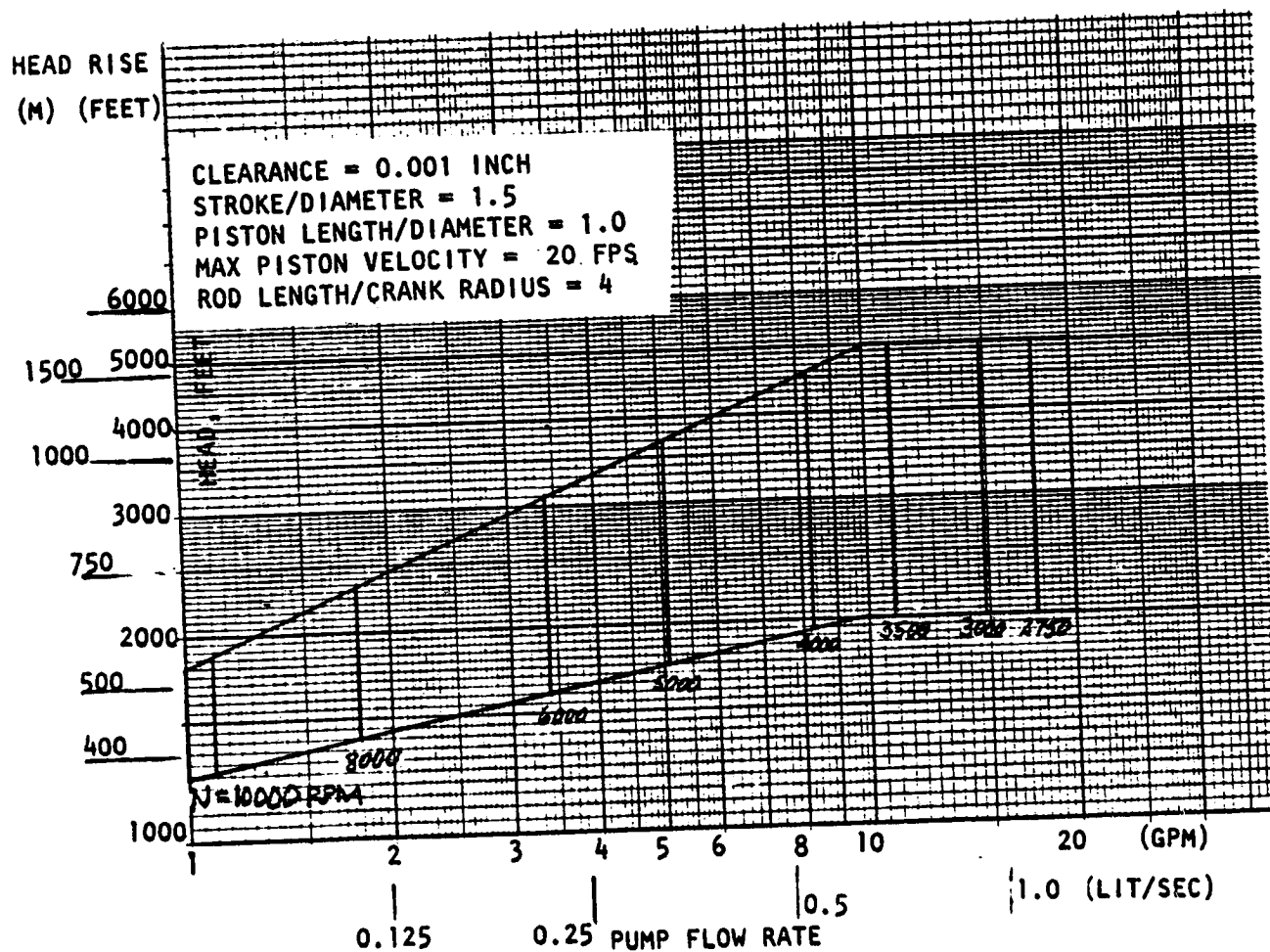


Figure A-144. Piston Methane Pump, Speed, NPSH = 6 Feet

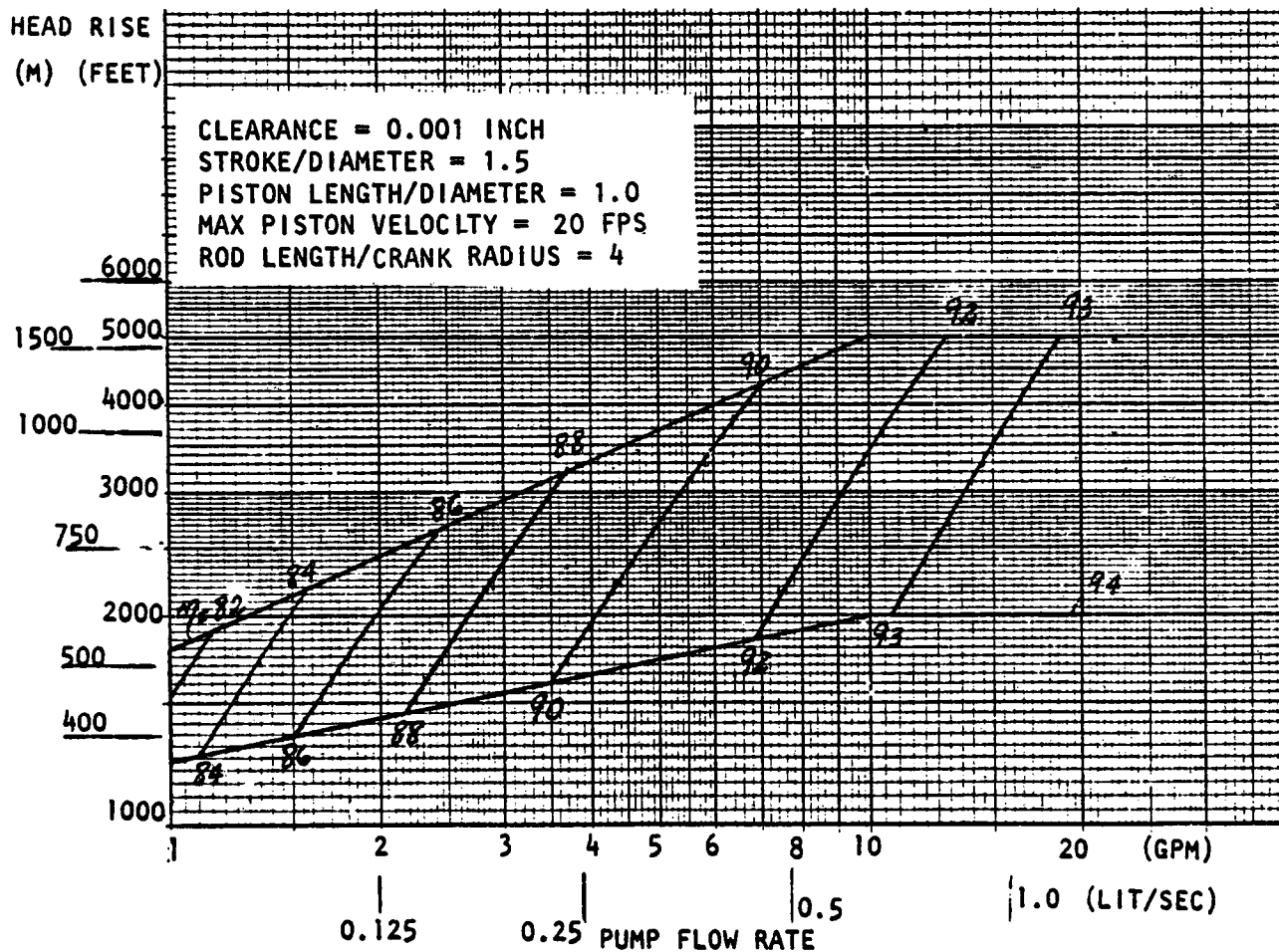


Figure A-145. Piston Methane Pump, Efficiency, NPSH = 6 Feet

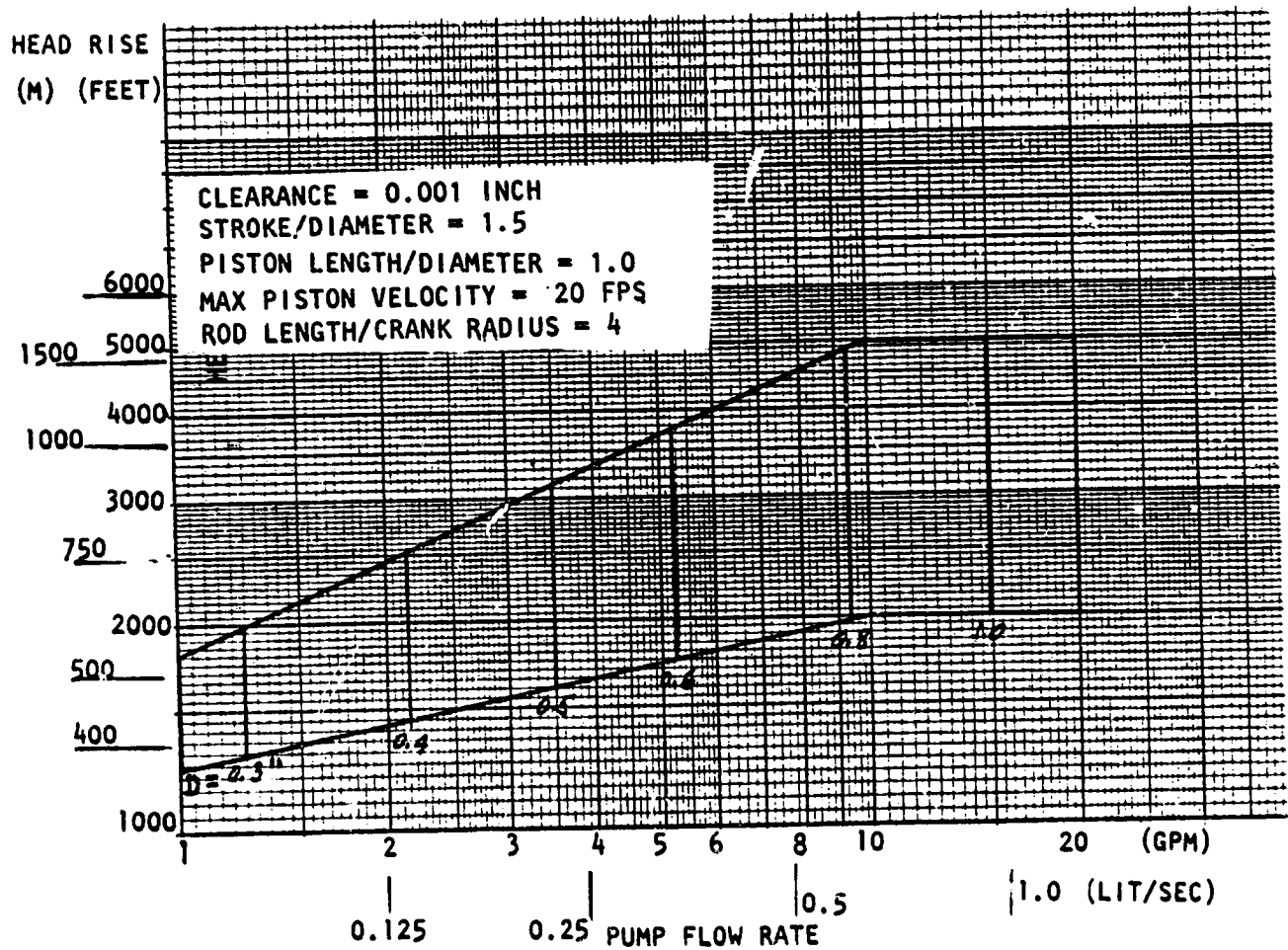


Figure A-146. Piston Methane Pump, Diameter, NPSH = 6 Feet

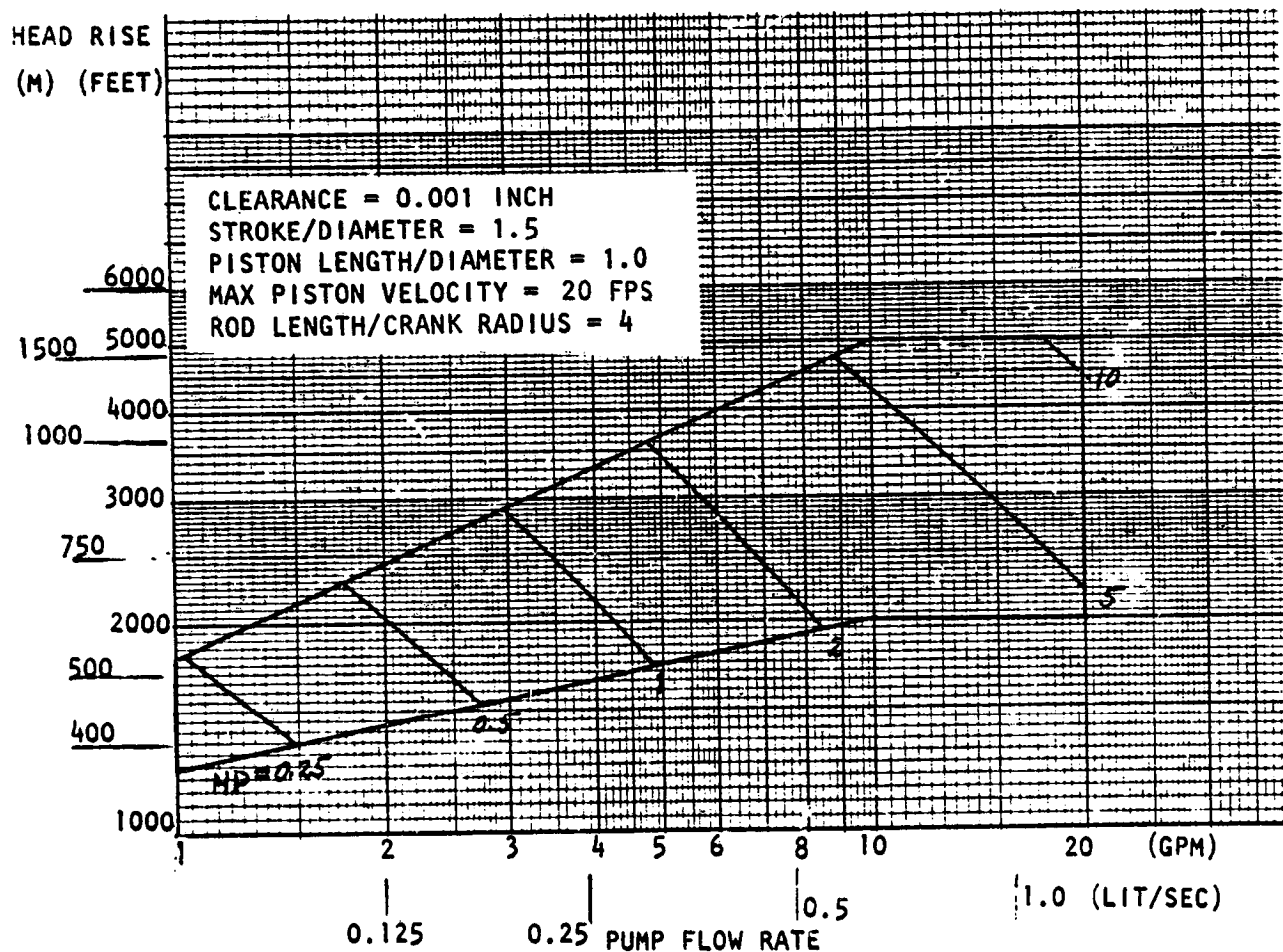


Figure A-147. Piston Methane Pump, Power, NPSH = 6 Feet

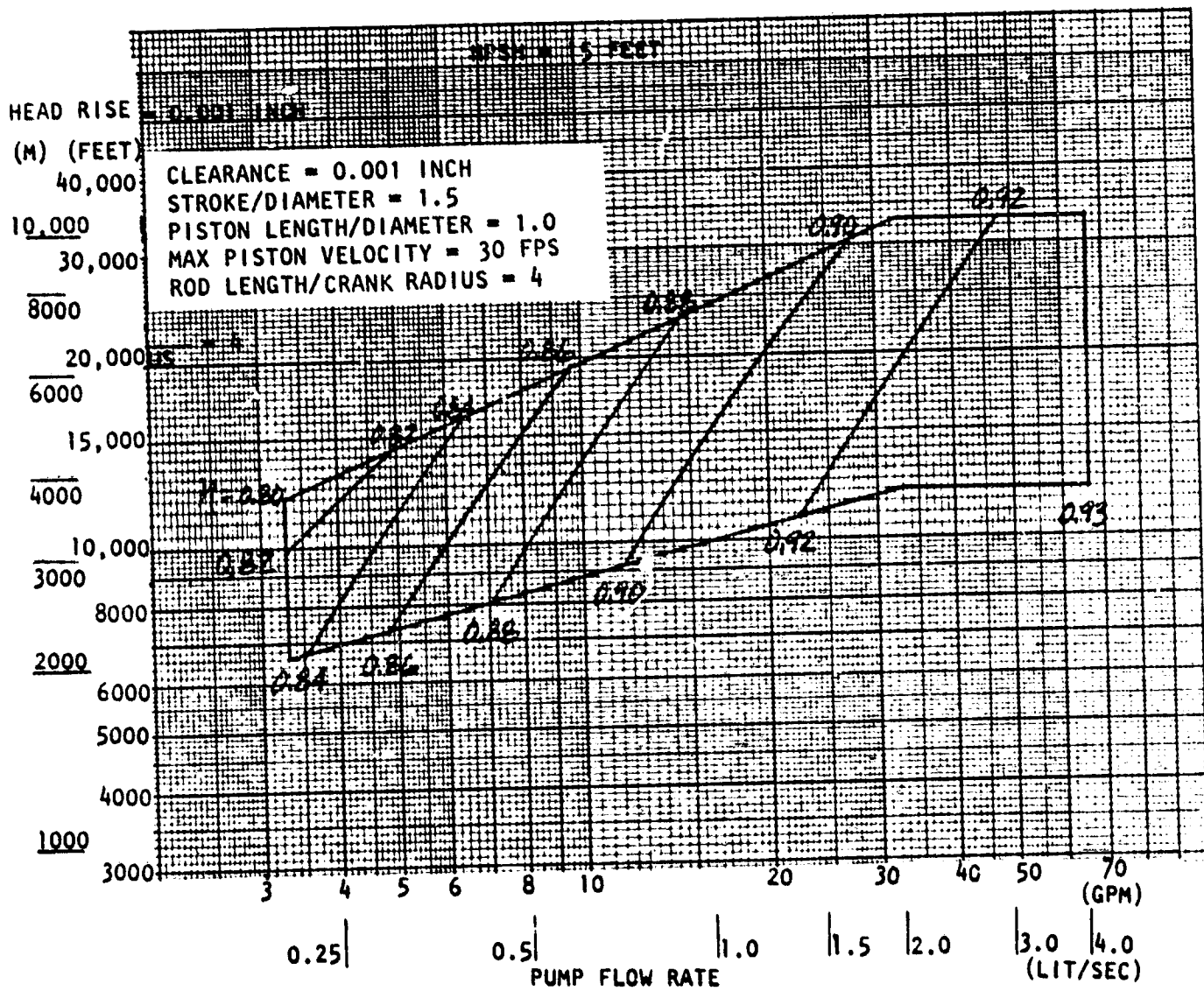


Figure A-149. Piston Hydrogen Pump, Efficiency

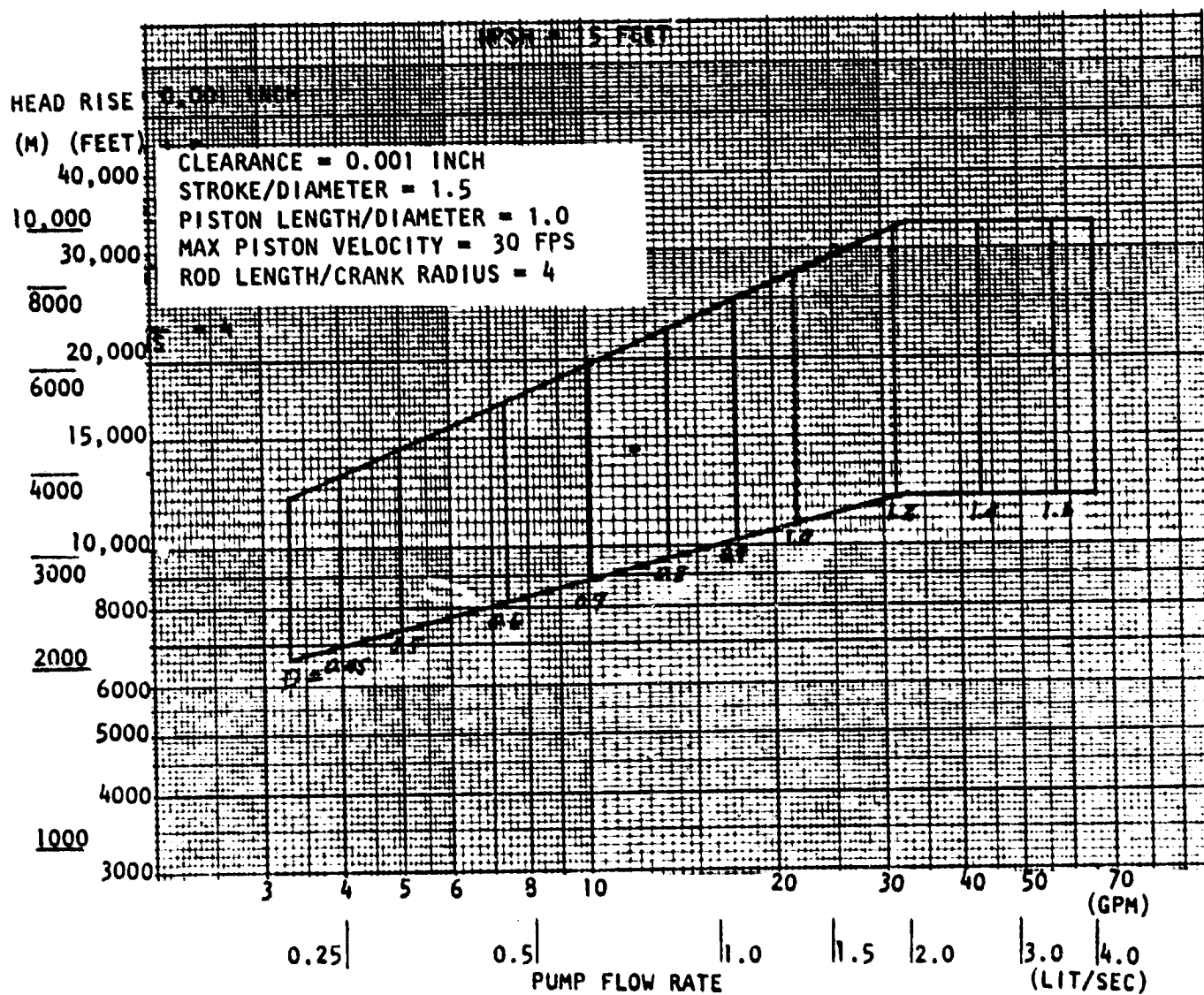


Figure A-150. Piston Hydrogen Pump, Diameter

ORIGINAL PAGE IS
OF POOR QUALITY

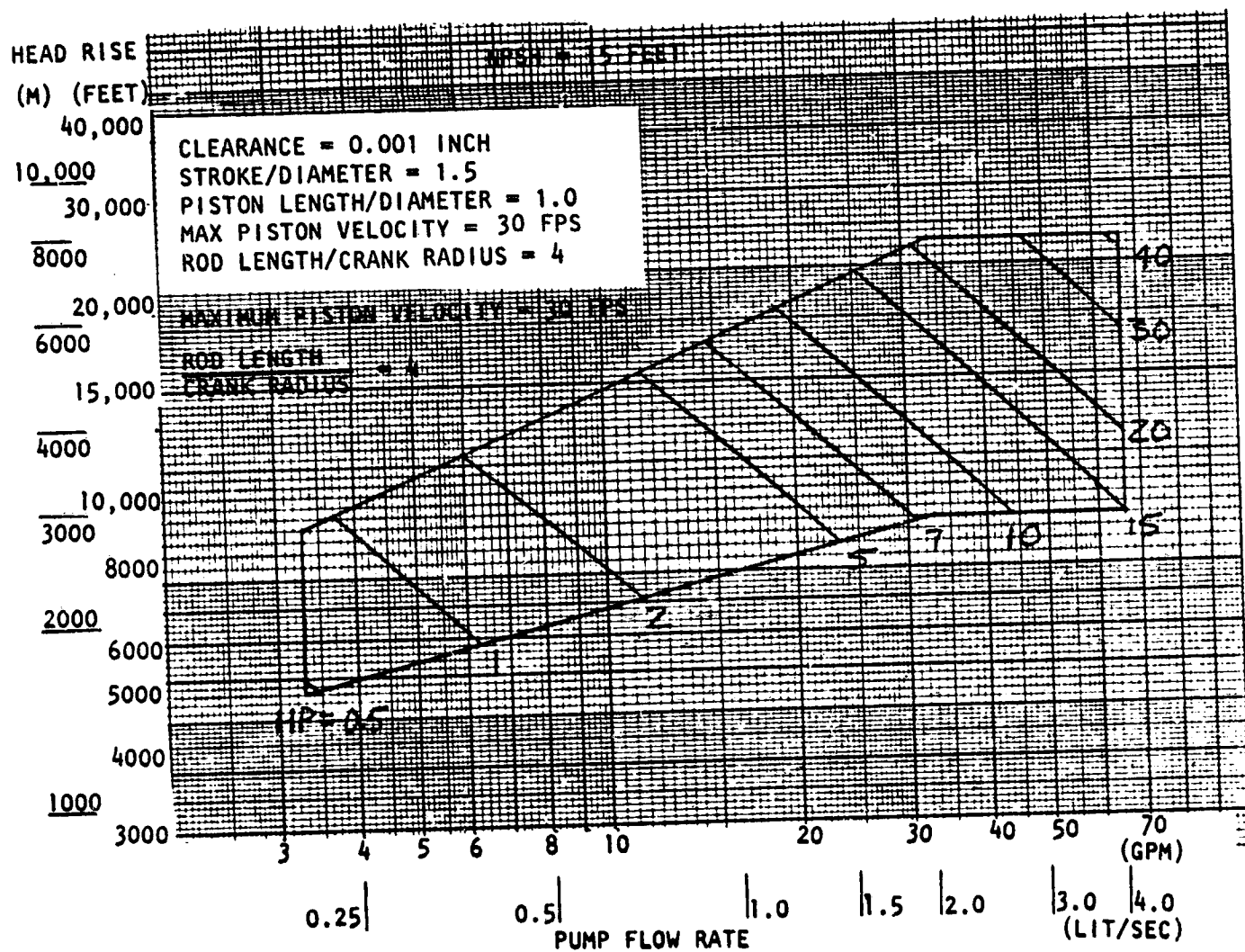


Figure A-151. Piston Hydrogen Pump, Power

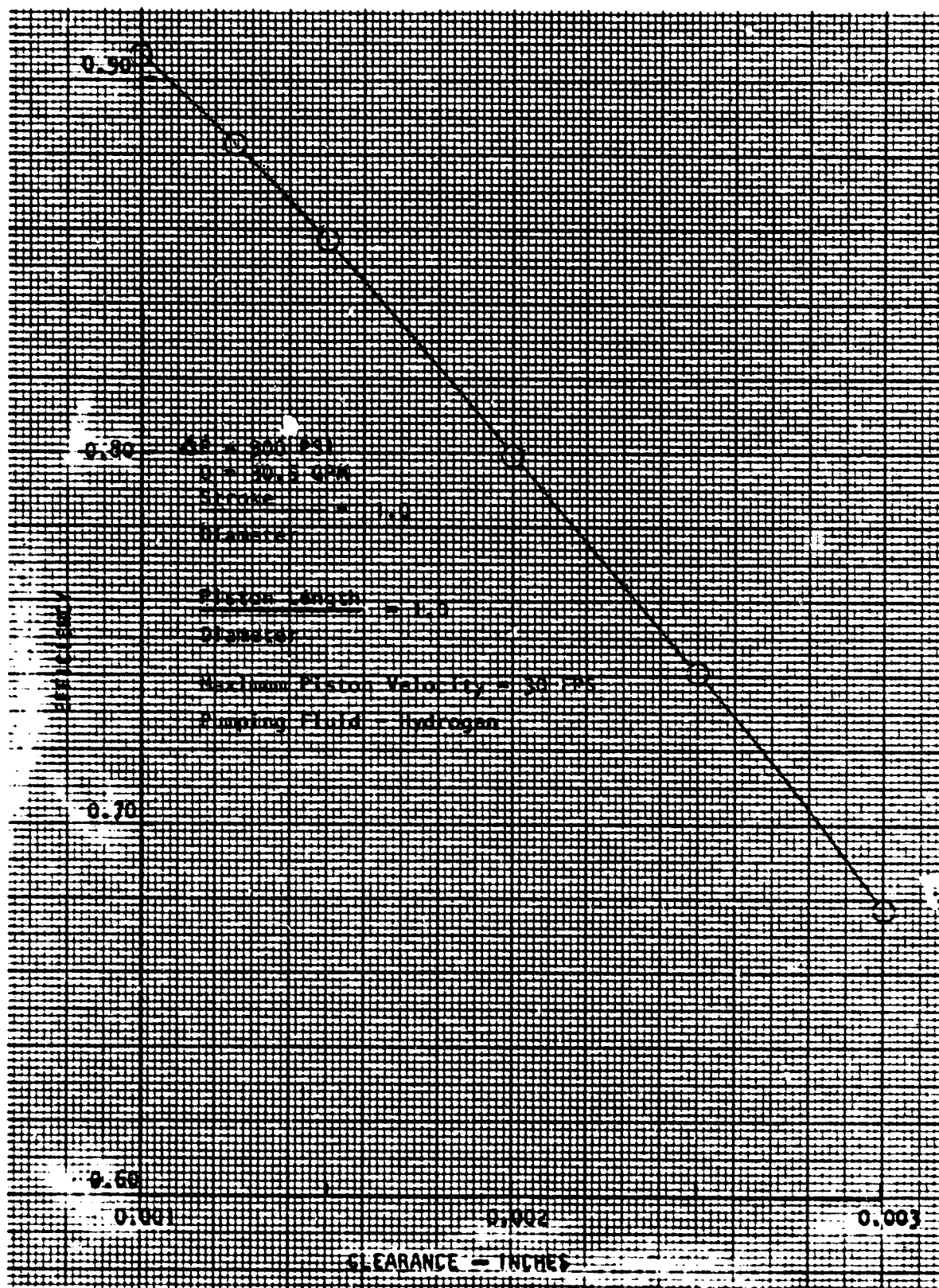


Figure A-152. Piston Hydrogen Pump, Effect of Clearance on Efficiency

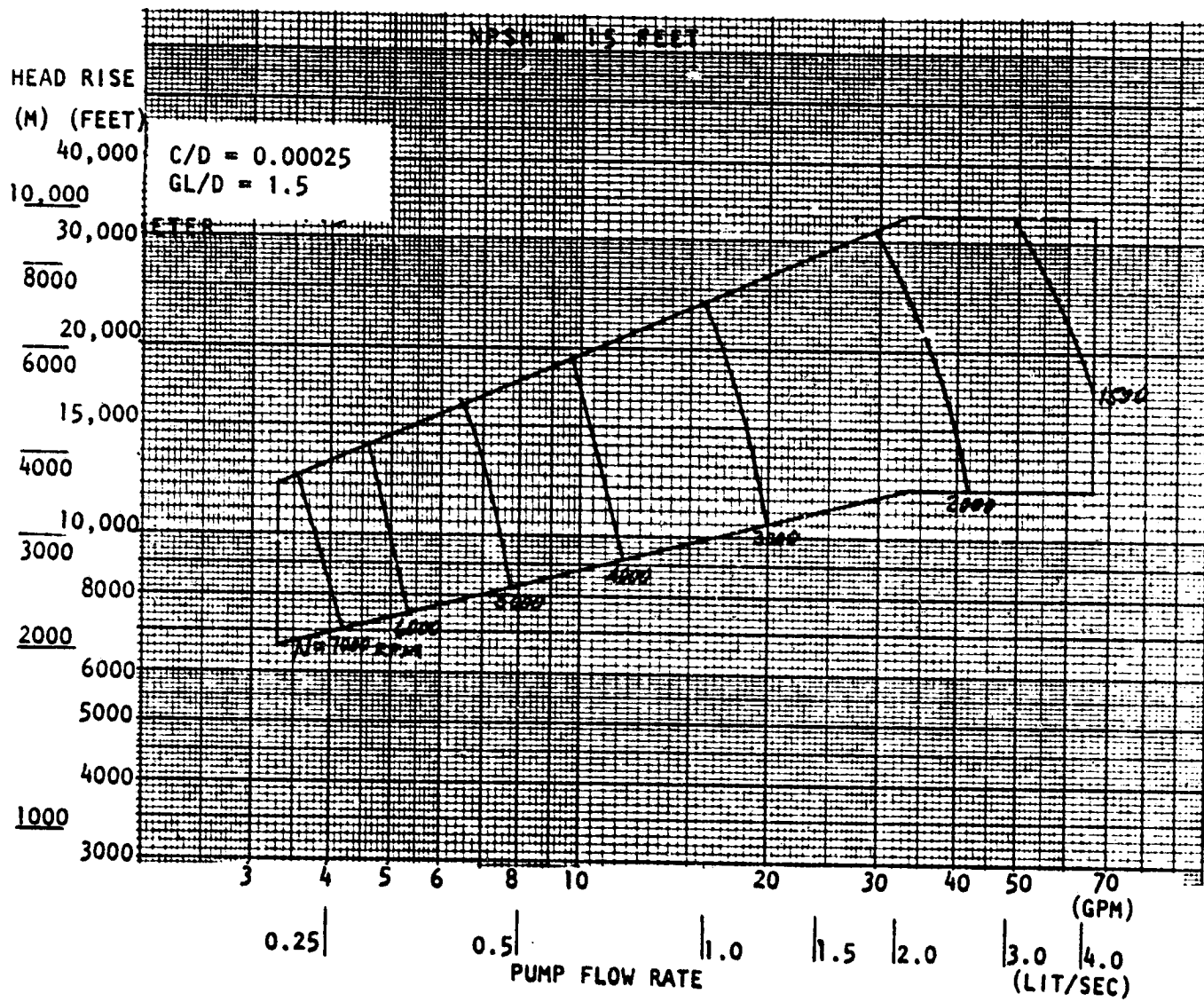


Figure A-153. Gear Hydrogen Pump, Speed

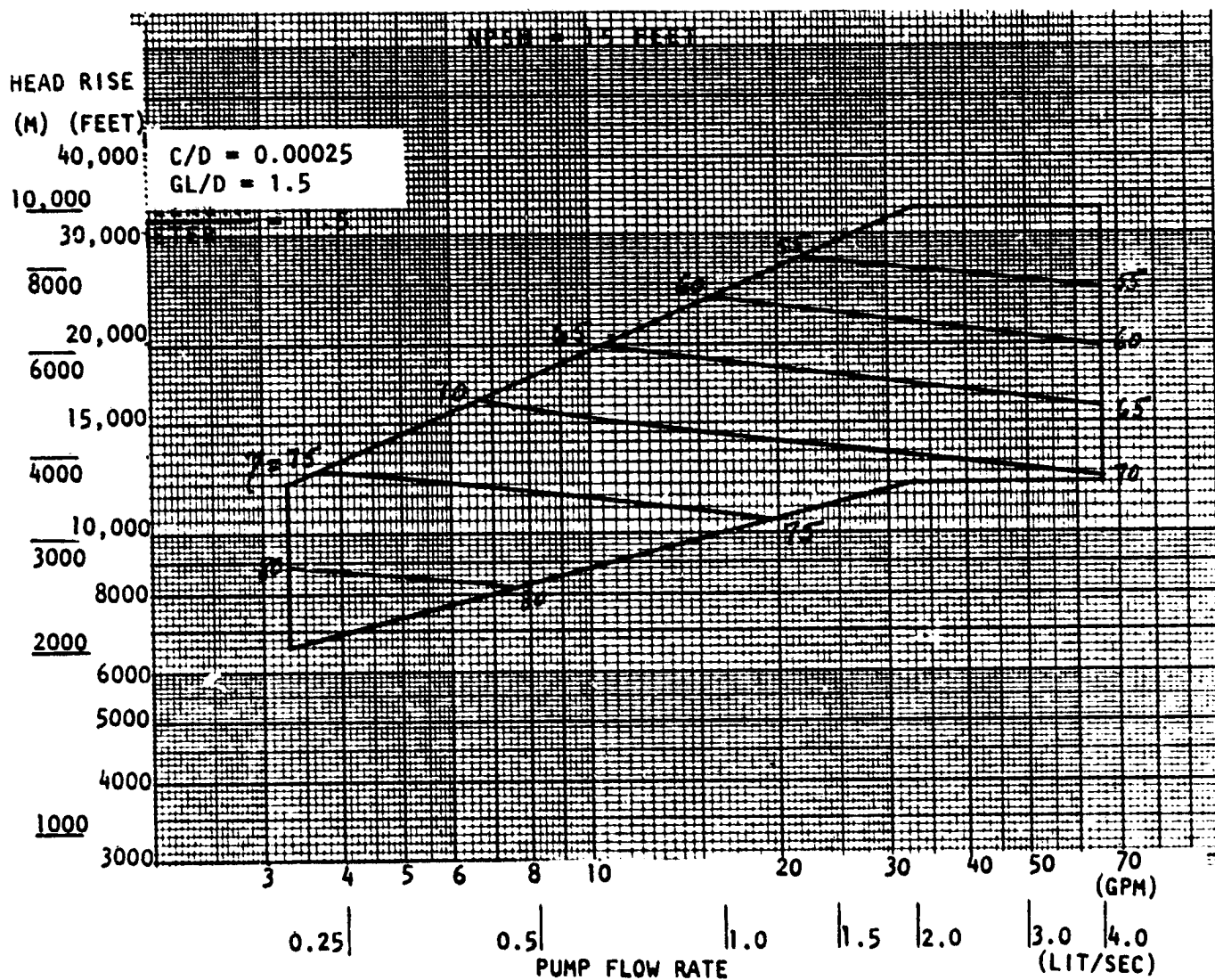


Figure A-154. Gear Hydrogen Pump, Efficiency

ORIGINAL PAGE IS
OF POOR QUALITY

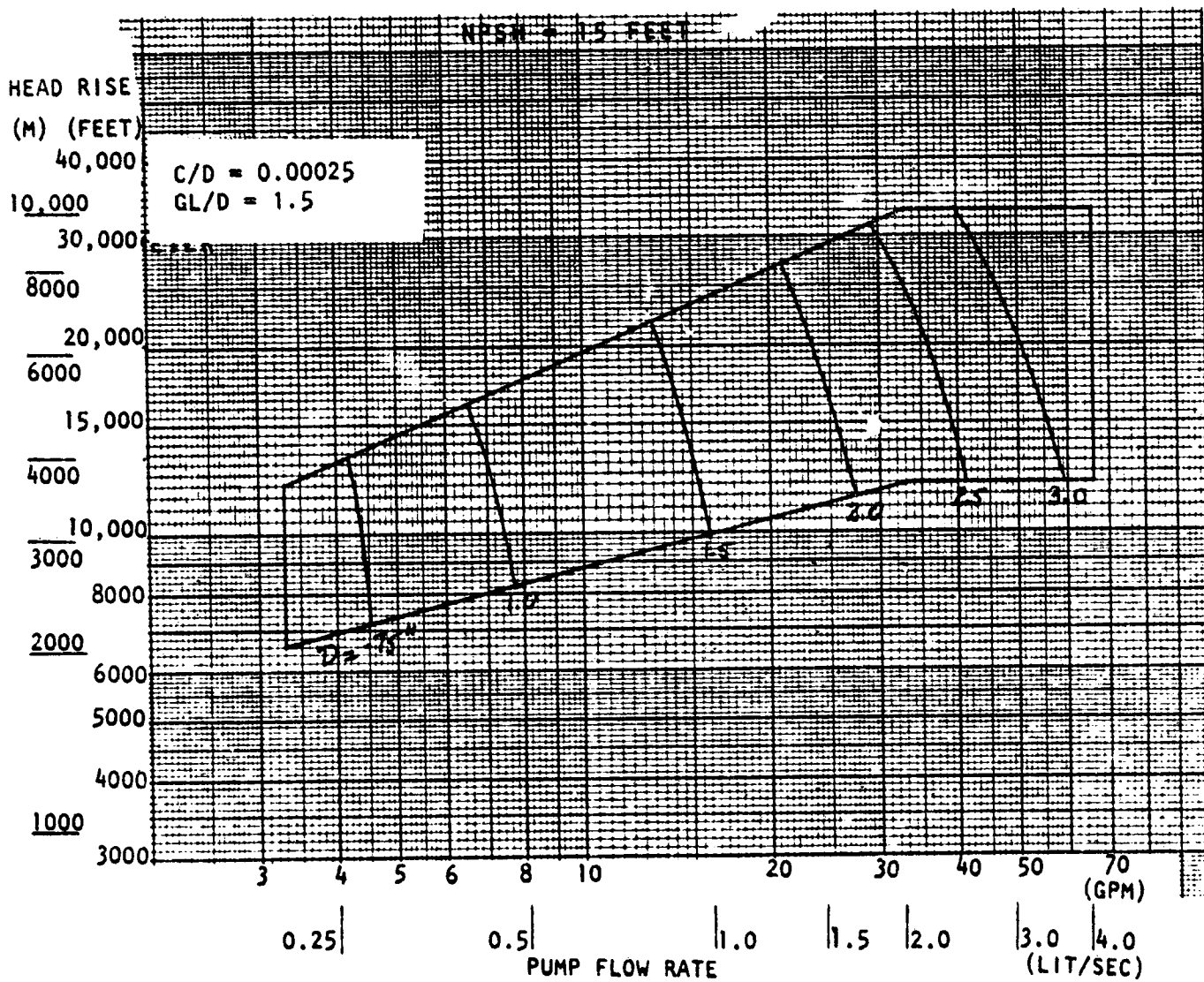


Figure A-155. Gear Hydrogen Pump, Diameter

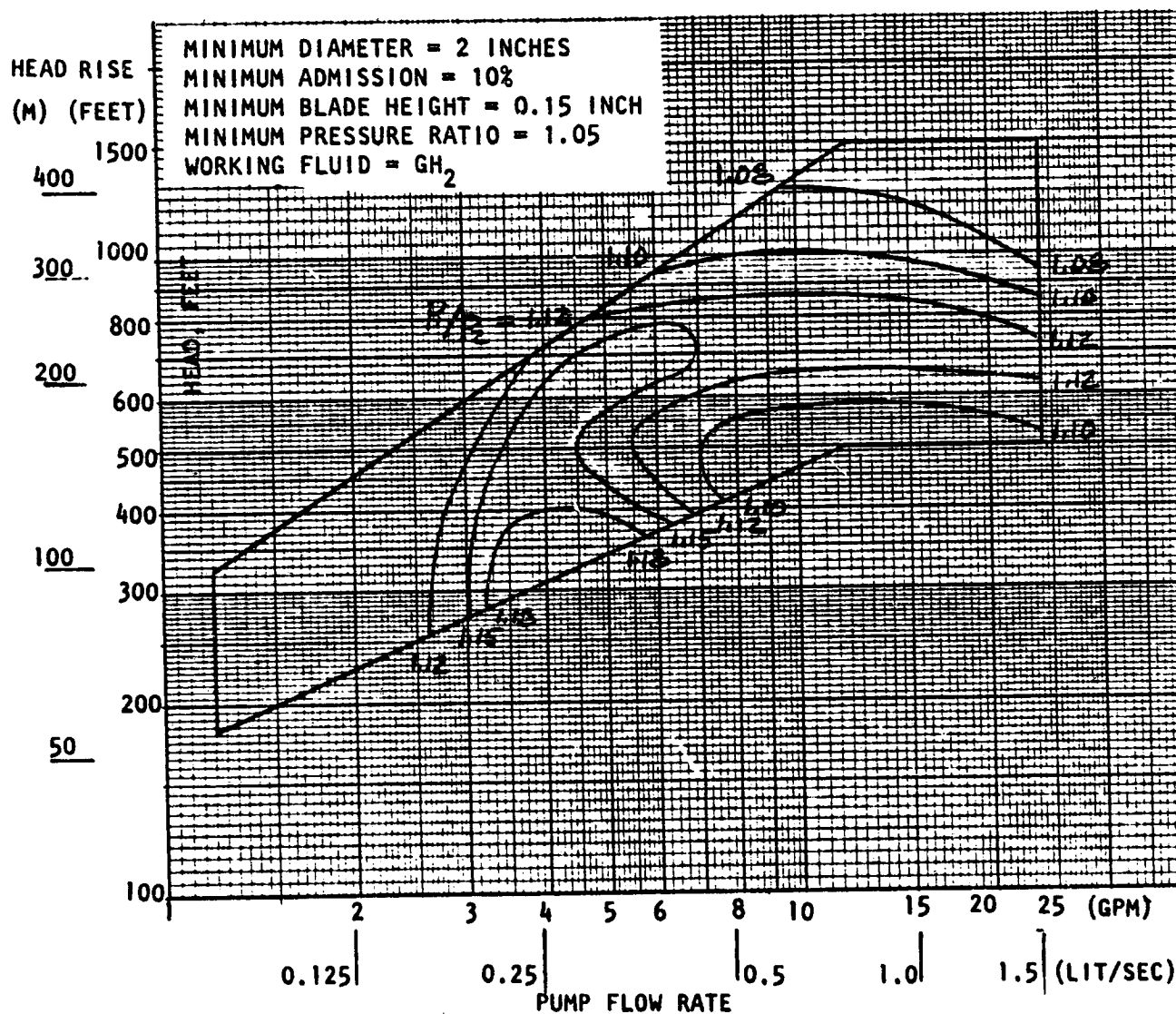


Figure A-156. Impulse Turbine Drive for Centrifugal LOX Pump, Pressure Ratio

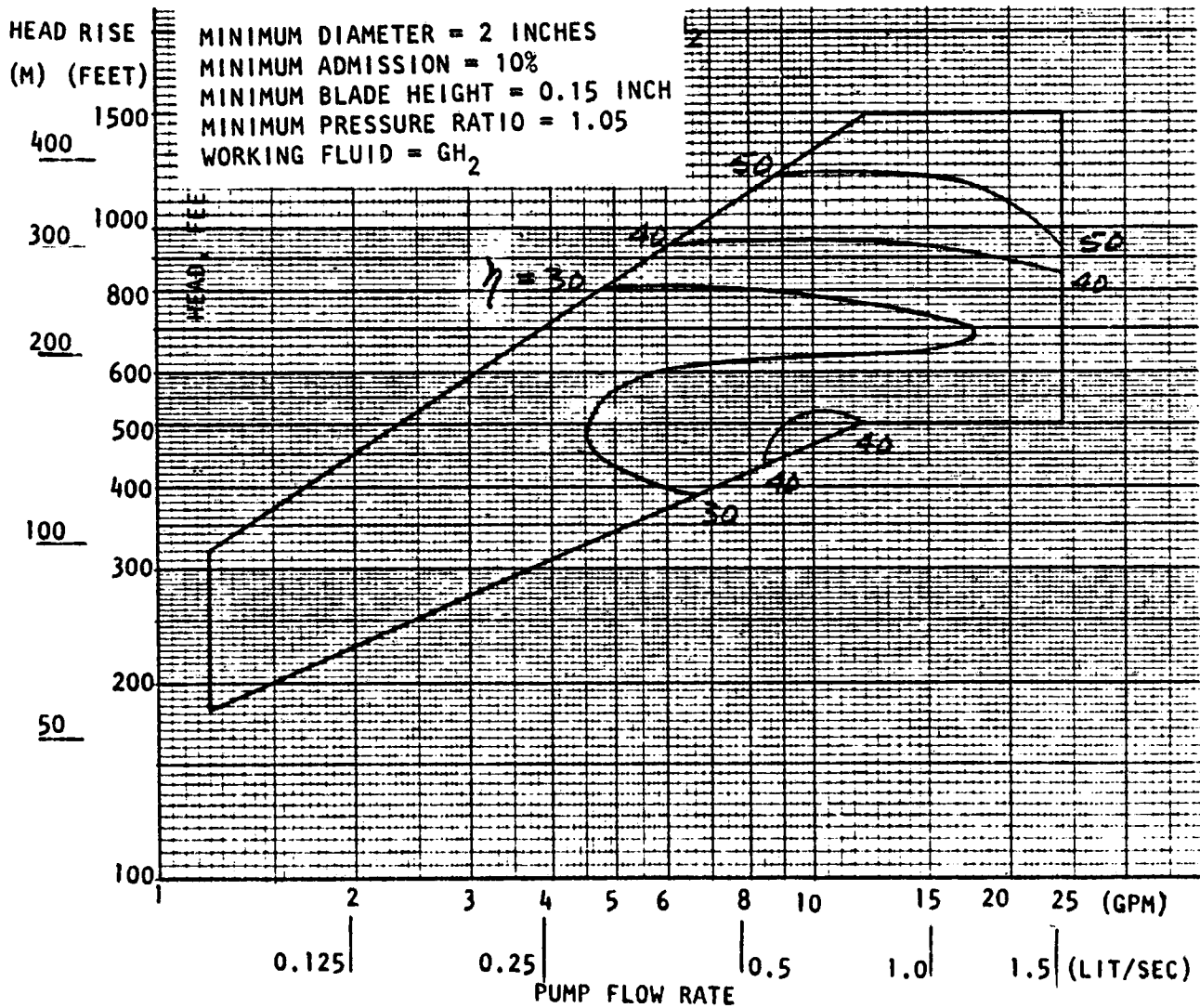


Figure A-157. Impulse Turbine Drive for Centrifugal LOX Pump, Efficiency

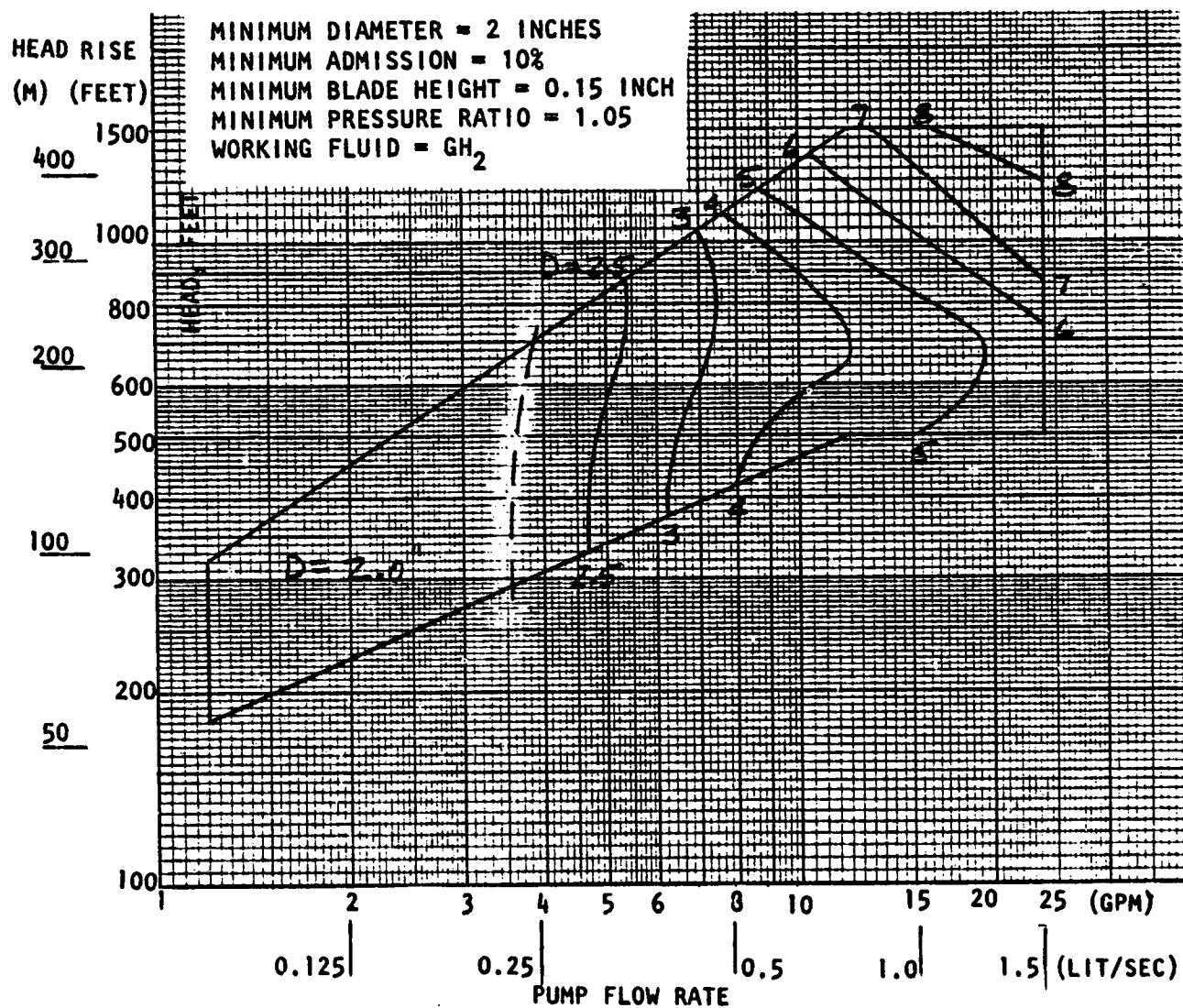


Figure A-158. Impulse Turbine Drive for Centrifugal LOX Pump, Diameter

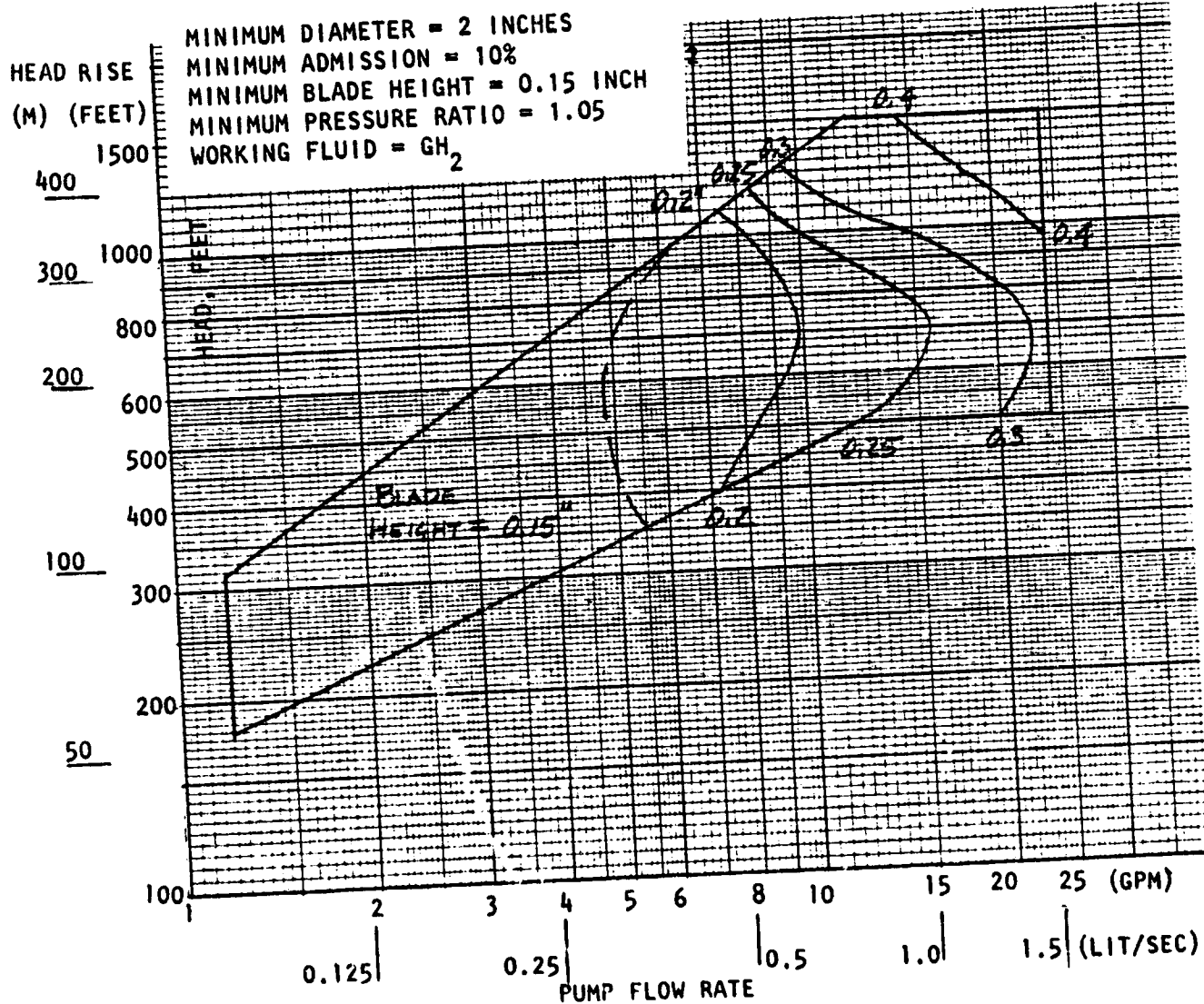


Figure A-159. Impulse Turbine Drive for Centrifugal LOX Pump, Blade Height

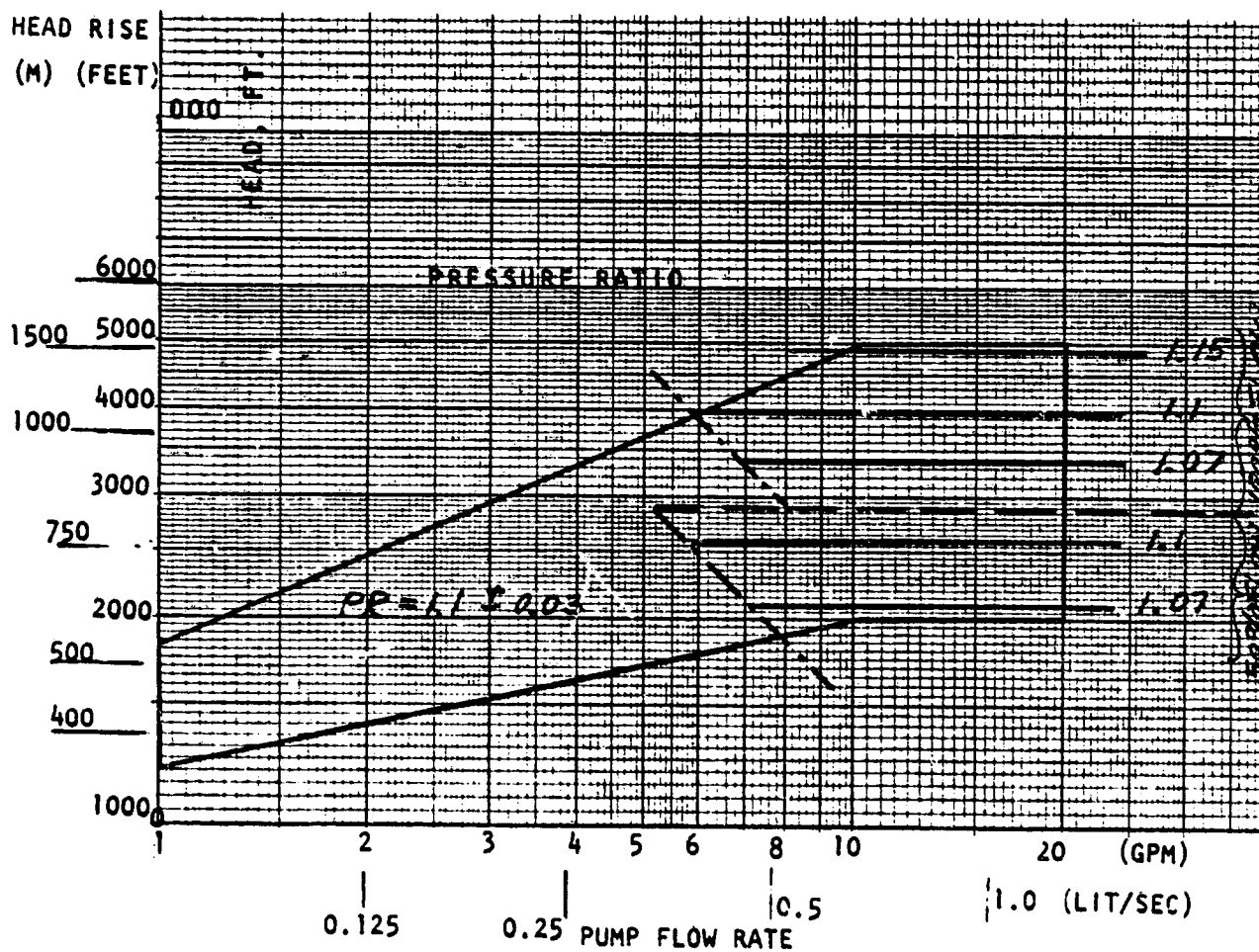


Figure A-160. Impulse Turbine Drive for Centrifugal Methane Pump, Pressure Ratio, NPSH = 6 Feet

ORIGINAL PAGE IS
OF POOR QUALITY

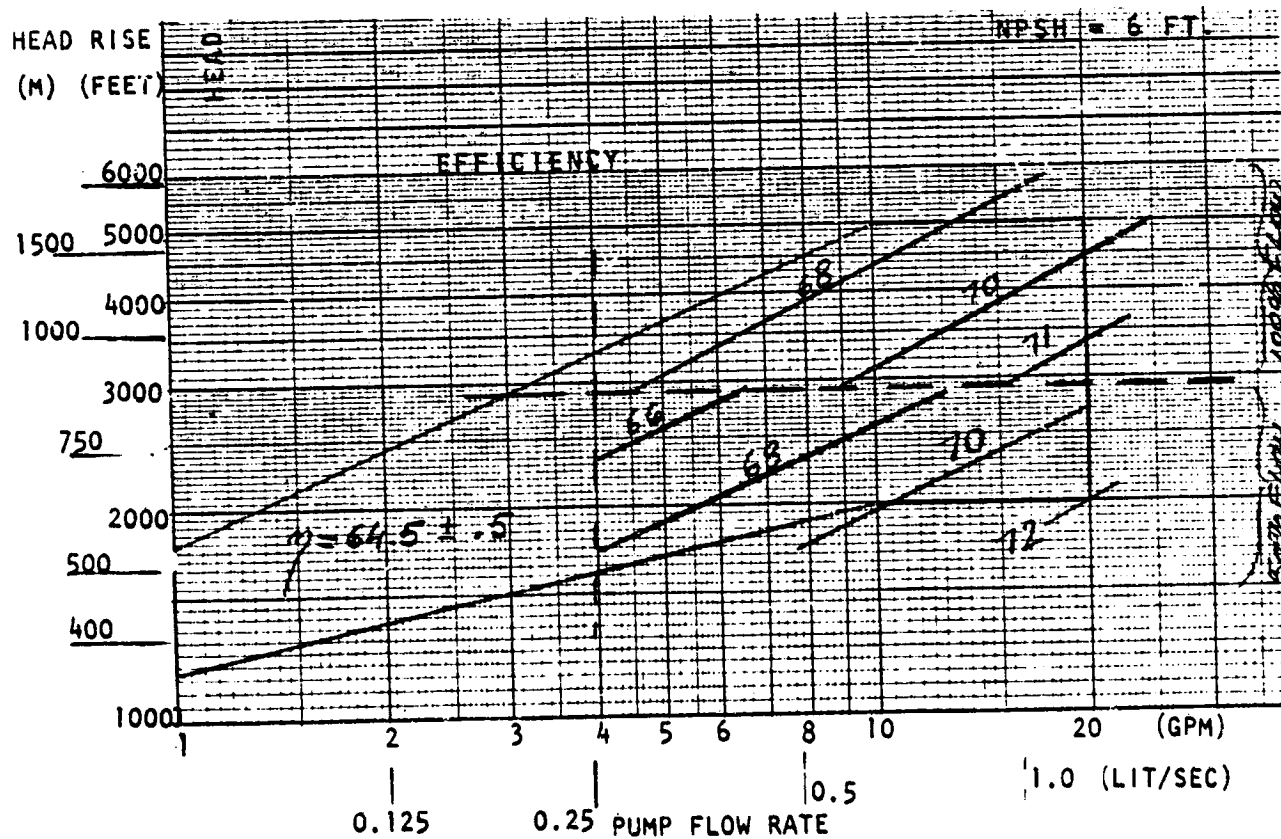


Figure A-161. Impulse Turbine Drive for Centrifugal Methane Pump, Efficiency

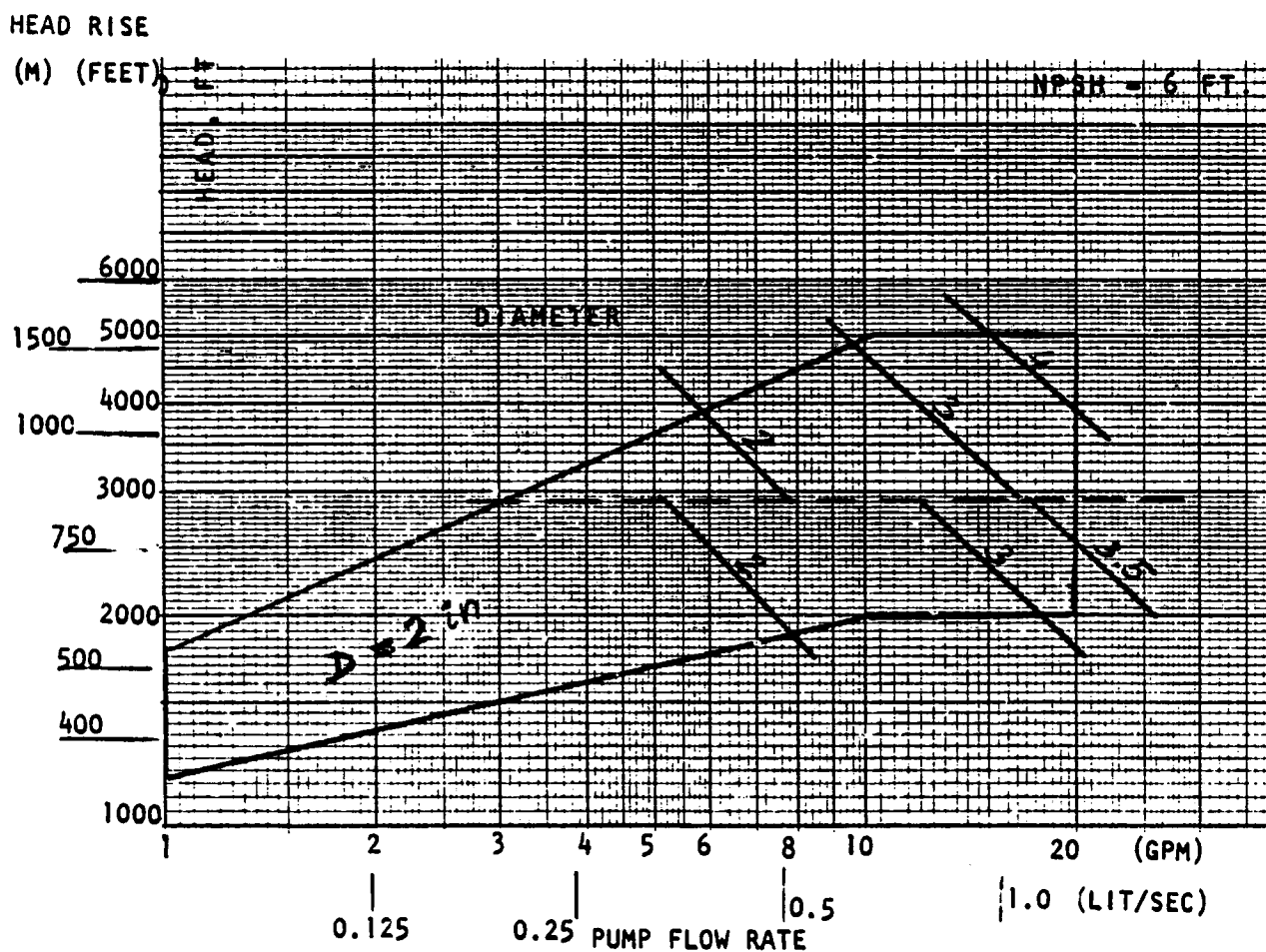


Figure A-162. Impulse Turbine Drive for Centrifugal Methane Pump, Diameter

ORIGINAL PAGE IS
"POOR QUALITY"

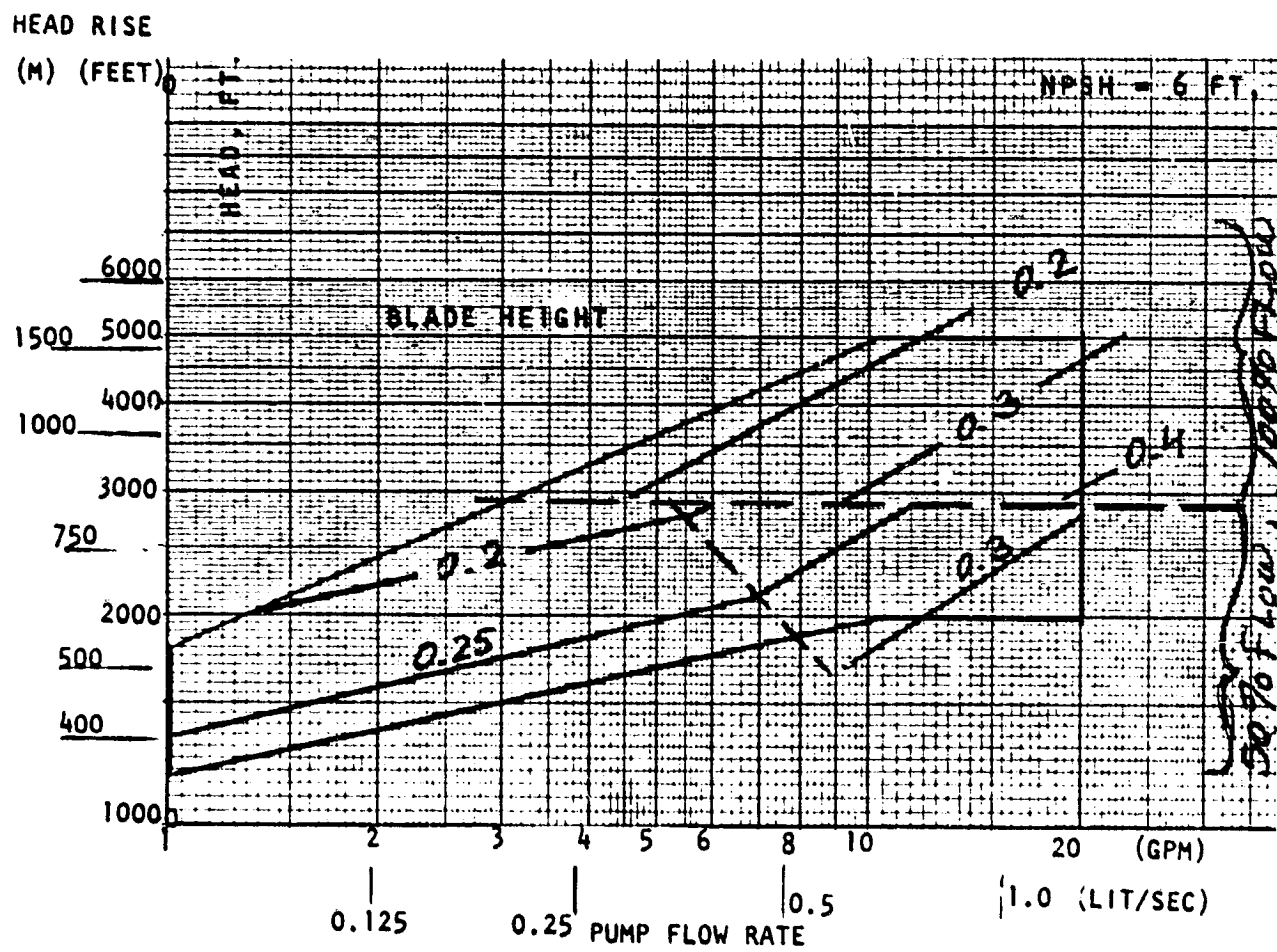


Figure A-163. Impulse Turbine Drive for Centrifugal Methane Pump, Blade Height

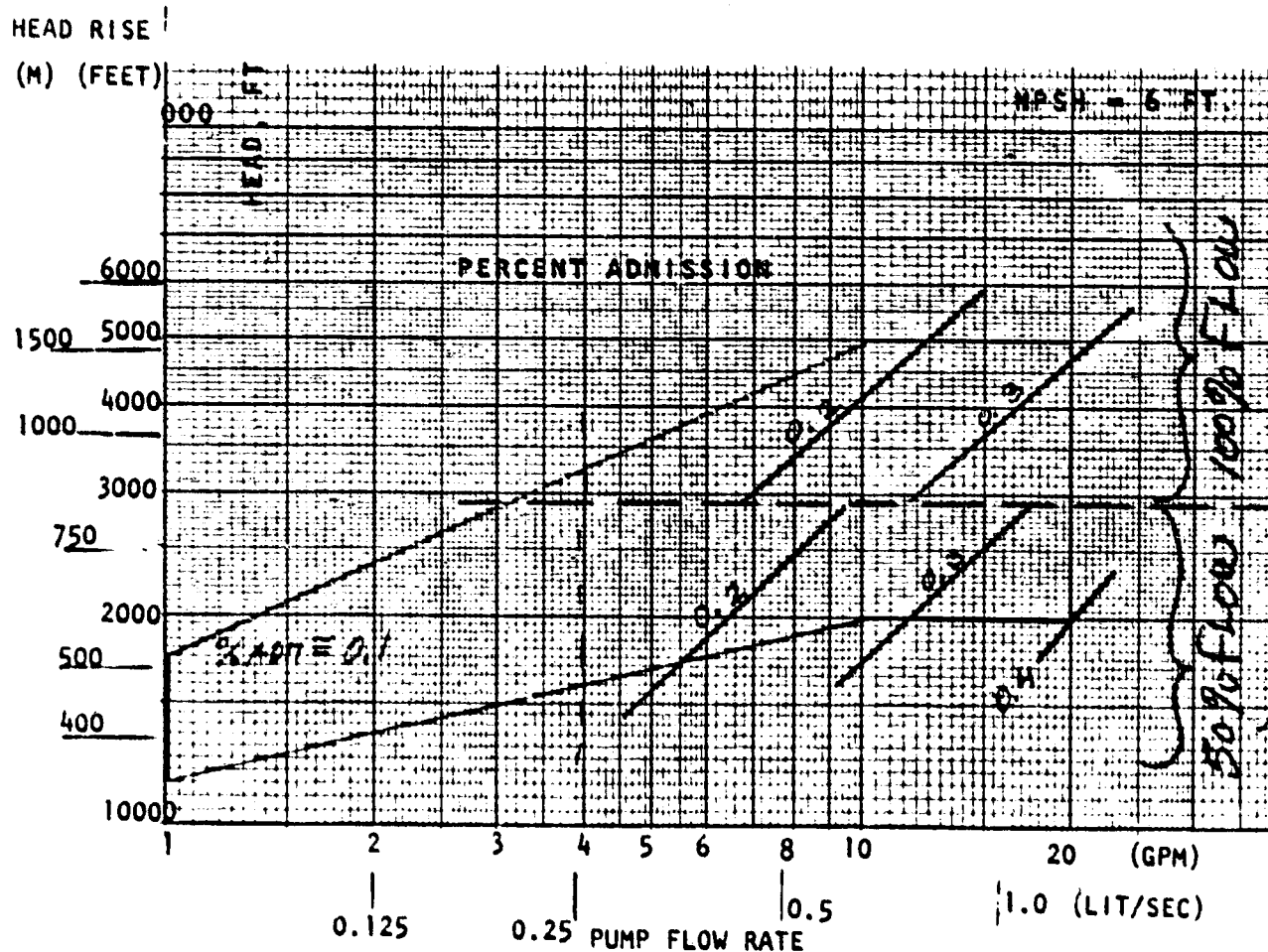


Figure A-164. Impulse Turbine Drive for Centrifugal Methane Pump, Percent Admission

ORIGINAL PAGE IS
OF POOR QUALITY

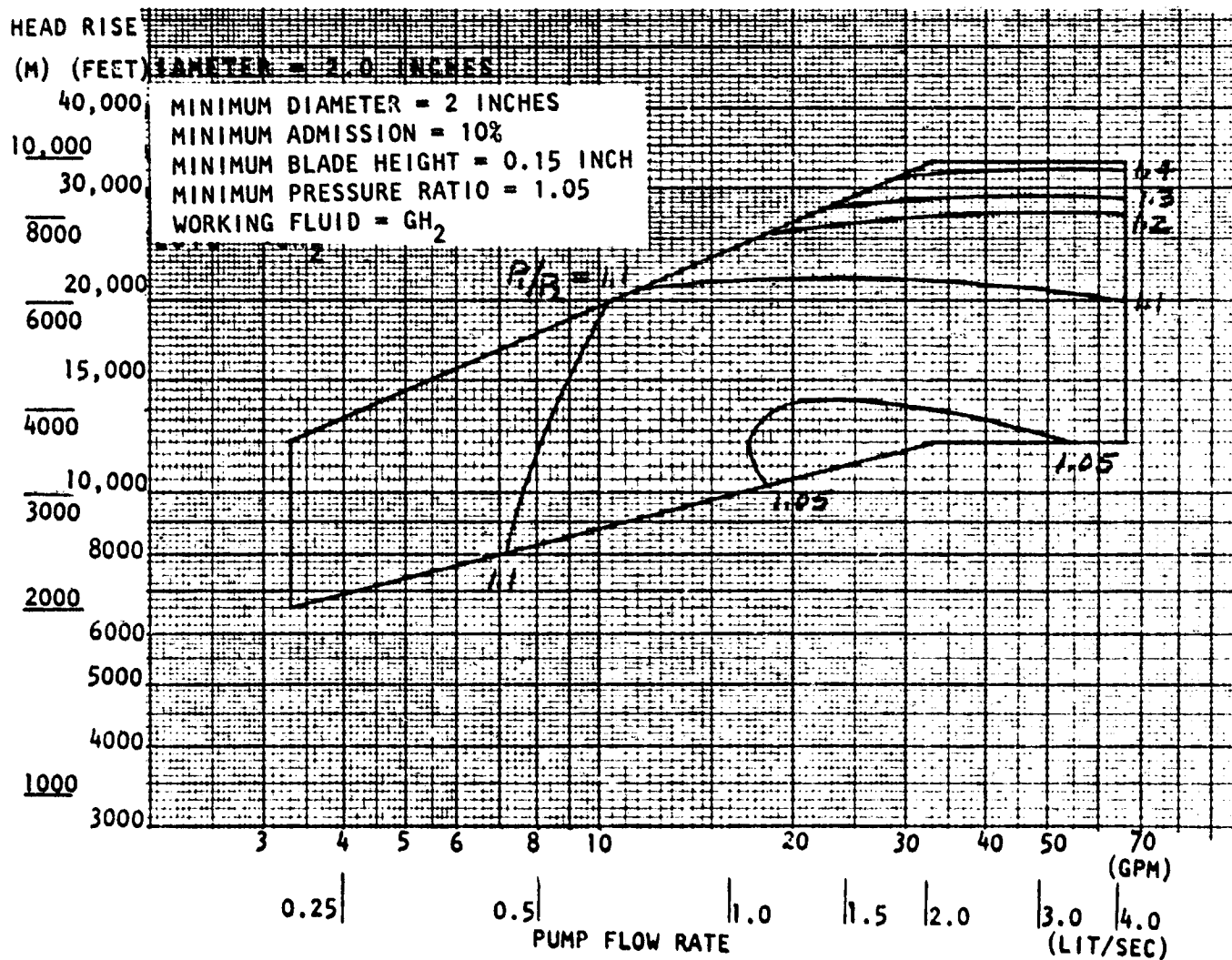


Figure A-165. Impulse Turbine Drive for Centrifugal Hydrogen Pump, Pressure Ratio

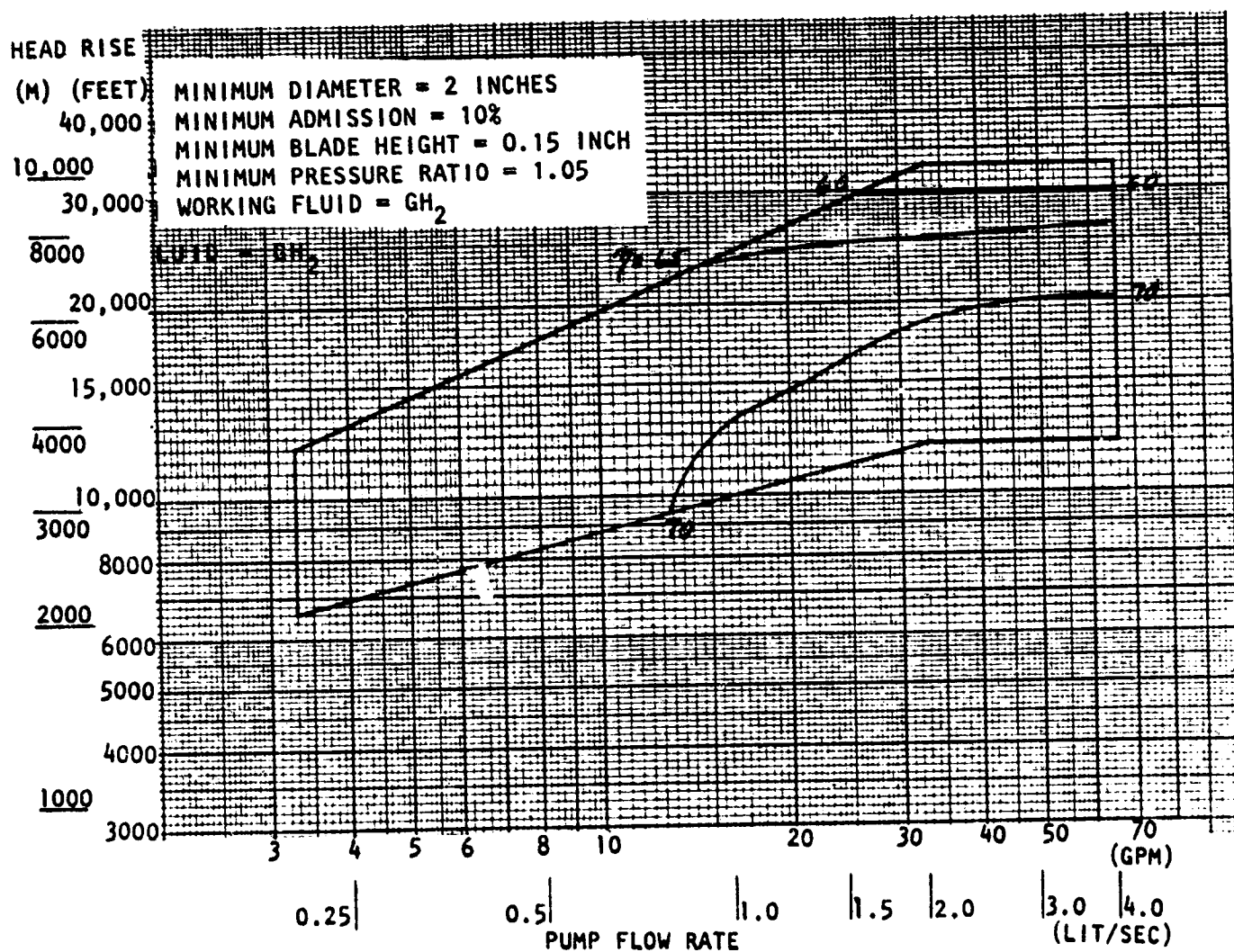


Figure A-166. Impulse Turbine Drive for Centrifugal Hydrogen Pump, Efficiency

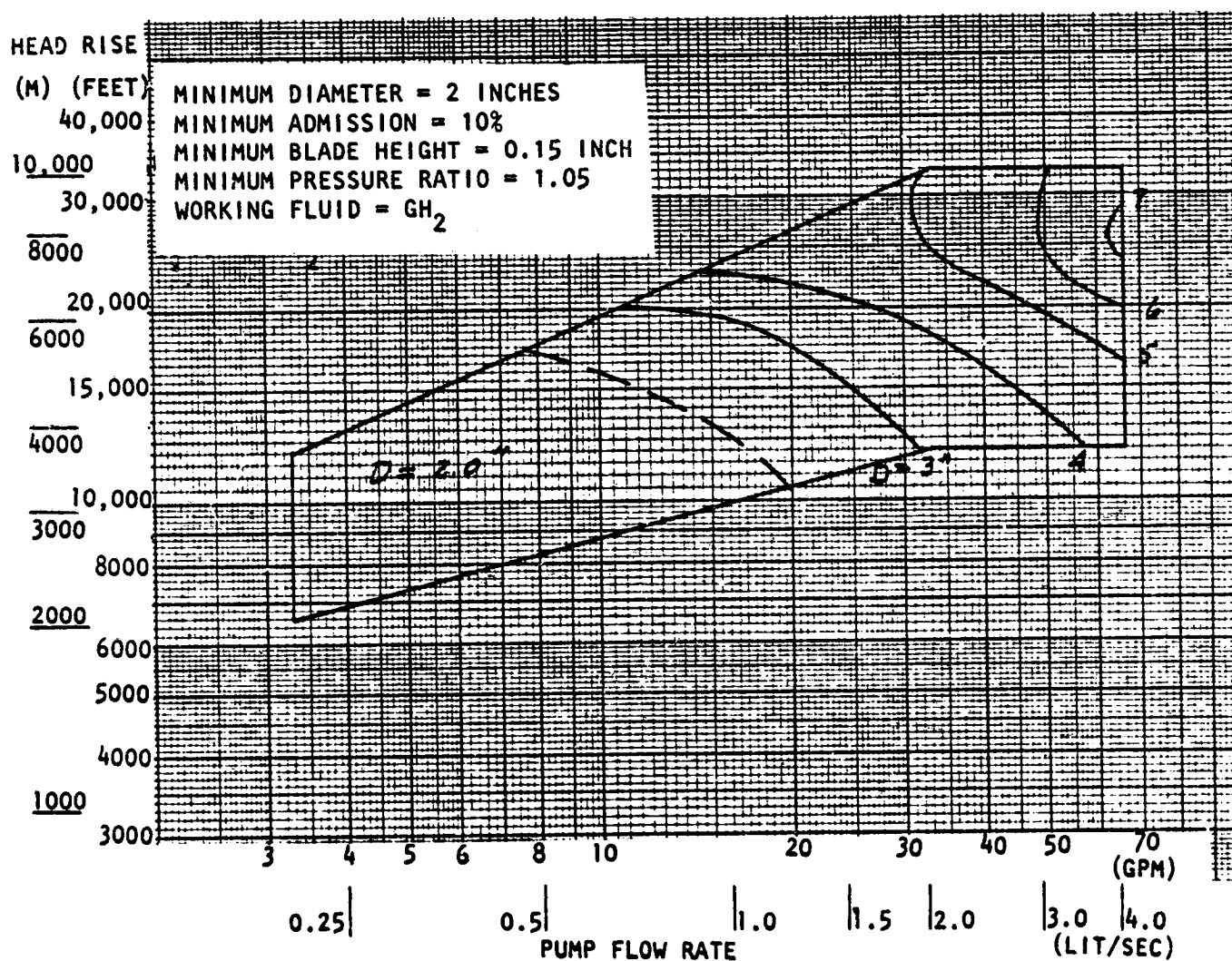


Figure A-167. Impulse Turbine Drive for Centrifugal Hydrogen Pump, Diameter

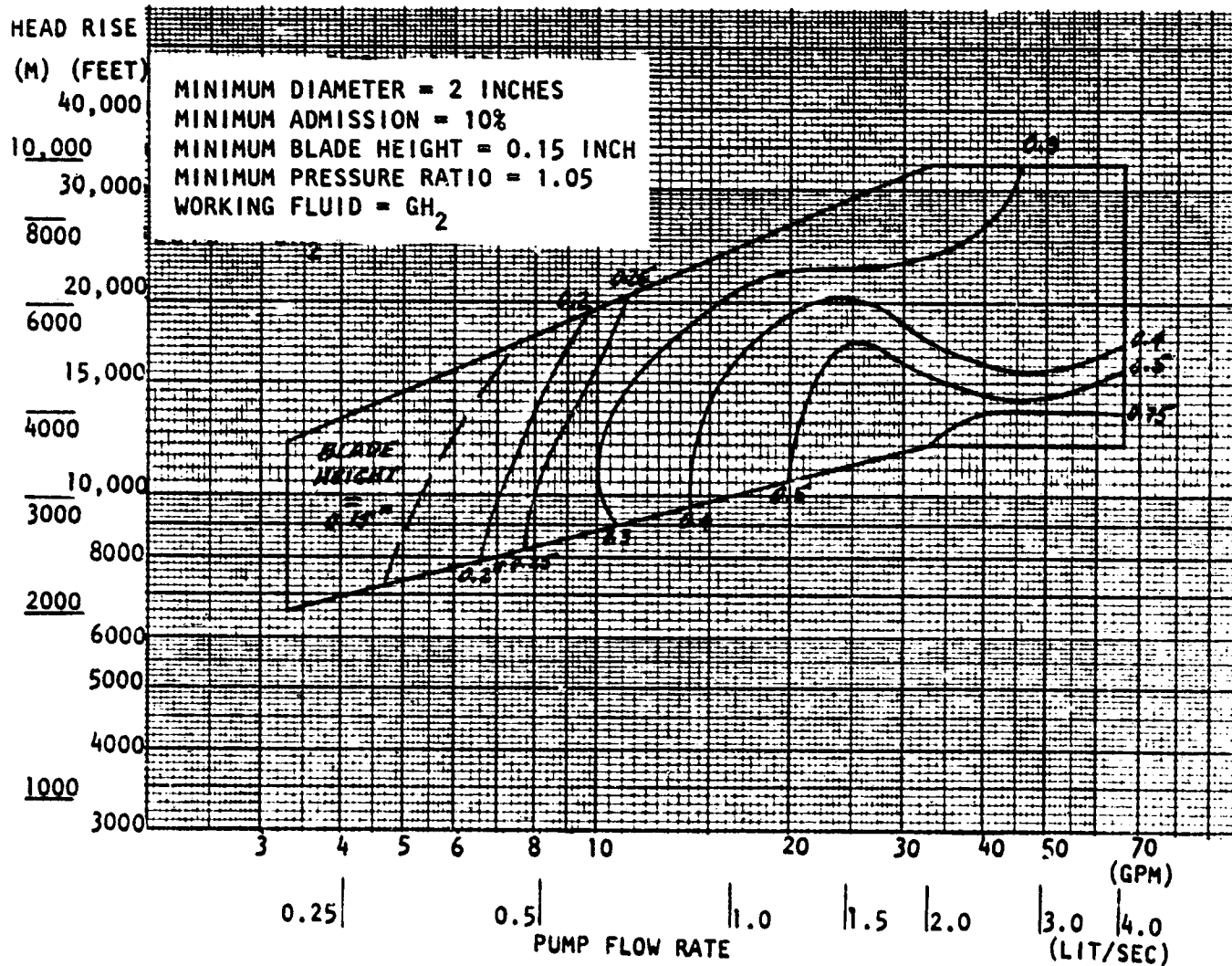


Figure A-168. Impulse Turbine Drive for Centrifugal Hydrogen Pump, Blade Height

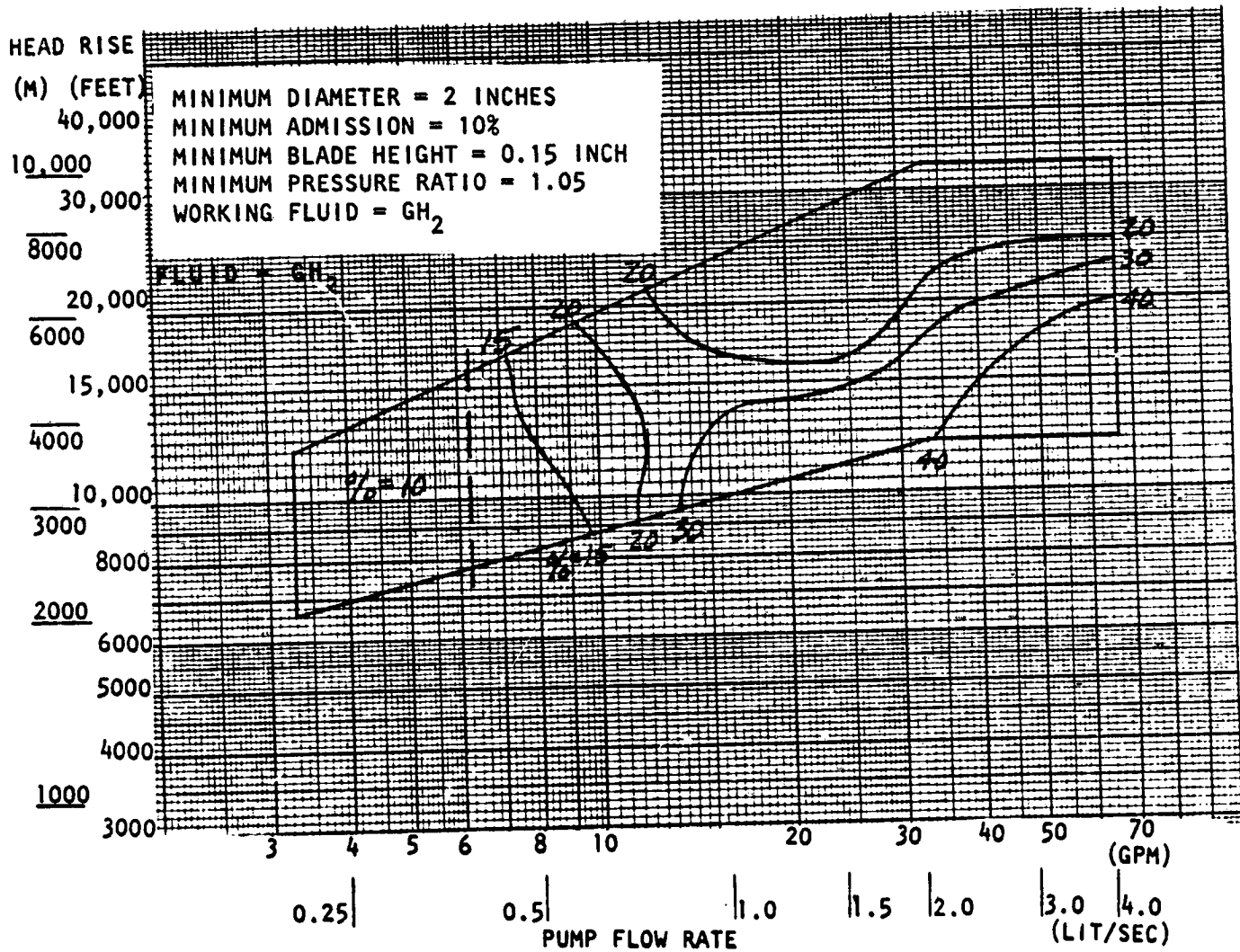


Figure A-169. Impulse Turbine Drive for Centrifugal Hydrogen Pump, Percent Admission

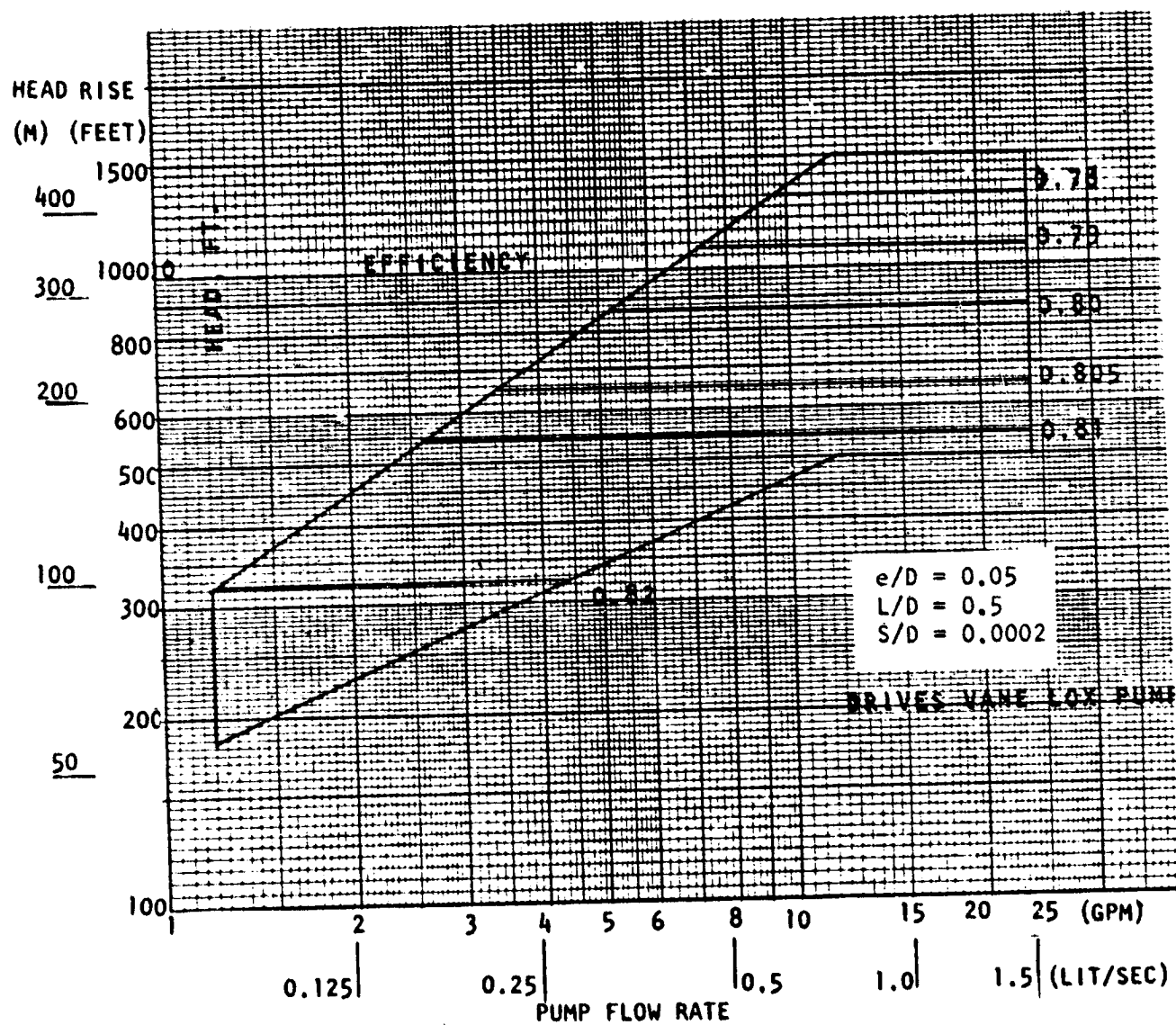


Figure A-170. Vane Expander for Vane LOX Pump, Efficiency

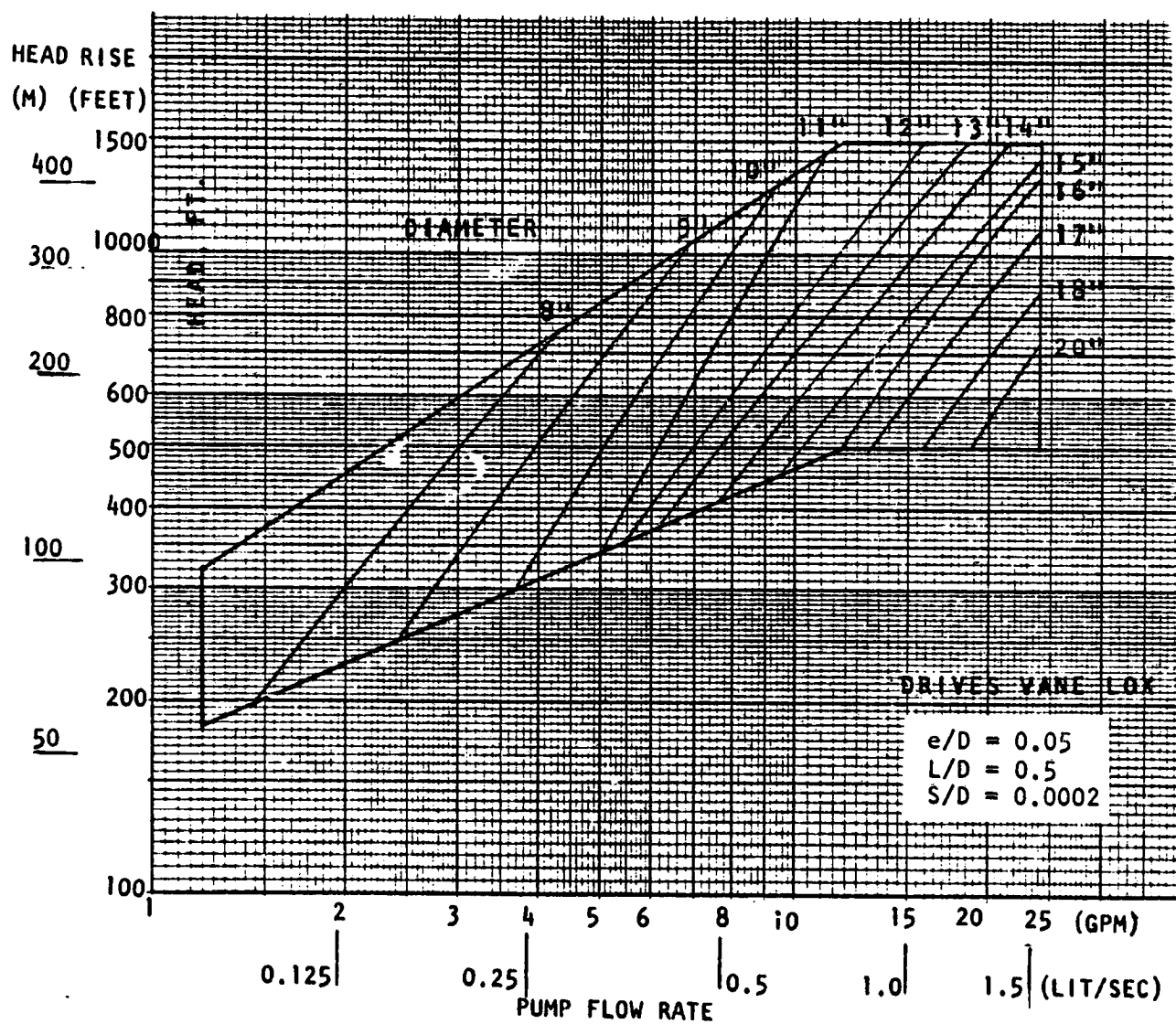


Figure A-171. Vane Expander for Vané LOX Pump, Diameter

ORIGINAL PAGE IS
OF POOR QUALITY

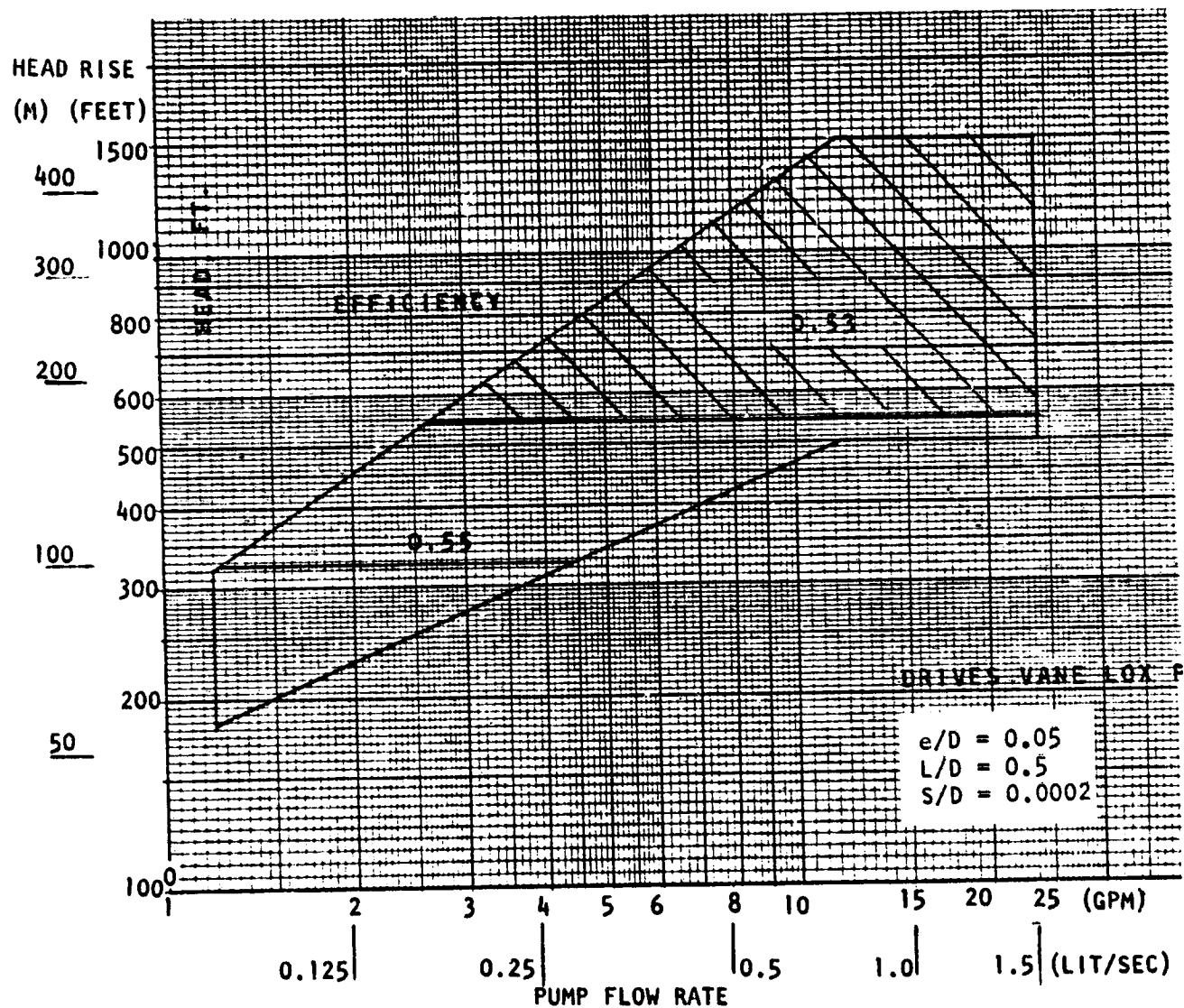


Figure A-172. Vane Expander for Vane LOX Pump, Efficiency
($P_1/P_2 = 1.3$)

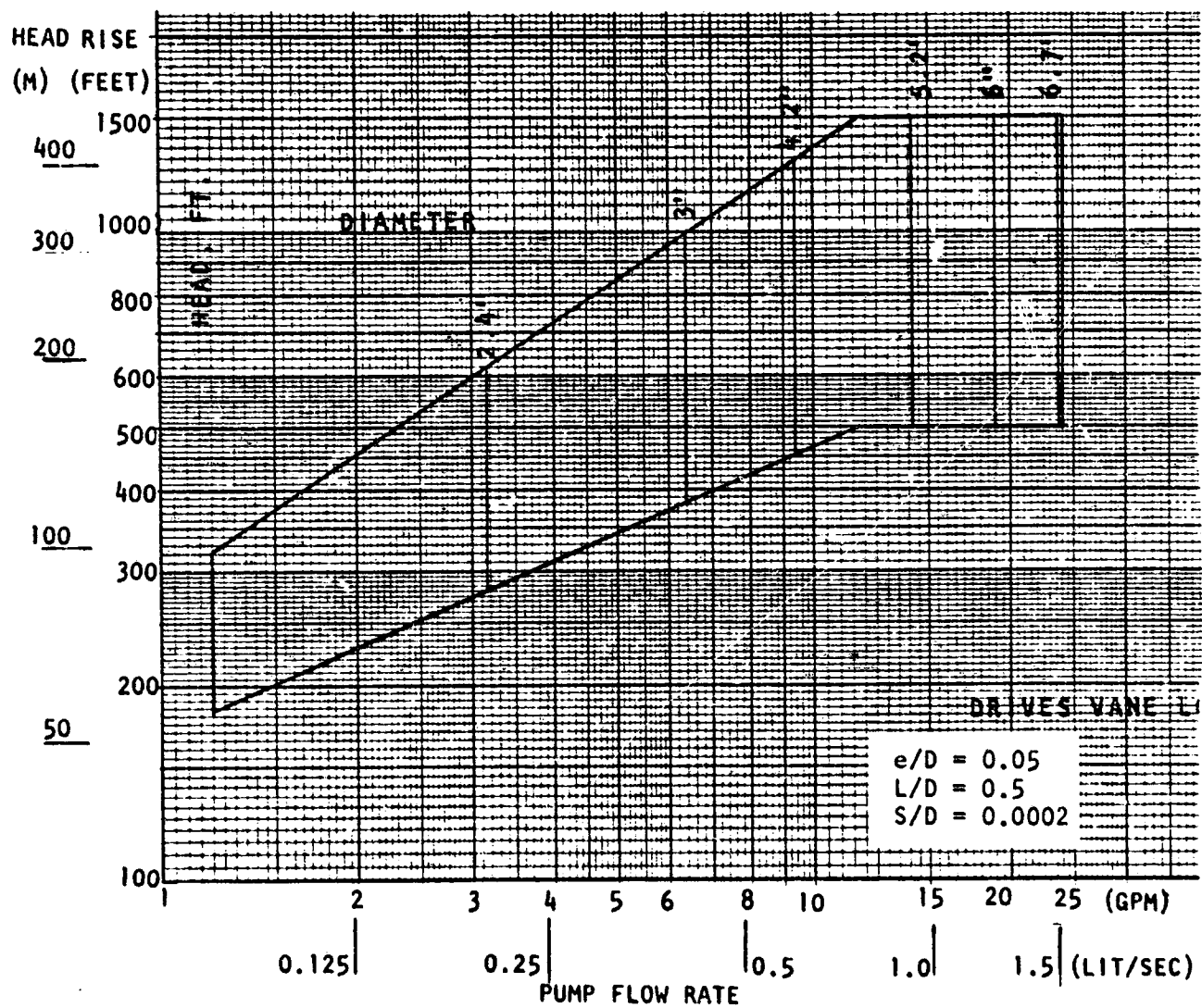


Figure A-173. Vane Expander for Vane LOX Pump, Diameter
($P_1/P_2 = 1.3$)

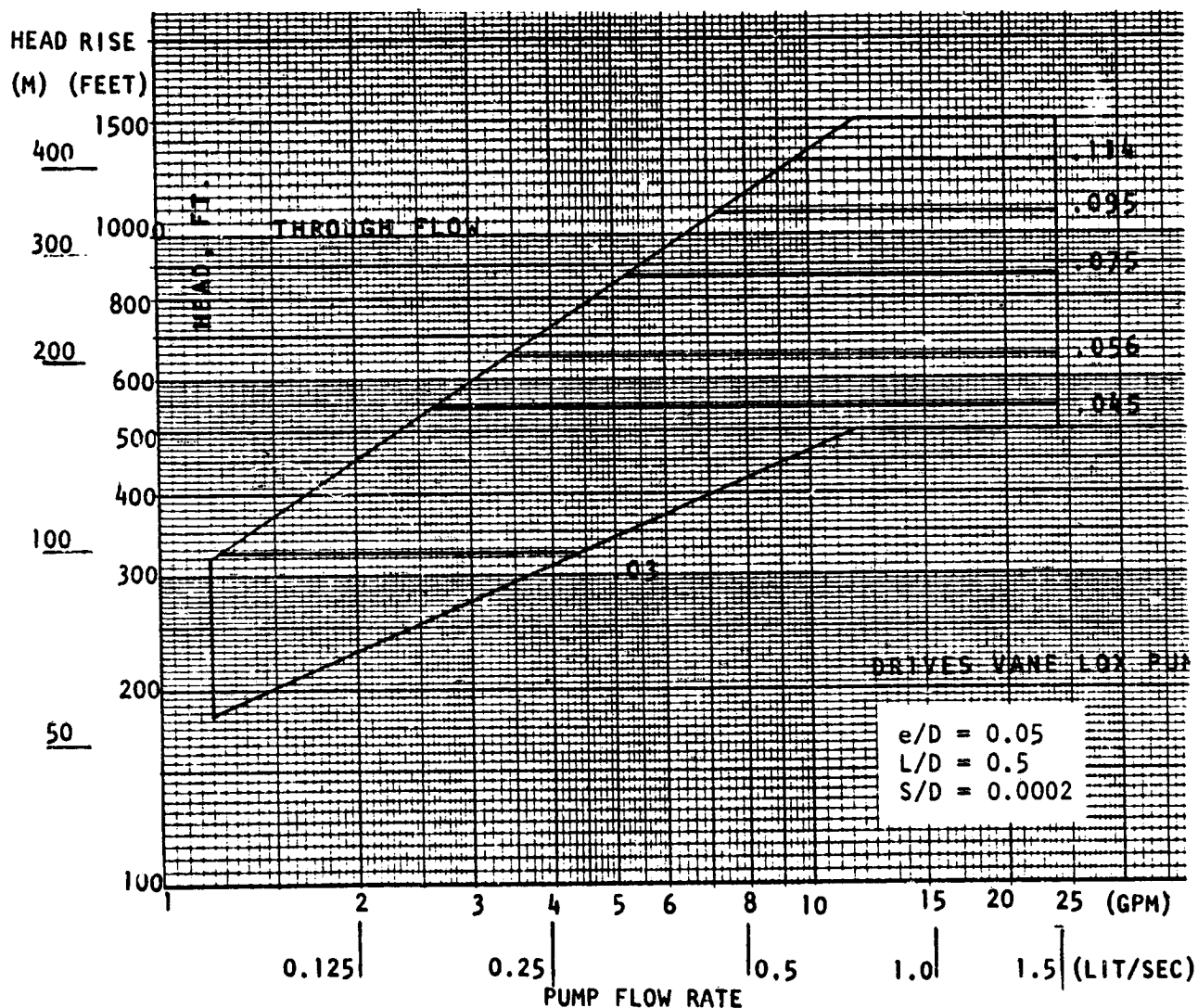


Figure A-174. Vane Expander for Vane LOX Pump, Through Flow
($P_1/P_2 = 1.3$)

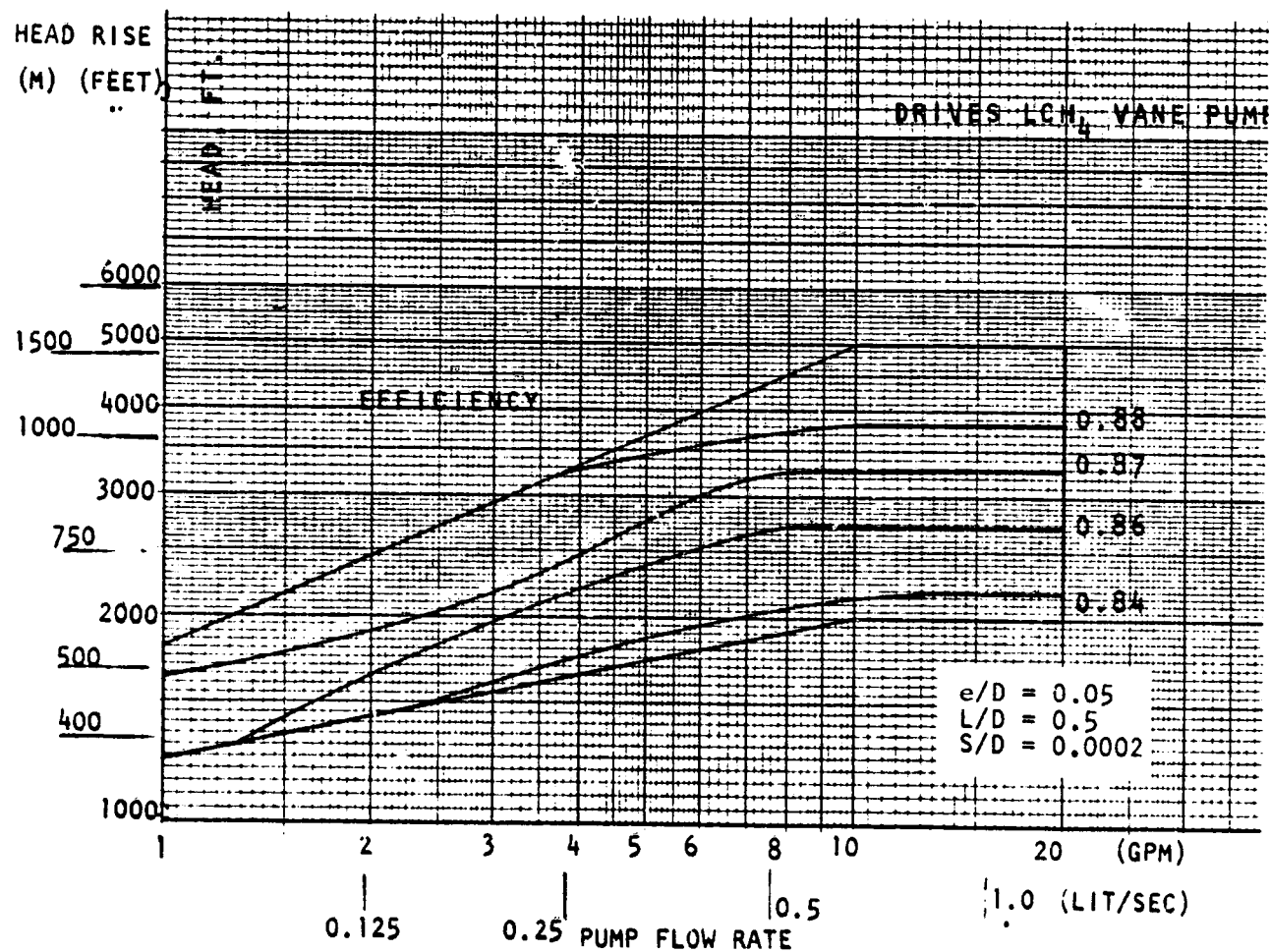


Figure A-175. Vane Expander for Vane Methane Pump, Efficiency

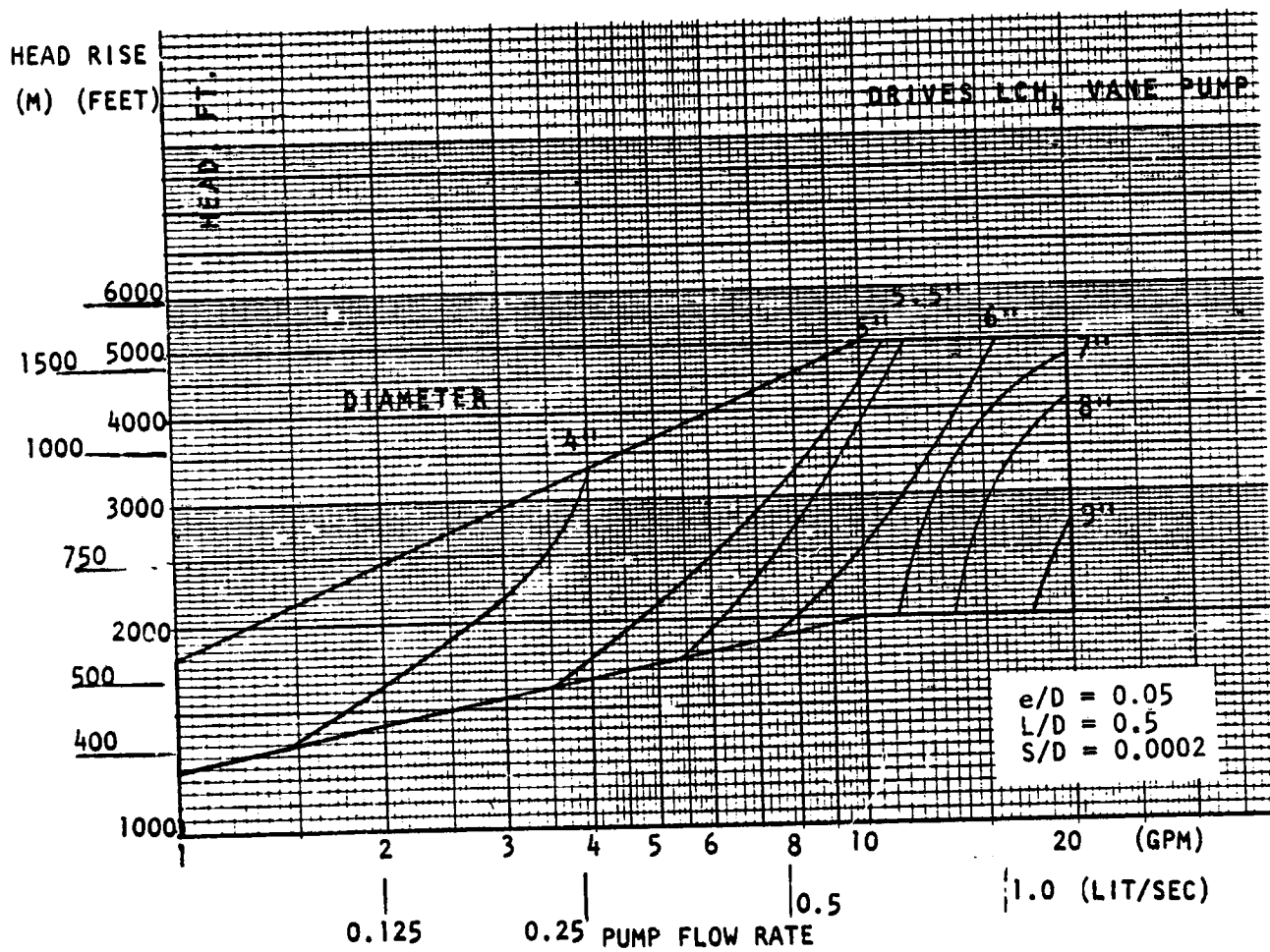


Figure A-176. Vane Expander for Vane Methane Pump, Diameter

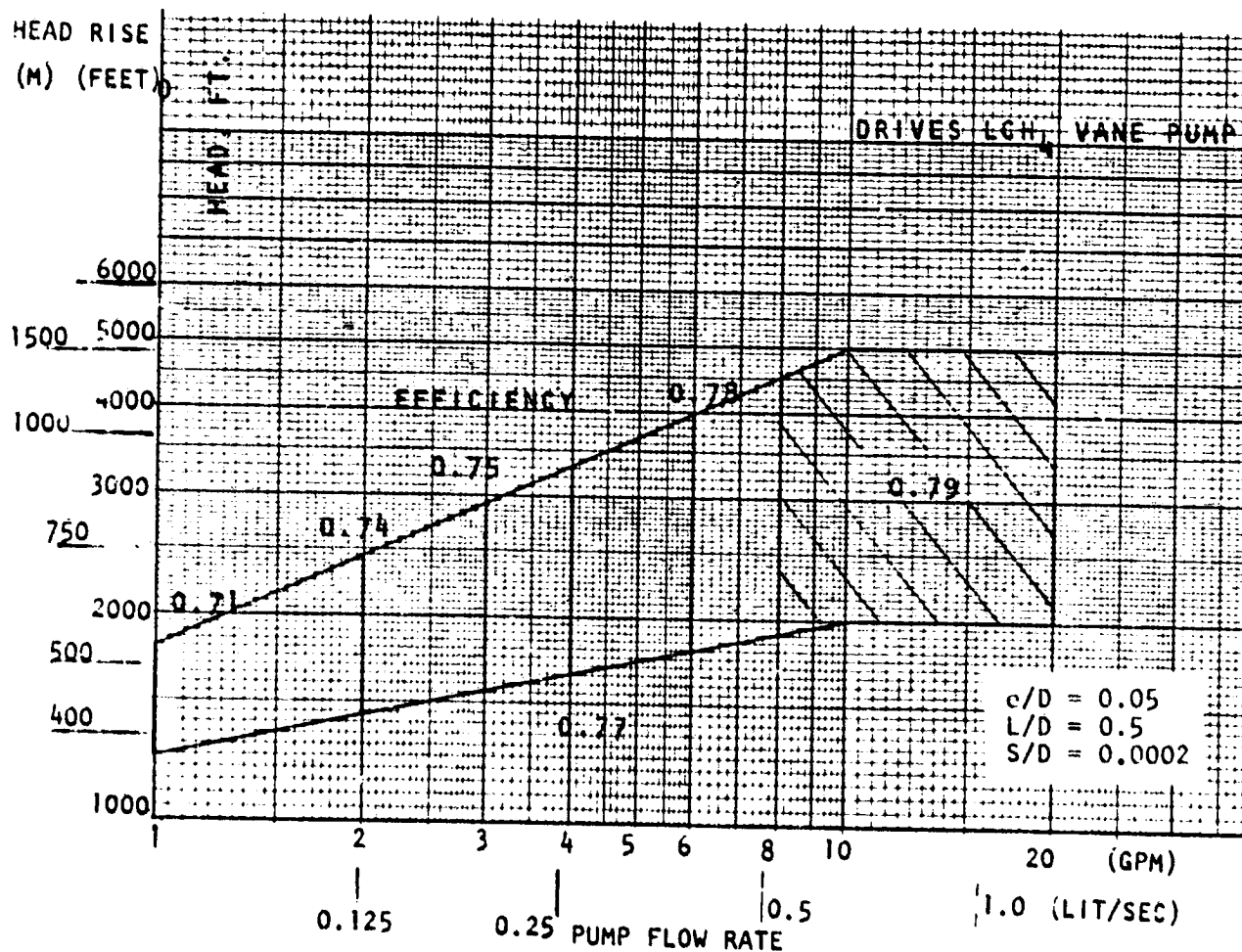


Figure A-177. Vane Expander for Vane Methane Pump, Efficiency
($P_1/P_2 = 1.3$)

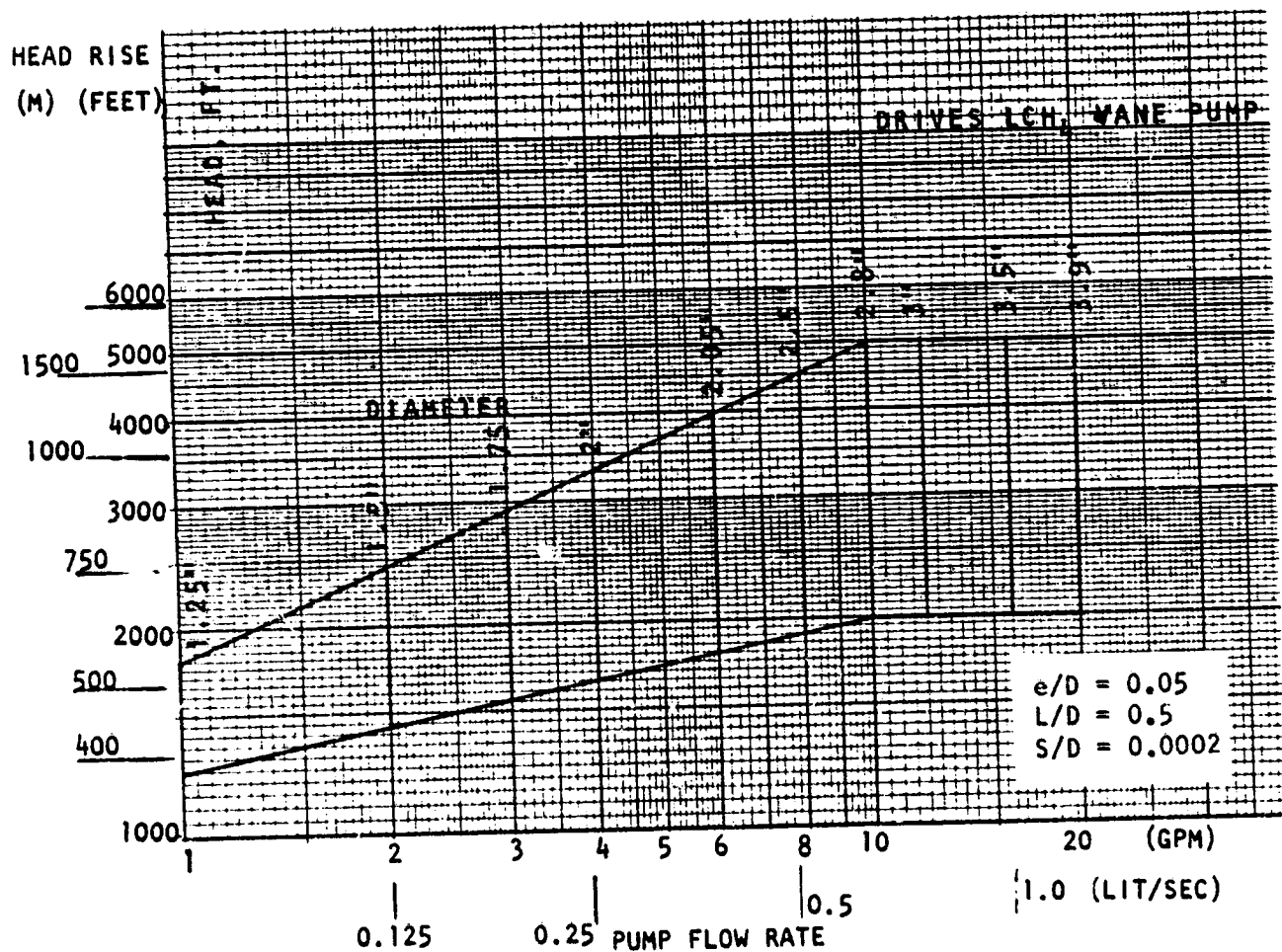


Figure A-178. Vane Expander for Vane Methane Pump, Diameter
($P_1/P_2 = 1.3$)

ORIGINAL PAGE IS
OF POOR QUALITY

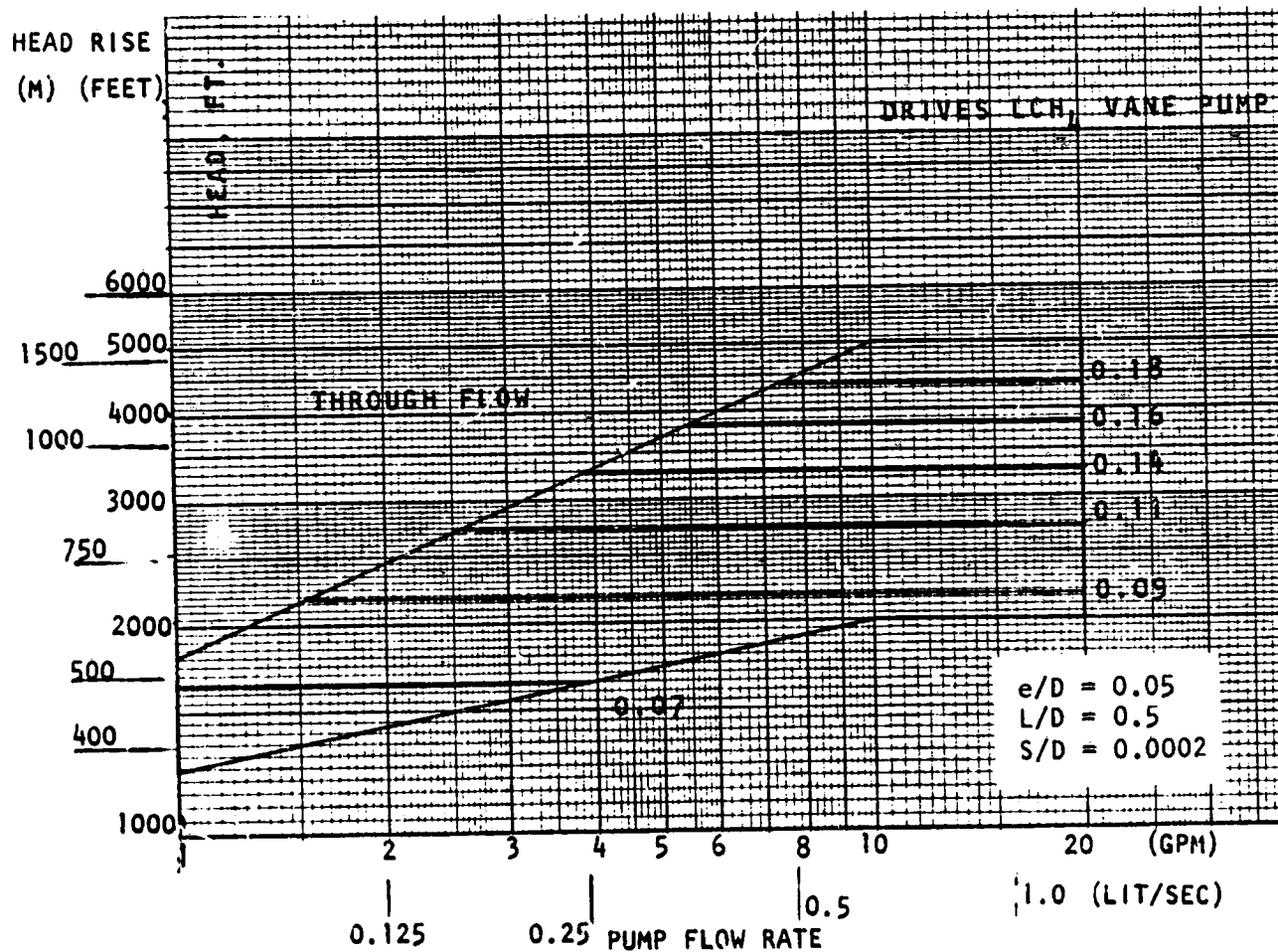


Figure A-179. Vane Expander for Vane Methane Pump, Through Flow
($P_1/P_2 = 1.3$)

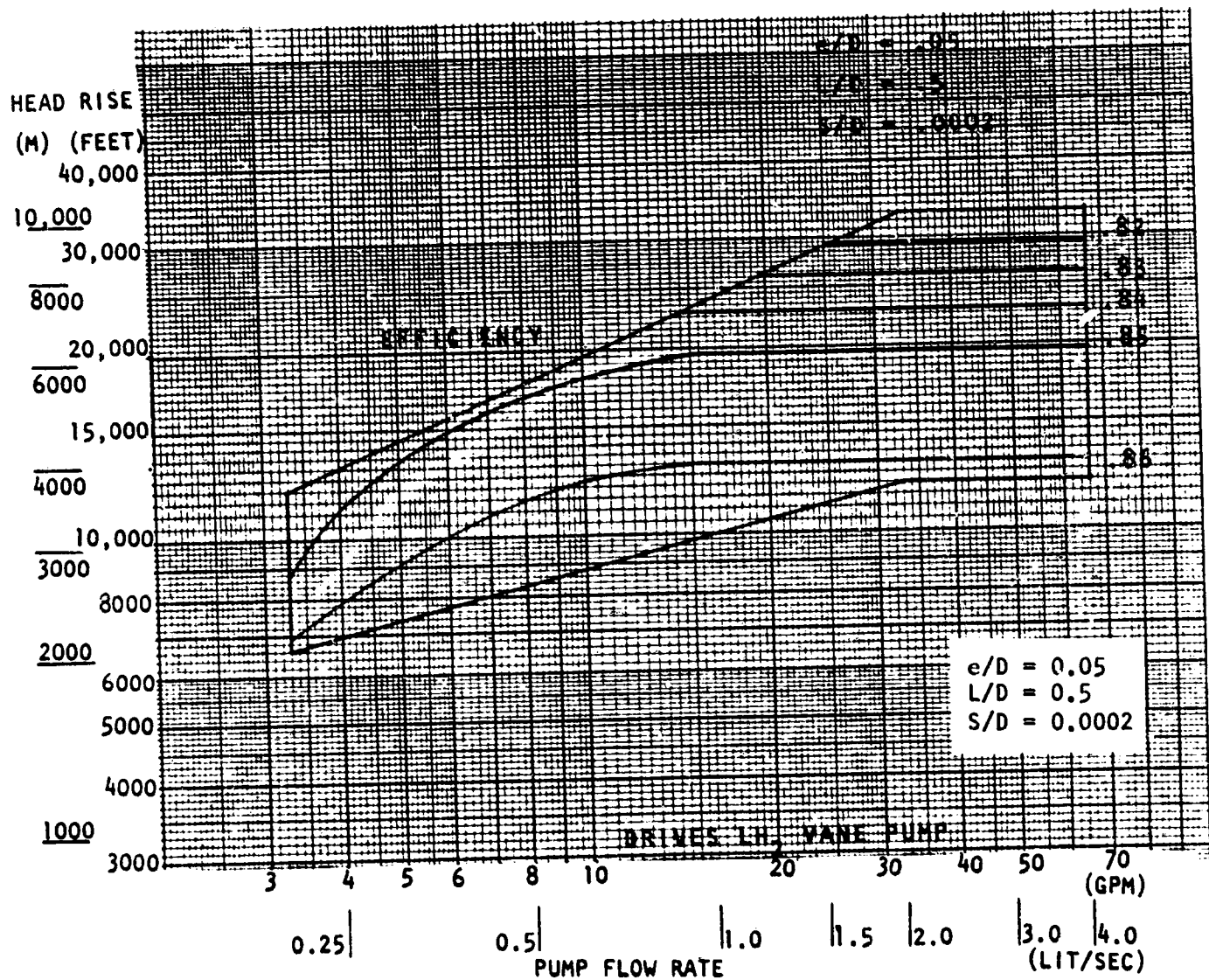


Figure A-180. Vane Expander for Vane Hydrogen Pump, Efficiency

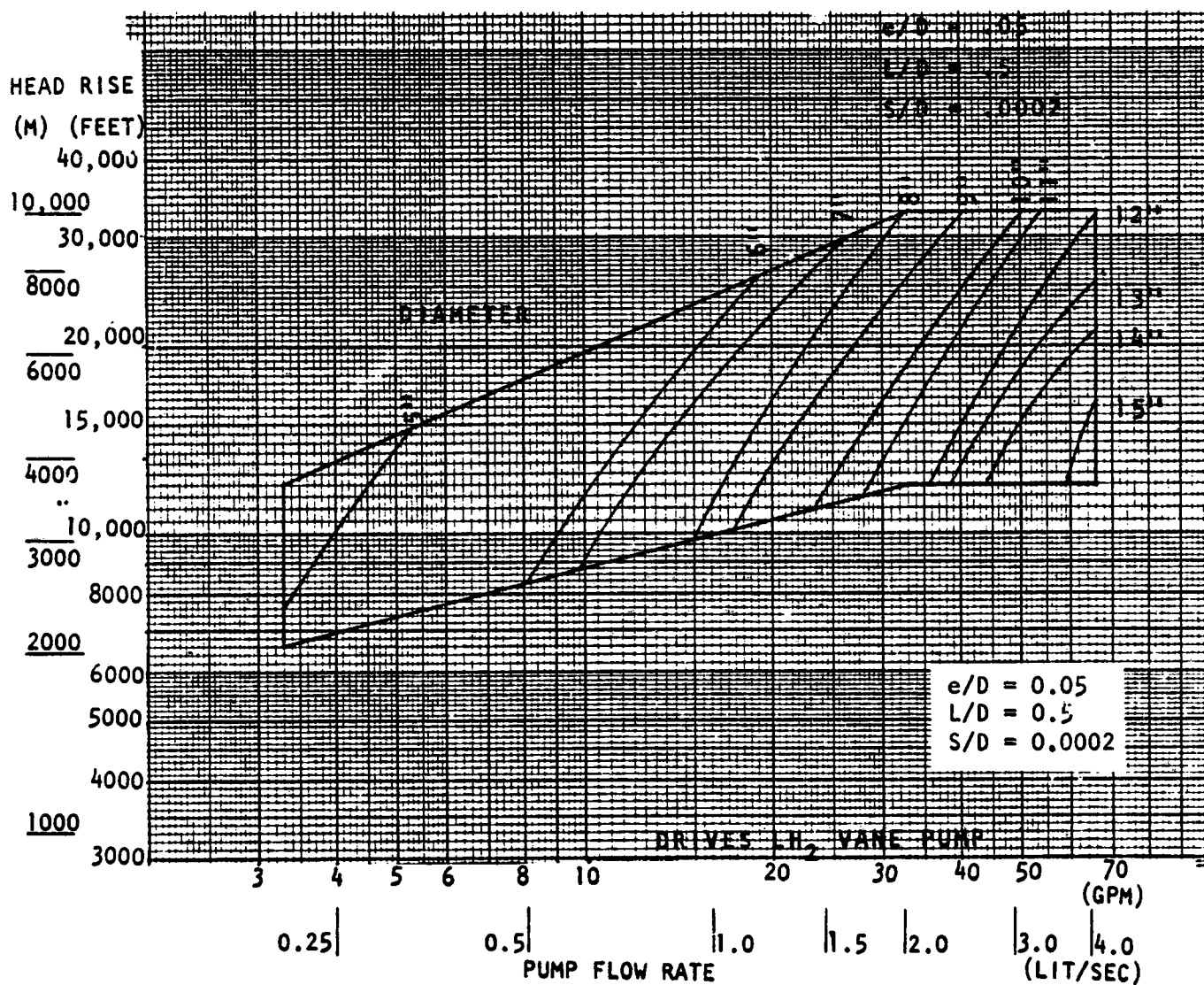


Figure A-181. Vane Expander for Vane Hydrogen Pump, Diameter

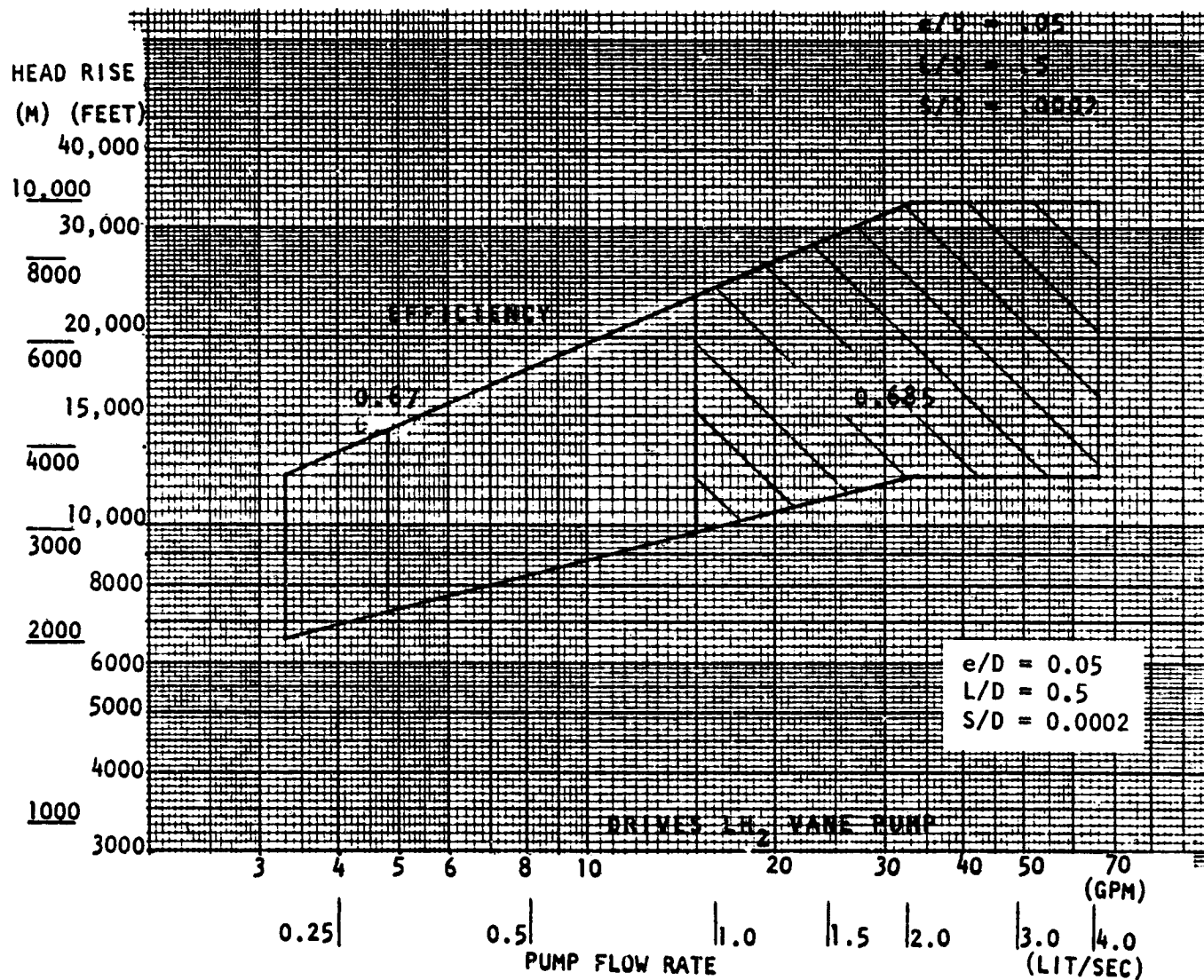


Figure A-182. Vane Expander for Vane Hydrogen Pump, Efficiency
($P_1/P_2 = 1.3$)

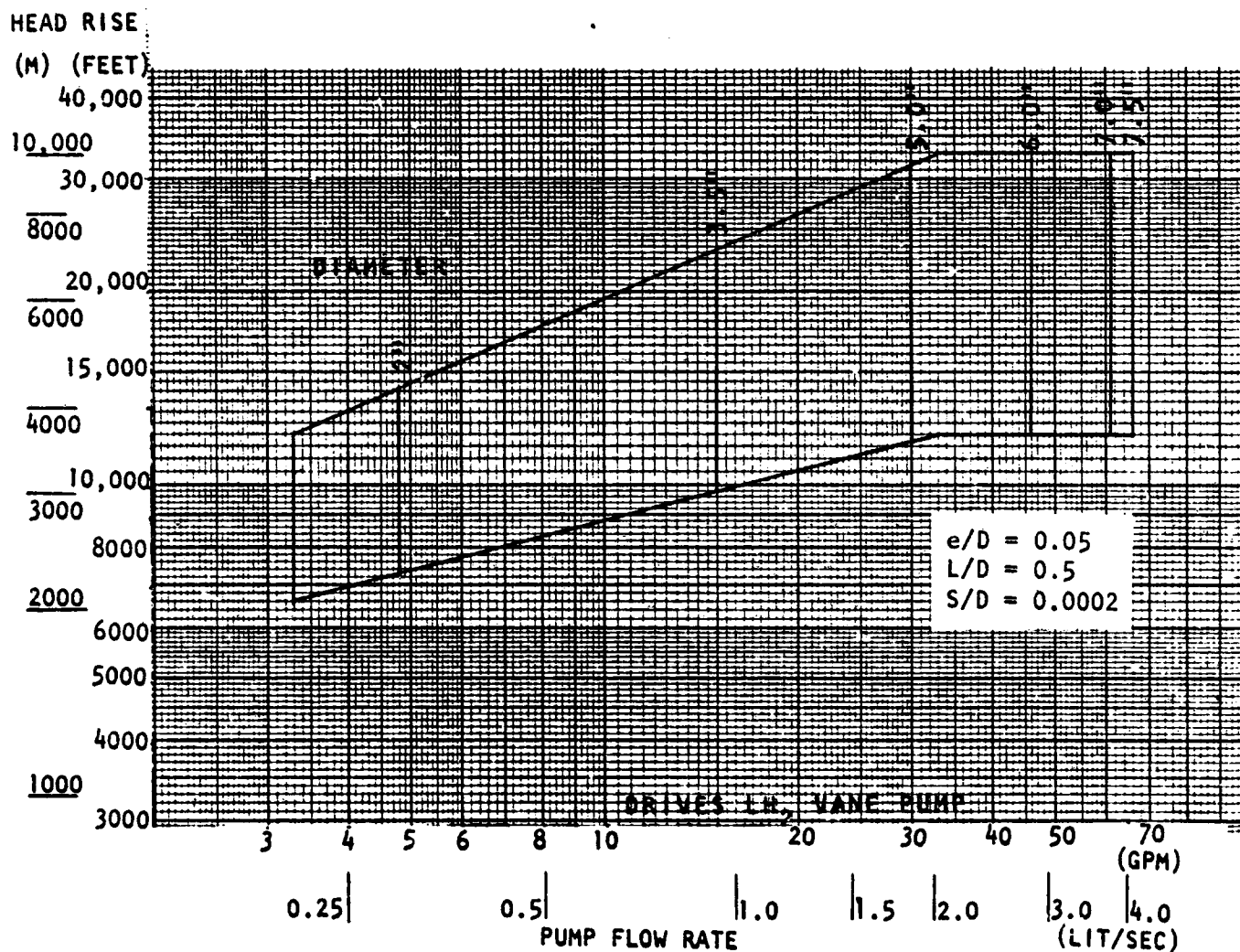


Figure A-183. Vane Expander for Vane Hydrogen Pump, Diameter
($P_1/P_2 = 1.3$)

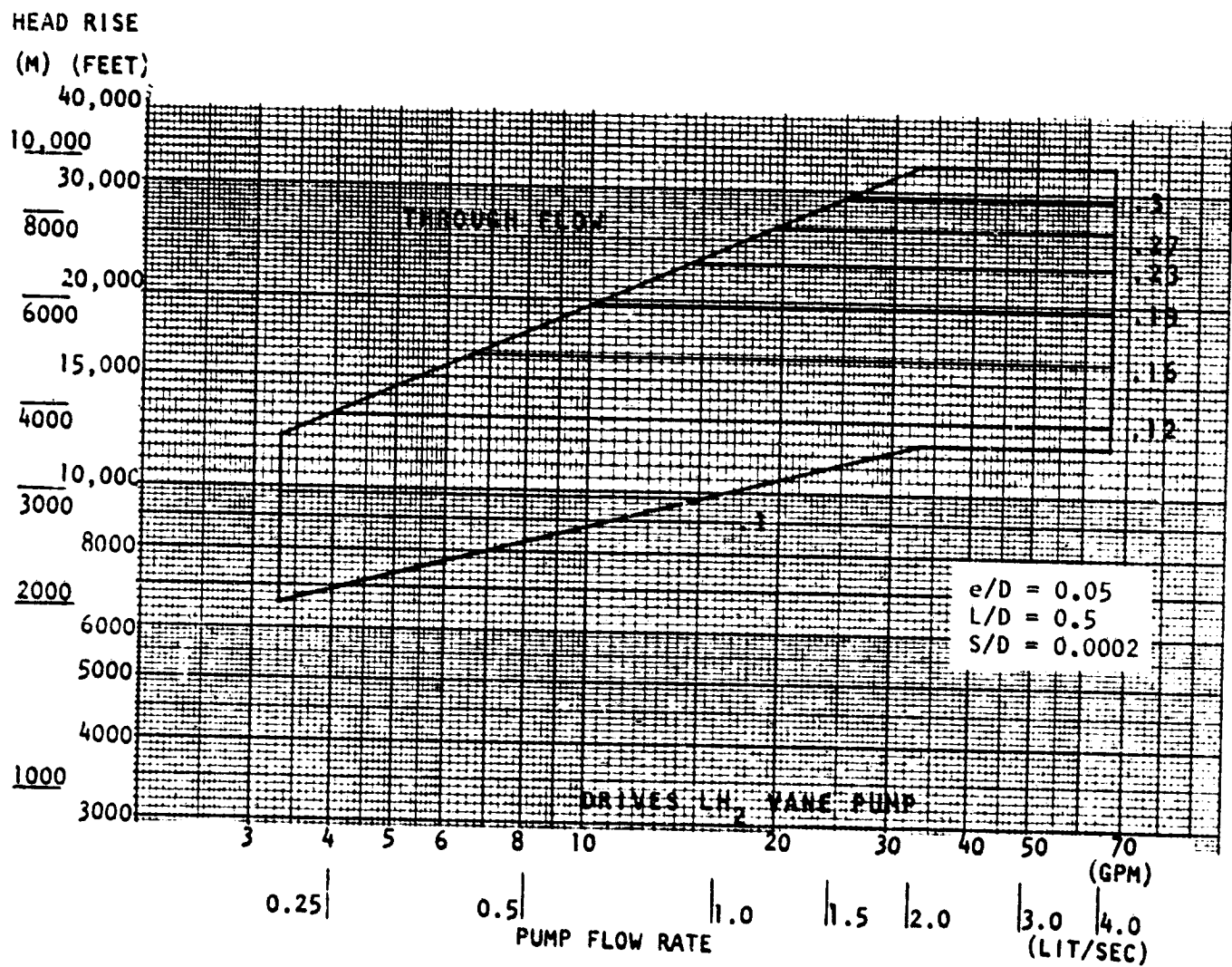


Figure A-184. Vane Expander for Vane Hydrogen Pump, Through Flow
($P_1/P_2 = 1.3$)

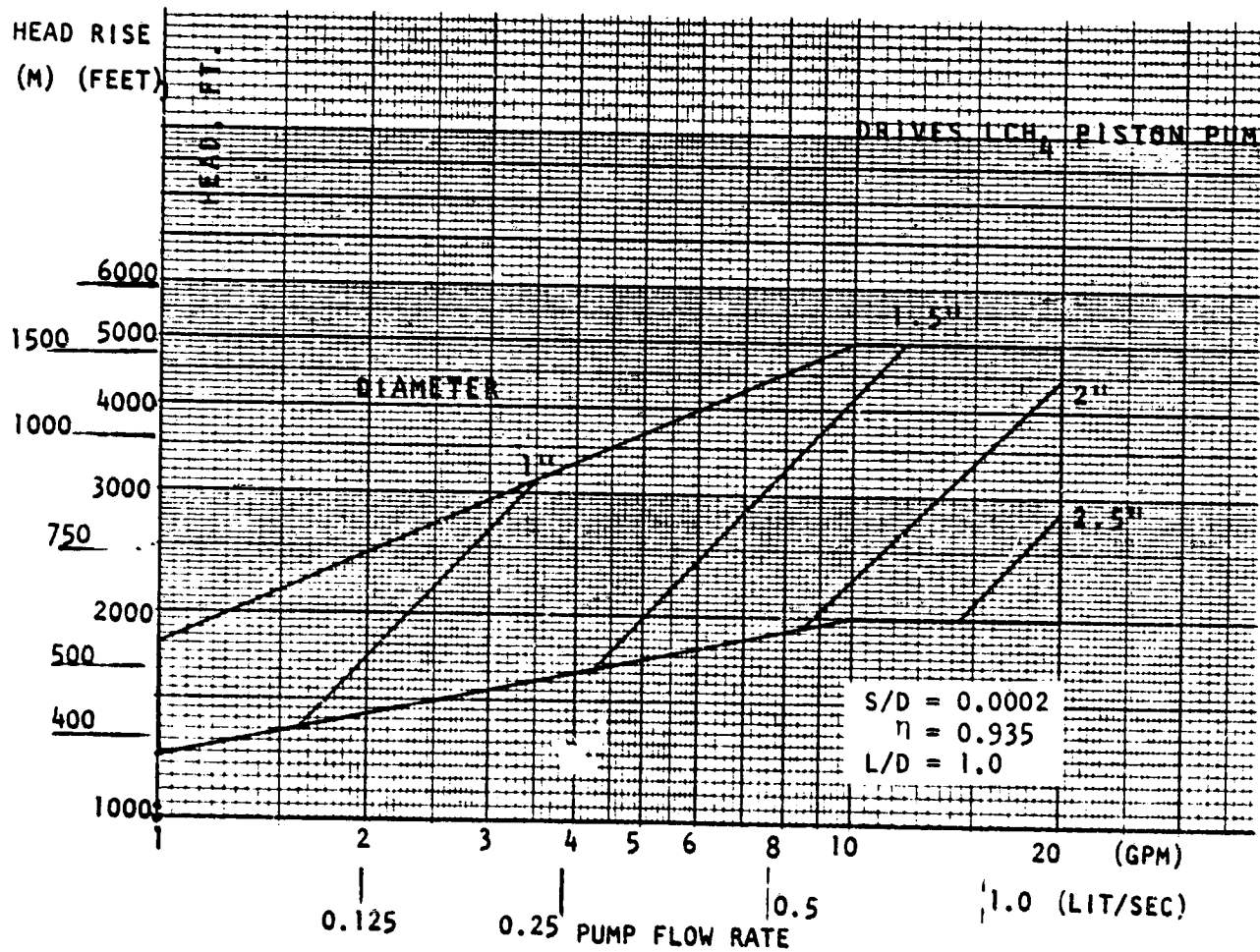


Figure A-185. Piston Expander for Piston Methane Pump, Diameter

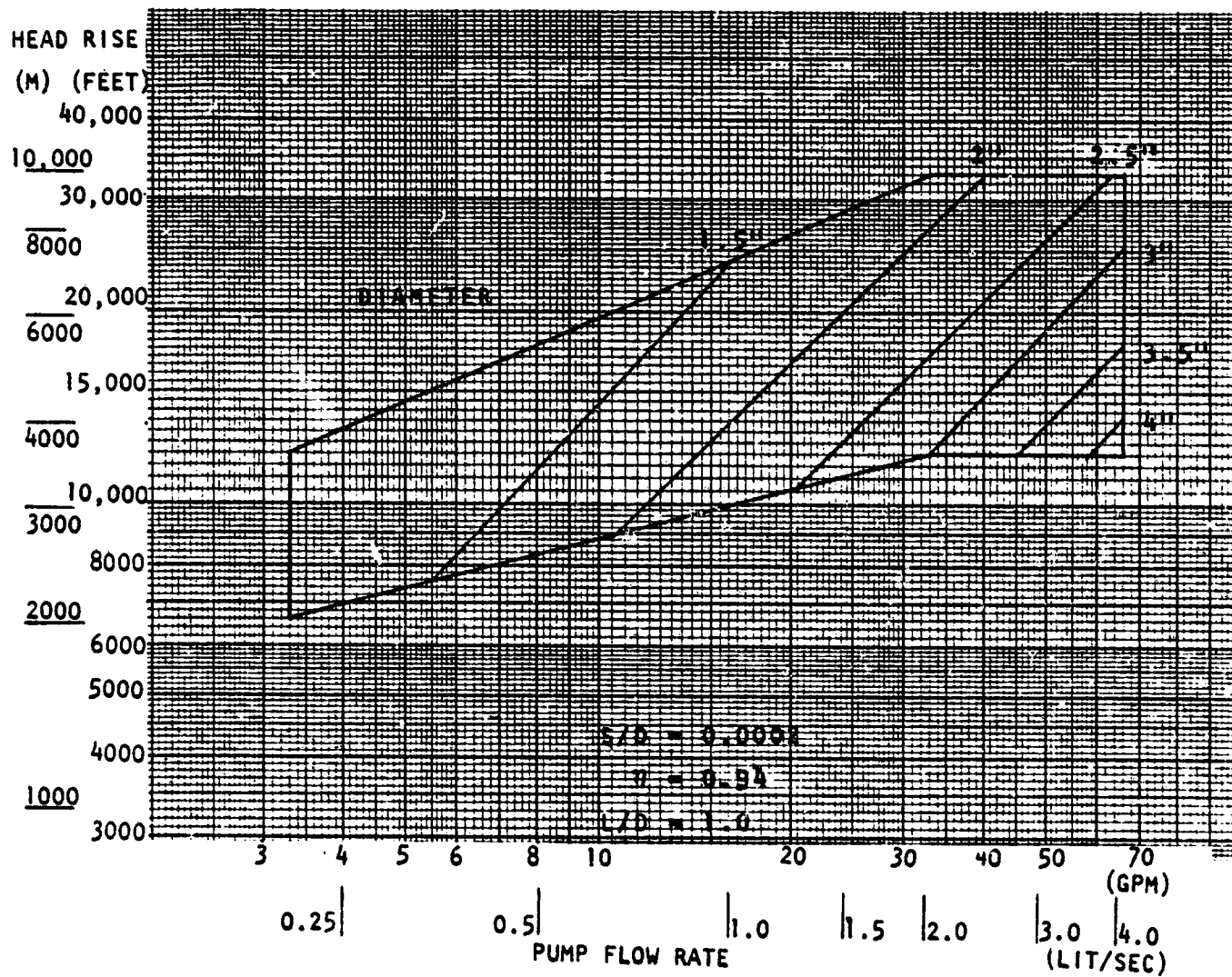


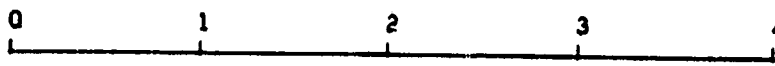
Figure A-186. Piston Expander for Piston Hydrogen Pump, Diameter

APPENDIX B

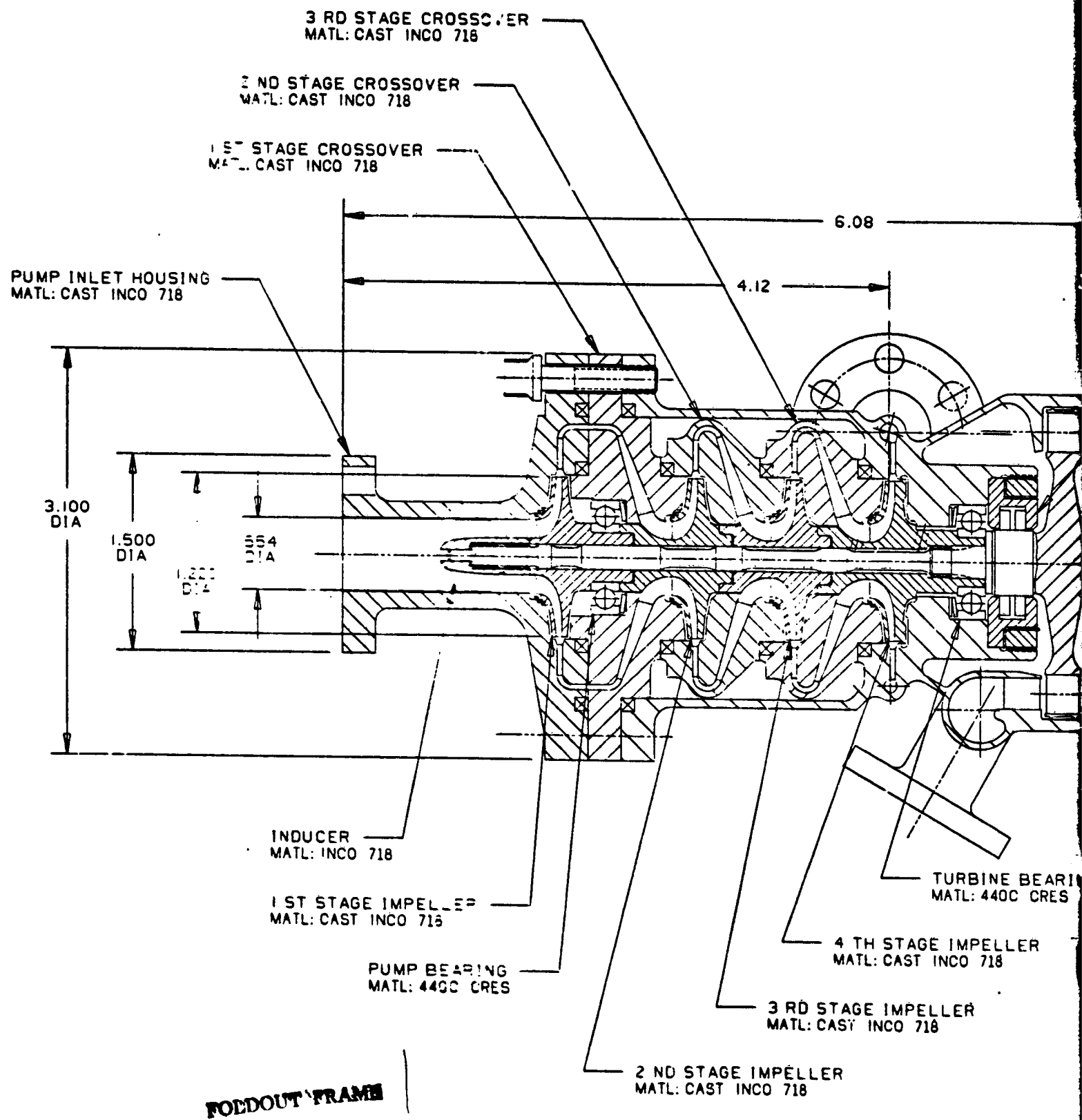
TASK III DRAWINGS

- Figure B-1. Design 1, Hydrogen Turbopump Assembly
- Figure B-2. Design 1, Exploded View, Hydrogen Turbopump
- Figure B-3. Design 2, Hydrogen Turbopump Assembly
- Figure B-4. Design 2, Exploded View, Hydrogen Turbopump
- Figure B-5. Design 3, Oxygen Turbopump Assembly
- Figure B-6. Design 3, Exploded View, Oxygen Turbopump
- Figure B-7. Design 4, Oxygen Turbopump Assembly
- Figure B-8. Design 4, Exploded View, Oxygen Turbopump
- Figure B-9. Design 5, Hydrogen Vane Pump-Motor Assembly
- Figure B-10. Design 6, Methane Piston Pump-Drive Assembly

PRECEDING PAGE BLANK NOT FILMED



SCALE: INCHES

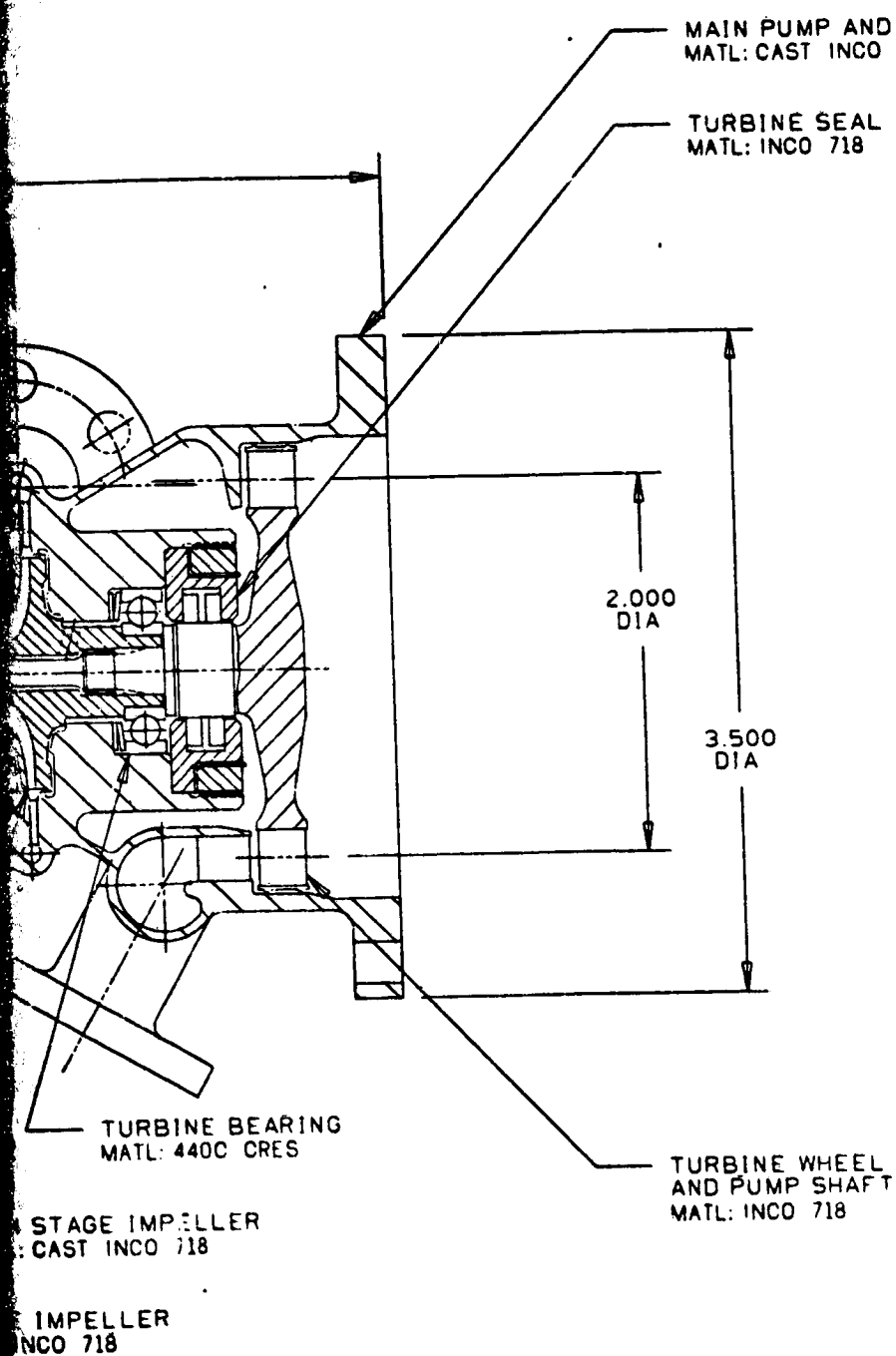


PODDOUT FRAME

PRECEDING PAGE BLANK NOT FILMED

NOTE: UNLESS OTHERWISE SPECIFIED

ON BMO MS		REVISIONS		DATE	APPROVED
REV	DESCRIPTION				
1	MAY BE REWORKED	3	RECORD CHANGE		
2	CANNOT BE REWORKED	4	NOW SHOP PRACTICE		
		5	PARTS MADE OK		



FOLDOUT FRAME

TURBOPUMP DESIGN 1

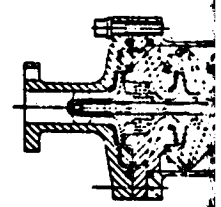
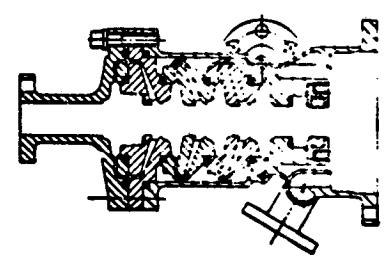
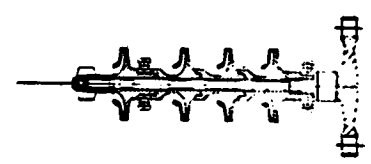
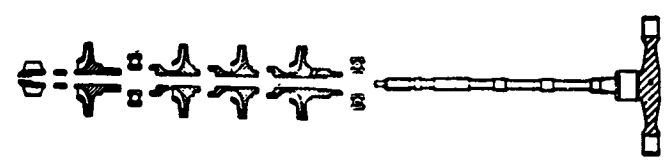
TYPE: 4 STAGE CENTRIFUGAL PUMP, AXIAL IMPULSE TURBINE
 SHAFT POWER= 17 HP
 N= 140,000 RPM
 PUMP:
 FLUID= LIQUID HYDROGEN
 Q= 9.9 GPM
 DELTA P= 950 PSI
 NPSH= 15 FT
 IMPELLER TIP WIDTH= .043 INCHES
 IMPELLER OD= 1.22 INCHES
 IMPELLER TIP SPEED= 745 FT PER SEC
 TURBINE:
 PERCENT ADMISSION= 7.0
 DRIVE GAS= GH2
 DRIVE GAS FLOW= .0926 POUNDS PER SEC
 INLET TEMP= 780 R
 DISCHARGE TEMP= 722 R
 INLET PRESSURE= 740 PSIA
 DISCHARGE PRESSURE= 479 PSIA
 PITCH DIA= 2.00 INCHES
 PITCH LINE VELOCITY= 1222 FT PER SEC
 BEARINGS:
 PUMP BEARING 10 MM. DN= 1.400.000
 TURBINE BEARING 10 MM. DN= 1.400.000

HEAT TREAT		UNLESS OTHERWISE SPECIFIED DIMENSIONS ARE IN INCHES AND APPLY PRIOR TO FINISH		CENTR		Figure B-1. Design 1, Hydrogen Turbopump Assembly	
FINISH		TOLERANCES ON ANGLES ± .01° DECIMALS ± .001" ± .002" ± .005" HOLES NOTED "DRILL"		DATE		DESIGN 1. HYDROGEN TURBOPUMP ASSEMBLY	
MATL		OVER THRU TOLERANCE		DATE		LOW THRUST CHEMICAL PROPULSION SYSTEM	
		0000 .0400 ± .0015 - .0010		DATE		SIZE PCLM NO DWG NO	
		0400 .1300 ± .0010 - .0010		DATE		D 02602	
		1300 .2200 ± .0015 - .0010		DATE		369	
		2200 .5000 ± .0010 - .0010		DATE		SCALE	
		5000 1.0000 ± .0010 - .0010		DATE		SHEET	
		1.0000 2.0000 ± .0120 - .0010		DATE			
		DO NOT SCALE PRINT					

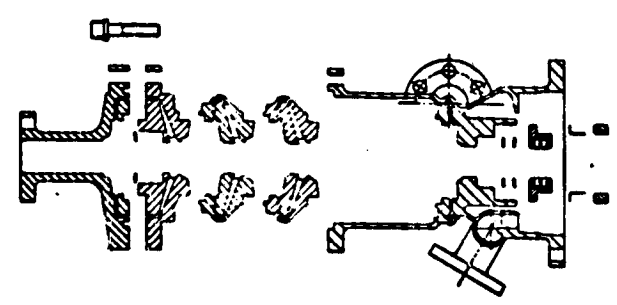
E
D
C
B
A

8 7 6 5 4

H
G
F
E
D
C
B
A



0 1 2 3



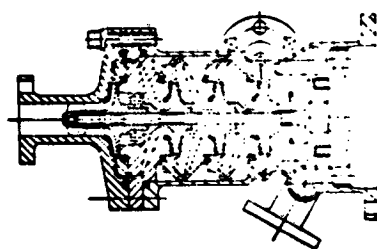
FOLDOUT FRAME

PRECEDING PAGE BLANK NOT FILMED

NOTE: UNLESS OTHERWISE SPECIFIED

8 7 6 5 4

REVISIONS		
REV	DESCRIPTION	DATE APPROVED
1	ONLY BE REMOVED	3 RECORD CHANGE
2	CANNOT BE REMOVED	4 NOW SHOP PRACTICE
3	PARTS MADE BY	



0 1 2 3 4 5 6 7
SCALE: INCHES

ORIGINAL PAGE IS
OF POOR QUALITY

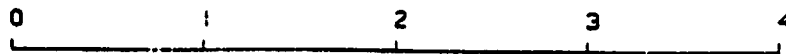
FOLDOUT FRAME

TURBOPUMP DESIGN 1
TYPE: 4 STAGE CENTRIFUGAL PUMP, AXIAL IMPULSE TURBINE
SHAFT POWER: 17 HP
N: 140,000 RPM
PUMP
FLUID: LIQUID HYDROGEN
Q: 8.8 GPM
DELTA P: 880 PSI
NPSH: 15 FT
IMPELLER TIP WIDTH: 0.43 INCHES
IMPELLER OD: 1.22 INCHES
IMPELLER TIP SPEED: 745 FT PER SEC
TURBINE
PERCENT ADMISSION: 7.0
DRIVE GAS: O₂
DRIVE GAS FLOW: 0.040 POUNDS PER SEC
INLET TEMP: 700 R
DISCHARGE TEMP: 722 R
INLET PRESSURE: 700 PSIA
DISCHARGE PRESSURE: 670 PSIA
PITCH DIA: 3.00 INCHES
PITCH LINE VELOCITY: 1222 FT PER SEC
BEARINGS
PUMP BEARING: 10 MM DIA 1,000,000
TURBINE BEARING: 10 MM DIA 1,000,000

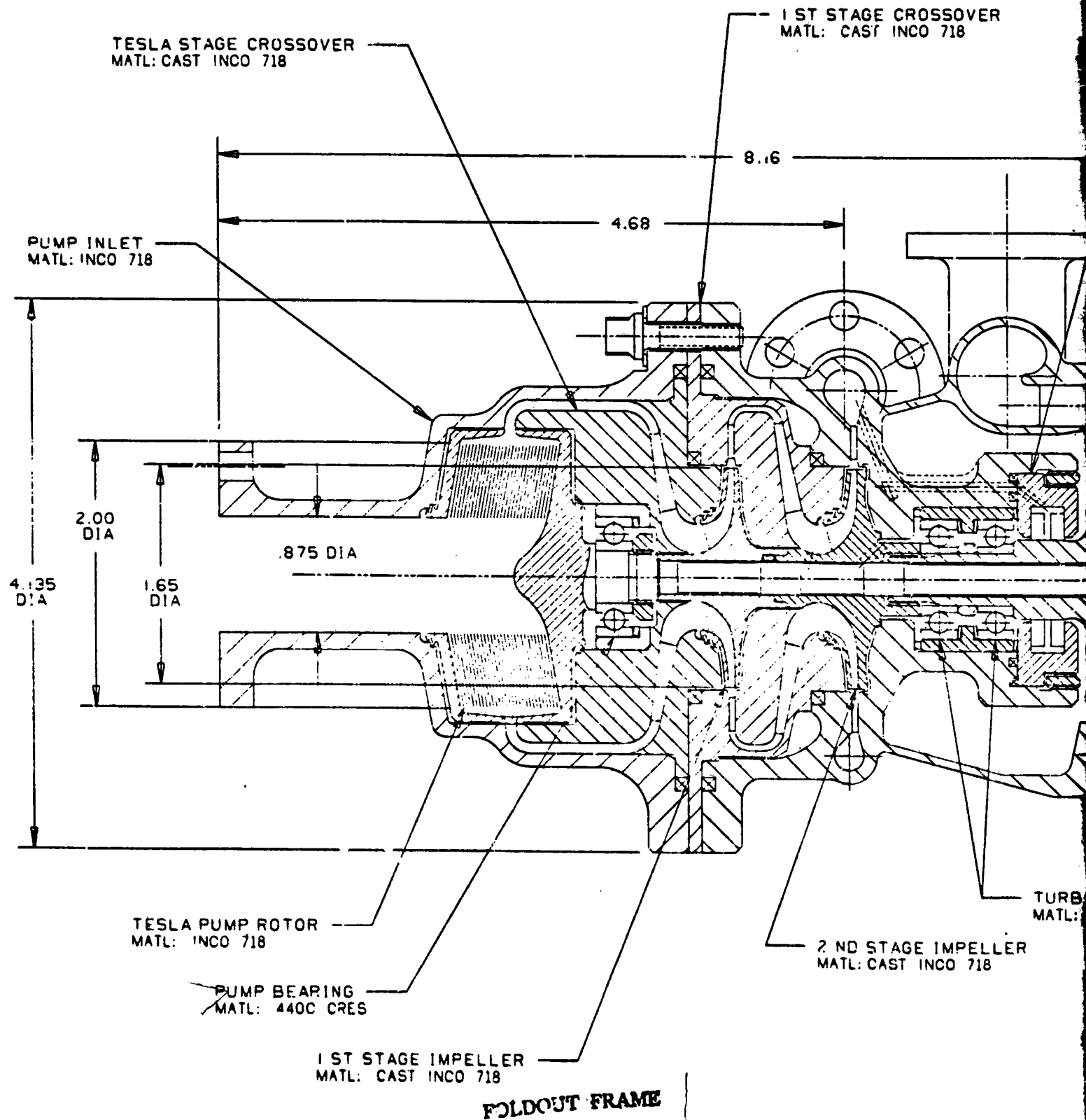
Figure B-2. Design 1, Exploded View,
Hydrogen Turbopump

DATE DRAWN CHECKED DESIGNED APPROVED BY	APPROVED VIEW UP LINE ASSEMBLY LOW THRUST CHEMICAL PRODUCTION SYSTEM
	E 02602
	371
	SCALE 1/1

NOTE: UNLESS OTHERWISE SPECIFIED



SCALE: INCHES



PRECEDING PAGE BLANK NOT FILMED

NOTE: UNLESS OTHERWISE SPECIFIED

REVISIONS			
REV	DESCRIPTION	DATE	APPROVED
1	MAY BE REWORKED		
2	CANNOT BE REWORKED		
3	RECORD CHANGE		
4	NOW SHOP PRACTICE		
5	PARTS MADE OK		

CROSSOVER
INCO 718

TURBINE SEAL
MATL: INCO 718

MAIN PUMP AND TURBINE HOUSING
MATL: CAST INCO 718

2.625
DIA

4.200
DIA

FOLDOUT FRAME

TURBINE BEARING
MATL: 440C CRES

TURBINE WHEEL
MATL: INCO 718

AGE IMPELLER
INCO 718

TURBOPUMP DESIGN 2

TYPE: TESLA - 2 CENTRIFUGAL STAGES PUMP, AXIAL IMPULSE TURBINE
SHAFT POWER= 58.6 HP
N= 110,000 RPM

PUMP:

FLUID= LIQUID HYDROGEN
Q= 50 GPM
DELTA P= 950 PSI
NPSH= 15 FT
IMPELLER TIP WIDTH= .045 INCHES
IMPELLER OD= 1.65 INCHES
IMPELLER TIP SPEED= 792 FT PER SEC
TESLA TIP SPEED= 950 FT PER SEC

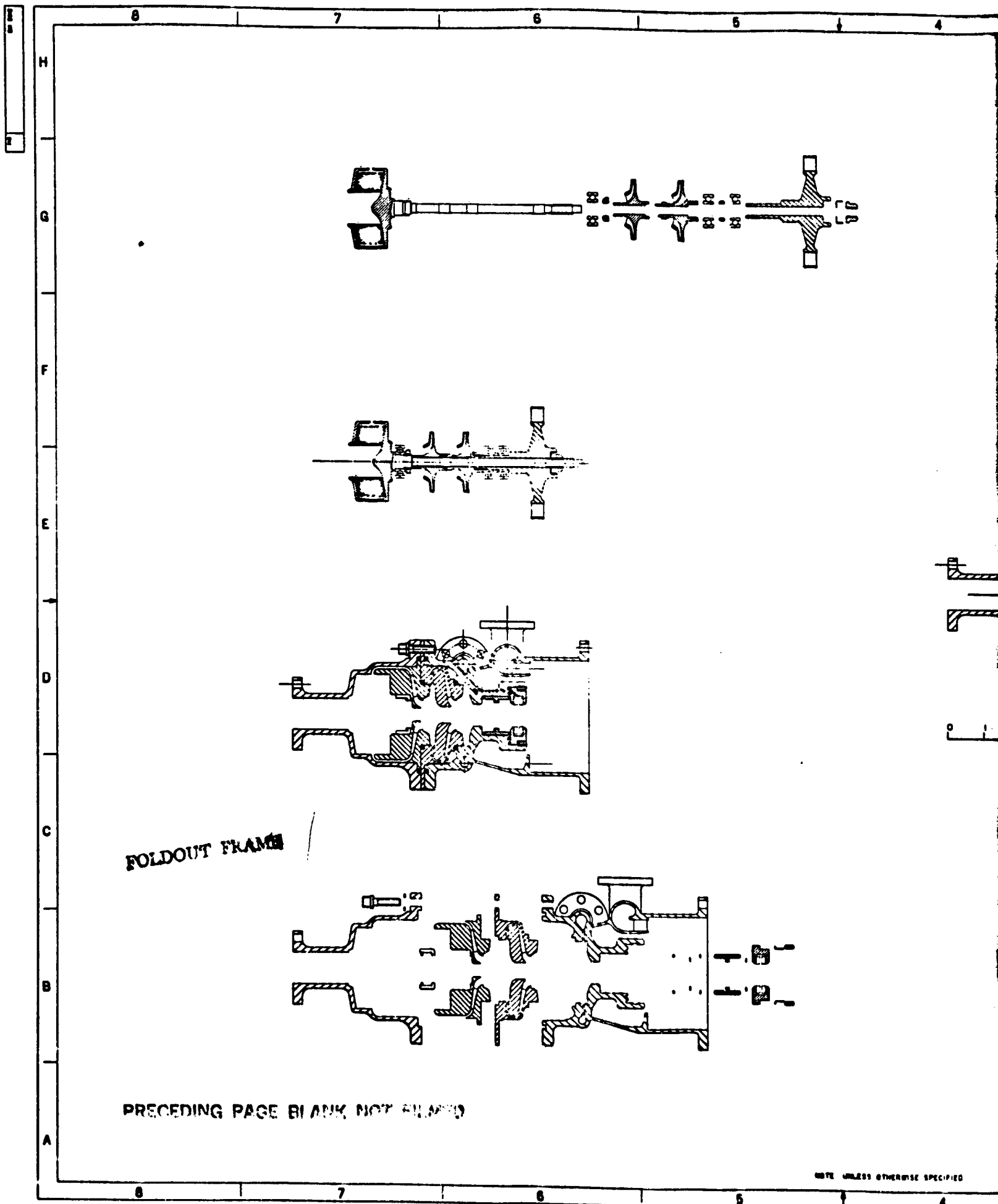
TURBINE:

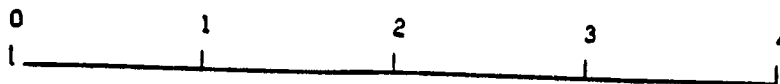
PERCENT ADMISSION= 30
DRIVE GAS= GM2
DRIVE GAS FLOW= .468 POUNDS PER SEC
INLET TEMP= 780 R
DISCHARGE TEMP= 754 R
INLET PRESSURE= 655 PSIA
DISCHARGE PRESSURE= 533 PSIA
PITCH DIA= 2.625 INCHES
PITCH LINE VELOCITY= 1260 FT PER SEC

BEARINGS:

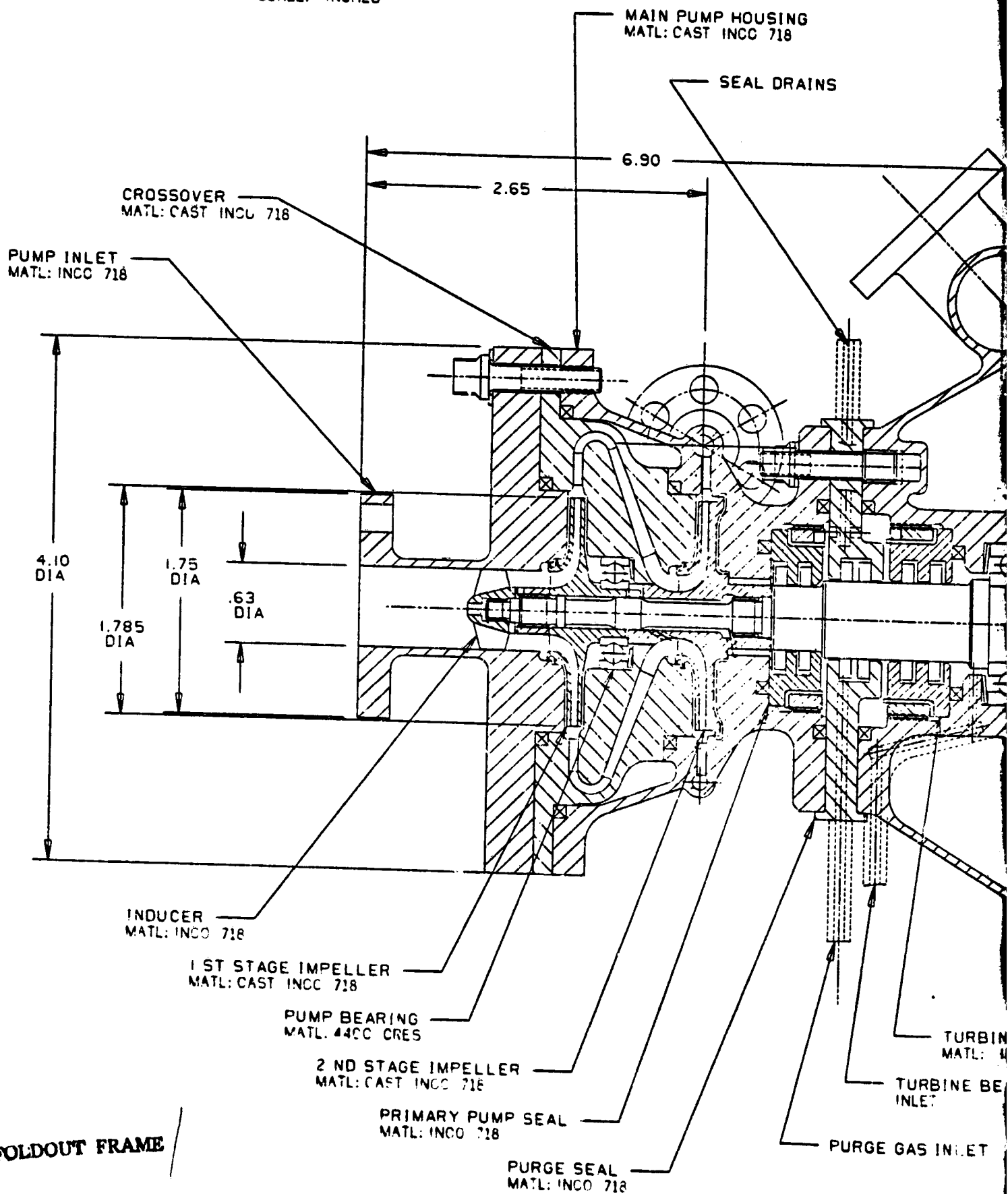
PUMP BEARING 10 MM. DN= 1,100,000
TURBINE BEARING 10 MM. DN= 1,100,000

HEAT TREAT	UNLESS OTHERWISE SPECIFIED DIMENSIONS ARE IN INCHES AND APPLY PRIOR TO FINISH 125/ MACH SURF ROUGHNESS	CONTR		Rockwell International Corporation Rockatdyne Division			
		DWN R SWAIAA DATE		Figure B-3. Design 2, Hydrogen Turbopump Assembly			
FINISH	TOLERANCES ON ANGLES OF 10 DECIMALS EX 2.51 EX 2.010 HOLDS NOTED "DRILL"	CHN		LOW THRUST CHEMICAL PROPULSION SYSTEM			
		DSGN		373			
MATL	OVER THRU TOLERANCE 0000 0400 + 0015 - 0010 0400 1300 + 0030 - 0010 1300 2250 + 0045 - 0010 2250 5000 + 0050 - 0010 5000 7500 + 0010 - 0010 7500 10000 + 0020 - 0010 10000 20000 + 0.20 0010	MATL		DO NOT SCALE PRINT			
		STRUCT		SCALE			
		DESIGN ACTIVITY APD DATE		SIZE FSCM NO DWG NO		SHEET	
				D 02602			





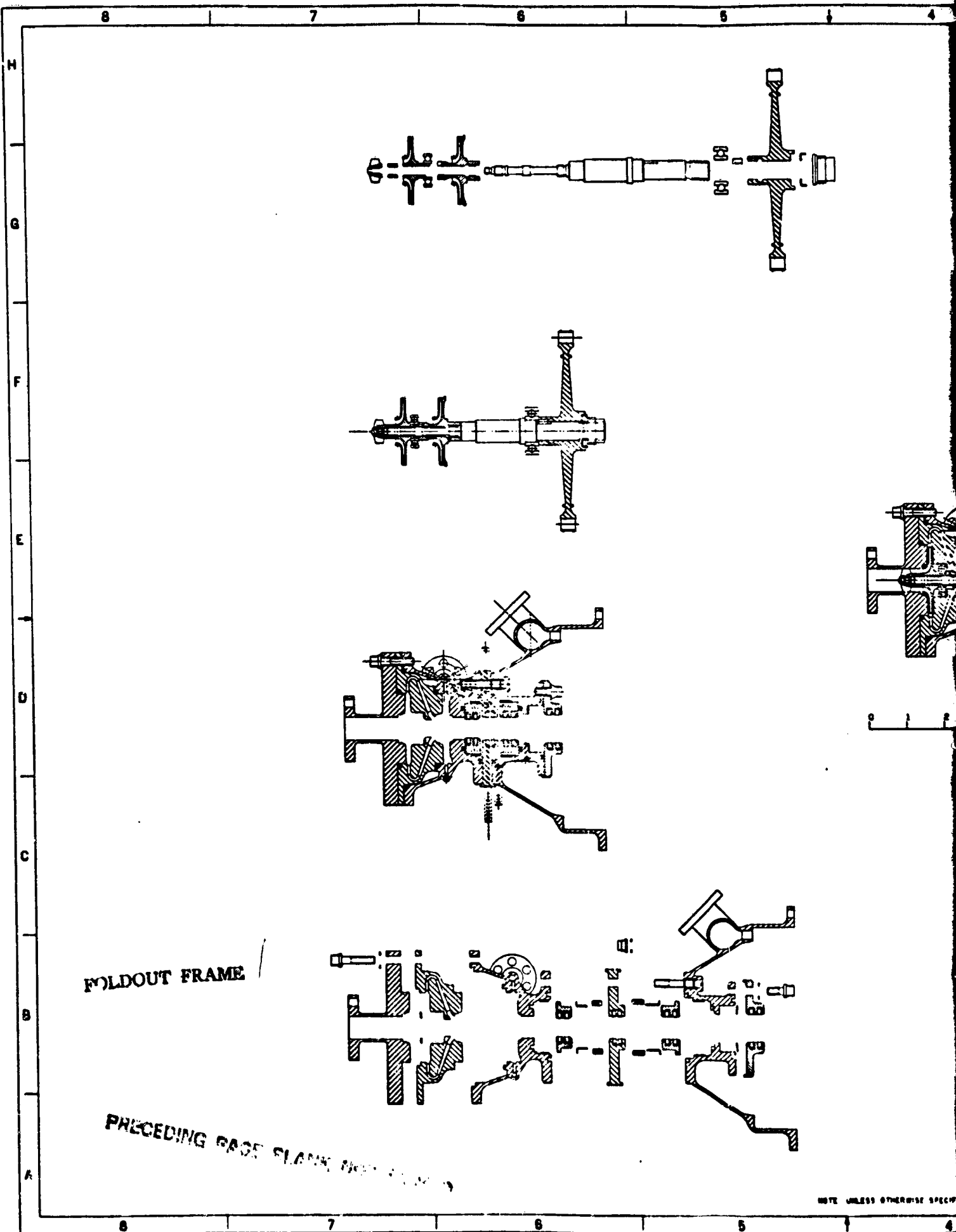
SCALE: INCHES



FOLDOUT FRAME

PRECEDING PAGE BLANK, NOT FILLED

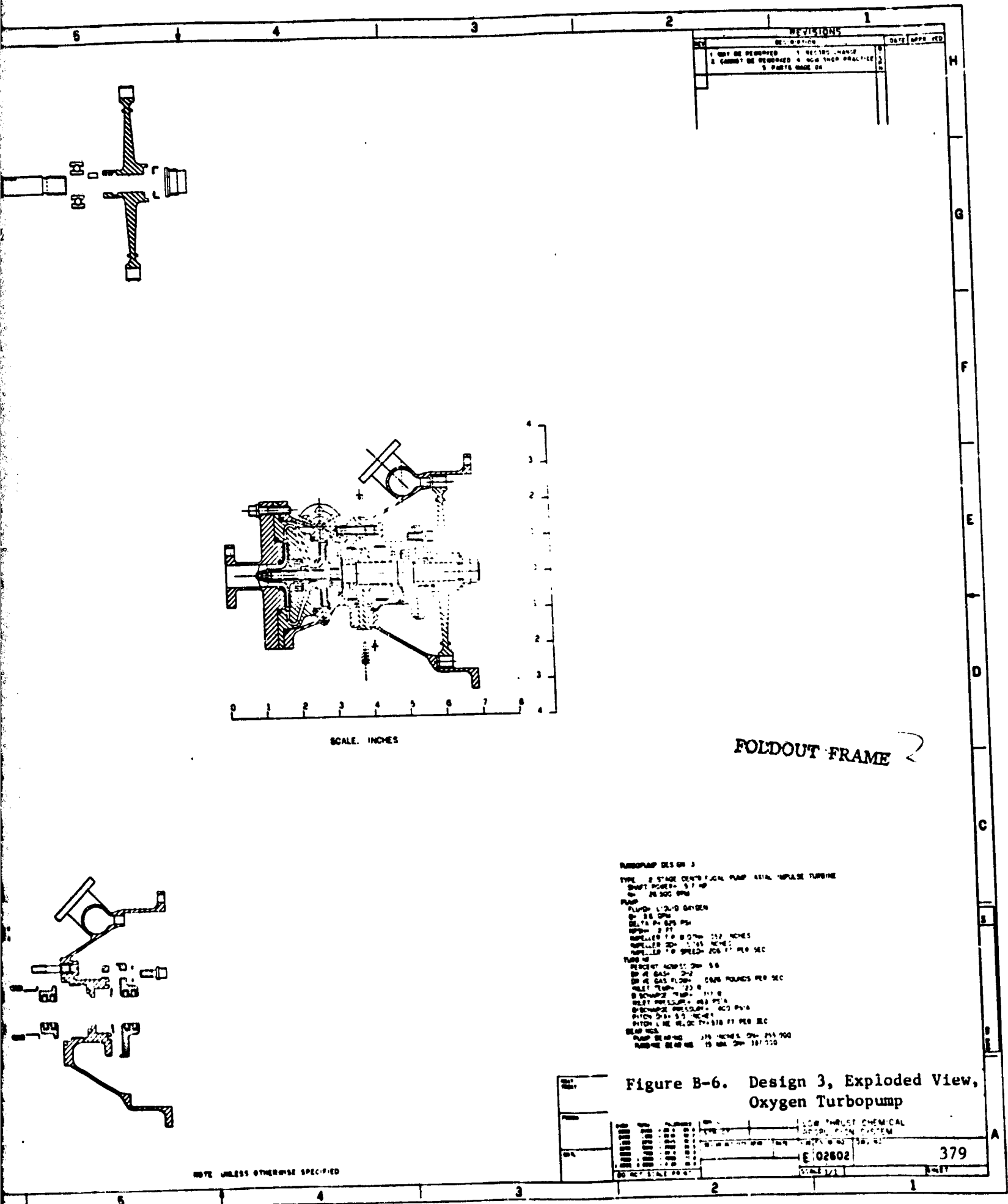
NOTE: UNLESS OTHERWISE SPECIFIED

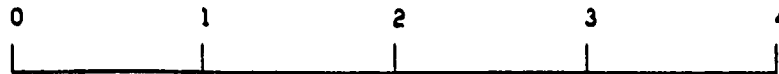


FOLDOUT FRAME

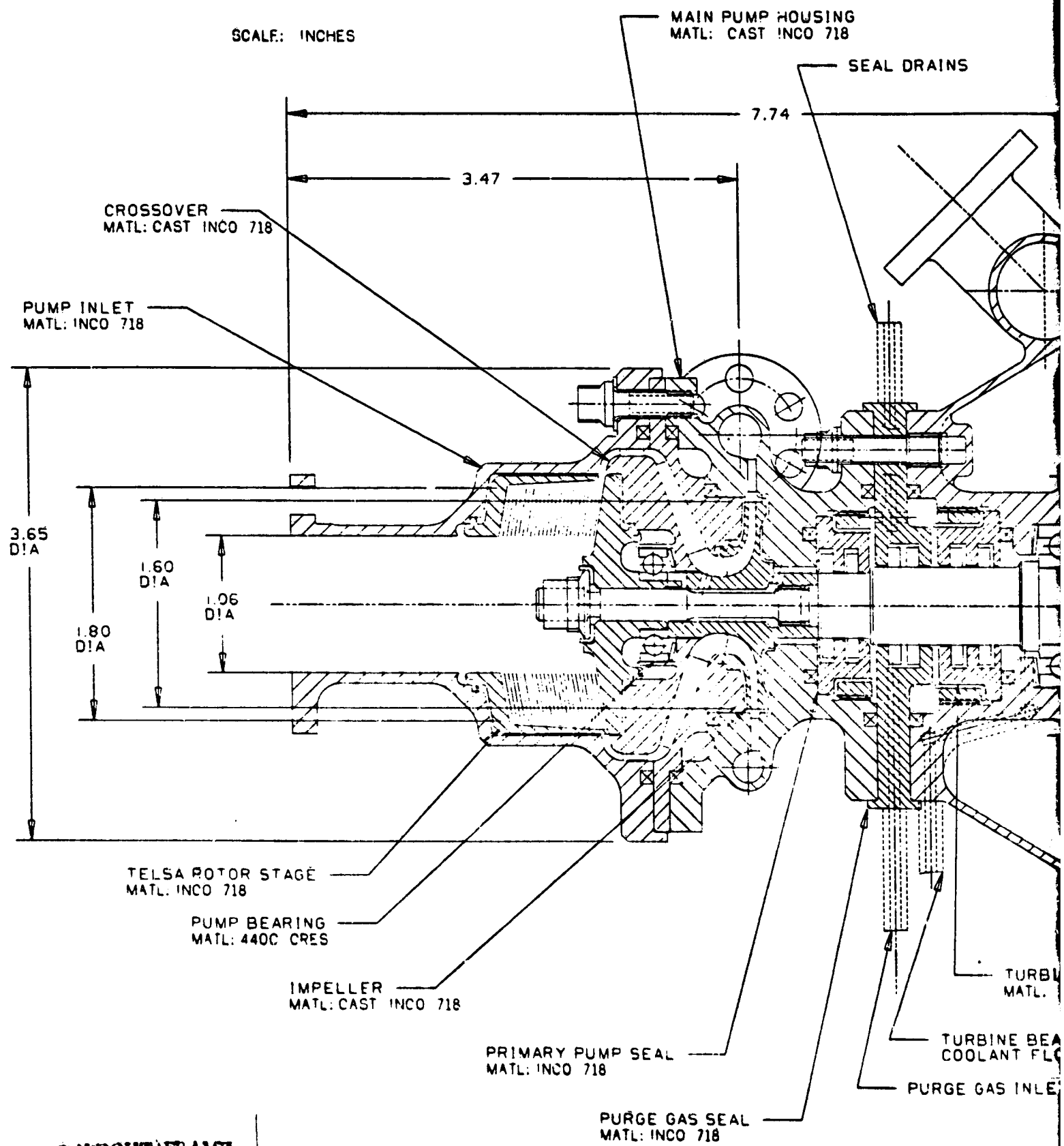
PRECEDING PAGE SLANK NOT SHOWN

NOTE: UNLESS OTHERWISE SPECIFIED





SCALE: INCHES



BOLDOUT FRAME

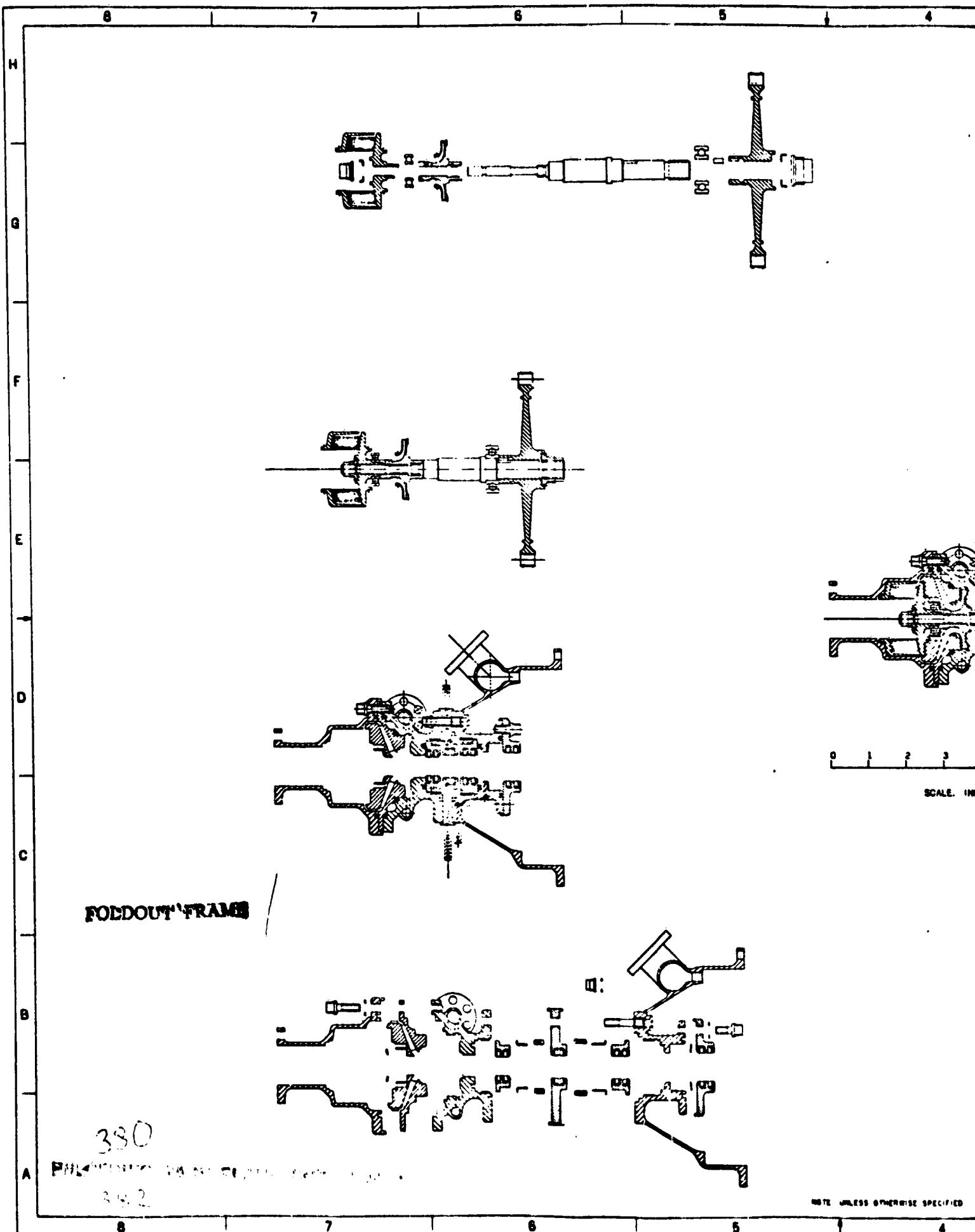
NOTE: UNLESS OTHERWISE SPECIFIED

DRAINS



HEAT TREAT	UNLESS OTHERWISE SPECIFIED DIMENSIONS ARE IN INCHES AND FINISH IS TO BE AS SHOWN 12/ MACH SURF ROUGHNESS:	CONTR	Rockwell International Corporation Ruckelshyne Division		
		DWG NO. 5	DATE	Figure B-7. Design 4, Oxygen Turbopump Assembly	
FINISH	TOLERANCES ON ANGLES ± 10° UNLESS NOTED OTHERWISE UNLESS NOTED OTHERWISE	CHK	DSGN		
		MATL	LOW THRUST CHEMICAL PROPULSION SYSTEM		
MATERIAL	OVER THIS TOLERANCE 0.000 0.000 ± 0.015 - 0.010 0.002 0.000 ± 0.010 - 0.010 0.005 0.000 ± 0.010 - 0.010 0.010 0.000 ± 0.010 - 0.010 0.015 0.000 ± 0.010 - 0.010 0.020 0.000 ± 0.010 - 0.010 0.025 0.000 ± 0.010 - 0.010 0.030 0.000 ± 0.010 - 0.010 0.035 0.000 ± 0.010 - 0.010 0.040 0.000 ± 0.010 - 0.010 0.045 0.000 ± 0.010 - 0.010 0.050 0.000 ± 0.010 - 0.010 0.055 0.000 ± 0.010 - 0.010 0.060 0.000 ± 0.010 - 0.010 0.065 0.000 ± 0.010 - 0.010 0.070 0.000 ± 0.010 - 0.010 0.075 0.000 ± 0.010 - 0.010 0.080 0.000 ± 0.010 - 0.010 0.085 0.000 ± 0.010 - 0.010 0.090 0.000 ± 0.010 - 0.010 0.095 0.000 ± 0.010 - 0.010 0.100 0.000 ± 0.010 - 0.010 0.105 0.000 ± 0.010 - 0.010 0.110 0.000 ± 0.010 - 0.010 0.115 0.000 ± 0.010 - 0.010 0.120 0.000 ± 0.010 - 0.010 0.125 0.000 ± 0.010 - 0.010 0.130 0.000 ± 0.010 - 0.010 0.135 0.000 ± 0.010 - 0.010 0.140 0.000 ± 0.010 - 0.010 0.145 0.000 ± 0.010 - 0.010 0.150 0.000 ± 0.010 - 0.010 0.155 0.000 ± 0.010 - 0.010 0.160 0.000 ± 0.010 - 0.010 0.165 0.000 ± 0.010 - 0.010 0.170 0.000 ± 0.010 - 0.010 0.175 0.000 ± 0.010 - 0.010 0.180 0.000 ± 0.010 - 0.010 0.185 0.000 ± 0.010 - 0.010 0.190 0.000 ± 0.010 - 0.010 0.195 0.000 ± 0.010 - 0.010 0.200 0.000 ± 0.010 - 0.010 0.205 0.000 ± 0.010 - 0.010 0.210 0.000 ± 0.010 - 0.010 0.215 0.000 ± 0.010 - 0.010 0.220 0.000 ± 0.010 - 0.010 0.225 0.000 ± 0.010 - 0.010 0.230 0.000 ± 0.010 - 0.010 0.235 0.000 ± 0.010 - 0.010 0.240 0.000 ± 0.010 - 0.010 0.245 0.000 ± 0.010 - 0.010 0.250 0.000 ± 0.010 - 0.010 0.255 0.000 ± 0.010 - 0.010 0.260 0.000 ± 0.010 - 0.010 0.265 0.000 ± 0.010 - 0.010 0.270 0.000 ± 0.010 - 0.010 0.275 0.000 ± 0.010 - 0.010 0.280 0.000 ± 0.010 - 0.010 0.285 0.000 ± 0.010 - 0.010 0.290 0.000 ± 0.010 - 0.010 0.295 0.000 ± 0.010 - 0.010 0.300 0.000 ± 0.010 - 0.010 0.305 0.000 ± 0.010 - 0.010 0.310 0.000 ± 0.010 - 0.010 0.315 0.000 ± 0.010 - 0.010 0.320 0.000 ± 0.010 - 0.010 0.325 0.000 ± 0.010 - 0.010 0.330 0.000 ± 0.010 - 0.010 0.335 0.000 ± 0.010 - 0.010 0.340 0.000 ± 0.010 - 0.010 0.345 0.000 ± 0.010 - 0.010 0.350 0.000 ± 0.010 - 0.010 0.355 0.000 ± 0.010 - 0.010 0.360 0.000 ± 0.010 - 0.010 0.365 0.000 ± 0.010 - 0.010 0.370 0.000 ± 0.010 - 0.010 0.375 0.000 ± 0.010 - 0.010 0.380 0.000 ± 0.010 - 0.010 0.385 0.000 ± 0.010 - 0.010 0.390 0.000 ± 0.010 - 0.010 0.395 0.000 ± 0.010 - 0.010 0.400 0.000 ± 0.010 - 0.010 0.405 0.000 ± 0.010 - 0.010 0.410 0.000 ± 0.010 - 0.010 0.415 0.000 ± 0.010 - 0.010 0.420 0.000 ± 0.010 - 0.010 0.425 0.000 ± 0.010 - 0.010 0.430 0.000 ± 0.010 - 0.010 0.435 0.000 ± 0.010 - 0.010 0.440 0.000 ± 0.010 - 0.010 0.445 0.000 ± 0.010 - 0.010 0.450 0.000 ± 0.010 - 0.010 0.455 0.000 ± 0.010 - 0.010 0.460 0.000 ± 0.010 - 0.010 0.465 0.000 ± 0.010 - 0.010 0.470 0.000 ± 0.010 - 0.010 0.475 0.000 ± 0.010 - 0.010 0.480 0.000 ± 0.010 - 0.010 0.485 0.000 ± 0.010 - 0.010 0.490 0.000 ± 0.010 - 0.010 0.495 0.000 ± 0.010 - 0.010 0.500 0.000 ± 0.010 - 0.010 0.505 0.000 ± 0.010 - 0.010 0.510 0.000 ± 0.010 - 0.010 0.515 0.000 ± 0.010 - 0.010 0.520 0.000 ± 0.010 - 0.010 0.525 0.000 ± 0.010 - 0.010 0.530 0.000 ± 0.010 - 0.010 0.535 0.000 ± 0.010 - 0.010 0.540 0.000 ± 0.010 - 0.010 0.545 0.000 ± 0.010 - 0.010 0.550 0.000 ± 0.010 - 0.010 0.555 0.000 ± 0.010 - 0.010 0.560 0.000 ± 0.010 - 0.010 0.565 0.000 ± 0.010 - 0.010 0.570 0.000 ± 0.010 - 0.010 0.575 0.000 ± 0.010 - 0.010 0.580 0.000 ± 0.010 - 0.010 0.585 0.000 ± 0.010 - 0.010 0.590 0.000 ± 0.010 - 0.010 0.595 0.000 ± 0.010 - 0.010 0.600 0.000 ± 0.010 - 0.010 0.605 0.000 ± 0.010 - 0.010 0.610 0.000 ± 0.010 - 0.010 0.615 0.000 ± 0.010 - 0.010 0.620 0.000 ± 0.010 - 0.010 0.625 0.000 ± 0.010 - 0.010 0.630 0.000 ± 0.010 - 0.010 0.635 0.000 ± 0.010 - 0.010 0.640 0.000 ± 0.010 - 0.010 0.645 0.000 ± 0.010 - 0.010 0.650 0.000 ± 0.010 - 0.010 0.655 0.000 ± 0.010 - 0.010 0.660 0.000 ± 0.010 - 0.010 0.665 0.000 ± 0.010 - 0.010 0.670 0.000 ± 0.010 - 0.010 0.675 0.000 ± 0.010 - 0.010 0.680 0.000 ± 0.010 - 0.010 0.685 0.000 ± 0.010 - 0.010 0.690 0.000 ± 0.010 - 0.010 0.695 0.000 ± 0.010 - 0.010 0.700 0.000 ± 0.010 - 0.010 0.705 0.000 ± 0.010 - 0.010 0.710 0.000 ± 0.010 - 0.010 0.715 0.000 ± 0.010 - 0.010 0.720 0.000 ± 0.010 - 0.010 0.725 0.000 ± 0.010 - 0.010 0.730 0.000 ± 0.010 - 0.010 0.735 0.000 ± 0.010 - 0.010 0.740 0.000 ± 0.010 - 0.010 0.745 0.000 ± 0.010 - 0.010 0.750 0.000 ± 0.010 - 0.010 0.755 0.000 ± 0.010 - 0.010 0.760 0.000 ± 0.010 - 0.010 0.765 0.000 ± 0.010 - 0.010 0.770 0.000 ± 0.010 - 0.010 0.775 0.000 ± 0.010 - 0.010 0.780 0.000 ± 0.010 - 0.010 0.785 0.000 ± 0.010 - 0.010 0.790 0.000 ± 0.010 - 0.010 0.795 0.000 ± 0.010 - 0.010 0.800 0.000 ± 0.010 - 0.010 0.805 0.000 ± 0.010 - 0.010 0.810 0.000 ± 0.010 - 0.010 0.815 0.000 ± 0.010 - 0.010 0.820 0.000 ± 0.010 - 0.010 0.825 0.000 ± 0.010 - 0.010 0.830 0.000 ± 0.010 - 0.010 0.835 0.000 ± 0.010 - 0.010 0.840 0.000 ± 0.010 - 0.010 0.845 0.000 ± 0.010 - 0.010 0.850 0.000 ± 0.010 - 0.010 0.855 0.000 ± 0.010 - 0.010 0.860 0.000 ± 0.010 - 0.010 0.865 0.000 ± 0.010 - 0.010 0.870 0.000 ± 0.010 - 0.010 0.875 0.000 ± 0.010 - 0.010 0.880 0.000 ± 0.010 - 0.010 0.885 0.000 ± 0.010 - 0.010 0.890 0.000 ± 0.010 - 0.010 0.895 0.000 ± 0.010 - 0.010 0.900 0.000 ± 0.010 - 0.010 0.905 0.000 ± 0.010 - 0.010 0.910 0.000 ± 0.010 - 0.010 0.915 0.000 ± 0.010 - 0.010 0.920 0.000 ± 0.010 - 0.010 0.925 0.000 ± 0.010 - 0.010 0.930 0.000 ± 0.010 - 0.010 0.935 0.000 ± 0.010 - 0.010 0.940 0.000 ± 0.010 - 0.010 0.945 0.000 ± 0.010 - 0.010 0.950 0.000 ± 0.010 - 0.010 0.955 0.000 ± 0.010 - 0.010 0.960 0.000 ± 0.010 - 0.010 0.965 0.000 ± 0.010 - 0.010 0.970 0.000 ± 0.010 - 0.010 0.975 0.000 ± 0.010 - 0.010 0.980 0.000 ± 0.010 - 0.010 0.985 0.000 ± 0.010 - 0.010 0.990 0.000 ± 0.010 - 0.010 0.995 0.000 ± 0.010 - 0.010 1.000 0.000 ± 0.010 - 0.010 1.005 0.000 ± 0.010 - 0.010 1.010 0.000 ± 0.010 - 0.010 1.015 0.000 ± 0.010 - 0.010 1.020 0.000 ± 0.010 - 0.010 1.025 0.000 ± 0.010 - 0.010 1.030 0.000 ± 0.010 - 0.010 1.035 0.000 ± 0.010 - 0.010 1.040 0.000 ± 0.010 - 0.010 1.045 0.000 ± 0.010 - 0.010 1.050 0.000 ± 0.010 - 0.010 1.055 0.000 ± 0.010 - 0.010 1.060 0.000 ± 0.010 - 0.010 1.065 0.000 ± 0.010 - 0.010 1.070 0.000 ± 0.010 - 0.010 1.075 0.000 ± 0.010 - 0.010 1.080 0.000 ± 0.010 - 0.010 1.085 0.000 ± 0.010 - 0.010 1.090 0.000 ± 0.010 - 0.010 1.095 0.000 ± 0.010 - 0.010 1.100 0.000 ± 0.010 - 0.010 1.105 0.000 ± 0.010 - 0.010 1.110 0.000 ± 0.010 - 0.010 1.115 0.000 ± 0.010 - 0.010 1.120 0.000 ± 0.010 - 0.010 1.125 0.000 ± 0.010 - 0.010 1.130 0.000 ± 0.010 - 0.010 1.135 0.000 ± 0.010 - 0.010 1.140 0.000 ± 0.010 - 0.010 1.145 0.000 ± 0.010 - 0.010 1.150 0.000 ± 0.010 - 0.010 1.155 0.000 ± 0.010 - 0.010 1.160 0.000 ± 0.010 - 0.010 1.165 0.000 ± 0.010 - 0.010 1.170 0.000 ± 0.010 - 0.010 1.175 0.000 ± 0.010 - 0.010 1.180 0.000 ± 0.010 - 0.010 1.185 0.000 ± 0.010 - 0.010 1.190 0.000 ± 0.010 - 0.010 1.195 0.000 ± 0.010 - 0.010 1.200 0.000 ± 0.010 - 0.010 1.205 0.000 ± 0.010 - 0.010 1.210 0.000 ± 0.010 - 0.010 1.215 0.000 ± 0.010 - 0.010 1.220 0.000 ± 0.010 - 0.010 1.225 0.000 ± 0.010 - 0.010 1.230 0.000 ± 0.010 - 0.010 1.235 0.000 ± 0.010 - 0.010 1.240 0.000 ± 0.010 - 0.010 1.245 0.000 ± 0.010 - 0.010 1.250 0.000 ± 0.010 - 0.010 1.255 0.000 ± 0.010 - 0.010 1.260 0.000 ± 0.010 - 0.010 1.265 0.000 ± 0.010 - 0.010 1.270 0.000 ± 0.010 - 0.010 1.275 0.000 ± 0.010 - 0.010 1.280 0.000 ± 0.010 - 0.010 1.285 0.000 ± 0.010 - 0.010 1.290 0.000 ± 0.010 - 0.010 1.295 0.000 ± 0.010 - 0.010 1.300 0.000 ± 0.010 - 0.010 1.305 0.000 ± 0.010 - 0.010 1.310 0.000 ± 0.010 - 0.010 1.315 0.000 ± 0.010 - 0.010 1.320 0.000 ± 0.010 - 0.010 1.325 0.000 ± 0.010 - 0.010 1.330 0.000 ± 0.010 - 0.010 1.335 0.000 ± 0.010 - 0.010 1.340 0.000 ± 0.010 - 0.010 1.345 0.000 ± 0.010 - 0.010 1.350 0.000 ± 0.010 - 0.010 1.355 0.000 ± 0.010 - 0.010 1.360 0.000 ± 0.010 - 0.010 1.365 0.000 ± 0.010 - 0.010 1.370 0.000 ± 0.010 - 0.010 1.375 0.000 ± 0.010 - 0.010 1.380 0.000 ± 0.010 - 0.010 1.385 0.000 ± 0.010 - 0.010 1.390 0.000 ± 0.010 - 0.010 1.395 0.000 ± 0.010 - 0.010 1.400 0.000 ± 0.010 - 0.010 1.405 0.000 ± 0.010 - 0.010 1.410 0.000 ± 0.010 - 0.010 1.415 0.000 ± 0.010 - 0.010 1.420 0.000 ± 0.010 - 0.010 1.425 0.000 ± 0.010 - 0.010 1.430 0.000 ± 0.010 - 0.010 1.435 0.000 ± 0.010 - 0.010 1.440 0.000 ± 0.010 - 0.010 1.445 0.000 ± 0.010 - 0.010 1.450 0.000 ± 0.010 - 0.010 1.455 0.000 ± 0.010 - 0.010 1.460 0.000 ± 0.010 - 0.010 1.465 0.000 ± 0.010 - 0.010 1.470 0.000 ± 0.010 - 0.010 1.475 0.000 ± 0.010 - 0.010 1.480 0.000 ± 0.010 - 0.010 1.485 0.000 ± 0.010 - 0.010 1.490 0.000 ± 0.010 - 0.010 1.495 0.000 ± 0.010 - 0.010 1.500 0.000 ± 0.010 - 0.010 1.505 0.000 ± 0.010 - 0.010 1.510 0.000 ± 0.010 - 0.010 1.515 0.000 ± 0.010 - 0.010 1.520 0.000 ± 0.010 - 0.010 1.525 0.000 ± 0.010 - 0.010 1.530 0.000 ± 0.010 - 0.010 1.535 0.000 ± 0.010 - 0.010 1.540 0.000 ± 0.010 - 0.010 1.545 0.000 ± 0.010 - 0.010 1.550 0.000 ± 0.010 - 0.010 1.555 0.000 ± 0.010 - 0.010 1.560 0.000 ± 0.010 - 0.010 1.565 0.000 ± 0.010 - 0.010 1.570 0.000 ± 0.010 - 0.010 1.575 0.000 ± 0.010 - 0.010 1.580 0.000 ± 0.010 - 0.010 1.585 0.000 ± 0.010 - 0.010 1.590 0.000 ± 0.010 - 0.010 1.595 0.000 ± 0.010 - 0.010 1.600 0.000 ± 0.010 - 0.010 1.605 0.000 ± 0.010 - 0.010 1.610 0.000 ± 0.010 - 0.010 1.615 0.000 ± 0.010 - 0.010 1.620 0.000 ± 0.010 - 0.010 1.625 0.000 ± 0.010 - 0.010 1.630 0.000 ± 0.010 - 0.010 1.635 0.000 ± 0.010 - 0.010 1.640 0.000 ± 0.010 - 0.010 1.645 0.000 ± 0.010 - 0.010 1.650 0.000 ± 0.010 - 0.010 1.655 0.000 ± 0.010 - 0.010 1.660 0.000 ± 0.010 - 0.010 1.665 0.000 ± 0.010 - 0.010 1.670 0.000 ± 0.010 - 0.010 1.675 0.000 ± 0.010 - 0.010 1.680 0.000 ± 0.010 - 0.010 1.685 0.000 ± 0.010 - 0.010 1.690 0.000 ± 0.010 - 0.010 1.695 0.000 ± 0.010 - 0.010 1.700 0.000 ± 0.010 - 0.010 1.705 0.000 ± 0.010 - 0.010 1.710 0.000 ± 0.010 - 0.010 1.715 0.000 ± 0.010 - 0.010 1.720 0.000 ± 0.010 - 0.010 1.725 0.000 ± 0.010 - 0.010 1.730 0.000 ± 0.010 - 0.010 1.735 0.000 ± 0.010 - 0.010 1.740 0.000 ± 0.010 - 0.010 1.745 0.000 ± 0.010 - 0.010 1.750 0.000 ± 0.010 - 0.010 1.755 0.000 ± 0.010 - 0.010 1.760 0.000 ± 0.010 - 0.010 1.765 0.000 ± 0.010 - 0.010 1.770 0.000 ± 0.010 - 0.010 1.775 0.000 ± 0.010 - 0.010 1.780 0.000 ± 0.010 - 0.010 1.785 0.000 ± 0.010 - 0.010 1.790 0.000 ± 0.010 - 0.010 1.795 0.000 ± 0.010 - 0.010 1.800 0.000 ± 0.010 - 0.010 1.805 0.000 ± 0.010 - 0.010 1.810 0.000 ± 0.010 - 0.010 1.815 0.000 ± 0.010 - 0.010 1.820 0.000 ± 0.010 - 0.010 1.825 0.000 ± 0.010 - 0.010 1.830 0.000 ± 0.010 - 0.010 1.835 0.000 ± 0.010 - 0.010 1.840 0.000 ± 0.010 - 0.010 1.845 0.000 ± 0.010 - 0.010 1.850 0.000 ± 0.010 - 0.010 1.855 0.000 ± 0.010 - 0.010 1.860 0.000 ± 0.010 - 0.010 1.865 0.000 ± 0.010 - 0.010 1.870 0.000 ± 0.010 - 0.010 1.875 0.000 ± 0.010 - 0.010 1.880 0.000 ± 0.010 - 0.010 1.885 0.000 ± 0.010 - 0.010 1.890 0.000 ± 0.010 - 0.010 1.895 0.000 ± 0.010 - 0.010 1.900 0.000 ± 0.010 - 0.010 1.905 0.000 ± 0.010 - 0.010 1.910 0.000 ± 0.010 - 0.010 1.915 0.000 ± 0.010 - 0.010 1.920 0.000 ± 0.010 - 0.010 1.925 0.000 ± 0.010 - 0.010 1.930 0.000 ± 0.010 - 0.010 1.935 0.000 ± 0.010 - 0.010 1.940 0.000 ± 0.010 - 0.010 1.945 0.000 ± 0.010 - 0.010 1.950 0.000 ± 0.010 - 0.010 1.955 0.000 ± 0.010 - 0.010 1.960 0.000 ± 0.010 - 0.010 1.965 0.000 ± 0.010 - 0.010 1.970 0.000 ± 0.010 - 0.010 1.975 0.000 ± 0.010 - 0.010 1.980 0.000 ± 0.010 - 0.010 1.985 0.000 ± 0.010 - 0.010 1.990 0.000 ± 0.010 - 0.010 1.995 0.000 ± 0.010 - 0.010 2.000 0.000 ± 0.010 - 0.010 2.005 0.000 ± 0.010 - 0.010 2.010 0.000 ± 0.010 - 0.010 2.015 0.000 ± 0.010 - 0.010 2.020 0.000 ± 0.010 - 0.010 2.025 0.000 ± 0.010 - 0.010 2.030 0.000 ± 0.010 - 0.010 2.035 0.000 ± 0.010 - 0.010 2.040 0.000 ± 0.010 - 0.010 2.045 0.000 ± 0.010 - 0.010 2.050 0.000 ± 0.010 - 0.010 2.055 0.000 ± 0.010 - 0.010 2.060 0.000 ± 0.010 - 0.010 2.065 0.000 ± 0.010 - 0.010 2.070 0.000 ± 0.010 - 0.010 2.075 0.000 ± 0.010 - 0.010 2.080 0.000 ± 0.010 - 0.010 2.085 0.000 ± 0.010 - 0.010 2.090 0.000 ± 0.010 - 0.010 2.095 0.000 ± 0.010 - 0.010 2.100 0.000 ± 0.010 - 0.010 2.105 0.000 ± 0.010 - 0.010 2.110 0.000 ± 0.010 - 0.010 2.115 0.000 ± 0.010 - 0.010 2.120 0.000 ± 0.010 - 0.010 2.125 0.000 ± 0.010 - 0.010 2.130 0.000 ± 0.010 - 0.010 2.135 0.000 ± 0.010 - 0.010 2.140 0.000 ± 0.010 - 0.010 2.145 0.000 ± 0.010 - 0.010 2.150 0.000 ± 0.010 - 0.010 2.155 0.000 ± 0.010 - 0.010 2.160 0.000 ± 0.010 - 0.010 2.165 0.000 ± 0.010 - 0.010 2.170 0.000 ± 0.010 - 0.010 2.175 0.000 ± 0.010 - 0.010 2.180 0.000 ± 0.010 - 0.010 2.185 0.000 ± 0.010 - 0.010 2.190 0.000 ± 0.010 - 0.010 2.195 0.000 ± 0.010 - 0.010 2.200 0.000 ± 0.010 - 0.010 2.205 0.000 ± 0.010 - 0.010 2.210 0.000 ± 0.010 - 0.010 2.215 0.000 ± 0.010 - 0.010 2.220 0.000 ± 0.010 - 0.010 2.225 0.000 ± 0.010 - 0.010 2.230 0.000 ± 0.010 - 0.010 2.235 0.000 ± 0.010 - 0.010 2.240 0.000				

1
2
3
4
5
6
7
8
9
10
11
12
13
14
15
16
17
18
19
20
21
22
23
24
25
26
27
28
29
30
31
32
33
34
35
36
37
38
39
40
41
42
43
44
45
46
47
48
49
50
51
52
53
54
55
56
57
58
59
60
61
62
63
64
65
66
67
68
69
70
71
72
73
74
75
76
77
78
79
80
81
82
83
84
85
86
87
88
89
90
91
92
93
94
95
96
97
98
99
100

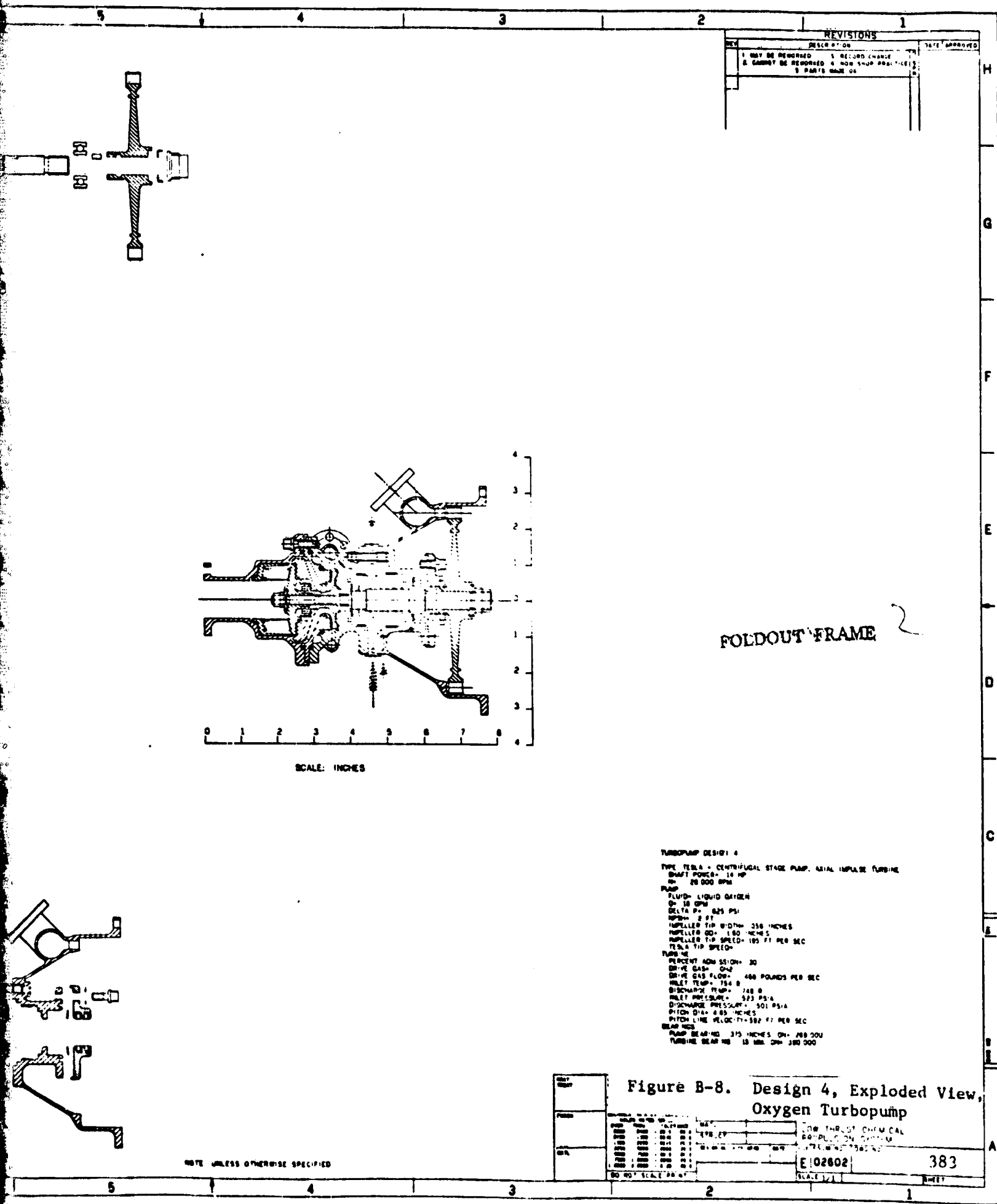


FOLDOUT FRAME

380

382

NOTE: UNLESS OTHERWISE SPECIFIED

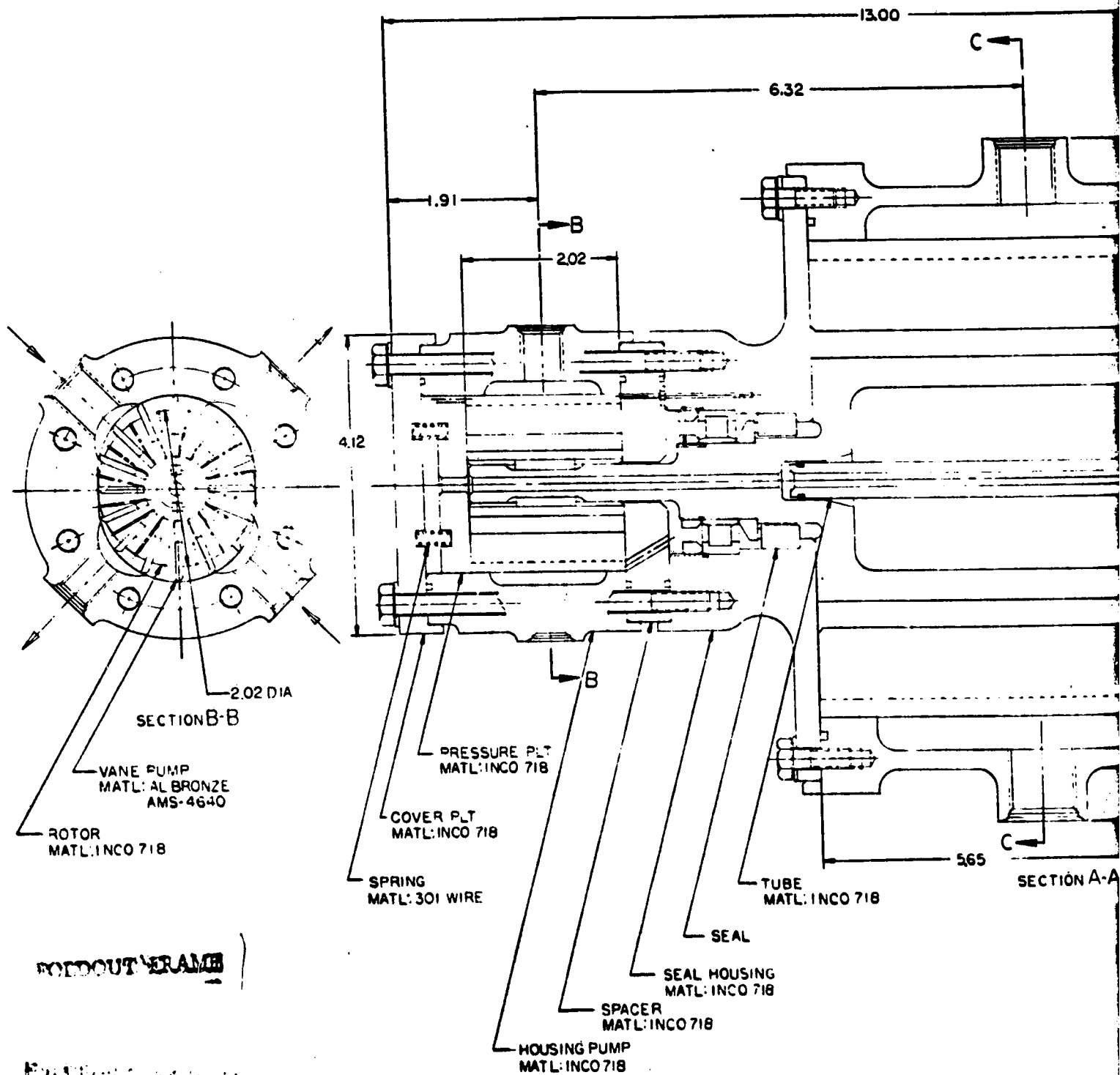


REVISIONS		DATE	APPROVED
REV	DESCRIPTION		
1	NOT BE REQUIRED		
2	REWORK CHANGE		
3	CANNOT BE REQUIRED		
4	NON-SHAFT PARTS		
5	PARTS NAME		

TURBOPUMP DESIGN 4
 TYPE: TELBA - CENTRIFUGAL STAGE PUMP, AXIAL IMPELLER TURBINE
 SHAFT POWER: 14 HP
 RPM: 20,000 RPM
 PUMP
 FLUID: LIQUID OXYGEN
 Q: 18 GPM
 DELTA P: 825 PSI
 RPM: 20,000
 IMPELLER TIP WIDTH: 358 INCHES
 IMPELLER OD: 180 INCHES
 IMPELLER TIP SPEED: 185 FT PER SEC
 TELBA TIP SPEED:
 TURBINE
 PERCENT AGE: 30
 DRIVE GAS: O₂
 DRIVE GAS FLOW: 480 POUNDS PER SEC
 INLET TEMP: 754 R
 DISCHARGE TEMP: 748 R
 INLET PRESSURE: 523 PSIA
 DISCHARGE PRESSURE: 501 PSIA
 PITCH DIA: 4.85 INCHES
 PITCH LINE VELOCITY: 582 FT PER SEC
 BEARINGS
 PUMP BEARING: 375 INCHES DIA, 200,000
 TURBINE BEARING: 18 INCH DIA, 100,000

FIGURE	B-8	DESIGN	4	EXPLODED VIEW	OXYGEN TURBOPUMP
DATE	10/26/02	BY	383	SCALE	1/2"
NO.	1	SCALE	1/2"	SHEET	1

NOTE: UNLESS OTHERWISE SPECIFIED



VANE PUMP-MOTOR 5
 TYPE 16 VANE DOUBLE FLOODED PUMP
 24 VANE DOUBLE FLOODED MOTOR
 POWER=25 HP
 N=2500 RPM

PUMP
 FLUID=LIQUID HYDROGEN
 Q=33 GPM
 DELTA P=950 PSI
 NPSH=15 FT
 VANE TIP SPEED=22 FT/SEC

MOTOR
 DRIVE GAS=GH₂
 DRIVE FLOW=309 LB/SEC
 INLET TEMP=780 R
 INLET PRESSURE=655 PSIA
 DISCHARGE PRESSURE=617 PSIA

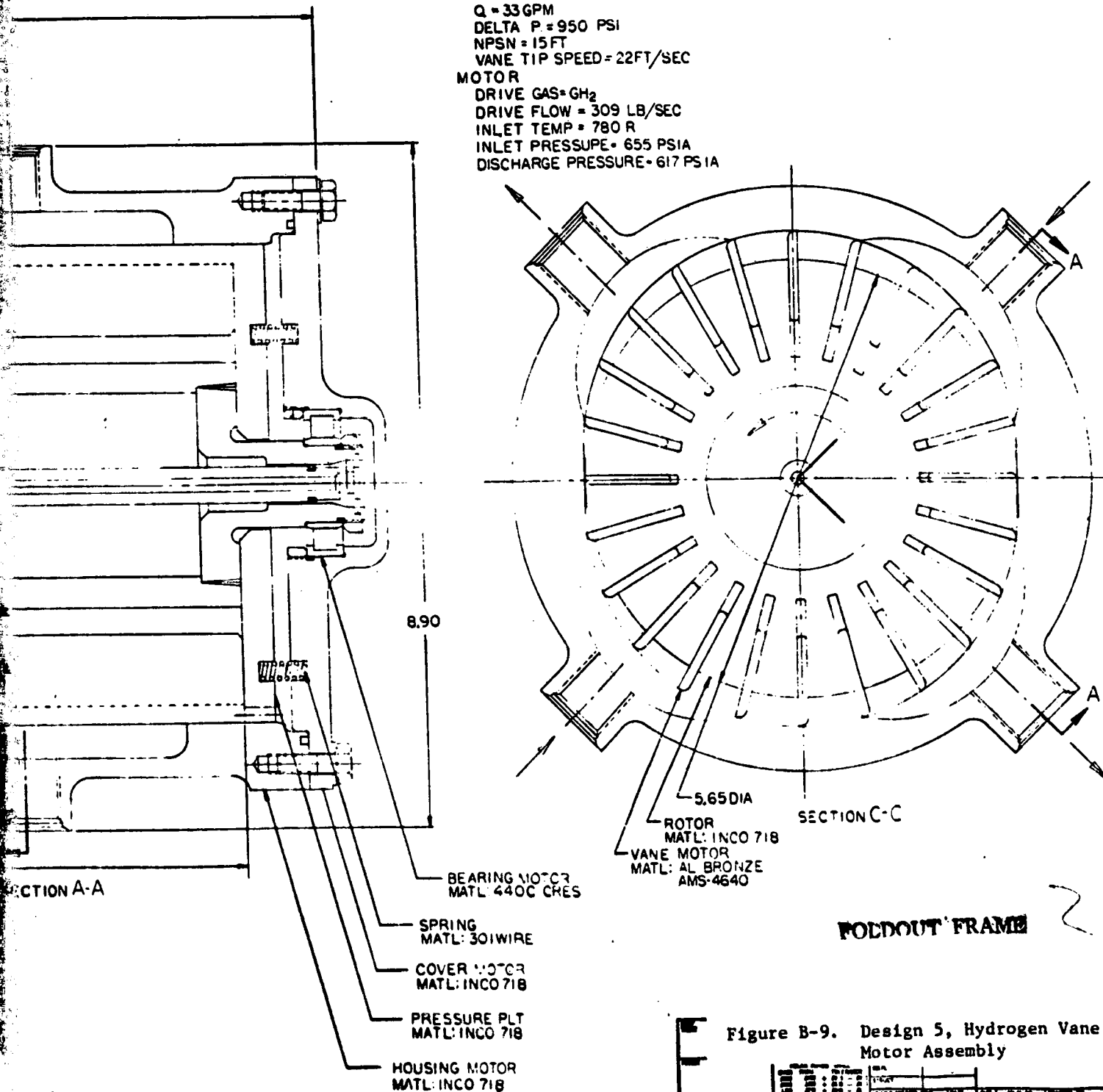
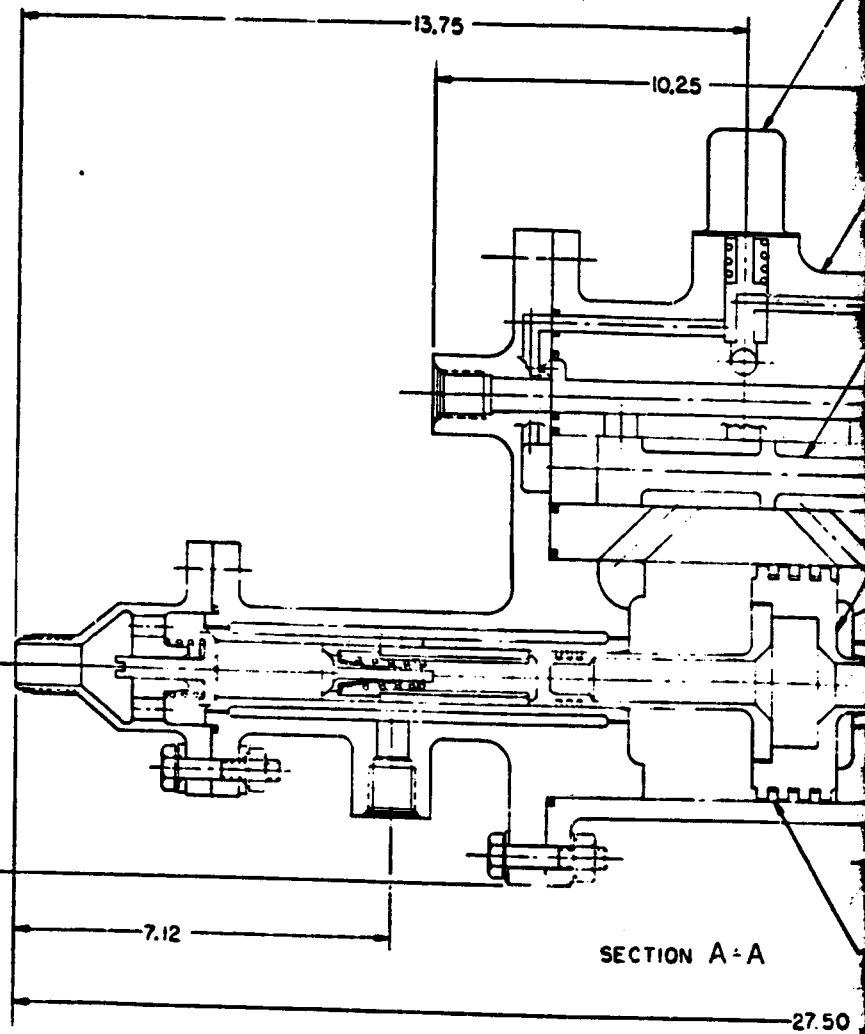
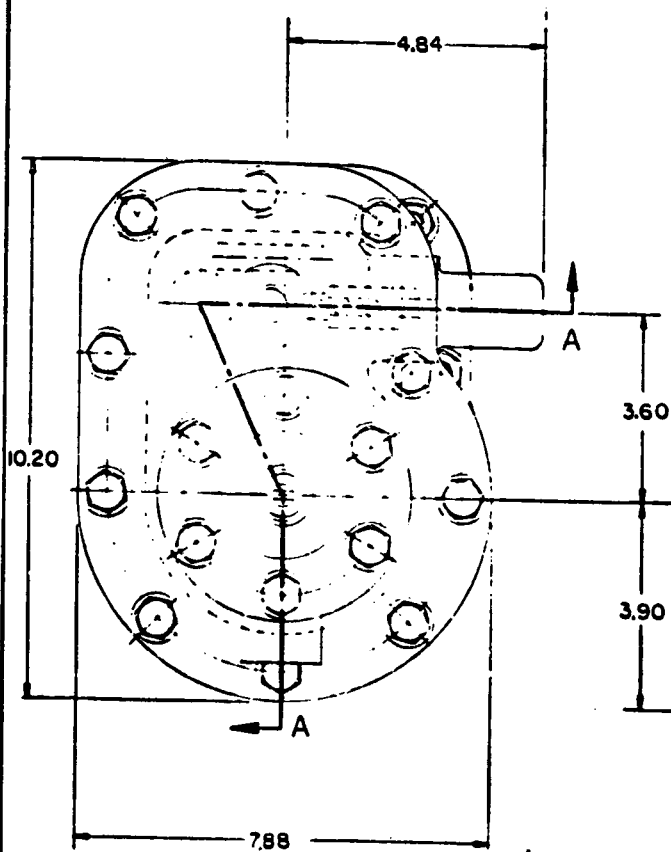


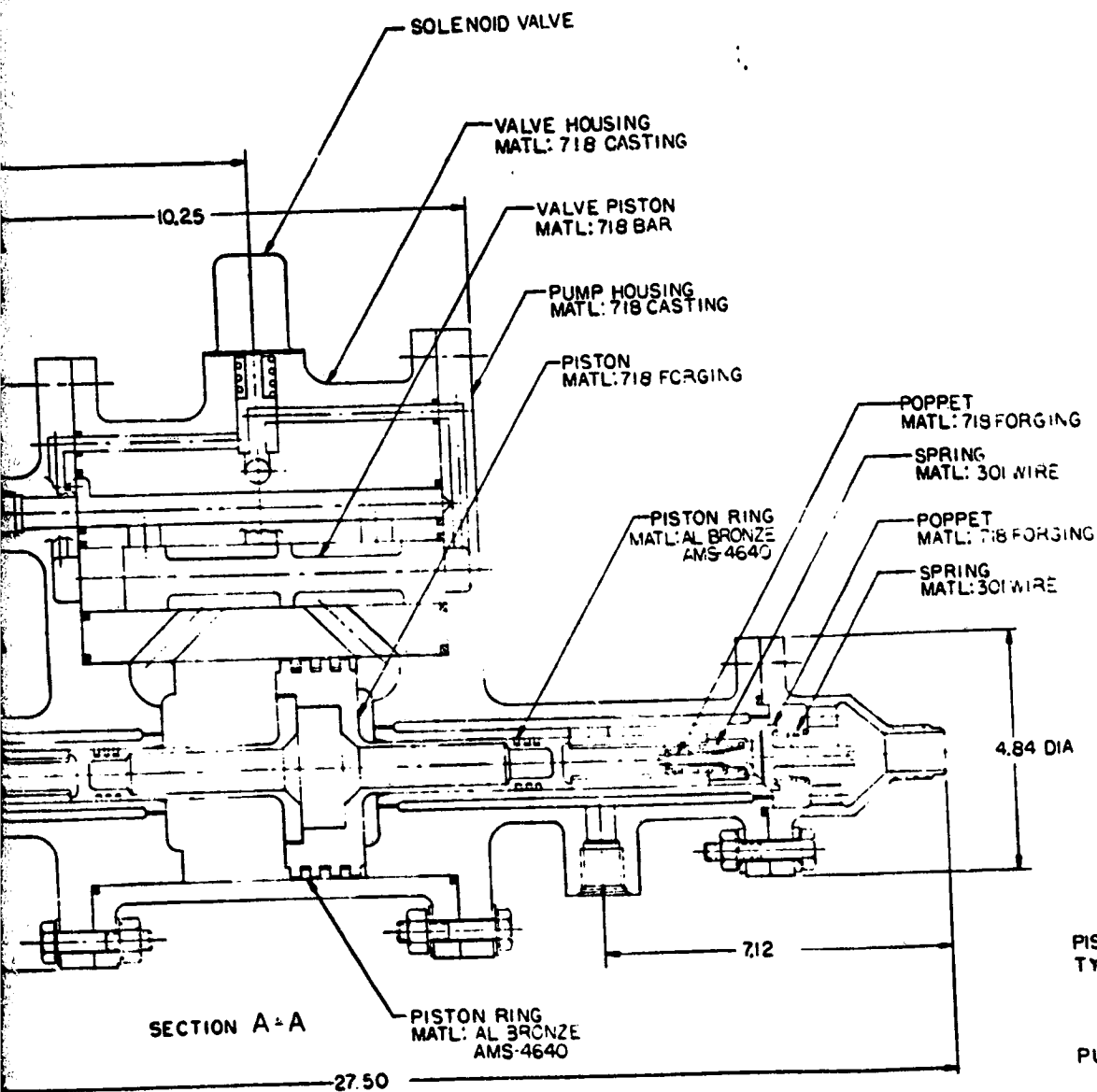
Figure B-9. Design 5, Hydrogen Vane Pump-Motor Assembly

REV	DATE	BY	CHKD	QTY	385
1	10/10/60	J. H. HARRIS	J. H. HARRIS	02602	
2	11/10/60	J. H. HARRIS	J. H. HARRIS		
3	12/10/60	J. H. HARRIS	J. H. HARRIS		



BOULDER FRAME

FLANGE AND FLANGE MOUNTING



FOLDOUT FRAME

PISTON PUMP-DRIVE 6
TYPE: DUAL PUMPS DOUBLE ACTING
DRIVE: FREE PISTON
POWER: 8 HP
N: 625 CPM

PUMP
FLUID: LIQUID METHANE
Q: 10 GPM
DELTA P: 950 PSI
NPSH: .38 FT
DIAMETER: 1.076 IN
STROKE: 2 IN
AVE VELOCITY: 3.5 FT/SEC

DRIVE
DRIVE GAS: CH_4
DRIVE FLOW: 612 LB/SEC
INLET TEMP: 650 °R
INLET PRESSURE: 655 PSIA
DISCHARGE PRESSURE: 585 PSIA

Figure B-10. Design 6, Methane Piston Pump-Drive Assembly

DESIGN	02602	387
DATE		
BY		
CHECKED		
APPROVED		
REVISIONS		
1		
2		
3		
4		
5		
6		
7		
8		
9		
10		